GEOLOGICAL SURVEY OF CANADA
DEPARTMENT OF ENERGY, MINES AND RESOURCES, OTTAWA

PAPER 75-1B

REPORT OF ACTIVITIES
PART B

1975

Technical editing and compilation
R.G. Blackadar
P.J. Griffin
Helen Dumych

Production editing and layout
Leona R. Mahoney
Angelica Koops

Printed from text typed by:
Janet Gilliland
Sharon Parnham

Energy, Mines and Resources Canada
Énergie, Mines et Ressources Canada

GEOLOGICAL SURVEY
PAPER 75-1B

REPORT OF ACTIVITIES
PART B

1975

Available by mail from *Information Canada*, Ottawa, K1A 0S9

from the Geological Survey of Canada
601 Booth St., Ottawa, K1A 0E8

and

Information Canada bookshops in

HALIFAX — 1683 Barrington Street
MONTREAL — 640 St. Catherine Street W.
OTTAWA — 171 Slater Street
TORONTO — 221 Yonge Street
WINNIPEG — 393 Portage Avenue
VANCOUVER — 800 Granville Street

or through your bookseller

A deposit copy of this publication is also available
for reference in public libraries across Canada

Price - Canada: $5.00
Other Countries: $6.00

Catalogue No. M44-75-1B

Price subject to change without notice

Information Canada
Ottawa
1975

CONTENTS

ADDENDUM

(The following papers were received after production of this report had begun on April 9, 1975)

INTRODUCTION

In January 1958 the Geological Survey issued a 23-page informal report summarizing the field work undertaken by its staff during the 1957 field season. In the following four years similar reports were issued, each being somewhat larger than its predecessor. The results of the 1962 field season were released as Paper 63-1 — "Summary of Research: Field, 1962" — and being published in the Paper series of the Survey were brought to the attention of a much wider audience. Not all of the Survey's work derives from field studies, and a second part, released in the summer and comprising mainly reports resulting from office and laboratory studies, was also started in 1963. Succeeding years have seen the evolution of these reports from a collection of brief, summary reports to a series that includes many papers comparable in scope and quality to those appearing in the principal scientific journals. This development is most visible in the sheer bulk of the recent versions of the report and to assist in making volumes more manageable for production, more convenient for the reader and more flexible for the contributor, it has been decided to publish the Report of Activities series in three parts. These will be:

Part A: released in January and including many of the reports based on the preceding field season.

Part B: released in June and serving as a publication medium for short scientific contributions from staff members.

Part C: released in November and designed to facilitate early release of significant data obtained during the field season and also as a publication outlet for short scientific reports.

It is probable that Part A will continue to be the largest but it is hoped that the new publication schedule will to some extent at least, reduce the crisis atmosphere that usually prevails in the editorial offices during "Report of Activities time" — mid-October to late November.

R. G. Blackadar
Chief Scientific Editor

ERRATUM

Geological Survey Paper 74-1, Part B, p. 53

G.E.M. Aslin
Resource Geophysics and Geochemistry Division

The data pertaining to silver content of samples collected on Little Cornwallis Island and presented by Allan (1974) have been found to be in error. The method of analysis used was atomic absorption spectroscopy where, for silver, background correction is a necessity, especially when limestone samples are involved. It appears this correction was overlooked, leading to erroneously high values. The analysis was repeated and the revised Tables 1 and 2 are shown below. A value of 0.3 ppm is given for all samples below the detection limit of 0.5 ppm Ag. All samples shown on Figure 4 contain less than 0.5 ppm Ag.

Revised Table 1, p. 53, Geol. Surv. Can., Paper 74-1, Part B

	ppm SILVER								
DEPTH	(1)	(2)	(3)	(4)	(5)	(6)	(7)	(8)	(9)	(10)
0-15	13.5	0.3	2.5	2.0	2.9	7.6	0.3	0.3	0.3	0.3
15-30	0.8	0.3	2.8	1.0	3.3	11.0	0.3	0.3	0.3	0.3
30-45	4.4	0.3	2.2	1.7	3.1	11.0	0.3	0.3	0.3	0.3

Revised Table 2, p. 53, Geol. Surv. Can., Paper 74-1, Part B

Sample Number	Silver
(11)	0.3
(12)[2]	7.6
(13)[2]	9.3
(14)[2]	0.3
(15)[2]	0.3
(16)	0.3
(17)[3]	0.3
(18)[3]	0.3
(19)[3]	0.3
(20)	0.3
(21)[4]	2.9
(22)[5]	0.3
(23)[5]	0.3
(24)[5]	0.3

Reference:

Allan, R.J.
1974: Trace Metal Dispersion in an Arctic Desert Landscape: a Pb-Zn Deposit on Little Cornwallis Island, District of Franklin; *in* Report of Activities, November 1973 to March 1974, Geol. Surv. Can., Paper 74-1, Pt. B, p. 51-56.

1. STUDIES IN "STANDARD SAMPLES" OF SILICATE ROCKS AND MINERALS

Project 690089

Sydney Abbey
Central Laboratories and Administrative Services Division

Over 70 laboratories, located in about 20 different countries, indicated their willingness to collaborate in the analysis of the two Bancroft syenites and the Mount Royal gabbro. To date, over 50 of these laboratories have reported anywhere from one to 160 individual results. The available data have been tabulated, and calculations made for the establishment of some recommended values - mainly for the major, minor and more common trace elements. Less reliable values were deduced for a number of additional trace elements. The first report on these operations is in the advanced stage of preparation. Additional data continue to arrive, and it may therefore be necessary to publish a second report a year or two after the first.

Work was also continued on the compilations of data on reference rock samples originating elsewhere. New data were received on samples originating in the United Kingdom and in Scandinavia, and errors in earlier compilations corrected. All of this new information, combined with some results from our own laboratories, are included in a paper, now in press.

Reference

Abbey, Sydney
Studies in "standard samples" of silicate rocks and minerals, Part 4. 1974 edition of "usable" values; Geol. Surv. Can., Paper 74-41. (In press)

2. COMPREHENSIVE ANALYSIS OF SILICATE ROCKS BY X-RAY FLUORESCENCE SPECTROSCOPY

Project 690090

J.-L. Bouvier and G.R. Lachance
Central Laboratories and Administrative Services Division

In June 1974, the 12-year-old ARL VXQ multichannel X-ray Quantometer was replaced by a Philips PW 1450 automatic sequential X-ray spectrometer. The older instrument permitted the determination of only eight elements and those could not be varied; the new one is almost infinitely flexible in terms of the number of elements that can be determined. Also acquired was a Claisse Fluxer - a semi-automatic apparatus for preparing reproducible fusions of samples.

With this new equipment, it was possible to develop a more nearly "complete" method of rock analysis, only carbon dioxide, water and ferrous iron still requiring chemical determination.

The new scheme consists of three steps:

(a) The mixture (0.5 g of sample and 3.0 g of a lithium metaborate-tetraborate mixture) is fused in a Pt-Au crucible and the melt poured into a mould to produce a clear glass disc. This takes about eight minutes.

(b) The disc is irradiated with primary X-rays in the spectrometer and the intensities of characteristic fluorescent and background radiations are measured for Si, Al, Fe, Mg, Ca, Na, K, Ti, P, S, Cr, Mn and six additional "trace" elements selected by the submitter. Output of intensities is in the form of a numerical print-out and a punched paper tape. About 30 minutes are required for these operations.

(c) The punched tape data are reduced in an off-line minicomputer to give a print-out of concentration for each oxide. This step includes corrections for background, spectral line interference, instrumental drift, varying matrices and the effect of those components which are determined chemically. This takes only one minute.

The discs appear to be stable and are therefore available for further analysis. Accuracy of results is comparable to that obtained by the "neo-classical" scheme, in which silica is determined gravimetrically and most other components by atomic absorption or colorimetry.

3. USE OF AN INTEGRATOR AND MINICOMPUTER TO IMPROVE THE EFFICIENCY OF DATA PROCESSING IN CHEMICAL ANALYSIS

Project 690090

J.-L. Bouvier and R.J.J.M. Guillas
Central Laboratories and Administrative Services Division

In analysis by atomic absorption spectroscopy, maximum precision and accuracy can be attained by measuring the area under the curve representing the analytical signal, particularly in "total-volatilization" techniques, such as the Govindaraju "screw-rod" method. A major advance in both speed and accuracy was attained by introducing an integrating device, incorporating a digital read-out.

In the above application, and in others involving final measurement by instrumentation (e.g. in use of a selective-ion electrode meter), it is generally necessary to take readings on a series of standards, to plot a calibration graph, and to read off the values for the unknowns from that graph. Such procedures are not only slow and tedious, but are also subject to human error.

In order to accelerate and simultaneously improve the operation, use of a minicomputer was introduced. Programs were written whereby, in effect, the equations of linear regression curves are calculated from readings on the standards. Standard deviations are also calculated, standards with the largest deviations rejected, and new curves calculated, from which the values for the unknowns are deduced.

4. A "NEO-CLASSICAL" SCHEME OF ROCK ANALYSIS

Project 690090

J.-L. Bouvier, R.J.J.M. Guillas and Sydney Abbey
Central Laboratories and Administrative Services Division

In the proposed scheme, the sample is fused with a threefold excess of lithium metaborate and the fusion disintegrated in hydrochloric acid. Methanol is added and the mixture evaporated to volatilize borate and to dehydrate the bulk of the silica. After filtration, the silica is determined in the conventional gravimetric manner. The residue from the HF treatment of the silica is fused with a little more lithium metaborate, dissolved in HCl and combined with the filtrate. Aliquots of the resulting solution, or of two dilutions of it, are used to determine unprecipitated silica and phosphorus colorimetrically, and Al, total Fe, Mg, Ca, Na, K, Ti, Mn, Ba, Sr, Cr and Ni by atomic absorption.

As originally applied, the atomic absorption part of the new scheme involved the use of standard solutions, prepared from pure reagents. In order to reduce the number of standard solutions, and to ensure that knowns and unknowns were of similar chemical composition, portions of all available international reference samples of silicate rocks were taken through the decomposition procedure, and the resulting solutions used as standards. Only 500 mg of each reference sample was used, and the standard solutions thus produced can be used in the analysis of dozens of unknowns.

The major difficulties observed in the scheme were:

(1) The silica results tended toward a positive bias. That was thought to be due to incomplete volatilization of boric acid at the methanol stage, but experiments have not confirmed that suspicion. Further work is needed.
(2) With samples containing relatively high titanium values, it was very difficult to obtain a clear solution from the fusion of the residue from the HF treatment of the separated silica. Spectrographic examination revealed that the residue consisted almost entirely of titanium dioxide. The fusion of that residue with lithium metaborate was therefore replaced by fusion with potassium pyrosulphate, which readily gives a clear solution with dilute sulphuric acid. That solution is set aside, and an aliquot of it combined with one of the main solution only for titanium determination.
(3) Occasional erratic results are obtained in the determination of Al and Ca by atomic absorption, but the causes have not been ascertained at this writing.

All calculations involving atomic absorption in the proposed scheme were done by means of the computer system described in the preceding note.

5. APPLICATION OF SPECTROCHEMICAL METHODS TO TRACE ELEMENT DETERMINATIONS IN GEOLOGICAL MATERIALS

Project 690090

W.H. Champ, K.A. Church, F.W. Jones and Laboratory Staff
Central Laboratories and Administrative Services Division

Optical components of the Jaco Direct Reading Spectrometer have been completely realigned and additional exit slits installed to provide a total of 41 read-out channels, which is the physical limit of the instrument for our purposes.

Re-calibration of the instrument is underway to establish a revised general rock analysis scheme comparable to the current photographic spectrographic method. This will produce rapid analytical determinations for 30 elements per sample, replacing the former 20-element system. The new solid state electronic system provides greater stability and precision in operation.

Greater accuracy will be obtained through computer-controlled corrections for various spectral line interferences and through monitoring of curve displacements by use of control standards. Programs in "Basic" computer language for controlling these operations in the laboratory with the Datagen minicomputer have been devised.

A minicomputer program is also now in regular use to derive spectral line intensity ratios from densitometric measurements of photographic plates taken by any of our analytical methods. An extension of this program has been completed for obtaining element concentrations from the intensity ratios for the elements most often requested by our general silicate analytical method. This work is continuing and we expect eventually to have all of our quantitative spectrographic methods "computerized" to a high degree. The logical extension of this approach is to obtain automatic densitometric apparatus for reading the original photographic plates. This very complex and expensive installation has been considered for possible future action.

As a supporting base for these procedures, and for the additional analytical methods both photographic and direct reading that have been planned for the future, the laboratory staff has prepared a one kilogram "high purity" synthetic rock base and 144 individual synthetic standards covering 22 elements for establishing quantitative working curves and determining or correcting inter-element interferences in recorded spectra.

We have also successfully completed the synthesis and analyses of four very complex multi-element secondary "control" standards, made up in four different rock matrices and incorporating trace elements in known concentrations at varying levels. These have been made in sufficient amounts for daily use in monitoring the direct reading spectrometer, and also for use with our other photographic analytical methods.

6. CORRELATION BETWEEN COAL RANK, PALEOTEMPERATURE AND PETROLEUM OCCURRENCES IN ALBERTA[1]

Project 680133

P.A. Hacquebard
Institute of Sedimentary and Petroleum Geology, Calgary

The degree of organic metamorphism (D.O.M.) of producing oil and gas pools in Alberta has been obtained from rank variations of subsurface and near-surface coals. Of the former, which are coals of the Lower Cretaceous Mannville Formation, the rank was determined from vitrinite reflectance measurements of thirty samples, collected from coreholes along a 338-km (210-mile) section across the eastern flank of the Alberta syncline. The coals lie at depths of between 600 and 330 m (1968-10 826 ft.) and increase in rank from 0.4 to 1.6 per cent Ro, from east to west (Section A-B, Figs. 1 and 2A).

The near-surface coals, of younger formations, show a similar increase in rank, which is illustrated with the isomoisture contour maps of Figure 2. The east-west changes are from 30 to 5 per cent in moisture content.

The maximum depth of burial of the near-surface coals has been obtained from moisture-overburden correlations established in Germany by Kutzner (1960), and Patteisky and Teichmüller (1960). By adding this depth to the present subsurface position of the Mannville coals, the original (maximum) overburden of these coals also is obtained. When this depth is plotted against the reflectance data of the coals, a smooth curve results (Fig. 3).

The procedure followed in plotting the Mannville coalification curve is illustrated with coal A, which has a reflectance of 0.62 per cent and lies 1402 m (4599 ft.) below the present surface, where near-surface coal B has 20 per cent moisture. A coal with 20 per cent moisture correlated with an overburden of 1463 m

FIGURE 1.

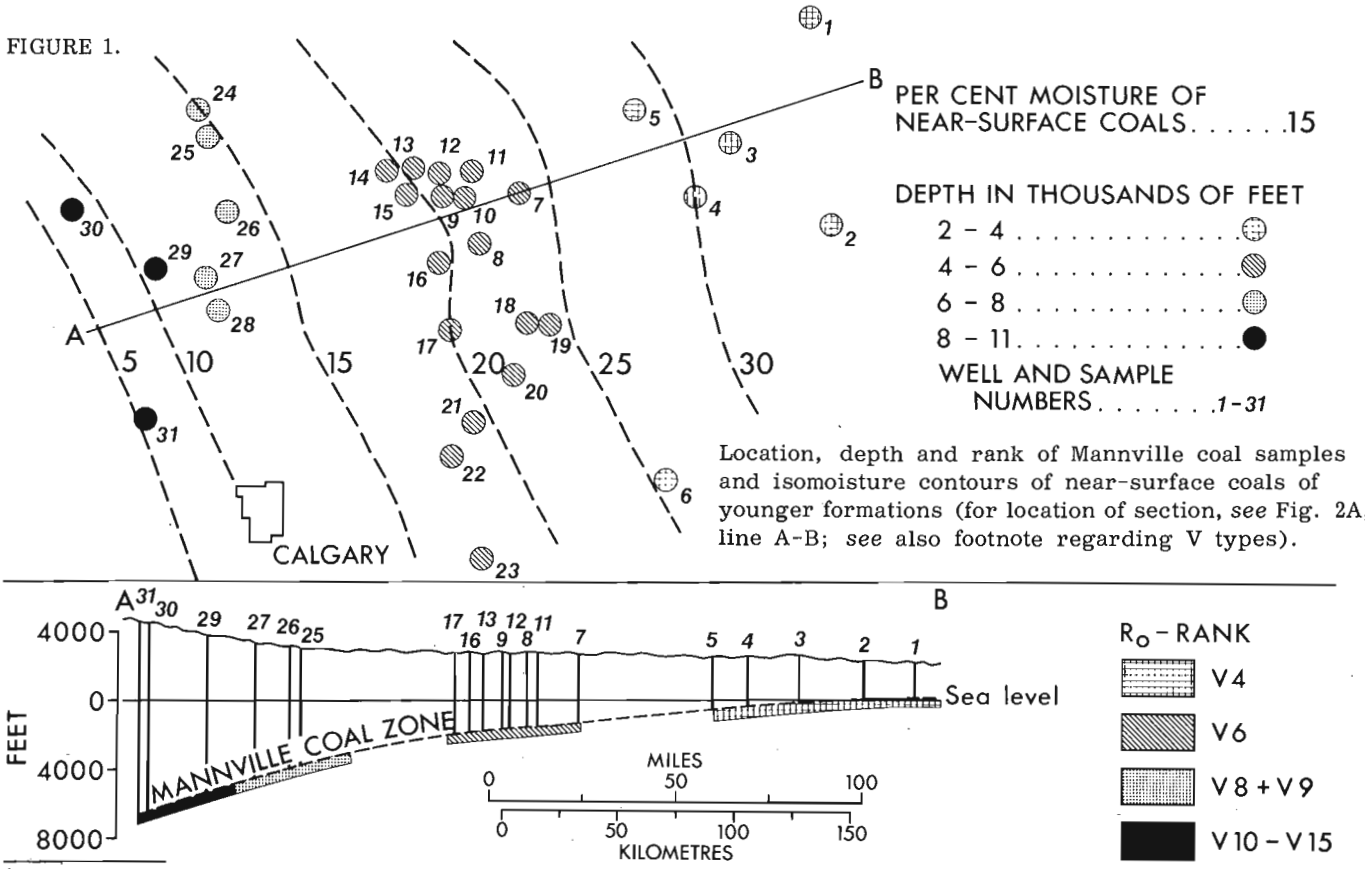

Location, depth and rank of Mannville coal samples and isomoisture contours of near-surface coals of younger formations (for location of section, *see* Fig. 2A, line A-B; *see* also footnote regarding V types).

[1]This report is a shortened version of a paper submitted to the 8th Carboniferous Congress, Moscow, 1975. The vitrinite reflectance measurements were carried out by J.R. Donaldson, formerly with the Geological Survey of Canada, presently with Energy Research Laboratories of CANMET in Ottawa. The Mannville coal samples were provided by N.L. Ball of the Institute of Sedimentary and Petroleum Geology in Calgary.

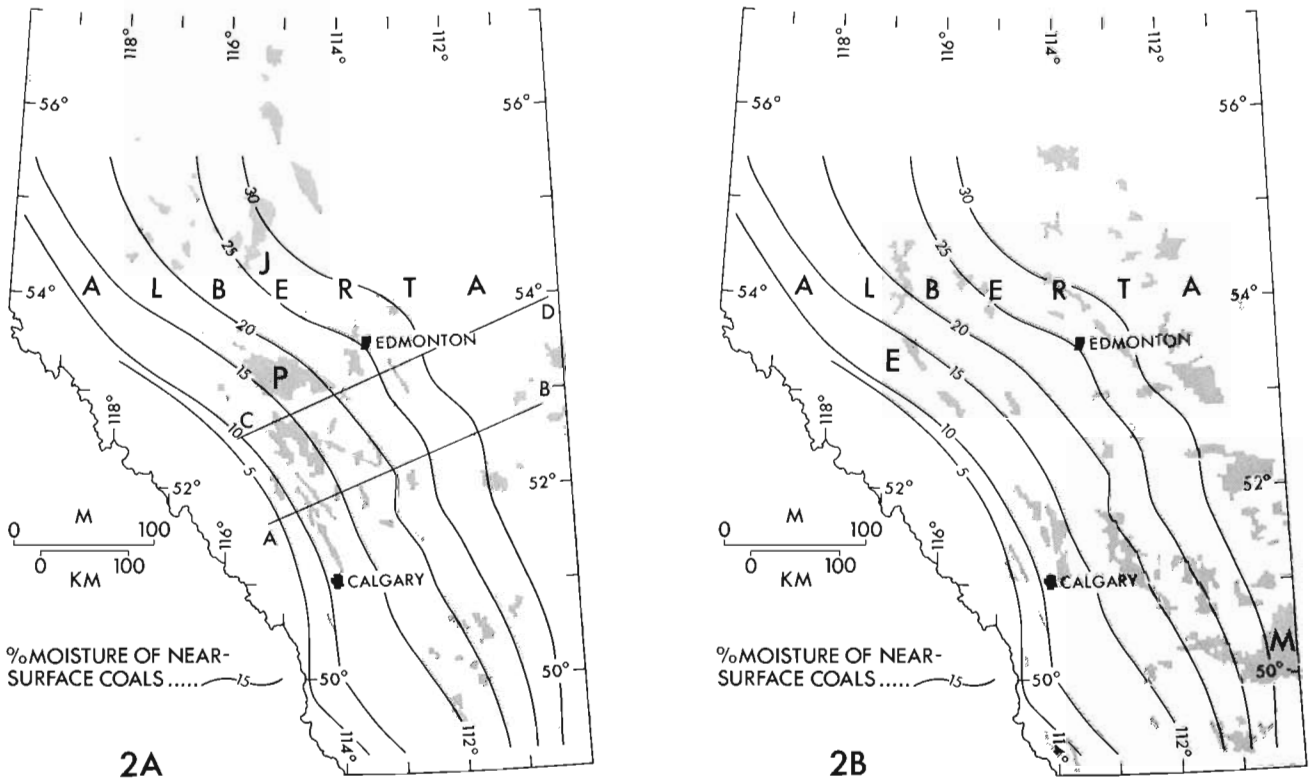

Figure 2. Maps of Alberta showing isomoisture contours of near-surface coals and locations of crude oil pools (2A) and natural gas pools (2B) (after Steiner *et al.*, 1972, Fig. 5; and Energy Resources Conservation Board, 1973).

(4800 ft.). The maximum depth of burial of coal A, therefore, is 1402 + 1463 = 2865 m (4599 + 4800 = 9399 ft.), which is shown on the ordinate of Figure 3.

The other 29 coals used for the diagram have been plotted in the same way. The resultant curve shows that a good correlation exists between rank and maximum depth of burial. However, the Mannville coalification curve relates only to lateral changes along an east-west section that is 338 km (210 miles) long. For an insight into the vertical changes in rank above and below the curve, additional information on coalification time and paleotemperatures is required.

This additional information has been obtained from the coalification models of Karweil (1956) and Bostick (1973), which relate coal rank to temperature and duration of heat. With these data, the isoreflectance contours (dashed lines in Fig. 3) have been drawn; they permit rank assignments at various depths above and below the Mannville curve. They also provide information required to calculate the paleogeothermal gradients, which are shown in the uppermost abscissa of Figure 3.

With the addition of the isoreflectance contours, Figure 3 now presents a three-dimensional picture of the changes in rank. Apart from the vertical changes, it also relates to regional changes, because the diagram is tied in with the isomoisture contours of Figure 2, which cover most of Alberta.

The method followed in obtaining the D.O.M. of the producing petroleum fields is best illustrated with the four pools especially indicated in Figures 2 and 3, by the letters J, P, M and E, and the numbers 1, 2, 3 and 4, respectively.

The Judy Creek oil pool (1), which geographically underlies the isomoisture contour of 26 per cent (Fig. 2), is plotted at this position in Figure 2 to its producing depth of 2743 m (9000 ft.), where it lies at a rank level of 0.8 to 0.9 per cent Ro, or V8[1]. The Pembina oil pool (2) is plotted at the 17 per cent moisture position. It produces from an average depth of 1524 m (5000 ft.), which correlates with a rank of V6. The Medicine Hat gas pool (3) at 30 per cent moisture and a depth of 610 m (2000 ft.) plots through to V4. The Edson gas field (4), which underlies the 14 per cent moisture contour by 3048 m (10 000 ft.), is correlated with a rank of V10.

Of these fields, those below the Mannville curve produce from Paleozoic strata, while those that lie above it have production from the Cretaceous or Tertiary. Since the former are below the Paleozoic unconformity, the question arises: can their rank position be projected from the considerably younger Mesozoic coals? The answer to this question is related to the maximum depth of burial, because it controls the rank of coal. An increase in depth of burial can cause an increase in rank, but a decrease will not affect

[1] V types represent increments of vitrinite reflectance that range from 0.40-0.49 per cent for V4, from 0.50-0.59 per cent for V5, etc.

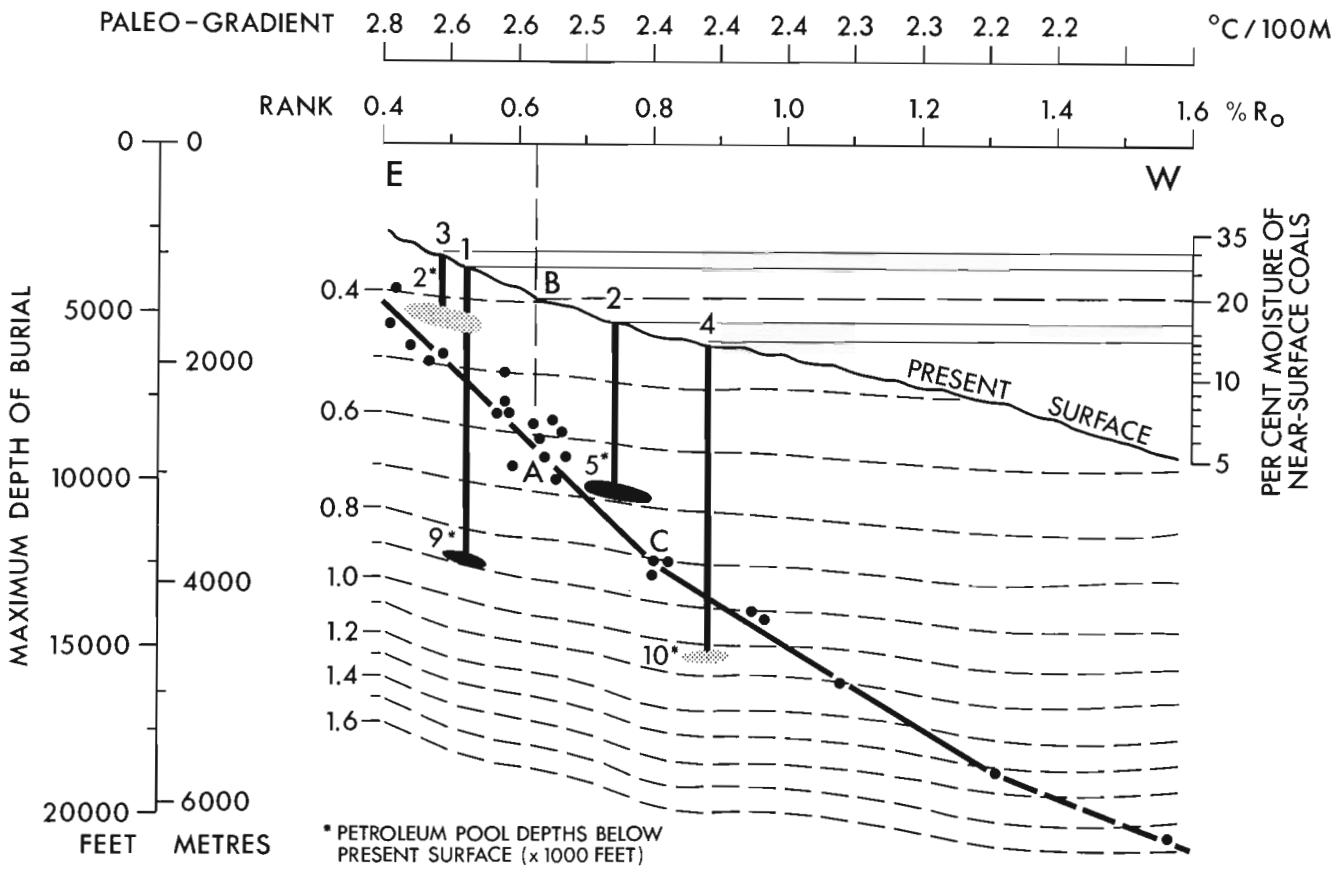

Figure 3. Coalification diagram applicable to entire Alberta Plains region, based on Mannville coalification curve, with rank assignments of four petroleum pools. (The oil pools are: 1. Judy Creek; 2. Pembina, and the natural gas pools; 3. Medicine Hat; 4. Edson.)

it, because the coalification process is irreversible; once a specific rank has been attained, it cannot be diminished.

It seems reasonable to assume that the maximum depth of burial took place in post-Mannville time, and that this depth exceeded the amount of overburden that was removed by erosion during the time represented by the unconformity. Rank projections from the Cretaceous into the underlying Paleozoic, therefore, appear to be in order.

Coal rank assignments of the oil and gas pools known in Alberta in 1973 have been made in the same manner as was explained previously for the four selected fields shown in Figure 3. A total of 78 oil pools and 66 gas pools have been considered, and of each the calculated initial reserves has been plotted against the projected coal rank, which is given in terms of reflectance by V types. For each V type, moreover, the corresponding paleotemperatures [obtained from Karweil's (1956) coalification model, using 35 m.y. as the duration of coalification of the Mannville coals at their maximum depth of burial] have been recorded also. The data on initial reserves, depth of producing zones and their geological ages were obtained from the publication by the Energy Resources Conservation Board of Alberta (1973) on oil and gas reserves. The results are shown in Figure 4.

The diagram reveals that, in Alberta, 88 per cent of the initial (in place) oil reserves have a D.O.M. comparable to a coal rank of 0.5 to 0.9 per cent Ro (V5 to V8), with about half (41%) of this occurring at V6. The paleotemperatures in this interval range from 68 to 116°C, with the bulk occurring between 82 and 96°C. No oil was found above V12, or above 143°C. These results conform rather well with published data of Landes (1966), Wassojewitch *et al.* (1969), Tissot (1971) and Teichmüller (1974), which indicate that significant hydrocarbon generation begins at about 65°C (0.5% Ro) and destruction of liquid hydrocarbons takes place above 135-150°C (1.2% Ro). This interval has been called "liquid window" by Pusey (1973). In Alberta, the liquid window lies essentially between 52 and 131°C (or between 0.4 and 1.1% Ro). When expressed in thickness of potential sediments, the window averages about 3000 m (9842 ft.), as deduced from Figure 3.

An interesting observation is that, while the Paleozoic oil occurs in about the same quantities at the rank levels of V6, V7 and V8, the Cretaceous oil is found predominantly at V6. Furthermore, heavy Cretaceous oil is found at V4, a level at which one normally does not expect oil to be present, since it lies below the minimum generation temperature of 65°C. Up-dip migration of Cretaceous oil would place it in a

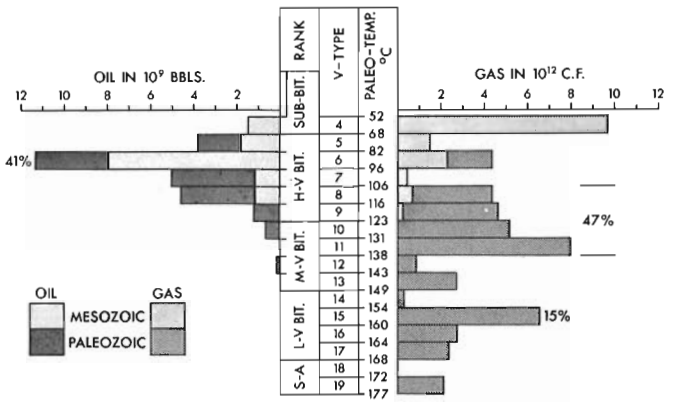

Figure 4. Coal rank assignments and paleotemperatures of initial petroleum reserves in producing fields of Alberta.

lower rank interval, because this reduces the depth of oil below the surface. Recent organic geochemistry studies of Alberta oils, carried out by Institut Français du Pétrole in co-operation with the Geological Survey of Canada, give strong support to an eastern migration of Cretaceous oil. This would not be the case with the Paleozoic oil, because it is confined mainly to coral reef deposits of limited areal extent.

As regards the D.O.M. of natural gas pools, large quantities of (biogenic?) methane occur at a coal rank of V4, or between temperatures of 52 and 68°C. Thermal gas ranges over a much larger rank interval; it is abundant particularly between V8 and V11 (47% of total gas) and substantial quantities also lie at V15 (15%). The temperature range of the thermal gas is from about 106 to 177°C. According to Landes (1966), gas is found between 120 and 204°C. So here also, the Alberta occurrences are within the broad temperature limitations previously published.

In general terms, it can be stated that, in Alberta, the D.O.M. of most of the oil is comparable with a rank of V5 to V8, or with high volatile "C" to high volatile "A" bituminous coal. Gas compares with V8 to V19, or with middle of high volatile "A" bituminous coal to semianthracite.

In conclusion, it can be stated that the present comparative study of coal rank and petroleum occurrences supports the view that both oil and gas occur within specific ranges of organic metamorphism. These ranges are defined by the paleotemperatures and this temperature interval can be deduced from the rank of coal and also from the rank of dispersed coaly particles in associated sediments. Rank determinations, therefore, are an important tool in petroleum exploration. They can outline areas with a favourable degree of organic metamorphism, and also indicate the subsurface position of the petroleum "floor" beyond which exploration drilling should not be extended.

References

Bostick, N.H.
1973: Time as a factor in thermal metamorphism of phytoclasts (coaly particles); Comptes Rendus, 7me Congrès Int. de Stratigraphie et de Géologie du Carbonifère, Krefeld 1971, Tome 2, p. 183-192.

Energy Resources Conservation Board of Alberta
1973: Reserves of crude oil, gas, natural gas liquids and sulphur - Province of Alberta; Rept. 73-18.

Karweil, J.
1956: Die Metamorphose der Kohlen vom Standpunkt der physikalischen Chemie; Z. Deut. Geol., Ges. 107, p. 132-139.

Kutzner, R.
1960: Änderungen in der Beschaffenheit der Braunkohle des Hambacher Forstes in Abhängigkeit von ihrer Tiefen Lage und palàographischen Situation; Geol. Meldearbeit der Techn. Hochschule Aachen. *See* also "Coal and coal-bearing strata", D.G. Murchison and T.S. Westoll (eds.), Oliver and Boyd Ltd., Edinburgh and London, 1968, Ch. 11, p. 243, Fig. 8.

Landes, K.K.
1966: Eometamorphism can determine oil floor; Oil Gas J., May 2, 1966, p. 172-177.

Patteisky, K. and Teichmüller, M.
1960: Inkohlungs-Verlauf, Inkohlungs-Maszstäbe und Klassification der Kohlen auf Grund von Vitrit-Analysen; Brennstof-Chemie 41, no. 3, p. 79-84; no. 4, p. 97-104; no. 5, p. 133-137.

Pusey, W.C. III
1973: The ESR-kerogen method; A new technique of estimating the organic maturity of sedimentary rocks; Pet. Times, Jan. 12, 1973, p. 21-24.

Steiner, J., Williams, G.D. and Dickie, G.J.
1972: Coal deposits of the Alberta Plains; Proc. First Geol. Conf. on Western Canadian Coal, Res. Counc. Alberta, Inf. Ser. 60, p. 85-96.

Teichmüller, M.
1974: Entstehung und Veränderung bituminöser Substanzen in Kohlen in Beziehung zur Entstehung und Umwandlung des Erdöls; Fortschr. Geol. Rheinl. u. Westf., Bd. 24, p. 65-112.

Tissot, B., Califet-Debyser, Y., Deroo, G. and Oudin, J.L.
1971: Origin and evolution of hydrocarbons in early Toarcian shales, Paris Basin, France; Am. Assoc. Pet. Geol., Bull. 55, no. 12, p. 2177-2193.

Wassojewitch, N.B., Kortchagina, J.I., Lopatin, N.W., Tchernichev, W.W. and Tchernikov, K.
1969: Die Hauptphase der Erdölbildung; Z. Angew. Geol., Bd. 15, p. 611-622.

7. MARINE SEISMIC REFRACTION PROFILING KAY POINT, YUKON TERRITORY

Project 730006

J.M. Carson[1], J.A. Hunter[1] and C.P. Lewis[2]

A shallow marine refraction survey in the Kay Point area of the Yukon Territory was carried out during the 1974 field season as part of a study of sediments and sedimentary processes along the Beaufort Sea coast, jointly sponsored by the Geological Survey, the Beaufort Sea Project, and the Environmental-Social Program, Northern Pipelines (*see* also Lewis, 1975 and Forbes, 1975). Approximately 80 reversed seismic refraction profiles were obtained along survey lines in the Babbage River estuary and seaward of the Kay Point spit and coastal cliff areas (Fig. 1). The objectives of the survey were to map the occurrence of sub-seabottom frozen ground, to infer from refractor velocities the type of frozen material, and to relate this information to such coastal processes as delta formation and shoreline recession.

The marine refraction technique employed in the study has been described by Hunter (1973). Unlike previous surveys, a "reversed" profiling technique was used, with explosive charges placed on both ends of the 200-metre 12-channel hydrophone array. This resulted in good definition of refractor velocities because the effects of dipping layers could be accounted for by standard interpretive techniques.

Velocity-depth structure for the profiles is illustrated in Figure 2. Velocities in layer 1 range from 1460 to 1800 metres/second (m/s) and are characteristic of unfrozen sediments of various grain sizes. Those of layer 2 range from 1800 to 2300 m/s and can be interpreted to be frozen ice-saturated sand. Velocities in layer 4 range from 3350 to 4600 m/s and are characteristic of frozen ice-rich gravels and coarse sand.

The refraction data, together with borehole logs and geomorphic observations (Forbes, 1975; Lewis 1975) suggest that the following sequence of events may have led to the formation of the present Babbage delta and estuary:

1. Development of a gravel and coarse sand outwash plain - fed through the Deep Creek valley from late-Wisconsin ice at King Point, 25 kilometres southeast of Kay Point, and from the Babbage River basin - which extended northwest into Herschel Basin where a lake may have been ponded, and then out to the lower sea level of that time: represented in Figure 2 by layer 4 and a portion of layer 3; the present estuary and nearshore areas would have been a part of the subaerial outwash plain and, therefore, frozen.

2. Retreat of the ice from King Point, leading eventually to decreased river competence and capacity and accompanied by rising sea level and resultant marine transgression until at least the mid-Holocene; deposition of sand in and in front of river channels and of silt and fine sand elsewhere on the delta and river flood plains: remainder of layer 3, much of layer 2 and possibly of portion of layer 1; the present estuary and nearshore areas would have been subaerial or very shallow marine and, therefore, frozen, perhaps containing considerable massive ground ice.

3. Formation of the modern delta and estuary under relatively stable late-Holocene sea level conditions and continued decreasing sediment supply; deposition of sand in channel areas and silt and fine sand elsewhere: layer 1 in Figure 2; some permafrost degradation may have occurred but probably quite slowly in water which, today, is shallow enough to freeze to the bottom in winter.

This history implies that layer 2 is more likely to be frozen silt and very fine sand than to be unfrozen gravel or coarse sand. The validity of this interpretation is untested, but is based on the presence, side by side at the same depths, of layer 3 which definitely is frozen (*see* profile BY11, Fig. 2) and layer 2, which is, therefore, likely to be frozen as well.

Contemporaneously with the development of the Babbage delta and estuary, the cliffs on the northeast side of the Kay Point peninsula (Fig. 1) were being cut back by marine wave erosion, resulting in the migration landward over the river and estuary deposits of the sandy gravels of Kay Point spit (*see* Lewis, 1975). This rapid migration continues today: 25 to 88 metres between 1952 and 1970 (McDonald and Lewis, 1973), and, with warm river water confined largely to the area behind the spit, has enabled the preservation of sub-seabottom frozen ground off both the spit and cliffs (Fig. 2).

References

Forbes, D.L.
1975: Sedimentary processes and sediments, Babbage River delta, Yukon coast; *in* Report of Activities, Pt. B, Geol. Surv. Can., Paper 75-1, pt. B, p. 157.

Hunter, J.A.
1973: Shallow moving refraction surveying in the Mackenzie Delta and Beaufort Sea; *in* Report of Activities, November 1972 to March 1973, Geol. Surv. Can., Paper 73-1, pt. B, p. 59-66.

[1]Resource Geophysics and Geochemistry Division.

[2]Terrain Sciences Division.

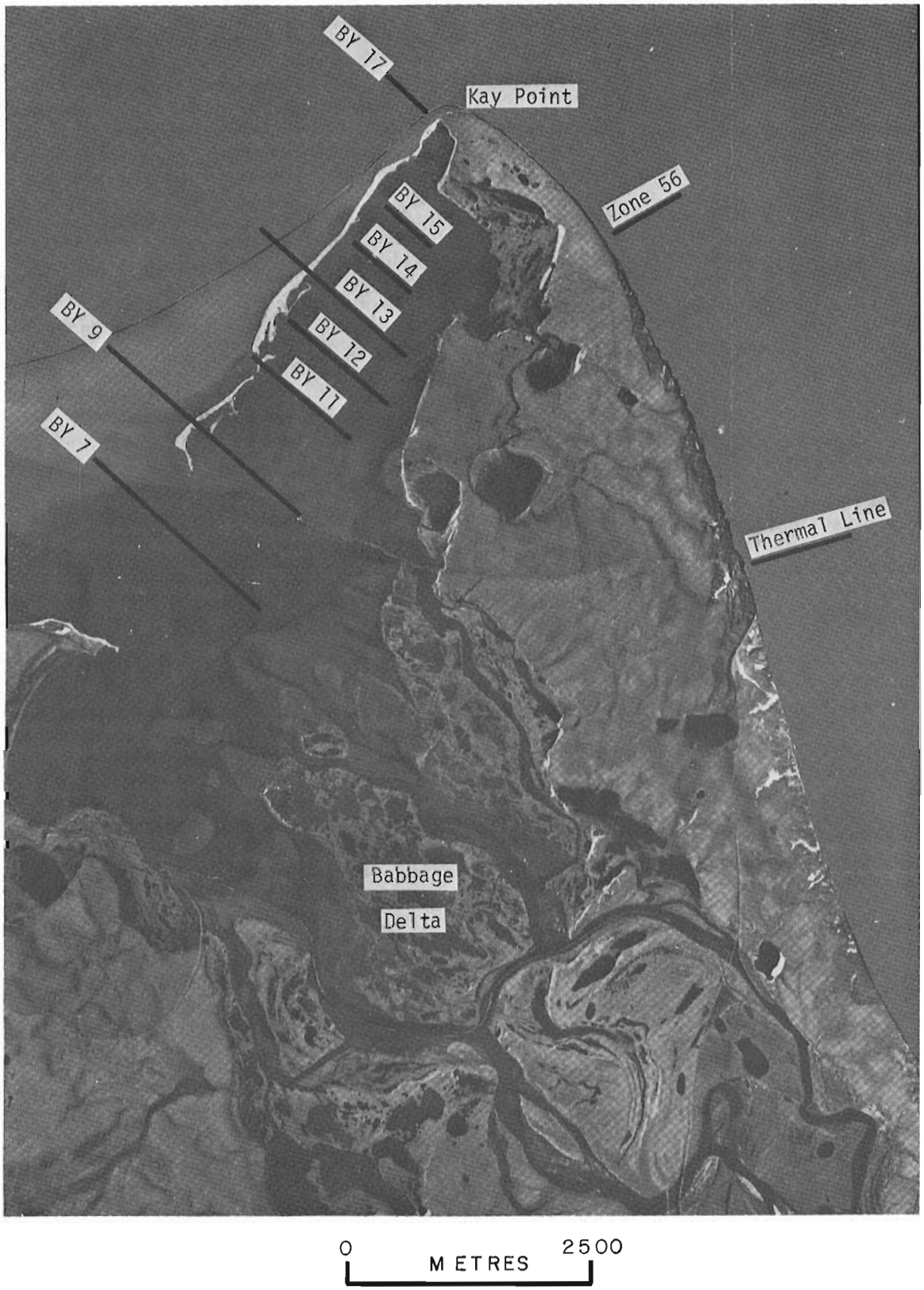

Figure 1. Location of marine seismic refraction lines at Kay Pt., Yukon Territory.

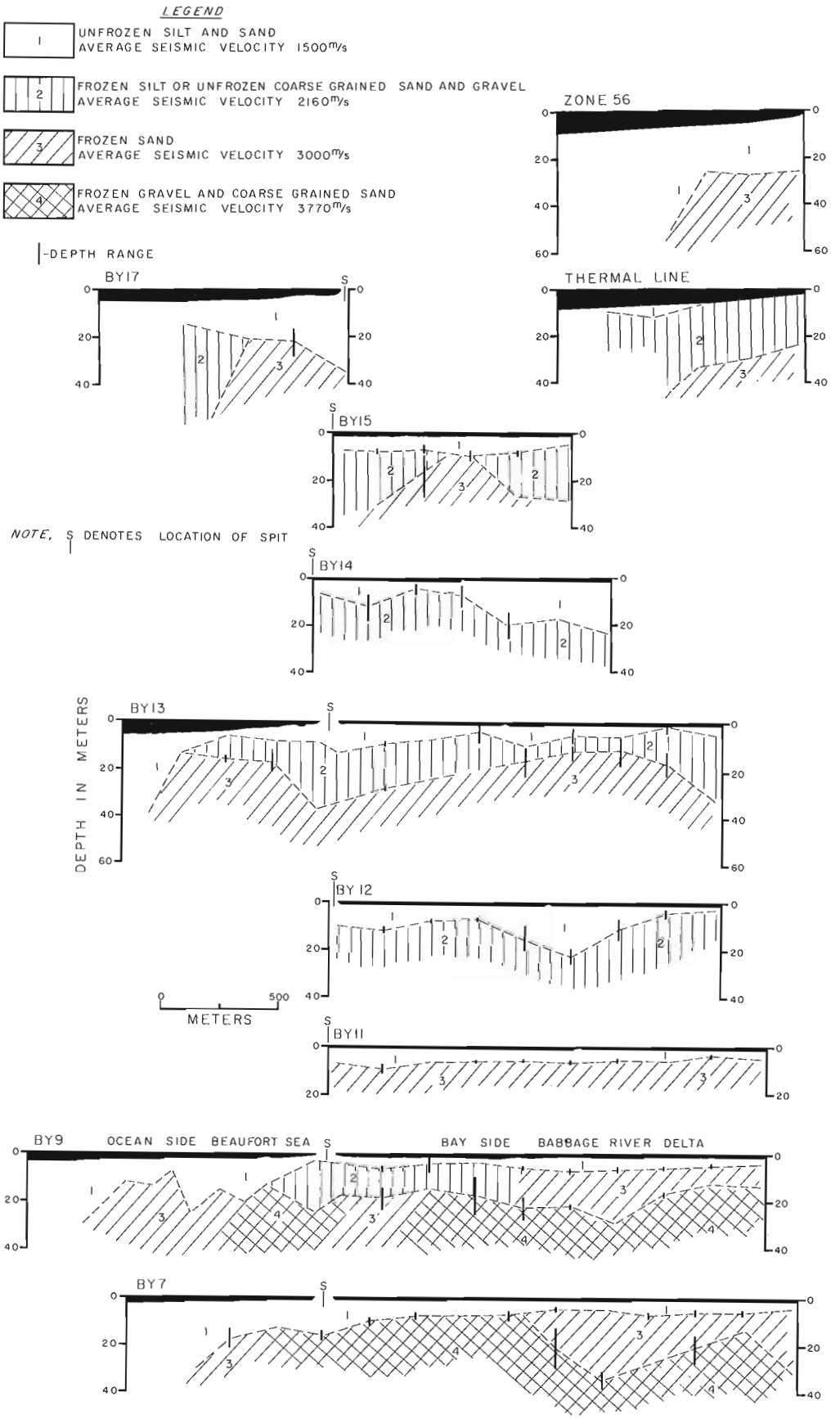

Figure 2. Interpretation of seismic profiles. Black shading denotes water layer.

Lewis, C.P.
1975: Sediments and sedimentary processes, Yukon Beaufort Sea coast; *in* Report of Activities, Pt. B, Geol. Surv. Can., Paper 75-1, pt. B, p.165.

McDonald, B.C. and Lewis, C.P.
1973: Geomorphic and sedimentologic processes of rivers and coast, Yukon coastal plain; Environmental-Social Committee, Northern Pipelines, Task Force on Northern Oil Development, Government of Canada, Report No. 73-39, 245 p.

8. HAMMER SEISMIC STUDIES OF SURFICIAL MATERIALS, BANKS ISLAND, ELLESMERE ISLAND, AND BOOTHIA PENINSULA, N.W.T.

Project 680037

R.M. Gagne and J.A. Hunter
Resource Geophysics and Geochemistry Division

During the field season of 1974, a shallow seismic program was conducted in co-operation with a drilling program carried out by J. Veillette of the Terrain Sciences Division, at selected sites on north Banks Island, Bjorne Peninsula, Ellesmere Island and near Spence Bay, Boothia Peninsula. Detailed seismic refraction profiling was carried out with a Huntec FS-3 hammer seismograph over some of the drill sites to obtain seismic velocities of surficial materials in permafrost.

A layered refraction interpretation of the seismic data was carried out as a field check, however the data was re-analyzed in the office using a time-distance curve-filling routine described by Hunter (1971). Seismic data quality was good despite poor ground coupling of the hammer source resulting from the high water content of the active layer.

The locations of survey sites are listed in Table 1 and the velocity-depth curves are compared to the generalized geological logs in Figures 1, 2 and 3 for the three areas. Velocities increase from a surface layer of 300-850 m/s (the active layer) to velocities in excess of 3000 m/s. The velocities of materials within 2 metres of the surface are relatively low; the rate of increase appears to be much more apparent in ice-rich material. In general, fine-grained materials exhibit lower seismic velocities than ice-rich sands and consolidated rock. No apparent velocity differences could be found between frozen ice-bonded coarse-grained materials and bedrock of sandstone or shale. The frozen till observed at site no. 6 in Figure 3 exhibited an unusually high velocity probably as a result of ice bonding of coarse-grained fraction.

Figure 4 shows the correlation between measured ground temperature and seismic refraction results at a drill-site described by Veillette (1975). Shown also are the typical velocity depth curves for ice saturated sand and clay for the measured temperatures after Aptikaev (1964). The observed velocity-depth curve shows velocity less than the range of ice saturated materials at depths close to surface suggesting that the material in that zone may be undersaturated. Nakano and Arnold (1973) have shown in laboratory studies that the degree of ice saturation strongly affects the acoustic velocity of the material at temperatures below $0^{\circ}C$. The velocity-depth curves from all of the test sites probably are affected by the large near-surface negative temperature gradient as well as the degree of ice saturation.

A comparison of seismic velocities and volume per cent moisture was attempted from samples taken from the boreholes (J. Veillette, pers. comm.). For samples taken below the active layer, a velocity value was interpolated from the velocity-depth curve at each sample

TABLE 1

LOCATIONS OF BORE HOLES AND SEISMIC PROFILES

BANKS ISLAND

NUMBER	LAT.	LONG.
B-1	73°30.8'	121°21.5'
B-2	73°21'	120°14'
B-3	73°21.5'	119°58.5'
B-4	73°21.3'	119°55.5
B-5	73°22.5'	119°55'
B-6	73°25'	119°54'
B-9	73°22.8'	120°05'
B-12	73°17.5'	120°39'
B-13	73°17.75'	120°39'
B-14	73°23'	121°33.5'

ELLESMERE ISLAND

NUMBER	LAT.	LONG.
E-1	79°59.7'	85°51'
E-2	80°01.5'	85°46'
E-5	80°03.5'	86°00'
E-6	80°02.2'	85°58'
E-8	79°54.3'	85°16'
E-9	79°55.8'	84°56'
E-10	79°58.5'	84°48'
E-11	79°57.1'	84°49'
E-12	79°58'	84°45'
E-13	79°58.2'	85°12'
E-14	79°59.3'	85°43'

BOOTHIA

NUMBER	LAT.	LONG.
BO-1	68°30.8'	93°14'
BO-2	69°30'	92°52'
BO-4	69°59.8'	94°42'

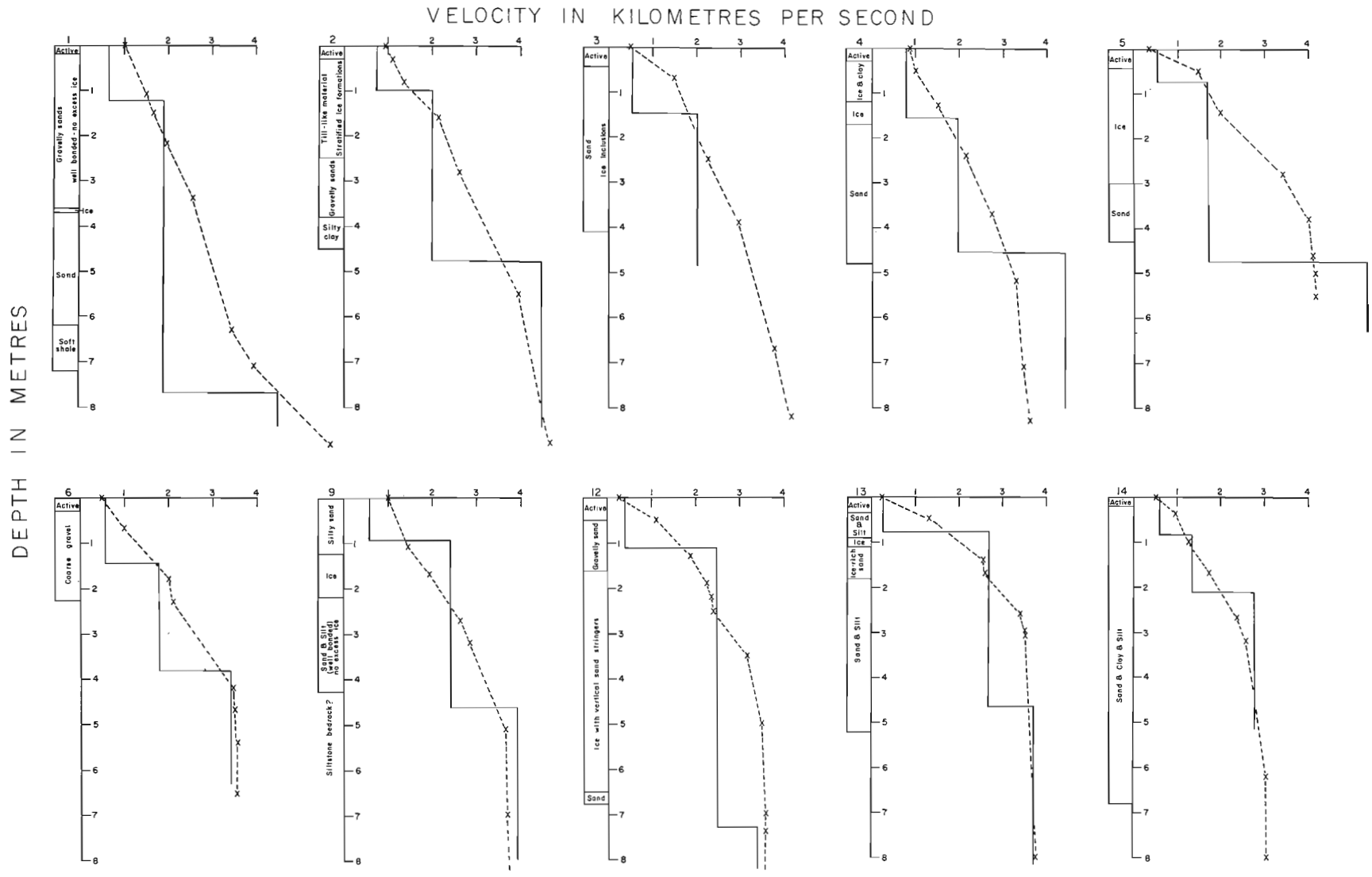

Figure 1. A comparison of seismic velocity-depth results with the generalized geological logs for the Banks Island sites. Solid lines denote the layered interpretation; dashed lines represent the velocity-depth curve interpretation.

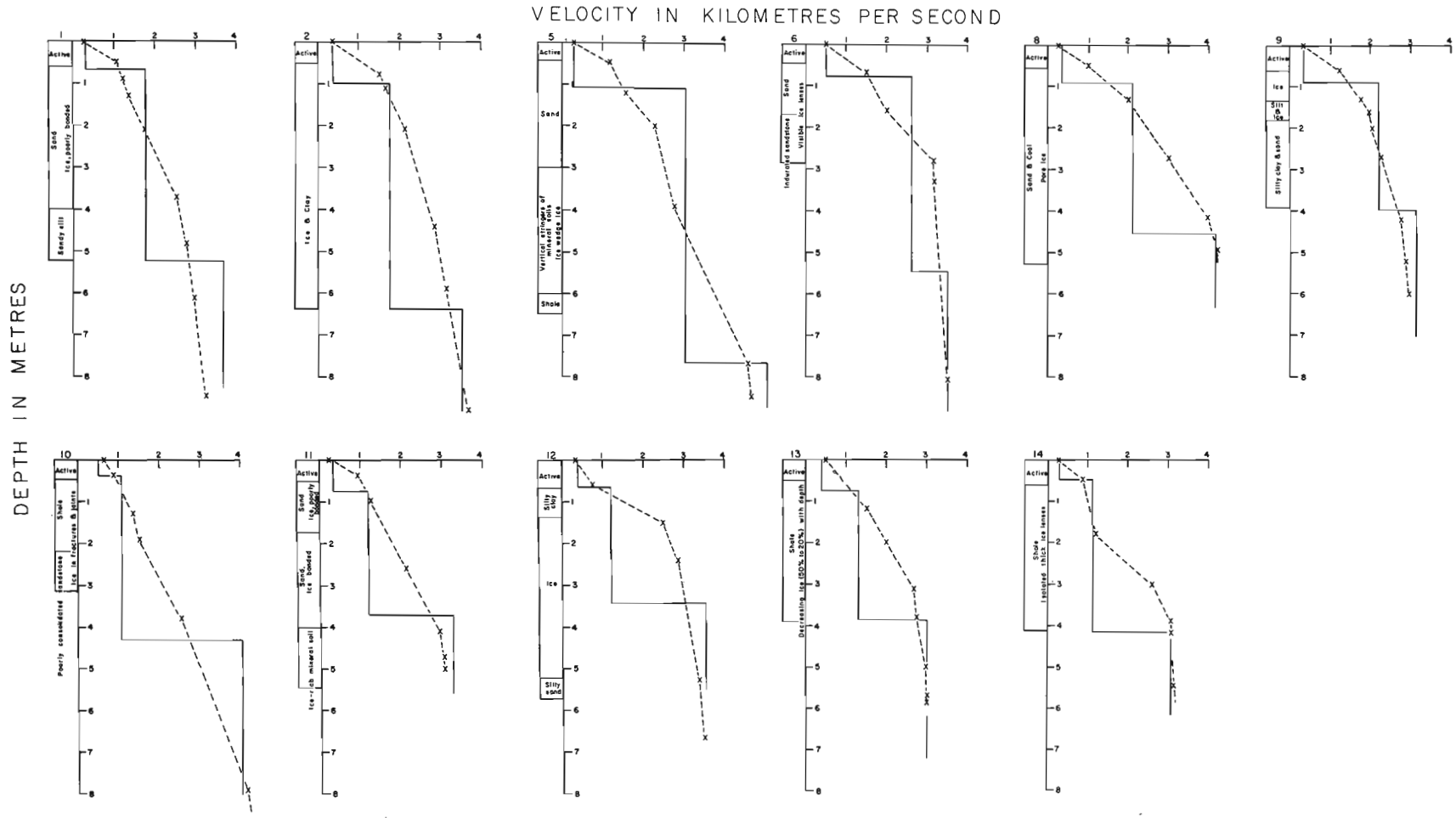

Figure 2. A comparison of seismic results with generalized geological logs for the Ellesmere Island sites.

depth. Inherent in the correlation is the assumption that the sample is representative of the material at that depth and over the volume of material through which the seismic velocity is measured. The comparison of moisture content and seismic velocity measurements is shown in Figure 5 for 30 observations with ice contents between 7 and 34% by volume. No representative samples at high ice contents (> 50%) could be found. Although there is a considerable scatter of the data, a trend towards higher ice content at higher velocities is indicated, and a linear regression analysis of seismic velocity on volume moisture was attempted. This standard deviation of the regression is $\sigma = 0.41$ with a correlation factor $R = 0.76$. It is encouraging to obtain a correlation of these variables from a variety of different types of material containing probable variations in the degree of ice saturation and temperatures. This analysis suggests that ice content is probably a major factor controlling the seismic velocity of surficial materials at low permafrost temperatures.

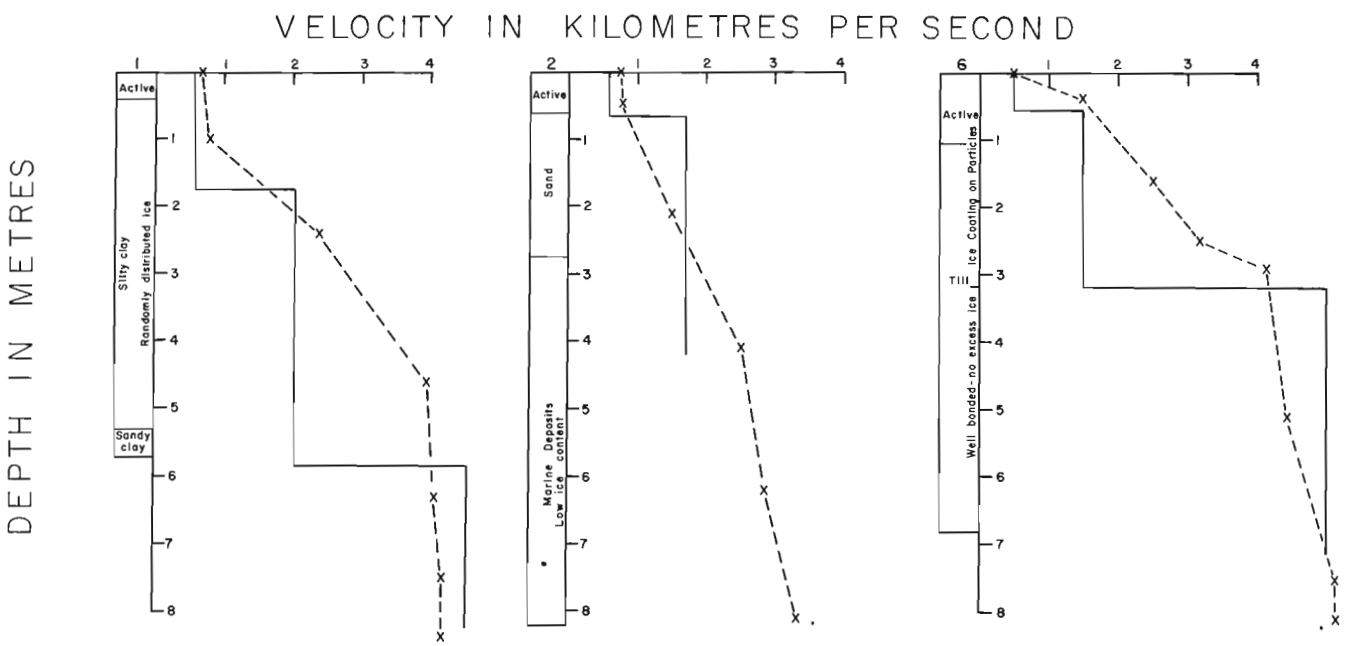

Figure 3. A comparison of seismic results with generalized geological logs for the Boothia Peninsula sites.

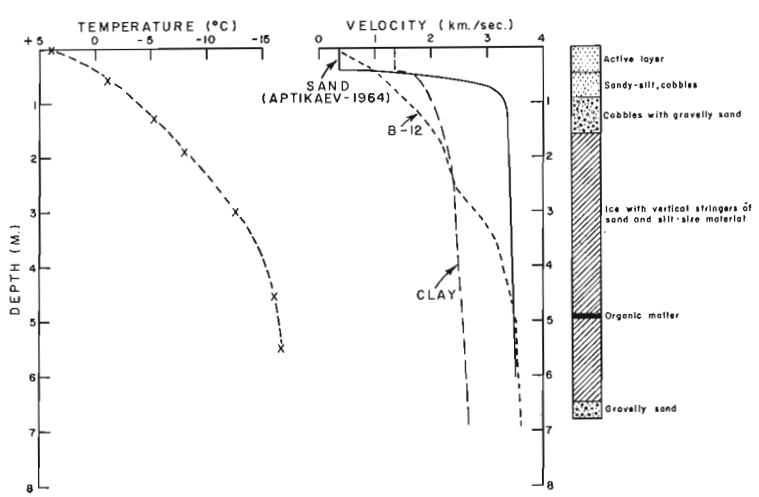

Figure 4.

A comparison of observed and computed (after Aptikaev 1964) velocity-depth functions with the geological and temperature logs at Banks Island site no. B-12.

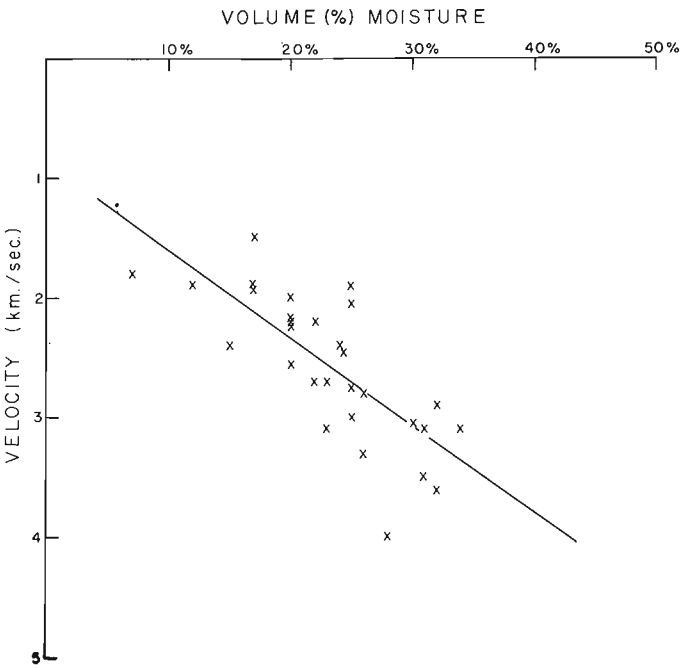

Figure 5. A comparison of observed seismic velocities and volume % moisture of the drill hole samples. The best fitting line is: velocity = 0.87 + 0.07 x (Volume % Moisture).

Acknowledgments

We wish to thank C. Broomfield and D. Boicey for their help in acquiring the field data and J.S. Vincent, D. Hodgson and A.N. Boydell for their logistics support.

References

Aptikaev, F.F.
1964: Temperature field effect on the distribution of seismic velocities in the permafrost zone; *in* Adakemiia Nauk SSSR Sibirskop otd-ie. Inst. merzlotovedeniia. Teplovve protsessy v merzlykh. (In Russian)

Hunter, J.A.M.
1971: A computer method to obtain the velocity-depth function from seismic refraction data; *in* Report of Activities, November 1970 to March 1971, Geol. Surv. Can., Paper 71-1B, p. 40-48.

Nakano, Y. and Arnold, R.
1973: Acoustic properties of frozen Ottawa sand; Jour. Water Resources Research, v. 9, no. 1, p. 178-184.

Veillette, J.
1975: Stabilization of ground temperature in a shallow bore hole; *in* Report of Activities, April to October 1973, Geol. Surv. Can., Paper 74-1A, p. 371-372.

A SHALLOW MARINE REFRACTION SURVEY, CUNNINGHAM INLET, SOMERSET ISLAND, N.W.T.

Project 730006

J.A. Hunter and R.J. Godfrey
Resource Geophysics and Geochemistry Division

A shallow marine refraction survey was conducted in the area of Cunningham Inlet, Somerset Island, August 15-28, 1974, in co-operation with coastal processes studies reported by Taylor and Lewis (1975). The objective of the survey was to obtain velocity structure of the nearshore sediments to identify type of material and possible permafrost (frozen material) conditions.

The marine refraction technique employed here has been described by Hunter (1973). A 200-m 12-hydrophone array (15 m spacing) was used with an S.I.E. RS-4 seismograph. The seismic source used was, alternately, a three-electrode sparker operated at 300 joules or ½ lb geogel explosive. Work was done from a 30-ft. enclosed barge (Taylor and Lewis, 1975); positioning of survey lines was accomplished by radar and transponders.

Figure 1 shows the location of survey lines and shot positions. Reconnaissance lines were run in the inlet to produce both transect and longitudinal sections. Much of the survey was concentrated over a bathymetrical high area at the western side of the inlet close to a possible land-fall point for a proposed submarine gas-pipeline across Barrow Strait.

Record quality throughout the survey was good despite unfavourable wave conditions and frequent contact between hydrophones and seabottom in shallow areas. On many of the records three refraction layers were interpreted. Figure 2a shows a typical case with velocities of 1460 m/s, 2950 m/s and 5900 m/s.

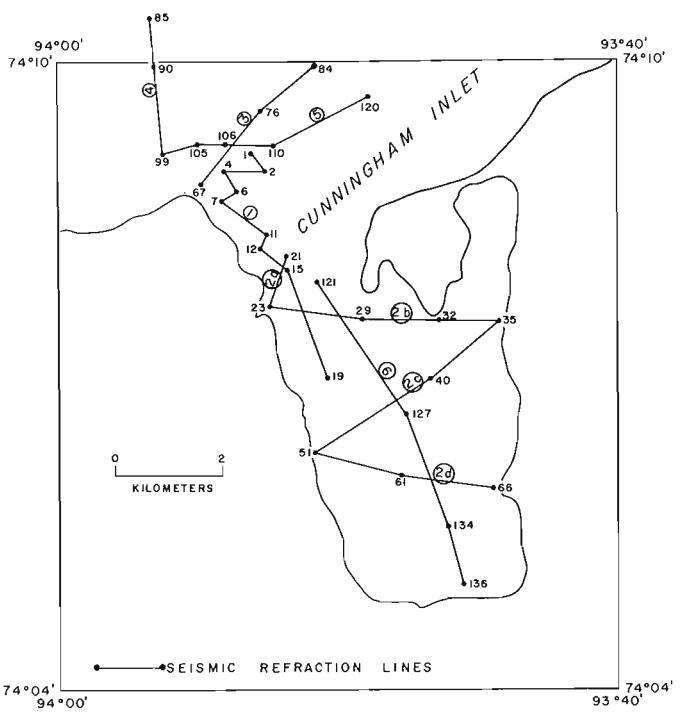

Figure 1. Location of seismic refraction profiles, Cunningham Inlet, northern Somerset Island.

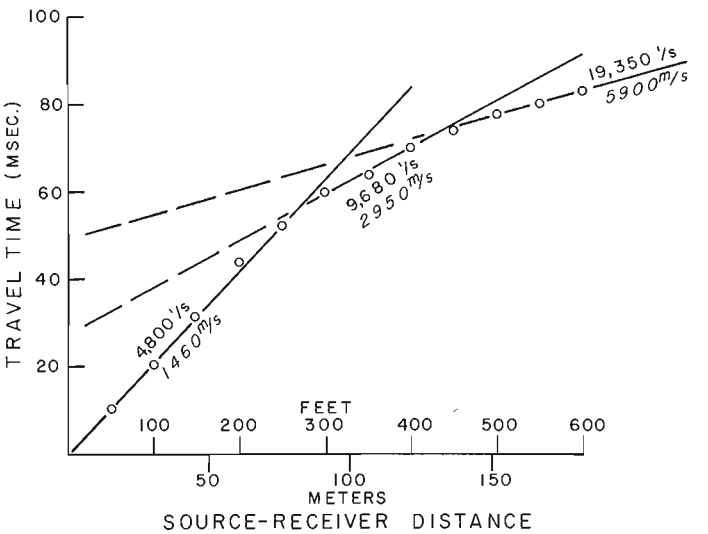

Figure 2a. A first arrival time-distance plot of a marine refraction record showing a three layer interpretation.

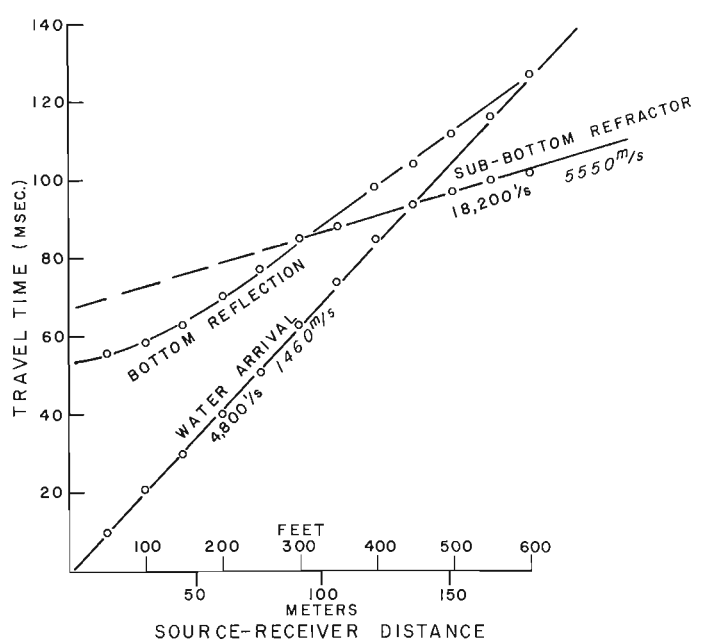

Figure 2b. A time-distance plot showing a "hidden layer" case where the intermediate refractor velocity is not seen as a first arrival.

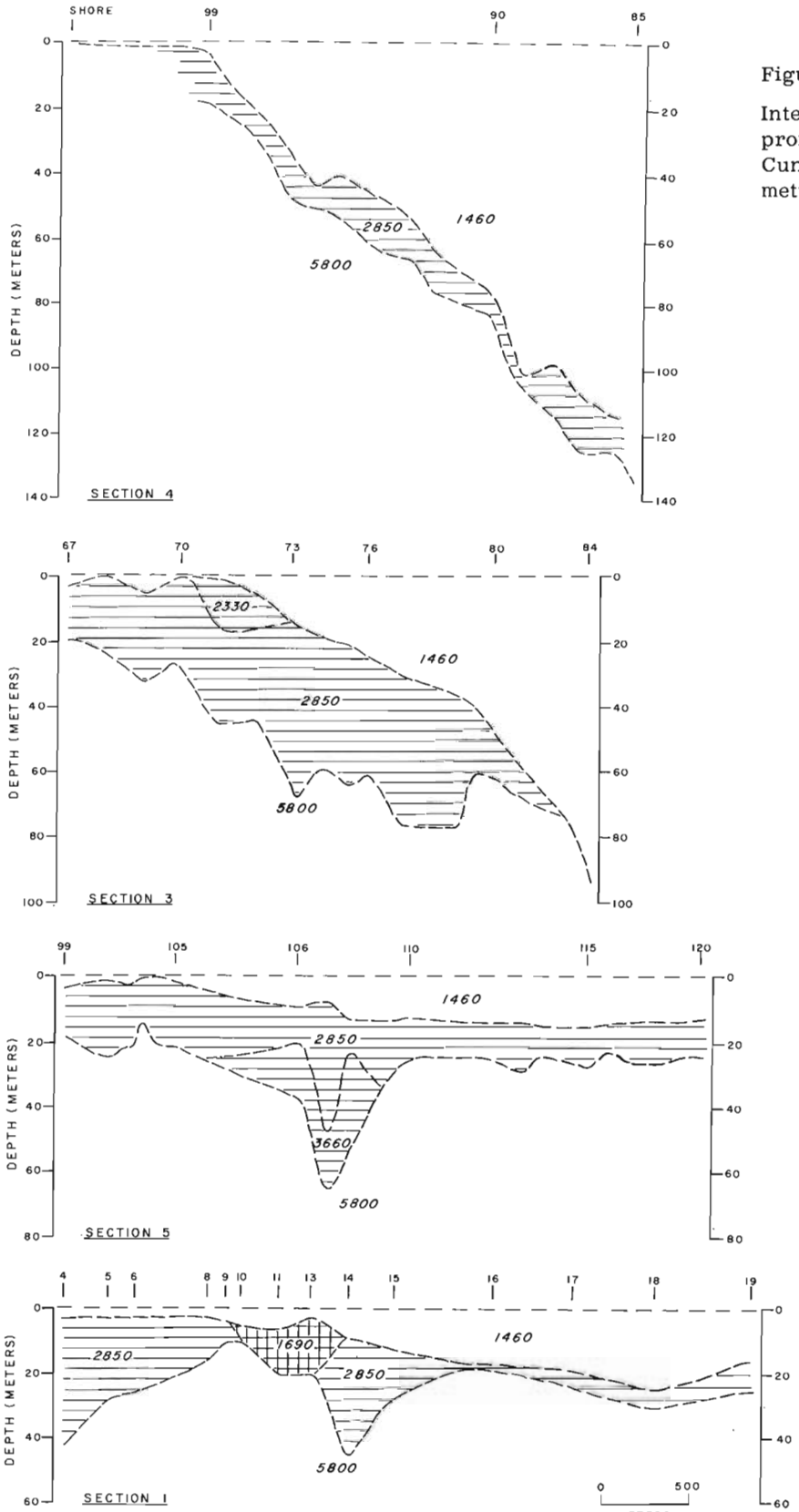

Figure 3.

Interpreted sections from refraction profiling for lines at the entrance to Cunningham Inlet. Velocities are in metres/sec.

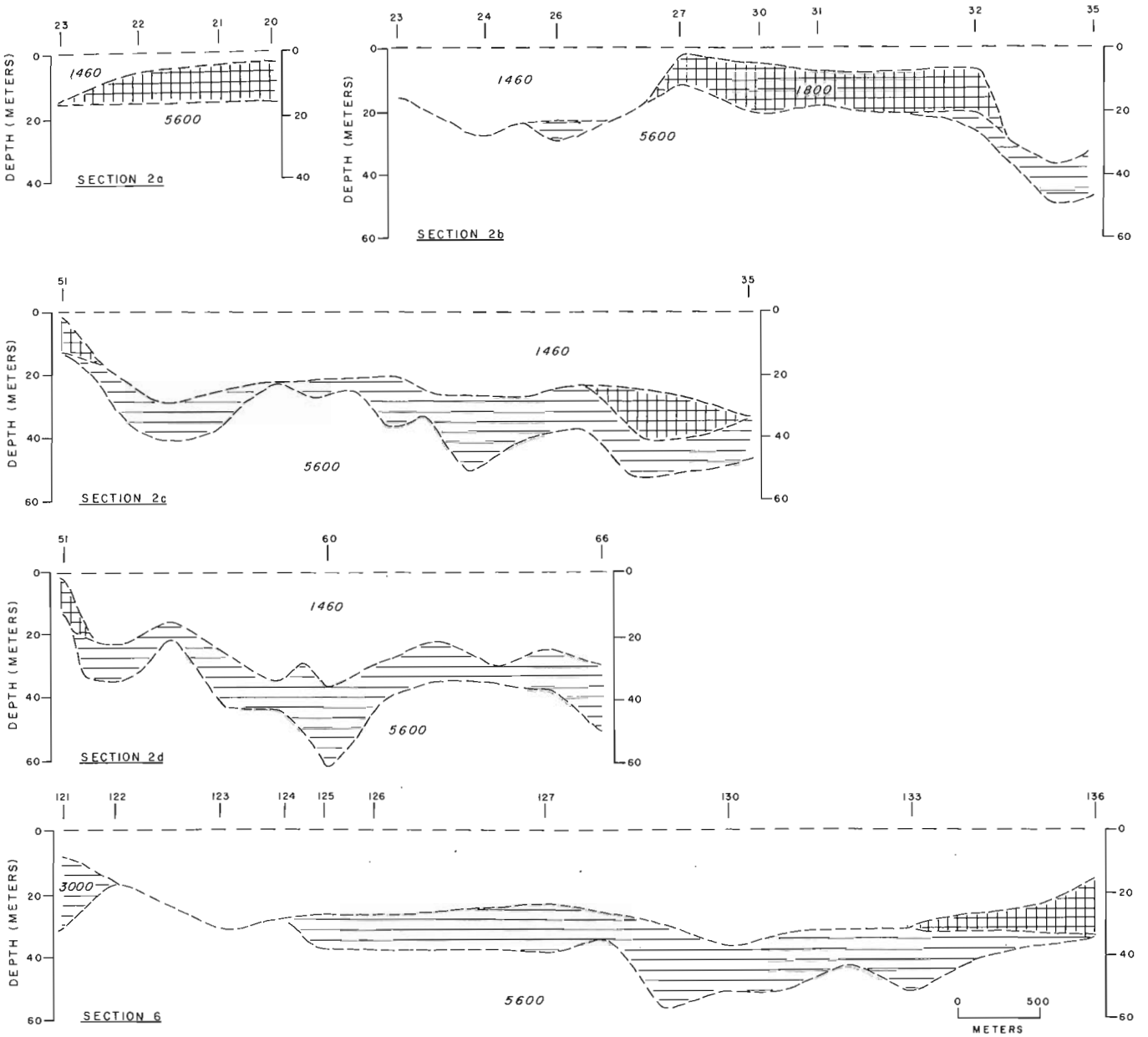

Figure 4. Interpreted sections for seismic lines in Cunningham Inlet. Velocities are in metres/sec.

On some of the records, a wide angle reflection was observed which was interpreted to be generated at the water-sediment interface and which compared well in many cases with the water depth given by the ship's fathometer. In water deeper than 15 m this event was well separated from the first arrival "water break"; it was also found that often in these conditions the refracted event for the intermediate layer was missing (*see* Fig. 2b). A marked difference between the intercept-time values of the wide angle reflection and the high velocity refractor can be considered evidence for the existence of an intermediate layer or zone with indeterminant velocity structure. The "hidden layer" problem in refraction interpretation has been discussed by Green (1962) who suggests that considerable error in depth determinations could occur if the "hidden" refracted event is overlooked in the analysis. Because of high amplitude interfering events closely following the first arrival refracted waves, the hidden layer refractor is often impossible to identify. In this survey area, the hidden layer refraction is only occasionally seen and depth determinations must be made from the wide angle reflection. In the absence of reliable velocities for the hidden layer, a minimum thickness (hence minimum depth to the underlying layer) was computed by using the wide angle reflection depths and computing the depth to the high velocity basal interface from the first arrival refracted waves.

Figure 3 shows sections from lines 1, 3, 4 and 5 for the area around the mouth of the inlet. The inter-

mediate layer has an average velocity of 2850 m/s; in some locations (sections 3 and 5) structure within this layer is detected. At water depths greater than 15 m and layer thicknesses less than 15 m this unit becomes a hidden layer. This material is interpreted to be a cobble-boulder bed and is probably derived from nearby land outcrops. Bottom sampling in the area confirmed that hard bottom conditions existed; some subangular cobbles were recovered. Frozen ice-saturated gravel exhibits, in general, velocities in the range of 4000-5000 m/s (Roethlesberger, 1972); since seismic velocities of the intermediate layer are much less, it is suggested the ice-content is low and possibly the layer is not frozen. On section 1, a localized occurrence of a low velocity material was mapped; from seismic velocities this unit is probably silt or sand. The deepest refractor is interpreted to be bedrock with an average velocity (over these sections) of 5800 m/s. The apparent velocity variation along this refractor results from the single-ended profiling technique employed, since corrections for local topographic anomalies on the refractor, or for a dipping interface, cannot be made. The observed velocities are in the range of that given for well consolidated argillaceous limestone and correlates well with the Silurian Read Bay Formation outcropping on land. An infilled topographic low on the bedrock surface has been mapped on sections 5 and 1 and is probably continuous between the sections. This trough is approximately parallel to the western shore of the inlet.

Figure 4 shows sections from lines 2 and 6. On most records a wide angle reflection was observed, which is interpreted to be from the top of the cobble-boulder bed. In the same areas a low velocity layer with a velocity close to that of water was observed (line 2b). In some sections, the velocity was not significantly different than water, (line 2(c)) and the thickness of this layer is based on the difference in depths between the seabottom as given by the fathometer, and the reflection from the top of the boulder-bed. This layer is interpreted to be composed of fine grained material (silts and sands) with considerable gravel content where velocities increase to 1800-2000 m/s on line 2(b). Bedrock topography varies between 11 m and 60 m below sea level. A topographic high is associated with the shoal area (record 29) on line 2(b) and probably extends north beneath the tombolo. Topographic bedrock lows occur in the centre and towards the eastern side of the inlet.

References

Green, R.
1962: The Hidden Layer Problem; Geophysical Prospecting, v. 10, no. 2, p. 166-170.

Hunter, J.A.
1973: Shallow Marine Refraction Surveying in the Mackenzie Delta and Beaufort Sea; *in* Report of Activities, Geol. Surv. Can., Paper 73-1, pt. B, p. 59-66.

Roethlesberger, Hans
1972: Seismic Exploration in Cold Regions; Cold Regions Research and Engineering Laboratory Report, Corps. of Engineers, U.S. Army, Hanover, New Hampshire.

Taylor, R.B. and C.F.M. Lewis
1975: Nearshore Marine Geological Reconnaissance at Cunningham Inlet, Somerset Island, N.W.T.; *in* Report of Activities, April to October 1974, Geol. Surv. Can., Paper 75-1A, p. 505-507.

10. EVALUATION OF HIGH RESOLUTION AEROMAGNETIC SURVEY DATA OVER A TEST RANGE IN THE TIMMINS AREA, ONTARIO

Project 720080

L. J. Kornik, P. H. McGrath, M. T. Holroyd and P. J. Hood
Resource Geophysics and Geochemistry Division

Introduction

The Geological Survey of Canada has been involved in the development of aeromagnetic survey techniques and equipment since the late 1940's. During this interval a major portion of the Canadian Shield has been surveyed and approximately 7000 aeromagnetic maps which incorporate more than four million line miles have been published. It has become apparent that these standard sensitivity maps which are contoured at 10-gamma intervals, while compatible with reconnaissance scale (1: 250 000) geological mapping are not entirely suitable for detailed (1: 50 000) mapping. A considerable amount of information that is geologically significant is, in fact, lost in the compilation of the standard 10-gamma interval maps. The amount of information retrievable below the 10-gamma interval range is increased with the use of higher sensitivity instruments. In order to advance the state-of-the-aeromagnetic survey art the Geological Survey in 1968 took the necessary steps to acquire a high resolution aeromagnetic capability. A Beechcraft Queenair aircraft was purchased and equipped with a self-orienting optical absorption magnetometer which was mounted in a 10-foot tail boom. Much effort was expended in the compensation of the aircraft, and a digital recording system was incorporated so that the map compilation process and any subsequent data processing could be computerized.

A project was initiated in 1972 to evaluate the usefulness of the resultant high resolution aeromagnetic data as an aid to detailed geological mapping programs. A test range was established in Godfrey Township, 10 miles northwest of Timmins, in the District of Cochrane, Ontario. The location of Timmins, which is in the famous Porcupine - Val d'Or mining area, is indicated in Figure 1. The test range is situated in parts of National Topographic Sheets 42 A/5 and 42 A/12 and part of the Ontario Department of Mines and Geological Survey of Canada Aeromagnetic Map 2299G. Ontario Department of Mines Preliminary Geophysical Series Map P. 639 (1971) includes a geological compilation of the test range and surrounding areas as well as a résumé of previous geological mapping history. Prospecting activity in the surrounding region has been extensive since the nineteen twenties, first for gold and more recently for base metals and nickel. A variety of airborne and ground geophysical surveys have been carried out in the region. For a summary of these activities *see* Paterson (1957), Pyke and Middleton (1971), and Middleton (1973, 1974).

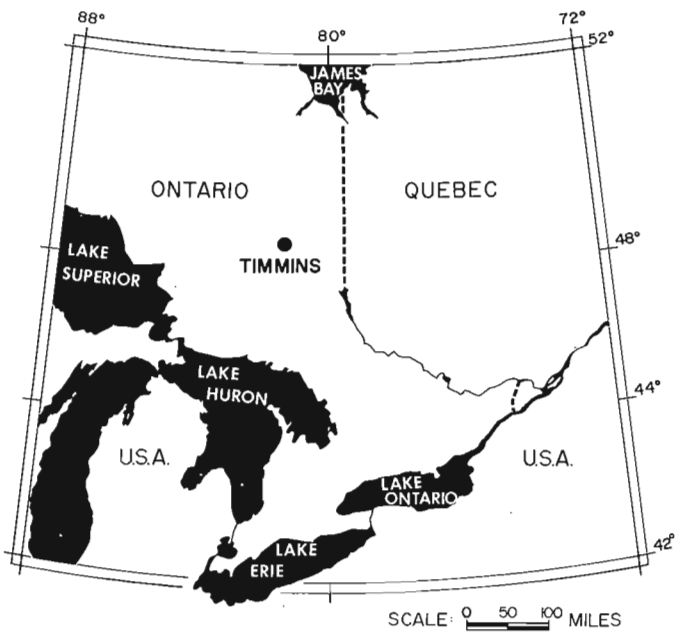

Figure 1. Map showing location of Timmins, Ontario.

Timmins Test Range

The test range consists of seven subparallel lines oriented 055°E, spaced 500 feet apart, and 15 000 feet long which were cut through the bush. Survey stations were staked every 50 feet along each line.

The grid is situated within the Abitibi 'greenstone' belt of Precambrian age. A geological map of the test range is presented in Figure 2a. A major portion of the test range is underlain by acid volcanic rocks. An intermediate intrusive unit occurs near the middle of the grid along with three adjacent areas of basic volcanic rocks. All of these rock types are cut by younger diabase dykes which strike 340-360°. Following the geological mapping of the test range, several different types of ground magnetic survey were carried out, namely total and vertical field surveys together with an in situ magnetic susceptibility survey (Fig. 2b). In addition oriented 1. 25-inch drill cores were collected for subsequent remanent magnetization and magnetic susceptibility determinations in the laboratory.

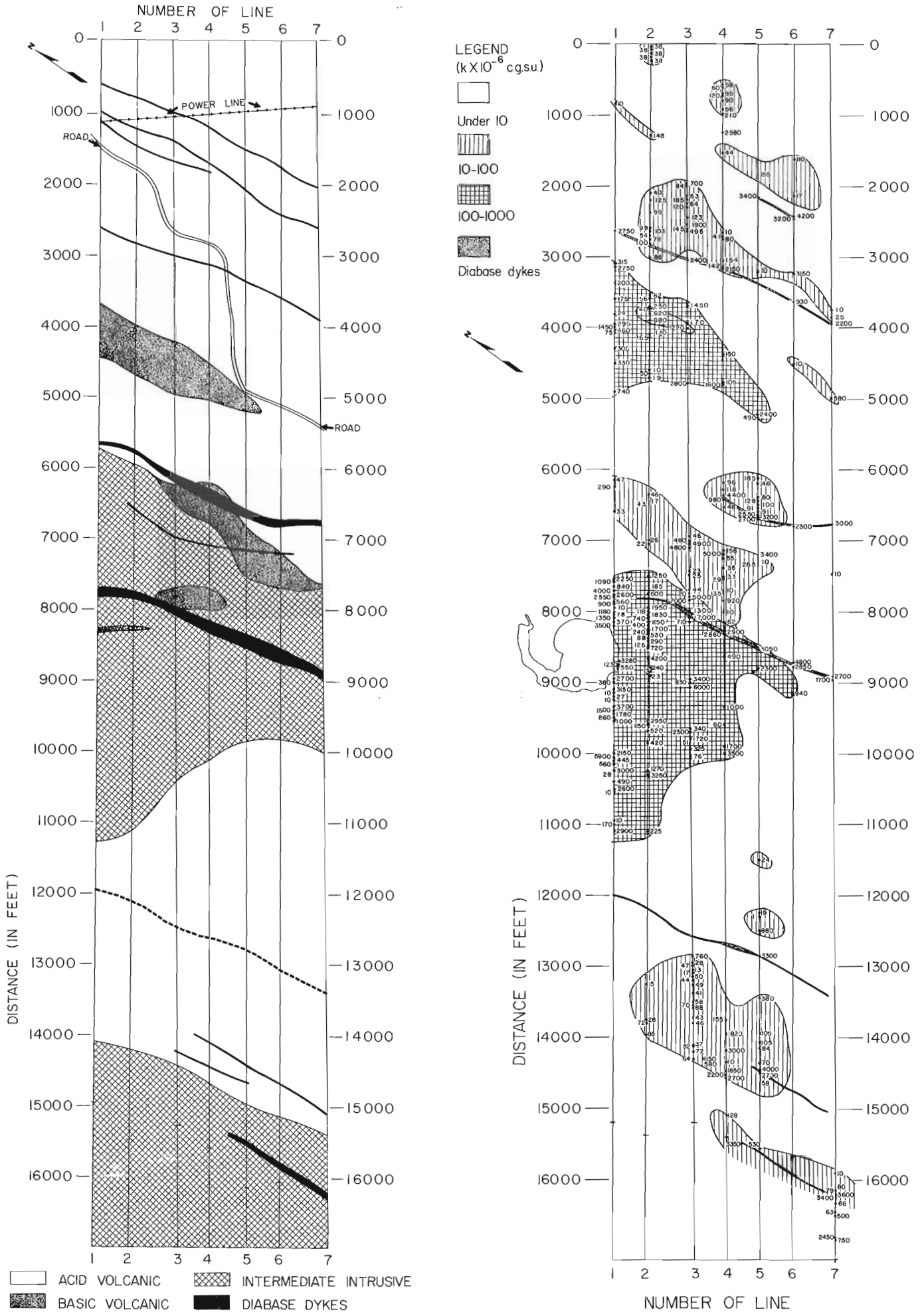
NUMBER OF LINE
1 2 3 4 5 6 7
0
1000
2000
3000
4000
5000
6000
7000
8000
9000
10000
11000
12000
13000
14000
15000
16000
POWER LINE
ROAD
ROAD
DISTANCE (IN FEET)
LEGEND
(k X 10⁻⁶ c.g.s.u.)
Under 10
10-100
100-1000
Diabase dykes
ACID VOLCANIC
INTERMEDIATE INTRUSIVE
BASIC VOLCANIC
DIABASE DYKES
NUMBER OF LINE

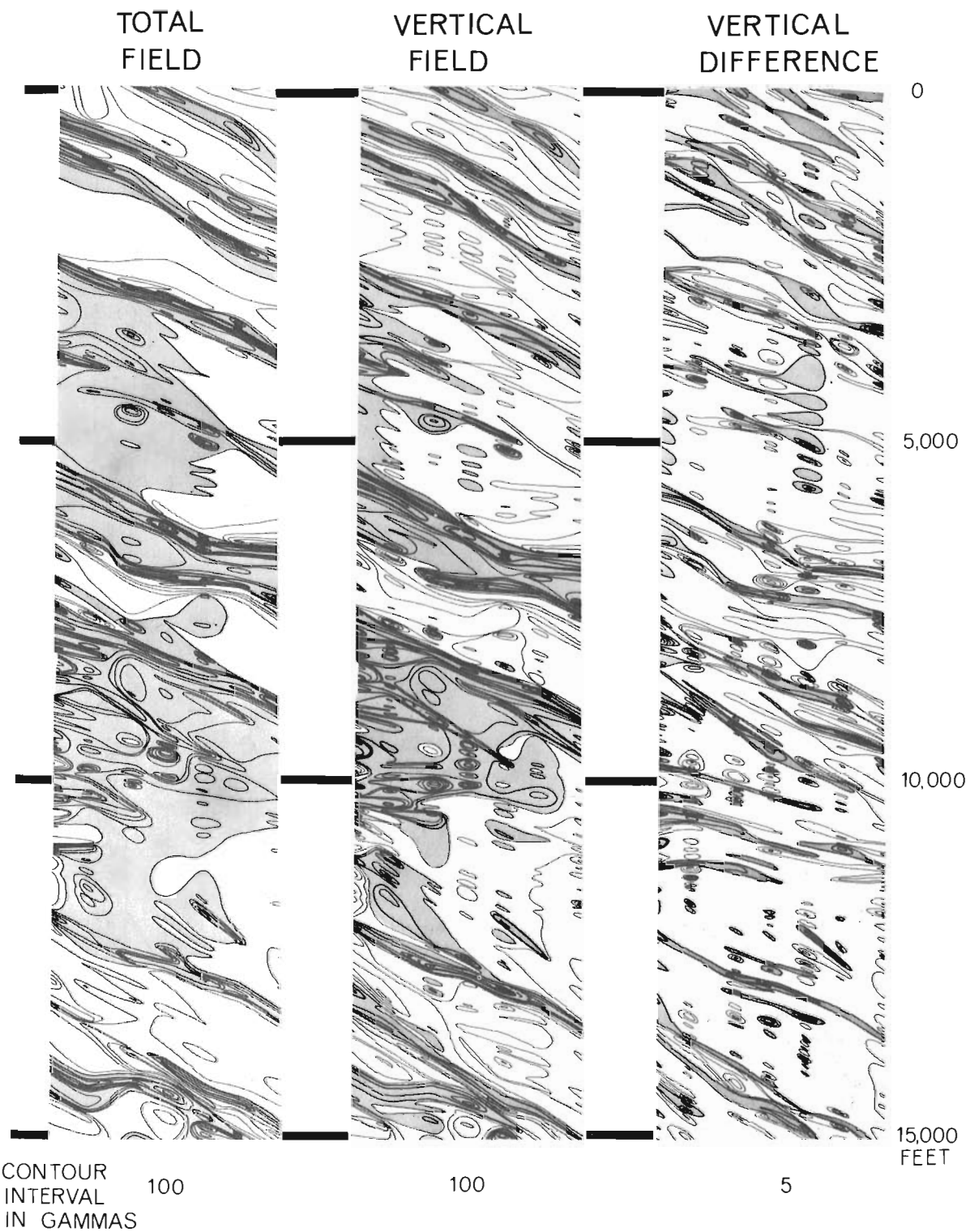

Figure 3.

Ground magnetometer maps of Timmins test range;

(a) total field, (b) vertical magnetic field, (c) vertical difference in the total magnetic field over a 5-foot interval.

Figure 2 (opposite)

(a) Geological map of the Timmins test range.

(b) In-situ magnetic susceptibility map of the Timmins test range. Magnetic susceptibility values shown are in units of 10^{-6} emu/cm^3.

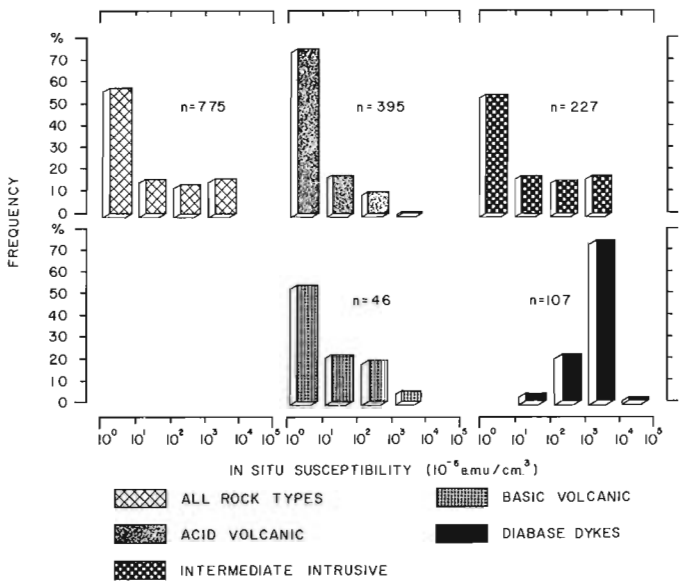

Figure 4 (above).

Graphs showing range and distribution of in-situ magnetic susceptibility measurements for the various geological units.

Figure 5 (right)

Location of oriented diamond drill cores. The arrows point in the direction of natural remanent magnetization and the numbers by the arrows indicate the inclination of this direction from the vertical.

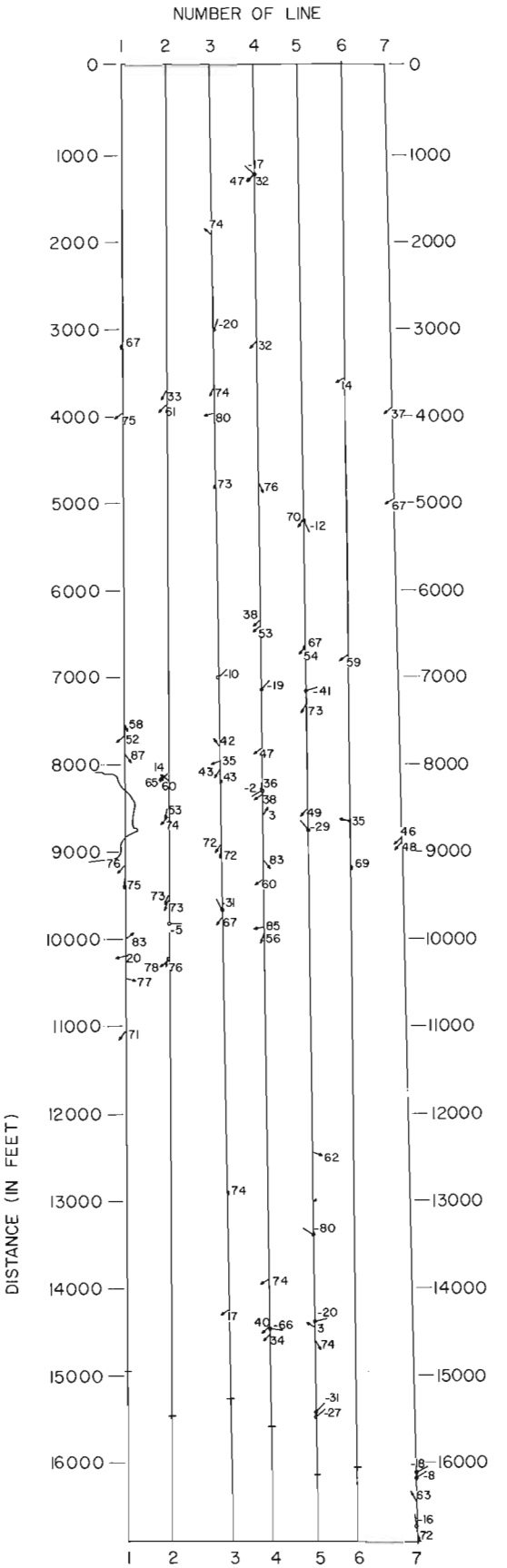

Ground Surveys

Two Scintrex MF-1 fluxgate magnetometers were employed for the vertical field survey. One magnetometer was used for traversing, while the other was connected to a strip chart recorder and used at a fixed base station to continuously monitor daily variations in the earth's magnetic field. An external probe was connected to the base station magnetometer and it was mounted in a vertical position during the vertical field survey. The base station was established in an area of low magnetic gradient about 200 feet from the initial station on line 5 which had been selected to be the reference station for the entire survey. At the beginning of each day the traverse magnetometer was adjusted to read 500 gammas while occupying the reference station on line 5. At the same time the reading on the strip chart recorder at the base station was also assigned a value of 500 gammas. At the end of each day the traverse magnetometer was reread at the reference station. Due to varying rates of drift, differences between the two magnetometers of a few tens of gammas were often observed. For purposes of correcting the data, the base station magnetometer was assumed to have a zero drift, while the traverse magnetometer was assigned a linear drift. After correction for instrument drift, the data was further corrected

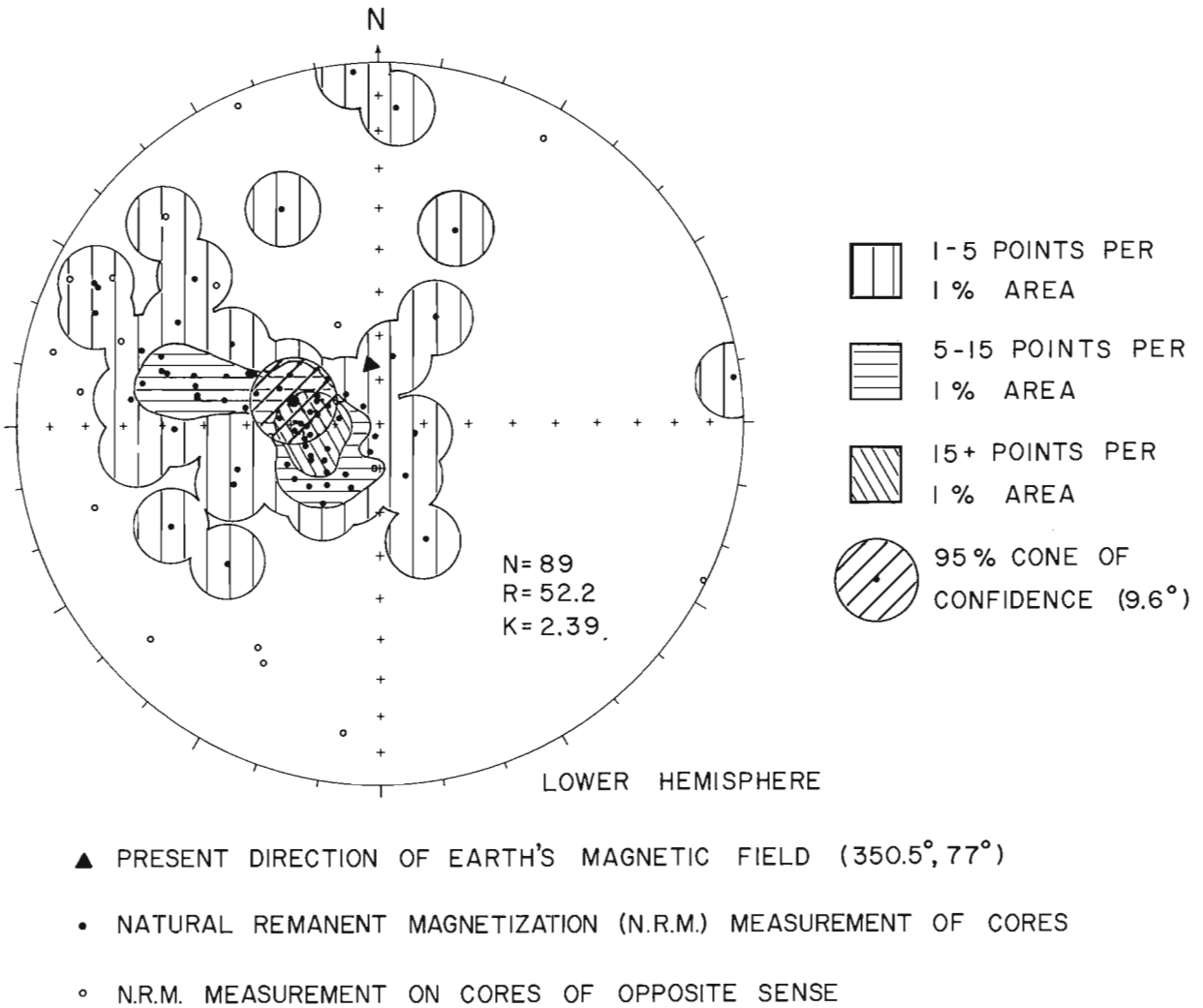

Figure 6. Lower hemisphere of a Schmidt equal area plot of natural remanent magnetization directions.

for diurnal variations in the geomagnetic field using the base station record.

A Sander NPM-3 proton precession instrument was used for total field magnetometer surveys at two heights. The surveys were performed at the same time with readings being taken with the sensor at elevations of 3 and 8 feet above the ground at each occupied station. The difference between these two readings enabled a vertical difference map to be prepared which would correspond in a general way to the vertical gradient of the total magnetic field at ground level. For the total field surveys, the external probe at the base station was aligned in the direction of the geomagnetic field vector. This was accomplished by adjusting the external probe until a maximum reading was obtained. Again the initial station on line 5 was used as a reference station. A value of 59 735 gammas was assigned to this station and each day's readings were tied to this value. The adjusted readings were then corrected for instrument drift and diurnal variations.

The corrected magnetic data are presented in map form in Figure 3. The shaded areas on these maps represent the areas of positive anomalies. The map on the left is the total magnetic field obtained with the proton precession magnetometer. The contour interval is 100 gammas with the 60 000 gamma contour separating the shaded positive areas from the areas of lower magnetic intensity. The centre map is the vertical magnetic field obtained with the fluxgate magnetometer. The contour interval on the map is also 100 gammas. The 1400 gamma (relative) contour separates the areas of shaded positive magnetic anomalies from the unshaded negative areas. The map on the right of Figure 3 is the vertical difference map derived by subtracting the value of the 8-foot elevation reading of the proton precession magnetometer from the 3-foot elevation reading and dividing by the vertical separation of the two readings. These vertical difference values are contoured in 5 gammas per foot intervals. The positive vertical difference areas are shaded on the map.

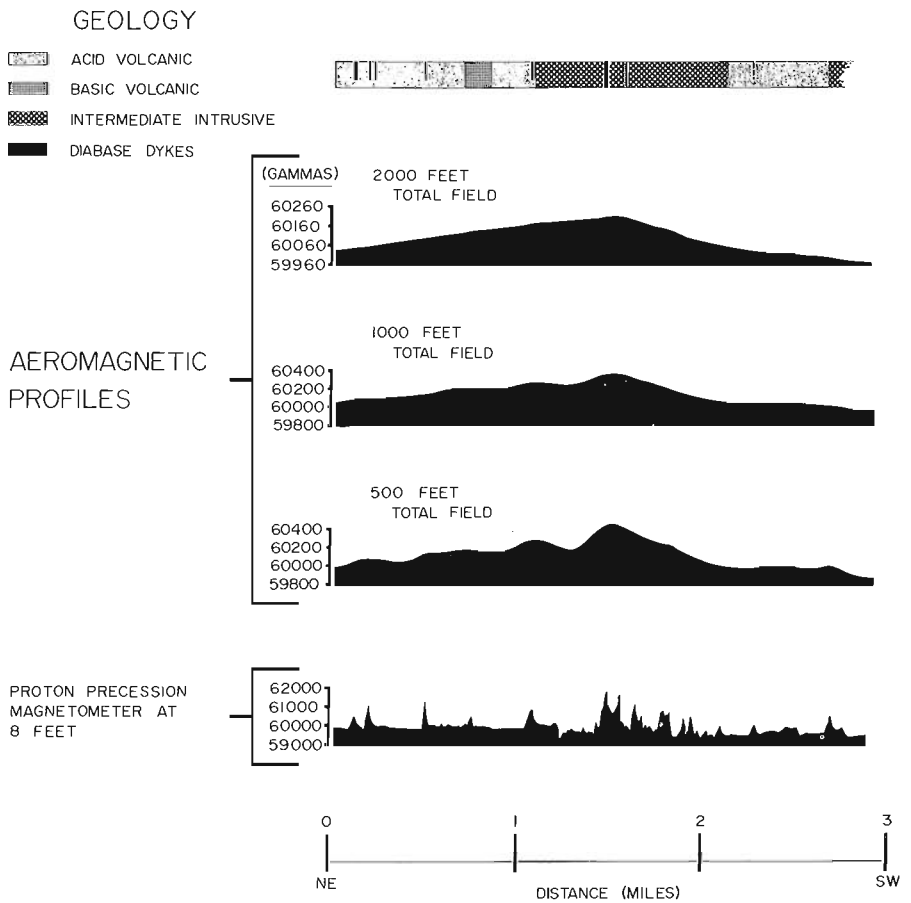

Figure 7.

Profiles along line 1 of the Timmins test range of ground proton precession magnetometer data, aeromagnetic data at the three survey altitudes, with accompanying geological data.

The magnetic patterns in the total field and vertical field maps shown in Figure 3 are similar. The vertical field map appears to contain a large number of single station anomalies as evidenced by the large number of small highs and lows. These are not apparent in the total field map and probably are a reflection of the different sensitivities of the two magnetometers. The proton precession instrument yielded results which were reproducible with a resolution of 0.5 gamma if the measurements were taken in a quiet field. The resolution of the fluxgate magnetometer at best was ten gammas.

The most prominent feature in these three maps is the strong correlation of magnetic anomalies with the occurrence of diabase dykes of Figure 2a. Also there is some suggestion that the intermediate intrusive is more magnetically active than are the basic and acidic volcanic units. The great amount of variation and lack of coherency in the ground magnetic data, however, precludes an adequate presentation. This is a direct result of undersampling, in other words the 50-foot sampling interval used in the survey was not sufficient to obtain an accurate representation of the rapid variations in the magnetic field occurring at ground level. This is further complicated by the 500-foot line spacing used in the survey, especially when one attempts to transform the profile data into map form. As a result, it was necessary to contour these data by hand, since none of the automatic computer contouring programs at our disposal could handle such incoherent data. In order to adequately sample variations in the magnetic field at such close proximity to the causative bodies, a sampling interval of approximately two feet (McGrath, in press), would be required. Such a sampling density is not feasible over a large heavily treed area and the cost would be excessive, hence we are obliged to work with undersampled data in most ground magnetometer surveys. Also since the vertical differencing process tends to enhance the smaller anomalies in the data, the problem is even more severe, as can be seen in Figure 3c where the data appear to be approaching complete incoherency.

The in-situ magnetic susceptibility measurements obtained using a Scintrex SM-4 susceptibility meter have been contoured using four units in Figure 2b, namely under 10, 10 to 100, 100 to 1000 and over 1000 ($k \times 10^{-6}$ cgsu.). The major part of the test range, which is the unpatterned portions on the map, has values below 10 units, and correlates mainly with that portion of the test range underlain by acid volcanic rocks. Smaller enclosed areas having values between 10 and 100 units, the areas with vertical ruling, also

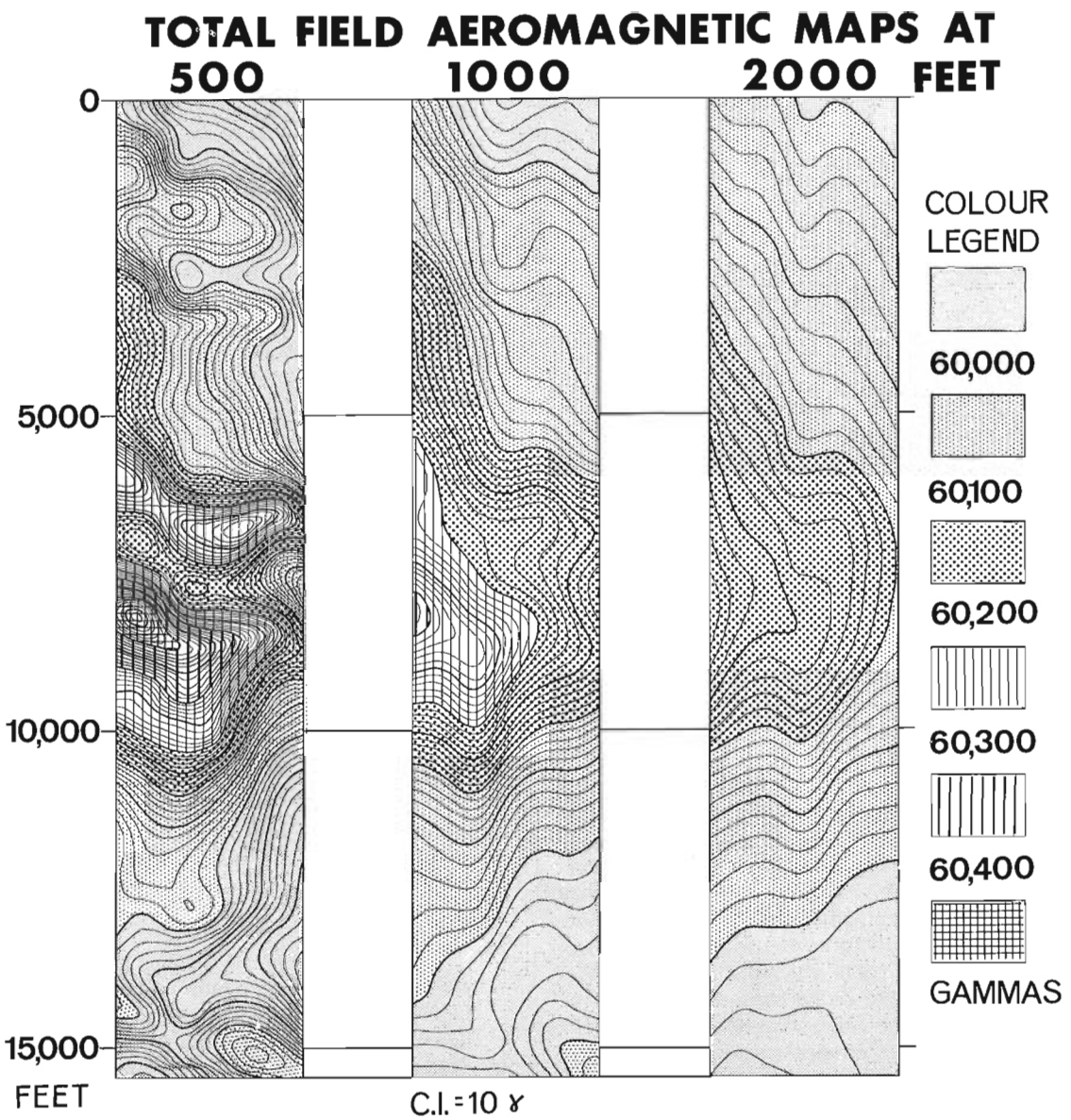

Figure 8. Total field aeromagnetic maps of the test range at the three survey altitudes. Contour interval (C.I.) is 10 gammas.

occur within the acid volcanic rocks. Two areas of higher magnetic susceptibility where values range between 100 and 2000 units occur in areas underlain by basic volcanic rocks and intermediate intrusive rocks. These areas are cross-hatched on the map of the magnetic susceptibility. The areas of diabase dykes have much higher susceptibilities, up to 10 000 susceptibility units, and are shown as heavily hatched linear features on the diagram. There is a one-to-one relationship between magnetic susceptibilities and magnetic anomalies. Areas of high magnetic intensities correlate with areas of high magnetic susceptibilities and similarly with the lows. The ranges of values of the in-situ magnetic susceptibility determinations for the various rock types are similar to those obtained by Middleton (1973) in nearby Robb and Jamieson townships.

A statistical treatment of the in-situ susceptibility measurements is summarized in Figure 4. This diagram shows the range and distribution of the magnetic susceptibility values plotted with frequency percentages on the vertical axis against the magnetic susceptibility values along the horizontal axis using a logarithmic scale in 10^{-6} cgs units, which is also 10^{-6} emu/cm^3. The 'n' on the diagram is the number of measurements obtained on each rock type. The majority of the samples have low magnetic susceptibility values with the larger frequency percentages clustered at the low end of the magnetic susceptibility range. The plot of the in-situ magnetic susceptibility measure-

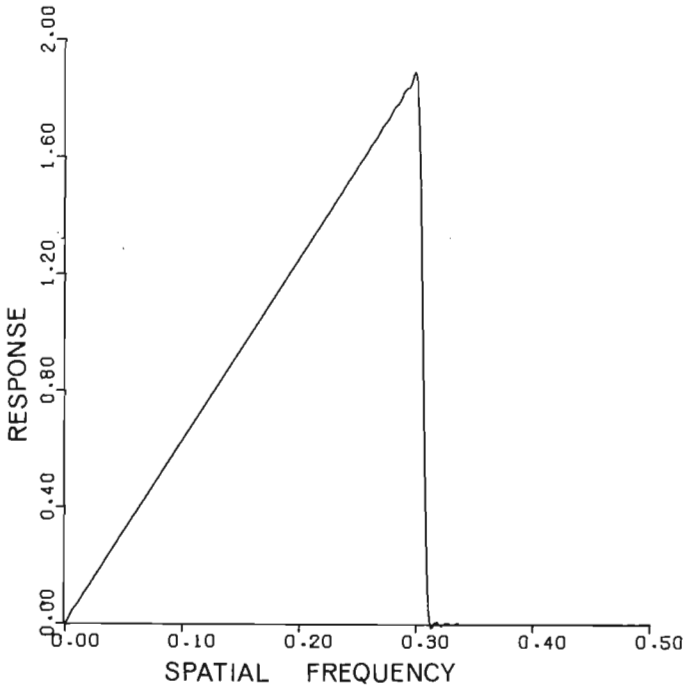

Figure 9. Recovered transfer function (calculated response) for 201 point first vertical derivative operator: $\mu_c = 0.3$ cycles per sampling interval, $\Delta\mu = 0.013$ cycles per sampling interval.

ments of all rock types is in the top left hand corner of Figure 4 and illustrates the preponderance of these low susceptibility values. The acid volcanic rocks are basically non-magnetic with the majority of the values below 10 susceptibility units. The basic volcanic rocks have higher susceptibility values and a greater number of these values occur in the weakly magnetic area of the plot (below 1000 susceptibility units). The intermediate intrusive rocks have a more uniform distribution in the higher magnetic susceptibility range. The diabase dykes have a concentration of values in the 1000 to 10 000 susceptibility unit range. These results also agree closely with the results obtained by Middleton (1973).

Oriented cores were collected with a portable diamond drill from those outcrop areas which had measurable magnetic susceptibilities. These outcrops occurred mainly in the areas of intermediate intrusive rocks, basic volcanic rocks and the diabase dykes. The location of these samples are shown in Figure 5 where the direction of the arrow indicates the direction of natural remanent magnetization and the number by the arrow indicates the dip of this direction from the vertical.

The remanent magnetism determined on these cores is plotted on the lower hemisphere of a Schmidt equal area net (Fig. 6). The resultant plot shows that the remanent magnetism directions have a small scatter, and have an average direction within 20 degrees of the present earth's magnetic field, which is represented as a solid triangle in the plot. Remanent magnetization measurements by Middleton (1973) from Robb and Jamieson townships indicates a close cluster of measurements near the centre of the net within about 20 degrees of the present earth's magnetic field. However, the centre of the cluster of measurements from the Timmins test range occurs in the southwest quadrant, whereas the centre of the cluster from Robb and Jamieson townships (Middleton, 1973) occurs in the northeast quadrant. The ratio of remanent magnetism to induced magnetism, the Koenigsberger ratio, for two-thirds of the rocks collected was below 0.3. The Koenigsberger ratio for the more magnetic third of the rocks averaged 2.4. Thus, in the majority of the rock samples, the induced magnetism is the more important component which contributes to the observed magnetic anomalies.

These surveys indicate that a good correlation exists between the geology and the variation in the anomaly patterns of the ground magnetometer data. However, in spite of the usefulness of the ground magnetic data, difficulties are encountered with this type of survey. First, because of water-covered areas it is difficult to obtain uniform coverage. Secondly, ground magnetometer surveys are generally considerably more expensive and time consuming than a comparable airborne survey. Thirdly, local inhomogenieties in the magnetization of near surface rocks makes it difficult to adequately sample the rapid variations in the magnetic field at ground level. Removing the magnetometer some distance from the sources eliminates the local variations by averaging and the resultant anomalies reflect magnetization contrasts between larger masses of rocks. Airborne surveys provide more uniform coverage at a reduced cost and permits mapping of large areas in a reasonable length of time and overcomes the undersampling problem present in most ground magnetometer surveys.

Aeromagnetic Surveys

The seven lines of the test range were flown at 500, 1000 and 2000 feet altitude using the Geological Survey's high resolution aeromagnetic survey system previously described. The sampling rate was 0.5 second (132 feet) and readings were averaged for 0.2 second (53 feet). From an analysis of the effects of upward continuation on white noise (McGrath, in press), it can be demonstrated that these parameters are adequate to properly sample all significant frequency components which are contained in the aeromagnetic data at flight elevations of 500 feet or higher.

The profile data along the southeastern side of the test range (line 1, Fig. 2a) is shown in the central part of Figure 7. Also shown in this figure are the total field ground profile, and a geological cross-section along the same line. The aeromagnetic profiles illustrate the loss of definition and amplitude with increasing height of the sensing system. Note the superior resolution of the ground magnetic data compared to the aeromagnetic data and that each diabase dyke has a corresponding magnetic anomaly. In general, dyke anomalies present in the ground data are not readily apparent in the airborne data. In particular, adjacent dyke anomalies are not resolved as individual anomalies in the airborne profile data. Figure 8 presents the total field aeromagnetic maps of the test range at

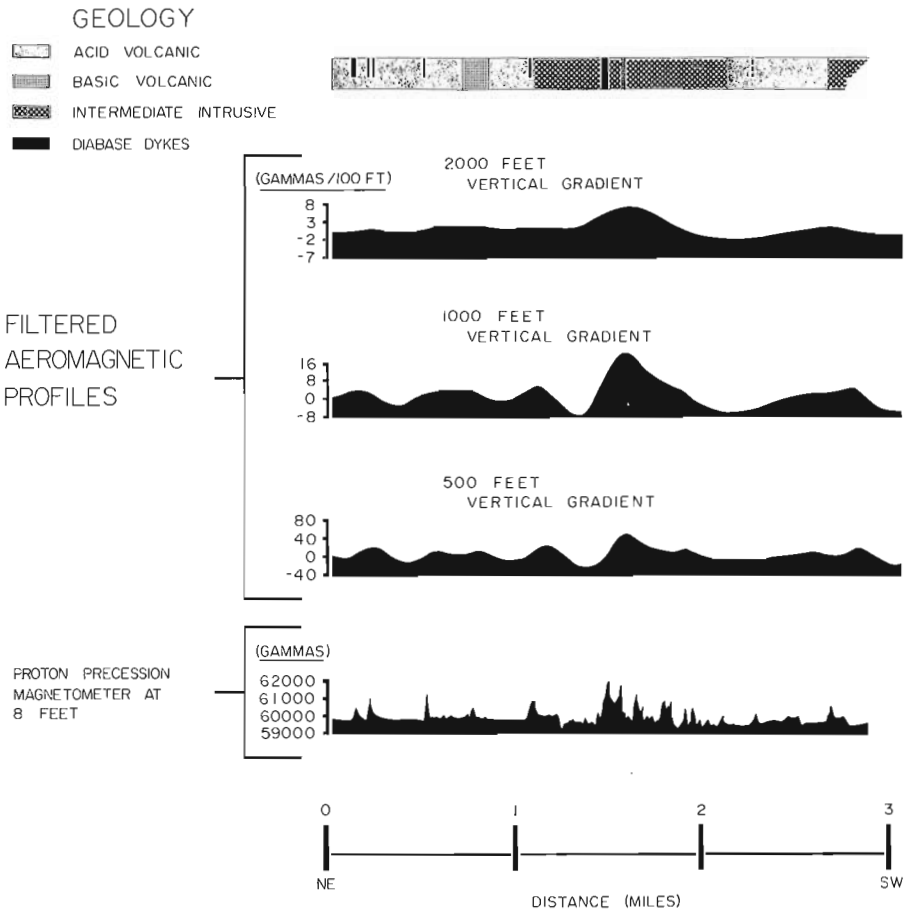

Figure 10.

Profiles of ground proton precession magnetometer survey data, filtered aeromagnetic data at the three survey altitudes and geological data along line 1 of the Timmins test range.

the three survey altitudes. The contour interval is 10 gammas. Again on these maps we can see the effect of height on the amplitude and resolution of the magnetic anomalies. As a means of comparison of the magnetic data at the various elevations, there is a 4000 gamma range of variation in the ground data, 1300 gammas in the 500-foot map, 700 gammas in the 1000-foot map and 250 gammas at 2000 feet. The occurrence of dykes is only readily apparent on the ground data and on the 500-foot map.

Data Processing of Aeromagnetic Measurements

Up to now we have discussed state-of-the-art techniques for the magnetic method. In an attempt to maximize the geologically meaningful information that can be derived from high sensitivity data, it was decided to investigate the application of digital filters to the aeromagnetic data.

In order to improve the resolution of the aeromagnetic data, tests using vertical derivative, downward continuation and band pass filter operators were conducted. Each operator was one-dimensional, and consisted of an array of 201 weights. A roll-off length of 0.013 cycles per sampling interval was used as required. The filter weights were calculated using a finite Fourier series (equation 1, from Hamming, 1962).

$$W(x) = \frac{A_o}{2} + \sum_{k=1}^{N-1} A_k \cos\frac{\pi k x}{N} + \frac{A_k}{2}\cos \pi x \qquad (1)$$

where $W(x)$ = the weighting function, $x = -100$ to 100,
A_k = the Fourier coefficients
N = the number of terms in the Fourier Series.

All of the filters used in this study possess weighting functions which are symmetrical about the central weight, hence all of the B coefficients in the Fourier Series are zero, and thus there are no sine terms in equation 1.

Comparison of the filter operators obtained using this approximation method with the same operators obtained from exact analytical expressions (McGrath and Bower, 1973) indicate that N = 500 is an acceptable value. The main advantage in generating the weighting functions in this manner is the great variety of operators which can be obtained for which no analytical expressions exist.

The Fourier coefficients, A_k, were obtained by digitizing the transfer function R (u), of a given filter at an interval of 0.001 cycles per sampling interval. For example the transfer function of a first vertical derivative filter operator can be defined as follows:

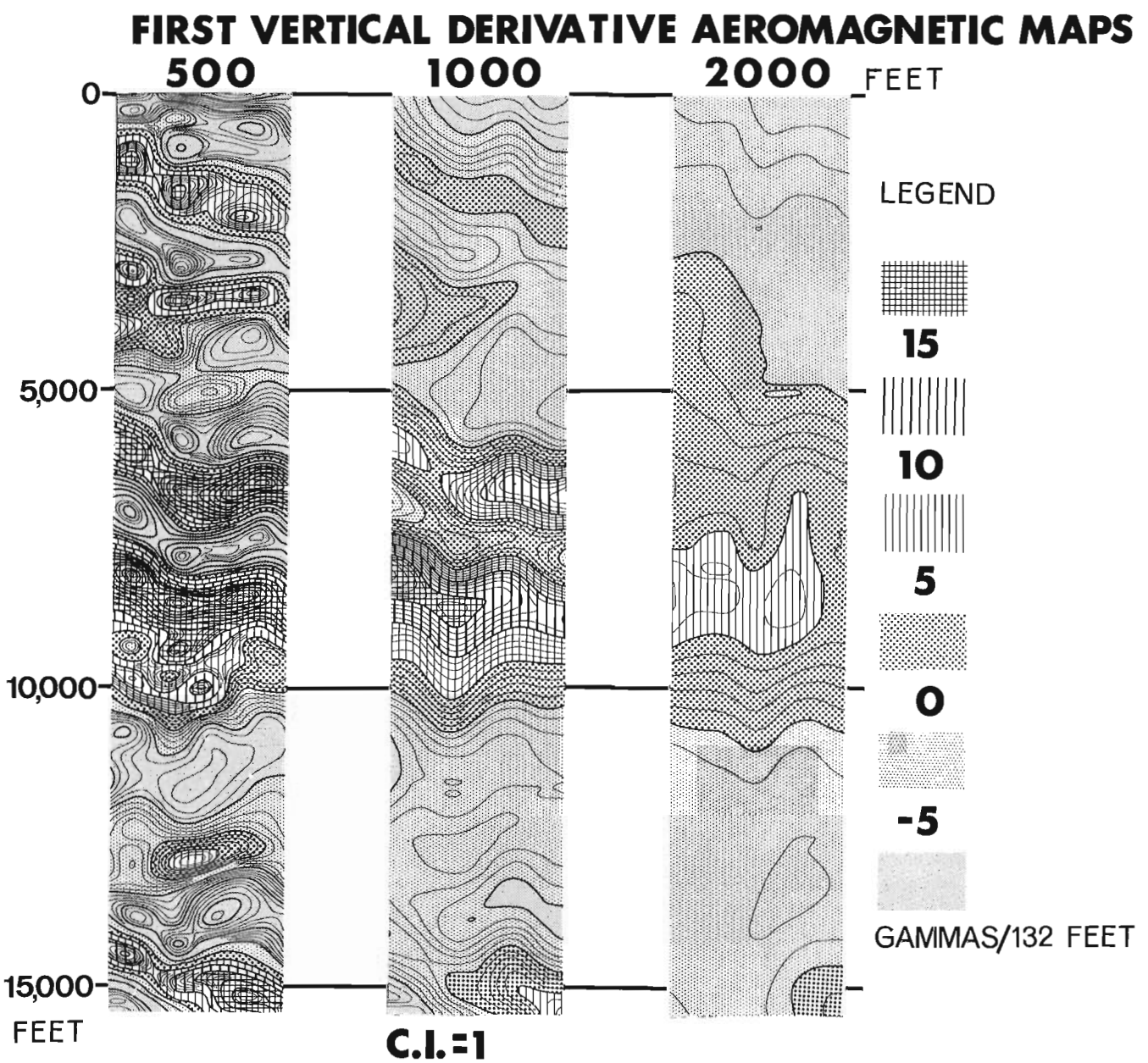

Figure 11. Calculated first vertical derivative maps of the test range at the three survey altitudes. Contour interval (C.I.) is 1 gamma per 132 feet.

$$R(u) = \begin{cases} 2\pi u & , \ 0 \leq u \leq u_c \\ 2\pi u_c \cos^2 \left[\dfrac{\pi(u-u_c)}{2\Delta u} \right] & , \ u_c \leq u \leq u_c + \Delta u \\ 0 & , \ u_c + \Delta u < u \end{cases} \qquad (3)$$

where

- u = spatial frequency in cycles per sampling interval,
- u_c = the cut-off frequency in cycles per sampling interval,
- Δu = the roll-off length in cycles per sampling interval.

The recovered transfer function for the resultant 201 point operator which was derived using equation 2 is illustrated in Figure 9. Based on the value of the spatial frequency, u, it can be subdivided into three regions. Between values of u = o, u_c, the transfer function follows the theoretical response of the first vertical derivation process, $2\pi u$. Between values of u_c and $u_c + \Delta u$, a cosine bell (Kanasewich, 1973) is used as the filter roll-off, and from $u_c + \Delta u$ up to u = 0.5, the Nyquist frequency, the response is zero. Values of 0.3 and 0.013 cycles per sampling interval, were assigned to u_c and Δu respectively. This assured that the geological signal in the aeromagnetic data was enhanced by the derivation process while at the same time the sam-

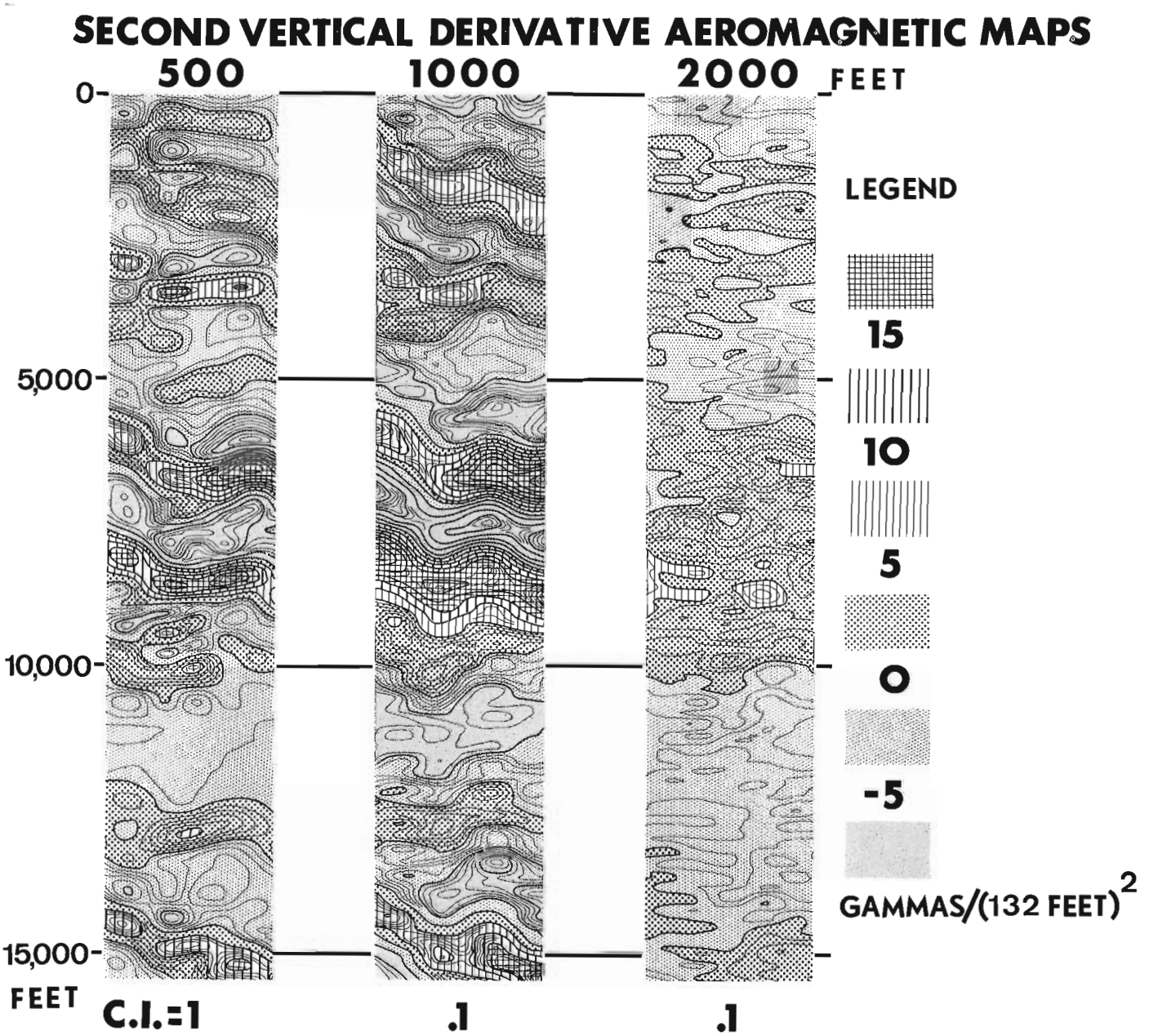

Figure 12. Calculated second vertical derivative maps at the three survey altitudes. Contour intervals (C. I.) are 1 or 0. 1 gammas per $(132)^2$.

pling noise at the Nyquist frequency was suppressed. In a similar way, second and third vertical derivative, as well as band pass and downward continuation operators were designed using the above procedure with the appropriate theoretical response, K(u), where

K(u) = $^2\pi u$, for first vertical derivative operators,
= $(2\pi 4)^2$, for second vertical derivative operators,
= $(2\pi u)^3$, for third vertical derivative operators,
= 1, for band pass operators,
= $e+^2\ \pi$ hu, for downward continuation operators, and h equals the distance of downward continuation.

All of these responses were combined with the cosine bell roll-off as in equation 2, to produce the desired operators.

Initially the aeromagnetic data were filtered using a 201 point first vertical derivative operator which was obtained using the previously described procedure. The calculated response of the operator is shown in Figure 9. The results of the convolution of the filter

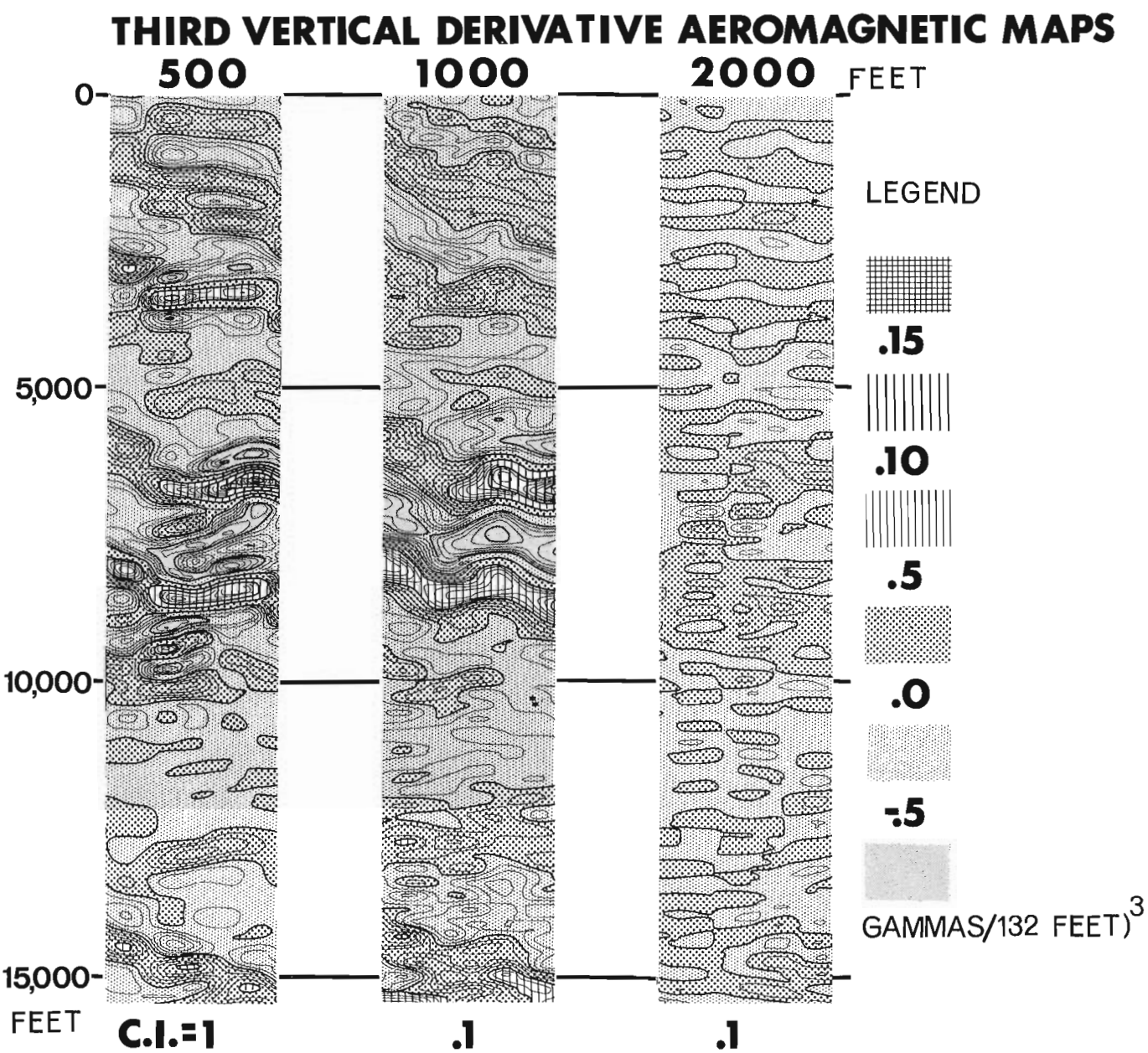

Figure 13. Calculated third vertical derivative maps at the three survey altitudes. Contour intervals (C.I.) are 1 or 0.1 gammas per (132 feet)^3.

weights with the aeromagnetic data shown in Figure 9 are illustrated in the middle of Figure 10. Also Figure 11 shows the calculated first vertical derivative maps of the test range at the three survey altitudes. Comparison of the calculated derivative data (Figs. 10 and 11) with the original total field data (Figs. 7 and 8) demonstrates the improved resolution of the smaller magnetic anomalies in the derived data, however not nearly as good as that of the ground total magnetic data which is shown at the bottom of Figure 7 and in map form in Figure 3. The poorer resolution of the airborne data is partially the result of the vertical scale used in Figure 7 (*see* for instance Olson, 1974), however it is mainly due to the increased separation between the sensor and the causative bodies. As the distance between the sensor and source increases, the amplitudes of the higher frequency components in the data are preferentially suppressed, eventually becoming lost in the noise level of the measuring system. Therefore, it is not possible to recover all of the information using high frequency enhancement filter operators on the data, e.g. vertical derivation. Thus the resolution of high level airborne data can never be as good as that of comparable lower level or ground level magnetic surveys. This assumes of course that all surveys have adequate sampling parameters (McGrath, in press).

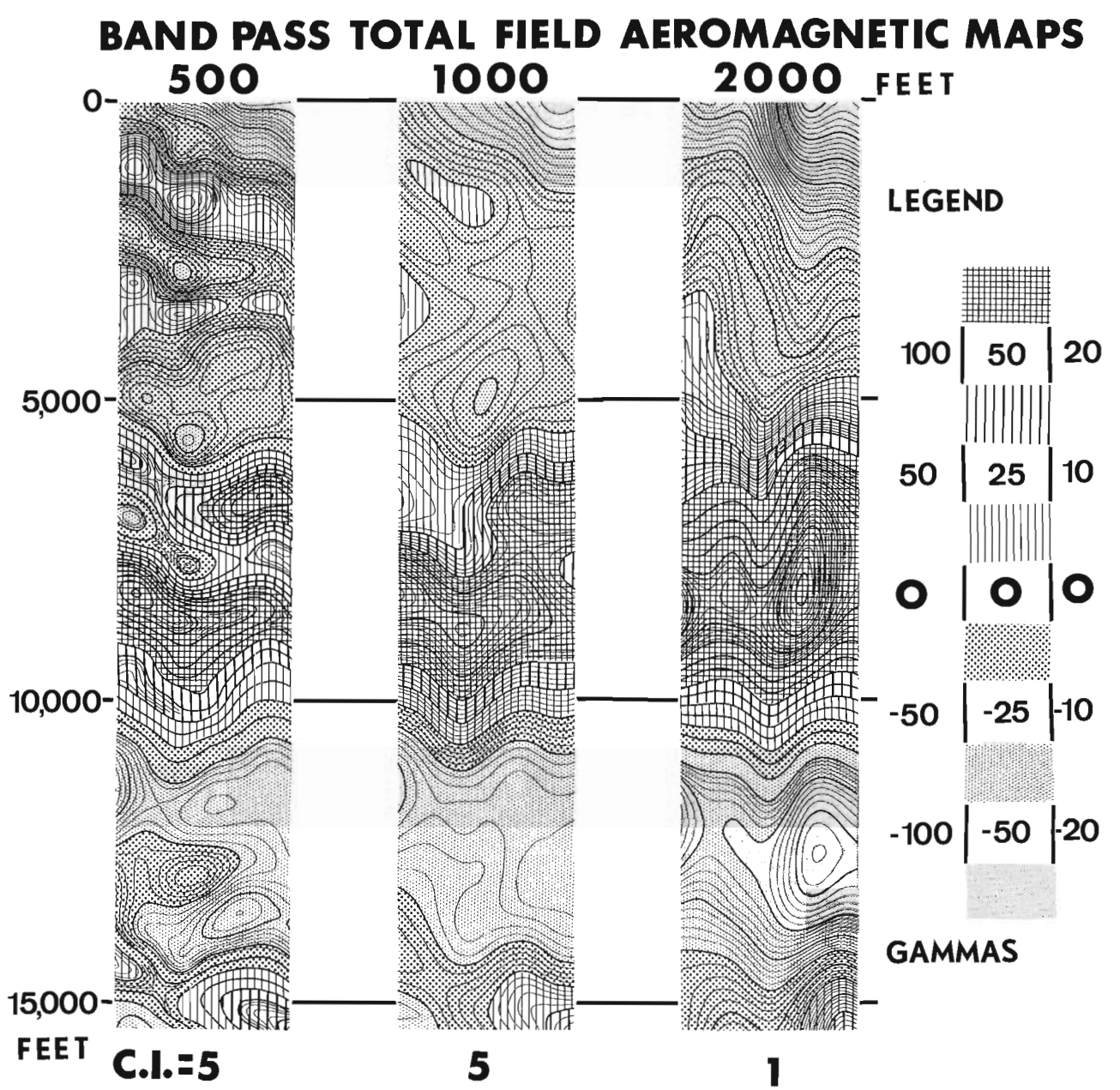

Figure 14. Band pass filtered maps at the three survey altitudes. Contour intervals (C.I.) are 5 or 1 gammas.

It is also apparent from Figure 10 that at least two advantages are gained by flying surveys at a lower altitude. Firstly, there is an obvious improvement in resolution at lower altitudes, and secondly the maximum dynamic range of the derivative anomalies calculated for 500-, 1000- and 2000-foot flight elevations decreases by an order of magnitude being 80, 24, and 8 gammas per sampling interval respectively. Hence these results indicate that there are significant improvements in the derivative data, both in improved resolution and in the amplitude of the geological signal, in flying low level surveys. A consideration of the optimum survey altitude, however, must also be concerned with the fact that at lower altitudes the resultant data, especially vertical derivative data, are much less coherent than for surveys at higher altitudes. Thus low level surveys require a closer flight line spacing in order to alleviate ambiguity problems in contouring the data, so that survey costs per square mile increase proportionately. Moreover there are safety factors to be considered in flying low level surveys, especially in rugged terrain.

The calculated second vertical derivative maps at the three survey elevations are presented in Figure 12. The filter designed in this case was a low pass operator with a cut-off at 0.3 cycles per sampling interval. The cut-off was required to prevent sampling noise in the data, whose frequency is near the Nyquist frequency (0.5) from degrading the resultant second vertical derivative maps. There is only a marginal

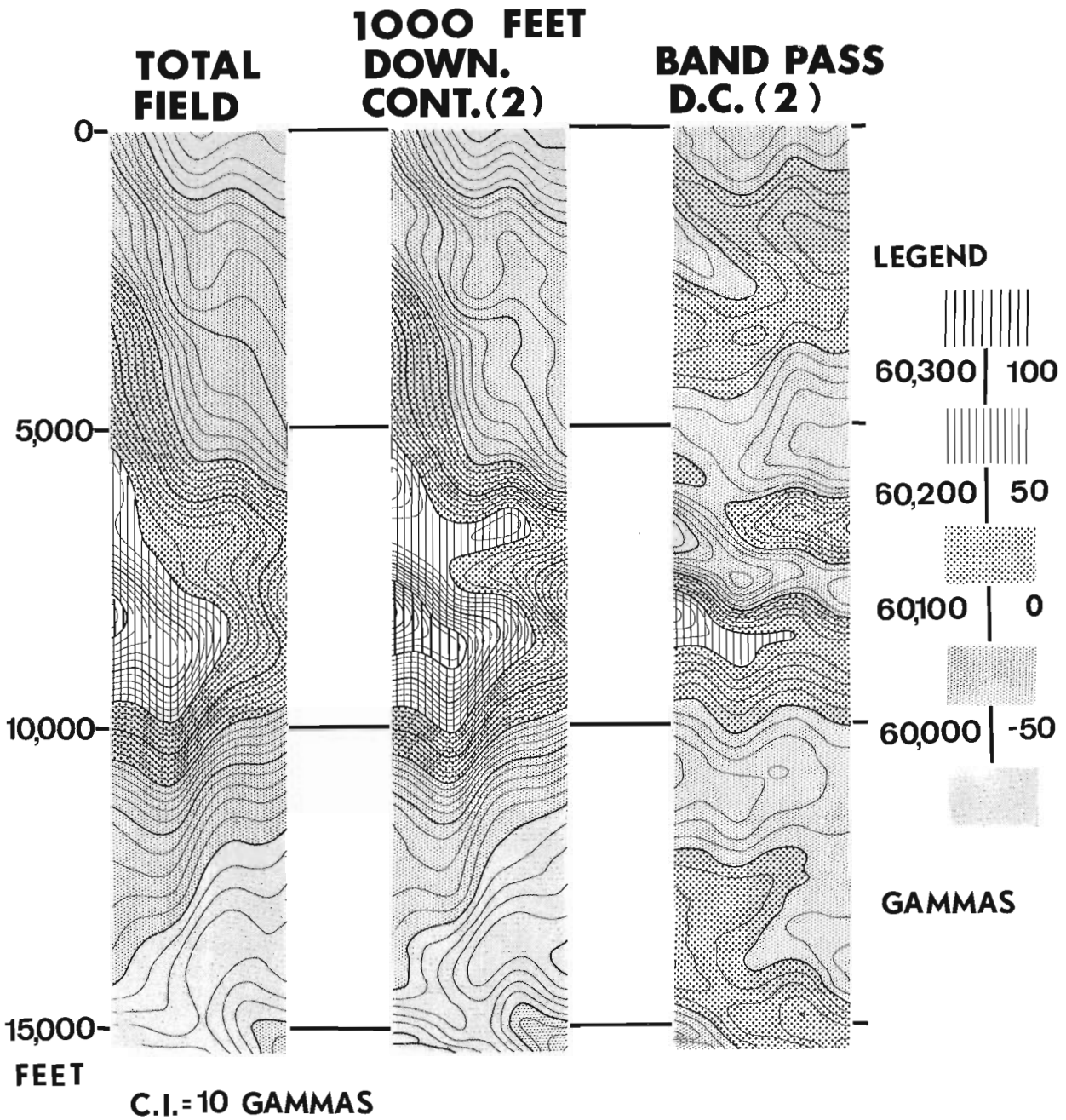

Figure 15. Comparison of the total field aeromagnetic maps for the 1000 foot data with maps of the same data downward continued and bandpass downward continued to 735 feet.

improvement in resolution over the first vertical derivative maps. The data at 2000 feet have become incoherent as the geological signal is lost in instrument and aircraft-produced magnetic noise. Similar conclusions can be drawn from Figure 13 which consists of low pass third vertical derivative maps. Also apparent in Figures 11, 12 and 13 is the enhancement of features which strike at high angles across the flight lines, and the suppression of features which are subparallel to the flight lines. This difficulty is a property of one-dimensional vertical derivative operators as has already been shown for the Timmins high resolution survey (Hood *et al.*, 1975). In spite of the undesirable biasing of one-dimensional operators however, the conclusion that very little is to be gained by going to the higher order derivatives remains unaffected.

Figure 14 shows the result of band pass filtering the airborne data. The band pass operator was designed to pass all frequency components in the data having frequencies from 0.015 to 0.3 cycles per sampling interval. The resolution of the filtered anomalies is not as good as was obtained using the vertical derivative operator.

The third type of filter applied to the airborne data was downward continuation. The results of the test for

data obtained at the 1000-foot flight elevation are shown in Figure 15. On the left side of the diagram is the total intensity map, and in the centre panel a map of the same data continued downward two sampling units (264 feet), again using an operator with a low pass cut-off of 0.3 cycles per sampling interval. The resolving power of the downward continuation filter is lessened because unlike the vertical derivation process, it passes the longer wavelength components in the data. It was decided, therefore, to try a band pass downward continuation filter. The logic behind such a filter was that the operator would reject the longer frequency components in the data as well as the magnetic noise caused by the instrument and the aircraft. The operator was to pass and enhance information caused by near surface sources. The results of this test is shown in the right panel of Figure 15, where the total field data were continued downward two sampling units (264 feet), and the band pass was from 0.025 to 0.3 cycles per sampling interval with a roll-off length of 0.013 cycles per sampling interval. The band pass downward continuation filter yields maps which have better resolution than either the straight band pass (*see* centre panel, Fig. 14) or simple downward continuation operators (*see* centre panel, Fig. 15) are capable of. The resolution of the band pass downward continuation operation is comparable to that obtained by the vertical derivation process (*see* centre panel, Figs. 11, 12 and 13).

Summary and Conclusions

A test range was established in Godfrey Township, near Timmins, Ontario. Lines were surveyed and cut, and several different types of magnetic surveys were performed. The test range was also flown at 500, 1000 and 2000 feet using the Geological Survey of Canada's Queenair aircraft which is equipped with a high sensitivity optical absorption magnetometer. The common form of presentation of survey data in the past has been total field maps. However, total field magnetic maps represent only one form of presentation. These maps tend to portray the dominant magnetic features, for instance, in a particular locality the small scale anomalies may be masked by large scale regional gradients. To obtain an optimum presentation to support geological mapping programs it is necessary to enhance the high frequency content in the aeromagnetic data. This can be accomplished through the use of a suitable digital filter and a proper selection of the vertical and horizontal scales. It is clear that a much improved resolution of the near surface sources is possible through the application of vertical derivative, band pass and downward continuation digital filter operators to the airborne data. The resolution obtainable is however not of the same quality as that found in ground surveys. This is a direct result of the filtering effect on the high frequency components by increased distances to the sources in the airborne surveys. Because much of the high frequency information is suppressed into the noise level of the measuring system, it is not recoverable by high frequency enhancement techniques, e.g. vertical derivation. Hence airborne surveys can never possess the same resolution of an equivalent ground survey. However, the maps yielded by the various digital filters show a remarkable improvement in resolution when compared to the original total field maps. In particular it appears as though the first vertical derivative operator is the most practical of all of the operators tested because it suppresses the long wavelength anomalies while enhancing the high frequency information in the data. The higher vertical derivative operators while marginally improving the resolution, also enhance noise in the data to a greater degree, e.g. compensation errors, thus increasing the difficulties in contouring the data into map form. The resolution of the band pass downward continuation operator was comparable to that of the vertical derivative filter, however because of the additional complexity of the band pass used with the downward continuation process we recommend the use of the simpler first vertical derivative operators to enhance anomalies caused by near-surface sources. As a result the Geological Survey of Canada has constructed an inboard gradiometer system on the Queenair aircraft (Sawatzky and Hood, 1975) in which the sensors are vertically separated by about two meters. The resultant measured vertical gradient values are objective repeatable diurnal-free potential field values and can be used as a starting point for subsequent filter processing. In parallel with the development of a gradiometer system, the Geological Survey of Canada is continuing to evolve digital filtering techniques as an additional tool to be utilized in future detailed geological mapping programs.

References

Hamming, R.W.
1962: Numerical methods of scientists and engineers; New York, McGraw-Hill.

Hood, P.J., McGrath, P.H. and Kornik, L.J.
1975: Evaluation of derived vertical gradient results in the Timmins area, Ontario; *in* Report of Activities, April to October 1974, Geol. Surv. Can., Paper 75-1, pt. A, p. 111-115.

Kanasewich, E.R.
1973: Time sequence analysis in geophysics; Univ. of Alberta Press, 352 p.

McGrath, P.H. and Bower, M.E.
1973: Martin-Graham Digital Filters; *in* Report of Activities, November 1972 to April 1973, Geol. Surv. Can., Paper 73-1, pt. B, p. 71-74.

McGrath, P.H.
Sampling parameters for high sensitivity magnetic surveys: Some consideration based on the upward continuation of white noise; Geophysics. (In press)

Middleton, R.S.
1973: Magnetic survey of Robb and Jamieson townships, District of Cochrane; Ont. Div. Mines, Geophys. Rept. 1, 56 p.

Middleton, R. S.
1974: Magnetic survey of Loveland and Macdiarmid townships, District of Cochrane; Ont. Div. Mines, Geophys. Rept. 2, 26 p.

Olson, D. G.
1974: Procedure for the field checking of digitally recorded high resolution aeromagnetic data; *in* Report of Activities, Pt. A, April to October 1973, Geol. Surv. Can., Paper 74-1, pt. A, p. 91-94.

Paterson, N. R.
1957: A sulphide discovery, Robb-Jamieson area, Ontario; p. 246-259 *in* Methods and case histories in mining geophysics, 6th Commonwealth Mining and Metallurgical Congress, Montreal, 359 p.

Pyke, D. R. and Middleton, R. S.
1971: Distribution and characteristics of the sulphide ores of the Timmins area; Bull. Can. Inst. Min. Met., v. 64, no. 710, p. 55-66.

Sawatzky, P. and Hood, P. J.
1975: Fabrication of an inboard digital-recording vertical gradiometer system for aeromagnetic surveying, A Progress Report; *in* Report of Activities, April to October 1974, Geol. Surv. Can., Paper 75-1, pt. A, p. 139-140.

11. THE IMPLICATIONS OF GEOPHYSICAL STUDIES ON THE PERMAFROST REGIME AND SURFICIAL GEOLOGY, MELVILLE ISLAND AND BYAM CHANNEL, N.W.T.

Projects 730020, 730006, 670041

P. McLaren[1], W.J. Scott[2] and J.A. Hunter[2]

Introduction

Seismic and resistivity techniques were utilized by J.A. Hunter and W.J. Scott respectively to investigate the occurrence of offshore permafrost. This was in conjunction with a coastal process study (McLaren, 1974a), 1975) on the east coast of Melville and west coast of Byam Martin Island. Unfortunately, unusually bad ice conditions precluded the use of marine surveying and studies were limited to selected dive-hole (DH) locations (Fig. 1).

Survey Techniques

A shallow seismic refraction technique was employed in the survey areas to determine velocity-depth relationships. A twelve-channel marine refraction cable was used in conjunction with an SIE RS-4 amplifier and camera. One-quarter pound sticks of Geogel immediately below the ice produced the explosion. At one site (DH 1, Fig. 1), array positioning was done by divers through a hole in the sea ice. At the other locations, the array was placed on the bottom through open leads. Array lengths varied between 40 and 100 m with up to 12 equispaced hydrophones. For each location, a time-distance plot and velocity-depth function were computed using a technique described by Hunter (1971).

Vertical electrical soundings were taken using a Schlumberger array, with potential electrode half-spacings of 0.15 m, 0.465 m and 4.65 m, and current electrode half-spacings from 0.465 m to 465 m. Electrodes were ¾-inch square brass rods hammered into the ice to depths of about 30 cm. A McPhar R 103 transmitter was used to obtain currents of up to 2.5 amperes at a frequency of 0.3125 Hz. The resulting potentials were read from a McPhar resistivity receiver. The results were interpolated both by curve-matching and by using an inversion routine supplied by Zohdy (U.S.G.S. pers. comm.). The interpretations for both the seismic and resistivity techniques described here are not final and may be subject to change.

At each location, the bottom was observed and sampled by the use of SCUBA diving (McLaren, 1974b; McLaren and Frobel, 1975).

Onshore Observations

Frost table profiles were obtained by hand augering on a system of beach profiles established on both the Byam Martin and Melville Island coasts. Above high water line the frost table was characteristically less than one metre below the surface, with minor fluctuations dependent on the sorting and grain size of the facies. Generally the fine, well sorted deposits such as silt and clay found in uplifted lagoons had lower frost table levels (up to 2 m). In poorly sorted beach deposits, this level rose to approximately 0.5 m. However, hand augering showed the frost table to become rapidly deeper in the intertidal and offshore. In most cases it was below the depth possible to obtain by augering (> 2.5 m).

Figure 1.

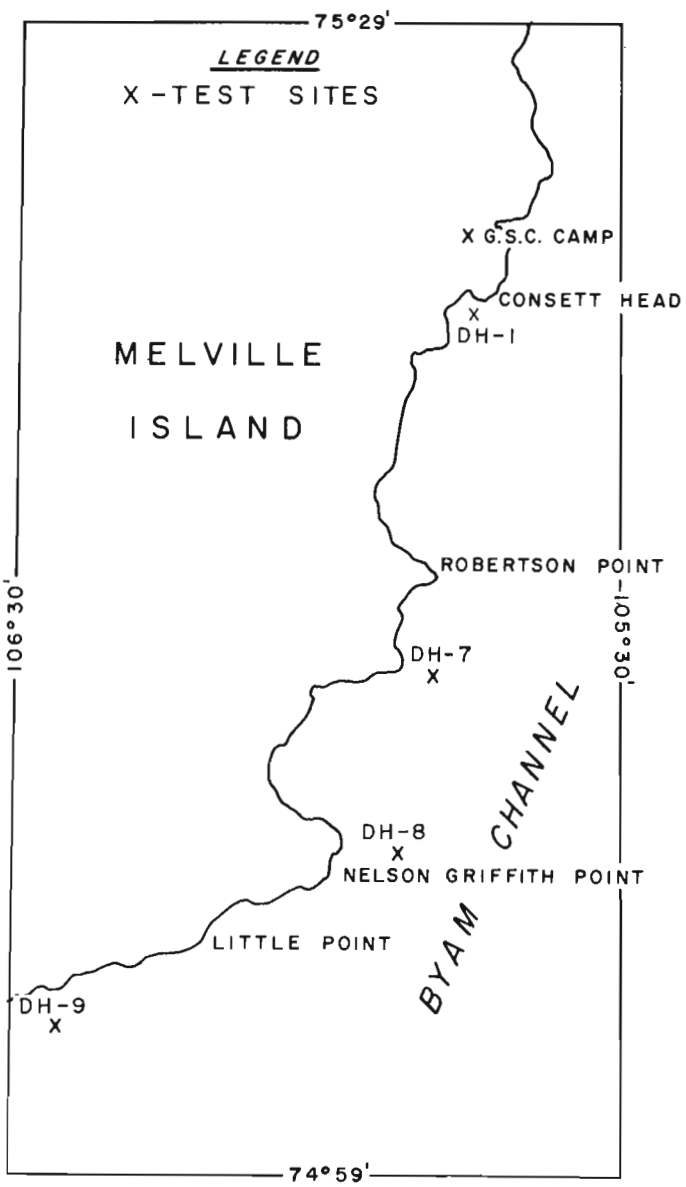

[1]Terrain Sciences Division.

[2]Resource Geophysics and Geochemistry Division.

Figure 2.

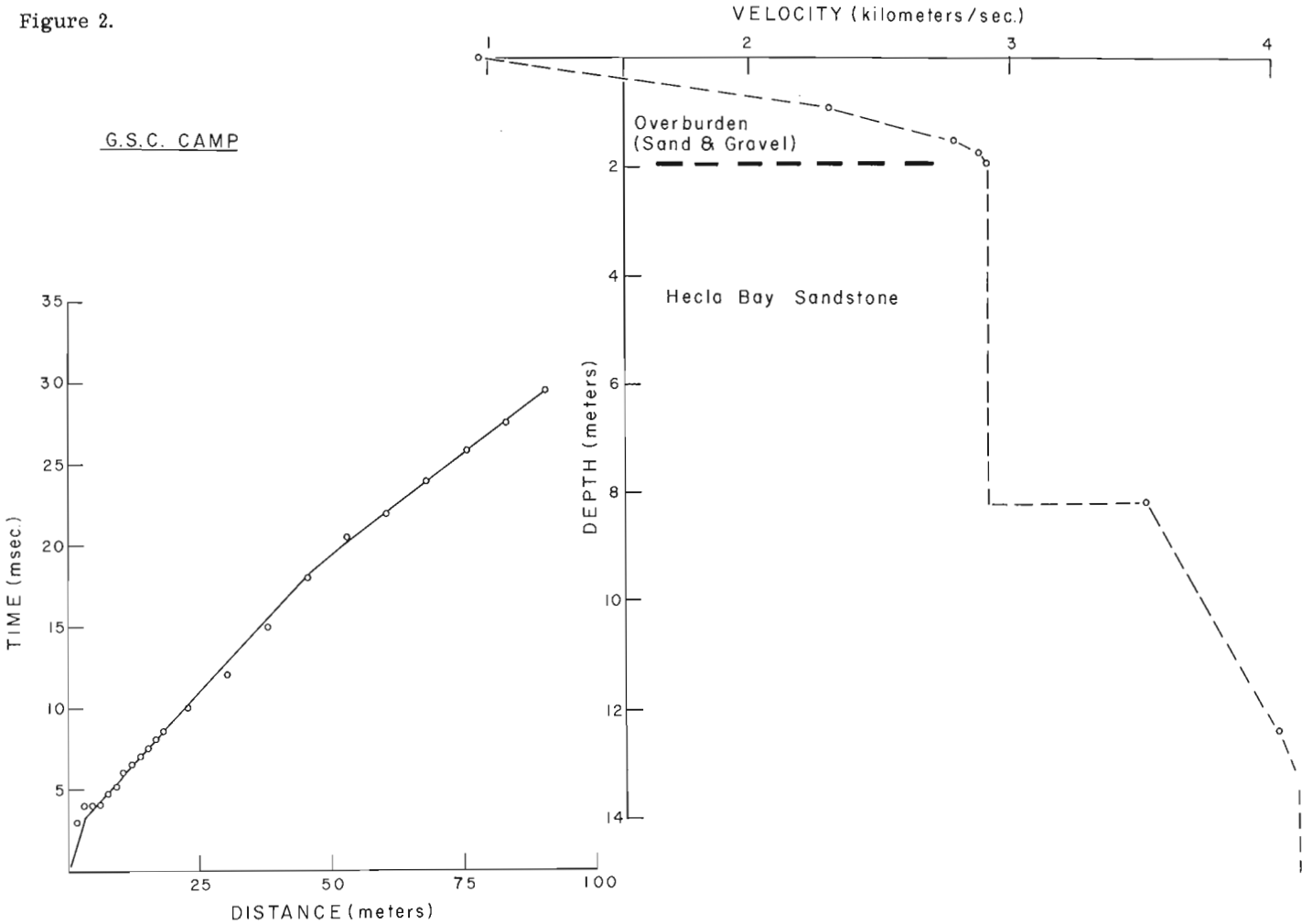

Figure 3.

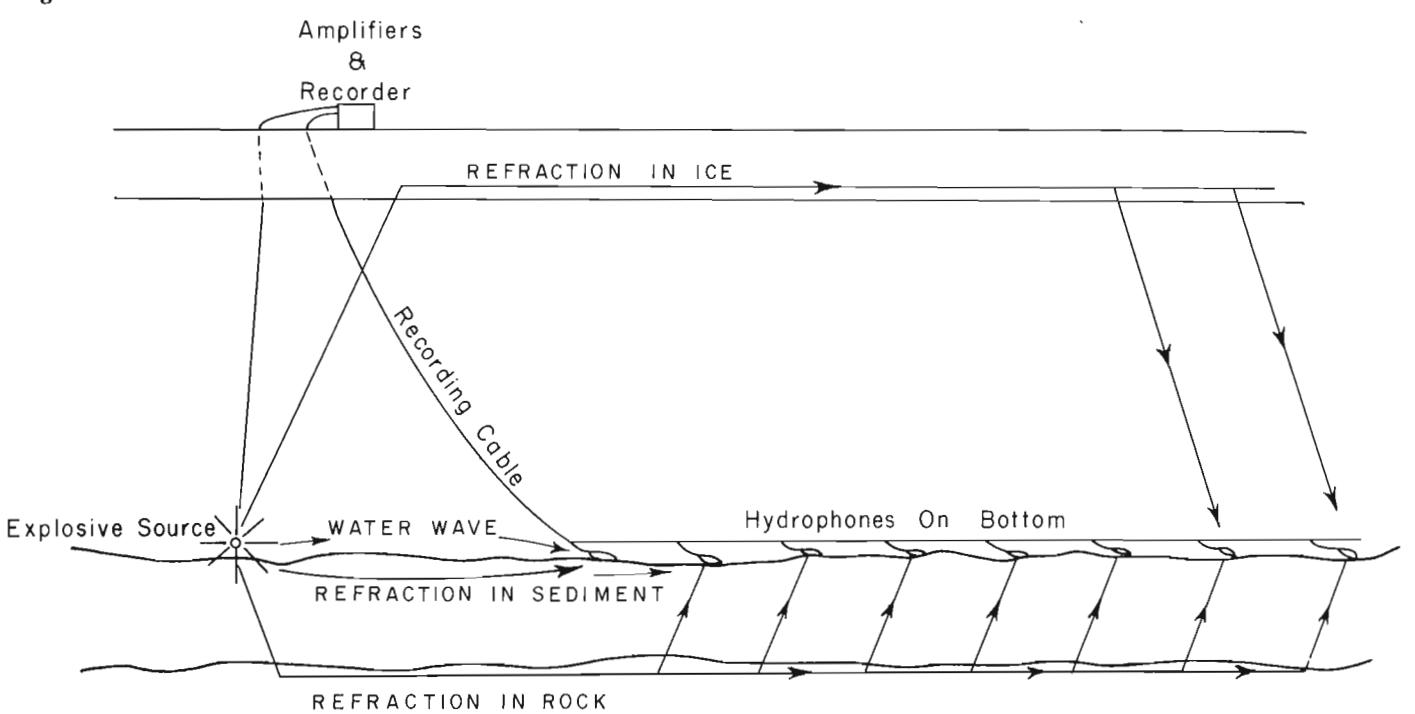

TABLE 1. G.S.C. CAMP

Depth to base of layer (m)	Resistivity (ohm-metres)	Remarks
0.2	120	overburden (sand and gravel)
0.3	300	
1.3	540	
2.8	230	
3.7	65	Hecla Bay sandstone (unlithified, with unfrozen, high saline brines ?)
5.0	32	
8.0	79	
9.2	1000	Hecla Bay sandstone (lithified, with unfrozen, high saline brines?)
12.2	870	
20.0	540	
33.0	490	
54.0	430	
86.0	360	
?	325	

Two onshore drillholes at Rea Point through Recent, well sorted, uplifted delta sand deposits, showed the base of permafrost being 18.9 and 12.8 m (Confidential Report). The holes were at 34 m and 5 m from the shoreline respectively, suggesting that the permafrost may be pinching out towards the channel.

Refraction profiles were shot near the Geological Survey camp (Fig. 1) in order to obtain representative velocities of bedrock known to be frozen. These velocities were then correlated with those observed offshore. Figure 2 illustrates the time-distance plot and velocity-depth function for the site. The bedrock, Upper Devonian Hecla Bay Formation, is an extremely well sorted, clean quartz sandstone, thought to have had an aeolian origin (Tozer and Thorsteinsson, 1964; Kerr, 1974). When unfrozen, the Hecla Bay Formation is often unlithified and it is unknown whether this is due only to surficial weathering. This is overlain by varying thicknesses (.75 m to 3.0 m) of poorly sorted sand and gravel overburden which was originally deposited in a recent nearshore marine environment. However, stream activity, solifluction and deflation have caused the deposit to be extensively reworked. The depth to permafrost was approximately 45-60 cm.

The velocity gradient (Fig. 2) in the overburden is probably due to both the scatter of travel-time data and decreasing temperatures with depth. Bedrock velocities range from 2925 m/sec to 4120 m/sec.

Table 1 shows resistivity values as a function of depth at approximately the same location. The overburden, measuring 2.8 m, ranges in resistivity from 120 ohm-metres to 540 ohm-metres. The dependence of resistivity on depth is probably related to vertical temperature changes and possibly with changes in unfrozen water content. Below 2.8 m, values less than 100 ohm-metres are anomalously low for a frozen sandstone. It is suggested that there may be unfrozen brine within the sandstone which is of a sufficiently high salinity to prohibit freezing. Since the coast has been uplifted, it can be speculated that when the bedrock was below sea level, the highly porous sandstone became saturated with brine. On emergence, freezing would expel high saline brines that would remain trapped within the bedrock. If this is the case, it is an indication that no permafrost was present in the offshore, otherwise it would have been impossible to saturate the bedrock with brine. Such a model might indicate that no permafrost would be present today in the offshore. The principal argument against the existence of high saline brines is the possibility that they would escape by diffusion (as they do in sea ice) over the period of several thousand years that this site has been uplifed.

Below 8 m, the resistivity values, although higher, are still rather low for a permafrost sandstone. It is suggested that below this point the bedrock is more lithified which would account for the marked increase in both velocity and resistivity.

Offshore Observations

Introduction

In shallow water areas, the depth of penetration of the refraction array is limited by water depth, and the velocity contrast between sea water and ice. This is caused by the possibility of interfacing refracted waves transmitted from the source on the bottom, through the ice layer to the hydrophone array (Fig. 3). The average velocity of sea ice in the survey area was measured to be 2250 m/sec, a value anomalously low indicating that the ice was water saturated. Attempted construction of dive holes with chain saws earlier in the season proved this to be true. Based on this average velocity, the travel time of the ice refraction was plotted on all travel-time distance plots for each of the marine sites. In all cases, the ice refraction arrived much later than the observed refracted events. Seismic soundings were obtained at DH 1, DH 7, DH 8 and DH 9 (Fig. 1, Fig. 4-7).

Four electrical soundings were made through the sea ice at DH 1, DH 7, DH 8 and DH 9. However, the sounding near Robertson Point (DH 7) was not completed due to instrument problems. The resistivity values as a function of depth and the geological interpretations are shown on Table 2 to Table 4.

Offshore drilling and piston coring in Byam Channel indicated that permafrost was not present in the top 1 to 8 m (Confidential Report). One exception to this occurred approximately 20 m from the Byam Martin coast where 6.5 m of frozen till lay above sandstone bedrock. This till was described as being predominantly clay and had a relatively high wet density of 2.2 gm/cc.

Figure 4.

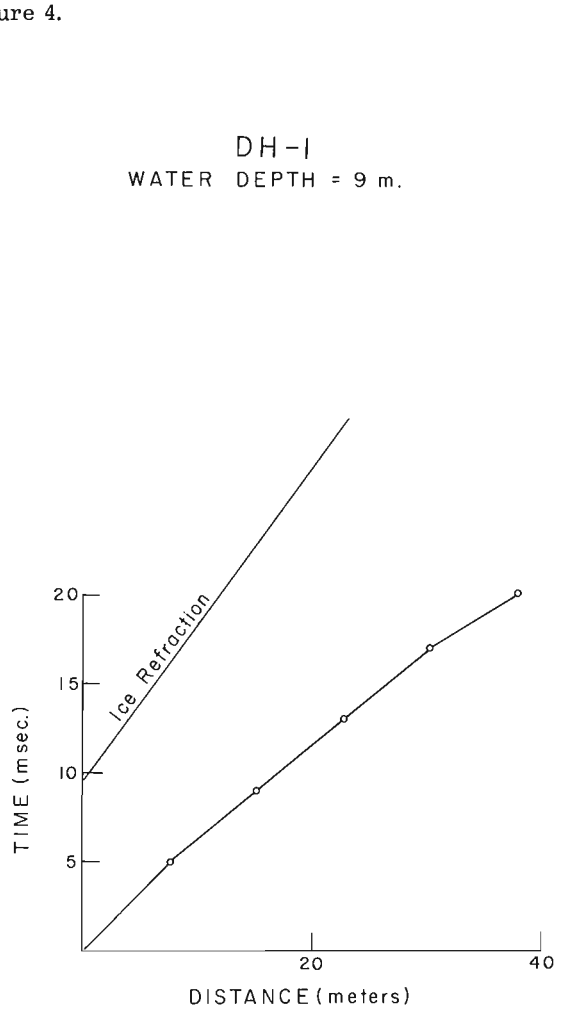

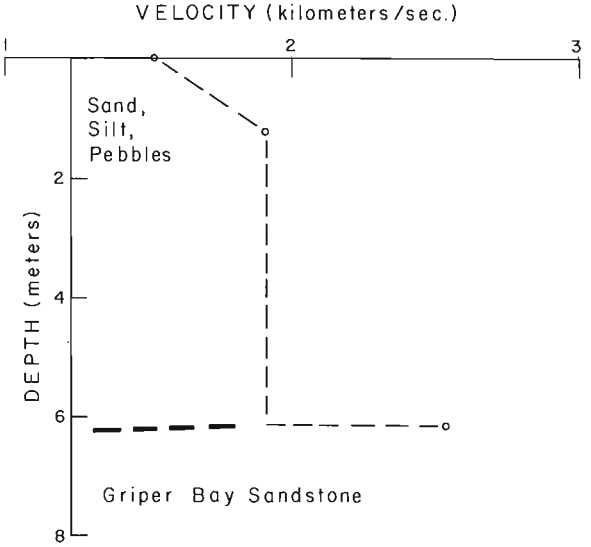

TABLE 2. DH 1

Depth of base of layer (m)	Resistivity (ohm-metres)	Remarks
1.4	120	ice, porous and saline
2.6	6.5	
6	30	sea water
12	1.5	bottom sediments
100	7.4	Griper Bay sandstone
150	12	
210	19	
?	35	

DH 1

Figure 4 and Table 2 show the seismic and resistivity results respectively. Based on bottom samples obtained by diving, the sediments consisted of 22% sand, 52% silt and 26% clay with scattered pebbles both on the surface of the bottom and within the sediment. Under ice observations indicating that ice rafting of pebbles does not appear to be a sedimentary process in Byam Channel, and the fact that the pebbles invariably reflected the bedrock of the region, has led to the tentative interpretation of this being a glacial marine deposit. It is suggested that it was derived from the break-up of the Innuitian Ice Sheet (Blake, 1970) which originated to the northeast of the area. Movement across Bathurst and Byam Martin Islands would have been parallel to the bedrock strike thus accounting for the lithologies of the pebbles.

The underlying bedrock, the Griper Bay Formation, is also an Upper Devonian, predominantly nonmarine sandstone. It would not be expected to have widely different seismic and resistivity properties to the Hecla Bay Formation.

The resistivity data agree well with seismic results, although the water depth differs by 3 m. This is probably not unreasonable since it represents an average over the central part of the sounding. The resistivity of the underlying sandstone rises with increasing depth which could be explained by near-surface invasion of salt water, decrease in temperature with increasing depth and consequent increase in ice content, or as a change in lithology with depth. Only drill or temperature control would give a satisfactory solution.

DH 7

The facies at this location (Fig. 5) has a sand-silt-clay ratio of 58%, 31% and 11%. The increase in sand may account for the higher velocities than those observed at DH 1. No resistivity measurements were taken for this site.

Figure 5.

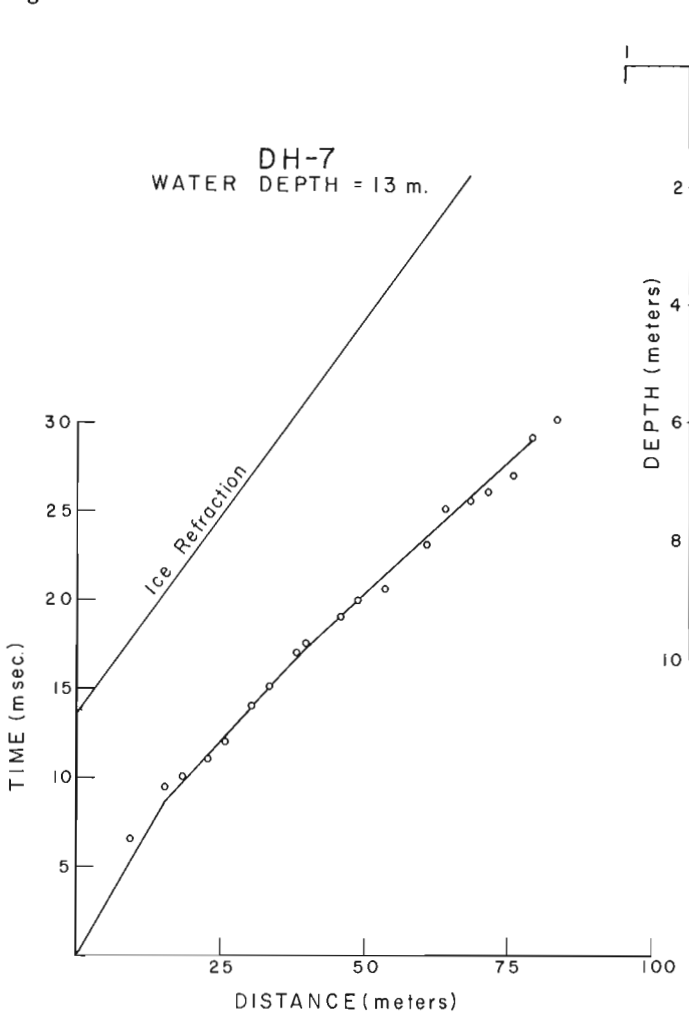

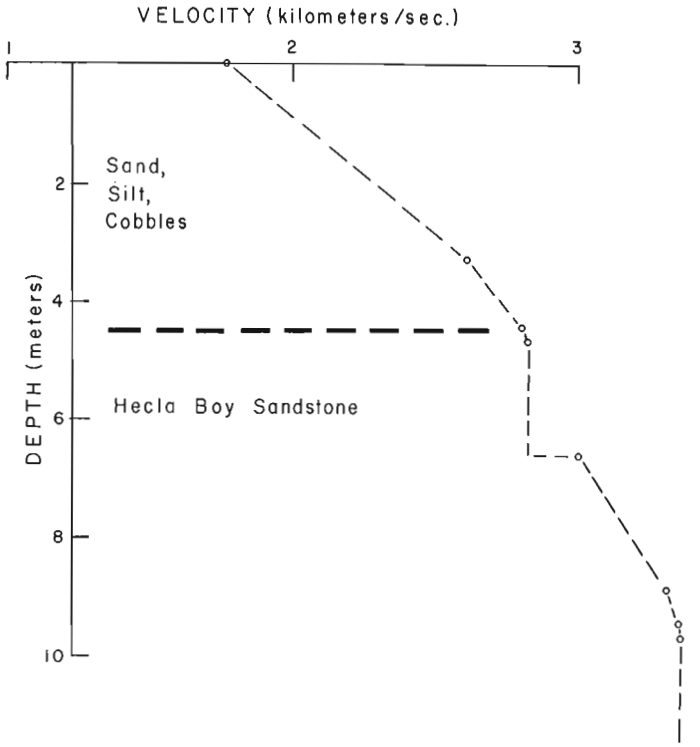

TABLE 3. DH 8

Depth to base of layer (m)	Resistivity (ohm-metres)	Remarks
0.6	1000	ice, less saline
2.0	315	than other sites
13.7	1.3	water (brackish ?)
27	40	Hecla Bay sand-stone
50	83	
110	150	
?	420	

DH 8

Diving observations showed the bottom to be Hecla Bay sandstone with no sedimentary cover. Both seismic and resistivity interpretations (Fig. 6 and Table 3) indicate this to be the case. The resistivity values for both the ice and water suggest less salinity than elsewhere which is explained by the site being close to the outflow of Nelson Griffiths River. The resistivities interpreted for the bedrock compare well with those observed onshore.

DH 9

The seismic velocities (Fig. 7) suggest the occurrence of two facies. The uppermost appears to be the same observed at DH 1 and DH 7 with a sand-silt-clay ratio of 31%, 41% and 28%. Below 6 m a higher velocity layer occurs that is thought to be a more dense till. A very compact till was observed on the south coast of Melville Island at Z1 (McLaren, 1974a). It had a sand-silt-clay ratio of 11%, 54% and 35% and could be similar to the earlier mentioned frozen till found in the borehole. The high density would account for the increase in velocity. It is suggested that this till may have been derived from the Wisconsin Laurentide ice-sheet which is known to have impinged onto the south coast of Melville Island (Craig and Fyles, 1960).

The resistivity measurements (Table 4) do not agree with the seismic interpretation. The water depth is much less than that measured by the seismic method which is the same as that recorded by diving. The interpreted presence of a thin bottom surface layer of 61 ohm-metre resistivity is difficult to explain. It

Figure 6.

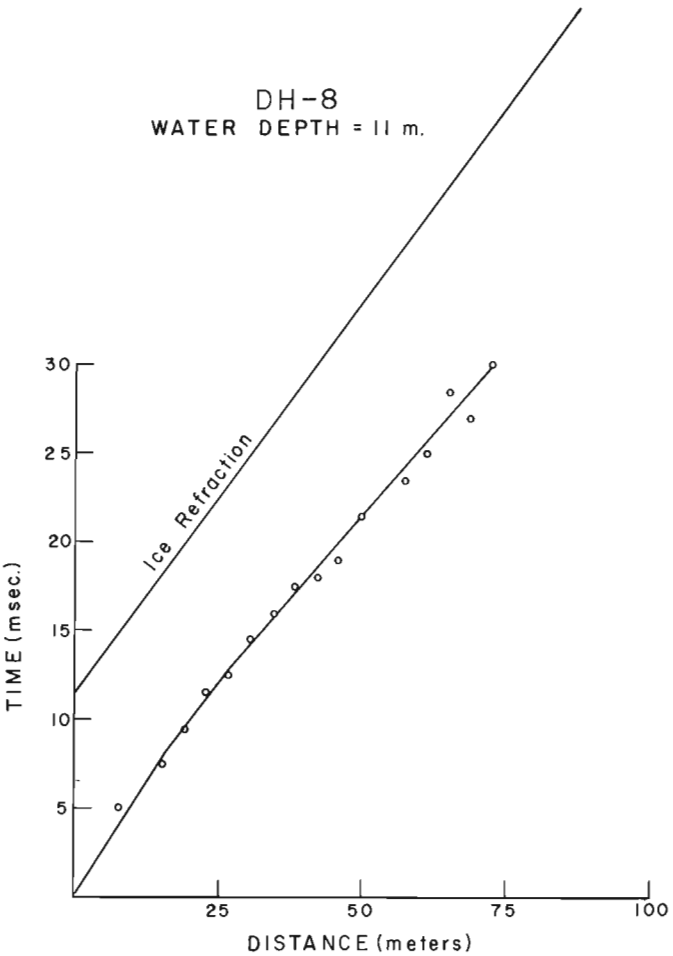

TABLE 4. DH 9

Depth to base of layer (m)	Resistivity (ohm-metres)	Remarks
3.0	270	ice, porous and saline
3.4	3.3	
6.0	0.18	sea water
7.8	61	?
18	5.5	Griper Bay sandstone
27	18	
42	63	
?	84	

may be the result of lateral variations in ice thickness along the line of the sounding, since it does not agree with sediment depths of > 2 m that divers obtained by hand augering.

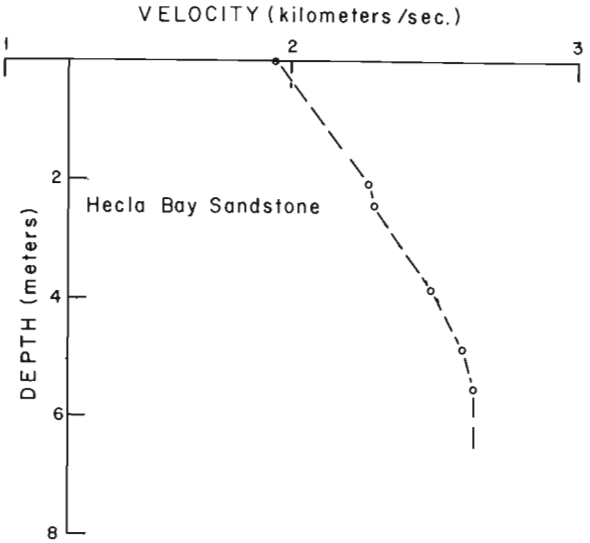

Conclusions

A sea-bottom refraction technique operated from the sea-ice surface has successfully mapped velocity-depth structure of unconsolidated material and bedrock. In general, the velocity of the sea-bottom sediments is relatively low, 1500-1950 m/sec, and corresponds well to poorly sorted sand, silt and clay with scattered pebbles and cobbles. This has been interpreted as a till. The velocities observed for bedrock known to be frozen range from 2925 m/sec to 4120 m/sec. Offshore, the velocities lie between 2360 m/sec and 3350 m/sec, slightly lower than those found on land. Although lower velocities would be expected if permafrost was absent in the offshore, there is too much overlap in the ranges to differentiate clearly between frozen and unfrozen sub-marine bedrock.

Except for DH 9, resistivity measurement agreed well with the seismic interpretations. Soundings through sea ice can give information on ice thickness, water depth, and sub-bottom characteristics. All the offshore soundings indicate increases in resistivity with increasing sub-bottom depth. Although this is consistent with results obtained onshore in known permafrost conditions, it could also be due to invasion of salt water or changing lithologies.

The geological interpretation favours the absence of permafrost in Byam Channel. The drillhole data, and the anomalous onshore resistivities suggest that permafrost would pinch out quickly in the channel. The amalgamation of geological and geophysical methods has given rise to some answers, several possibilities and many questions. Further developmental work is planned for the coming season.

Acknowledgments

The authors would like to thank R.L. Good, D. Eberle and D. Frobel for their valuable assistance in the seismic, resistivity and diving programs respectively.

Figure 7.

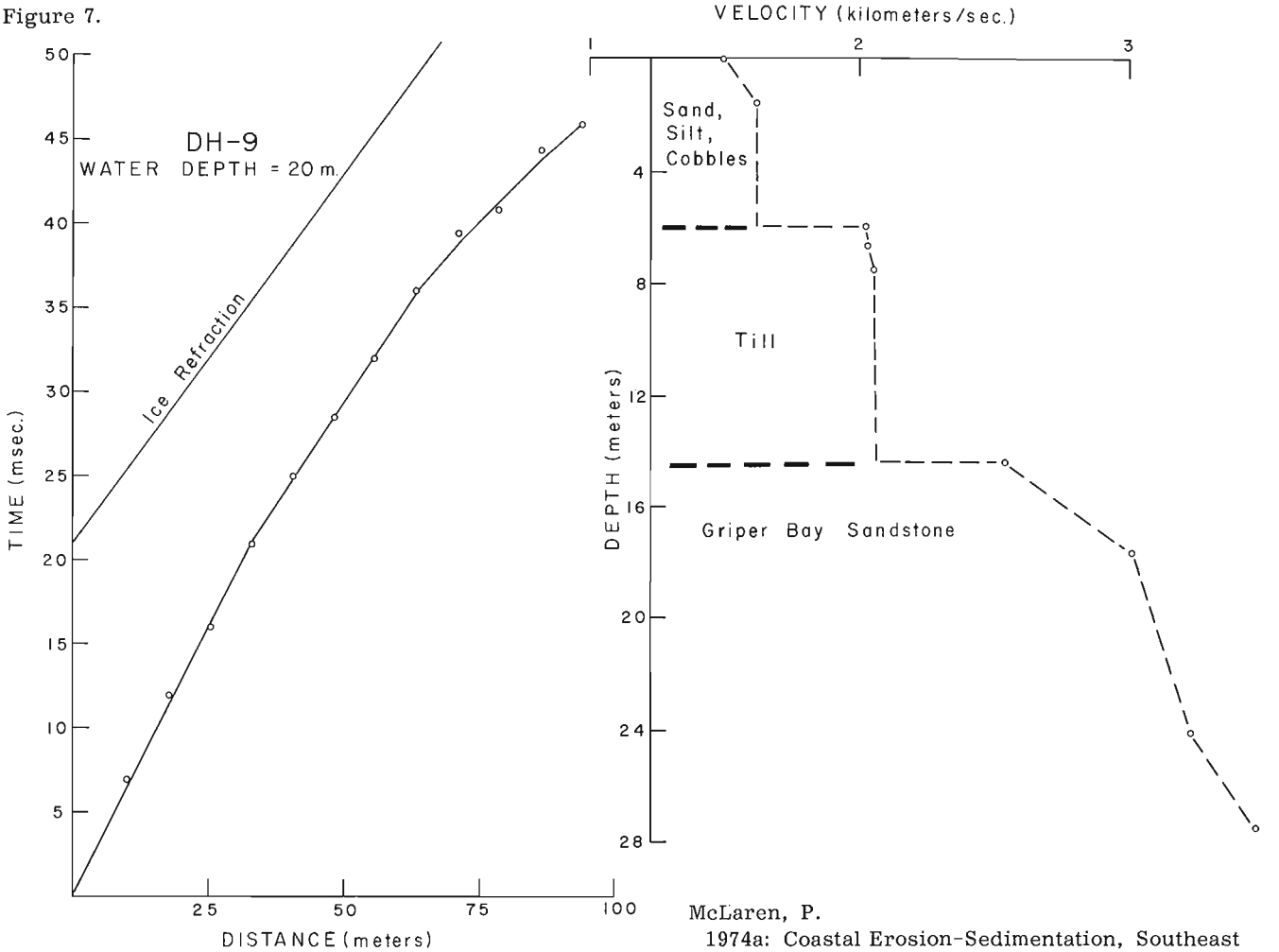

References

Blake, W., Jr.
1970: Studies of glacial history in Arctic Canada. I. Pumice, radiocarbon dates, and differential postglacial uplift in the eastern Queen Elizabeth Islands; Can. J. Earth Sci., v. 7, no. 2 (Pt. 2), p. 634-664.

Craig, B.G. and Fyles, J.G.
1960: Pleistocene Geology of Arctic Canada; Geol. Surv. Can., Paper 60-10, 21 p.

Hunter, J.A.
1971: A Computer Method to obtain the Velocity-Depth Formation from Seismic Refraction Data; *in* Report of Activities, Pt. B, November 1970 to March 1971, Geol. Surv. Can., Paper 71-1B, p. 40.

Kerr, J.W.
1974: Geology of Bathurst Island Group and Byam Martin Island, Arctic Canada; Geol. Surv. Can., Mem. 378, 152 p.

McLaren, P.
1974a: Coastal Erosion-Sedimentation, Southeast Melville and Western Byam Martin Islands, District of Franklin; *in* Report of Activities, Pt. A, April to October 1973; Geol. Surv. Can., Paper 74-1A, p. 267.

1974b: Arctic Diving Observations at Resolute Bay, N.W.T. and the North Pole; *in* Report of Activities, Pt. B, November 1973 to March 1974, Geol. Surv. Can., Paper 74-1B, p. 257-258.

1975: Under-Ice Diving Observations in the Coastal Environments of Southeast Melville and Western Byam Martin Islands; *in* Report of Activities Pt. A, April to October 1974, Geol. Surv. Can., Paper 75-1A, p. 475-477.

McLaren, P. and Frobel, D.
1975: Under Ice SCUBA Techniques for Marine Geological Studies; Geol. Surv. Can., Paper 75-18, p. 13.

Tozer, E.T. and Thorsteinsson, R.
1964: Western Queen Elizabeth Islands, Arctic Archipelago; Geol. Surv. Can., Mem. 332, 242 p.

12. LITTORAL PROCESSES AND SEDIMENT DYNAMICS, MAGDALEN ISLANDS, QUEBEC: NOVEMBER, 1974

Project 740009

E. H. Owens
Atlantic Geoscience Centre, Dartmouth

Introduction

As a continuation of investigations reported earlier (Owens, 1975) two study sites were reoccupied during November 1974 on the Magdalen Islands to determine seasonal variations in processes and morphology on two barrier beaches.

Data Collection

Meteorological, wave, tide and groundwater variables were monitored at each site every three hours from November 12 to 30. Due to storm waves, prior to this phase of the operations, only one of the four wave towers installed during the summer phase of the operations remained undamaged (tower 4 on the east site). Five current meters were installed in the nearshore zones (Fig. 1) and a wave pressure sensor was placed at the site of the former no. 1 wave tower on the west coast. At the termination of the winter study only one of these instruments, the outer east site current meter, was retrieved. This was due to burial of the instruments (up to 1 m of deposition at one location) and unfavourable sea conditions which severely restricted boat operations. Attempts to locate and retrieve these instruments are planned for spring 1975.

Beach profiles were surveyed at both sites throughout the winter study period and echo-sounder profiles were recorded twice on the east site. Wave conditions did not permit satisfactory echo-sounder surveys on the west site. In addition to the observed process variables, volumes of longshore sediment transport were computed from breaker angle and breaker height data. These volumes were derived from a formula (adopted from Galvin, US Army Coastal Engineering Research Center; pers. comm., 1974) which involved calculation of the immersed weight of sediment and the longshore component of wave energy flux to determine the immersed-weight transport rate.

Preliminary Data Analysis

During the 19-day period of observations, six low pressure centres passed through the southern Gulf of St. Lawrence. Minimum pressures of 990, 987 and 971 mb were recorded for the three most intense storms. In general, low pressure centres which passed to the west and north of the islands generated winds onshore to the east barrier. Centres which were to the east and south of the islands generated onshore winds on the west coast. In microtidal environments (tidal range <2 m) one of the usual effects of storms is the generation of wind tides. However in this case, tidal data recorded adjacent to the west coast study site showed that onshore winds did not cause significant rises in water level and that wave height was the principal factor in causing water level changes. The absence of wind tides must result from the lack of enclosing land areas on this island barrier complex, so that water is not trapped against the coast.

On both barriers wave height was closely related to the onshore wind component. An example is given by the storm of November 26-27 (Fig. 2) which passed directly over the Magdalen Islands. With onshore winds on the 26th (Fig. 3) significant wave height increased with wind velocity on the east-facing coast.

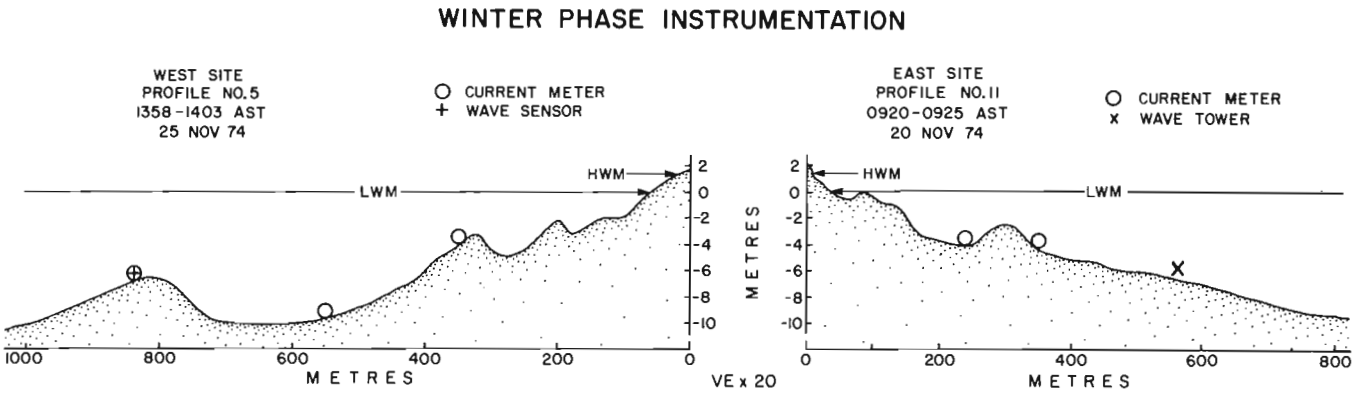

Figure 1. Location of instruments and winter beach-nearshore profiles of the west and east study sites (cf. Figs. 1 and 2; Owens, 1975).

As the low pressure centre crossed the islands wind direction reversed to offshore and wave height diminished rapidly. Wave period remained constant until approximately 24 hours after the wind reversal when longer-period swell waves out of the west reached this site.

Beach profile surveys at the west site show that a wide (50 m), flat low-tide terrace was present throughout the study period. Beach morphology was not greatly modified during storms as waves greater than 2 m in height broke on the nearshore bars, up to 880 m from the swash line. Greater variation was observed at the east site where storm waves eroded the beach (Fig. 4) to a flat profile which was followed by onshore migration of ridge and runnel systems in the post-storm recovery period (Fig. 5). More significant on this beach was the change in the morphology of the inner nearshore bar during storms. Beach protuberances developed behind these bars during periods of low wave activity. With an increase in wave height longshore currents were deflected by the protuberances and eroded rip channels through the bars while new bars were deposited in less energetic environments at the sites of former rip channels. With the development of protuberances on the lee of the new bars, longshore currents generated by the next storm were again deflected and eroded rip channels through the new bars. Thus in one cycle of two storms the morphology of the beach and nearshore bars had returned to its initial pattern. This cyclic oscillation of bars is the same as that reported by Davis and Fox (1972) on eastern Lake Michigan beaches. During the Magdalen Islands winter study, three complete cycles were observed at the east site during a 19-day period in response to six low pressure systems which crossed the region.

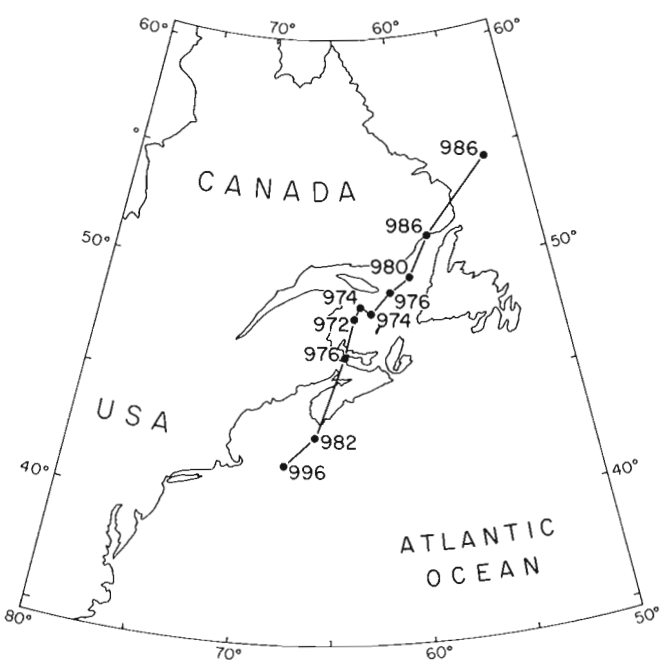

Figure 2.

Track of low pressure system 0200 AST November 26, 1974 to 0800 AST November 28, 1974. Pressure, in millibars, is shown at the centre of the storm every 6 hours.

Summary

A summary of selected data (Table 1) shows that the dominant and prevailing wind direction during this phase of the study was out of the west. The net longshore current direction was to the north on the west coast and to the south on the east coast. Computed volumes of the hourly longshore sediment transport rates (Table 2) indicate the great differences between the

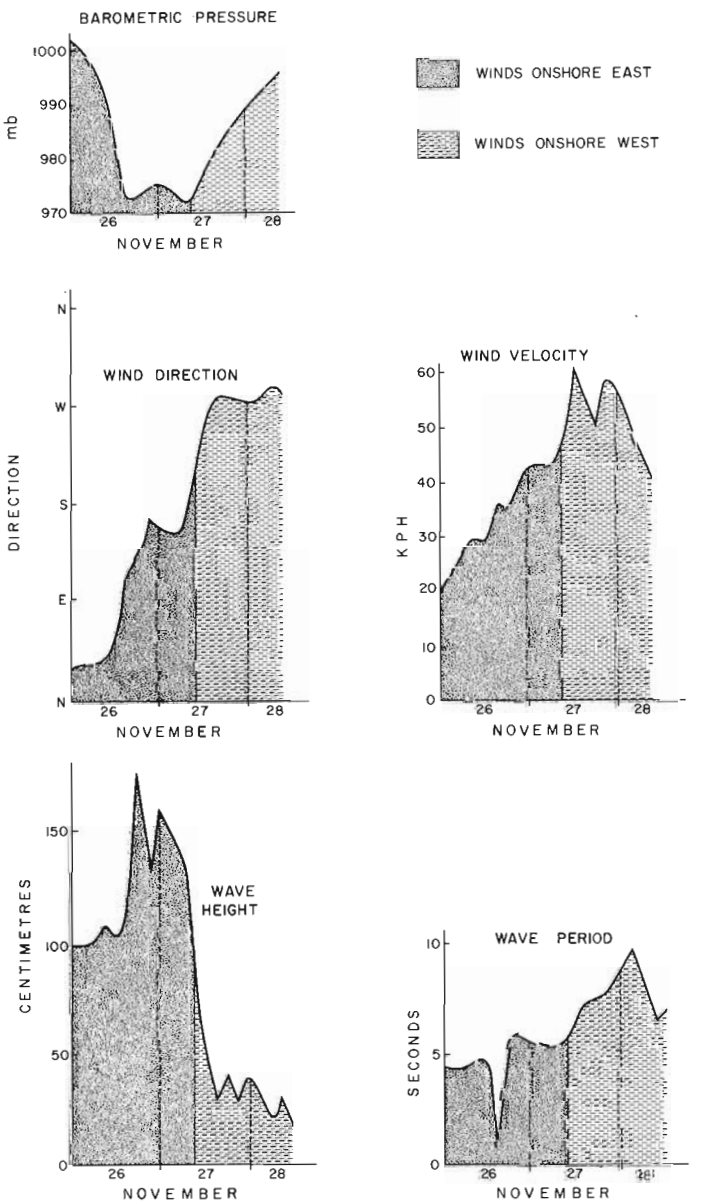

Figure 3.

Meteorological variables recorded at Grindstone and wave parameters recorded at the east study site during the storm of November 26-27, 1974.

Table 1a - Summary of onshore wind data, November 12-30, 1974.

		Hours	% Time	Ave. Speed (kph)	Max. Speed (kph)	Wind Run (km)	% Time Speed >25 kph	Longest Period onshore winds >25 kph (hrs)
Onshore Winds	East	159	40	41.6	77	5184	81.0	42
	West	411	60	34.4	62	8040	76.0	60

Table 1b - Summary of wave data recorded on east study site.

		Ave. Significant Wave Ht. (cm)	Max. Significant Wave Ht. (cm)	% Time Significant Wave Ht. > 90 cm	Ave. Wave Period (seconds)
Wave Data	East*	98	350	43.9	5.9

Table 1c - Longshore current data.

			Hours	% Time	Ave. Speed (cm/sec)	Max. Speed (cm/sec)	Current Run (km)	% Time Current >50 cm/sec
Longshore Currents	East	to North	192	46	25.3	99	159	12.1
		to South	225	54	36.0	123	224	18.7
	West	to North	183	48	56.5	125	311	47.1
		to South	201	42	54.2	124	263	42.2

* No. 4 Wave Tower (see Fig. 2d, Owens 1975)

NOTE: Wind run and current run are the multiples of velocity and time.

Figure 4.

East study site, profile line 11, at 1630, November 21, 1974. Under normal conditions, waves rarely reached the berm crest, at the most seaward of the three groundwater pipes (Fig. 5). During this storm a small erosion scarp was cut into the base of the foredune ridge. At the time of the photograph significant wave height was 2.6 m.

Table 2

Summary of computed longshore sediment transport rates

a. Summer longshore sediment transport:

		Total Transport (m^3)	Period (hours)	Hourly Rate (m^3/hour)	Net Daily Rate (m^3/day)
East	to North	11 149	219	51	195.36
	to South	5 626	150	38	-
West	to North	34 903	240	145	415.14
	to South	12 904	141	92	-

b. Winter longshore sediment transport:

East	to North	21 569	84	257	-
	to South	38 501	126	306	933.84
West	to North	117 708	192	613	1 244.16
	to South	112 034	222	504	-

c. Approximate annual (ice-free period) sediment transport rates:

East: gross transport: 534 896 m^3/year
net transport: 101 080 m^3/year to the south

West: gross transport: 1 999 058 m^3/year
net transport: 227 117 m^3/year to the north

Figure 5.

East study site, profile line 9, at 1300 on November 5, 1974. Following this echo-sounder survey the ridge and runnel system welded onto the beach face. The two wave towers are visible in the upper left of this photograph.

summer and winter phases and between the east and west study sites. On the east site the winter rate was five times greater than that computed from the summer data but at all times the rates were only half those computed from the west site data. This major difference in the two barrier environments is also shown by the estimated annual net sediment transport rates.

The differences in the two energy environments are significant in terms of variations in sediment transport volumes and in the patterns of nearshore morphology. During periods of storm waves breakers formed up to 800 m from the beach on the west study site and maximum sediment transport was in the nearshore zone. On the east coast the mean breaker distance was 120 m and as a result, greater variation in morphology occurred on the inner bars.

References

Davis, R.A., Jr. and Fox, W.T.
1972: Coastal processes and nearshore sand bars; J. Sed. Petrol., v. 42(2), p. 401-412.

Owens, E.H.
1975: Littoral processes and sediment dynamics, Magdalen Islands, Quebec: July-August, 1974; *in* Rept. of Activities, April to October 1974, Geol. Surv. Can., Paper 75-1, Pt. A, p. 157-160.

13. OCCURRENCE OF ZINC IN DEVONIAN METALLIFEROUS SHALES, PINE POINT REGION, DISTRICT OF MACKENZIE

Project 710033

R. W. Macqueen and E. D. Ghent[1]
Institute of Sedimentary and Petroleum Geology, Calgary

Anomalously high values of zinc and uranium were reported by Macqueen *et al.* (1975) from 12 subsurface core samples of shales and mudstones either in, or in close stratigraphic proximity to, the Bituminous Member of the Middle Devonian Pine Point Formation in the Great Slave Lake area (Norris, 1965; this unit appears to be the F-facies of Cominco's Pine Point property; *see* Skall, 1975; also H. Skall, pers. comm., 1975). Because these sediments may have acted as a source bed for Zn mineralization at Pine Point, it is of interest to determine where the Zn resides within the samples (in sulphides, organic matter, adsorbed on clays, carbonate lattice, or chloride complexes). Recent work has focussed on this problem; in addition, samples were analyzed for Cu content. Other compositional data were given earlier (Macqueen *et al.*, 1975, Tables 1, 2).

Analytical Methods

Two approaches were used to try to determine where Zn resides within the shales and mudstones: a) leaching of separate sets of samples with 4 NHCl and with H_2O_2 (*see* Table 1); and b) analysis of 4 samples rich in Zn and organic matter by electron microprobe. The probe work was done with an ARL EMX-SM model microprobe, located in the Geology Department, University of Calgary. Electron beam-scanning of selected areas and the observation of Pb, Zn, and S K α scanning images were undertaken with the microprobe. With this technique, high concentrations of Zn coincident with high concentrations of S demonstrate the presence of sphalerite; similarly, high concentrations of Fe and S indicate pyrite. Sample current imagery was used also; this method provides a map of the distribution of the mean atomic numbers of the constituents, and gives better spatial resolution than X-ray scanning imagery.

Copper contents were determined by atomic absorption spectrophotometry (*see* Table 1).

Results

Leaching results, as shown in Table 1, were moderately successful using 4 NHCl, but unsuccessful using H_2O_2, apparently owing to oxidation of Zn to a state not detected by atomic absorption analysis. Some of the Zn-rich samples yielded half or more of the Zn on treatment with HCl (samples 4, 5, 6, 12); others did not (samples 7, 8).

Microprobe analysis detected minute crystals of sphalerite in 3 of the 4 samples analyzed. Lead was not detected above background values in any of the samples. It is important to note that the area of the samples analyzed ranges from 7 to 17 mm in stratigraphic thickness (samples cut normal to bedding), and from about 14 to 20 mm in width. Within these sample areas, smaller areas were scanned with the electron beam (Figs. 1-5); not all of the areas available were scanned completely because of surface irregularities or other limitations.

In samples 4 and 12, the sphalerite crystals are associated with carbonate shell material, and range from about 2 to 8 microns in size (Figs. 1, 3, 4). If the small areas analyzed are representative, sphalerite crystals are rare. None were detected in the matrix (comprising carbonate, quartz, organic matter, and clay minerals) of samples 4 and 12. Sphalerite was not detected in sample 7, which has the highest reported values of both Zn and organic matter (Table 1). Sphalerite is very rare in Sample 6; two minute sphalerite crystals ($\simeq$2 microns) were detected in the matrix of this sample. Pyrite is ubiquitous, and is readily identified in all samples (Figs. 2, 5).

Copper values reported in Table 1 are generally low, with higher values tending to follow higher values of organic matter, as earlier reported for Zn, U_3O_8, and Pb (Macqueen *et al.*, 1975, Table 2).

Interpretation

The amounts of sphalerite identified by microprobe in samples 4 and 12 may be sufficient to account for most or all of the Zn determined by atomic absorption analysis of these samples (Table 1). Considering the microprobe analyses as representative, sample 6 from the Bituminous Member and sample 7 from the Horn River Formation apparently contain more Zn than can be accounted for by sphalerite. The most reasonable interpretation is that the Zn resides within the abundant organic matter characteristic of these samples. The incomplete extraction of Zn from sample 7 using hot HCl treatment (Table 1) suggests that Zn is not merely adsorbed on organic matter, but may be tightly bound within the organic structure, perhaps as clathrate compounds. Carbonates, clay minerals, and chloride complexes as Zn sites seem unlikely, unless these materials are very tightly sheathed by organic matter. Crushing of samples should have negated this factor.

[1]Department of Geology, The University of Calgary, Calgary, Alberta, T2N 1N4.

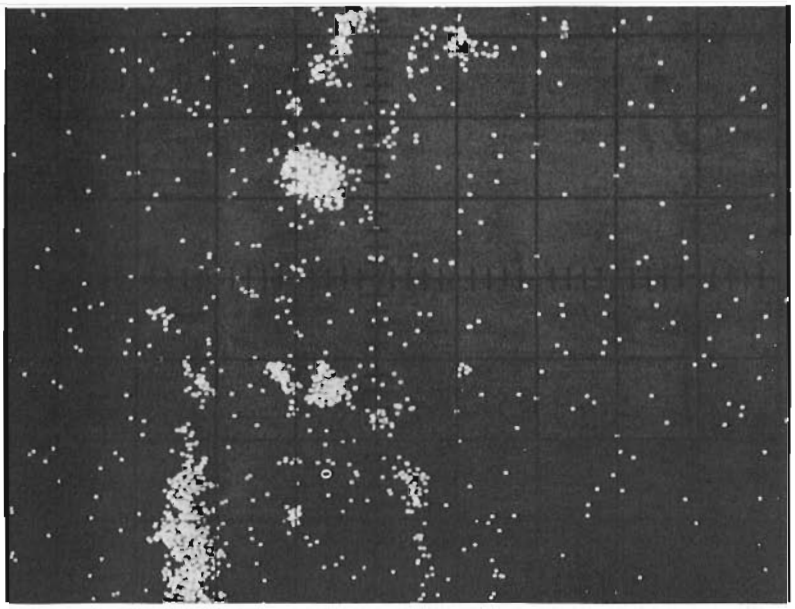

Figure 1.

Zn K α X-ray scanning photograph showing Zn distribution in part of sample 4, Bituminous Member. Clusters of points are sphalerite crystals, confirmed by S K α scan of same area (Fig. 2). Sphalerite crystals fringe carbonate skeletal material. Single grid square = 10 x 10 microns; field of photo 100 microns wide.

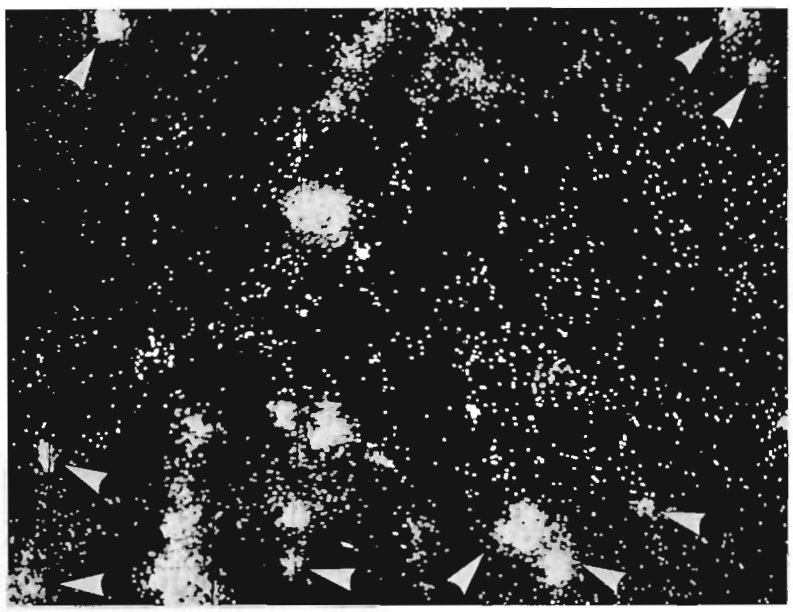

Figure 2.

S K α X-ray scanning photograph of same area shown in Figure 1. Clusters of points marked by arrows are pyrite; remaining clusters coincide with Zn K α image shown in Figure 1, and are sphalerite. Scale as Figure 1.

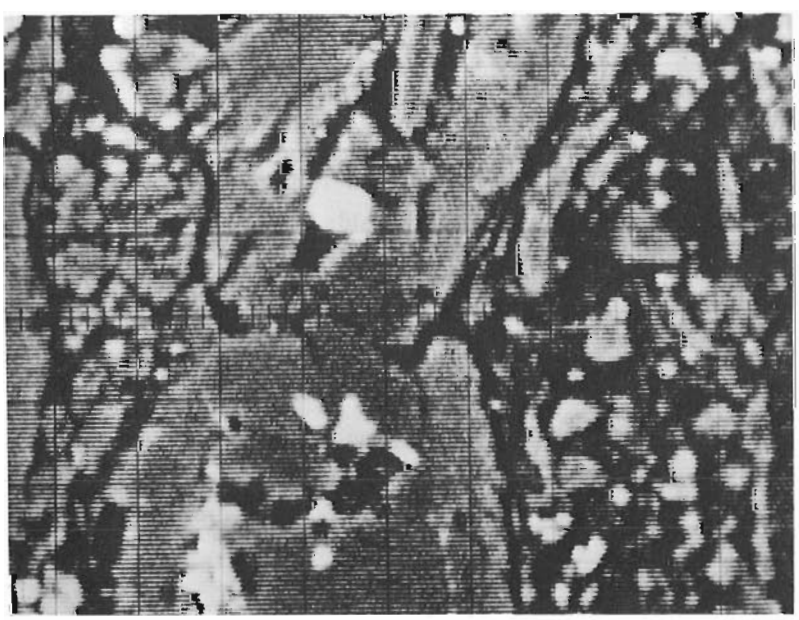

Figure 3.

Sample current image of same area shown in Figures 1, 2. Brightest spots are sphalerite crystals, which have a relatively high mean atomic number compared to the surrounding material. Scale as Figure 1.

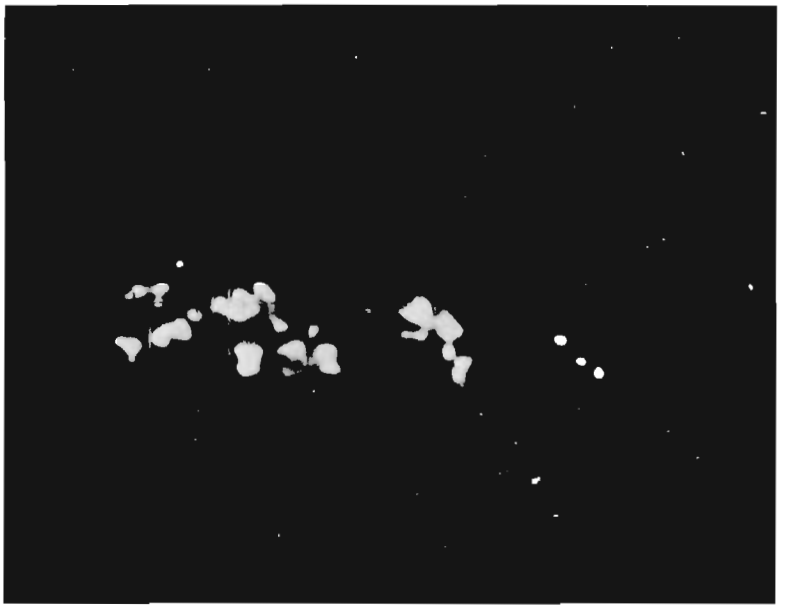

Figure 4.

Sample current image of part of sample 12, showing delicate sphalerite crystals, associated with carbonate skeletal material. Bituminous Member.
Single grid square = 10 x 10 microns;
field of photo = 100 microns wide.

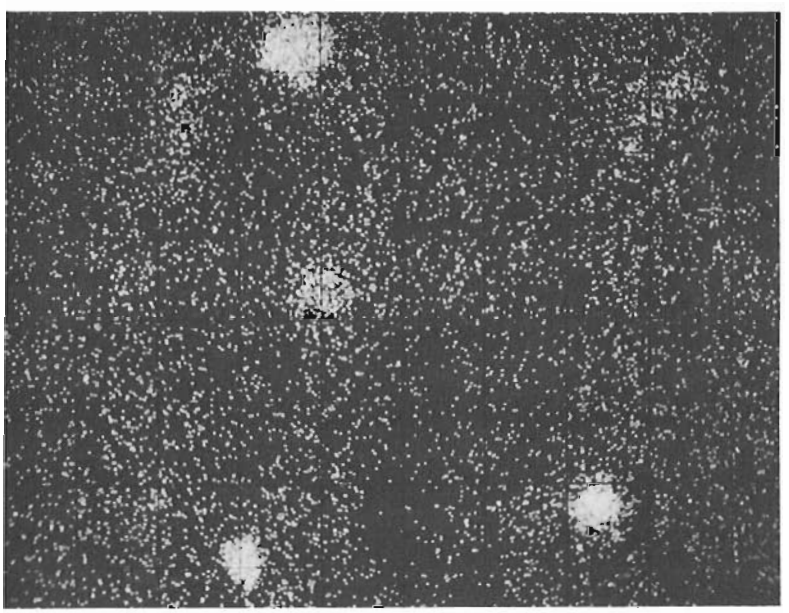

Figure 5.

S K α X-ray scanning photograph showing S distribution in part of sample 7, Horn River Formation. Clusters of points are pyrite. Zn not detected above background level in this sample by probe analysis. Single grid square = 5 x 5 microns; field of photo 50 microns wide.

Discussion and Speculation

Billings *et al.* (1969) reported the occurrence of Zn-rich subsurface brines in Middle Devonian carbonate units about 350 km downdip from the Pine Point orefield. Their calculations suggest that basinal shales of the Mackenzie basin (using Western Canada basin compositional data) should contain amounts of Zn well beyond those necessary to produce the Pine Point orefield, given the passage of metal-bearing brines through the Presqu'ile barrier-complex conduit. Such calculations can be made for shales at other stratigraphic levels in the Western Canada basin. To date, however, the most promising mineralization known occurs in Middle Devonian rocks of the Interior Platform and Rocky Mountains (e.g. Pine Point - Skall, 1975; Robb Lake area - Taylor *et al.*, 1975). Perhaps metal-rich source beds are a necessary prerequisite for mineralization found within marginal settings of carbonate platforms of Pine Point and Robb Lake type (although these two occurrences are very different).

If sediments at the approximate level of the Bituminous Member acted as source beds for Pine Point orefield mineralization, the fact that Zn is abundant whereas Pb is not could point to selective mobilization of Pb from the shales and mudstones, addition of Pb from other sources at Pine Point, or both. High Zn values in the shales and mudstones analyzed (Table 1) suggest that much Zn remains within these rocks. Perhaps, however, the process of mobilization of Zn is an inefficient one, akin to processes of flushing of hydrocarbons from argillaceous source beds (Baker, 1962, quoted in Dott and Reynolds, 1969, p. 196).

Table 1

Compositional data and Zn extractability, Devonian shales and mudstones, Pine Point region

Sample[1] No.	Well	Location	Depth	Stratigraphic Unit	Organic[2] Matter (%)	Cu[3] (ppm)	Zn (total)[4] (ppm)	Zn (acid)[5] (ppm)	%Zn extracted
1	McDermott *et al.* Sulphur Point 0-7	65°57'N; 114°45'W	340 ft.	Bituminous Mbr., Pine Point Fm.	3.6	24	80	24	30
2	"	"	345 ft.	"	6.3	36	208	66	32
4	McDermott *et al.* Hay River I-47	61°01'N; 115°38'W	760 ft.	"	13.7	100	1312	663	51
5	"	"	810 ft.	"	9.9	72	992	600	67
6	"	"	814 ft.	"	11.2	52	1296	650	50
8	Central Del Rio Mills Lake B-75	61°14'N; 117°29'W	1465 ft.	"	12.3	52	640	70	11
9	Central Del Rio Mills Lake A-70	61°09'N; 117°56'W	2101 ft.	"	15.8	72	208	109	52
12	Cities Service Laferte River M-16	61°46'N; 118°34'W	1184 ft.	"	8.5	28	960	575	60
3	McDermott *et al.* Hay River I-47	61°01'N; 115°38'W	740 ft.	Buffalo R. Mbr., Pine Point Fm.	1.9	--	56	19	34
7	Central Del Rio Mills Lake B-75	61°46'N; 118°34'W	1457 ft.	Horn River Fm.	40.8	716	3216	363	11
10	Cities Service Laferte River M-16	61°46'N; 118°34'W	1070 ft.	"	7.0	64	240	134	56
11	"	"	1090 ft.	"	3.7	76	272	113	42

[1]For compositional data, map locations and stratigraphic cross-section, *see* Macqueen and others, 1975. Samples are listed in stratigraphic order within wells which are listed from southeast to northwest; samples are grouped in table according to stratigraphic units.

[2]From Table 1, Macqueen and others, 1975.

[3]Determined by atomic absorption; procedures in Macqueen and others, 1975, Table 2. Accuracy as a percentage of values stated is estimated as ±5%. Analyst R. R. Barefoot, Geochemistry Section, Institute of Sedimentary and Petroleum Geology, Calgary.

[4]From Table 2, Macqueen and others, 1975.

[5]Zn ppm values represent the amount of Zn extracted by heating 200 mg of crushed sample in 40 ml of 4 NHCl in a steaming water bath for 24 hours. This treatment ensures dissolution of all carbonates; however, the values stated are a composite of Zn extracted from carbonates, most of the metallic sulphides, and some of the less well-bound Zn from organic matter. Analyst R. R. Barefoot.

The presence of minor amounts of sphalerite in some of the samples, and the probable presence of tightly bound Zn associated with organic compounds, suggest that these rocks in their present form may not yield Zn or other metals easily to formation fluids under natural conditions, although this requires further study. Recently, Carpenter *et al.* (1974) have attributed anomalously high Zn and Pb values in oil field brines in Mississippi to cross-formational migration of potash-rich fluids expelled from the underlying Upper Jurassic Louann Salt. They suggested that the potash-rich fluids obtain metal ions from clays within shales of the Upper Jurassic Cotton Valley Group. The situation is similar in some respects to that of the Bituminous Member and closely associated stratigraphic units, which also are underlain locally by evaporites of the Chinchaga sequence.

The nature of the organic matter, regional and stratigraphic distribution of metals, and additional data on the precise location of metals, including Zn are yet to be determined for the Middle Devonian shales.

References

Baker, D. R.
1962: Organic Geochemistry of Cherokee Group in southeastern Kansas and northeastern Oklahoma; Bull. Am. Assoc. Pet. Geol., v. 46, p. 1621-1624.

Billings, G. K., Kesler, S. E. and Jackson, S. A.
1969: Relation of zinc-rich formation waters, northern Alberta, to the Pine Point ore deposit; Econ. Geol., v. 64, p. 385-391.

Carpenter, A. B., Trout, M. L. and Pickett, E. E.
1974: Preliminary report on the origin and chemical evolution of lead- and zinc-rich oil field brines in Central Mississippi; Econ. Geol., v. 69, p. 1191-1206.

Dott, R. H., Sr. and Reynolds, M. J. (compilers)
1969: Sourcebook for Petroleum Geology; Am. Assoc. Pet. Geol., Mem. 5.

Macqueen, R. W., Williams, G. K., Barefoot, R. R. and Foscolos, A. E.
1975: Devonian metalliferous shales, Pine Point region, District of Mackenzie; *in* Report of Activities, Part A, April to October 1974, Geol. Surv. Can., Paper 75-1, pt. A, p. 553-556.

Norris, A. W.
1965: Stratigraphy of Middle Devonian and older Paleozoic rocks of the Great Slave Lake region, Northwest Territories; Geol. Surv. Can., Mem. 322.

Skall, H.
1975: The paleoenvironment of the Pine Point lead-zinc district; Econ. Geol., v. 70, p. 22-47.

Taylor, G. C., Macqueen, R. W. and Thompson, R. I.
1975: Facies changes, breccias, and mineralization in Devonian rocks of Rocky Mountains, northeastern British Columbia (94B, G, K, N); *in* Report of Activities, Part A, April to October 1974, Geol. Surv. Can., Paper 75-1, pt. A, p. 577-585.

GEOLOGY OF RARE-EARTH DEPOSITS OF CANADA: A NOTE ON DETECTING RARE-EARTH OCCURRENCES IN CENTRAL AND WESTERN CANADA

Project 670028

E. R. Rose
Regional and Economic Geology Division

A new field method for detecting rare-earth elements, being developed by the writer, was used in 1973/74, and found useful in checking a variety of rock formations and mineral deposits in central and western Canada for rare-earths. The test method will be described in detail in a separate paper to be issued shortly. It consists essentially of dissolving a small powdered sample of rock, mineral or other material, in a small amount of concentrated hydrochloric acid (HCl) or nitric acid (HNO_3), and bringing a small drop of the resulting acid solution into contact with a piece of Arsenazo III paper[1]. The violet coloured Arsenazo III paper will quickly turn green in the presence of any or all of the rare-earth elements, and also in the presence of uranium, thorium and to some extent scandium, in solution with concentrations of 0.5% or more rare-earth elements.

Numerous occurrences of rare-earth minerals are recorded in the Precambrian Shield area of central Canada, but in the large, geologically younger, region of Canada west of the Canadian Shield, only a handful of occurrences have been reported. By means of the test described above, traces of rare elements were indicated in a number of rock formations and mineral deposits, in central and western Canada, in which they were previously unknown. All of these occurrences probably carry less than 0.5% rare-earth elements, and none are likely to be of economic importance in that regard, but, when verified by more precise analytical methods they will add a measure to knowledge of the distribution and nature of rare-earth elements in these regions.

[1] Arsenazo III paper, prepared as described in detail in a forthcoming report indicated above.

15. IMPORTANT CHARACTERISTICS OF SOME CANADIAN CORDILLERA PORPHYRY DEPOSITS

Project 750033

A. E. Soregaroli
Regional and Economic Geology Division

Detailed studies of several Canadian Cordillera porphyry deposits have established the multistage relationship between igneous activity, fracturing (breccias, veins, faults), mineralization and alteration. Mineralization within these deposits is predominantly fracture-controlled and, by careful recording of cross-cutting relations, the age of each stage relative to other stages has been documented. Each stage of mineralization occupies or is related to unique sets of fractures, has a unique mineralogy, is accompanied by the development of specific alteration assemblages as envelopes in vein walls, and has a unique spatial distribution. The "stockworks" of many porphyry deposits on closer scrutiny can be seen to consist of several superimposed stages of mineralization and alteration. All stages of mineralization are not uniformly distributed throughout a deposit. Some stages are limited to one part of the deposit, and thus indicate variable distribution in space as well as time. Relative ages in such deposits are established in areas where stages overlap.

Figures 1 and 2 are schematic diagrams representing different stages of hypogene mineralization and alteration that have been identified in some British Columbia porphyry deposits. Although there are some apparent correlations between stages from the different deposits, the figures are not designed to indicate equivalence in time or duration of stages between different deposits. Stages merely represent relative ages as reported at each deposit.

For the sake of simplicity the only sulphides shown in Figures 1 and 2 are pyrite (Py), chalcopyrite (Cpy-includes bornite) and molybdenite (Mo). Quartz is the most abundant vein mineral in many deposits. Other minerals, such as magnetite, galena, sphalerite, scheelite, etc., may be present in significant amounts but

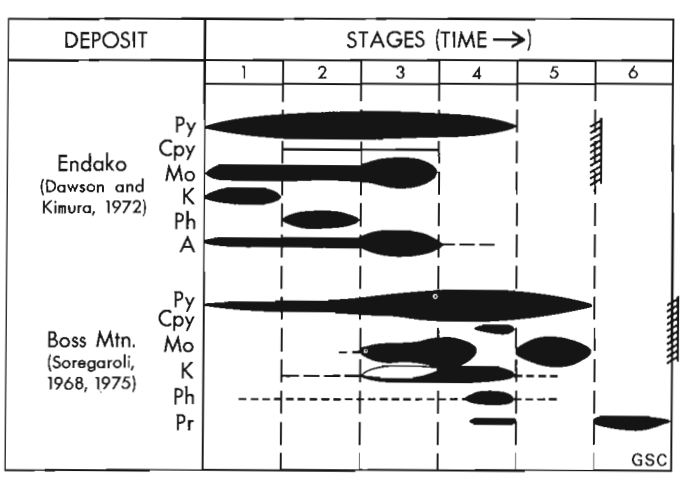

Figure 1. Stages of hypogene mineralization and alteration; Mo deposits.

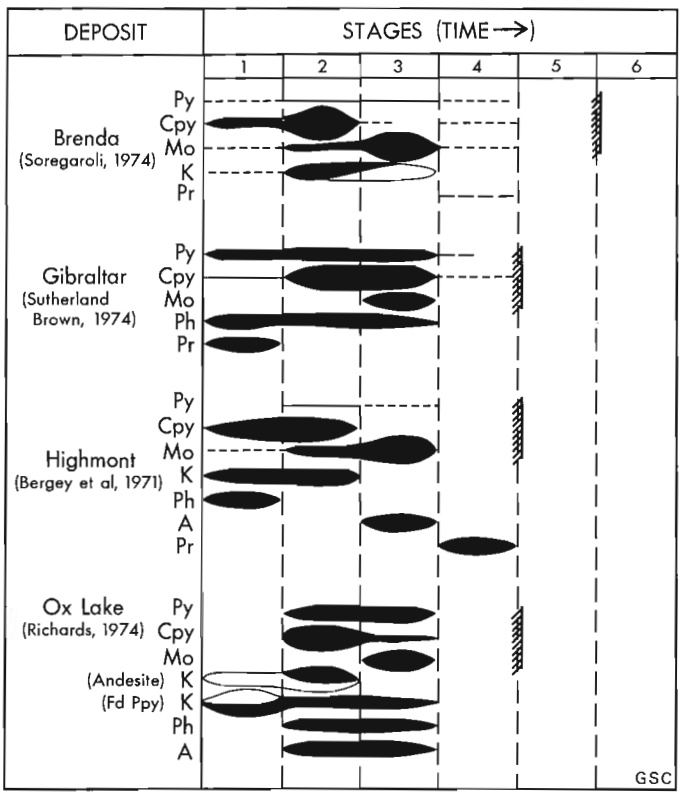

Figure 2. Stages of hypogene mineralization and alteration; Cu-Mo deposits.

are not included in the figures. In the figures the relative volume of mineralization and alteration at each stage is represented by the thickness of the symbol. Hachure marks on the right signify the end of the mineralizing event.

Alteration has been correlated with specific stages of mineralization and is shown as potassic (K), phyllic (Ph), argillic (A), and propylitic (Pr). Potassic alteration includes both biotite and potash feldspar. Biotite is represented by an open symbol (white) which distinguishes it from potash feldspar (black). Phyllic alteration as used here denotes the presence of sericite. Argillic is equated to clays and/or poorly ordered micas and propylitic alteration merely indicates the presence of chlorite, epidote, zoisite, albite, and/or carbonate.

These standard alteration terms are not entirely satisfactory for some alteration assemblages, but are used to keep figures simple. Detailed listing of alteration minerals and compositions of host rocks would be much more meaningful, but this is beyond the scope of this article.

Porphyry Molybdenum Deposits

Only two porphyry molybdenum deposits, Endako (Dawson and Kimura, 1972) and Boss Mountain (Soregaroli, 1968, 1975) have published data available which define the stages of mineralization and alteration. Detailed studies of other deposits, such as Hudson Bay Mountain (Kirkham (1967) and Jonson *et al.* (1968)), have recorded evidence of multistage development in the form of cross-cutting veins and intermineral intrusions, but have not established a relationship to alteration.

The multistage development of molybdenum deposits has been established at many deposits and the degree of complexity is considered by some as a critical parameter in the evaluation of prospects. Wallace *et al.* (1968) lucidly portrayed the sequential development of the Climax orebodies and drew attention to the importance of intermineral dykes and the close genetic ties of mineralization and intrusive activity. In British Columbia similar relationships were established at Boss Mountain (Soregaroli, 1968, 1975), Endako (Drummond and Kimura, 1969; Dawson and Kimura, 1972), Hudson Bay Mountain (Kirkham, 1967; Jonson *et al.*, 1968), and B.C. Molybdenum (Giles, 1975), but the details of sequential stages of mineralization with concommitant alteration are recorded only for the Boss Mountain and Endako. Intermineral intrusions and breccias have also been reported at British Columbia porphyry copper deposits by Kirkham (1972) and Carter (1974).

There are few similarities between the sequential evolution at Endako and Boss Mountain. Endako shows a 3-stage history of molybdenum introduction. Chalcopyrite, which is only of mineralogic interest, accompanies molybdenite in stages 2 and 3. Pyrite is ubiquitous in all stages, except the latest barren stage (5). No single type of alteration can be correlated as most significantly related to molybdenite. Argillic alteration persists through all stages of molybdenite introduction, but is only of major importance during stage 3, the most important period of molybdenite introduction.

Boss Mountain deposit appears somewhat more complex in that a "barren" (no molybdenum), intermineral stage is recorded between molybdenum-producing stages. Potassic alteration (both biotite and potash feldspar), as well as sericite show important genetic and spatial relationship to molybdenite. Stages 1 through 4 are considered as the first phase of mineralization which is directly related to a Cretaceous quartz monzonite intrusion, the Boss Mountain Stock. Stage 5 is interpreted as the initial stage of mineralization related to a second intrusive source, either a differentiate of the Boss Mountain Stock or a second intrusion. Intrusive activity, brecciation, veining, mineralization, and alteration form a complex, overlapping sequence of events in the deposits (Soregaroli, 1975).

Porphyry Copper - Molybdenum Deposits

Multistage development of veins and alteration have been established at four British Columbia porphyry copper-molybdenum deposits; Brenda, Gibraltar, Highmont and Ox Lake (Fig. 2). Brenda (Soregaroli, 1974) and Gibraltar (Sutherland Brown, 1974; Drummond *et al.*, 1973) deposits were developed in a single intrusive host rock of intermediate composition in which almost all hypogene mineralization is fracture controlled (veins). These features have permitted recognition of cross-cutting relations and identification of alteration envelopes with a minimum of difficulty. Early studies at Gibraltar by Drummond *et al.* (1973), which were based on drill core and supergene zone studies, were slightly modified by Sutherland Brown (1974) when hypogene mineralization was exposed in the pit. Such exposures permitted better definition of alteration assemblages related to each stage of mineralization.

The Highmont deposits were for the most part formed in one phase (quartz diorite) of the Guichon Creek Batholith, but some mineralization also occurs in a granodiorite phase (Bergey *et al.*, 1971). The prominent fracture control of mineralization and veins with prominent alteration envelopes again have permitted identification of several discrete stages of mineralization.

Perhaps of most significance is the documentation by Richards (1974) of the simultaneous development of two distinct alteration assemblages in two different host rocks (andesite and feldspar porphyry (rhyodacite)). Potassic alteration accompanied stage 1 (biotite) and stage 2 (potash feldspar and biotite) veins in andesite. In the feldspar porphyry, stage 1 is predominantly biotite with lesser amounts of potash feldspar, but in stage 2 potash feldspar is accompanied by phyllic and propylitic assemblages.

Observations and Interpretations

Although the available data are limited, a few generalizations are suggested.

1. Porphyry copper and molybdenum deposits are formed by multistage events which relate intrusive activity to fracturing, sulphide mineralization, and alteration. It is suggested that in order to achieve an economic concentration of ore minerals, the overlap of several stages of mineralization are necessary. One stage can be dominant, as in the Brenda deposit, but the lesser contributions by other stages are necessary to achieve economic grades.
2. There are changes in mineralogy ("ore" and alteration) with each successive stage. This can be explained in several ways, but there are two main alternatives: a) a systematic evolutionary change in the composition of the hydrothermal fluids at their sources combined with changes resulting from reactions with wall-rocks (preferred by the author) or b) a constant, uniform composition of the hydrothermal solution at the source, combined with progressive change in physical and chemical conditions in the wall-rocks resulting in different mineralogy at each stage.
3. Each system is a little different in detail, but there are some general similarities.

a. In porphyry copper-molybdenum deposits (Fig. 2) the bulk of the copper is deposited before the bulk of the molybdenum. Molybdenite is late in the mineralizing event at Island Copper (Cargill, 1975), Ingerbelle (Macauley, 1973) and at Valley Copper (Osatenko, pers. comm.) and the author has observed molybdenite-bearing quartz veins and "slips" which cut chalcopyrite-bearing veins at Bethlehem, Lornex, Bell Copper, Granisle, Dorothy, Okeover, Corrigan Creek, and several other British Columbia prospects.

b. Sulphide mineralization and alteration generally are limited in initial stages, become progressively more intense and then gradually or in some cases abruptly diminish with time. Most copper and molybdenum are deposited in two or three stages which follow an initial weak stage and in many deposits are followed by a late barren or weakly mineralized stage.

4. If we recognize that each successive stage is superimposed upon preceding stages and each stage occupies unique sets of fractures which are developed in response to structural adjustments within a changing stress field, then each successive stage can be spatially displaced from, but typically overlaps, the area of preceding stages. This displacement can cause eccentricity in the resulting deposit and need not result in concentric zoning around a single core area as suggested by some modern models (Lowell and Guilbert, 1970; Sillitoe, 1973).

5. The attitudes of the veins representing the various stages of mineralization in the deposits are not shown here, but are detailed in the references on individual deposits. Examination of their attitudes by the author, combined with the various author's interpretations on development, suggest the following:

a. Mineralization within porphyry deposits related to stocks, plugs and dykes (the Phallic and Volcanic porphyries of Sutherland Brown, 1972) is introduced into fractures created by intrusive and hydrothermal activity related to emplacement of a specific intrusive body and to a far lesser extent into pre-porphyry fractures derived from older regional tectonic activity. Ox Lake (Richards, 1974) and Boss Mountain (Soregaroli, 1968) are examples.

b. Mineralization within porphyry deposits in batholithic masses (the Plutonic porphyries of Sutherland Brown, 1972) is introduced into fractures created by intrusive and hydrothermal activity related to some specific intrusive event in the related intrusion and by contemporaneous regional tectonic activity. Various forms of compressional regional tectonics have been invoked to explain fracture development in deposits in batholithic masses, such as at Endako (Dawson and Kimura, 1972), Brenda (Soregaroli, 1974) and Gibraltar (Drummond *et al.*, 1973; Sutherland Brown, 1974).

A better framework is required for understanding the genesis and evolutionary history of hydrothermal systems related to porphyry deposits. Further detailed studies, such as those summarized in this paper, will help establish this framework.

Much more detailed information is required concerning the major and trace element geochemistry of each stage of mineralization. Logically, the trace element content of pyrite or any other mineral should be unique for each stage of mineralization. Collection of samples for geochemical studies without recognition that more than one age is present, could result in mixing of several unique pyrites (or other mineral) from different stages and cause erroneous or confusing results.

References

Bergey, W.R., Carr, J.M. and Reed, A.J.
1971: The Highmont copper-molybdenum deposits, Highland Valley, British Columbia; Can. Inst. Min. Met. Bull., v. 64, p. 68-76.

Cargill, D.G.
1975: Geology of Island Copper Mine, Port Hardy, British Columbia; unpubl. Ph.D. thesis, Univ. Brit. Columbia.

Carter, N.C.
1974: Geology and geochronology of porphyry copper and molybdenum deposits - West-central British Columbia; unpubl. Ph.D. thesis, Univ. Brit. Columbia.

Dawson, K.M. and Kimura, E.T.
1972: Endako; *in* Copper and molybdenum deposits in the Western Cordillera; 24th Int. Geol. Cong., Guidebook, Field Excursion A09-C09, p. 36-48.

Drummond, A.D. and Kimura, E.T.
1969: Hydrothermal alteration at Endako - A comparison to experimental studies; Can. Inst. Min. Met. Bull., v. 62, p. 709-714.

Drummond, A.D., Tennant, S.J. and Young, R.W.
1973: The interrelationship of regional metamorphism, hydrothermal alteration and mineralization at the Gibraltar Mines copper deposit in British Columbia; Can. Inst. Min. Met. Bull., v. 66, p. 48-55.

Giles, D.L. and Livingston, D.E.
1975: Geology and isotope geochemistry of the Lime Creek MoS_2 orebody, Alice Arm, B.C.; AIME Ann. Mtg., preprint 75-S-72.

Jonson, D.C., Davidson, D.A. and Daughtry, K.L.
1968: Geology of Hudson Bay Mountain molybdenum deposit, Smithers, B.C.; preprint, Can. Inst. Min. Met., Ann. Mtg., Vancouver, B.C.

Kirkham, R.V.
1967: Glacier Gulch; B.C. Min. Mines Ann. Rept., 1966, p. 86-90.

1972: Intermineral intrusions and their bearing on the origin of porphyry copper and molybdenum deposits; Econ. Geol., v. 66, p. 1244-1249.

Lowell, J. D. and Guilbert, J. M.
1970: Lateral and vertical alteration zoning in porphyry ore deposits; Econ. Geol., v. 65, p. 373-408.

Macauley, T. N.
1973: Geology of the Ingerbelle and Copper Mountain deposits at Princeton, British Columbia; Can. Inst. Min. Met. Bull., v. 66, p. 105-112.

Oriel, W. W.
1972: Detailed bedrock geology of the Brenda copper-molybdenum mine, Peachland, B. C.; unpubl. M. Sc. thesis, Univ. Brit. Columbia.

Richards, G. G.
1974: Geology of the Ox Lake Cu-Mo porphyry deposit; unpubl. M. Sc. thesis, Univ. Brit. Columbia.

Sillitoe, R. H.
1973: The tops and bottoms of porphyry copper deposits; Econ. Geol., v. 68, p. 799-815.

Soregaroli, A. E.
1968: Geology of the Boss Mountain Mine, British Columbia; unpubl. Ph. D. thesis, Univ. Brit. Columbia.

1974: Geology of the Brenda copper-molybdenum deposit in British Columbia; Can. Inst. Min. Met. Bull., v. 67, p. 76-83.

1975: Geology and genesis of the Boss Mountain molybdenum deposit, British Columbia; Econ. Geol., v. 70, no. 1, p. 4-14.

Sutherland Brown, A.
1972: Morphology and classification of porphyry deposits in the Canadian Cordillera (abst.); Proceedings, Western Inter-University Geol. Conf., Vancouver.

1974: Gibraltar; GEM, 1973, B. C. Dept. Mines Pet. Resour., p. 299-318.

16. X-RAY POWDER PATTERN RECOGNITION BY MINICOMPUTER

Project 680023

M. Bonardi and R. J. Traill
Central Laboratories and Administrative Services Division

The identification of crystalline substances by X-ray powder diffraction is based on the fact that every crystalline substance gives a characteristic X-ray pattern consisting of a set of arcs (lines) whose measured spacings (d-spacings) and relative intensities are the identification criteria. The identification is made by visually comparing the film with a file of reference films of known compounds, or by comparing its measured d-spacings and estimated relative intensities with those of a standard pattern. Patterns of the more common minerals can be easily identified by an experienced analyst by direct observation of the film. Complex and less common patterns however may require careful measurements and a long and tedious search through reference data in cards or books. In order to eliminate the time-consuming manual search, we have created a magnetic tape file of our reference data for the identification of minerals, and written a computer program to search and compare the data with those of an unknown pattern. The program is written in Fortran II, for use with a Hewlett Packard minicomputer.

A print out of part of the magnetic tape file is shown in Table 1. The file may be extended and updated at any time, and initially it contains data for 901 minerals. For each reference pattern, the d-spacings and relative intensities of the five strongest lines are recorded along with an abbreviated mineral name and catalogue number. The abbreviated mineral names, for the most part, are those used in Index Alphabétique de Nomenclature Minéralogique published by the Bureau de Recherches Géologiques et Minières, Paris, in 1968. The catalogue number refers to data given in Geological Survey of Canada Paper 75-8, A Catalogue of X-ray Powder Patterns and Specimen Mounts on file at the Geological Survey of Canada, which lists the minerals used to prepare the standard patterns, and gives literature references to more precise and complete X-ray data. The standard patterns were obtained using nickel-filtered copper radiation and a 57.3 mm diameter Debye-Scherrer camera. The measured d-spacings have not been corrected for film shrinkage or expansion, and the relative intensities were estimated visually.

The search program, listed in Table 2, permits recognition of X-ray powder patterns, based on input of measured d-spacings of the five strongest lines on the pattern. In our service laboratory, X-ray mounts are prepared routinely from mineral grains examined under a microscope and as a result of this procedure more than 80 per cent of the patterns we examine are of single phase minerals. Preliminary identification of many of these patterns can be made from measured d-spacings of only two or three of the strongest lines. In the case of mixtures, however, more lines must be measured. To perform a search, the user must input the following information:

K,	the number of standard patterns to be searched,
MNF,	the minimum number of matches required for an identification,
U(1) to U(5),	d-spacings of the five strongest lines of the unknown pattern,
TOL,	the amount of tolerance permitted in matching d-spacings.

TABLE 1

d	I/Io	d	I/Io	d	I/Io	d	I/Io	d	I/Io	Min.Name	Catalogue No.
3.08	7	2.84	7	2.59	10	2.44	9	2.37	9	ACANTH	1
4.90	9	2.99	9	2.70	8	2.46	10	1.62	9	ADAMIT	2
7.90	7	3.14	9	2.71	9	2.56	10	2.13	8	AENIGM	3
4.04	10	3.69	3	3.23	7	2.73	7	2.13	5	AERINI	4
3.19	9	2.84	10	2.72	9	2.15	7	1.93	7	AFWILL	5
3.66	10	3.19	9	2.87	9	1.96	4	1.76	3	AIKINI	6
6.18	9	4.11	9	3.09	10	2.94	7	2.81	9	AJOITE	7
4.23	4	3.71	4	3.09	4	2.87	10	1.76	5	AKERMA	8
3.01	2	2.61	10	1.84	9	1.50	3	1.30	1	ALABAN	9
2.25	3	2.12	4	1.99	10	1.55	1	1.31	1	ALGODO	10
3.71	9	3.27	7	3.05	10	2.91	6	2.51	7	ALLACT	11
3.56	6	2.94	10	2.72	5	2.63	5	1.65	5	ALLANI	12
3.26	6	3.15	7	2.87	8	2.61	7	1.81	10	ALLEGH	13
3.58	4	2.91	10	2.76	6	2.13	5	1.28	5	ALLEMO	14

TABLE 2

```
FTN,B
      PROGRAM XFILE
      DIMENSION S(5),U(5)
    2 WRITE(2,10)
   10 FORMAT("PROG. FOR X-RAY MIN.IDENT.,INPUT K=NO.OF STANDARDS  *")
      CALLPTAPE(7,2,0)
      READ(1,*)K
   13 WRITE(2,40)
   40 FORMAT("INPUT MNF,U(1),U(2),U(3),U(4),U(5),TOL    *")
      READ(1,*)MNF,U(1),U(2),U(3),U(4),U(5),TOL
      WRITE(2,30)
   30 FORMAT(/"NFIT",X,5(2X,"D",4X,"I",2X)3X,"MIN.",8X,"NO",/)
      TOL=TOL+(.005)
      DO 29 JN=1,K
      READ(7,20)S(1),INT1,S(2),INT2,S(3),INT3,S(4),INT4,S(5),INT5,
     1NA,NB,NC,MIN
   20 FORMAT(5(F5.2,X,I2,2X)3X,A2,A2,A2,4X,I5)
      NFIT=0
      DO 9 I=1,5
      DO 19 J=1,5
      DEL=U(I)-S(J)
      IF(DEL)21,23,23
   21 DEL=DEL*(-1.)
   23 IF(DEL-TOL)25,25,19
   25 NFIT=NFIT+1
   19 CONTINUE
    9 CONTINUE
      IF(NFIT-MNF)29,28
   28 WRITE(2,70)NFIT,S(1),INT1,S(2),INT2,S(3),INT3,S(4),INT4,
     1S(5),INT5,NA,NB,NC,MIN
   70 FORMAT(X,I2,2X,5(F5.2,X,I2,2X)3X,A2,A2,A2,3X,I5)
   29 CONTINUE
      WRITE(2,80)
   80 FORMAT(/"SEARCH COMPLETED"/)
      REWIND 7
      GO TO 2
      END
      END$
```

K was introduced to allow for partial searches of the reference data and to permit additions to the file. The value chosen for MNF affects the number of possible identifications made by the search. If MNF = 5, the output is restricted to only those patterns for which the d-spacings of all 5 lines match those of the unknown, within the chosen tolerance. If MNF = 3, the output will list all patterns for which 3 or more lines are in agreement. A TOL value of .02 means that the d-spacing of the standard and the unknown will be considered to be in agreement if they match to within ±0.02 angstrom units. A value of .02 is generally suitable, but TOL may need to be increased to .03 or .04 when attempting to match a pattern with broad lines or large d-spacing values. Changes in output as a result of varying MNF and TOL are illustrated in Table 3. The first column, NFIT, indicates the number of lines of the standard pattern that agree with lines in the unknown. The five strongest lines used as input were 6.92, 3.48, 2.42, 2.70, 2.62, and the mineral was subsequently identified as posnjakite, POSNJA. If the search fails to find enough matching lines to meet the MNF criterion, the program will write only "SEARCH COMPLETED". Patterns listed as output by the search program must be compared visually with the unknown in order to ensure a positive identification. The visual comparison will reveal any extra lines in the unknown pattern that may be due to the presence of other minerals. The d-spacings of the extra lines may then be measured and used as input for further searches to identify additional phases present.

TABLE 3

```
PROG. FOR X-RAY MIN.IDENT.,INPUT K=NO.OF STANDARDS  *
901
INPUT MNF,U(1),U(2),U(3),U(4),U(5),TOL   *
5 6.92 3.48 2.42 2.70 2.62 .02           X-47657

NFIT   D    I    D    I    D    I    D    I    D    I     MIN.          NO

  5   6.92 10   3.47  6   2.68  3   2.60  2   2.42  4     POSNJA        653

SEARCH COMPLETED


INPUT MNF,U(1),U(2),U(3),U(4),U(5),TOL   *
3 6.92 3.48 2.42 2.70 2.62 .02           X-47657

NFIT   D    I    D    I    D    I    D    I    D    I     MIN.          NO

  3   3.46  5   2.81 10   2.71  6   2.64  3   1.95  4     APATIT         37
  3   4.02  5   2.90 10   2.68  7   2.60  5   2.40  5     EPIDOT        279
  3   3.50  9   3.02  2   2.86 10   2.72  8   2.42  2     GRAFTO        362
  5   6.92 10   3.47  6   2.68  3   2.60  2   2.42  4     POSNJA        653

SEARCH COMPLETED


INPUT MNF,U(1),U(2),U(3),U(4),U(5),TOL   *
3 6.92 3.48 2.42 2.70 2.62 .03           X-47657

NFIT   D    I    D    I    D    I    D    I    D    I     MIN.          NO

  3   3.46  5   2.81 10   2.71  6   2.64  3   1.95  4     APATIT         37
  3   4.02  5   2.90 10   2.68  7   2.60  5   2.40  5     EPIDOT        279
  3   3.50  9   3.02  2   2.86 10   2.72  8   2.42  2     GRAFTO        362
  3   3.45  6   2.71 10   2.41  4   2.33  4   1.76  7     MARCAS        510
  3   4.27  6   3.20 10   2.73  7   2.65  4   2.41  4     PFERRI        633
  5   6.92 10   3.47  6   2.68  3   2.60  2   2.42  4     POSNJA        653
  3   4.49 10   3.46  6   2.43  7   2.39  7   2.32  6     PSMALA        661

SEARCH COMPLETED
```

17.

CLAY MINERAL VARIATIONS IN THE BELL COPPER PORPHYRY COPPER DEPOSIT, BABINE LAKE AREA, B.C.

Project 700041

J.L. Jambor[1] and R.N. Delabio[2]

Unlike most porphyry copper deposits in the southwestern United States and other parts of the world, deposits of this type in Canada show little evidence of significant oxidation and supergene enrichment. Although the potentially productive Casino deposit in Yukon Territory, is an exception in that it has an economically important blanket of supergene chalcocite, the development of all Canadian deposits producing currently has been dependent on their grades of hypogene copper sulphides. The Bell Copper deposit in the Babine Lake area of northern British Columbia (Fig. 1) is no exception to this rule, but the upper part of the deposit does have a significant oxidized zone in which supergene chalcocite is not only present, but is sufficiently abundant to be of economic importance. Within the mine pit, the lowest benches have now reached the apparent megascopic bottom of the oxidation profile, which is marked by the cessation of occurrences of dark brown iron oxides. The optimum pit outline is enclosed by the 2500- to 2550-foot contours at surface; as the depth of overburden is about 30 feet, the lower limit of iron oxidation as exposed along the face of the 2340 bench is thus about 150 feet below the original bedrock surface.

A study of oxidized samples from the pit, and of samples from deep diamond-drill holes below the pit, is in progress in order to determine the mineralogy of the oxide zone and to establish the depth limits of supergene effects. That the latter has been a matter of some debate is attributable in large part to the presence at Bell Copper of very strong quartz-sericite alteration within major portions of the 0.3% Cu zone. The position and intensity of this alteration, unique amongst the Babine deposits, are apparently megascopically similar to those of clayey materials in the oxidized parts of non-Canadian deposits. However, the alteration at Bell Copper has been interpreted by Carson and Jambor (1974) as being a primary, hydrothermal effect that was superimposed on a pre-existing, partly obliterated zone of hydrothermal biotitization. Thus, in addition to the study of the supergene effects mentioned above, the clay mineralogy of samples from outside the 0.3% Cu zone was also examined.

Procedures

Hand specimens from the pit and pieces of drill core were crushed to -200 mesh, and 2 grams of each sample were mixed with a 5 g/l sodium metaphosphate solution in 100 ml Nalgene centrifuge tubes. Residues from the third and fourth centrifuge runs were combined, and small amounts dispersed on glass slides and allowed to dry at room temperature. For each of the 80 samples studied, X-ray diffraction patterns were obtained from an air-dried mount, a glycerated mount, and a mount heated at 600°C for 15 minutes. Charts were recorded with an XRD-G.E. diffractometer using Cu radiation at 45 kv and 16 ma, and a scan rate of 2 degrees 2θ per minute for the 2θ range 2½ to 35°.

Differences in the ratios of clays present in each sample were obtained by measurement of the net peak heights of (001) diffraction lines. For air-dried samples, chlorite, illite, and [kaolinite (001) + chlorite (002)] were measured at approximately 6.2, 8.1, and 12.4° 2θ, respectively. Where chlorite was present, its (001) and (002) lines were assigned equal intensities; to obtain kaolinite (001), the combined peak of [kaolinite (001) + chlorite (002)] was reduced by an amount equal to chlorite (001). For montmorillonite abundances, the (001) peak was measured at about 4.9° 2θ for glycerated material. When montmorillonite was detected, all clay ratios were determined from the glycerated slide.

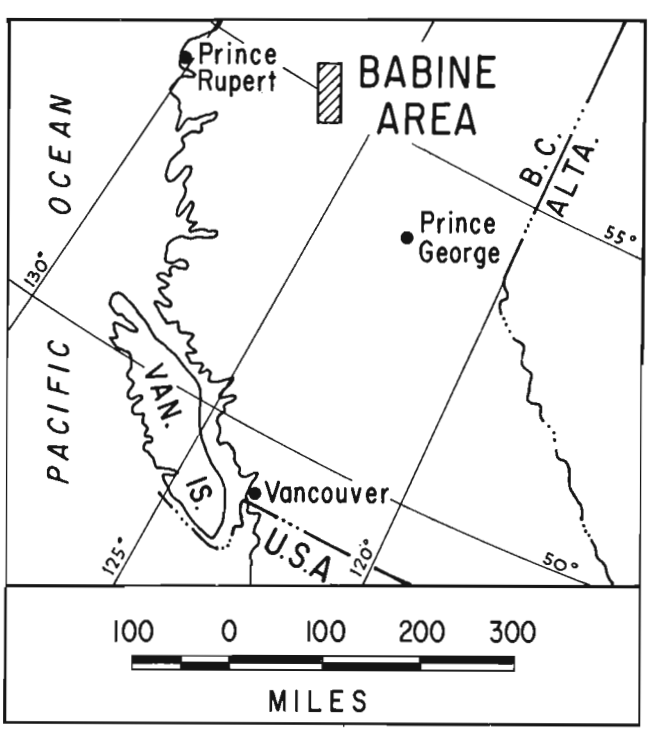

Figure 1. Location of the Babine Lake area, British Columbia.

[1] J.L. Jambor, Regional and Economic Geology Division.

[2] R.N. Delabio, Central Laboratories and Administrative Services Division.

Table 1

Results of X-ray diffraction analyses of clay mineral fraction of Bell Copper samples, excluding those shown in cross-section Figure 2.

Sample No. & Footage	Clay Mineral Ratios			
	Illite	Kaolinite	Montmorillonite	Chlorite
N 208-343'	37	63		
N 209- 92'	35	65		
N 220- 91'	36	64		
-130'	57	43		
-165'	40	60		
N 219-200'	55	41		4
N 221- 78'	66	34		
-200'	65	35		
F- 4-13'	56	44		
F-13-19'	100			
F-14-13'	100			
F-16-12'	63	37		
F-17- 7'	100			
N 70- 72'	100			
-652'	78	22		
N 158-562'	52	48		
N 170-553'	26	74		
N 172-599'	15	55	30	
N 18-1405'	36	39	25	
Pit Samples				
N 874	100			
N 875	100			
N 876	100			
N 877	100			
2340-1-1	81	19		
-2	66	34		
-3	52	48		
2340-2-2	100			
-4	68	32		
2340-3-1	100			
-2	100			
N 74-8	58	42		

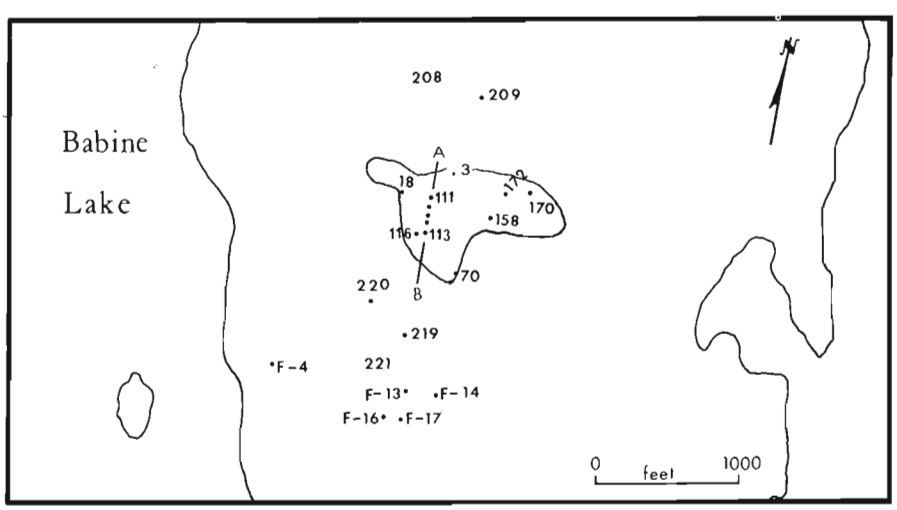

Figure 2.

Distribution of Bell Copper samples examined for clay mineral content. Additional samples from within the 0.3% Cu zone are listed in Table 1 and shown in the A-B cross-section of Figure 3.

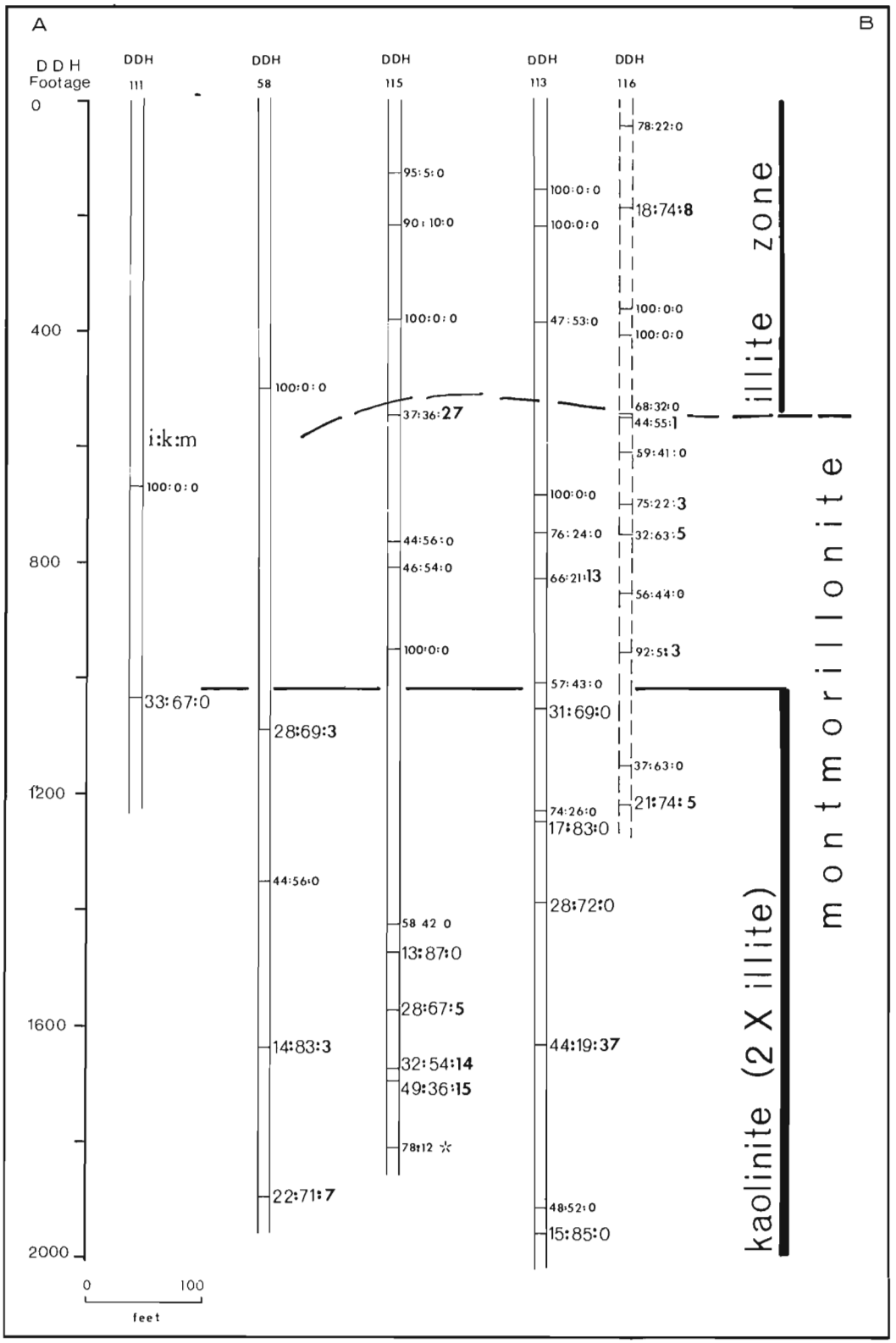

Figure 3. Results of clay mineral X-ray analyses in vertical drill holes 111 to 113 (section A-B, Fig. 2, with DDH 116 added). The lowermost zone contains most of the samples in which kaolinite exceeds illite by more than 2X.

*sample contains 10% chlorite.

Results

The locations of the drill core samples are shown in Figure 2. A part of the results is listed in Table 1, and the remainder is shown in cross-section Figure 3. The data may be summarized as follows:

(1) Samples outside the 0.3% Cu zone contain illite, or illite plus kaolinite, but no montmorillonite. The ratio of illite to kaolinite is variable and no simple pattern is evident.

(2) Not only do all samples containing montmorillonite occur within the 0.3% Cu zone, but of the 17 occurrences, 16 are at depths exceeding 540 feet, regardless of horizontal position within the copper zone.

(3) The proportion of kaolinite in the clay fraction shows a well-defined increase with depth (Fig. 3) - 12 of the 14 samples in which the ratio of kaolinite: illite = >2 lie at depths greater than 1000 feet.

The above results suggest strongly that kaolinite and montmorillonite are part of the hydrothermal alteration assemblage, and that their varying proportions may be a sensitive indicator of vertical zonation in the Bell Copper deposit. The possibility that sulphides also have a systematic vertical variation is being studied in a suite of polished sections comparable to the samples shown in Figure 3.

Reference

Carson, D.J.T. and Jambor, J.L.
1974: Mineralogy, zonal relationships and economic significance of hydrothermal alteration at porphyry copper deposits, Babine Lake area, British Columbia; Can. Inst. Min. Met. Bull., v. 67, p. 110-133.

Project 700041

J. L. Jambor
Regional and Economic Geology Division

Meneghinite, $Cu_2S \cdot 26PbS \cdot 7Sb_2S_3$, is a relatively common sulphosalt that in natural occurrences has been found always to contain small amounts of copper, theoretically 1.45 weight per cent. Although Palache *et al.* (1947) attributed the copper to impurities and suggested that meneghinite is $Pb_{13}Sb_7S_{23}$, a crystal structure study of the mineral by Euler and Hellner (1960) showed that Cu was bound within the structure. Indications that the element might be necessary to stabilize the structure were also found in the study of the Pb-Sb-Cu-S system by Hoda and Chang (1974), who reported that meneghinite has an elongate region of solid solution, the two ends corresponding to $Cu_2S \cdot 26PbS \cdot 7Sb_2S_3$ and $1 \cdot 1\ Cu_2S \cdot 4.6PbS \cdot 4.3Sb_2S_3$. Thus the role of copper in meneghinite could be construed as being similar to the role of the 2.71 weight per cent Fe essential in jamesonite, $Pb_4FeSb_6S_{14}$.

Despite the above evidence, Wang (1973) reported that crystals grown from the original synthetic Phase II of Salanci and Moh (1970) gave X-ray powder diffraction patterns differing from those of the starting material, but corresponding to the pattern of meneghinite. Although Wang did not publish powder diffraction data for the crystals, he reported that they have a unit cell equal to the subcell of meneghinite. According to Euler and Hellner (1968), the unit cell of natural meneghinite is $a = 11.363$, $b = 24.057$, $c = 24 \times 4.128$Å, space group $Pn2_1m$, and the subcell is a, b, $c = 4.128$Å, space group $Pbnm$.

In order to add new data points to the density determinative curve for lead sulphantimonides (Jambor, 1967), synthesis of $2PbS \cdot Sb_2S_3$ was attempted. This composition is close to Garvin's (1973) Phase IV, and is the formula reported for Wang's (1973) Phase IV, which is a different compound. Wang's Phase IV is apparently identical to Phase II of Craig *et al.* (1973), but Phase II is reported to be $3PbS \cdot 2Sb_2S_3$ whereas Wang gave his formula as $2PbS \cdot Sb_2S_3$. As outlined below, two attempts to obtain a 2:1 compound gave heterogeneous products, one of the phases being Wang's (1973) copper-free meneghinite. Although the phase was present as abundant acicular crystals having a maximum length of 4 mm, a grain mount of several crystals showed that all were composite, parallel growths. Zero-level precession photographs of several grains also gave multiple-crystal diffraction effects, but the magnitudes of the cell dimensions were appropriate for the subcell of meneghinite.

New X-ray powder diffraction data obtained for meneghinite from Bottino, Tuscany (National Mineral Collection) were indexed with the subcell parameters, and the results were used for comparative indexing of the copper-free phase (Table 1). Cell volumes obtained from the calculated cell dimensions are $1109A^3$ for the synthetic phase, and $1123A^3$ for the natural material.

TABLE 1. *X*-RAY POWDER DIFFRACTION DATA FOR MENEGHINITE (BOTTINO, TUSCANY) AND FOR THE SYNTHETIC COPPER-FREE PHASE

	meneghinite			Cu-free synthetic phase		
hkl	d_{meas} Å	d_{calc} Å	I_{est}	d_{meas} Å	d_{calc} Å	I_{est}
100*				11.2	11.3	½
120	8.2	8.24	<½	8.3	8.24	<½
-	7.5		<<½			
-	7.0		<<½			
130	6.53	6.54	1	6.54	6.53	2
040	6.05	6.01	<½	6.02	5.99	<½
200	5.68	5.67	<½	5.66	5.67	<½
140	5.32	5.31	<½	5.30	5.30	<½
220	5.14	5.12	<½	5.13	5.13	1
150	4.42	4.42	1	4.42	4.42	½
240	4.13	4.12	5	4.13	4.12	5
060				3.98	4.00	<½
101	3.88	3.88	½	3.85	3.84	½
310	3.740	3.731	8	3.742	3.734	8
121	3.681	3.690	2	3.666	3.657	6
320	3.599	3.602	1	3.610	3.605	<½
131	3.489	3.490	6	3.462	3.461	7
330	3.411	3.416	½			
170	3.274	3.284	10	3.280	3.278	10
141				3.233	3.233	3
231	3.080	3.079	3	3.062	3.060	4
270				2.934	2.931	4
241	2.922	2.916	9	2.900	2.899	9
410				2.817	2.815	<½
311	2.773	2.768	3	2.763	2.755	5
251	2.741	2.740	4	2.726	2.725	4
280	2.656	2.653	3	2.653	2.649	2
440	2.563	2.562	<½	2.557	2.563	<½
341	2.534	2.527	<½	2.520	2.517	<<½
081	2.429	2.428	<½	2.406	2.415	<½
271	2.393	2.392	½			
181	2.374	2.374	1	2.364	2.362	1
421	2.292	2.292	2	2.287	2.286	1
431	2.244	2.242	3	2.238	2.235	2
470	2.179	2.184	1	2.184	2.184	1
371				2.152	2.155	
540	2.122	2.120	½	2.124	2.121	½
0.10.1	2.077	2.076	3	2.069	2.067	3
002	2.063	2.064	2	2.042	2.041	2
461	2.020	2.017	<½			
0.12.0	2.002	2.002	<½			
511	1.975	1.980	2	1.977	1.976	2
560		1.972			1.972	
2.10.1	1.949	1.949	<½	1.944	1.942	<½
531	1.929	1.928	1	1.924	1.924	1
391		1.927			1.921	
600	1.890	1.888	2	1.890	1.890	2
481	1.845	1.843	½	1.840	1.839	1
	1.827		<½	1.821		½
	1.804		1	1.796		1
	1.781		<½	1.776		½
	1.758		<½			
	1.746		1	1.733		½
	1.721		2	1.715		1
	1.700		½	1.700		<½
	1.688		<½	1.677		½

Camera diameter 114.6 mm, Ni-filtered Cu radiation. Intensities estimated visually.

*Not permitted in the space group (*Pbnm*) of the meneghinite subcell.

The latter gives a calculated density of 6.47 g/cm^3, in fairly good agreement with the density of 6.44 g/cm^3 calculated by Euler and Hellner (1960) for the same formula.

Microprobe analyses of the synthetic material (Table 2) suggest that the compound is non-stoichiometric, and that its formula, rather than being $Pb_{13}Sb_7S_{23}$, is $Pb_{13}Sb_{8.35}S_{24.93}$. The validity of the analyses is not questioned, and the excess of $Sb_{1.35}S_{1.93}$ beyond the "ideal" formula is believed to be real. As shown below for the additional analyses of synthetic

products, variations in Pb-Sb-S ratios in "single phase" sulphosalts do not seem to be unusual. Such variations have been found not only among synthetic sulphosalts studied previously and not discussed here, but also in natural phases, especially boulangerite. Studies being done in the Mineralogy Section, CLAS Division, though not yet complete, have given strong indications that the existing fundamental concept of ideal, stoichiometric formulas for lead sulphantimonides may require modification.

Syntheses

Preparation of the synthetic lead sulphantimonides was done at the Canada Centre for Mineral and Energy Technology (Mines Branch) by J.H.G. Laflamme under the supervision of L.J. Cabri; their efforts are gratefully acknowledged.

Because of difficulty in synthesizing Sb_2S_3, all samples were prepared from pure metals weighed out in stoichiometric proportions and sealed in evacuated silica tubes. Phase 1 of Craig *et al.* (1973), stated to be $3PbS \cdot Sb_2S_3$ and stable between 610 ± 10°C and 642 ± 2°C, did not form after heating the appropriate mixture for 3 days at 635°C. The temperature was checked with a calibrated thermocouple, and the charge ground under acetone and heated at the same temperature for an additional 3 weeks. The product was quenched in ice, and examined in polished section and by microprobe. A homogeneous phase corresponding to Phase I was not present.

Two runs were done with material corresponding to $2PbS \cdot Sb_2S_3$. The first was heated for 5 days at 550°C, then 2 days at 500°C. The charge was ground and pelletized, then heated at 500°C for 11 days, quenched, ground and pelletized, and heated for an additional week at 550°C. The product consisted of Cu-free meneghinite and an unidentified phase.

In the second run, the charge was heated at 500°C for 3 days, then 550°C for 4 days, quenched, ground and pelletized, and reheated at 550°C for 100 days. Microprobe analyses of the product (Table 3) indicate that Pb:Sb is variable; none of the four X-ray mounts prepared from the fired charge corresponds to the powder data given by Wang (1973) for $2PbS \cdot Sb_2S_3$.

TABLE 2. THEORETICAL COMPOSITIONS OF MENEGHINITE AND MICROPROBE ANALYSES OF THE COPPER-FREE SYNTHETIC PHASE

	$CuPb_{13}Sb_7S_{24}$	$Pb_{13}Sb_7S_{23}$	synthetic phase*			
wt %			1	2	3	recalc. to 100% and averaged
Pb	61.51	62.88	59.80	59.81	59.75	59.72
Cu	1.45					
Sb	19.46	19.91	22.62	22.70	22.43	22.55
S	17.58	17.21	17.88	17.73	17.62	17.72
	100.00	100.00	100.30	100.24	99.80	99.99

*Microprobe analyses by A.G. Plant. Ten spots analyzed on each of three grains; galena and stibnite used as standards; results corrected by EMPADR VII program.

TABLE 3. RESULTS OF MICROPROBE ANALYSES OF SYNTHETIC SULFOSALT (starting composition $2PbS \cdot Sb_2S_3$)*

	weight per cent			atomic proportions		
	1	2	3	1	2	3
Pb	47.01	50.93	54.55	0.223	0.241	0.260
Sb	32.20	29.03	25.84	0.260	0.233	0.210
S	20.78	20.04	19.61	0.636	0.612	0.604

*second run

Analyses by J.H.G. Laflamme, CANMET. Original data recalculated using EMPADR VII. Analyses represent the extremes and an intermediate of 15 spot analyses in a polished section.

Formulas	Approximations	Approx.	$PbS:Sb_2S_3$
1. $Pb_{22.3}Sb_{26.0}S_{63.6}$	1. $22.3PbS \cdot 13Sb_2S_{3.18}$	1.	22:13
2. $Pb_{24.1}Sb_{23.3}S_{61.2}$	2. $24.1PbS \cdot 11.7Sb_2S_{3.17}$	2.	24:12
3. $Pb_{26.0}Sb_{21.0}S_{60.4}$	3. $26PbS \cdot 10.5Sb_2S_{3.28}$	3.	26:11

Acknowledgments

The writer is most grateful to A.G. Plant and G. Pringle for microprobe analyses, to A. Roberts for running X-ray powder patterns, and to the personnel of CANMET for their significant contributions to this study.

References

Craig, J.R., Chang, L.L.Y., and Lees, W.R.
1973: Investigations in the Pb-Sb-S system; Can. Mineral., v. 12, p. 199-206.

Euler, R. and Hellner, E.
1960: Über Complex zusammengesetzte sulfidische Erze VI. Zur Kristallstruktur des Meneghinits, $CuPb_{13}Sb_7S_{24}$; Zeits. Krist., v. 113, p. 345-372.

Garvin, P.L.
1973: Phase relations in the Pb-Sb-S system. Neues Jahrb Mineral. Abt., v. 118, p. 235-267.

Hoda, S.N. and Chang, L.L.Y.
1974: Phase relations in the systems $PbS-Cu_2S-Bi_2S_3$ and $PbS-Cu_2S-Sb_2S_3$; Geol. Soc. Am., Program Abstr., 1042.

Jambor, J.L.
1967: New lead sulfantimonides from Madoc, Ontario - Part 1; Can. Mineral., v. 9, p. 7-24.

Palache, C., Berman, H. and Frondel, C.
1944: The System of Mineralogy, v. 1, p. 402-404.

Salanci, B. and Moh, G.
1970: The pseudobinary join galena-antimonite, $PbS-Sb_2S_3$; Neues Jahrb Mineral. Mh., H. 11, p. 524-528.

Wang, N.
1973: A study of phases on the pseudobinary join $PbS-Sb_2S_3$; Neues Jahrb Mineral. Mh. H. 2, p. 79-81.

19. PRIMARY PRECIPITATION OF CONCENTRATED DEPOSITS OF MAGMATIC ORES

Project 590283

T.N. Irvine[1]
Regional and Economic Geology Division

Recent work on the Muskox intrusion has revealed a mechanism that appears to have been essential to the formation of chromitite layers in several major stratiform ultramafic-gabbroic intrusions and that may also have importance in the genesis of certain magmatic sulphide deposits. The purpose of this report is to give a brief description of the mechanism and to point out features that are possibly indicative of its operation and therefore of interest in mineral exploration work.

The Contamination Mechanism

In general, when oxide or sulphide phases precipitate from basic or ultrabasic magmas, they form concurrently with various silicate minerals in only minor quantities, and consequently even under conditions of fractional crystallization, they end up as only disseminated, "varietal" or "accessory" minerals of little or no economic interest. Thus chromite crystallized simultaneously with olivine typically forms only 1-3 per cent of the precipitate; magnetite precipitated with pyroxenes and plagioclase amounts to only 3-5 per cent; and ilmentite, formed in similar circumstances, to just 4-6 per cent (cf. Irvine and Smith, 1969). When immiscible sulphide liquid coprecipitated with olivine, pyroxene, plagioclase, and oxide minerals in the Skaergaard intrusion, it formed less than 2 per cent of the total cumulate (Wager and Vincent, 1959).

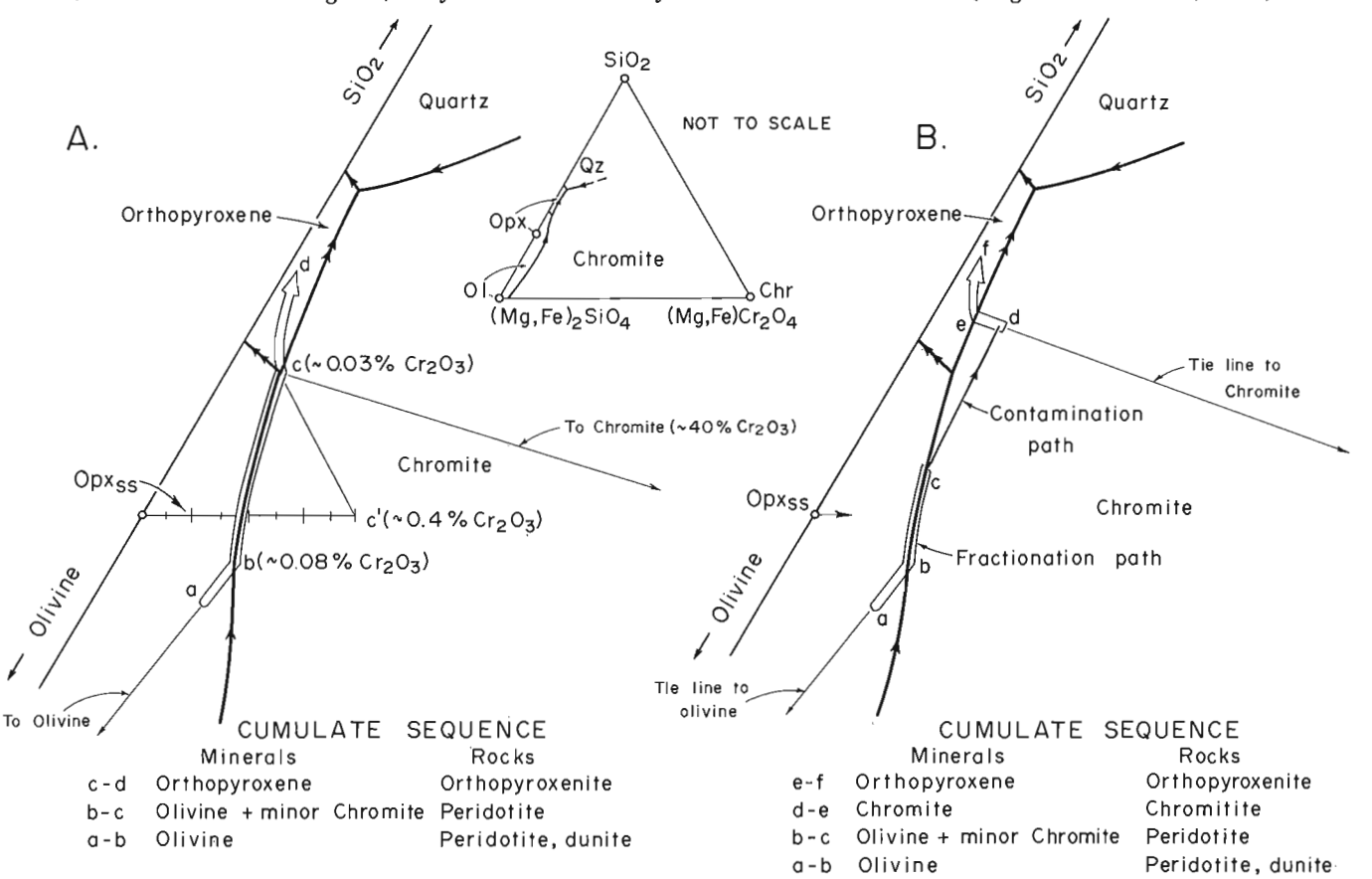

CUMULATE SEQUENCE

	Minerals	Rocks
c-d	Orthopyroxene	Orthopyroxenite
b-c	Olivine + minor Chromite	Peridotite
a-b	Olivine	Peridotite, dunite

CUMULATE SEQUENCE

	Minerals	Rocks
e-f	Orthopyroxene	Orthopyroxenite
d-e	Chromite	Chromitite
b-c	Olivine + minor Chromite	Peridotite
a-b	Olivine	Peridotite, dunite

Figure 1. Schematic projections illustrating the apparent phase relations of olivine, orthopyroxene and chromite in subalkaline basic and ultrabasic magmas, and showing (A) a "normal" fractional crystallization path for a liquid starting in the olivine field and (B) the path followed when contamination of the magma by salic material causes precipitation of a chromitite layer. Modified from Irvine (1975a, b).

[1]Geophysical Laboratory, 2801 Upton St., N.W.
Washington, D.C., U.S.A. 20008.

These low values reflect in large degree the very low saturation limits of oxides and sulphides in magmas in terms of certain key constituents in their compositions. In basaltic liquid, for example, saturation with chromite is reached at Cr_2O_3 values of only 0.05-0.1 per cent, with magnetite at Fe_2O_3 values of just 2.5-3.0 per cent, and with ilmenite at TiO_2 values of 4.0-4.5 per cent (Irvine and Smith, 1969). Sulphide saturation is reached at sulphur contents of only about 0.03-0.2 per cent (Skinner and Peck, 1969; Naldrett, 1973; Haughton *et al.*, 1974). Thus, if the ore phases are to continue to coprecipitate with silicate minerals over any extended period, as generally is required by phase relations, they can form only in small percentages. It is implied, therefore, that unless they begin to form before the silicate minerals, a situation that seems rarely to occur[1], they cannot be precipitated in concentrated deposits by the familiar process of magmatic differentiation by fractional crystallization. Some additional mechanism or process is necessary.

One of the potentially most powerful mechanisms in this regard from a chemical standpoint, and certainly one of the most likely geologically, is contamination. From general principles of phase equilibria, it can be said that if the appropriate magma is contaminated by the right material, in the right way and at the right time, the precipitation of ore-grade deposits of oxides or sulphides can be induced. There are certain obvious possibilities in this regard — contamination by oxygen will generally enhance the crystallization of oxide minerals containing ferric iron such as magnetite and chromite; contamination by sulphur should tend to promote the formation of a sulphide phase. Another possibility, however, less obvious but perhaps equally effective and almost certainly more common, is contamination by salic material — that is, by material rich in silica, alumina and alkalis as might be derived from granitic rocks, acidic volcanic rocks, or pelitic or arenaceous sediments. It was this type of contamination that evidently caused precipitation of the two chromitite layers and associated sulphides in the Muskox intrusion. It appears that the crystallization of the basaltic magma in the intrusion released enough heat at sufficiently high temperatures to melt large amounts of salic material from its roof, and that on two occasions, major quantities of this melt were rapidly mixed into the magma with the effect that for brief periods, chromite and immiscible sulphide liquid were precipitated to the exclusion of silicate minerals and so could accumulate in concentration. This mechanism, which was identified through comparison of Muskox data with theoretical inferences and experimental data, appears also to apply to the much larger, economically important chromitite layers of the Bushveld Complex and Great Dyke in southern Africa and of the Stillwater Complex in Montana, and it may also have been a major factor in the formation of the Sudbury Cu-Ni sulphide ores (Irvine, 1975a, b).

[1]It appears that most basic magmas are saturated with at least one silicate mineral when they arrive in the crust.

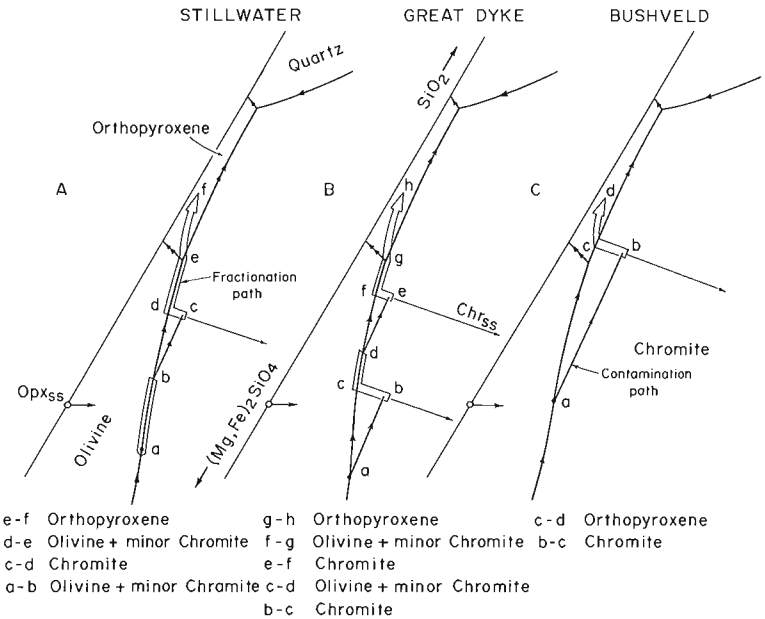

Figure 2. Variations on the model in Figure 3C illustrating formation of the more common stratigraphic sequences involving chromitite layers in the Stillwater, Great Dyke, and Bushveld complexes.

The chemical principles of the mechanism as applied to chromitite layers are illustrated schematically in Figures 1 and 2. Figure 1A illustrates a "normal" fractional crystallization path for a subalkaline basic or ultrabasic liquid in which olivine is the first mineral to form. Chromite shortly joins olivine along the path but is never precipitated in amounts of more than a few per cent, and both minerals cease to crystallize with the appearance of orthopyroxene because of reaction relationships. The sequence of cumulates produced is found in two cyclic units in the Muskox intrusion and is closely approximated in numerous cyclic units in the Stillwater, Bushveld and Great Dyke[2].

By contrast, Figure 1B shows the type of path that was evidently followed by the Muskox magma when the chromitite layers were formed. The liquid starts off on the same course as in A but because of salic contamination is suddenly shifted into the chromite liquidus field. Chromite then precipitates alone until the liquid is driven back to the silicate liquidus, by which stage, because of the enrichment in silica, orthopyroxene crystallizes instead of olivine. The succession of cumulates from this path is that observed in the Muskox cyclic units containing the chromite-rich layers. Figure 2 shows alternative paths that simulate some of the main layer sequences involving chromitite in the

[2]Cyclic units are repeated stratigraphic divisions in stratiform ultramafic-gabbroic intrusions in which the succession of rock layers reflects directly the order of crystallization of the magma (Jackson, 1961; Irvine, 1970). In most cases their repetition appears to reflect the repeated introduction of fresh magma into the intrusion (Irvine and Smith, 1967).

Stillwater, Great Dyke and Bushveld. It is seen that the sequence can differ considerably depending on the timing and degree of the contamination. The thickness of the chromitite layer produced depends on the bulk composition of the parental magma as well as its Cr-content, and on the amount of magma affected and the nature and degree of the contamination.

Figure 3 is an attempt to define the main physical processes relating to the mechanism. Diagram A depicts "normal" conditions during solidification of a stratiform intrusion; B and C portray events relating to episodes of contamination. Note that convection currents play an integral role in both the crystallization of the magma and the deposition of the crystals. The important feature in A is that, because the minerals crystallized in the intrusion entirely accumulate on its floor, the roof contact is continuously exposed to the high temperature of the basic magma. Thus salic rocks at the roof would be expected to melt, yielding a granitic liquid that would tend to float at the top of the intrusion and remain separate because of its low density and high viscosity. In the Muskox and Bushveld intrusions, melt of this type appears to be represented by thick zones of granophyre (*see* Irvine, 1975b for details). In diagrams B and C, the basic magma is contaminated by mixing with large amounts of the salic melt. The mixing in B might be associated, for example, with tectonic disturbance of the intrusion; that in C occurs during the influx of fresh magma prior to formation of a new cyclic unit. The possibility that the salic melt might form or spread beneath large areas of the roof is considered important in explaining the great lateral extent of stratiform chromite deposits, many of which can be traced for tens of kilometres. Direct evidence that salic melt was involved is found inside the concentrated chromite crystals in the form of tiny, spheroidal, composite silicate inclusions rich in silica and alkalis, apparently representing droplets of the melt trapped at various stages of mixing and assimilation, and in various stages of reaction with the host chromite (Irvine, 1975a, b).

The possibility that the contamination mechanism might yield magmatic sulphide deposits stems from the long-standing observation that sulphide solubility in silicate melts is strongly dependent on silica content, decreasing as silica increases (Vogt, 1917). The importance of this effect is strikingly illustrated in the fundamental system FeS-FeO-SiO_2 shown in Figure 3A, where it is seen that the addition of silica to liquids in the part of the fayalite (iron-olivine) field that compares most closely with basic magmas just undersaturated in sulphide can induce the precipitation of immiscible sulphide liquid to the exclusion of olivine. In Figure 3B this effect is adapted to a model phase diagram for natural magmas and shows how it might yield a sequence of cumulates with a concentration of sulphide in a stratigraphic position equivalent to that of the Muskox chromite-rich layers (cf. Fig. 1). Other sequences analogous to those shown for chromite in Figure 2 can similarly be derived. It is important to note in addition that, although the sulphide may be precipitated in layers, the fact that it is liquid gives rise to a further possibility, not applicable to chromite, that it subsequently can be extensively redistributed by flow in response to magmatic or tectonic stresses. The suggestion that the mechanism might apply to the Sudbury Cu-Ni sulphide ores arises from evidence that the basic magma of the Sudbury irruptive was extensively contaminated with salic melt formed by the impact of a meteorite just prior to emplacement of the irruptive (*see* Irvine, 1975b, for further details).

Effects of Oxidation and Reduction

As presented above, the contamination mechanism for producing magmatic ore deposits is primarily dependent on the effect of silica and alkalis to reduce the solubility of the ore phases. There may also be other effects, however, relating to other aspects of the contamination process, and those of oxidation and reduction are potentially of sufficient importance to warrant specific consideration.

It is well established experimentally that oxidation will tend to promote the crystallization of magnetite and chromite in basic and ultrabasic magmas (e.g. Muan and Osborn, 1954; Osborn, 1959; Hill and Roeder, 1975). This process has been advocated by several authors as a possible means of precipitating chromitite layers, and it could be effected in the present model if the contaminant melt were at a higher degree of oxidation than the basic magma. To date, however, evidence to support this possibility has not been forthcoming. One might expect it to show, for example, through higher Fe_2O_3/FeO ratios in the concentrated chromite as compared with disseminated chromite precipitated at a preceding stage, but no such increase could be found in the Muskox intrusion (Irvine, 1975b), and none is apparent in the data presently available on chromites from other stratiform intrusions. In fact, in Muskox there is a possibility that the salic melt was more reduced than the basic magma, because some of the granophyre contains graphite (Smith, 1962).

With regard to sulphides, it is generally considered that sulphur dissolves in silicate melts by bonding to ions such as Fe^{2+} that can simultaneously bond to oxygen ions in the transient silicon-oxygen framework of the melt (Richardson and Fincham, 1954). Thus any process that will lower the concentration of Fe^{2+} in the melt may be expected also to lower the solubility of sulphide. Oxidation and reduction both qualify as such processes.

The effect of reduction is perhaps most easily visualized. In very simple terms, it tends to separate Fe^{2+} from the oxygens that hold it in the melt, thus causing it to precipitate together with sulphur, either as an immiscible sulphide liquid or as a sulphide mineral, depending on temperature and other factors. This effect appears well represented in experimental data presented by Haughton *et al.* (1974, Fig. 4A). A natural situation in which it may have been significant is an occurrence of Cu-Ni sulphides in a subsiduary intrusion of the Duluth Complex recently described by Mainwaring and Naldrett (1974), who postulate that the sulphides were

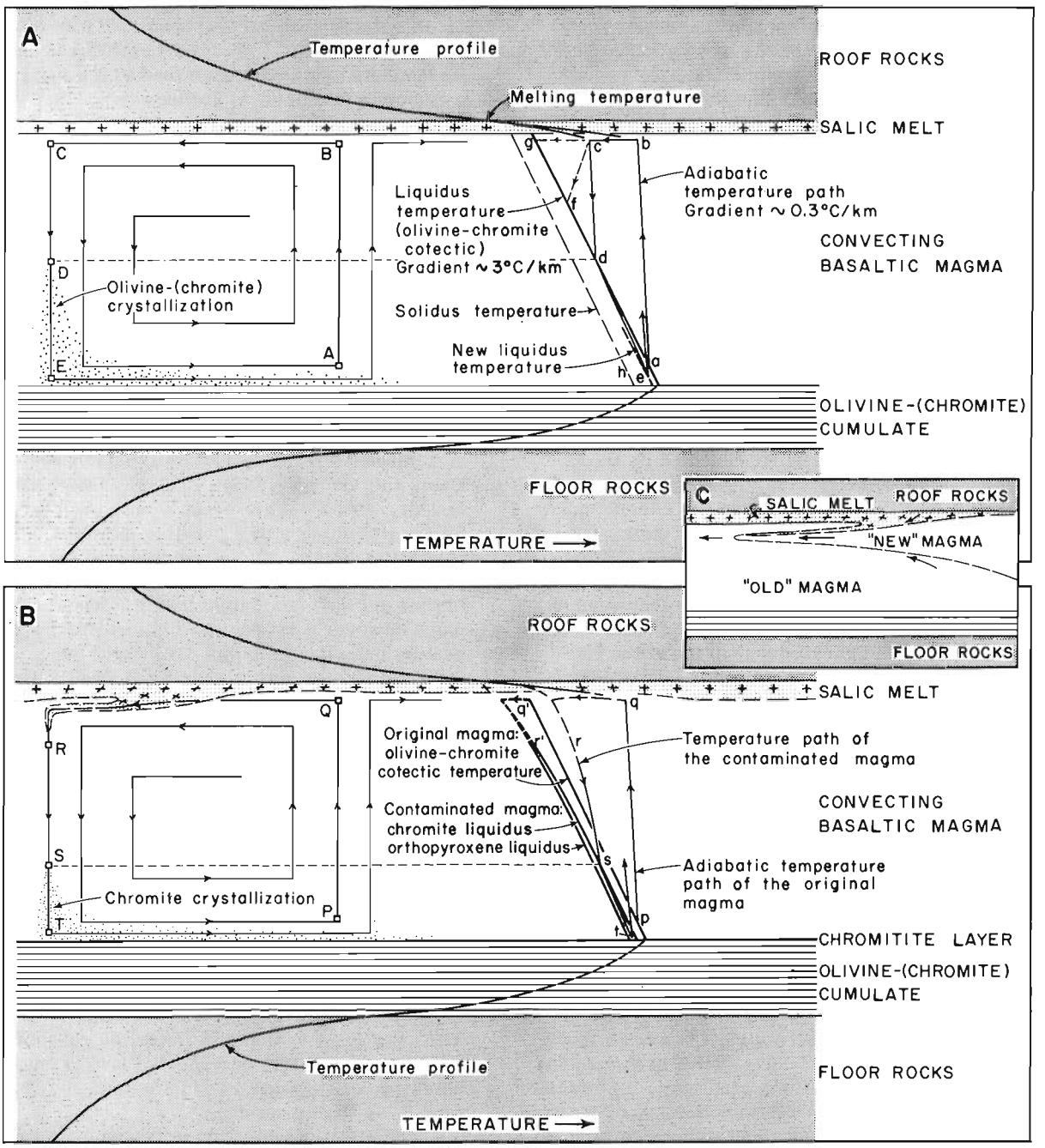

Figure 3. Diagrams illustrating the physical processes that are probably involved in formation of chromitite layers. It is assumed that the roof of the intrusion consists at least partly of rocks such as granite or pelitic schist that will yield salic melt at temperatures well below the liquidus of the basic magma. In A, abcde is a possible temperature path for the basic magma moving in the convection path ABCDE; crystallization ideally should begin at D and continue to E. Branch cf exemplifies the temperature path if the liquid were to descend a cooling wall; branch cg would obtain if the magma cooled to its liquidus as it moved along the roof. Comparable paths in B illustrate possible effects of contamination. Diagram C portrays contamination during lateral influx of fresh magma into the part of the intrusion under consideration.

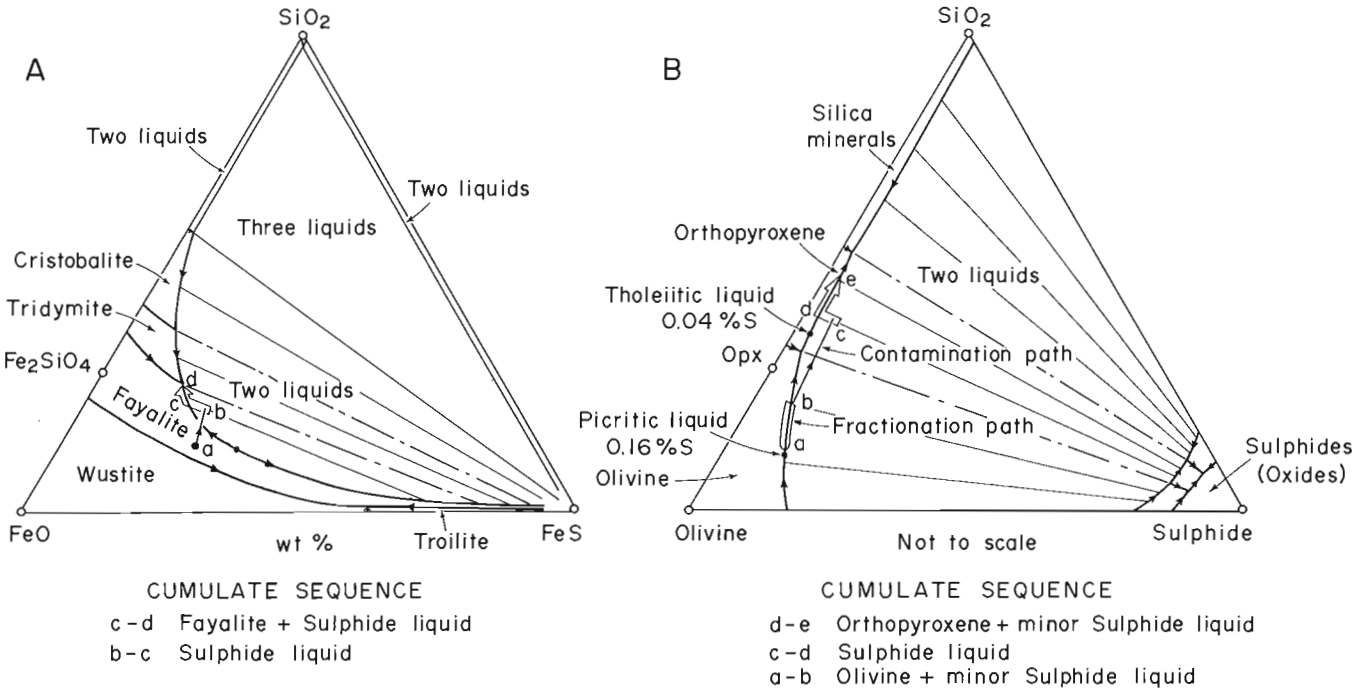

Figure 4. A) Liquidus relations in the system FeS-FeO-SiO_2, after MacLean (1969), showing how the addition of silica to certain liquids in the fayalite field can lead to precipitation of immiscible sulphide liquid. B) Schematic diagram showing how similar relations in subalkaline magmas could yield a concentrated deposit of sulphides like that associated with the Muskox chromite-rich layers. Compare with Figures 1 and 2.

formed because the intrusion was contaminated with sulphide-bearing graphitic slate.

In the case of oxidation, the sulphur in the melt is displaced from its bonds to Fe^{2+} by oxygen, with the effect that its activity is increased until, if the process is carried far enough, the sulphur can in effect "wrest free" metals such a Fe, Cu and Ni and precipitate as sulphide. This effect is apparent in the phase relations of the system FeS-FeO-Fe_2O_3-SiO_2 (MacLean, 1969) and has been suggested as a mechanism of origin for the Lynn Lake Cu-Ni sulphide ores in northern Manitoba (Emslie and Moore, 1961).

Critical Factors

From present knowledge, it appears that three conditions must be satisfied if the contamination mechanism is to produce an economically significant concentration of chromite or sulphide.

1. A large amount of magma must be affected. This factor is a direct consequence of the very low saturation limits of the ore phases noted above. Thus in the case of chromite, if half the chromium in the liquid could be caused to precipitate, then to form a 1-foot (30-cm) layer of chromitite containing 40 per cent Cr_2O_3 would require contamination of 1000 feet (300 m) of basaltic liquid like the Muskox chilled margin containing 0.08 per cent Cr_2O_3. A comparable degree of upgrading is indicated for sulphides.

2. The contamination must occur rapidly in comparison with the rate at which the intrusion is crystallizing. From the phase relations in Figures 1, 2, and 4, it can be inferred that slow, gradual assimilation will tend only slightly to increase the proportion of chromite or sulphide that will precipitate with the silicate minerals. To produce a concentrated deposit, the liquid composition must be shifted abruptly into the primary field of the ore phase. It is because of this factor that the notion that stratiform intrusions first melt their roof rocks and then assimilate the melt is particularly attractive. The heat requirements of the actual contamination process are thus minimized, and so it can go on rapidly. The situation at Sudbury would seem even more favourable if the salic melt was largely formed in advance of the basic intrusion by the meteorite impact.

3. The contamination must occur at a stage when the critical metal is at a relatively high concentration in the magma. For Cr and Ni, this means early, because they are strongly depleted even by "normal" crystallization, but a later stage might be more appropriate for Cu. The situation may be complicated, however, if the intrusion was open to additions of fresh magma, as stratiform intrusions seem commonly to have been. Under these circumstances, the contamination may be relatively late in terms of the over all history of the intrusion, but early with respect to the crystallization of a particular batch of magma.

One other factor of concern is the degree of contamination. As yet, no concrete information is available in this regard, but from relations in Muskox and some of the other stratiform intrusions in which the mechanism

seems to have been effective, it appears that perhaps 5 per cent contamination is necessary for there to be a significant result.

Diagnostic Criteria

Given that the salic melt contamination mechanism is a viable means of producing a magmatic ore deposit, it is of considerable practical interest to be able to recognize situations in which it might have functioned. One cannot expect to anticipate all the ramifications of the mechanism or the complications that might be related to its implementation, but there are several features observed in intrusions in which it has evidently been effective that would seem diagnostic. The mechanism pertains specifically to mafic-ultramafic intrusions in which cumulates are a major component, and it may be suspected in the following situations:

1. In intrusions emplaced in granitic rocks, acidic volcanics, or pelitic or arenaceous sediments.

2. In intrusions containing substantial amounts of granophyre, either as discrete units, especially along roof contacts, or as interstitial material in olivine-free pyroxenite and gabbro units. (Granophyre will generally not form in olivine-bearing ultramafic and gabbroic rocks because the olivine is usually magnesian and, therefore, incompatible with quartz.)

3. In intrusions containing large amounts of orthopyroxene (bronzite-hypersthene), especially as a cumulus phase in orthopyroxenite or norite. It is noted in this regard that, among basic lavas that appear to have come more or less directly from the upper mantle, orthopyroxene rarely crystallizes before augite. (The lavas of Mauna Loa volcano, Hawaii, for example, are one of the few exceptions among Cenozoic volcanic rocks.) Thus the occurrence of cumulus orthopyroxene without associated cumulus augite represents a somewhat anomalous situation, and it is an anomaly that could arise through contamination of basic magma by salic material.

4. In intrusions showing conspicuous evidence of contamination, such as xenoliths of salic rocks. At present, however, this type of evidence would not seem to be as common or important as one might expect. The cumulates of stratiform intrusions containing chromitite layers only rarely include fragments of foreign rock. (The Bushveld chromitite layers commonly contain fragments of anorthosite, but these are cognate inclusions, indigenous to the complex itself.) A probable reason is that most salic rocks will float in basic or ultrabasic liquids, and thus it is only on rare occasions when convection in the liquid is especially strong that they are carried down to where they can be buried in cumulates. From relations in the Muskox intrusion, a more significant indication of contamination would seem to be the presence of fragments of quartzite in granophyre, representing a residue of country rock material that was too refractory to melt even at the temperature of the basic magma.

5. In intrusions showing more subtle evidence of contamination, such as very high $^{87}Sr/^{86}Sr$ ratios, or U-Pb isotopic relations that are atypical of mantle derived magmas. Presently available data on Sr-isotopic relations in the Muskox, Bushveld and Great Dyke show some favourable signs in this respect (Irvine, 1975b) but more detailed investigations are needed. A particularly critical problem arises from the recent discovery that the oxygen in the granophyric rocks of several layered intrusions has been extensively altered isotopically by exchange with meteoric waters circulating through the intrusions in the later stages of their cooling histories (e.g. Taylor, 1974). Inasmuch as Sr, U and Pb are only trace elements, whereas oxygen is a major constituent, there is a strong possibility that their concentrations and isotopic compositions may also have been modified. For the present, the other criteria listed above appear more reliable, as well as being easier to apply.

References

Emslie, R.F. and Moore, J.M
1961: Geological studies of the area between Lynn Lake and Fraser Lake; Man. Dep. Mines Nat. Resour., Mines Br. Publ. 59-4.

Haughton, D.H., Roeder, P.L. and Skinner, B.J.
1974: Solubility of sulfur in mafic magmas; Econ. Geol., v. 69, p. 451-567.

Hill, R. and Roeder, P.L.
1975: The crystallization of basalt as a function of oxygen fugacity; J. Geol., v. 82, p. 709-730.

Irvine, T.N.
1970: Crystallization sequences in the Muskox intrusion and other layered intrusions--I. Olivine-pyroxene-plagioclase relations; Geol. Soc. S. Africa, Spec. Publ. 1, p. 441-476.

1975a: Chromitite layers in stratiform intrusions; Carnegie Inst. Washington Year Book 73, p. 300-316.

1975b: Crystallization sequences in the Muskox intrusion and other layered intrusions--II. Origin of chromitite layers and of similar deposits of other magmatic ores; Geochem. Cosmochem. Acta, v. 39 (in press).

Irvine, T.N. and Smith, C.H.
1967: The ultramafic rocks of the Muskox; *in* P.J. Wyllie, ed., Ultramafic and related rocks; New York, John Wiley and Sons, Inc., p. 38-49.

1969: Primary oxide minerals in the layered series of the Muskox intrusion; Econ. Geol. Monogr. 4, p. 76-94.

Jackson, E. D.
1961: Primary textures and mineral associations in the ultramafic zone of the Stillwater Complex, Montana; U. S. Geol. Surv. Prof. Paper 358, 106 p.

Mainwaring, P. R. and Naldrett, A. J.
1974: Genesis of Cu-Ni sulfides in the Duluth Complex; Geol. Soc. Am., Abstracts with Programs, v. 6, No. 7, p. 854-855.

Nuan, A. and Osborn, E. F.
1956: Phase equilibria at liquidus temperatures in the system $MgO-FeO-Fe_2O_3-SiO_2$; J. Am. Ceram. Soc., v. 39, p. 121-140.

Naldrett, A. J.
1973: Nickel sulphide deposits -- their classification and genesis, with special emphasis on deposits of volcanic association; Can. Inst. Min. Met., Trans. LXXVI, p. 183-201.

Osborn, E. F.
1959: Role of oxygen pressure in the crystallization and differentiation of basaltic magma; Am. J. Sci., v. 257, p. 609-647.

Richardson, R. D. and Fincham, C. J. B.
1954: Sulphur in silicate and aluminate slags; J. Iron Steel, v. 178, p. 4-14.

Skinner, B. J. and Peck, D. L.
1969: An immiscible sulfide melt from Hawaii; Econ. Geol., Monogr. 4, p. 310-320.

Smith, C. H.
1962: Notes on the Muskox intrusion, Coppermine River area, District of Mackenzie; Geol. Surv. Can., Paper 61-25, 16 p.

Taylor, H. P., Jr.
1974: Oxygen and hydrogen isotope evidence for large-scale circulation and interaction between ground waters and igneous intrusions, with particular reference to the San Juan volcanic field, Colorado; Carnegie Inst. Washington, Publ. 634, p. 299-324.

Vogt, J. H. L.
1917: Die sulfid: Silicatschmelzlosungen; Kristiania Vid.-Selksk. I. Mat. - Nat. Klasse, No. I.

Wager, L. R., Vincent, E. A. and Smales, A. A.
1957: Sulphides in the Skaergaard intrusion, East Greenland; Econ. Geol., v. 52, p. 855-903.

20. AXELGOLD LAYERED GABBRO INTRUSION McCONNELL CREEK MAP-AREA, BRITISH COLUMBIA

Project 650288

T. N. Irvine[1]
Regional and Economic Geology Division

This report gives a brief description of the Axelgold gabbro intrusion, with a map and structural sections, and presents some first results from a petrologic study of the body presently underway at the Geophysical Laboratory. The report is based on field work done in 1973 (Irvine, 1974).

Field Characteristics

As mapped (Fig. 1), the intrusion is elliptical in plan, trending north-northwesterly, with a short arcuate "tail" extending to the north. Its total length is about 7.5 miles (12 km); its maximum width, just under 3 miles (4.5 km). At the present level of exposure, the body is almost entirely layered, and the main rock type is olivine gabbro. There are a few prominent picritic (olivine-rich) and anorthositic (plagioclase-rich) layers, 30-100 feet (10-30 m) thick, in the northeast, and several thinner anorthositic layers, not distinguishable at the scale of the map, in the south. Small amounts of two-pyroxene gabbro have been found through thin section studies. On the basis of the layering and of textural features, the rocks can generally be readily identified as cumulates — that is, they have formed by accumulation of minerals through processes of crystal settling and magmatic sedimentation (cf. Wager and Brown, 1968). The cross-sections in Figure 2 show the over all structure of the intrusion; the field photographs in Figure 3 illustrate the terrane and the layering.

The intrusion is emplaced in a complex assemblage of Cache Creek Group rocks in the northern tip of the Stuart Lake belt of Permian oceanic crust that extends for several hundred miles to the south-southeast, past Pinchi and Fort St. James (cf. Paterson, 1974). The Pinchi fault system, which delimits the eastern edge of the Stuart lake belt and in places contains metamorphic rocks of blueschist facies, underlies the Omineca River valley immediately to the east (*see* Fig. 1). The host rocks of the intrusion are mainly graphitic sedimentary schists and amphibolitic metavolcanic rocks, with minor ribbon chert (now quartzite) and crystalline limestone (fine-grained marble), plus several bodies of alpine-type ultramafic rocks and a small pluton of foliated granodiorite. Where the edges of the gabbro intrusion are exposed, a high-temperature contact metamorphic aureole about 1000 feet (300 m) wide can generally be distinguished in which the sedimentary schists have been converted to hypersthene- and olivine-bearing hornfels, the metavolcanics to diopside-garnet-plagioclase rocks, and the granodiorite to a biotitic gneiss.

The Axelgold intrusion cannot be dated geologically beyond its relationships to its immediate host rocks, but it is exceptionally fresh and underformed and thus gives strongly the impression of being much younger. This impression is supported by radiometric age dates recently determined in the laboratories of the Geological Survey. K-Ar dates have been obtained for two biotite-hornblende pairs from the intrusion, one pair from a micaceous facies of the gabbro along the southeast edge of the intrusion, the other from a reaction rim around a granitic xenolith in the central interior. The two biotites and one of the hornblendes gave essentially concordant dates ranging from 98 to 108 m.y., corresponding to a mid-Cretaceous assignment, and this is taken to be the age of the intrusion (R. K. Wanless, written comm., 1975). The other hornblende gave an apparent age of 155 m.y., which is a late Jurassic date, but in view of the concordance of the other data, this value is thought to reflect the presence of excess argon in the hornblende.

The actual contacts of the Axelgold intrusion with its host rocks are only rarely exposed, but they can be traced within narrow limits over several ridges 100-500 feet (30-150 m) in relief, and they appear in all places to be approximately vertical. The layering in the intrusion has a spoon- or bowl-shaped structure discordant to the contacts, dipping inward at 30-60 degrees from the perimeter on the east and north, and flattening, and eventually slightly reversing dip, to the west and south. The visible stratigraphic thickness of layered rocks is about 5000 feet (1500 m), but the base of the section does not appear to be exposed, and the top has been lost through erosion, so the total original thickness could have been much greater. It is apparent that the intrusion must in some way "bottom out" at depth, probably by becoming funnel shaped, in order for there to have been a base for accumulation of the layers, but no clear indication of such a configuration can be seen in outcrop. In a gross way the structure of the intrusion is reminiscent of that of the famous Skaergaard intrusion in East Greenland (cf. Wager and Deer, 1939; Wager and Brown, 1968), but unlike Skaergaard, Axelgold has no chilled margins and no marginal border group; its layering extends right out to the contacts.

The "tail" mapped at the north end of the intrusion requires specific comment because its form might suggest that the magma was emplaced into a ring-dyke type of fracture system. This form, unfortunately, depends heavily on the interpretation of several small outcrops of hornfels along the concave western side of the tail. On the map, these outcrops (which are much exaggerated in size for purposes of illustration) are treated as parts of the walls of the intrusion. There is an alternative possibility, however, that they only

[1]Geophysical Laboratory, 2801 Upton St., N.W., Wash., D.C., U.S.A. 20008

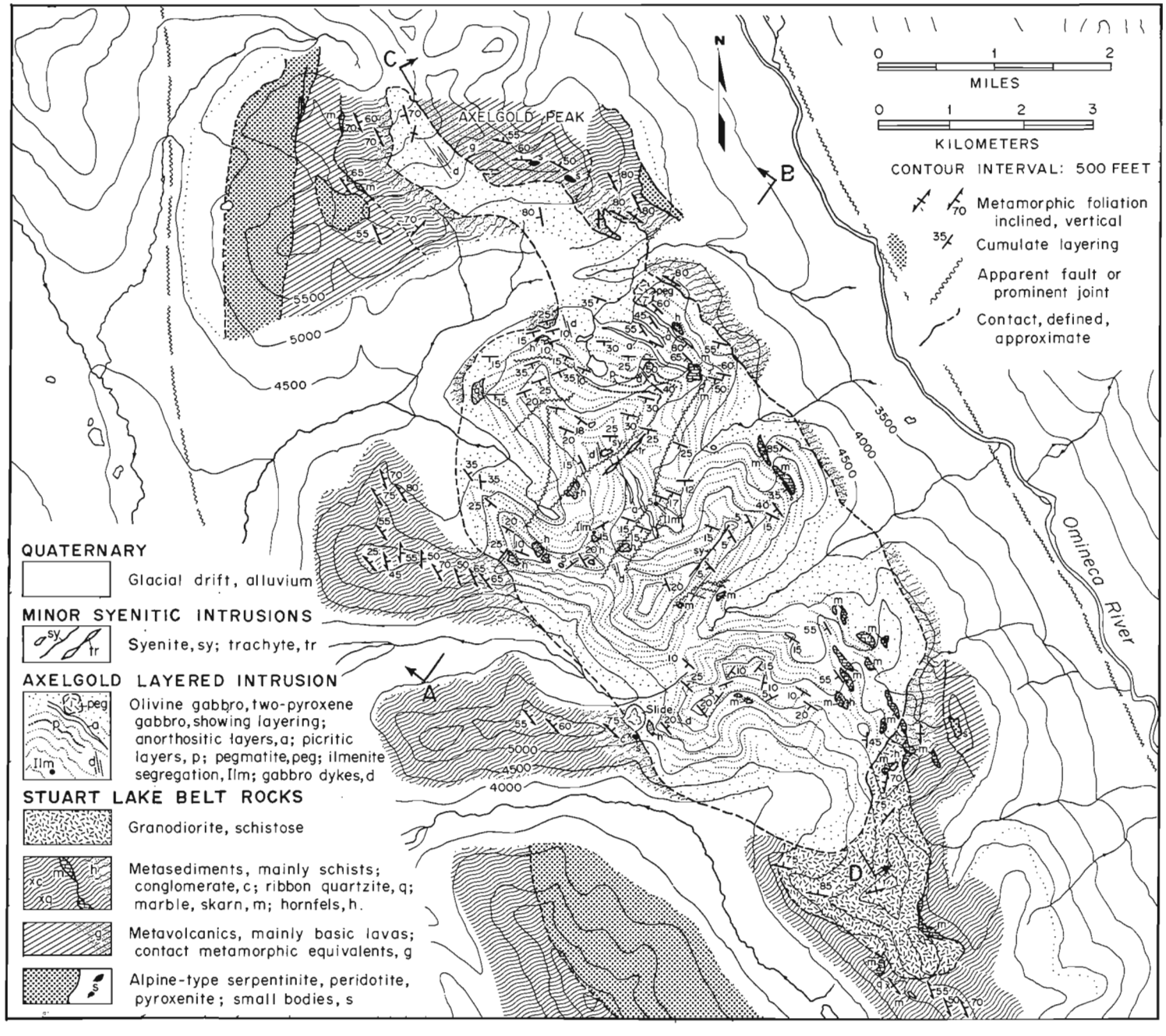

Figure 1. Preliminary geological map of the Axelgold layered gabbro intrusion.

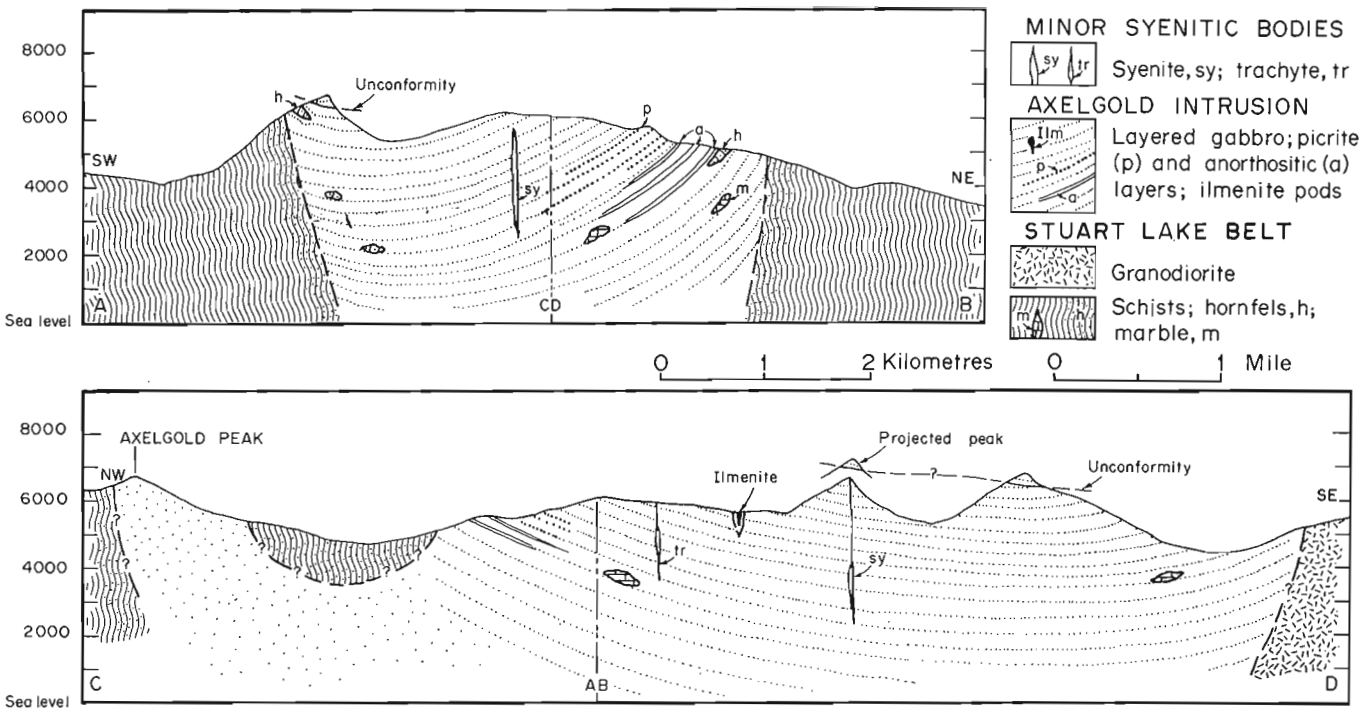

Figure 2. Structural cross-sections of the Axelgold intrusion. The lines of section are shown on the map in Figure 1.

represent large xenoliths similar to other hornfels xenoliths common within the intrusion (*see* below). If this alternative applies then the western contact of the intrusion could be much straighter, and the tail perhaps non-existent. The aeromagnetic map of the area (Geol. Surv. Can. Map 5270G) has not been helpful in resolving this problem because the gabbro intrusion has little or no magnetic expression. The magnetic anomaly pattern is dominated by the effects of the alpine-type ultramafic bodies among the country rocks, in which secondary magnetite has been produced in relatively large amounts during serpentinization.

An attempt has been made on the map to delineate the outcrop trace or trend of the layering in order both to illustrate its distribution and to establish a general stratigraphic framework. It was found, however, that although most of the intrusion is layered, there are few distinctive stratification units that can be used as marker horizons, and none that can be traced throughout the body. Most layers are only vaguely defined and tend to pinch and fade over relatively short distances. Thus the correlations represented in the mapped trend lines are frequently tenuous, especially between the sections of rock contained in the three main ridges that cross the intrusion. On the other hand, the over all structure of the layering appears relatively simple, and the intrusion does not seem to be broken by any major faults that might greatly invalidate the correlations.

The layering itself, as viewed from a distance, generally appears to be defined by stratification units 10-30 feet (3-10 m) thick that in places show a vague cyclic repetition (Fig. 3). Close at hand, it distinguished mainly a discontinuous lamination of pyroxene and olivine in plagioclase (Fig. 3C). There are a few layers that well graded modally, typically 3-10 feet (1-3 m) thick with mafic minerals concentrated in their basal parts and plagioclase towards their tops, but they are greatly in the minority. More commonly the sorting of minerals is diffuse or indefinite, and the general style of the layering contrasts markedly with the classic, very regular, rhythmic layering of the Skaergaard intrusion (cf. Wager and Brown, 1968). Some of the Axelgold layering does, however, show slight crossbedding, and the lamination frequently has a winnowed appearance, so there is no doubt that the layering was produced by sedimentation of crystals from magmatic currents.

At least two angular unconformities can be seen in the layered rocks, as indicated in the cross-sections (Figs. 2, 3B). In each case the discordance is only about 10 degrees, and it appears that the breaks record only mild episodes of disturbance of the inrusion during solidification. There are no outstanding changes of lithology at the unconformities as might indicate the introduction of fresh magma.

A major feature of the intrusion is the presence of numerous large xenoliths of country rock. About two dozen occurrences are shown on the map comprising blocks ranging from about 50 to 650 feet (15 to 200 m) in length, and many more are undoubtedly present at depth, as suggested schematically in the cross-sections (Fig. 2). Numerous examples can be seen both to rest on layered gabbro and to be covered by younger layers, and it is clearly evident that the xenoliths were shed or stoped repeatedly from the walls or roof of the intrusion as the layers accumulated. In many cases, the blocks have disturbed the layering structure, presumably through their weight and impact as they came to rest-- or to some extent simply by their presence. In

A. Panorama of the central interior, view to the south. Locations of a marble xenolith (m), ilmenite pods (il), a hornfels xenolith (h), a syenitic plug (sy).

B. Angular unconformity (u) in layering near the south end of the intrusion, view to the southeast. Intrusion contact, c; Slide s.

C. Typical lamination in olivine gabbro.

Figure 3. Layering in the Axelgold gabbro intrusion.

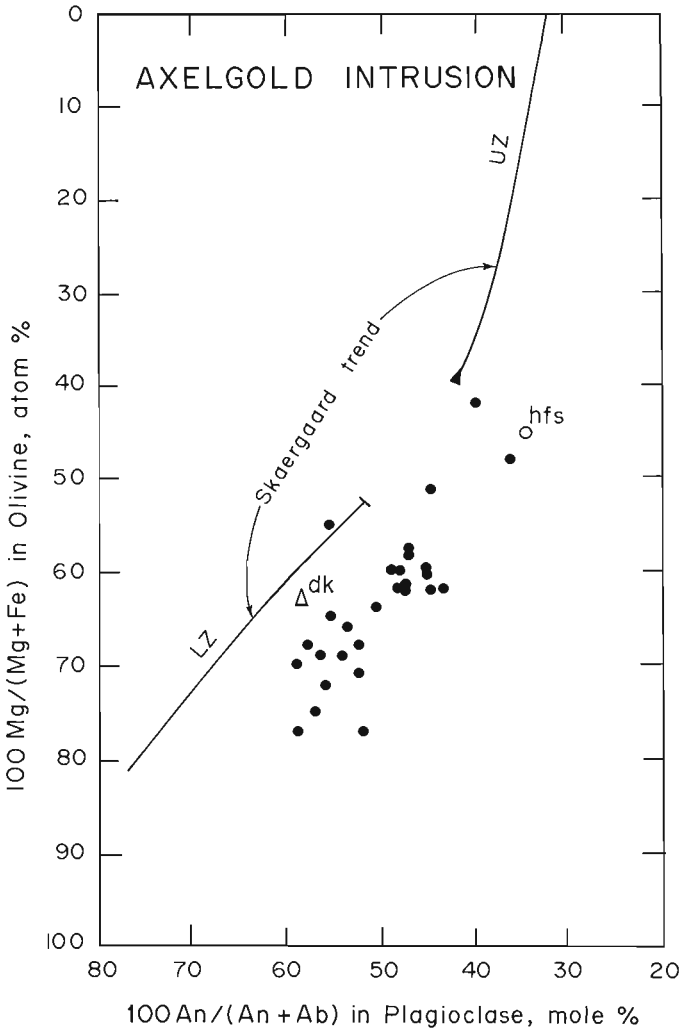

Figure 4. Plot of Mg/(Mg+Fe) in olivine vs An/(An+Ab) in coexisting plagioclase in Axelgold gabbro and related rocks. The trend of variation reported for the Skaergaard intrusion by Wager and Brown (1968) is shown for comparison (LZ, lower zone; UZ, upper zone).

the western half of the intrusion, most xenoliths consist of biotitic hypersthene- and olivine-bearing hornfels similar to that derived from sedimentary schists in the metamorphic aureole along the west contact. In the east, however, blocks of fine-grained marble are predominant; in fact, there is much more marble or limestone included in the intrusion than can be seen among its country rocks for distances up to several miles from its contacts, a feature that would suggest that the process by which the xenoliths were taken into the intrusion was for some reason selective. It is interesting also, although perhaps fortuitous, that the marble xenoliths are mostly contained in a relatively thin stratigraphic zone that is roughly aligned on the map with a contorted, discontinuous limestone unit intersected by the south end of the intrusion. The impression is that the limestone unit was the main source of the blocks. The small granodiorite pluton in the country rocks is also emplaced against the limestone and appears similarly to have included pieces of it.

The distribution of the xenoliths is of interest in that it suggests a possible explanation for the difference between the Axelgold layering and that in the Skaergaard intrusion. In Skaergaard the layering was apparently deposited by a very regular system of convection currents, with the magma circulating across the floor in the same general direction (from north to south) throughout the accumulation of most of the layered series (Wager and Brown, 1968; and personal observations). In Axelgold, however, it would appear that the xenoliths alternately tumbled into the magma, first from one side (or end) of the intrusion and then the other, and in view of their large size, it seems likely that they would have considerably stirred the magma, producing complex circulation patterns. The layering therefore, may reflect this complexity.

The Axelgold gabbro is cut by numerous dykes of darker, finer grained gabbro, some with phenocrysts of plagioclase. These dykes typically are 6 inches to 3 feet (0.1 to 1 m) in width and generally trend north-northwesterly, parallel to the axis of the main intrusion, and dip steeply. They are mineralogically similar to their host gabbro, and since they have neither been found outside the main intrusion nor show chilled contacts against it, they would appear to be in some way related to it. Possibly they represent intercumulus liquid (i.e. liquid from between the settled crystals in the layered gabbro) that was segregated into fractures during the last stages of solidification of the main intrusion.

Gabbro like that in the dykes is especially common in the northern tip or tail of the intrusion, just south of Axelgold Peak, and accordingly the presence of dykes is indicated in that area (Fig. 1). It should be noted, however, that the outcrops are rubbly, so the dykes are not clearly defined.

The Axelgold gabbro is also cut by three small intrusions of syenitic rocks. One is a northeasterly trending dyke, about 1800 feet (550 m) long and 10-30 feet (3-10 m) wide, composed of a fine-grained, grey rock appropriately termed trachyte, containing tiny phenocrysts of oligoclase and green biotite and traces of interstitial quartz. The other two bodies are composed of medium grained white syenite consisting almost entirely of well twinned plagioclase. The largest is a bottle-shaped pipe, about 150 feet (45 m) in diameter that can be seen to cut up through several hundred feet of layered gabbro (Fig. 3A); the other is a narrow dyke extending for some 1500 feet (450 m) parallel to the trachyte dyke.

As noted previously (Irvine, 1974), sulphide minerals are very lightly disseminated through the Axelgold intrusion with slight concentrations developed locally in the inner part of the contact metamorphic aureole. The intrusion also contains two small segregations of massive ilmenite (Figs. 1, 3A). The most southwesterly occurrence is very small; the other is a

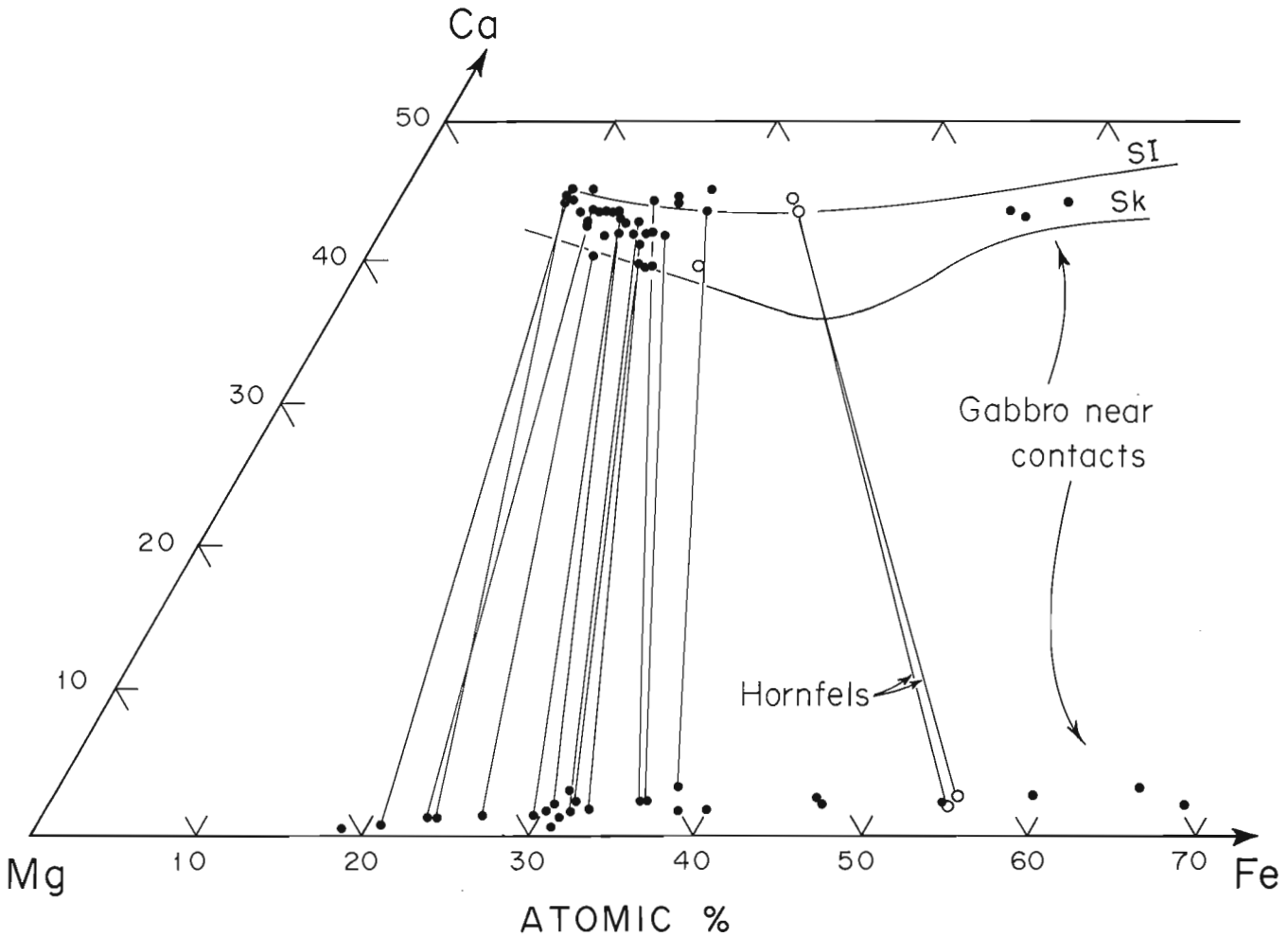

Figure 5. Ca-Mg-Fe plot of pyroxenes in Axelgold gabbro and related rocks. A representative selection of the data points for coexisting pyroxenes are joined by tie lines. Sk, trend of Skaergaard augites; SI, trend of augite crystallized from alkali basalt in Shiant Isles Sills.

branching pod extending over an area about 30 feet (10 m) square associated with a small zone of pegmatitic gabbro. A larger zone of pegmatitic gabbro without visible ilmenite concentrations occurs near the northeast edge of the intrusion (Fig. 1).

Petrography and Mineralogy

The olivine gabbro that makes up most of the Axelgold intrusion is essentially a cumulate of plagioclase, augite and olivine. On the average, these minerals occur in relatively "normal" modal proportions of approximately 55: 35: 10, respectively, but owing possibly to the sorting of plagioclase from the mafic minerals during formation of the layering, the rock tends to have a leucocratic or anorthositic aspect. Orthopyroxene is commonly but not invariably present, occurring principally as thin rims or small grains around the olivine. In the two-pyroxene gabbro, orthopyroxene occurs to the exclusion of olivine in amounts of about 15 per cent, and in some samples it shows abundant exsolution blebs of augite in patterns indicative of inversion from pigeonite. The presence of the orthopyroxene suggests that the parental magma was subalkaline in composition, but there is an alternative possibility that it formed because the magma was extensively contaminated with siliceous material. Other evidence of contamination is discussed below.

Ilmenite is widespread in the gabbro and appears sufficiently abundant in many places to be a cumulus phase although it almost invariably has an "interstitial" habit. It is commonly separated from the major silicate phases by thin rims of brown hornblende. In the gabbro that has been examined microscopically, apatite is a conspicuous accessory phase in most material collected from within about 1500 feet (450 m) of the edge of the intrusion. From its textural relations, the apatite frequently appears to be cumulus, but its distribution seems more closely related to the contacts of the intrusion than to its stratigraphy.

Some of the electron microprobe data that have been obtained on mineral compositions are illustrated

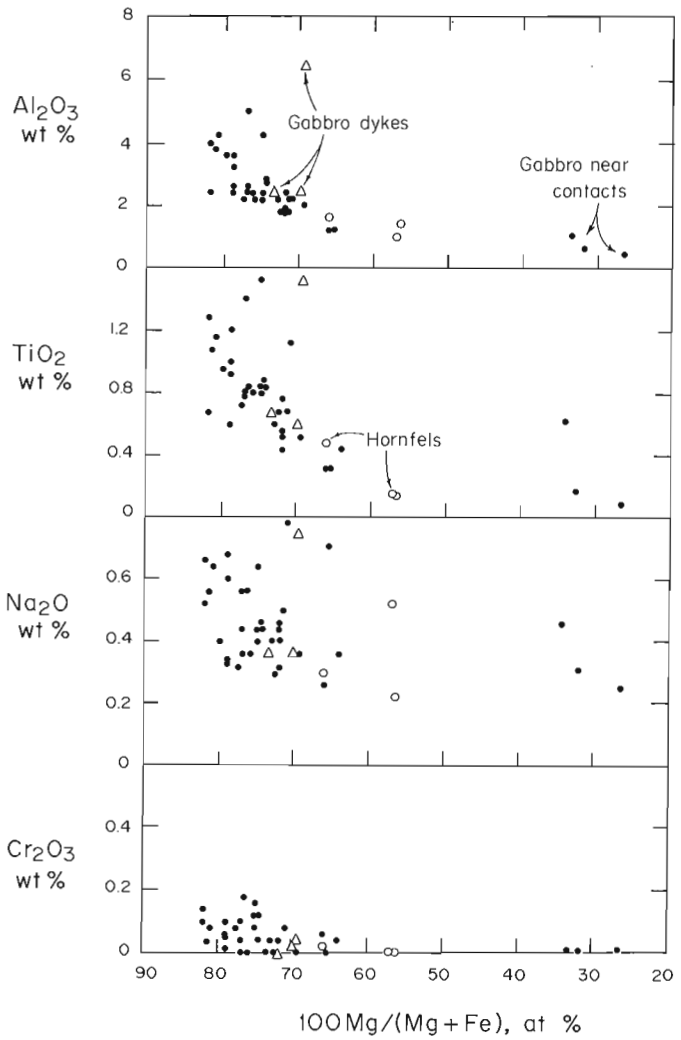

Figure 6. Plots of the variations of Al_2O_3, TiO_2, Na_2O and Cr_2O_3 with Mg/(Mg+Fe) in augites from Axelgold gabbro and related rocks.

in Figures 4, 5 and 6. To date, 40 samples have been investigated, from 2 to 5 minerals being analyzed in each. Wherever possible, analyses have been made of 3 separate grains of each mineral and the results averaged. The olivines and pyroxenes are practically homogeneous within any given sample; their principle end-member components seldom range over more than 0.5 mole per cent. Plagioclase shows some local variation, up to about 1.5 mole per cent in An-content, but even part of this variation is analytical, stemming from the difficulties inherent in electron microprobe analysis of the light elements.

Figure 4 illustrates the relationship between the Mg/(Mg+Fe) ratio of the olivine and the An-content of the plagioclase in comparison with that reported for the Skaergaard intrusion by Wager and Brown (1968). Closely similar relationships have been found for augite and plagioclase and for orthopyroxene and plagioclase. It is seen that the ranges of the plotted ratios are relatively small, and although there is some correlation between them as expected from the phase relations of the minerals and general principles of crystal-liquid equilibrium and fractional crystallization, the correlation is comparatively weak. There is even less correlation, however, between the mineral variations and stratigraphic height. The data are not yet sufficient to illustrate this feature in detail, but among the presently analyzed samples, the most calcic plagioclase comes from one of the stratigraphically highest points in the intrusion, and some of the olivines in the middle and upper parts of the exposed section are just as magnesian as those from the bottom. Despite the extensive development of layering, it appears that fractional crystallization due to settling of the minerals to the floor of the intrusion was only a relatively minor factor in the development of the mineral variations.

The data on pyroxene compositions in Figures 5 and 6 point to the same conclusion. Figure 5 demonstrates a close approach to equilibrium between coexisting pyroxenes in terms of Mg/(Mg+Fe) ratio, and taking this ratio as a differentiation index, the variations in Figure 6 might reasonably be ascribed to fractional crystallization. (Thus, the weak trends of decrease of Al_2O_3 and Na_2O could be due to fractionation of plagioclase along with the pyroxene; the decrease of TiO_2 to fractionation of ilmenite; and the decrease of Cr_2O_3, to fractionation of the pyroxene itself.) However, when plotted against stratigraphic height, none of these variations is systematic.

What appears to be a more important factor than crystallization differentiation is contamination by country rock material, either by assimilation or by exchange reactions. This possibility is suggested by the data in Figure 5 in that all of the most iron-rich pyroxenes that have been analyzed from the gabbro are from samples collected close to contacts, either the outer contacts of the intrusion as a whole, or internal contacts with large xenoliths. An even stronger indication, however, comes from the oxide minerals. The only oxide phase that has been found in significant quantity in the intrusion is ilmenite; no appreciable occurrence of magnetite has been detected, a feature that accords with the previously noted absence of an aeromagnetic anomaly over the intrusion. In investigating this matter, it has been found that many of the hornfels xenoliths in the intrusion contain graphite, leading to the suggestion that the magma assimilated enough of the graphite to reduce its Fe_2O_3 content to such an extent that magnetite could not precipitate. The graphite could have been taken into the magma by direct assimilation of hornfels, but a perhaps better possibility is that it was absorbed through processes whereby it reacted with water (derived from either the hornfelsed schist or the magma) to form CO, CO_2 and H_2, which then dissolved in the magma where they could react further to reduce Fe_2O_3 to FeO.

The possibility that the Axelgold intrusion has been extensively contaminated is of some interest from a mineral exploration viewpoint. As described in the preceding report, contamination of basic and ultrabasic magmas is theoretically an extremely powerful mechanism

for inducing precipitation of concentrated deposits of certain magmatic ores, and contamination by a reducing material such as graphite may be particularly effective as a means of precipitating sulphide. Mainwaring and Naldrett (1974) have described an occurrence of Ni-Cu sulphides in association with magnetite-free, ilmenite-bearing olivine gabbro and troctolite in a subsidiary intrusion in the Duluth Gabbro Complex where the sulphides appear to have formed because of contamination of basic magma by sulphide-bearing graphitic slate. Although sulphides are not prominent in the Axelgold intrusion, and Ni seems rare (the most Ni-rich silicate mineral in the gabbro, the olivine, seldom shows as much as 0.05 weight per cent (NiO), the possibility of significant concentrations of Ni sulphides at depth should not be ruled out.

Regional Correlations

No volcanic rocks have been reported from the McConnell Creek map-area of the appropriate age and composition to be considered as possible volcanic equivalents of the Axelgold intrusion. The best possibility in this regard would seem to be feldspathic augite porphyry volcanics of Lower Cretacous age (Skeena Group) reported by Richards (1973) in the Hazelton map-area immediately to the south.

To the writer's knowledge, the Axelgold intrusion has no plutonic counterpart in the Canadian Cordillera, but it is remarkably similar to the Crillon-La Perouse layered gabbro intrusion in the Alaska Fairweather Range, described by Rossman (1963). This intrusion, which is also thought to be Cretaceous, is much larger than Axelgold, measuring about 17 miles (27 km) by 7-8 miles (~ 12 km) with an estimated exposed stratigraphic thickness of 32 000 feet (10 000 m), but it has the same shape and structure and exhibits the same style of layering; it is closely similar in lithology, showing the same lack of correlation between mineral variations and stratigraphy; it similarly contains abundant ilmenite and no magnetite; and perhaps not coincidentally, it too is intruded close to a major fault system into host rocks that comprise a typical oceanic crust assemblage. It should be noted also that there is an important Ni-Cu sulphide deposit close to the lower edge of the Crillon-La Perouse intrusion (MacKevett, *et al.*, 1971).

References

Irvine, T.N.
1974: Ultramafic and gabbroic rocks in the Aiken Lake and McConnell Creek map-areas, British Columbia; *in* Report of Activities, Part A, April to October, 1973, Geol. Surv. Can., Paper 74-1A, p. 149-152.

MacKevett, E.M., Jr., Brew, D.A., Hawley, C.C., Huff, L.C. and Smith, J.G.,
1971: Mineral resources of Glacier Bay National Monument, Alaska; U.S. Geol. Surv. Prof. Paper 632, 90 p.

Mainwaring, P.R. and Naldrett, A.J.
1974: Genesis of Cu-Ni sulfides in the Duluth complex; Geol. Soc. Am., Abstracts with Programs, v. 6, no. 7, p. 854-855.

Paterson, I.A.
1974: Geology of Cache Creek Group and Mesozoic rocks at the northern end of the Stuart Lake Belt, Central British Columbia: *in* Report of Activities, Part B, November 1973 to March 1974, Geol. Surv. Can., Paper 74-1, p. 31-42.

Richards, T.A.
1973: Hazelton east-half (93 M east half); *in* Report of Activities, Part A, April to October, 1973, Geol. Surv. Can., Paper 74-1A, p. 35-37.

Rossman, D.L.
1963: Geology and petrology of two stocks of layered gabbro in the Fairweather Range, Alaska; U.S. Geol. Surv. Bull. 1121-F, 50 p.

Wager, L.R. and Brown, G.M.
1968: Layered igneous rocks; Oliver and Boyd, Edinburgh and London, 588 p.

Wager, L.R. and Deer, W.A.
1939: The petrology of the Skaergaard intrusion, Kangerdlugssuag, East Greenland; Medd. Grønland, v. 105, no. 4, p. 1-352.

21.

GNEISS DISTINCTIONS IN THE HAYES RIVER REGION: MAGNETIC AND GEOCHEMICAL PARAMETERS

Project 720062

Mikkel Schau
Regional and Economic Geology Division

Introduction

The Churchill Structural Province has always been considered a complex region which was last deformed during the Hudsonian "orogeny" (Stockwell, 1963; Davidson, 1972). In a regional study (Schau, 1974, 1975) of the Prince Albert Group in the northern Churchill Province the original assignment of this group to the Archean is confirmed (Heywood, 1961). This permits us to subdivide the Archean because in favoured regions it is possible to separate different gneisses on the basis of their geologic relations to the Prince Albert Group. In a previous paper (Schau and Campbell, 1974) a clustering technique borrowed from numerical taxonomy was used to classify some gneisses from map-area 56 J, K. In this study, which focusses on a small part of map-areas 56 K 9, 15, 16 and 56 J 12, 13, 14, the different types of Archean (?) gneisses, previously separated, are studied in greater detail.

Geology

The geology of the area, displayed in Figures 1, 2, is divisible into three regions whose boundaries are parallel to the northeasterly structural grain of the area. "New" gneisses flank a central region of complicated geology featuring "old" gneiss, tightly folded supracrustal units of the Prince Albert Group, "new" gneiss and acid and basic intrusions.

Gneisses of region A were once porphyroblastic high grade gneisses featuring biotite-hornblende-sphene-plagioclase-potash feldspar-quartz paragenesis (Winkler, 1974, p. 298) which have been subsequently retrograded to middle and lower grade gneisses characterized by abundant new minerals such as epidote, chlorite, actinolite, calcite, sphene overgrowths, sericite alteration of feldspars, as well as new mortar textures, annealed shear textures and rotated or strained older mineral grains. These gneisses are considered "new" because they cut, along the southern boundary, the deformed Prince Albert Group. Since supracrustal rocks have not been recognized in the region, the gneisses have not been extensively studied and their protolith is unknown.

Region B is recognizably complicated because here preserved supracrustal rocks and dykes allow a sequence of events to be established. "Old" gneiss underlies structurally (and to the southwest, stratigraphically, (Schau, 1974) rocks of the Prince Albert Group and "new" gneiss is partly generated from these rock groups. Granite cuts all these units. One type, an almandine, muscovite, graphic granite and its associated pegmatites is thought to be a culmination of the "new" gneiss-making event. A northerly trending metagabbro dyke cuts the previously described rock assemblages. Another type, a red weathering, biotite-bearing granite with scattered grains of fluorite alters the metagabbro dyke and the other units. Petrographic investigations indicate that many mineral assemblages in the area are of medium grade, but also that a later period of crushing, straining, recrystallization and reorientation and new growth of minerals occurred irregularly, but in all rock units except of younger granite. Almandine-andalusite-muscovite-biotite-bearing schist is an indicator of the grade of the first episode of metamorphism. New actinolite, sphene, ilmenite, oligoclase and calcite growing within, but not everywhere destroying, the original diabasic texture of the northerly trending metagabbro dyke is a clear example of the second episode. In other rocks amphiboles or biotites may grow across previous fabrics or may be degraded, but the time of new mineral growth is not as clear as in the two examples given above. Biotites formed during this episode of metamorphism yields Hudsonian ages (Heywood, 1961).

Gneisses of region C are now tentatively classified as "new" although they contain abundant evidence of a complicated history of deformation. Fluorite-bearing red stained biotite granite cuts the gneiss, providing an upper bound to their age. There generally gently dipping, well developed gneissosity, with a coarse extremely porphyroblastic fabric and widespread pegmatites, differentiates them from gneisses in regions A and B. In this region a large magnetic anomaly, discussed later, is found. In thin section mafic minerals are degraded and associated with fluorite and grain boundaries are often annealed or crushed. These observations suggest the degradation is associated with emplacement of the youngest type of granite (Hudsonian?). This brief summary of geologic elements of the region emphasizes that although recrystallization and minor movement of grain and rock units accompanied the Hudsonian event, a prior metamorphic and deformational event was by far the most important in the history of these rocks.

Magnetic Studies

Samples collected along a line through the different units mentioned above have been analyzed using magnetic and chemical methods. Magnetic parameters studied include total magnetic field over the region

under study, magnetic susceptibility and magnetic anisotropy determinations for cores from the sample sites, as well as an unsuccessful attempt to determine the paleomagnetic pole associated with the emplacement of the metagabbro dyke.

The total field (Fig. 3) is characterized by two anomalously high regions. One occurs in area B over supracrustals of the Prince Albert Group; the other occurs in area C in a region of gneisses. The magnetic fields sensed by magnetometers one thousand feet above ground over these two anomalous regions are equivalent because the field generated by a given volume of quartzose metasediment with thin beds of maghemite-magnetite-quartz iron formation (Table 3B), is similar to the field generated by the same volume of gneissic granite or granitic gneiss (Table 3A) with 7 per cent magnetite. To the east-northeast of the southern anomaly, there are iron formations noted by Heywood (1961) and one wonders whether gneisses of area C include rocks of Prince Albert Group parentage to yield these locally magnetic gneisses and gneissic granites.

Magnetic susceptibility determinations vary greatly and are summarized in Table 1. In these samples magnetite is the only magnetic mineral as determined by Curie point determinations. The abundance of magnetite, in weight per cent, and magnetic susceptibility are related by a highly significant linear equation. The large variations in magnetic susceptibility thus reflect an irregular distribution of magnetite in the samples. Both this variability and the volume problem mentioned above indicate that caution in the interpretation of aeromagnetic maps is necessary.

Magnetic anisotropy determinations are more difficult to summarize and interpret. The method measures the arrangement of magnetic material in a specimen. Using a geometrical analogy, if a magnetic susceptibility determination in a rock with a random arrangement of magnetic material is thought of as a sphere with the radius proportional to the susceptibility, then the magnetic anisotropy measures the extent that magnetic mineral arrangements in a rock causes departure from this reference sphere. Magnetization can be isotropic (spherical analogue) or anisotropic (prolate spheroid, ellipsoid, or oblate spheroid analogues). In Table 2 the samples are divided into these four categories. Two factors important in determining the nature of magnetic anisotropy are grain shape and crystallographic orientation. In magnetite the former is important, whereas in pyrrhotite the latter has a greater influence. Since magnetite is the most important magnetic mineral, it follows that the parameter measured is really a magnetite lineation or foliation. The orientations of these lineations (prolate spheroids), foliations (oblate spheroids) and lineation-in-foliations (ellipsoids) are plotted in Figure 4. An old lineation (A) lies athwart the main gentle to medium plunging northeast trending features (B) associated with the main deformation phase. Foliations of gneiss rock (C) lie along the great circle to (B). Foliations in meta-peridotite (D) and magnetite lineations in the metagabbros have very different orientations. These lineations plunge east-southeastward at medium angles nearly within the plane defined by the foliation. The relative age of this east-southeast plunging lineation is thus post-gabbro emplacement. It is probably associated with the second period of metamorphism because this is the age of the recrystallization and orientation of the magnetite grains yielding the fabric. This finding is of interest because megascopic structures have orientations similar to those of the magnetite. The relative ages of the mineral lineations and minor folds where seen are the same as the magnetite; that is, early northeast trending

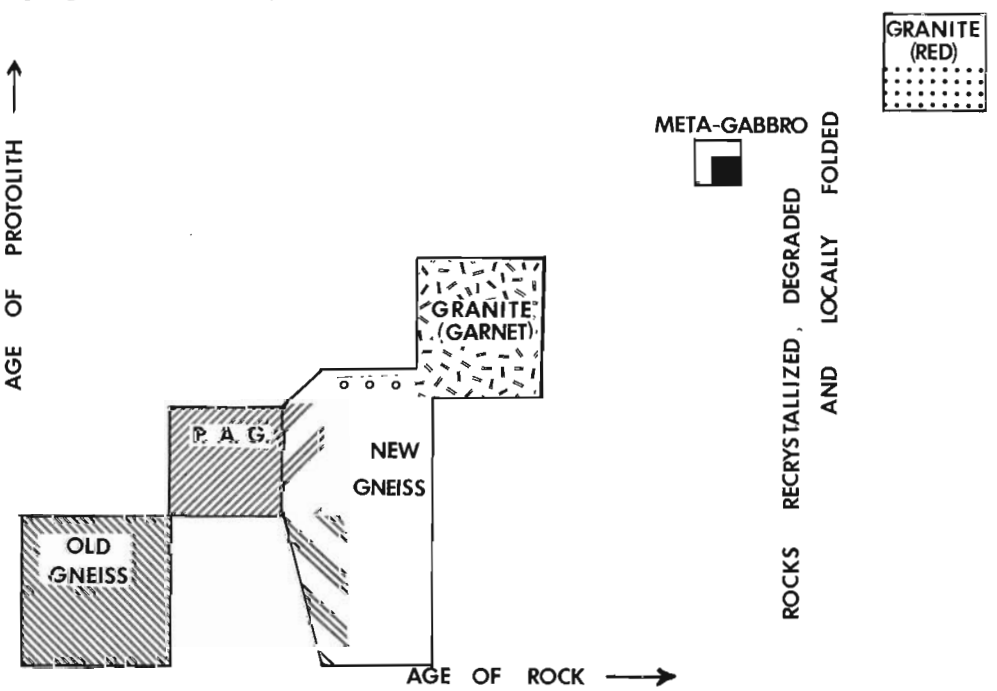

Figure 1. Hayes River region lithologies and legend for Figure 2.

lineations are deformed around southeast plunging folds. The magnetic anisotropy data thus reinforces field observations and confirms the speculation that the later deformation post-dates the gabbro emplacement. Many minor folds have the southeast plunge, whereas major rock units are generally arranged around the earlier northeast trending axes, again suggesting that the second deformation was important only in local rearrangements such as minor folding and shearing of metagabbro dykes or ultramafic schists.

Paleomagnetic pole determinations from the metagabbro were unreliable and unstable. The recrystallization of the opaque oxides into sphene, ilmenite and iron-bearing amphibole destroyed the thermoremanent components. X-ray diffraction studies and Curie point determinations indicate that a small amount of magnetite and magnetic pyrrhotite are present. The latter mineral is responsible for the extremely unstable character of the weak remanent component. These data again confirm that the recrystallization of the metagabbro was a

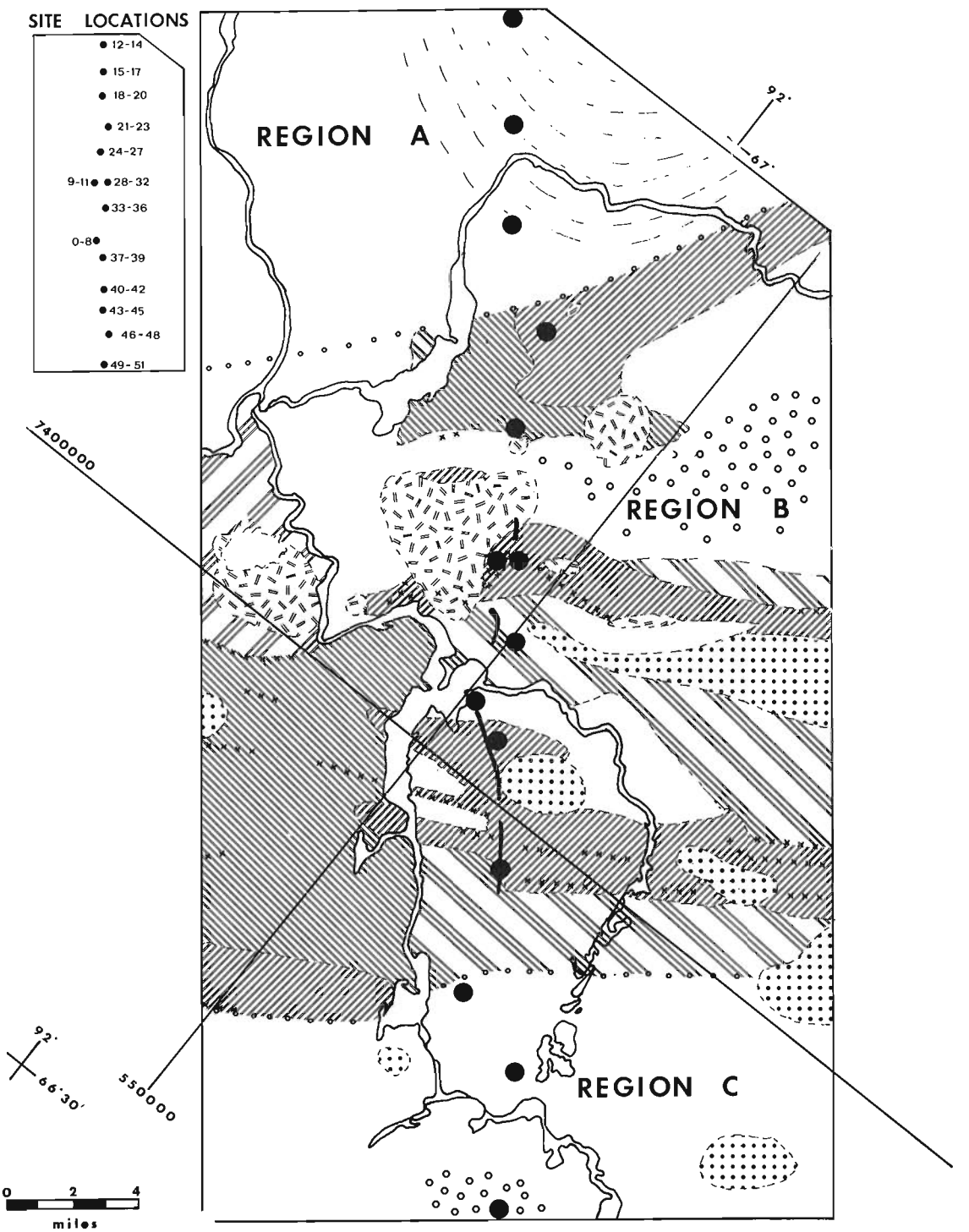

Figure 2. Sketch map of Hayes River region.

middle or low grade phenomena of considerable efficiency.

Magnetic studies have thus helped with assigning relative ages to various minerals. They reinforce the assertion based on geologic evidence that two periods of deformation and recrystallization are separated by sufficient time to allow emplacement of a now metagabbroic dyke. The latter event is Hudsonian, and arguing by analogy to other regions where the Prince Albert Group is involved in deformation, the first event is "Kenoran". The "old" and "new" gneisses must thus both be Archean in age.

Chemical Studies

Chemical studies of the gneisses have involved determination of 33 elements in samples taken from the three regions (Table 1). The gross similarity of

Table 1

Magnetic susceptibility of cores

Sites	Rock type	Region	Number of Determinations	Range of susceptibility Values in cgs units
0-8	Metagabbro	B	17	912 - 1 843
9-11	Metaperidotite	B	6	greater than 100 000
12-14	Gneiss, "New"	A	6	627 - 1 208
15-17	Gneiss, "New"	A	6	9 390 - 10 750
18-20	Gneiss, "New"	A	6	1 547 - 2 303
21-23	Gneiss, "New"	B	6	180 - 250
24-27	Gneiss, "Old"	B	8	9 870 - 15 480
28-32	Actinolite schist	B	9	1 032 - 8 280
33-36	Metaperidotite	B	6	51 400 - 63 000
37-39	Metasediment	B	6	less than 100
40-42	Metagabbro	B	6	1 162 - 2 399
43-45	Gneiss, "New"	C	6	526 - 1 648
46-48	Gneiss, "New"	C	5	825 - 2 600
49-51	Granite gneiss, "New"	C	5	31 500 - 47 000

Table 2

Rock types classified according to magnetic anisotropy

	Isotropic	Anisotropic		
	sphere	prolate spheroid	ellipsoid	oblate spheroid
New gneiss Region A	5	-	4	9
Do - Region B	-	4	2	-
Do - Region C	10	3	0	3
Old gneiss Region B	1	5	2	-
Metasediment	-	-	-	-
Actinolite schist	6	2	-	1
Metaperidotite	-	-	-	6
Metagabbro	11	10	1	1

Specimens are judged anisotropic if the F ratio given in Larochelle's Magnetic Anisotropy Program is greater than 99. This is a very cautious estimate - i.e. some of the material reported isotropic may well be thought to be slightly anisotropic by other workers.

Figure 3.

Surface of magnetic intensity in Hayes River region.

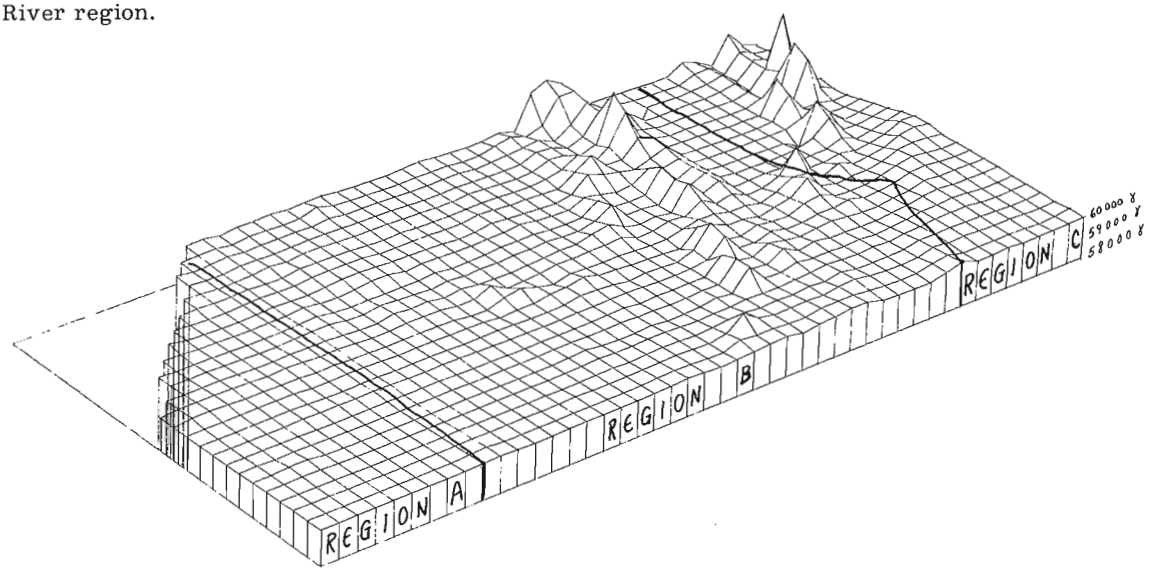

Table 3A

Selected analyses of Archean gneiss

Oxides	New Gneiss[1] Region A	New Gneiss[2] Region B	New Gneiss[3] Region C	Old Gneiss[4] Region B	Average[5] Gneiss
SiO_2	64.37	68.88	66.47	71.77	66.9
Al_2O_3	15.05	15.94	15.69	15.26	15.5
Fe_2O_3	1.41	0.13	.94	.49	.9
FeO	3.60	2.30	2.70	1.07	3.3
MgO	2.75	1.38	1.73	.79	1.5
CaO	4.97	3.48	3.53	1.90	2.9
Na_2O	4.27	4.06	4.38	4.91	3.7
K_2O	1.71	2.76	2.96	2.85	3.7
$H_2O_{(T)}$	.98	.60	.93	.45	.8
TiO_2	.64	.33	.48	.23	.55
P_2O_5	.23	.16	.22	.08	.20
MnO	.10	.04	.07	.04	.07
CO_2	.00	.00	.00	.00	.00
S	.00	.07	.01	.01	NM

[1]Average of 9 gneisses from sites 12-20.

[2]Average of 3 gneisses from sites 21-23.

[3]Average of 9 gneisses from sites 43-51.

[4]Average of 4 gneisses from sites 24-27.

[5]Average from Eade and Fahrig, 1971, p. 49 taken from Northern Keewatin district. Analyses by X-ray fluorescence and chemical analysis, Analytical Chemistry Section, Geol. Surv. Can.

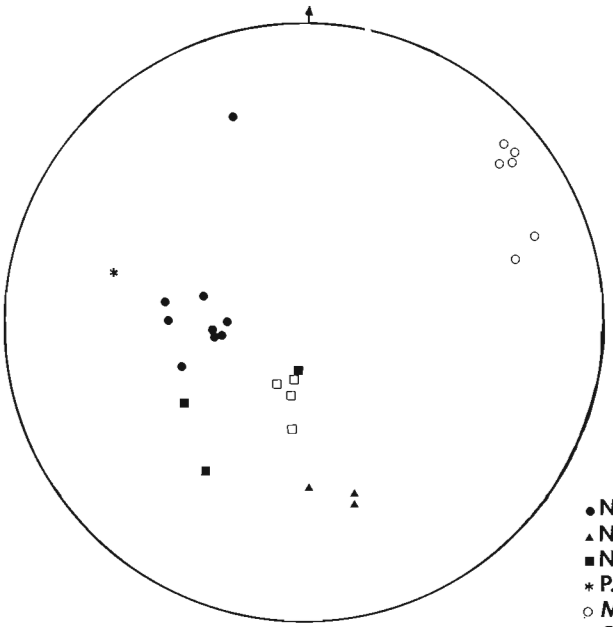

Figure 4A. Poles to foliation.

LEGEND

- NEW GNEISS (A)
- NEW GNEISS (B)
- NEW GNEISS (C)
- P.A.G. (B)
- METAPERIDOTITE (B)
- OLD GNEISS (B)
- METAGABBRO

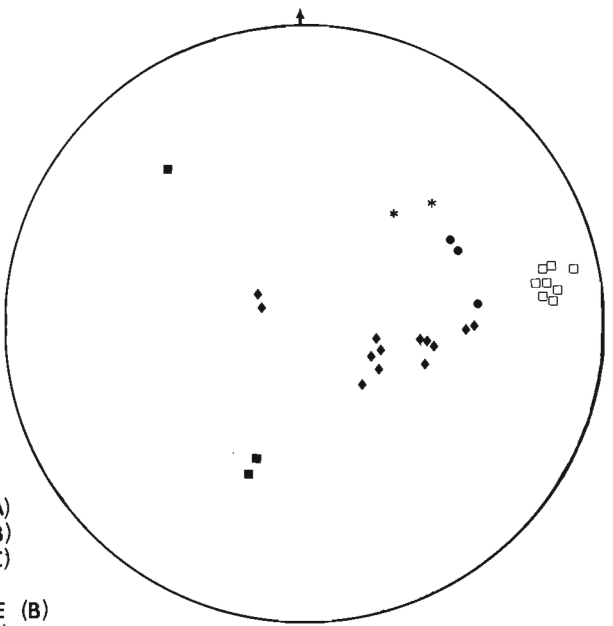

Figure 4B. Lineations.

Table 3B

Selected analyses of Archean supracrustals

Oxides	Quartzite[1] Region B or environs	Metasediment[2] Region B	Iron-formation[3] Region B	Actinolite[4] Schist Region B	Meta-komatiites[5] Region B + environs
SiO_2	98.7	70.72	39.70	44.93	43.7
Al_2O_3	.5	13.31	.78	12.21	6.6
Fe_2O_3	0	.07	36.10	5.51	2.8
FeO	0	3.73	18.00	11.82	8.6
MgO	0	1.89	1.90	7.16	20.90
CaO	.2	2.57	3.00	11.93	9.0
Na_2O	.1	3.41	.05	1.40	.54
K_2O	.2	2.71	.05	.75	.15
$H_2O_{(T)}$	.2	.80	.05	1.80	4.66
TiO_2	.09	.47	.02	1.56	.43
P_2O_5	0	.17	.24	.06	.05
MnO	0	.07	.05	.25	.25
CO_2	0	.00	.00	.00	1.46
S	0	.05	.04	.00	.20

[1]Quartzite from Eade and Fahrig, 1971, p.

[2]Metasediment from sites 37-39 (average of 3).

[3]Iron-formation from northern magnetic anomaly mentioned in text.

[4]Actinolite schist from sites 28-32 (average of 4).

[5]Average meta-komatiite (Schan, 1975).

Analyses by X-ray fluorescence and chemical anlysis, Analytical Chemistry Section, Geol. Surv. Can.

Table 4

Trace elements (in ppm) in selected Aarchean units

	New Gneiss Region A	New Gneiss Region B	New Gneiss Region C	Old Gneiss Region B	Metasediment Region B
Sr	347	523	515	342	342
Ba	420	616	1178	642	853
Cr	29	9.6	12	5	79
Zr	225	131	281	142	256
V	147	51	78	13	98
Ni	32	5	5	5	17
Cu	23	14	7	2	31
Y	10	10	18	10	10
Co	11	5	6	5	5
Sc	11	3.6	8.5	3.2	8.6
Zn	80	46	49	43	55
Pb	5.7	15.6	15.6	13	19
Sn	1.8	2.9	1.9	1.2	1.4
Ag	.033	.025	.025	.025	.046
Cl	1.5	1.0	1.3	1.5	
F	5.2	5.0	7.1	7.0	5.0
Rb	71	97	117	120	106
N	9	3	9	4	3

Analyses by spectrographic lab., Analytical Chemistry Section, Geol. Surv. Can.

Figure 5.

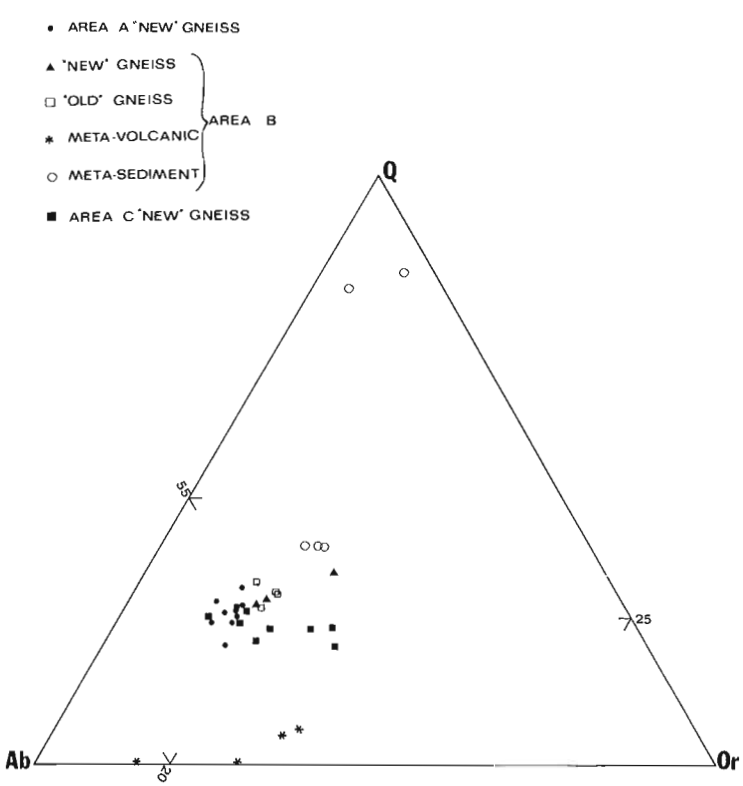

gneisses is noted - both with each other and with Eade and Fahrig's (1971, p. 49) average gneiss for this area. In Figure 5 the gneisses and selected supracrustals are plotted on a normative, cation-equivalent Q-Ab-Or diagram. "New" gneisses are generally homogeneous and not very different from "old" gneisses or any other gneiss, for that matter. Supracrustals (Table 3B) show the spread expected of compositionally distinct rocks such as meta-komatiites (Schau, 1975) or quartzites. Discriminant analyses of major elements show that gneisses cannot be easily distinguished. Trace elements may be of some help, however, in characterizing geologically separate groups. In region B, for instance, "new" and "old" gneiss differ in that Cr, V, Pb and S are significantly (using a discriminant function) higher in the "new" gneiss. Using these criteria one-half of the gneisses from the flanking regions are of "old" origins. If on the other hand we lump all the "new" gneiss together and contrast these with the preserved "old" gneiss, we find that V is much higher, CaO, Sr, MgO and Cr_2O_3 are higher, and Pb slightly lower in "new" gneiss compared to the older. Apparently V and Cr are useful in distinguishing gneisses from each other. The "new" gneiss from differing regions can be characterized using half the analyzed elements but the most important elements are Ni, Y, Pb and S. Possibly these variations in trace elements reflect the various proportions of old gneiss, supracrustal Prince Albert Group material and new added material that were mixed together to make the new gneiss. Presumably gneiss from region A with

a higher content of Ni has assimilated more of the ultramafic material than have the others. Pb and S are more abundant in metasediments and the "new" gneiss from regions B and C. If all 16 elements are utilized, new gneiss of region A and region B are more closely related to each other than either are with region C, a finding that agrees with the geology. It is apparent from these comments that it may be possible, with a larger sample, to utilize such elemental variations to provide quantitative limits to our geological speculations.

Conclusions

This pilot project has shown that gneisses can be separated from each other using a variety of techniques. In this case, detailed geologic observations confirmed by magnetic studies lead to the establishment of different groups of gneisses which, when analyzed, show minor but significant chemical differences. Whether these procedures applied in the opposite order would yield the same result is not known.

In terms of geological history of the small region studied in the northern Churchill Province, the complex history is now better understood. The region was underlain by "old" gneiss upon which supracrustal units of the Archean Prince Albert Group were deposited and emplaced. This sequence was then deformed during the Kenoran (?) about shallow plunging northeast axes, eventually leading to a high grade gneiss forming event which culminated in the emplacement of local granitic plutons. The rocks cooled and a gabbroic dyke was emplaced in the region. Later local adjustments about southeast axes led to minor folding and slippage along schistose planes of décollement as well as to low to medium grade crystallization throughout the region was accompanied by emplacement of small granitic plutons during the Hudsonian 700 m.y. later. Subsequent events, such as maghematization of iron-formations and faulting did not alter the geology of the region substantially.

Acknowledgments

Acknowledgments are gratefully extended to E. Schwarz for his interest and help with all the magnetic methods. G. Campbell drilled the sites, G. Freda and L. deBie processed some of the samples. Computer programs used were from BMD and divisional libraries. G. Martin helped with DDD program used to plot magnetic field map. Critical remarks by J.B. Henderson improved manuscript.

References

Davidson, A.
1972: Churchill Province; *in* Variations in Tectonic Styles, edited by R.A. Price and R.J.W. Douglas; Geol. Assoc. Can., Spec. Paper 11.

Eade, K.E. and Fahrig, W.F.
1971: Geochemical evolutionary trends of continental plates - A Preliminary Study of the Canadian Shield; Geol. Surv. Can., Bull. 179, 51 p.

1973: Regional, lithological, and temporal variation in the abundances of some trace elements in the Canadian Shield; Geol. Surv. Can., Paper 72-46, 46 p.

Heywood, W.W.
1961: Geological notes, northern District of Keewatin; Geol. Surv. Can., Paper 61-18, 9 p.

Schau, Mikkel
1974: Volcanic rocks of the Prince Albert Group, District of Keewatin; *in* Report of Activities, Part A, April to October 1973, Geol. Surv. Can., Paper 74-1, Pt. A, p. 187-188.

1975: Komatiitic and other ultramafic rocks in the Prince Albert Group, Hayes River Region, N.W.T. *in* Report of Activities, April to October 1974, Geol. Surv. Can., Paper 75-1, Pt. A, p. 363-367.

Schau, Mikkel and Campbell, S.W.
1974: Gneiss distinctions in the Hayes River Region, District of Keewatin; *in* Computer use in projects of the Geological Survey of Canada, (eds.) Terry Gordon and W.W. Hutchison, Geol. Surv. Can., Paper 74-60, p. 49-54.

Stockwell, C.H.
1963: Second report on Structural Provinces orogenies and time classification of rocks of the Canadian Precambrian Shield *in* Lowdon, J.A., Stockwell, C.H., Tipper, H.W. and Wanless, R.K., Age determinations and geologic studies; Geol. Surv. Can., Paper 62-17, p. 123-133.

Winkler, H.G.F.
1974: Petrogenesis of Metamorphic Rocks; 3rd Edition, Springer Verlag, N.Y., 320 p.

22. ASSESSMENT OF TERRAIN PERFORMANCE IN THE MACKENZIE VALLEY AND THE ARCTIC ISLANDS

Project 740046

P. J. Kurfurst
Terrain Sciences Division

This project was initiated in May 1974 as an extension of Project 710077, which was located in the Mackenzie Valley (Heginbottom and Kurfurst, 1972, 1973; Kurfurst, 1974). The main objective for the field season was a reconnaissance study of different types of man-caused and natural disturbances in the Arctic Islands with special reference to man-made structures such as airfields, access roads, old oil well sites, abandoned campsites, and related activities. Special emphasis was placed upon the investigation of terrain and permafrost conditions and ground ice content in various surficial materials and the possible implications for pipeline and other construction activities in the Arctic.

Several weeks of detailed study of sequential aerial photographs preceded field investigation in order to evaluate all terrain changes resulting from traffic, engineering, and construction activities.

Approximately four weeks were spent in the Arctic Islands during the 1974 summer. Two weeks of field investigation was conducted on Cornwallis Island around Resolute Bay, ten days were spent around Cambridge Bay on Victoria Island with a short visit to Eureka on Ellesmere Island. Two short reconnaissance trips were made to Bathurst Island but detailed field work was postponed until summer 1975 due to bad weather conditions and heavy snow cover. Ten sites with terrain

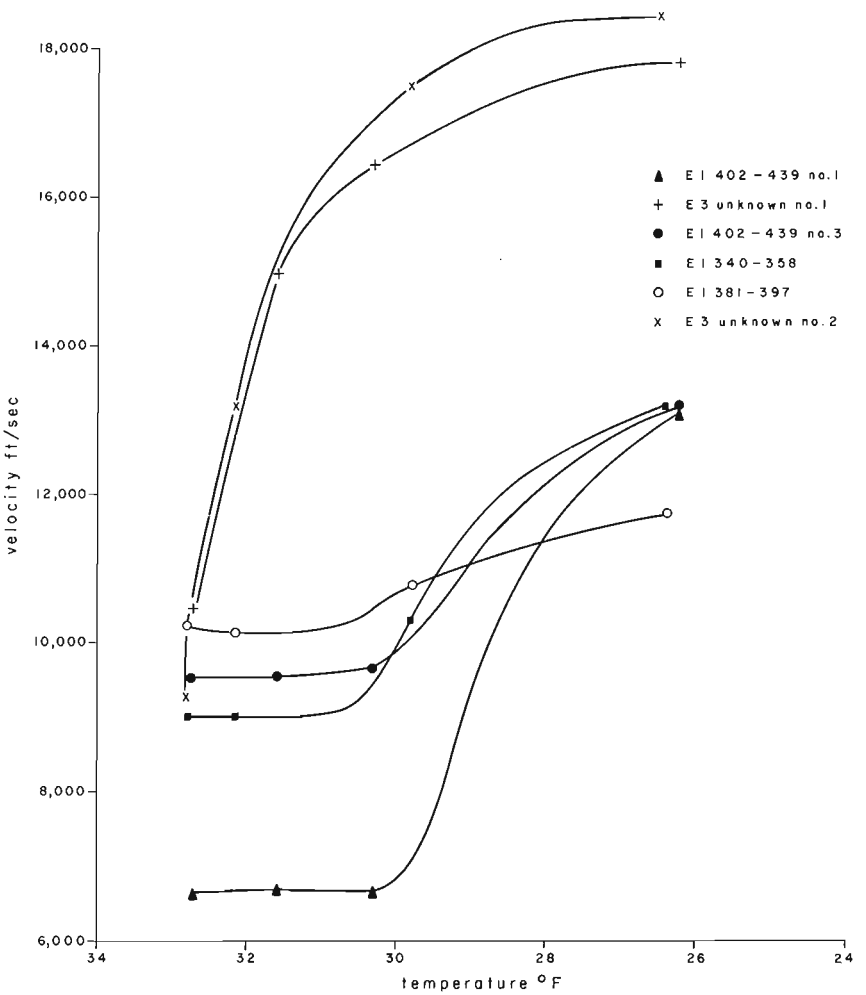

Figure 1. Compressional wave velocities vs. temperature

likely susceptible to disturbance were identified as potential drill sites for the 1975 field season.

Additional more detailed studies of sequential black and white as well as colour aerial photographs followed field investigation with the main emphasis being placed on particular areas of old and fresh man-made and natural disturbances that were identified in the field. This stage has been almost completed and results are in the process of being evaluated.

No final conclusions can be drawn at this stage, but preliminary field observations and results of the aerial photographs study seem to indicate that the rate of terrain change due to man-made disturbances is slower in the Arctic Islands than in the Mackenzie Valley. This is probably due to lower mean annual air and ground temperatures, shorter summers, and hence a thinner active layer.

A number of frozen core samples from various geomorphological units were recovered from several drill sites around Eureka where shallow seismic measurements were conducted. The samples were kept frozen for further laboratory ultrasonic tests and for determination of their engineering properties (natural moisture content, Atterberg limits, and sand-silt-clay ratio) in the soil testing laboratory. The samples varied from silty sands to sandy and clayey silts with moisture content ranging between 17 and 61 per cent.

Ultrasonic velocities measured on samples in the laboratory showed sharp increase with decrease in temperature at temperatures below 31°F. Typical results are shown in Figure 1. These results were compared with the results obtained from shallow seismic profiles shot in the field at the sampled drill sites at the time of drilling. The values of field velocities lie within the range of laboratory measurements (Table 1) and therefore prove that the laboratory tests provide a measure of control in the interpretation of the seismic records.

Table 1

Drill site	Material	Compressional wave velocities ft/sec	
		Field data	Laboratory data
E1 340	sandy loam	9900	10307
E1 381			10758
E1 402-1			9864
E1 402-3			6651

References

Heginbottom, J.A. and Kurfurst, P.J.

1972: Terrain sensitivity evaluation and mapping — Mackenzie Valley Transportation Corridor; *in* Report of Activities, Part A, Geol. Surv. Can., Paper 72-1, pt. A, p. 145-146.

1973: Terrain sensitivity evaluation and mapping — Mackenzie Valley Transportation Corridor; *in* Report of Activities, Part A, Geol. Surv. Can., Paper 73-1, pt. A, p. 226-229.

Kurfurst, P.J.

1974: Terrain sensitivity evaluation and mapping — Mackenzie Valley Transportation Corridor; *in* Report of Activities, Part A, Geol. Surv. Can., Paper 74-1, pt. A, p. 279.

23. QUATERNARY LANDSCAPES: PRESENT AND PAST — AT MARY HILL, COQUITLAM, BRITISH COLUMBIA (92G/2f)

Project 730153

John E. Armstrong and Stephen R. Hicock
Terrain Sciences Division, Vancouver

Introduction

The Fraser Lowland, which forms the southwest corner of the mainland of Canada, is a triangular shaped area of low relief with its apex 105 km east of the Strait of Georgia. It is bounded on the north by the Coast Mountains and on the southeast by the Cascade and Chuckanut Mountains, and has an area of approximately 3500 km^2, of which approximately 2600 km^2 are north of the Canada-United States boundary. The dominant geomorphological feature of the Fraser Lowland is the Fraser River which occupies a late glacial and post-glacial valley up to 5 km wide and 225 m deep. This river terminates in a growing delta 31 km long and 24 km wide. North and south of Fraser River valley, the Fraser Lowland consists mainly of flat topped and gently rolling low hills, separated by wide, flat-bottomed valleys. Most of the hills consist of unconsolidated deposits and do not exceed 155 m in elevation, although 3 bedrock hills exceed 300 m. The hills range in area from about 3 to 400 km^2.

In the western part of the Fraser Lowland these hills normally consist of unconsolidated deposits laid down during several major advances and retreats of continental glaciers and during several non-glacial or interglacial intervals. Each major ice advance and retreat was accompanied by eustatic and isostatic sea level changes of up to 230 m. Armstrong (1975) has stated that five major Pleistocene formational units, each probably representing a major geologic-climatic unit, are exposed in the Fraser Lowland. He also tabled a pre-last glaciation stratigraphic succession consisting of 26 lithologic units. Revisions since last summer (1974) show that additional units may be identified. No one stratigraphic section is found illustrating all these older units. The reason is that all the hills in the western part of the Fraser Lowland are in fact composite hills. Each contains within it, parts of one or more buried older hills that represent buried and eroded Quaternary landscapes. Consequently the unravelling of the stratigraphic succession becomes very complex (especially as lithologic units of different chronologic ages may closely resemble one another), and without absolute chronologic ages, may be impossible to separate. Mary Hill, one of the smaller hills (about 5 km^2), best illustrates these problems.

Mary Hill

Mary Hill is surrounded by wide, flat-bottomed valleys of the Fraser, Pitt, and Coquitlam rivers. The hill is approximately 3050 m long, 1500 m wide, and 95 m in elevation. The southern part of the hill has been the site of a major gravel and sand operation since 1928. The pit is approximately 750 m by 1200 m in area and over the years at least 20 million m^3 of material has been removed. The present operator of the pit is Construction Aggregates Ltd. who will terminate the operation in 1975 because of zoning regulation. Armstrong examined the pit on many occasions between 1951 and 1965 and drew many cross-sections, revising them each time new information was obtained. The reconstructed cross-section (Fig. 1) incorporates this previous material obtained by Armstrong with that observed by both writers in 1974. Hicock established the contact between the Quadra Sediments and Semiahmoo Drift, and in so doing uncovered a buried landscape.

The topographic form of Mary Hill results from late glacial and postglacial river erosion and from marine erosion during the deglaciation period of the last major glaciation. The hill is not recognizable as a glacial geomorphological landform.

Mary Hill Stratigraphy

The cross-section demonstrates that Mary Hill is underlain by deposits related to two major glaciations and, depending on the terminology accepted, two interglacial or interstadial sedimentary sequences (Fig. 1); Armstrong, 1953, 1956, 1957, 1965, 1975; Leaming, 1968). These four major geologic-climatic units are separated by unconformities, which are in part non-depositional buried landscapes and in part modified by later stream or ice erosion.

The following stratigraphic succession has been established:

Fraser Glaciation (11 000 - 22 000 radiocarbon years B.P.)

- Capilano Sediments - glaciomarine sediments and marine lag gravels.
- Vashon Drift - at least three tills, glaciofluvial and ice-contact deposits.

Olympia Interglaciation (22 000 - 44 000? radiocarbon years B.P.)

- Quadra Sediments - proglacial and fluvial sand and gravel, organic sediments, silt, and fine sand. Radiocarbon dates:
  GSC - 2107, 27 400 ± 420;
  GSC - 536, 27 180 ± 460;
  GSC - 124, 26 450 ± 520.

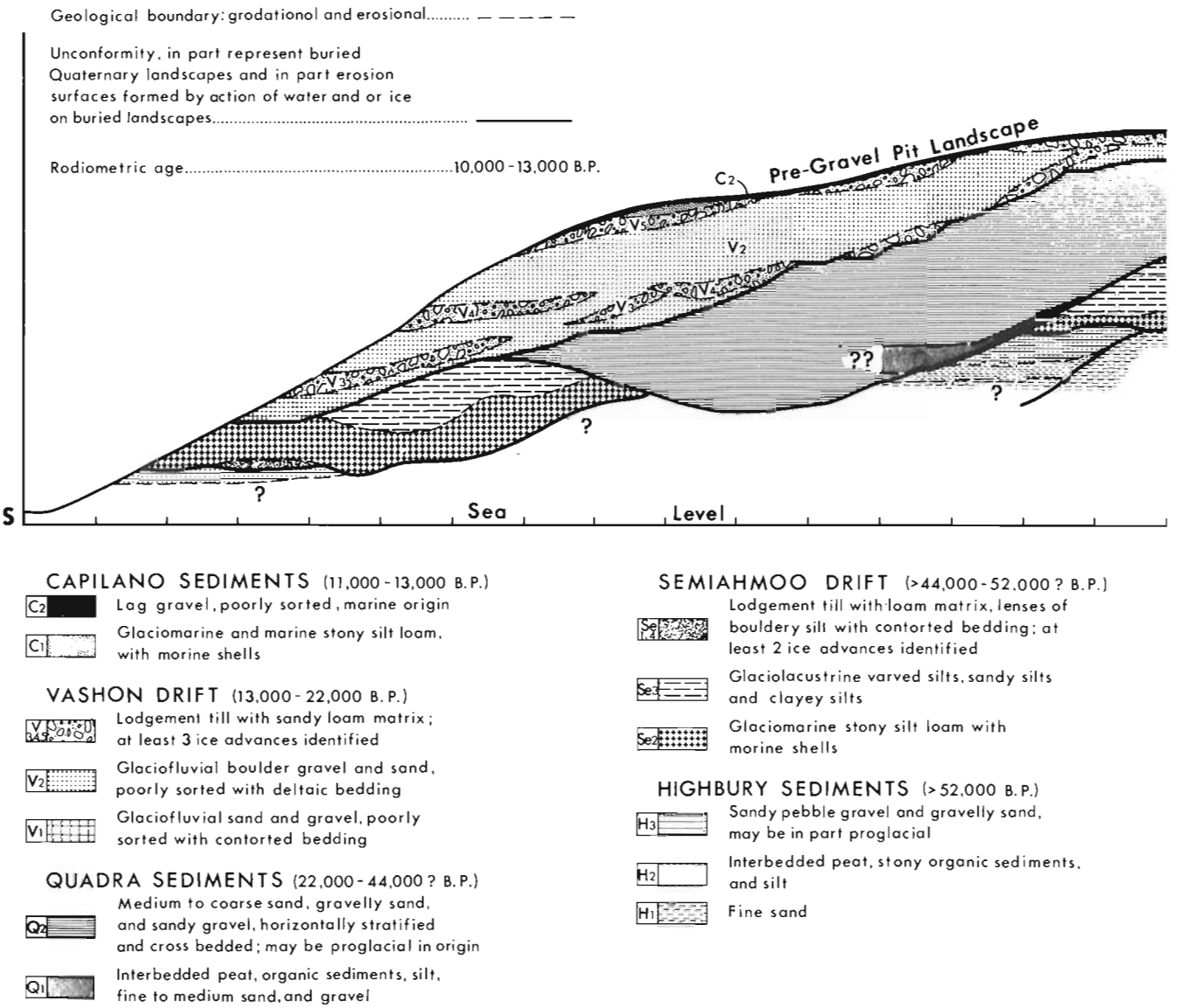

Figure 1. Reconstructed composite section Mary Hill Gravel Pit, Coquitlam, British Columbia.

Major Glaciation (> 44 000 - 52 000)

Semiahmoo Drift - at least two tills, glaciomarine, glaciolacustrine, and glaciofluvial sediments. Radiocarbon date: GSC - 2091, > 44 000; GSC - 2120, > 48 000.

Interglaciation or Interstadial (> 52 000 radiocarbon years B.P.)

Highbury Sediments - fluvial sand and gravel, organic sediments, silt, and fine sand.

The major ice sheets that deposited the Vashon and Semiahmoo Drifts moved southward from the Coast Mountains. This direction of ice movement was apparently the cause of very thick Vashon drift deposits accumulating on the south slope of Mary Hill where at least three southward dipping Vashon tills and thick glaciofluvial sandy gravels are exposed. Each Vashon till is truncated by the next youngest till. Similar Vashon Drift is found on the southern slopes of many other hills in the western part of the Fraser Lowland. At Mary Hill (and elsewhere) the youngest Vashon till mantles the hill, except where completely eroded by late glacial and postglacial marine action, which suggests that the hills had approximately their present landforms when the last ice advance took place.

The Semiahmoo Drift is much more poorly exposed; where the drift is seen however, it appears to have the same southward dip and also seems to have been deposited on a pre-Semiahmoo Pleistocene hill that only in part was modified by the ice advance. Closely

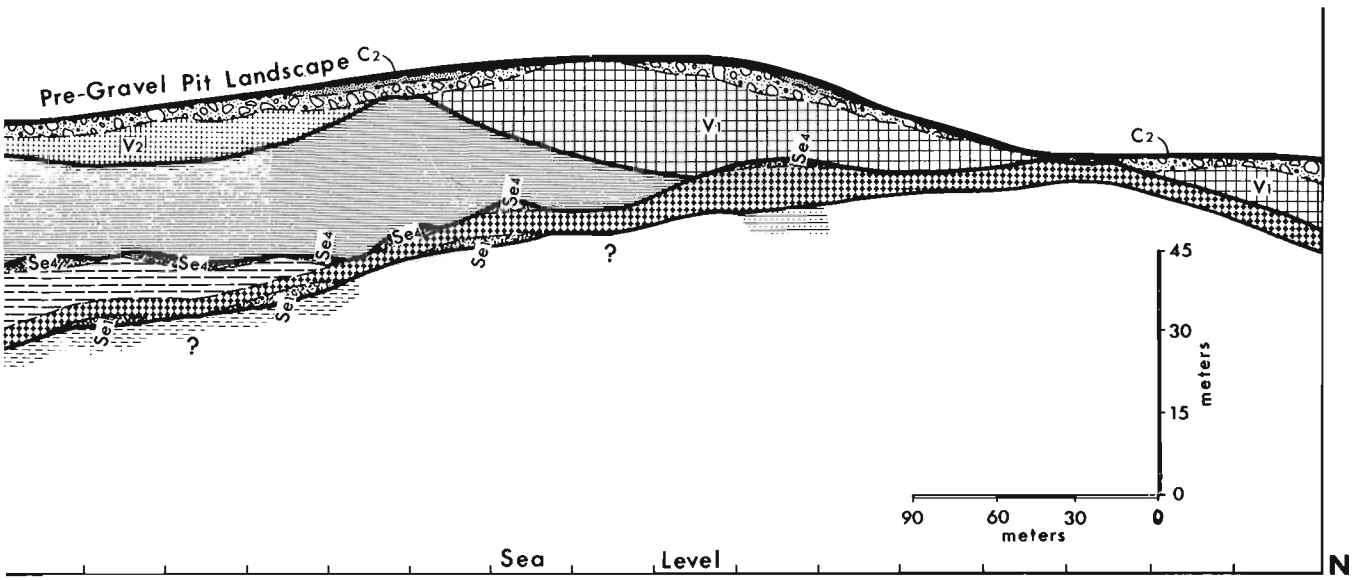

associated with the Semiahmoo tills are glaciomarine and glaciolacustrine sediments which may represent an ice standstill.

The two interglacial or interstadial sedimentary sequences are similar. Both contain thick sections of organic sediments exposed at approximately the same elevations in the pit. At first they were thought to be correlatives of the same age, however, Hicock has been able to show they are separated by a marked unconformity as illustrated in the cross-section (Fig. 1). Both are exposed in gullies, about 120 m apart, in the centre of the pit between elevations of 30 and 65 plus m. The two sequences are as follows (elevations are to the nearest 0.5 m):

Quadra Organic Sediments (ca. 27 000 radiocarbon years B.P.)

Elevation	Lithographic Unit
49-65 m	Cross-bedded sand, minor gravel; organic layer about 3 cm thick at 63 m.
48-49 m	Fibrous peat containing wood fragments and leaves.
39-49 m	Stony silty organic sediment containing wood and peat fragments, also clasts of glaciolacustrine sediments. This material, which has a maximum thickness of 1.5 m, has been deposited on a paleoslope believed to be part of a buried Quaternary landscape. The deposit probably was formed by a mud slide. It is overlain on both sides of the gully by sand and gravel.
38-39 m	Fibrous peat with logs and tree trunks; largest log observed is 3 m by 0.6 m. Also contains fossil beetles.
37-38 m	Silt and sand containing finely disseminated organic debris.
36.5-37 m	Fibrous peat with wood fragments.
34-36.5 m	Silt and sand containing finely disseminated organic debris.
33.5-34 m	Fibrous peat with wood fragments.
30-33.5 m	Silt and sand containing finely disseminated organic debris.

Highbury Organic Sediments (Probably more than 52 000 radiocarbon years B.P.)

37-39 m	Sandy gravel containing a thin layer (3 cm) of peat with wood at 38 m.
33.5-37.0 m	Massive peat with fragments of wood that appears to have been deposited on a buried slope. The thickness of the peat is not known. It is overlain on both sides of the gully by fine silt and sand between 33.5 and 35 m and by sandy gravel from 35 to 37 m.
32.5-33.5 m	Massive peat with fragments of wood.
3-32.5 m	Stony organic sediment with boulder up to 1 m in diameter. Probably deposited along a shoreline of a pond into which an intermittent stream was flowing, carrying the stones.
30-31 m	Fine brown sand containing organic debris.
29-30 m	Massive peat with wood fragments.

No pollen studies have been undertaken on either of these organic sequences.

The Quadra organic sediments are overlain by at least 30 m of cross-bedded sand and gravel that may be partly proglacial in origin. These have been included in the lithologic unit called Quadra. The contact between the Quadra Sediments and the Vashon Drift is mainly erosional; however, the writers believe that at the end of the Quadra, a hill existed at Mary Hill and that the contact, in part, is an eroded older landscape. Also, at the close of Semiahmoo glaciation a hill existed in this area and the contact mapped is a pre-Quadra non-depositional landscape and a pre-Quadra landscape that has been eroded by Quadra streams. Similarly when the Semiahmoo ice advanced, it rode over a pre-Semiahmoo landscape modifying it by erosive action.

Quaternary History

Commencing with the oldest sediments exposed the geological history of Mary Hill may be summarized as follows:

1. The oldest Highbury Sediments found in the pit are organic deposits. They were formed in a swamp overlapping an older hilly landscape as evidenced by the buried slope and by the boulders in some of the organic sediments. These boulders possibly may be attributed to intermittent streams flowing off a higher slope into the swamp. The climate at this time may have been as warm as the present day climate, however, only pollen and insect studies will confirm this.

2. The Highbury swamp deposits are overlain by fluvial sediments laid down by streams which eroded the pre-existing hilly landform. These fluvial deposits, which also have been mapped as Highbury, are possibly proglacial in origin, representing a climatic interval between a relatively warm climate and a glacial climate. A landscape was developed on these sediments.

3. A major glaciation, represented by the Semiahmoo Drift, resulted from this cooling climate. During the first Semiahmoo ice advance, basal till and glaciofluvial sediments were deposited and the pre-existing landscape was partly eroded; however much of the pre-Semiahmoo hill is preserved. This first Semiahmoo ice advance brought about an isostatic depression of the land of at least 65 m as seen at Mary Hill and probably at least 200 m as surmised elsewhere in the Fraser Lowland. Following this ice advance, the area was invaded by the sea and glaciomarine deposits were laid down to elevations of 55 m. As the land rose above sea-level, a glaciomarine environment was replaced by a glaciolacustrine environment and varved silts were deposited to elevations of 55 m. Wood from these silts gave radiocarbon dates of greater than 44 000 years. In this area a second Semiahmoo ice advance moulded and ploughed up the earlier sediments and deposited a basal till.

4. As a result of climatic warming, the Semiahmoo glaciation came to a close. A hilly landscape had once again been formed.

5. The Quadra Sediments of the Olympia Interglaciation were deposited during this second warm period which may have lasted 25 000 years. These sediments consist of fluvial and swamp deposits with many characteristics similar to those of the Highbury Sediments. Some fluvial sediments are older and some younger than the swamp deposits. During their initial deposition, the streams associated with them deeply eroded the Semiahmoo landscape and a basin-like depositional area was formed. In places the entire Semiahmoo Drift sequence was destroyed by stream erosion. Some of the swamp deposits were laid down at the margins of the basin. As already described, sliding occurred at this basin margin. The climate during this period is believed to have been similar or slightly cooler than the present day climate.

6. The Quadra organic deposits are overlain by thick fluvial sediments which were deposited by streams that channelled into the swamps. These fluvial sediments, which have been included in the Quadra lithologic unit, probably were laid down during the transitional period from a relatively warm to a glacial climate. They may be proglacial in origin, that is, the streams that carried them debouched from glaciers.

7. A continued cooling resulted in a glacial climate once again, commencing about 22 000 years ago and lasting about 11 000 years. The Mary Hill pit records three local advances of ice during this period, each accompanied by deposition of till and glaciofluvial sediments. The tills all appear to be basal and each seems to be moulded to a pre-existing, short-lived, hilly landscape. These landscapes were deeply eroded by ice and stream action, although this erosion has not obliterated the shapes of the original landforms. At the maximum advance of the Vashon glaciers, the land was isostatically depressed at 210 m and if eustatic lowering of the sea level is taken into account, this figure probably would be at least 310 m. During Vashon deglaciation the sea invaded the area and covered Mary Hill. An isostatic rebound and eustatic adjustments took place and the land rose to its present position and was mantled by glaciomarine sediments and lag marine gravel. These adjustments were not uniform and good evidence is available in the eastern part of the Fraser Lowland that two or more major marine invasions occurred. Although tectonic adjustments undoubtedly took place, their importance and magnitude are completely unknown.

Conclusion

The main purpose of this short paper is to illustrate the complex geological makeup of the hills in the western half of the Fraser Lowland. Mary Hill is only one example but is the best documented. The geology of Burrard, Surrey, and Port Moody uplands is equally complex, as is that of the lower slopes of the Coast Mountains. The writers hope that the cross-section (Fig. 1), which is part of a three dimensional study, demonstrates the unreliability of attempting to correlate Quaternary sediments seen in two dimensions only or

intersected in drillholes only. Correlations made on other than a three dimensional study at best are tentative and should be supported wherever possible by radiocarbon dates.

Because of the multiple unconformities found in the sediments underlying Mary Hill, drillhole information only could lead to completely misleading conclusions. Sixteen lithologic units have been mapped in the cross-section; however, no drillhole would penetrate more than 10 units and in places as few as four.

References

Armstrong, J.E.

1953: Geology of sand and gravel deposits in the Lower Fraser Valley, British Columbia; Can. Mining Met. Bull., April 1953, p. 1-8.

1956: Surficial geology of the Vancouver area, British Columbia; Geol. Surv. Can., Paper 55-40. 16 p.

Armstrong, J.E. (cont'd)

1957: Surficial geology of the New Westminster map-area, British Columbia; Geol. Surv. Can., Paper 57-5, 25 p.

1965: Pacific Northwest; Guidebook for Field Conf., INQUA, VIIth Cong., Nebraska Acad. of Sciences, p. 105-107.

1975: Quaternary geology, stratigraphic studies, and revaluation of terrain inventory maps, Fraser Lowland, British Columbia; *in* Report of Activities, Part A, Geol. Surv. Can., Paper 75-1, pt. A, p. 377-380.

Leaming, S.F.

1968: Sand and gravel in the Strait of Georgia area; Geol. Surv. Can., Paper 66-60, p. 46-47.

24.

INTERDISCIPLINARY ENVIRONMENTAL DATA PRESENTATION FOR EASTERN MELVILLE ISLAND: AN APPROACH

Projects 710041 and 710042

D. M. Barnett, S. A. Edlund and L. A. Dredge
Terrain Sciences Division

The integrated pilot mapping project of eastern Melville Island, initiated in 1973 (Barnett and Dredge, 1974), was designed to gather and correlate baseline data dealing with a range of environmental factors of possible concern for future environmental management including potential pipeline routing.

The approach was designed to produce a coherent environmental statement based on both field and air-photo interpretation for more than 6000 square miles mapped at 1: 125 000. Such a system is believed to be readily applicable throughout the Sverdrup Basin and possibly farther afield. This note deals with date presentation ancillary to the basic photomosaics.

The landscape of eastern Melville Island, like much of the Sverdrup Basin, is composed of folded sedimentary strata with generally little evidence of glacial modification and sparse glacial deposits. Many of the strata are either poorly or moderately lithified. The diversity of lithology and varying resistance to erosion creates a variety of distinct landscapes dominated by the geological structure. Vegetation is not abundant, but that which does occur commonly grows in the weathered mantle. The types of plant communities are directly influenced by the materials at the surface. Another major attribute of the landscape is the effect of postglacial marine submergence ranging up to 85 m above present sea level; it has left a discontinuous marine veneer which in many areas is strikingly picked out by vegetation and in others, is seen in more subtle ways. This veneer has led to a more complex landscape at the lower levels.

A three level hierarchy was formulated for presentation of the Melville Island data. Although rank is implicit in a hierarchy, in practice the ranks indicate degree of generalization of the data. The names as assigned to the levels are "Landscape Type", "Geobotanical Facies", and "Terrain Units", each being a natural subdivision of the rank above. In this way the user has a choice of the various aspects of the landscape which he may wish to examine and a choice of three levels of detail.

Regional Unit: LANDSCAPE TYPE. This basic unit of the landscape is based on published geological formation boundaries but it includes additional units such as Quaternary Alluvium and Quaternary (?) brown gravels. A characteristic geomorphology is inherent in this unit as well as distinctive vegetation. The expanded legend covers a range of information pertinent to the scale of the unit.

Intermediate Unit: GEOBOTANICAL FACIES. This unit is a natural subdivision of the Landscape Type unit having composite distinctive character, including vegetation, while retaining visible affinity with the larger unit, or bedrock unit masked by veneer of variable thickness showing some characteristics of the underlying unit.

Detailed Unit: TERRAIN UNIT. This unit is a subdivision of the Geobotanical Facies unit having distinctive character detectable on air photographs. These units recur on a variety of different landscape types. At this most detailed level, greatest judgment is required in order to limit the different units to a manageable number. The numerical format allows for the addition of further terrain units from other environments.

Eleven 1: 125 000 airphoto mosaics have been released using this hierarchical system for presentation on three map sheets. Twenty Landscape Type units were described and each assigned a letter code conforming to geologic convention. These units were subdivided into Geobotanical Facies represented by a single digit which follows a convention from 1 for Alluvium, then increasing in number from sea level upwards. Fifty-one distinct Terrain Units were recognized within the sum of the Geobotanical Facies. These units recur throughout eastern Melville Island. None are exclusive. Terrain Units are assigned a three digit number which follows a decimal point separating it from the Geobotanical Facies. In the Terrain Unit portion the lead digit indicates the primary basis for pattern recognition, with 0 indicating landform, 1 indicating veneer, and 2 indicating geobotanical pattern. In addition the landform group further is subdivided so that the second digit of the group of three is as follows: 0 indicates a fluvial environment, 2 a coastal environment, 4 a periglacial environment, 6 a glacial environment, 8 a bedrock controlled environment, and 9 a localized deposit. Each Terrain Unit within a Landscape Type, therefore, has a specific address (Fig. 1).

Accompanying the maps are expanded legends (sample section shown in Fig. 2) where the units are divided into four environmental variables which are treated at three ranks corresponding to the three mapping levels, to enable information storage and retrieval at each level (in anticipation of a range of questions requiring differing degrees of detail). The section

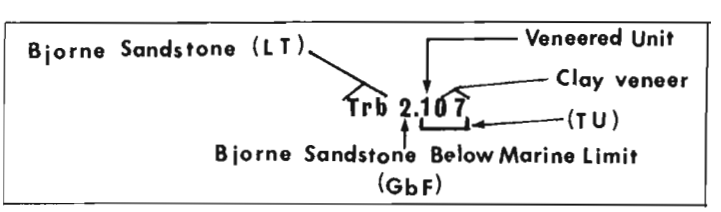

Figure 1. Example of address using the alpha-numeric code.

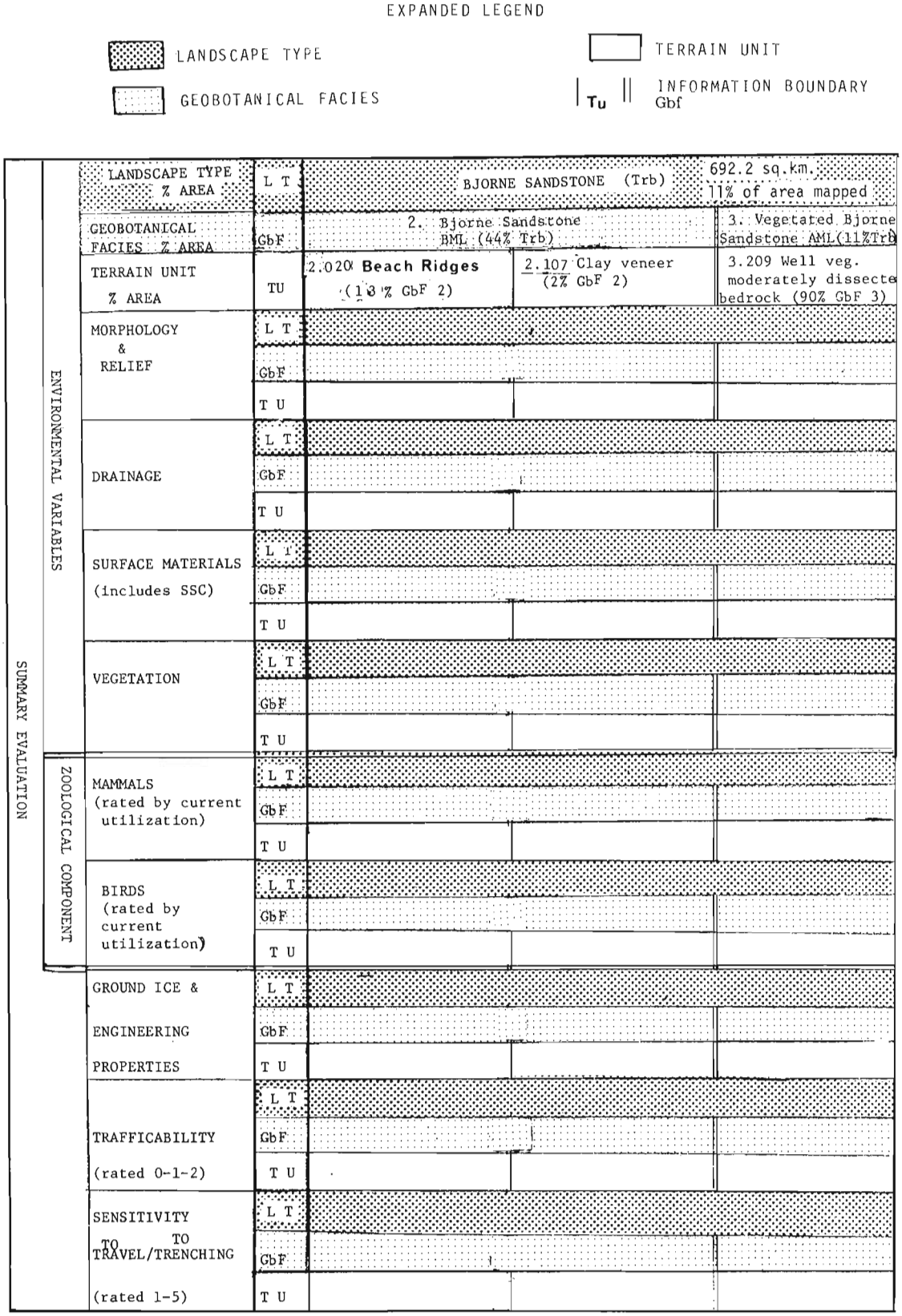

Figure 2. Each environmental component is treated at the three levels of detail (heavy stippling for Landscape Type, lighter stippling for Geobotanical Facies, no stippling for Terrain Units). This allows the user to select the required level of detail for each question posed.

designated "Summary Evaluation" involves value judgments based on both hard data and field experience, as the reconnaissance nature of the project did not permit more rigorous sampling. The maps and legends are available through G.S.C. Open File 252 (Barnett *et al.*, 1975). An encyclopedic text, corresponding to the legend format is part of the Open File and enables the user to obtain rapidly, specific answers to more detailed questions. Available information on any Terrain Unit type can be located in the text in 30 seconds by using the alpha-numeric code.

References

Barnett, D.M. and Dredge, L.A.
1974: Surficial geology and geomorphology of Melville Island, District of Franklin; *in* Report of Activities, Part A, Geol. Surv. Can., Paper 74-1, Pt. A, p. 239.

Barnett, D.M., Edlund, S.A., Dredge, L.A., Thomas, D.C. and Prevett, L.S.
1975: Terrain classification and evaluation, eastern Melville Island, N.W.T.; vols. I and II. Open File 252, Geol. Surv. Can., 747 and 571 p., incl. 3 map sheets and 3 legend sheets.

25. GLACIAL STYLE AND THE QUATERNARY STRATIGRAPHIC RECORD IN THE ATLANTIC PROVINCES, CANADA

Project 700056

D. R. Grant
Terrain Sciences Division

Quaternary sequences in Atlantic Canada are fragmentary and varied. Consequently, their interpretation has lagged while systematic terrain study commences to outline the causal events from other evidence. From ice-flow indicators a satisfactory account of the progress, pattern, and sequence of glacial movements now permits scattered deposits to be understood and integrated (Fig. 1). Given that glacial/interglacial cycles affected the landmass, the problem has been first to infer the probable terrestrial and marine effects, and then adduce the stratigraphic evidence. The glacial style in this region of uplands cut by deep submarine lowlands is characterized by growth and coalescence of separate ice caps, and their eventual incorporation by an advancing inland ice sheet. This model accounts for most features. As examples, superposed dissimilar tills are found where ice-flow reversal occurred, and subtill ancient organic beds occur in rugged areas of ice accumulation.

No deposits predating the last glacial cycle are recognized. The earliest is an emerged subtill marine bench and terrace in Cape Breton that tentatively is assigned to the Sangamon period of higher eustatic sea level. The controversial Bridgewater Conglomerate - a widespread but patchy iron-cemented gravel and a supposed correlative diamicton with glacial attributes - locally incorporated into younger tills, is arbitrarily assigned to the early Wisconsinan. All but one of twelve known buried organic deposits are beyond the limit of radiocarbon dating, and because their pollen indicate a nonglacial interval of cool boreal forest aspect, and because two rest on till on the Sangamon surface, these are placed in the early Wisconsinan St. Pierre Interstadial. The absence of similar beds of finite age dating from the mid-Wisconsinan Interstadial is taken to suggest that glacial cover persisted through this period, except perhaps in coastal areas where one bed, the intertill Salmon River Sand, contains a marine molluscan fauna dating 39 000 years B.P. (44 000 years by U/Th). The re-expansion of separate upland ice caps that began the late Wisconsinan Substage deposited tills of local derivation. As growth led to the maximal ice flood, a southward-moving ice sheet deposited the Lawrencetown Till whose distinctive red clay matrix and indicator erratics are of distant derivation. During deglaciation, shrinkage to local centres was interrupted by readvances ca. 12 700 and 10 500 years B.P. that emplaced local tills over outwash or marine beds, while in extraglacial areas a colluvial equivalent was accumulating. Ice withdrawal during the period 14 000 to 10 000 years B.P. was recorded in depressed coastal areas by a gravel/silt sequence, the Five Islands Formation, and by outwash trains in valleys leading to late centres. Finally, the sedimentary record of Holocene climatic improvement includes layered peat bogs, and an intertidal mud sequence and barrier dune episode related to the Flandrian transgression.

MAIN EVENTS	NEW BRUNSWICK	PRINCE EDWARD ISLAND	BAY OF FUNDY		MAINLAND NOVA SCOTIA						CAPE BRETON ISLAND				NEWFOUNDLAND		Stadials $ Interstadial	Sub-stages
			Minas Basin	Joggins	Salmon River	Cape St. Mary	Weymouth	Milford	Halifax	S. Shore	generalized	Whycocomagh R. Inhabitants	Castle Bay	Bay St. Lawrence	Bay St. George	N. Penin.		
eustatic and relative rise of sea level = estuarine sedimentation and barrier-building	tidal marsh	tidal marsh	tidal marsh	tidal marsh	intertidal marsh				intertidal marsh						Salt marsh			FLANDRIAN
local glacial readvance 10,5 - 11,400 y. B.P.											Mabou coll. Englishtown readvance	till				10-MILE FM	Y. DRYAS	Late Wisconsinan
moraine-building halt or readvance during recession, 12,700 y. B.P.			Parrsboro end moraine	local till					granite till	slate till				fan gravels, colluvium	Robinson's Head Drift	Piedmont moraines	"Port Huron"	
marine overlap on deglaciated depressed coasts <14,000 B.P.	emerged marine sand + gravel	emerged marine beds	Five Islands Formation		marine sand + gravel	marine sand + gravel			boulder horizon	erosional interval	outwash	outwash			Bay St George Delta	stony pelite		
glacial retreat by calving toward present coastline	coastal end moraines		till		till (from inland)	shale till	red-brown till	red clay till	Lawrencetown red drumlin till / local ground moraine	red clay drumlin till / local ground moraine			till		St. Georges River Drift	till		
re-expansion of local ice centres and development of regional ice sheet	till	till		till from N.B. local till	till from New Brunswick local till	Fe-cemented gravel ??	gravel brown sand till grey till	sand			till with molluscs 32,100 y. B.P.	till	till	till		----	< Erie ?	
glacial recession to upland ice caps; retreat from coastal regions marine incursion ca 40,000 y. B.P.		sand			Salmon R. Sand (molluscs) 38,600 y. B.P.	+			weathering; erosional interval ?		Middle R. mastodon 31,900 y. B.P.	(deglaciated offshore)	"peat"	stratified sediments, + marine shells ?			PLUM POINT / PORT TALBOT	Middle Wisconsinan
transition to regional ice sheet moving southeastward — — — — — growth of local ice caps		till			red till from New Brunsw. with marine molluscs	red-brown till with shells >38,000 y. B.P.	till with shells >39,000 y. B.P.	red silt till					till w. wood >52,000 y.					Early Wisconsinan
widespread cool nonglacial interval with organic accumulation	Hillsborough mastodon beds >43,000 y. B.P.				? marine mollusc source beds	?	?	woody silt >52000 y B.P.				various peaty beds >44,000 y B.P. > 49,000 ; 51,000	sand; peat >42,000 y.	peat + wood >38,270 y. B.P.			St. Pierre Interstadial	
glaciation (minor)						slate till		black till	oxidized till	"Bw. cgl." + till?		till		till				
bench-cutting and concordant terrace formation at +6m sea level deep weathering		Trout River Conglomerate ?				Bridgewater cgl. ?			Bridgewater cgl. ?	Bridgewater Conglomerate ?	marine bench	oxidized sand + gravel	bench and gravel terrace	rock bench				SANGAMONIAN

drg

CORRELATION CHART OF LATE QUATERNARY SEDIMENTARY FORMATIONS, ATLANTIC PROVINCES, CANADA

SURFICIAL GEOLOGY OF RED INDIAN LAKE MAP-AREA, NEWFOUNDLAND — A PRELIMINARY INTERPRETATION

Project 740072

D. R. Grant
Terrain Sciences Division

Surficial geology mapping and terrain analysis of the interior of mainland Newfoundland is continuing following field studies around the periphery of the island along the Trans-Canada Highway and coastal access roads.

The accompanying map (Fig. 1) has been prepared solely from airphoto interpretation, based upon knowledge of the origin, constitution, and texture of similar terrain types in adjacent areas already field-checked. It is important to note that heavy forest cover is confined to relatively small areas in the northwest and northeast corners, hence the small morphologic details that usually indicate origin and composition are clearly visible.

Rock

Areas of outcrop or bedrock covered only by vegetation comprise less than one-quarter of the area. Large tracts occupy the southern half and commonly are

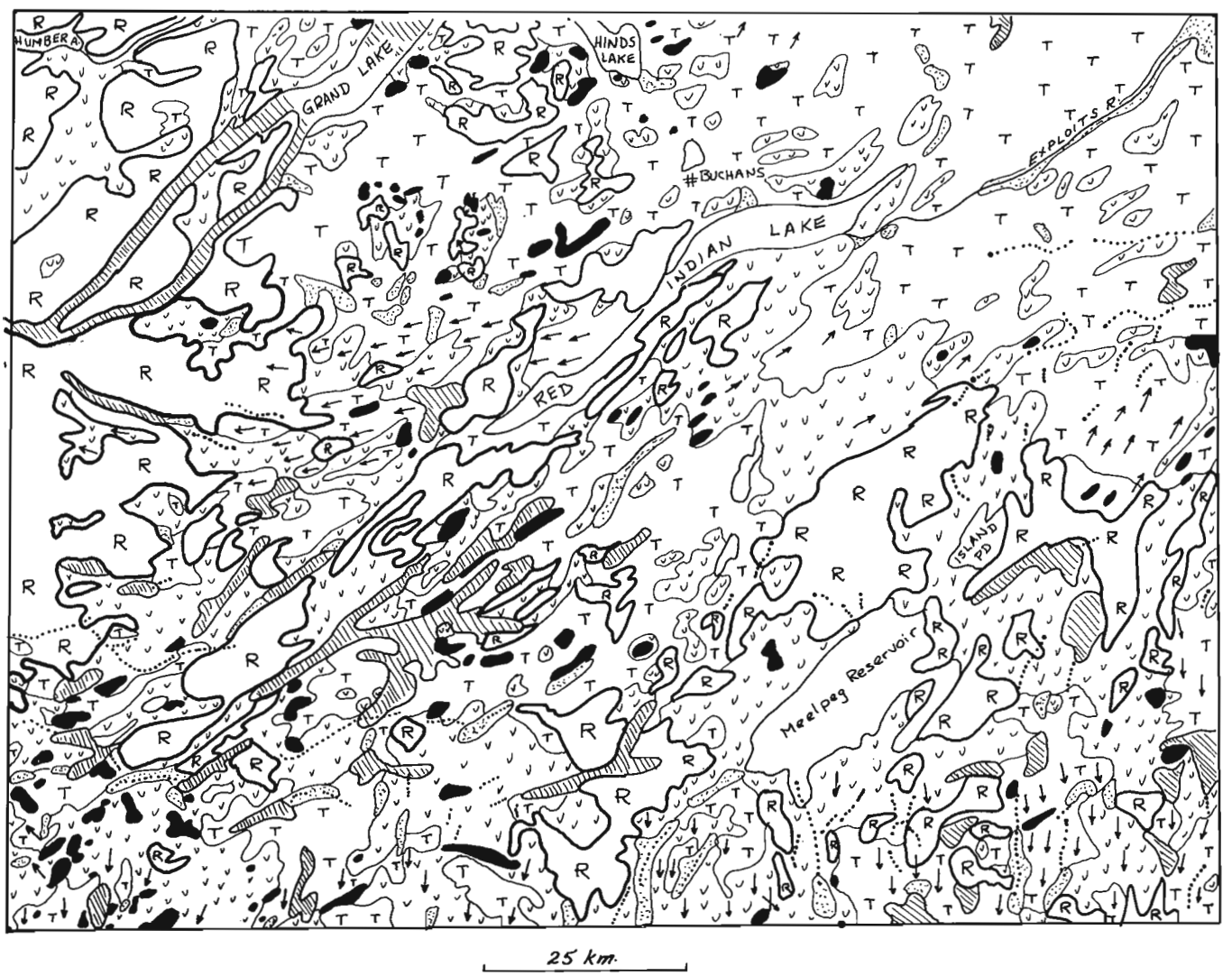

Figure 1. Surficial geology Red Indian Lake Map-Area (NTS 12A). (Bold outline and solid black = rock exposed or obscured with vegetation; T = till more than 2 m thick; usually drumlinized; v = till "veneer", i.e. less than 2 m thick; stippled areas = glaciofluvial sand and gravel; diagonal ruling = lakes; arrows = flutings and drumlins showing direction of last ice flow; dotted lines = eskers.)

composed of granite, or volcanic rocks of the Ordovician Glover Formation and others south of Red Indian Lake. There is usually a fairly sharp boundary between clearly visible rocky areas and adjacent till-covered tracts.

Till

The northern half and interior of the area is deeply covered with till, commonly moulded into long flutings and large drumlins from which the average thickness is inferred to be not less than 25 feet. The distribution corresponds to the occurrence of fine-grained and/or otherwise easily erodible rock types. However, anomalously thick deposits cover crystalline rocks of the Buchans Plateau, and are not readily explainable in terms of the glacial pattern. Elsewhere, the areas intervening between rock outcrops are thinly veneered with till through which the bedrock structural fabric, as expressed by positive and negative topographic elements, can be discerned. This thinner morainal mantle may display either a disorganized morphologic pattern or be organized into shallow flutings, discontinuous ridges (ribbed moraine) or true hummocky moraine. Towards the southern boundary the till sheet thins and discrete drumlins are detached from it, and are found isolated on the glaciated granite terrane.

Sand and Gravel

An inventory of granular resources has already been published for the entire island (Grant, 1974a) showing essentially all the occurrences in detail as to origin, thickness, and exploitability. To summarize this group for the area, most of the deposits occur in the southern half of the area as scattered small eskers and kame fields. Larger, more accessible eskers are found south of Exploits River, and apparently formed in an interlobate position at the junction of two remnant ice caps. Elsewhere important esker and outwash formations are localized along narrow valley floors of the Red Indian and Victoria lakes tributaries. Shallow patches of gravel produced by ice-marginal meltwater channels are found south of Buchans Plateau. Small, but commercially important, marine and fluvial gravels occur along Humber Arm and River. Finally, there is always the possibility of fluvial deposits that have been buried beneath till deposited by a readvance of the shrinking ice caps.

Glaciation

The map-area straddles the main ice shed for the island. Ice moved generally radially from this region, and an inferred ice divide trends diagonally from Island Pond to the southwest corner. The flow directions during the inception of the last glaciation are largely unknown, but during the maximal phase of that event the large, consistent trends of drumlinized till show that flow during advance as well as retreat was westward along the west margin, south along the south margin, northeast down Exploits Valley and northwest down Humber Valley. In the north-central area around Buchans, ice-flow evidence by till forms is at variance with ice flow during recession marked by sloping side-hill meltwater channels. In this area an ice lobe retreated northeastward in Red Indian Lake basin, while ice shrank back eastward over Buchans Plateau, southward across Hinds Lake, and ultimately disintegrated in Red Indian Lake basin. Minor ice caps shrank back northward to a centre north of Buchans Plateau, and southward to a late ice cap situated over Island Pond. This recessional pattern has been figured for the island as a whole (Grant, 1974b). It is hoped that future field work will produce data on direction and sequence of striations and rock dispersal to substantiate this preliminary construction.

References

Grant, D. R.

1974a: Granular resources inventory, Newfoundland; Geol. Surv. Can., Open File 194, scale 1:500 000.

1974b: Prospecting in Newfoundland and the theory of multiple shrinking ice caps; *in* Report of Activities, Part B, Geol. Surv. Can., Paper 74-1, Pt. B, p. 215-216.

27. SURFICIAL GEOLOGY MAPPING: OTTAWA VALLEY LOWLANDS (PARTS OF 31 G, B, F)

Project 740068

S.H. Richard
Terrain Sciences Division

Field investigation and mapping of the surficial geology of the Morrisburg (31 B/14) and of the east half of the Winchester (31 G/3) map-areas in southeastern Ontario during the summer of 1974 has revealed the presence of fossiliferous till and an associated drumlin field in the Newington area (Richard, 1975, p. 417). Terasmae (1965, p. 19) reported on similar drumlinized glacial deposits in the west half of the Cornwall map-area around Avonmore and Warina (adjacent to the Newington area) and his published surficial geology map of that area shows their location, distribution, size, and trend. The mapping of these drumlins by Terasmae revealed that they all trend south. This trend is quite distinct and different from the southeasterly movement attributed to the Fort Covington ice lobe from numerous till fabric analyses obtained at various sites throughout southeastern Ontario by MacClintock and Terasmae (MacClintock and Stewart, 1965; Terasmae, 1965, p. 14) and northern New York State by MacClintock (MacClintock and Stewart, 1965). This field evidence led Terasmae (1965, p. 19, 35) to explain the origin of these southerly trending drumlins by 'the remoulding of till by a post-Fort Covington ice readvance that superimposed them on the pre-existing ground moraine'.

In August 1974, in an attempt to determine when these drumlinized glacial sediments were deposited, the author identified fossil shells of the marine molluscs *Hiatella arctica, Balanus hameri,* and *Balanus crenatus* were recovered one mile south of Newington from the matrix of a till adjacent to deformed beds of fossiliferous beach gravels. A date of 11 200 ± 100 years B.P. (GSC-2108) was obtained for these shells (Table 1). This seems to indicate that not only did a readvance of ice, younger than either the Malone or the Fort Covington advance, occur in the area of southeastern Ontario between Cornwall and Port Johnstown as has already been suggested by Terasmae (1965, p. 35) but that this younger ice readvance took place during the time of the postglacial marine submergence of the area by the Champlain Sea. This late 'Newington ice lobe' must have readvanced into the marine waters of the Champlain Sea in order to be able to scoop up shells of marine molluscs and incorporate and disperse them throughout the glacial sediments.

Circa 11 200 years ago, parts of the Ottawa-St. Lawrence Lowlands had already been under marine submergence for as much as 1600 years. Table 2 lists Champlain Sea radiocarbon dates older than 11 200 years B.P., or before the Newington ice readvance took place in the Ottawa-St. Lawrence Lowlands. The location, elevation, and distribution of these ^{14}C dated marine sediment localities are shown in Figure 1. They occur mainly in two areas: 1) in the southwesternmost part of the Champlain Sea Basin between Brockville and Prescott in the south and Almonte and Clayton in the north; and 2) in the valley of the Gatineau River and of its tributaries between Kingsmere in the south and Martindale in the north. In these two areas, the marine sediments of the Champlain Sea lie at high elevations and commonly are well preserved and unmodified (except for the upper part of the marine sand deposits which in many places have been blown up into dunes by the wind), and no postdepositional deformations affecting them have been reported.

A late readvance of the Wisconsin ice sheet into the Champlain Sea ca. 11 200 years ago, therefore, could have occupied only certain areas of the Ottawa-St. Lawrence Lowlands and must not have reached these more remote parts of the basin where the marine sedimentation appears to have continued uninterrupted. The limit of advance of this late Wisconsin ice towards the west and southwest has been tentatively traced and is shown in Figure 1. This is based on field evidence reported by Terasmae (1965, p. 35) between Johnstown in the west and Cornwall in the east along the St. Lawrence valley, by Sharp (1974, pers. comm.) in the Merrickville map-area, and by the writer while mapping surficial geology between Pakenham and Newington from 1970 to 1975. Specific observations that have been made in the vicinity of Stittsville, Twin Elm, Richmond, Oxford Mills, Williamsburg, Finch, Newington,

Table 1

Champlain Sea radiocarbon date for marine molluscs from glacial sediments

Date No.	Date	Locality	Material	Collector	Reference
GSC-2108	11 200 ± 100	Newington, Stormont County, Ont.	Marine shells in fossiliferous glacial till at 106 m (330') a.s.l.	S.H. Richard	Unpublished 1975

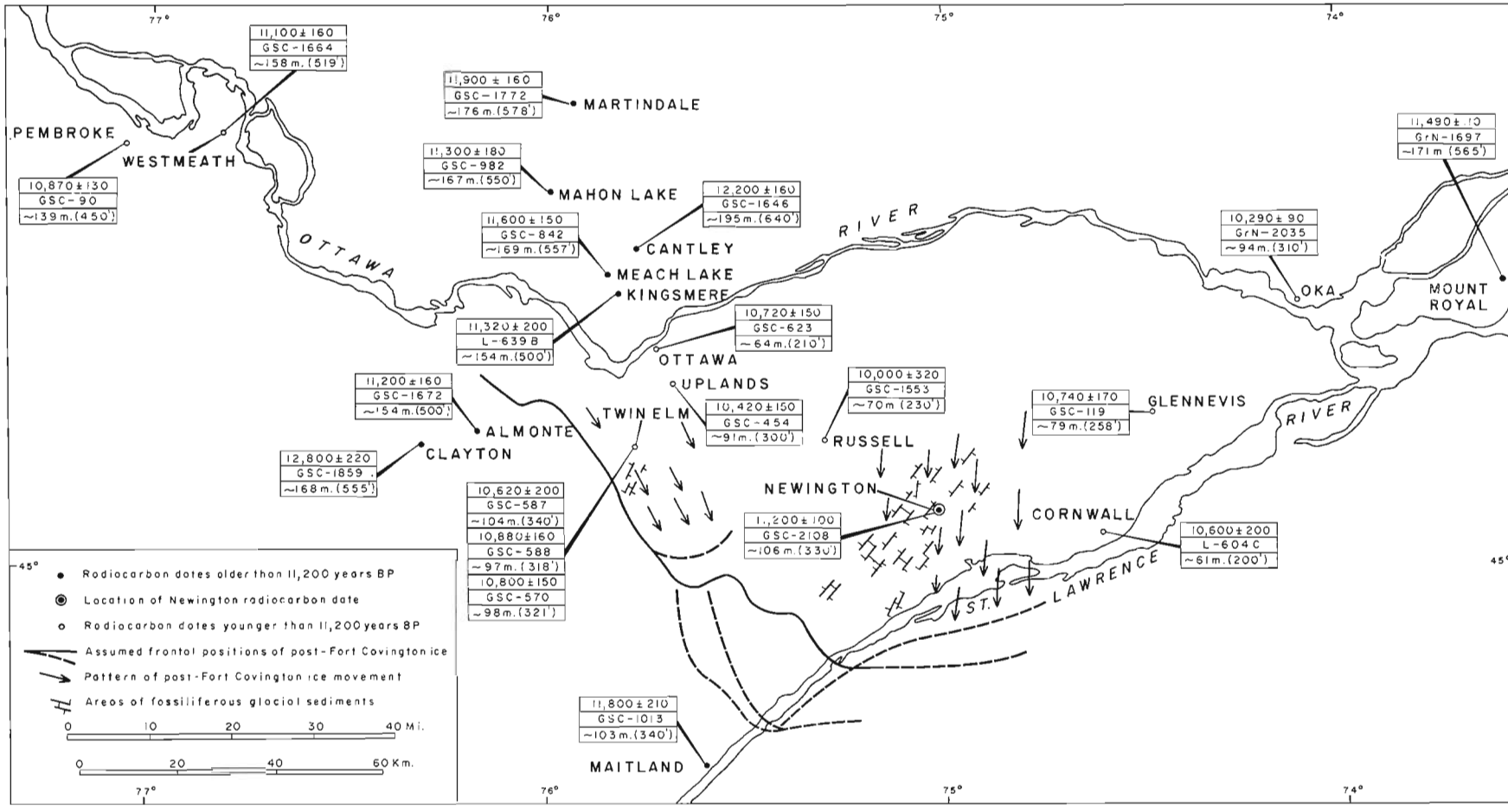

Figure 1. Location map of Ottawa-St. Lawrence Lowlands showing most localities where radiocarbon age determinations have been obtained, assumed configuration of ice-frontal positions of the post-Fort Covington ice readvance in the Champlain Sea basin, and the pattern of ice movements.

Table 2

Champlain Sea radiocarbon dates older than 11 200 years B.P. relating to marine limit

Date No.	Date	Locality	Material	Collector	Reference
GSC-1672	11 200 ± 160	Almonte, Ont.	Marine shells in beach gravels at 154 m (500') a.s.l.	S.H. Richard	Lowdon and Blake, 1973, p. 19.
GSC-982	11 300 ± 180	Mahon Lake, Que.	Marine shells in gravel at 167 m (550') a.s.l.	J.T. Buckley	Lowdon and Blake, 1970, p. 59
L-639B	11 320 ± 200	Kingsmere, Que.	Marine shells in beach gravels at 154 m (500') a.s.l.	N.R. Gadd	Gadd, 1964, p. 1250.
Grn-1697	11 490 ± 110	Mt. Royal, Que.	Marine shells in beach gravels at 171 m (565') a.s.l.	P. LaSalle	LaSalle, 1966, p. 91-128.
GSC-842	11 600 ± 150	Meach Lake, Gatineau Park, Que.	Marine shells in beach gravels at 169 m (557') a.s.l.	J.T. Buckley	Lowdon and Blake, 1970, p. 59.
GSC-1013	11 800 ± 210	Maitland, Ont.	Marine shells in beach gravels at 103 m (340') a.s.l.	E.P. Henderson	Lowdon and Blake, 1970, p. 60.
GSC-1772	11 900 ± 160	Martindale, Gatineau County, Que.	Marine shells in beach gravels at 176 m (578') a.s.l.	R. Romanelli	Lowdon and Blake, 1973, p. 17.
GSC-1646	12 200 ± 160	Cantley, Gatineau County, Que.	Marine shells in beach sands at 195 m (640') a.s.l.	R. Romanelli	Lowdon and Blake, 1973, p. 16-17.
GSC-1859	12 800 ± 220	Clayton, Lanark County, Ont.	Marine shells in beach gravels at 168 m (555') a.s.l.	S.H. Richard	Richard, 1974, p. 218.

Morrisburg, Avonmore, and Apple Hill include: deformed and overridden fossiliferous marine sediments, thin fossiliferous glacial till deposits overlying or adjacent to deformed fossiliferous marine sediments, fossiliferous till cored drumlins, and deformed pockets and lenses of fossiliferous glacial till or marine clay injected into bodies of unfossiliferous ice-frontal or ice-contact fluvioglacial or glaciodeltaic outwash deposits. Surficial geology maps of these areas, now in preparation, will show the location of these fossiliferous glacial deposits.

The direction of the late ice movement is shown in Figure 1. The duration of occupation of the marine basin by the ice is not yet known. Fossil shells of the marine molluscs *Macoma balthica*, recovered one mile south of Newington from unmodified beach gravels and sands lying at 350 feet a.s.l. and over the fossiliferous glacial sediments described above, have been submitted for dating to the Geological Survey of Canada radiocarbon laboratory. This date will throw some light on this problem by indicating the time at which the Champlain Sea waters had re-established themselves over this area after some recession towards the north of the post-Fort Covington ice front.

Following the final disintegration of the Newington ice, the Champlain Sea reoccupied its basin. Table 3 lists the most significant radiocarbon dates younger than 11 200 years B.P. relating to this younger period of marine submergence; their locations are plotted on Figure 1.

Terasmae (1965, p. 36) states: 'A correlation of the Malone and the Fort Covington ice-readvance to the eastward is even more obscure and considerable work is required before attempting a reliable correlation. The St. Narcisse moraine (Gadd, 1955; Karrow, 1957) is probably younger than the Fort Covington readvance. Whether the St. Narcisse readvance can be correlated with the Valders substage of the Wisconsin glaciation is still an unsolved problem, although it is a definite possibility (Terasmae, 1959). The post-Fort Covington readvance in the Prescott area may possibly belong in the Valders substage, too, but no absolute age for this readvance has yet been obtained'. This is no longer the case.

It is the author's opinion that the age of 11 200 ± 100 years B.P. for the fossiliferous glacial sediments dates the post-Fort Covington ice readvance in the Prescott-Newington-Cornwall area; it is further

Table 3

Champlain Sea radiocarbon dates younger than 11 200 years B.P.

Date No.	Date	Locality	Material	Collector	Reference
GSC-1664	11 100 ± 160	Westmeath, Renfrew County, Ont.	Marine shells in clayey sand at 158 m (519') a. s. l.	C. D. Allen and P. J. Howarth	Allen, 1971, 119 p.
GSC-588	10 880 ± 160	Twin Elm, Carleton County, Ont.	Marine shells in sands at 97 m (318') a. s. l.	R. J. Mott	Lowdon and Blake, 1970, p. 60; Mott, 1968, p. 322.
GSC-90	10 870 ± 130	Pembroke, Ont.	Marine shells in sand and silty clay at 139 m (450') a. s. l.	J. Terasmae	Dyck and Fyles, 1963, p. 44.
GSC-570	10 800 ± 150	Twin Elm, Carleton County, Ont.	Marine algae (kelp) in sands at 98 m (321') a. s. l.	R. J. Mott	Lowdon and Blake, 1970, p. 60; Mott, 1968, p. 322.
GSC-119	10 740 ± 170	Glennevis, Glengarry County, Ont.	Marine shells in near-shore sand at 79 m (258') a. s. l.	J. J. L. Tremblay	Dyck and Fyles, 1964, p. 167, 168.
GSC-623	10 720 ± 150	Ottawa, Ont.	Marine shells in clay at 64 m (210') a. s. l.	N. R. Gadd	Lowdon *et al.*, 1967 p. 161-2.
GSC-587	10 620 ± 200	Twin Elm, Carleton County, Ont.	Marine shells in sands at 104 m (340') a. s. l.	R. J. Mott	Lowdon and Blake, 1970, p. 60; Mott, 1968, p. 322.
L-604c	10 600 ± 200	Cornwall, Ont.	Marine shells in beach gravels at 61 m (200') a. s. l.	J. Terasmae	Dyck and Fyles, 1962.
GSC-454	10 420 ± 150	Uplands, Ottawa Ont.	Whale bone in marine sand at 91 m (300') a. s. l.	N. R. Gadd	Dyck *et al.*, 1966, p. 103.
GrN-2035	10 290 ± 100	Oka, Que.	Marine shells at 94 m (310') a. s. l.	P. LaSalle	LaSalle, 1966, p. 91-128.
GSC-1553	10 000 ± 320	Russell, Russell County, Ont.	Marine shells in beach sand at 70 m (230') a. s. l.	S. H. Richard	Lowdon and Blake, 1973, p. 19.

suggested that this event may correlate with the St. Narcisse readvance and that both would then belong in the Valders substage of the Wisconsin glaciation as had been anticipated with so much insight by Terasmae (1965).

References

Allen, C. D.
1971: The Westmeath-Beachburg esker complex; Unpubl. B.A. thesis, Dept. of Geography, McMaster University, 119 p.

Dyck, W. and Fyles, J. G.
1962: Geological Survey of Canada radiocarbon dates I; Radiocarbon, v. 4, p. 13-26.

Dyck, W. and Fyles, J. G. (cont'd)
1963: Geological Survey of Canada radiocarbon dates II; Radiocarbon, v. 5, p. 39-55.

1964: Geological Survey of Canada radiocarbon dates III; Radiocarbon, v. 6, p. 167-181.

Dyck, W., Lowdon, J. A., Fyles, J. G. and Blake, W. Jr.
1966: Geological Survey of Canada radiocarbon dates V; Radiocarbon, v. 8, p. 96-127.

Gadd, N. R.
1964: Moraines in the Appalachian region of Quebec; Bull. Geol. Soc. Am., v. 75, no. 12, p. 1249-1254.

LaSalle, P.
1966: Late Quaternary vegetation and glacial history in the St. Lawrence Lowlands, Canada; Leidse Geol. Mededel., v. 38, p. 91-128.

Lowdon, J.A. and Blake, W. Jr.
1970: Geological Survey of Canada radiocarbon dates IX; Radiocarbon, v. 12, p. 46-86.

1973: Geological Survey of Canada radiocarbon dates XIII; Geol. Surv. Can., Paper 73-7, 61 p.

Lowdon, J.A., Fyles, J.G. and Blake, W. Jr.
1967: Geological Survey of Canada radiocarbon dates VI; Radiocarbon, v. 9, p. 156-197.

MacClintock, P. and Stewart, D.P.
1965: Pleistocene geology of the St. Lawrence Lowland; New York State Mus. Sci. Serv., Bull. no. 394, Univ. State of New York, State Education Department, Albany, N.Y., 152 p.

Mott, R.J.
1968: A radiocarbon-dated marine algal bed of the Champlain Sea episode near Ottawa, Ontario; Can. J. Earth Sci., v. 5, p. 319-324.

Richard, S.H.
1974: Surficial geology mapping: Ottawa-Hull area (Parts of 31 F, G); *in* Report of Activities, Part B, Geol. Surv. Can., Paper 74-1, Pt. B, p. 218-219.

1975: Surficial geology mapping: Morrisburg-Winchester area (Parts of 31 B, G); *in* Report of Activities, Part A, Geol. Surv. Can., Paper 75-1, Pt. A, p. 417-418.

Terasmae, J.
1965: Surficial geology of the Cornwall and St. Lawrence Seaway Project areas, Ontario; Geol. Surv. Can., Bull. 121, and Map 1175A, 54 p.

Project 1135-D13-4-63/74

John A. Westgate[1]
Terrain Sciences Division

Wascana Creek Ash was first described and formally named by Christiansen (1961), who designated the west bank of Wascana Creek Valley at NE 9-29-18-21-W2 as the reference section*. This site is approximately 19 km northwest of Regina (Fig. 1). The silver grey (N 8.5) tephra occurs as discontinuous, irregular bodies within a well jointed clay, which is overlain by a soft, friable till and underlain by a weathered, firm, jointed, sandy till (Fig. 2). These tills have been identified respectively as the Battleford Formation and Floral Formation on the basis of lithology, structure, and electrical logs.

Granulometric analyses show that Wascana Creek Ash has a silty loam texture and is poorly sorted. Average sand, silt, and clay contents are 30, 60, and 10 per cent, respectively. These textural parameters are believed to resemble closely those of the original fall unit because all analyzed samples contained very little detrital contamination, suggesting that only slight reworking occurred subsequent to deposition. Platy, bubble-wall, and bubble-junction shards constitute the bulk of the tephra. Phenocrysts consist predominantly of sanidine, chevkinite, which is a titano-silicate of the cerium earths, magnetite, and colourless zircon, together with minor amounts of quartz, sodic plagioclase and the rare green hornblende and ilmenite. The volcanic glass has a calc-alkaline rhyolitic composition.

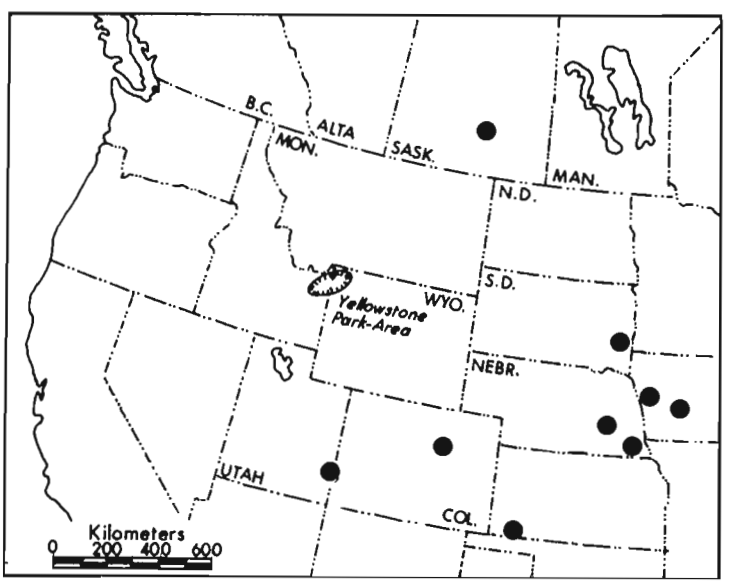

Figure 1. Location of Wascana Creek Ash in southern Saskatchewan and other Pearlette "O" tephra occurrences in the mid-continent region of the United States (*see* Boellstorff, 1973a). Filled circles represent tephra sites.

Figure 2. Stratigraphic setting of Wascana Creek Ash at its type section. 1. Battleford Formation; 2, clay; 3. Wascana Creek Ash; 4. Floral Formation. Measuring tape is 45 cm long.

Such a mineralogical assemblage, especially the presence of chevkinite, argues against a source in the Western Cordillera, which is the provenance of most Quaternary tephra in the Western Canadian Plains. Instead, it strongly supports equivalence with one of the Pearlette tephras, which are widespread in the mid-continent region of the United States (Powers *et al.*, 1958; Young and Powers, 1960). These tephras are now known to have come from Quaternary vents in Yellowstone National Park of Wyoming and Idaho (Izett *et al.*, 1970; Izett *et al.*, 1972), situated about 800 km southwest of the Wascana Creek locality in Saskatchewan (Fig. 1).

Three distinctive Pearlette tephras have been recognized; they are similar in composition and have been named, in order of decreasing age, Pearlette "B", Pearlette "S", and Pearlette "O" (Izett *et al.*, 1970; Izett *et al.*, 1972). Each has been correlated to a rhyolitic tuff at Yellowstone on the basis of mineralogy,

*In Christiansen (1961) the spelling of both the creek and ash was Waskana, but the correct spelling according to the topographic map is Wascana.

[1]This work was carried out while the author was at Department of Geology, University of Alberta, Edmonton.

Present address: Department of Geology, University of Toronto, and Scarborough College, University of Toronto, Toronto, Ontario.

Table 1. Fission-track age data for volcanic glass from Wascana Creek Ash

Sample	Spontaneous tracks		Induced tracks		Thermal neutron dose ($x10^{14}$n. cm^{-2})	Age+ (m.y.)	Age determination by
	Number counted	Apparent density, cm^{-2}	Number counted	Apparent density, cm^{-2}			
UA 256	91	2472	416	33871	1.32 ± 0.06	0.59 ± 0.07#	J. Boellstorff
"	83	2254	386	31481	1.32 ± 0.06	0.58 ± 0.07	"
UA 388	83	2254	372	29526	1.44 ± 0.08	0.67 ± 0.09	"
"	73	1983	384	31263	1.44 ± 0.08	0.56 ± 0.08	"
"	26	404	478	45163	11.0 ± 0.55	0.60 ± 0.12	J. Westgate*

Notes:

$\lambda_F = 6.85 \times 10^{-17} yr^{-1}$

* This fission-track date was determined at the United States Geological Survey laboratory at Denver, under the supervision of Dr. C. Naeser.

\+ Average of 5 age determinations is 0.60 ± 0.04 m.y.

\# Standard deviation based on sum of errors determined from number of spontaneous and induced tracks counted and from tracks in glass standards.

Etching conditions: Boellstorff used 24% HF at 23°C for 130 secs; Westgate used 24% HF at ~ 24°C for 40 secs.

chemistry, and age. Thus, Pearlette "B" tephra has been related to Huckleberry Ridge Tuff, Pearlette "S" to Mesa Falls Tuff, and Pearlette "O" to Lava Creek Tuff (Izett *et al.*, 1972; Christiansen and Blank, 1972). Sanidine from each Yellowstone tuff has been dated by the K-Ar method by J. D. Obradovich, United States Geological Survey, at 2.0 m.y., 1.2 m.y., and 0.6 m.y. respectively. Fission track ages of zircon and glass from each of the correlative Pearlette tephras in the mid-continent region are in good agreement with these K-Ar dates (Naeser *et al.*, 1973; Boellstorff, 1973b).

Electron microprobe analyses of glass, chevkinite, and magnetite from Wascana Creek Ash and the several Pearlette tephras strongly point to Wascana Creek Ash as being equivalent to the 0.6 m.y. old Pearlette "O" tephra (Westgate, 1970, 1973). However, this correlation initially was held suspect as the Floral Formation, which underlies Wascana Creek Ash, was generally thought to be much younger than 0.6 m.y. Two lines of stratigraphic evidence seemed to support an early Wisconsin age for this till. Firstly, at Fort Qu'Appelle, the Floral Formation overlies Echo Lake Gravel, which, on the basis of its vertebrate faunal content, was considered to be of Sangamon or Wisconsin age (Khan, 1970), and secondly, Mid-Wisconsin sediments occasionally occur between the Battleford and Floral formations (Christiansen, 1968).

To resolve this problem it was decided to attempt an age determination of Wascana Creek Ash itself. Initially, sanidines were concentrated from a large bulk sample of the tephra for a K-Ar date, but the fine sand size and presence of small amounts of detrital feldspar contaminants, which were presumably derived from glacial drift and therefore very likely of Precambrian age, made separation of a pure sanidine fraction a very laborious if not impossible task, and thus eventually was abandoned. Recent successes in the application of the fission track dating method to Quaternary tephra (Boellstorff, 1973a; Kohn, 1973; Naeser *et al.*, 1973; Seward, 1974) then prompted use of this dating technique, which is ideally suited to fine grained tephra as detrital contaminants can simply be avoided during the counting operation. The fission track age data for glass and zircon from Wascana Creek Ash are shown in Tables 1 and 2, respectively. The average of five age determinations on the glass is 0.6 ± 0.04 m.y., in good agreement with the zircon age of 0.68 ± 0.15 m.y. Hence, correlation of Wascana Creek Ash to Pearlette "O" tephra, first suggested by the mineralogical and chemical evidence, is confirmed.

Detailed stratigraphical studies by Christiansen at and around the type section show that Wascana Creek Ash is in situ; there is no evidence of glaciotectonic disturbance in the Quaternary sequence here. Thus, the Floral Formation — at least, as represented at this site — must be older than 0.6 m.y. In addition, it should be noted that this widespread Pearlette "O" tephra (Fig. 1) provides the opportunity for reliable correlation of part of the glacial sequence in southern Saskatchewan to that of the mid-continent region of the United States, where many of the type areas for the classical glacial-interglacial succession exist.

Table 2. Fission-track age data for zircon from Wascana Creek Ash

Sample	Number of grains	$\frac{\rho s}{\rho i}$*	Number of spontaneous tracks	Number of induced tracks	Thermal neutron dose $\times 10^{15}$ n. cm^{-2}	Age# (m.y.)
UA 388	5	0.0098	15	1534	1.135	0.68 ± 0.15

Notes:

This fission-track date was determined by J.A. Westgate, who worked under the supervision of Dr. C. Naeser, United States Geological Survey, Denver.

$\lambda_F = 6.85 \times 10^{-17} yr^{-1}$

* $\frac{\rho s}{\rho i} = \frac{\text{spontaneous track density}}{\text{induced track density}}$

\# Standard deviation based on sum of errors determined from number of spontaneous and induced tracks counted in sample and from tracks in glass standards.

Etching conditions: zircons were placed in NaOH solution (20g NaOH, 3.5 ml H_2O) at 280°C for 1 hr.

References

Boellstorff, J.D.
1973a: Tephrochronology, petrology and stratigraphy of some Pleistocene deposits of the Central Plains, U.S.A.; unpubl. Ph.D. dissertation, Louisiana State University.

1973b: Fission track dating Pleistocene tephra of the Central Plains, U.S.A.; Internatl. Union for Quaternary Res., 9th Cong., Christchurch, Abstracts, p. 33-34.

Christiansen, E.A.
1961: Geology and groundwater resources of the Regina area, Saskatchewan; Sask. Res. Council, Geol. Div., Rept. 2, 72 p.

1968: Pleistocene stratigraphy of the Saskatoon area, Saskatchewan, Canada; Can. J. Earth Sci., v. 5, p. 1167-1173.

Christiansen, R.L. and Blank, H.R., Jr.
1972: Volcanic stratigraphy of the Quaternary Rhyolite Plateau in Yellowstone National Park; U.S. Geol. Surv., Prof. Paper 729-B, 18 p.

Izett, G.A., Wilcox, R.E. and Borchardt, G.A.
1972: Correlation of a volcanic ash bed in Pleistocene deposits near Mount Blanco, Texas, with the Guaje pumice bed of the Jemez Mountains, New Mexico; Quaternary Res., v. 2, p. 554-578.

Izett, G.A., Wilcox, R.E., Powers, H.A. and Desborough, G.A.
1970: The Bishop ash bed, a Pleistocene marker bed in the western United States; Quaternary Res., v. 1, p. 121-132.

Khan, E.
1970: Biostratigraphy and Paleontology of a Sangamon deposit at Fort Qu'Appelle, Saskatchewan; Natl. Museum Natural Sci., Publ. in Palaeontology, no. 5, 82 p.

Kohn, B.P.
1973: Some studies of New Zealand Quaternary pyroclastic rocks; unpubl. Ph.D. thesis, University of Victoria, Wellington, 340 p.

Naeser, C.W., Izett, G.A. and Wilcox, R.E.
1973: Zircon fission track ages of Pearlette Family ash beds in Meade County, Kansas; Geology, v. 1, p. 187-189.

Powers, H.A., Young, E.J. and Barnett, P.R.
1958: Possible extension into Idaho, Nevada, and Utah of the Pearlette Ash of Meade County, Kansas; Geol. Soc. Amer., Bull., v. 69, p. 1631.

Seward, D.
1974: Age of New Zealand Pleistocene substages by fission-track dating of glass shards from tephra horizons; Earth Planetary Sci. Letters, v. 24, p. 242-248.

Westgate, J.A.
1970: Yellowstone Plateau pyroclastics of late Pleistocene age in southern Saskatchewan, Canada; Amer. Quaternary Assoc., 1st Meeting, Bozeman, Abstracts, p. 149.

1973: Mineralogical and chemical data bearing on the correlation of Wascana Creek Ash in southern Saskatchewan; *in* Quaternary geology and its application to engineering practice in the Saskatoon - Regina - Watrous area, Saskatchewan, Christiansen, E.A. (ed.), Geol. Assoc. Canada, Guidebook to field trip C, p. 54-63.

Young, E.J. and Powers, H.A.
1960: Chevkinite in volcanic ash; Amer. Mineralogist, v. 45, p. 875-881.

29. RADIOCARBON AGE DETERMINATIONS FROM THE KARUKULA SITE, SOUTHWESTERN ESTONIA, U.S.S.R.

Project 570148

W. Blake, Jr.
Terrain Sciences Division

Introduction

During a visit to the Soviet Union in the summer of 1973, the writer was able to make collections of the organic deposits at the Karuküla site, southwestern Estonian S.S.R. (Blake, 1974). This site, located some 30 km east of the Gulf of Riga (Fig. 1), has become an important one to studies of Quaternary chronology around the Baltic Sea and on the Russian Plain. It was of particular interest because the deposits there have been investigated in considerable detail, and a fairly large number of age determinations had been carried out prior to 1973. It was hoped that the wood and peat collected could be dated by at least two laboratories, thus providing a valuable cross-check on materials in the 40 000 to 50 000 year range. The purpose of this paper is to report on the new determinations made in early 1974 by the Radiocarbon Dating Laboratory at the Geological Survey of Canada.

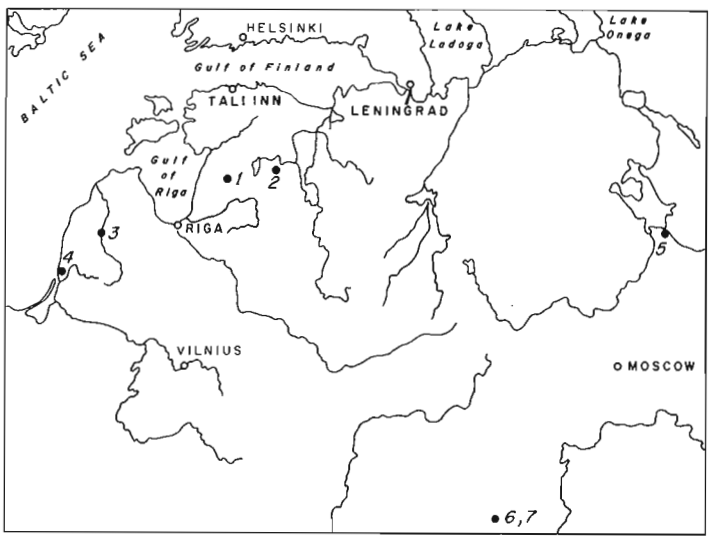

1. Karuküla 3. Desele 5. Chermenino 7. Mezin
2. Peedu 4. Purmaliai 6. Bryansk

Figure 1. Location map showing selected sites with radiocarbon-dated Late Pleistocene deposits in the northwestern part of the Russian Plain (adapted from Serebryanny *et al.*, 1970).

Site Description, Stratigraphy, and Vegetation

The Karuküla deposits are located near the periphery of the Sakala Heights, on a gently sloping drumlinoid hill (Serebryanny *et al.*, 1970). The site lies above a deep (> 150 m) buried valley which is oriented northeast-southwest and which leads to the Gulf of Riga. Drilling has revealed the presence of a complex series of deposits in the buried valley (Kajak *et al.*, 1970). The horizons under discussion here represent the uppermost organic strata, and they underlie the surface till. According to Raukas *et al.* (1971) ice of the Scandinavian Ice Sheet retreated from the belt of drumlin fields which are included in the Sakala Stage some 12 250 years ago.

The general stratigraphy at Karuküla is shown in Figure 2, which is reproduced from the paper by Kajak *et al.* (1970). Since the site is situated in a pasture adjacent to a farmhouse, a new excavation must be made each time collections are desired. The pit dug in 1973 revealed a stratigraphy similar to that displayed in Figure 2, and the organic layers were encountered at approximately the same depth as those in 1965 and 1969. The stratigraphic succession given in Figure 3, taken from Serebryanny *et al.* (1970) and based on the earlier report by Orviku and Pirrus (1965), is also similar. In addition, Figure 3 includes a pollen diagram and the following description of vegetation and pollen zones is summarized from Serebryanny *et al.* (1970).

Zone K_1, occurring in sand and silt, is interpreted as representing a periglacial environment. The vegetation cover consisted of stands of pine and birch, mainly *Betula nana* and *B. humilis*, together with herbaceous plant associations, including *Artemsia*, Cyperaceae, and Chenopodiaceae. Single pollen grains of *Ephedra* plus spores of *Selaginella selaginoides* and Bryales are present in these strata. The overlying sapropel and *Equisetum* peat (pollen zones K_2 and K_3) were deposited under milder climatic conditions. During zone K_2 time the Karuküla region was covered by a pine forest. This, in turn, gave way to a coniferous-broadleaved forest with alder groves (zone K_3). During deposition of the sediments in the latter zone, *Picea* and *Pinus* dominated, with a considerable admixture of *Tilia, Ulmus,* and *Quercus. Corylus* was present in the undergrowth (up to 5 per cent of total tree pollen), and pollen of *Tilia,* including both the thermophilic *Tilia platyphyllos* and *T. cordata* (now common in Estonia), were dominants (15 to 18 per cent) in the mixed oak portion of the zone K_3 assemblages. The coniferous-mixed oak forests represent the climatic optimum of this ice-free interval.

The pollen assemblages of the next zone, K_4, indicate a gradual deterioration of the climate. Coniferous trees encroached on the bog, and forest peat

Table 1

Previous radiocarbon age determinations from Karuküla

Material	Depth below surface (cm)	Laboratory dating no.[1,2]	Uncorrected age (conventional C^{14} years before 1950)	Collector and year	Reference
Woody peat	149-164	Mo-375	>33 000	R.O. Pirrus, 1963	Vinogradov *et al.*, 1968
Wood	150-170	TA-99	33 450 ± 800	K. Kajak, 1965	Punning *et al.*, 1966, 1968
Peat	150-170	TA-100	48 100 ± 1700		
Peat	195-215	TA-101	48 100 ± 1650		
Clayey sapropelite	235-225	TA-106	⩾45 000		
Wood	165	TA-275	40 800 ± 700		Kajak *et al.*, 1970
		Birm-249	>48 750		Shotton & Williams, 1973
Woody peat & woody detritus	205	TA-276	47 800 ± 1100	J.M. Punning, 1969	Kajak *et al.*, 1970
Equisetum peat	230	TA-277	48 800 ± 1200		Kajak *et al.*, 1970

[1]Laboratories:
Mo = V.I. Vernadsky Institute of Geochemistry and Analytical Chemistry, Academy of Sciences of the U.S.S.R., Moscow.
Ta = Institute of Zoology and Botany, Academy of Sciences of the Estonian S.S.R., Tartu.
Birm = The University of Birmingham, Birmingham.

[2]Birm-249 was determined on part of the same piece of wood used for TA-275.

Table 2

New radiocarbon age determinations from Karuküla

Material[1]	Field sample no.	Depth below surface (cm)	Laboratory dating no.	Uncorrected age (conventional C^{14} years before 1950)[2,3]	δC^{13} ‰	Corrected age (conventional C^{14} years before 1950)	Sample weight (g)	Counter (litres)	Pressure (atm)	No. of days counted
wood (*Pinus* sp., not *P. sylvestris*)	BS-73-40	160-170	GSC-1976	48 600 ± 1600	-23.6	48 700 ± 1600	43.0	5	4	8
rhizome-moss peat	BS-73-41	180-190	GSC-1985	>46 000	-28.3	>46 000	77.0	5	4	5

[1]Wood determined by L.D. Wilson (unpublished internal Wood Identification rep. 73-57). Peat constituents determined by Dr. M. Kuc: vascular plants dominant (mostly undeterminable remains, but also including rhizomes of *Carex* sp.). Mosses include: *Drepanocladus revolvens*, *D.* sp., *Calliergon giganteum*, *C.* sp., *Sphagnum* (at least 3 species), *Tomenthypnum nitens*, and *Meesea triquetra* (unpublished internal Bryological rep. 267).

[2]All age determinations from the Radiocarbon Dating Laboratory, Geological Survey of Canada, are based on a C^{14} half-life of 5568 ± 30 years and 0.95 of the activity of the NBS oxalic acid standard. Ages are quoted in conventional radiocarbon years before present (B.P.) where present is taken to be 1950. All finite age determinations from this laboratory are based on the 2σ criterion; i.e., there is a 95.5% probability that the correct age in conventional radiocarbon years lies within the stated limits of error. All "greater than" ages are based on the 4σ criterion (99.9% probability).

[3]The 8-day count for GSC-1976 was broken down into several individual counts, for which ages can be calculated as follows: 47 800 ± 1000 years (one 3-day count); 51 200 ± 1600 years (one 2-day count); and 45 500 ± 1200, >46 000, and 46 200 ± 1300 years (one 1-day count each). The 5-day count for GSC-1985 can be broken down as follows: 51 800 ± 1500 years (one 3-day count); and >48 000 and >45 000 years (one 1-day count each).

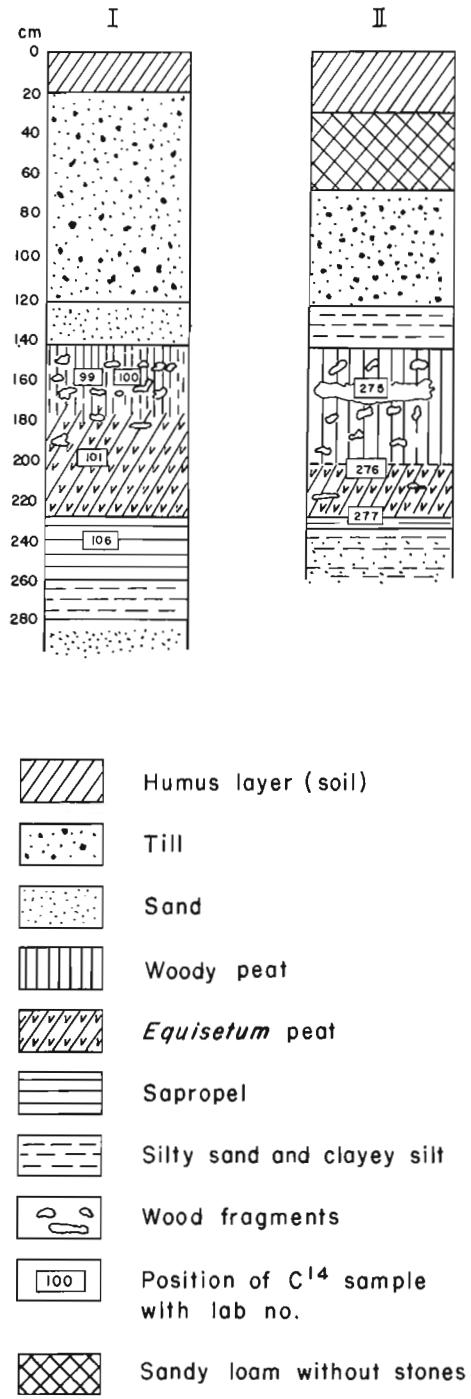

Figure 2. Cross-sections of the lacustrine-bog deposits at Karuküla (after Kajak *et al.*, 1970). Numbers refer to radiocarbon age determinations performed at Tartu in 1965 (section I) and 1969 (section II).

accumulated above the *Equisetum* peat. *Picea* and *Pinus* became the dominant species again, and broadleaved species disappeared locally. The sands within the limits of pollen zone K_5 accumulated during an even colder climate. A periglacial environment is indicated in the pollen diagram by the rise of *Betula nana*, *Artemisia*, and Chenopodiaceae, as well as by the reappearance of spores of *Selaginella selaginoides*.

Serebryanny *et al.* (1970) concluded their discussion of the Karuküla site by pointing out that these strata are distinctly different from typical Mikulino Interglacial deposits. For this reason Orviku and Pirrus (1965) proposed a possible correlation with the Brørup Interstadial, an early Weichselian interstadial named from the Brørup Hotel Bog in Denmark (Andersen, 1961; Andersen *et al.*, 1960).

The sample of peat from 180 to 190 cm depth collected by the writer was described by Kuc as rhizome (*Carex*)-moss peat (unpublished internal Bryological rep. 267). Kuc found that vascular plants dominated, and woody elements were absent, with the possible exception of some bark. The leaves in this strongly compressed holarctic, probably subarctic, peat were derived from dwarf shrubs, and the mosses are circumboreal types. This interpretation agrees well with the vegetation zones shown in Figure 3; i. e., zone K_4, the pollen zone to which the dated peat at 180 to 190 cm corresponds, is characterized by a deteriorating climate with spruce and pine becoming dominant, followed in zone K_5 by dwarf birch, etc.

Radiocarbon Age Determinations

The radiocarbon age determinations carried out up to 1969 by the laboratory at Tartu, as reported by Kajak *et al.* (1970), are listed in Table 1, and the position of the samples is indicated in Figure 2. The age determined by the University of Birmingham was on the same piece of wood used for TA-275, and the peat dated in Moscow, although its position is not indicated in Figure 3, is from about the middle of the forest peat unit.

Table 2 provides details of the new "high pressure" (4 atm versus 1 atm at which the 5-L counter is normally operated) age determinations carried out in Ottawa. As with most GSC "high pressure" age determinations, the pretreatment of both samples included a 1-hour leach in hot (just below boiling) NaOH, a 1-hour leach in hot HCl, and several rinses with distilled water. Details of the individual counts obtained on both samples are given in footnote 3 to Table 2.

The organic horizons at Karuküla originally were interpreted as representing interglacial pond and peat-bog deposits (cf. Orviku, 1960, and references therein). Although no radiocarbon age determinations were available when Orviku wrote his early papers, the assignment of interglacial rank has continued in current usage in the Soviet Union (e. g., *see* Serebryanny, 1969; Serebryanny *et al.*, 1970; Raukas and Serebryanny, 1972). However, Lundqvist (1974), in a recent summary entitled "Outlines of the Weichsel Glacial in Sweden", referred to the organic deposits at Karuküla as interstadial.

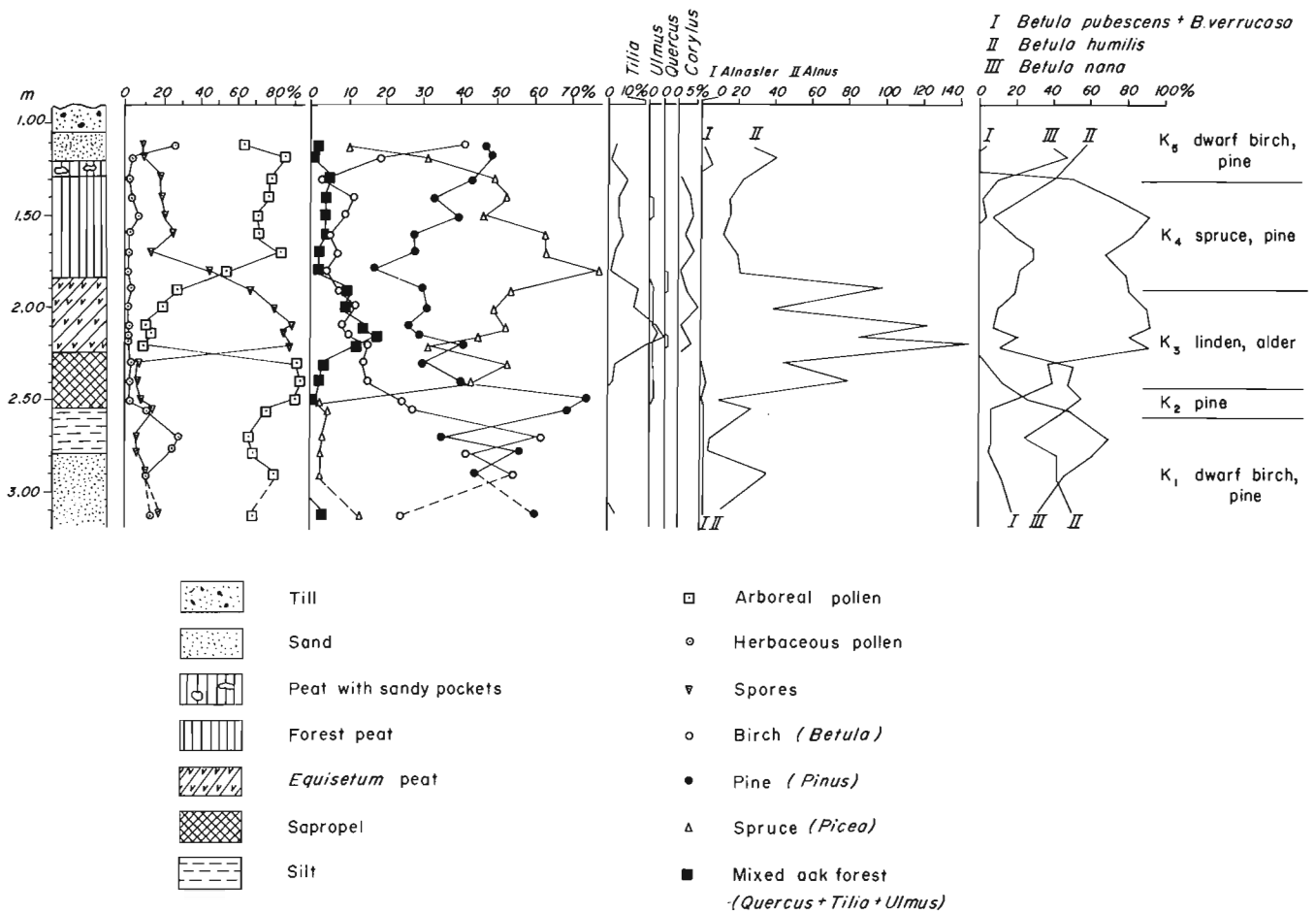

Figure 3. Pollen diagram of the "intermorainic" deposits at Karuküla, as analyzed by R. O. Pirrus in 1964; cf. Figure 5 in Orviku and Pirrus (1965) and Figure 1 in Serebryanny *et al.* (1970).

Discussion as to the ranking of the organic strata at Karuküla is not within the scope of the present report. It is apparent from the suite of age determinations available so far that there is a significant amount of wood and peat at Karuküla which is > 45 000 years old and it may well be that much of the material is > 50 000 years old.

The fact that the first age determined was only > 33 000 years (Mo-375) may simply reflect the limits of the laboratory at the Vernadsky Institute at that time, as none of the dates in their list V (Vinogradov *et al.*, 1968) exceeds > 35 000 years. The first determination on wood by the Tartu laboratory (TA-99) is more difficult to understand. Obviously organic deposits preserved at Karuküla must span a significant period of time, but was the region free of ice for as long as 15 000 years? The writer would feel more confident that this was indeed the case if some of the other determinations had resulted in values close to 35 000 years B. P., although it should be pointed out that Serebryanny *et al.* (1970) suggest that dates as young as approximately 25 000 years at Chermenino, Bryansk, and Mezin (cf. Fig. 1) mark the end of the Karuküla Interglacial. Another possibility is that the wood has become contaminated in some way by younger material, although it should have been less susceptible to contamination than the peat a few centimetres lower (cf. the detailed diagram on p. 335 in Serebryanny *et al.*, 1970). Perhaps the greatest enigma is the discrepancy between TA-275 (40 800 ± 700 years) and Birm-249 (> 48 750 years), determinations on the same piece of wood. Again, as pointed out already by Shotton and Williams (1973) it is the wood, not the peat, which has produced a date (TA-275) that appears to be too young.

Hopefully, more extensive excavations (trenching) can be made in the future so that detailed sampling can be carried out over a wider area. Additional age determinations on the variety of organic materials present at Karuküla, including the different constituents of wood, should permit definition of the exact time span represented by the deposits at this important site.

Acknowledgments

Appreciation is expressed to the Academy of Sciences of the U.S.S.R. for arranging my visit to Estonia, under the auspices of the Canada-U.S.S.R. General Exchanges Agreement, and in particular to Dr. M.G. Grosswald of the Academy's Institute of Geography, Moscow, for accompanying me there. Drs. A.V. Raukas and J.-M. Punning of the Geological Institute, Academy of Sciences of the Estonian S.S.R., ensured a most worthwhile visit to Tallinn and Karuküla. The age determinations in Ottawa were carried out under the direction of J.A. Lowdon, Mrs. L. Wilson and Dr. M. Kuc identified the wood and peat constituents, respectively, in the samples from Karuküla, and Dr. J.V. Matthews, Jr. provided helpful comments on the manuscript.

References

Andersen, Sv. Th.
1961: Vegetation and its environment in Denmark in the Early Weichselian Glacial (Last Glacial); Dan. Geol. Unders., Raekke 2, no. 75, 175 p.

Andersen, Sv. Th., Vries, Hl. de and Zagwijn, W.H.
1960: Climatic change and radiocarbon dating in the Weichselian Glacial of Denmark and the Netherlands; Geol. Mijnbouw, 39th Jaargang, p. 38-42.

Blake, W., Jr.
1974: Collection of samples for radiocarbon dating, U.S.S.R.; *in* Report of Activities, Part A, Geol. Surv. Can., Paper 74-1, Pt. A, p. 191-192.

Kajak, K., Punning, J.-M and Raukas, A.
1970: New data on the geology of the Karuküla profile (southwestern Estonia); Izvestia Akad. Nauk Estonian S.S.R., v. 19, Chemistry-Geology, no. 4, p. 350-357 (in Russian with summaries in Estonian and English).

Lundqvist, J.
1974: Outlines of the Weichsel Glacial in Sweden; Geol. För. i Stockholm Förh, v. 96, p. 327-339.

Orviku, K.K.
1960: Geology of the Pleistocene in Estonia; 21st Internatl. Geol. Cong., Copenhagen, 1960; Part IV, Proc. of Sect. 4, Chronology and Climatology of the Quaternary, p. 88-92.

Orviku, K.K. and Pirrus, R.O.
1965: Inter-morainic organic deposits at Karuküla (Estonian S.S.R.); in Lithology and stratigraphy of Quaternary deposits in Estonia (A contribution to the VIIth Internat. Cong. INQUA, U.S.A., 1965), K.K. Orviku (ed.); Tallinn, Geol. Inst., Akad. Nauk Estonian S.S.R., p. 3-21 (in Russian with summaries in Estonian and English).

Punning, J.-M., Ilves, E. and Liiva, A.
1966: Das Datieren der Proben Höheren Alters mittels der Radiokohlenstoff-Methode; Izvestia Akad. Nauk Estonian S.S.R., v. 15, Biological Ser., no. 4, p. 577-581 (in Russian with summaries in Estonian and German).

1968: Tartu radiocarbon dates II; Radiocarbon, v. 10, no. 1, p. 124-130.

Raukas, A., Rähni, E. and Miidel, A.
1971: Marginal glacial formations in north Estonia; Publishing House "Baltic": Tallinn, 225 p. (in Russian with extended summary in English).

Raukas, A. and Serebryanny, L.R.
1972: On the Late Pleistocene chronology of the Russian Platform, with special reference to continental glaciation; 24th Internatl. Geol. Cong., Montreal 1972, Sect. 12, Quaternary Geology, p. 97-102.

Serebryanny, L.R.
1969: L'apport de la radio-chronométrie à l'étude de l'histoire tardi-quaternaire des régions de glaciation ancienne de la Plaine russe; Revue de Géogr. physique et de géol. dynamique, v. XI, no. 3 (special volume for the VIIIth Internatl. Cong. INQUA, Paris, 1969) p. 293-302.

Serebryanny, L.R., Raukas, A. and Punning, J.-M.
1970: Fragments of the natural history of the Russian Plain during the Late Pleistocene with special reference to radiocarbon datings of fossil organic matter from the Baltic region; Baltica (Dept. of Geography, Acad. of Sci., Lithuanian S.S.R., Vilnius), v. 4, p. 351-366.

Shotton, F.W. and Williams, R.E.G.
1973: Birmingham University radiocarbon dates VI; Radiocarbon, v. 15, no. 1, p. 1-12.

Vinogradov, A.P., Devirts, A.L., Dobkina, E.I. and Markova, N.G.
1968: Radiocarbon dating in the Vernadsky Institute V; Radiocarbon, v. 10, no. 2, p. 454-464.

30. CONTEMPORARY POLLEN SPECTRA FROM THE EASTERN JAMES BAY AREA, QUEBEC

Project 690064

L. D. Farley-Wilson
Terrain Sciences Division

In September 1974 surface samples for pollen analysis were collected from several localities in the eastern James Bay area (Fig. 1) by R. J. Mott and J.-S. Vincent. Results of the analyses constitute the basis for the following report. All pollen identifications were done by the author.

There have been few studies made of modern pollen in surface sediments from northern Quebec and Labrador. In a study of bogs across Quebec Potzger and Courtemanche (1956) did not collect surface samples as such, but the uppermost sample in each profile is essentially modern. Several of their sites are located in the southwestern part of the present study area. Terasmae and Mott (1965) made an investigation of the modern pollen deposition to the east in the Nichicun Lake area of Quebec, and more recently Mott (1974) reported on the modern pollen spectra from west-central Labrador.

Physiography

All the sampling sites are in the Eastmain Lowland physiographic region of the Canadian Shield (Bostock, 1970) with the exception of one site, situated north of the boundary of this region but in a similar physiographic location. Igneous and metamorphic rocks of Archean and Proterozoic age underlie the area (Eade, 1966). The regional slope is towards the west and drainage into James Bay is through major river systems including La Grande, Opinaca, Eastmain, Rupert, Broadback, and Nottaway rivers. These river systems commonly are deeply incised and are responsible for some of the major differences in relief of the area.

Surficial geology of part of the area has been mapped by Lee *et al.* (1960) and Vincent (1973, 1974). The bedrock surface is overlain by glacial deposits including drumlins, eskers, drumlinoid ridges, end moraines and De Geer moraines. As the ice retreated towards the northeast, clays were deposited in glacial Lake Barlow-Ojibway. In parts of the area tills of the Cochrane readvance overlie the Barlow-Ojibway sediments. After the Cochrane, the Tyrrell Sea replaced glacial Lake Barlow-Ojibway and covered an extensive area east and southeast of James Bay. Marine clays and other sediments were deposited in this sea (Prest *et al.*, 1967). Rebound of the crust following deglaciation and washing of the glacial deposits has resulted in raised beaches. In the Sakami Lake area beaches are found at elevations up to 875 feet (ca. 267 m) a.s.l. (J.-S. Vincent, pers. comm.).

Extensive muskeg areas have developed on the poorly drained marine and lacustrine clay plains. Generally, lakes are in greater abundance at higher elevations to the east of the coast, although boggy areas are still common.

Climate

The climate of the region is severe although there is probably some ameliorating effect due to its proximity to James Bay. The mean daily January temperature is -23°C; the mean daily July temperature is 13°C. Winter lows of -40°C to -45°C, and summer highs up to 32°C, have been recorded (Meteorological Branch, 1960). Within the growing season of 140 to 150 days there is a frost-free period of less than 80 days. There are 180 days with measurable precipitation. The average annual total precipitation is 25 inches with a mean annual snowfall of 100 inches and an average annual rainfall of 15 inches. Prevailing winds are generally northwesterly for most of the year with summer winds frequently from the southwest (Thomas, 1953).

Vegetation

The area lies within three sections of the Boreal Forest Region: the Northern Clay Section, the East James Bay Section and the Fort George Section (Rowe, 1972).

The southern part of the area is characterized by vast stands of black spruce (*Picea mariana*) on the uplands as well as on the lowland flats where they alternate with extensive sedge (Cyperaceae) fens and sphagnum-heath (*Sphagnum*-Ericaceae) bogs. Tamarack (*Larix laricina*) is sparse except in young stands. Hardwood or mixed wood stands occur on well drained sites and consist of trembling aspen (*Populus tremuloides*), balsam poplar (*Populus balsamifera*), balsam fir (*Abies balsamea*), white spruce (*Picea glauca*), and black spruce. Jack pine (*Pinus banksiana*) is dominant on many of the drier sites, and white birch (*Betula papyrifera*) is prominent on sandy soils.

In the central part of the study area white and black spruce, balsam poplar, trembling aspen, white birch, and balsam fir grow to considerable size in the sheltered valleys. The rocky uplands with their thin cover of till support poor growths of black spruce, jack pine, and tamarack. There are restricted areas of low lying swamps back from the shoreline, and the subarctic type of open lichen-woodland appears on dry uplands. Eastward there is a decrease in the size, abundance, and quality of white spruce, balsam fir, and balsam poplar, species which apparently thrive in the moist conditions of the coastal area.

Extensive areas of open or closed stands of conifers on both upland and lowland characterize the area surrounding Sakami Lake. The hilly uplands support open, lichen-floored stands of black spruce, some white spruce, and balsam fir. Large areas of muskeg and open bog occur. North of La Grande Rivière there is less local relief. Jack pine is abundant on the low

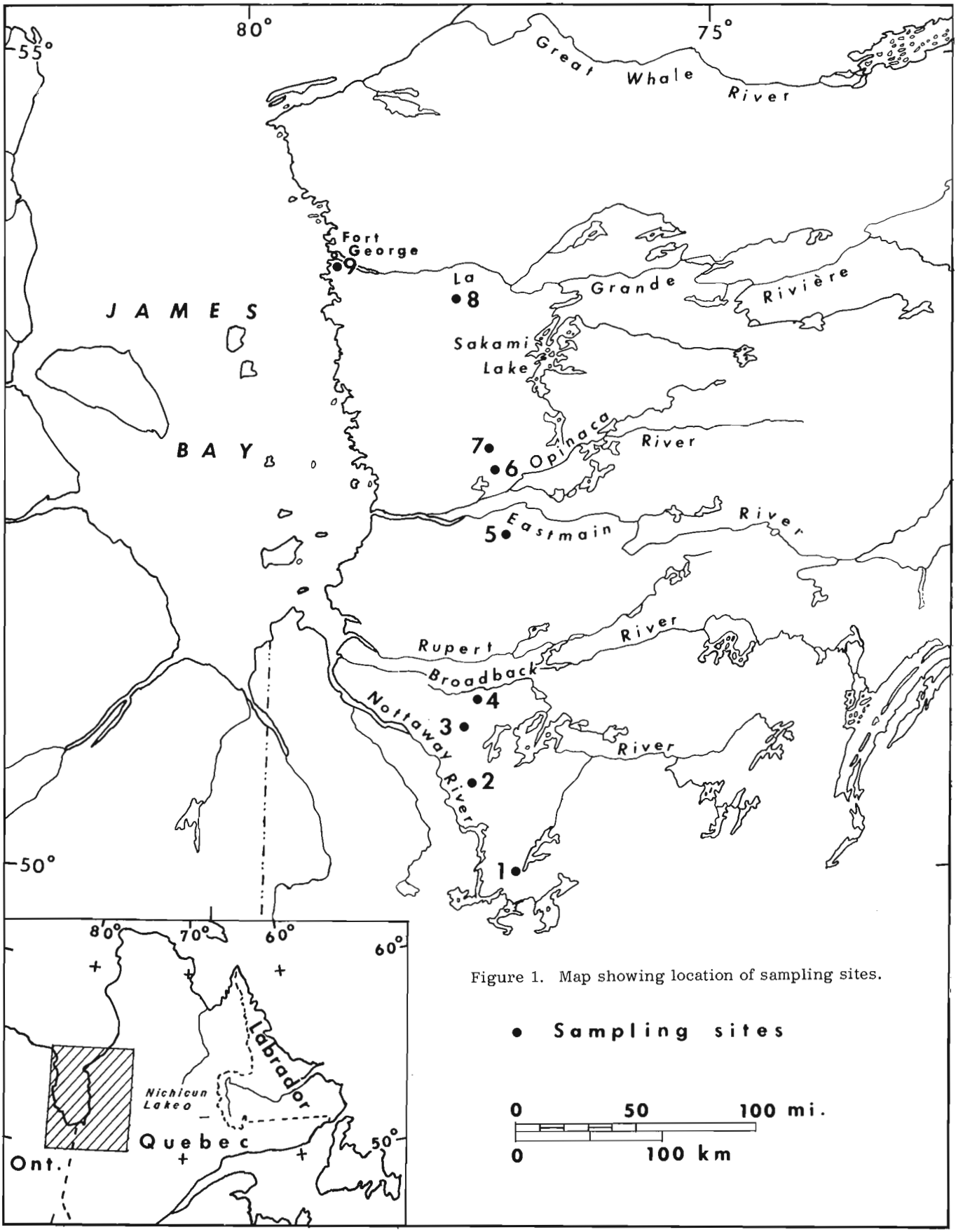

Figure 1. Map showing location of sampling sites.

Table 1

Site Locations

Site No.	Latitude	Longitude	Elevation* feet a. s. l.
1	50°01'40"	77°07'45"	875
2	50°35"40"	77°34'05"	950
3	50°54'35"	77°38'50"	890
4	51°05'45"	77°32'40"	780
5	52°04'35"	77°13'00"	790
6	52°31'00"	77°18'15"	820
7	52°40'40"	77°22'40"	570
8	53°33'35"	77°40'45"	540
9	53°47'32"	79°01'45"	35

*Elevations were determined by extrapolation from the 1: 50 000 NTS maps (contour interval 50 feet).

morainic ridges. The intervening clay-filled depressions, with their shallow organic soils, are occupied by black spruce and dwarf shrubs.

Sampling Sites

Sites 2, 3, 5 and 7 are small, shallow lakes. An Ekman dredge was used to collect samples at the mud/water interface. At sites 4 and 8, Brown cores (Brown, 1956) were collected from the top 100 cm (approximately) of lake bottom sediment and samples from the mud/water interface were removed in the laboratory. Collection of samples at sites 1 and 6, peat deposits, and at site 9, a palsa bog, was made by hand. Site locations and elevations are listed in Table 1, and locations are shown in Figure 1.

Results and Discussion

The pollen spectra from the nine sites are listed in Table 2. Taxa percentages are calculated from a sum of the total number of pollen grains and spores (exclusive of aquatics), and the pollen sum used for each sample is shown in the Table.

Spruce dominates the assemblages. No attempt was made to differentiate between white and black spruce, but the presence of both species was noted in the samples, and there appeared to be a preponderance of the black spruce pollen type. Next in prominence are jack pine and birch. Although present in the area, these taxa probably are overrepresented in the assemblages and likely do not occur locally at sites where lower percentages were obtained. White pine (*Pinus strobus*) was differentiated from the jack pine/red pine (*Pinus banksiana/resinosa*) type pollen on the basis of the presence of verrucae on the distal side of the grain between the bladders. Those grains that were lacking this portion and those that were not whole were identified as *Pinus*. Since the northern range of red pine is well to the south of this area, the majority of the grains identified as *Pinus banksiana/resinosa* are presumed to be jack pine. White pine and hemlock (*Tsuga canadensis*) do not grow in the area (Hosie, 1969), and their presence in the assemblages is the result of long distance wind transport. Small amounts of balsam fir and tamarack are present, reflecting their limited occurrence in the area. Although trembling aspen and balsam poplar grow in the region (Rowe, 1972), their presence in the assemblages is limited to three sites where one or two pollen grains were counted. This paucity of pollen may reflect either conditions of preservation in the sediments or the irregular distribution of these trees in the landscape. The presence of other hardwood genera in the assemblages is due to long distance transport, as their northern range lies well to the south of the study area.

Among the shrub pollen, alder (*Alnus*) is the most abundant. It is interesting to note that although willow (*Salix*) is present at most sites, a significant percentage is found at only the coastal site, reflecting its local abundance. Other shrubs appear in minor amounts. Heath plants appear to be greatly under-represented; low percentages were obtained despite their local abundance.

Although this region provides a suitable environment for various herbs and spore-bearing plants, only small percentages are found in the assemblages. One notable exception is ragweed type (Ambrosieae) pollen which is north of its range, and its presence here in the spectra can only be accounted for by long distance transport from areas to the south and southwest (Terasmae and Mott, 1965). As would be expected, sedge and *Sphagnum* have a varying abundance depending on their proximity to the sites. Other aquatics are poorly represented in the pollen spectra.

The results summarized here are similar to those found in Labrador (Mott, 1974) and at Nichicun Lake (Terasmae and Mott, 1965) and to those reported by Potzger and Courtemanche (1956) at their northern bog sites, with the exception of the percentages of pine. In the Labrador study pine percentages are minimal. Because the percentages in the Nichicun Lake analyses and those of Potzger and Courtemanche are calculated from the total number of arboreal pollen grains counted (as opposed to the total arboreal and non-arboreal pollen exclusive of aquatics as was done here and in the Labrador report), direct comparisons are difficult. Recalculation of the percentages of these earlier studies would lower the percentages in proportion to the number of shrubs and herbs counted. In the Potzger and Courtemanche assemblages, this recalculation would result in pine percentages that are similar to those obtained here. At Nichicun Lake the pine percentages also would be reduced. At that locality, however, another factor must be considered; i.e. the Nichicun Lake area is one of sparse vegetation so that any pollen introduced into the area by wind transport tends to be overrepresented in comparison to the pollen input from local vegetation.

Table 2

Pollen Spectra

Taxa	Site No. 1	2	3	4	5	6	7	8	9
Trees									
Picea	52.2	43.1	53.0	45.5	48.8	31.6	27.4	42.3	54.9
Pinus sp.		1.2	3.9	2.3	1.2	6.7	7.8	8.3	3.4
P. strobus	1.0	1.6	2.2	1.3	1.4	1.0	2.9	1.6	1.7
P. banksiana/resinosa	26.9	10.4	6.7	10.8	10.9	32.9	12.3	19.5	7.2
Abies balsamea	1.0	0.5	0.7	0.3		0.5	0.2	0.3	0.4
Tsuga canadensis					0.2				
Larix laricina		1.2		0.3	0.5		0.7	1.3	1.3
Betula	4.5	11.8	19.7	15.6	11.3	6.2	9.7	11.2	3.0
Populus		0.5				0.3			0.4
Quercus		2.3	1.3	1.0	1.2	0.5	0.7	2.1	
Ulmus		0.9	0.4		0.7				
Carya					0.2				
Acer		0.2	0.2						
Fraxinus	0.3	0.7	0.4		0.5			0.3	0.4
Carpinus/Ostrya		0.7	0.2				0.2		
Platanus		0.2							
Shrubs									
Juniperus/Thuja		0.5	0.2						
Alnus	8.0	13.7	4.8	14.0	9.9	5.1	26.9	9.1	4.7
Salix		0.2		1.0	0.9		1.2	0.5	10.2
Corylus		0.2				0.3	0.2		
Myrica				0.3	4.5		1.9	0.3	0.9
Ericaceae		1.2	0.9			8.7	1.5		0.4
Herbs									
Gramineae		1.2	1.3	0.3	0.5	0.5	0.7		0.4
Tubuliflorae	0.3				0.7				0.4
Ambrosieae	2.9	3.7	0.2	2.6	1.4	3.6	1.5	1.0	3.0
Artemisia	1.3	2.6	1.7	1.6	2.4	0.8	1.0	0.5	0.4
Chenopodiineae	0.6	0.2		1.0		0.5	0.2		1.3
Sarcobatus		0.2			0.2				
Rosaceae					0.2				
Rubus chamaemorus						0.3			
Potentilla							0.2		3.0
Caryophyllaceae				0.3					
Thalictrum				0.3					
Rumex				0.3					
Urtica							0.7	0.3	
Epilobium							0.2		
Lycopodium annotinum			0.2		0.5		0.7	0.8	0.4
L. clavatum			0.2		0.2				0.4
L. lucidulum			0.2						
Pteridophyta	0.6	0.5		0.3	0.5	0.3		0.3	
Polypodiaceae		0.2	0.7	0.7	0.5		0.7		
Unidentified N.A.P.	0.3	0.2	0.9		0.7	0.3	0.2	0.5	1.7
Pollen Sum (no. of grains)	312	432	462	308	424	389	413	385	235
Aquatics									
Cyperaceae	6.7	1.6	1.3	0.3	3.5	2.8	1.5	1.0	221.3
Isoetes		2.1	6.7	0.3	1.4		1.2		
Potamogeton								0.3	
Nuphar		0.2	1.5		1.7		0.5	0.3	
Menyanthes									2.1
Sphagnum	12.2	20.4	12.6	21.4	24.8	32.7	17.4	14.3	14.9

Percentages are based on total pollen (pollen sum) excluding aquatics.

Summary

The general vegetational characteristics of the forest region are reflected clearly in the modern pollen and spore assemblages obtained from the surface samples. These assemblages are dominated by spruce, jack pine, birch, alder, sedge, and *Sphagnum.*

The pollen frequencies here resemble those found in the Nichicun Lake area and in west-central Labrador, as well as those obtained by Potzger and Courtemanche in their study of bogs from the James Bay area. However, it is evident that the pine percentages are highest in the eastern James Bay area, where pine is locally present, and they decrease to the east with increasing distance of the sites from the northern range of the pine.

References

Bostock, H. S.
1970: Physiographic subdivisions of Canada; *in* Geology and Economic Minerals of Canada, R. J. W. Douglas (ed.); Geol. Surv. Can., Econ. Geol. Report No. 1, 5th ed., p. 10-30.

Brown, S. R.
1956: A piston sampler for surface sediments of lake deposits; Ecology, v. 37, p. 611-613.

Eade, K. E.
1966: Fort George River and Kaniapiskau River (west half) map-areas, New Quebec; Geol. Surv. Can., Mem. 339, 84 p.

Hosie, R. C.
1969: Native trees of Canada; Can. Forestry Serv., Dept. Fisheries and Forestry, 380 p.

Lee, H. A., Eade, K. E. and Heywood, W. W.
1960: Surficial geology of Sakami Lake (Fort George-Great Whale Area), New Quebec; Geol. Surv. Can., Map 52-1959.

Meteorological Branch
1960: The climate of Canada; Can. Dept. Transport, 74 p.

Mott, R. J.
1974: Modern pollen spectra from Labrador; *in* Report of Activities, Part B, Geol. Surv. Can., Paper 74-1, Pt. B, p. 232-234.

Potzger, J. E. and Courtemanche, A.
1956: A series of bogs across Quebec from the St. Lawrence valley to James Bay; Can. J. Bot., v. 34, p. 473-500.

Prest, V. K., Grant, D. R. and Rampton, V. N.
1967: Glacial map of Canada; Geol. Surv. Can., Map 1253A.

Rowe, J. S.
1972: Forest regions of Canada; Dept. Environment, Can. Forestry Serv., Publ. No. 1300, 172 p.

Terasmae, J. and Mott, R. J.
1965: Modern pollen deposition in the Nichicun Lake area, Quebec; Can. J. Bot., v. 43, p. 393-404.

Thomas, M. K.
1953: Climatological Atlas of Canada; Nat. Res. Council, Div. Bldg. Res. and Can. Dept. Transport, Meteorological Div., N. R. C. No. 3151, 253 p.

Vincent, J.-S.
1973: Géologie du Quaternaire et sensitivité du terrain d'une partie de la région en voie d'aménagement à l'est de la baie James; Geol. Surv. Can., Open File 178.

1974: Géologie du Quaternaire et sensitivité du terrain d'une partie de la région en voie d'aménagement à l'est de la baie James; Geol. Surv. Can., Open File 198. Includes an extended legend and four Quaternary geology maps: 33 E/9, 33 E/16, 33 F/12 and 33 F/13.

Project 690064

S. Lichti-Federovich
Terrain Sciences Division

Introduction

As part of a continuing investigation into the potential value of palynology as a means of analyzing samples from glaciers (Lichti-Federovich, 1974, 1975), surface snow samples from five widely distributed ice caps in the Canadian Arctic were analyzed. The samples were collected by Dr. R. M. Koerner (Polar Continental Shelf Project, Dept. of Energy, Mines and Resources, Ottawa) in April, May, and June 1974; pollen analyses made by the author. The collection sites are shown in Figure 1.

Field and Laboratory Methods

At each ice cap, an area of approximately 10 m x 5 m was sampled by pressing a 7.5 cm diameter ice corer several times into the snow to the depth of the 1973 melt surface. The weights of the samples are shown in Table 1. The samples were filtered and then processed in the laboratory by the special procedure set up to minimize contamination (Lichti-Federovich, 1975). Total pollen content of the samples was recorded.

Results

Table 1 shows the location, elevation, sample weights, and total pollen content; 142 pollen grains in 30 different taxa were recorded. Two have not yet been identified and 55 grains were degraded or fragmented to such an extent that identification was not possible. In addition, 29 moss spores, one *Lycopodium annotinum* and one Polypodiaceae spore were noted. The pollen totals are too small to permit useful quantitative comparisons, and it appears that larger samples will be required for any detailed analysis.

The feature common to all five spectra is the preponderance of exotic types with origins in boreal and temperate regions. A few records are of interest because of their rarity. *Plantago juncoides* was recorded

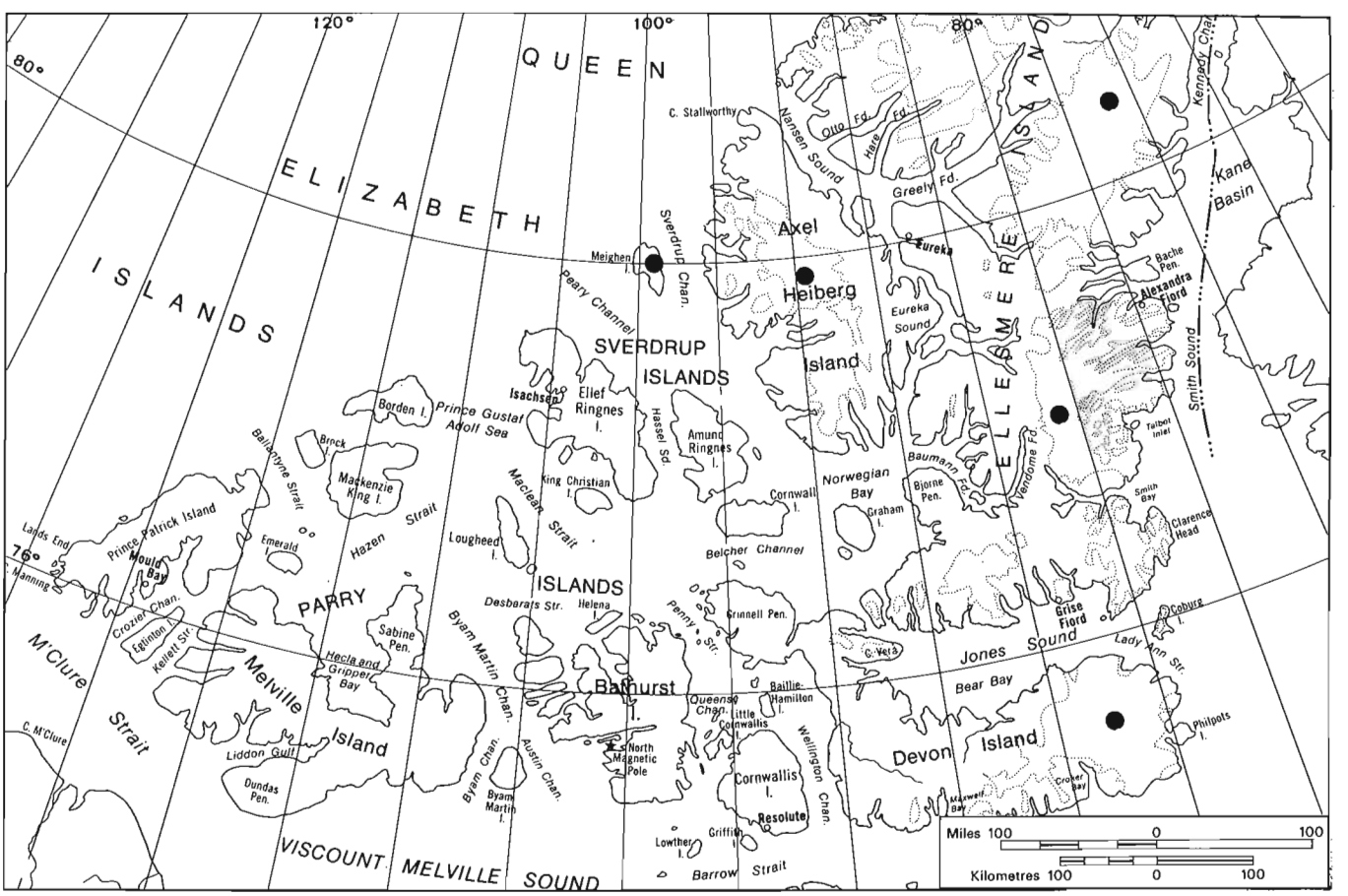

Figure 1. Location of sampling sites.

Table 1

Pollen and spore totals from snow samples of five Arctic Island ice caps

	DEVON ISLAND Ice Cap	ELLESMERE ISLAND South-central Ice Cap	ELLESMERE ISLAND North-central Ice Cap	AXEL HEIBERG ISLAND Ice Cap	MEIGHEN ISLAND Ice Cap
Elevation (ft. a. s. l.)	6 100	3 875	5 500	5 693	780
Sample weight (kg)	5. 67	7. 26	4. 31	3. 86	5. 67
Picea					2
Pinus	2				
Pinus banksiana			1		
Abies				1	
Thuja/Juniperus		2		2	3
Carya	1				
Quercus			1		
Ulmus	1			2	
Betula (tree)	8	2		5	3
Betula (shrub)	3		2	2	5
Alnus	5	3	1	4	11
Corylus			1		
Salix	3	1		3	
Ericaceae	1		1	3	1
Ephedra				1	
Cyperaceae	1				2
Gramineae	8	3	2	2	2
Artemisia	2	1	1	1	2
Ambrosieae	10	2	3	8	
Chenopodium	1	1			
Potentilla			2		
Dryas	1			2	
Rosaceae			2		
Saxifraga oppositifolia	1				
Saxifragaceae	1		1		
Oxytropis				1	
Oxyria digyna	1	1			
Ranunculus sulphureus	2				
Plantago juncoides			1		
Polygonum viviparum			4	1	
Musci			3	7	18
Unidentifiable NAP			2		
Lycopodium annotinum		1			
Polypodiaceae				1	
TOTAL	52	17	28	46	31
P. gr. degraded and fragmented	11	3	13	13	15
Fungal remains	+	+	++	+	+++
Tert. and older palynomorphs			2	2	8

from the north-central Ellesmere Island ice cap site. This species is anemophilous (pollinated by wind), but it is not a locally abundant plant anywhere in its arctic-subarctic range, which extends from Iceland and south-central Greenland to Labrador and Hudson Bay, with localities in southern Baffin Island and at Churchill and Great Bear Lake. It is absent from Ellesmere Island, and it does not occur in the Canadian Arctic Archipelago except at the southern tip of Baffin Island (Porsild, 1957). This occurrence, therefore, of an arctic species should be properly placed in the category of exotic origin.

The presence of one pollen grain of *Ephedra* is interesting and adds yet another station to the inventory of modern and late-Pleistocene occurrences of this shrub whose pollen grains are readily transported over great distances (Maher, 1964).

The number of exclusively arctic taxa recorded in the spectra is remarkably small (17) and, as in the case of *Plantago juncoides*, several might have been transported substantial distances. No geographic pattern is readily detectable in these data, although the sites are spread over a wide area.

The proportion of grains too deteriorated to be identified is high (> 25%). In many instances wall degradation appears to have been caused by microbial activity.

The limitations of these data are probably the result of the small sample sizes. Larger samples yield pollen sums amenable to more effective analysis and facilitate the discrimination between exotic, regional, and even local sources (Lichti-Federovich, 1974). The accumulation of data from snow surfaces and ice cap cores is proceeding (e.g., Fredskild and Wagner, 1974), and a firmer basis for interpretation is being established by these studies.

References

Fredskild, B. and Wagner, P.
1974: Pollen and fragments of plant tissue in core samples from the Greenland Ice Cap; Boreas, v. 3, p. 105-108.

Lichti-Federovich, S.
1974: Pollen analysis of surface snow from the Devon Island Ice Cap; *in* Report of Activities, Part A, Geol. Surv. Can., Paper 74-1, Pt. A, p. 197-199.

1975: Pollen analysis of ice core samples from the Devon Island Ice Cap; *in* Report of Activities, Part A, Geol. Surv. Can., Paper 75-1, Pt. A, p. 441-444.

Maher, L.J., Jr.
1964: *Ephedra* pollen in sediments of the Great Lakes region; Ecology, v. 45, p. 391-395.

Porsild, A.E.
1957: Illustrated flora of the Canadian Arctic Archipelago; Natl. Mus. Can., Bull. No. 146, 209 p.

32. INCONGRUENCE OF MACROFOSSIL AND POLLEN EVIDENCE: A CASE FROM THE LATE PLEISTOCENE OF THE NORTHERN YUKON COAST

Project 730027

John V. Matthews, Jr.
Terrain Sciences Division

Introduction

In a recent paper on the paleogeography and climatic history of Beringia, Hopkins (1972), using pollen data from Alaska and northwestern Canada, made some initial statements concerning possible Wisconsin age refugia for spruce, birch, and alder as well as their history of dispersal from such refugia during the late Pleistocene and Holocene. The conclusions expressed in that paper were necessarily of a preliminary nature; they depend, for testing and refinement, on a continuing flow of new paleobotanical-paleoecological information from Alaska and northwestern Canada. The northern coastal plain of Yukon Territory is a critical area for such work because, judging from the proximity of the northern limits of spruce, alder, and birch in that region (Fig. 1), it should be one of the more sensitive areas for discerning climatic induced vegetation changes involving those plants.

This paper deals with a small assemblage of plant and animal macrofossils and pollen from a coastal Yukon site near the Alaska border (Fig. 1). The fossils indicate a tundra environment. Dwarf birches were growing at the site, yet this fact is not clearly indicated by the pollen evidence. A similar case of incongruent pollen and macrofossil evidence from a site near Inuvik, N.W.T. is cited to illustrate a potential danger of relying on pollen evidence alone to plot the dispersal history of plants.

Methods

Except for the radiocarbon-dated wood, all of the fossils discussed here come from a 500 ml sample of peat submitted to the author by V.N. Rampton. A subsample of the peat was utilized for pollen analysis; the remainder was disaggregated and wet sieved using a 0.317 mm screen. The residue remaining on the screen was examined with a dissecting microscope, and all identifiable plant and animal fragments were isolated and stored in alcohol or mounted on macrofossil slides.

Insect fossils were identified by comparison with specimens in the author's own collection and the extensive collection in the Biosystematics Research Institute, Canada Department of Agriculture, Ottawa. Seeds and other plant macrofossils were identified by comparison with specimens in the Geological Survey's plant macrofossil reference collection. A list of macrofossils is presented in Table 1. All identifications were made by the author unless otherwise noted.

The pollen sample was processed by standard techniques, using NaOH, HF and acetolysis treatments. Pollen counts are presented in Table 2. The "Undet." category (undetermined pollen) includes pollen well enough preserved for identification, but not identified at this time. The "Indet." category (indeterminate pollen), excluded along with *Equisetum* and Polypodiaceae from the pollen sum, includes pollen recognized as such but with grains too degraded for identification.

Geological Setting

The sample site, first discovered and documented by V.N. Rampton, is located on the northern Yukon coast of 69°36'14" N; 140°36'12" W, approximately 7 km east of Clarence Lagoon (Fig. 1). It is outside the maximum limit of Laurentide glaciation (Hughes, 1972) and lies within the segment of coastline characterized by Rampton (1974) as having, at most exposures, 3 to 6 m of thermokarst sediments (peat, clay, fine sand) overlying marine or glaciomarine sediments. However, at the sample site — an exposure 4.5 m thick — the typical thermokarst over marine sequence is replaced laterally by fluvial (?), sandy gravels capped by approximately 0.5 m of peaty silt. Within the gravels at a level 2 m above the base of the exposure was a lens of autochthonous peat containing fragments of twigs (V.N. Rampton, field notes, 1974). One fragment, a branch 41 cm in length by 1 cm in diameter, identified by R.J. Mott as *Betula* sp. (Wood Ident. Rept. No. 74-42) was dated at 10 900 ± 80 years B.P. (GSC-1853).

Though presently coastal, the fossil locality likely was not so 10 900 years ago. Sediments and features thought to represent late Pleistocene and Holocene beaches have been recognized beneath the Beaufort Sea (J.M. Shearer, pers. comm., 1974; Shearer, 1971) but as yet are poorly dated. The sea level sequence near the Alaskan Bearing Sea coast is better known. There, several stillstands and one minor regression occurred during the late Wisconsin and Holocene rise of sea level (Hopkins, 1973). One Bering Sea shoreline at -30 metres evidently formed around 11 800 years ago and sea level in that area had reached -20 metres shortly after 10 000 years B.P. (Hopkins, 1973). Use of this data to delineate the position of the 10 900 year old Beaufort shoreline must be done with caution because of the possible effects of local tectonism (McDonald and Lewis, 1973) and Holocene sedimentation (cf. Shearer, 1972). It seems probable, however, that the level of the Beaufort Sea was between 20 and 30 metres lower than at present 10 900 years ago, and if so, the coast in the vicinity of the sample site would have been 4 to 15 km north of its present location (-20 to -30 m isobaths, Canadian Hydrographic Chart 7601, Siku Point to Kay Point).

Botanical Setting

Tundra, primarily poorly drained and dominated by sedges, characterizes the northern portion of the Yukon coastal plain today. According to Hultén (1968) both species of shrub birch, *Betula nana* L. and *B. glandulosa* Michx., occur along the Yukon coast; however, the former does not seem to have been recorded at Demarcation Point, just west of the Yukon-Alaska border (Wiggins and Thomas, 1962; Hultén, 1968). Thus the probable northern limit of shrub birches, especially *B. glandulosa,* is as indicated in Figure 1.

There seems to be slight disagreement on the northern limit of *Alnus*. Some authors show this genus extending all the way to the northern Yukon coast but others (e.g., Hultén, 1968) place the northern limit somewhat south of the coast. The line in Figure 1 is based on the observations, published and unpublished, of geologists and botanists who have worked in the area (e.g., V.N. Rampton, C.P. Lewis, L.R. Hettinger, J.M. Teversham, R.W. Wein).

Latest published observations on the northern distribution of spruce indicate the presence of isolated white spruce (*Picea glauca* [Moench] Voss) well down the Firth River valley to within 30 km of the coast. The actual position of spruce treeline, however, probably more closely coincides with the line drawn near the bottom of Figure 1. Even so, it is clear from Figure 1 that the northern limits of birch, alder, and spruce are closer to one another in the Northern Yukon than in Alaska. Perhaps nowhere in North America are the northern limits of these three plants so nearly coincident as in the northern Yukon.

Shingle Point, Stokes Point, and Komakuk Beach on the Yukon coast have meteorological stations, hence

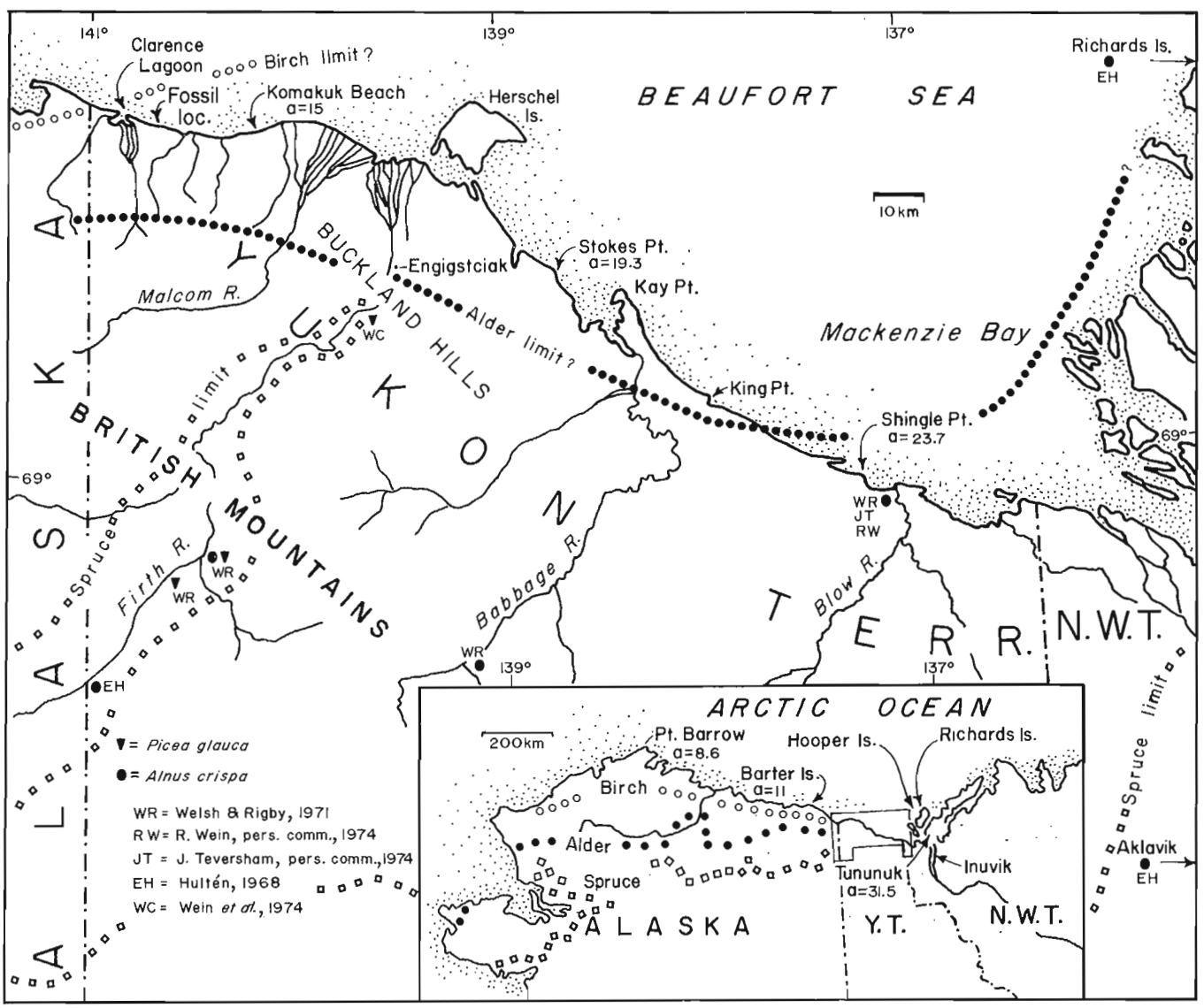

Figure 1. Location of sites mentioned in text and northern limits of spruce, alder, and birch. Numbers associated with some sites (e.g. a = 15) refer to a climatic parameter representing summer warmth (see text).

Table 1

MACROFOSSILS

Animals
- Vertebrata
  - Mammalia
    - Rodentia — isolated vertebra
- Insecta
  - Homoptera
    - Psyllidae
      - *Psylla* sp. [1]
  - Coleoptera
    - Carabidae
      - *Dyschirius* sp.
      - *Pterostichus pinguedineus* Eschz.
      - *Trichocellus mannerheimi* R. F. Sahlb. (Fig. 2b)
    - Hydrophilidae
      - *Cercyon marinus* C. J. Ths. [2]
    - Staphylinidae
      - *Stenus* sp.
      - *Olophrum latum* Makl.
      - Peaderinae — cf. *Lathrobium*
      - Aleocharinae — cf. *Atheta*
    - Lathridiidae
      - *Melanophthalma* ?
    - Chrysomelidae
      - Genus ?
    - Curculinoidae
      - *Lepidophorus lineaticollis* Kirby (Fig. 2c)
      - *Dorytomus* sp.
  - Diptera
    - Bibionidae
      - Genus ? (Fig. 2a)

Plants
- Pteridophyta
  - Equisetaceae
    - *Equisetum* sp.
- Angiospermae
  - Cyperaceae
    - *Carex* sp. (cf. *Carex aquatilis* Whalenb.) (Fig. 2e)
    - *Carex* sp.
  - Salicaceae
    - *Salix* sp.
  - Betulaceae
    - *Betula glandulosa* Michx. (Fig. 2d)
  - Rosaceae
    - *Dryas integrifolia* M. Vahl.

[1] Identified by W. R. Richards, Biosystematics, Agriculture Canada, Ottawa.

[2] Identified by A. Smetana, Biosystematics, Agriculture Canada, Ottawa.

they are sites for which some climatic data exist. Young (1971) has developed a system of tundra zonation which can be related to climatic data, particularly the parameter "a", the measure of total summer warmth in excess of 0°C (*see* Young, 1971 for details). According to his system, low arctic or Tundra, Zone 4 in which *Alnus* has its northern limit, includes sites like Shingle Point with "a" values ranging from 20 to 35 (Fig. 1) *Alnus* is found at Shingle Point, but the genus apparently is absent at Stokes Point and Komakuk Beach, whose "a" values are within the 12 to 20 range of sites in Tundra Zone 3, in which, according to Young, alder does not occur. *Betula* has its northern limit within Zone 3 and birch occurs at the Zone 3 sites of Stokes Point and Komakuk Beach. *Betula* species are absent in Zone 2 which includes such sites as Barter Island and Barrow. According to Figure 1, the fossil locality is probably within Young's Tundra Zone 3.

Insect Fossils

Even though the size of the peat sample was small, it contained a number of identifiable insect remains (Table 1), some of which have paleoecologic significance.

An outstanding characteristic of nearly all the fossils is their excellent state of preservation. For example, a few of the ground beetle fossils were partially articulated and the weevils (Curculionidae, Table 1) are represented by some specimens possessing much of the vestiture of scales and hairs that is often missing on fossils (Fig. 2c). These facts undoubtedly mean that the fossils are autochthonous.

The ground beetle *Trichocellus mannerheimi* is almost exclusively a tundra animal (Lindroth, 1968) and, like the weevil *Lepidophorus lineaticolis,* it can be collected today at dry fell-field sites such as those where *Dryas octopetala* and *D. integrifolia* are abundant. *L. lineaticollis* also is found at mesic to xeric sites within the limit of trees. Similarly, the ground beetle *Pterostichus pinguedineus* is only a facultative tundra inhabitant, but it occurs as far north as Herschel Island (Ball, 1966).

Cercyon commonly is not represented in northern insect assemblages, and then only rarely are the fossils well enough preserved for a specific determination. This sample included the head, pronotum, and elytra of one species, possibly a single individual. Characteristic colour patterns on the elytra show that it is from *Cercyon marinus,* a species which occurs today at several sites in the northern Yukon and Northwest Territories.

Species of the genus *Psylla* (jumping plant lice) feed on alder, willow, and birch (W. R. Richards, pers. comm., 1974). The weevil genus *Dorytomus* is associated with willow (*Salix* spp.) (O'Brien, 1970).

Plant Macrofossils

In addition to the dated *Betula* wood, the peat contained numerous samaras (winged seeds) and bracts from pistillate cones, as well as a few leaf fragments of *Betula.* The better preserved samaras possess

remnants of the "down" or tomentum regularly found at the base of the persistent styles in birch seeds (Katz *et al.*, 1965) and the wings, where present, are narrow as are those in the shrub species, *B. nana* and *B. glandulosa.* One leaf fragment has a cuneate, incompletely crenate base and the better preserved bracts have a raised area (resiniferous hump?) at the base of the median lobe (Fig. 2d). Both features are characteristic of *Betula glandulosa* Michx.

Like the insect fossils, the birch fossils also indicate that the peat is autochthonous, since some of the samaras were still attached to the bracts, an association which likely would not survive if the fossils had been transported before deposition.

Carex aquatilis (?) is represented by one poorly preserved achene with remnants of the perigynium (Fig. 2e). The species commonly is associated with poorly drained sites such as pond margins and river shorelines.

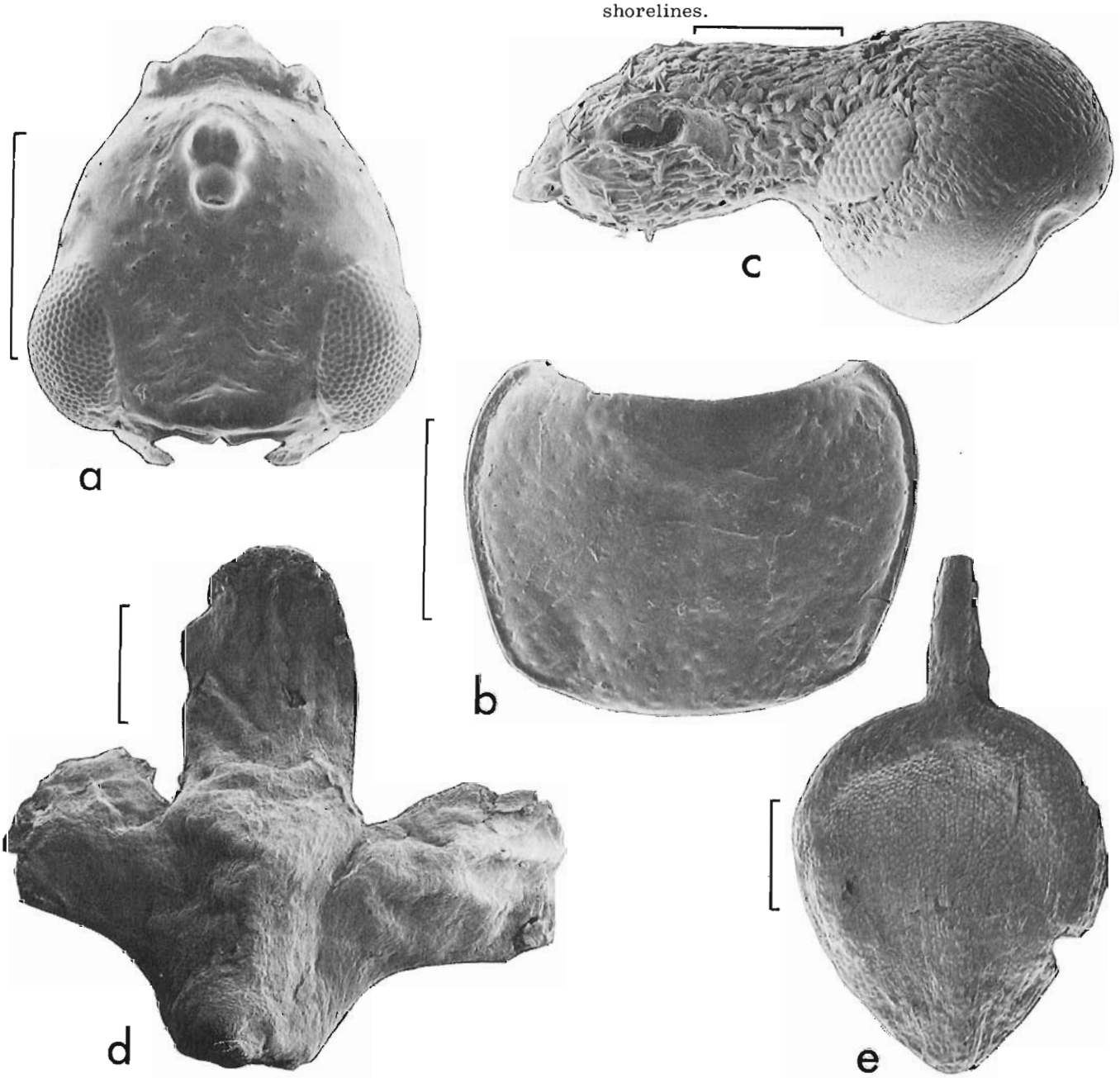

(a) head, Bibionidae (Diptera), female
(b) pronotum, *Trichocellus mannerheimi* Sahlb.
(c) head (side view), *Lepidophorus lineaticollis* Kirby. Note presence of scales, especially in front of the eye.
(d) pistillate bract, *Betula glandulosa* Michx. Lateral wings are not complete. Note presence of bulging area (resiniferous hump?) at base of median lobe.
(e) achene, *Carex*, sp. cf. *C. aquatilis* Wahlenb.

Figure 2. SEM photos of selected macrofossils. Scale bar equals 0.5 mm.

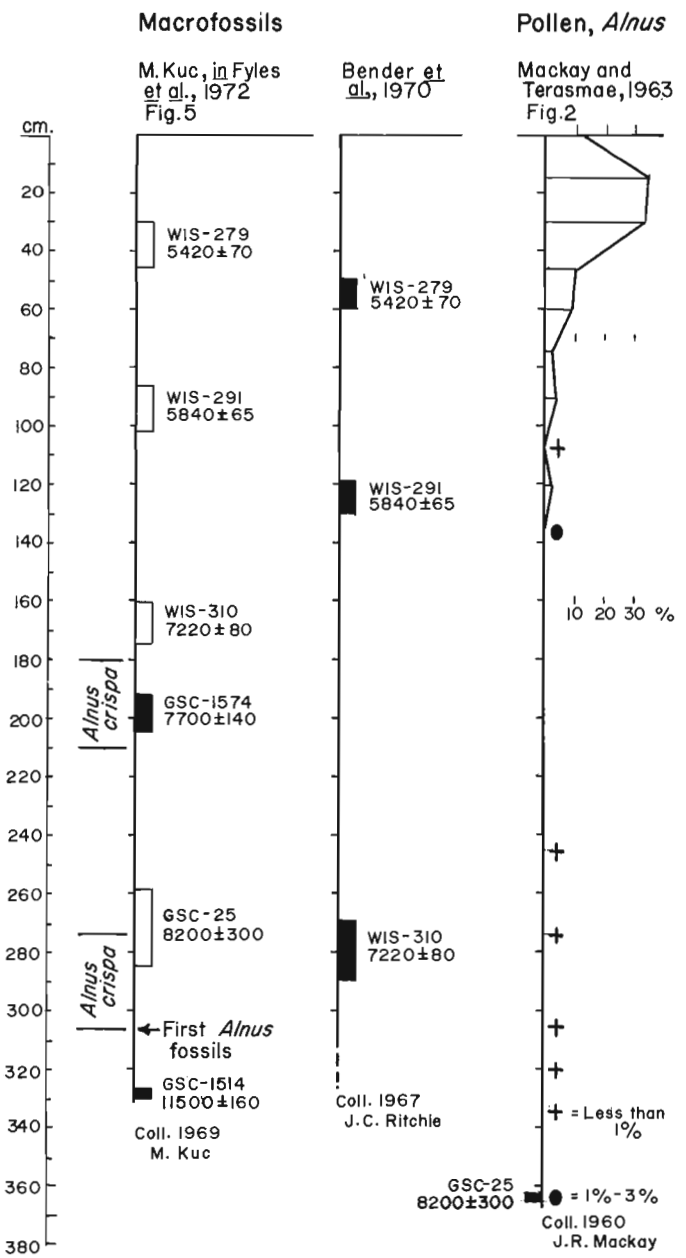

Figure 3. Comparison of radiocarbon dates with occurrence of alder macrofossils and pollen at Twin Lakes profile, near Inuvik (*see* text, footnote 1). Blackened bars are radiocarbon dates on samples collected in the year indicated below each sequence. Macrofossil diagram includes other dates as interpreted by Kuc, Fig. 5 in Fyles *et al.*, 1972. GSC-25 and GSC-1514 represent base of peat section as seen by Mackay and Kuc respectively. Base of peat observed by Ritchie was at 410 cm. Per cent *Alnus* recalculated on the basis of total pollen.

Table 2

Pollen Spectrum

Pollen or spore type	% (Σ = 335)[1]	% (Σ = 606)[2]
Alnus	+[3]	0.3
Betula	-	0.7
Picea	+	
Salix	2.7	
Artemisia	0.9	
Potentilla	0.6	
Cruciferae	2.4	
Liliaceae ?	1.2	
Gramineae	5.4	
Cyperaceae	84.0	
Undet.	2.4	99.0
Equisetum	6.3	
Polypodiaceae	3.0	
Indet.	12.5	

[1]Sum excludes *Equisetum*, Polypodiaceae, and Indet. pollen.

[2]Extended count tabulating only *Alnus*, *Betula*, and other (Undet.) pollen.

[3]+ = single grain.

Pollen

According to Table 1 at least two species of *Carex* were growing near the site, and this may account for the dominance of sedge pollen (Cyperaceae) in Table 2. Dwarf birch also was growing near the site, yet birch pollen accounts for only a fraction of the total pollen in the spectrum. Surface samples from tundra regions within the range of birch often contain higher percentages of *Betula* pollen than that reported in Table 2 (Ritchie, 1972), even in those cases where sedge pollen is greatly overrepresented (cf. Matthews, 1974b, Fig. 10, sample 74-67; Rampton, 1971, Fig. 4, sample B) Moreover, birch percentages are higher than that in Table 2 in surface spectra from Barrow, Alaska, which is far beyond the regional limit of *Betula* (Colinvaux, 1967). Thus the remarkably low per cent of *Betula* pollen in this sample, from a site at which birch was evidently growing, is puzzling.

Differential pollen preservation is not likely the cause of the anomaly. Birch pollen is more susceptible to degradation than some other types of tree pollen (Havinga, 1964), but it can be recognized in arctic assemblages, where no possibility of similar pollen exists, even when the grains are severely degraded. This means that if all of the pollen in the "Indet."

category in Table 2 were to be identified and shown to belong to the same pollen population as identified grains (i.e., no rebedded pollen), the revised percentage of *Betula* likely would be even lower than that indicated in Table 2.

Because neither overrepresentation by sedge pollen nor differential preservation of birch pollen seems to account entirely for the paucity of birch in Table 2, the author concludes that there must have been a deficit of *Betula* in the pollen rain at the sample site 10 900 years ago. The implications of this fact are mentioned below.

Discussion

The low percentage of *Picea* pollen in the pollen spectrum combined with the presence of macrofossils of *Betula glandulosa, Dryas integrifolia,* and *Trichocellus mannerheimi* suggest that the fossil locality was within a region of tundra 10 900 years ago. Alder pollen is also very rare in the pollen spectrum; however, in view of the anomalous situation presented by birch macrofossils and pollen, it seems best not to consider this as evidence of the regional absence of alder. The most that can be said is that *Alnus* was probably rare, and if any grew near the site they produced very little pollen.

The stratigraphic context of the peat (i.e., its occurrence in a sequence of inorganic, sandy gravels) and the fact that it contained fossils of *T. mannerheimi, Lepidophorus lineaticollis,* and *Dryas integrifolia* indicate a fell-field type of local environment, with only patchy vegetation. The peat itself may represent one such vegetated site.

Birches are known to produce abundant quantities of pollen (like alders), thus it is strange, even in the face of sedge pollen overrepresentation, that the per cent of birch pollen in the sample is not higher, for it seems certain in view of the macrofossil evidence that *Betula glandulosa* was growing at the site. A similar incongruence of pollen and macrofossil data occurs at Twin Lakes, near Inuvik (Fig. 1). There, the rise of alder percentages from about 3 to approximately 35 per cent (Fig. 3) occurred between ca. 5840 and 5420 years B.P., at least 2000 years after the first appearance of *Alnus* macrofossils at the lake (Fig. 3)[1]. At other Mackenzie Delta sites the alder pollen curves rise at about 5500 years B.P. (Ritchie, 1972) which is also well after the earliest appearance of Twin Lakes alder macrofossils. Such discrepancies between pollen and macrofossil evidence may be due to reduced pollen production by plants growing under climatic conditions inimical to sexual reproduction (Matthews, 1974a, 1974b). Whatever the cause or causes, cases such as these indicate the need for caution in reconstructing the dispersal history of a plant taxon on the basis of the earliest appearance of its pollen.

Such cases also illustrate the need for more detailed information on the growth and reproduction of plants at their distributional limit. For certain species information is already at hand, but as Hustich (1974) has pointed out, it is the common plants which should be receiving the most attention. Spruce, birch, and alder are especially critical in this regard because they play such an important role in northern paleoecological research. Geologists, zoologists, botanists, and archeologists working in areas near the northern limit of these taxa can contribute valuable information by examining any extralimital individuals that they encounter. The location of the plant should be recorded along with observations on its vigour – size, health, insect and wind damage. Evidence of reproduction such as seedlings or other nearby individuals should be noted and a few examples of any available fruits, staminate flowers, or cones should be collected. A soil sample or moss polster collected on the downwind side of the plant may help to indicate if pollen has been produced lately. Whatever other observations are made, they should do nothing which will enhance or compromise the plant's chances for continued survival, because such extralimital individuals someday may serve as sensitive indicators of short term climatic change.

---

[1] This statement and Figure 3 are based on a comparison of Figure 5 by Kuc (*in* Fyles *et al.*, 1972 with Figure 2 in Mackay and Terasmae (1963). Several comments are required if this comparison is to be meaningful.

In Mackay and Terasmae's report (1963) the captions for Figure 2 and Figure 3 are transposed. Thus Figure 2, not Figure 3, is the Twin Lakes diagram. Moreover, the date, GSC-25, should read 8200 ± 300 rather than 8000 ± 300 (Dyck and Fyles, 1962).

The macrofossil diagram by Kuc (Fyles *et al.*, 1972, Fig. 5) may give the impression that all of the radiocarbon dates are part of the same series. In fact only two, GSC-1514 and GSC-1574, were collected with the macrofossil samples (Lowdon and Blake, 1973). The position of the other dates, some of them based on samples collected as much as nine years before macrofossil sampling, is by interpolation or comparison of the macrofossil content of the original samples with the macrofossil profile (Fyles *et al.*, 1972, Fig. 5; M. Kuc, pers. comm., 1974). According to the macrofossil diagram alder (*Alnus crispa*) was present at Twin Lakes before 8200 ± 300 years B.P. (GSC-25), but inasmuch as GSC-25 is not part of the macrofossil sample series and GSC-1574 is, a safer conclusion would be that alder was there by 7700 years B.P. Comparison of the Wisconsin series of dates (Bender *et al.*, 1970) with the alder curve (re-computed as per cent of total pollen instead of tree pollen, Mackay and Terasmae, 1963) shows that alder percentages rise to significant values after 5840 ± 65 years B.P. (WIS-291), possibly as late as 5420 ± 70 years B.P. (WIS-279) (Fig. 3).

Acknowledgments

I thank V.N. Rampton for contributing the sample on which this report is based. V.N. Rampton, C.P. Lewis, J. Shearer, and R.J. Mott aided through helpful discussion of particular problems. L.R. Hettinger, J.M. Teversham, R.W. Wein, W.J. Cody, C.P. Lewis, and V.N. Rampton contributed information relating to the distribution of certain plant species. Members of the Coleoptera Unit, Biosystematics Research Institute (Agriculture Canada) allowed access to their collections and examined a few of the fossils. SEM photos were taken at Carleton University with the help of Louis Ling.

References

Ball, G.E.
1966: A revision of the North American species of the subgenus *Cryobius* Chaudoir (*Pterostichus*, Carabidae, Coleoptera); Opuscula Entomologica, Suppl. 28, 166 p.

Bender, M.M., Bryson, R.A. and Baerreis, D.A.
1970: University of Wisconsin Radiocarbon dates VII; Radiocarbon, v. 12, p. 335-345.

Colinvaux, P.A.
1967: Quaternary vegetational history of Arctic Alaska; *in* The Bering Land Bridge, D.M. Hopkins (ed.); Stanford Univ. Press, Palo Alto, California, p. 207-231.

Dyck, W. and Fyles, J.G.
1962: Geological Survey of Canada Radiocarbon dates I; Radiocarbon, v. 4, p. 13-26.

Fyles, J.G., Heginbottom, J.A. and Rampton, V.N.
1972: Quaternary geology and geomorphology, Mackenzie Delta to Hudson Bay; XXIV Internatl. Geol. Cong., Excursion A-30 Guidebook, 23 p.

Havinga, A.J.
1964: Investigation into differential corrosion susceptibility of pollen and spores; Pollen et Spores, v. 6, p. 621-635.

Hopkins, D.M.
1972: The paleogeography and climatic history of Beringia during late Cenozoic time; Inter-Nord, v. 12, p. 121-150.

1973: Sea level history in Beringia during the past 250 000 years; Quaternary Res., v. 3, p. 520-540.

Hughes, O.L.
1972: Surficial geology of northern Yukon Territory and northwest District of Mackenzie, Northwest Territories; Geol. Surv. Can., Paper 69-36, 11 p.

Hultén, E.
1968: Flora of Alaska and neighboring territories; Stanford Univ. Press, Palo Alto, Calif., 1008 p.

Hustich, I.
1974: Common species in the northern part of the Boreal region of Canada, an essay; Rept. Kevo. Subarctic Res., v. 11, p. 35-41.

Katz, N. Ja., Katz, S.V. and Kipiani, M.G.
1965: Atlas and keys of fruits and seeds occurring in the Quaternary deposits of the U.S.S.R. (in Russian); Acad. Nauk. U.S.S.R., Moscow 367 p.

Lindroth, C.H.
1968: The ground-beetles of Canada and Alaska, part 5; Opuscula Entomologica, Suppl. 23, p. 649-944.

Lowdon, J.A. and Blake, W., Jr.
1973: Geological Survey of Canada radiocarbon dates XIII; Geol. Surv. Can., Paper 73-7, 61 p.

Mackay, J.R. and Terasmae, J.
1963: Pollen diagrams in the Mackenzie Delta area, N.W.T.; Arctic, v. 16, p. 228-238.

Matthews, J.V., Jr.
1974a: Wisconsin environment of interior Alaska: pollen and macrofossil analysis of a 27 meter core from the Isabella Basin (Fairbanks, Alaska); Can. J. Earth Sci., v. 11, p. 828-841.

1974b: Quaternary environments at Cape Deceit (Seward Peninsula, Alaska): evolution of a tundra ecosystem; Geol. Soc. Am. Bull., v. 85, p. 1353-1385.

McDonald, B.C. and Lewis, C.P.
1973: Geomorphic and sedimentologic processes of rivers and coast, Yukon Coastal Plain; Environmental-Social Program, Northern Pipelines, Task Force on Northern Oil Development, Rept. no. 73-39, 245 p.

O'Brien, C.N.
1970: A taxonomic revision of the weevil genus *Dorytomus* in North America (Coleoptera; Curculionidae); Univ. of Calif. Publ. in Entomology, v. 60, 80 p.

Rampton, V.N.
1971: Late Quaternary vegetational and climatic history of the Snag-Klutlan area, southwestern Yukon Territory, Canada; Geol. Soc. Am. Bull., v. 82, p. 959-978.

Rampton, V.N. (cont'd)
1974: Terrain evaluation with respect to pipeline construction, Mackenzie corridor, northern part, Lat. 68°N to coast; Environmental-Social Program, Northern Pipelines, Task Force on Northern Oil Development, Rept. no. 73-74, 44 p.

Ritchie, J.C.
1972: Pollen analysis of late-Quaternary sediments from the arctic treeline of the Mackenzie River Delta region, Northwest Territories; *in* Mackenzie Delta Monograph, D.E. Kerfoot (ed.); Brock University, St. Catharines, Ontario, p. 29-50.

Shearer, J.M.
1971: Preliminary interpretation of shallow seismic reflection profiles from the west side of Mackenzie Bay, Beaufort Sea; *in* Report of Activities, Part B, Geol. Surv. Can., Paper 71-1, Pt. B, p. 131-138.

1972: Thickness of Recent (post-glacial?) mud in Beaufort Sea; Geol. Surv. Can., Open File 126.

Wein, R.W., Hettinger, L.R., Janz, A.V. and Cody, W.J.
1974: Vascular plant range extensions in northern Yukon Territory and northwestern Mackenzie District, Canada; Can. Field Nat., v. 88, p. 57-66.

Welsh, S.L. and Rigby, J.K.
1971: Botanical and physiographic reconnaissance of northern Yukon; Brigham Young Univ. Sci. Bull., Biological Series, v. 14, 64 p.

Wiggins, I.L. and Thomas, J.H.
1962: A Flora of the Alaskan Arctic Slope; Univ. of Toronto Press, Toronto, Canada, 425 p.

Young, S.B.
1971: The vascular flora of St. Lawrence Island with special reference to floristic zonation in the Arctic regions; Contrib. from the Gray Herbarium, Harvard Univ., no. 201, 115 p.

Project 690064

R. J. Mott
Terrain Sciences Division

Numerous samples of organic lake bottom sediments were collected during the summer of 1972 in the Red Lake area of northwestern Ontario by a team from the Resource Geophysics and Geochemistry Division to evaluate the usefulness of organic sediments for geochemical prospecting (Timperly *et al.*, 1973). The samples were collected from the mud/water interface at various water depths using an Ekman-Birge dredge. Since pollen surface data have not been reported from this area, these samples provided an opportunity to obtain information from a variety of lakes and from various water depths within a lake for comparison with the modern vegetation.

Not all of the samples collected for chemical analyses were used for pollen study. Those used for pollen analysis (Fig. 1) were chosen to provide the widest distribution in the area, or within the lake. For instance, three samples were selected from the very large and irregularly shaped Red Lake, and the same number were chosen from the relatively small Snib Lake, in the latter case to see if there were any differences between the shallower extremities and the deeper central part of the lake.

Previous pollen work in the Red Lake area is sparse. Terasmae (1967) reported two pollen diagrams from near Nungesser Lake but only one profile from a kettle bog extended to the surface. This one surface count has been recalculated to the same base used in this report and is listed in Table 1 as site 12. One surface sample from Bamaji Lake, collected by V. K. Prest in 1960 and reported as an unpublished internal report by J. Terasmae, is shown as site 11 in Table 1.

Physiography and Surficial Geology

The Red Lake area is situated within the Severn Upland Division of the James Physiographic Region of the Canadian Shield (Bostock, 1970). Crystalline Archean rocks underlie the area and form a gently rolling topography covered in part by glacial deposits and glacial lake sediments. Relief is low with prominent end moraines and eskers commonly forming the highest points in the landscape. The area is a topographic high characterized by numerous lakes; the major rivers flow from the upland eastward to James Bay, northward to Hudson Bay and westward to Lake Winnipeg in Manitoba.

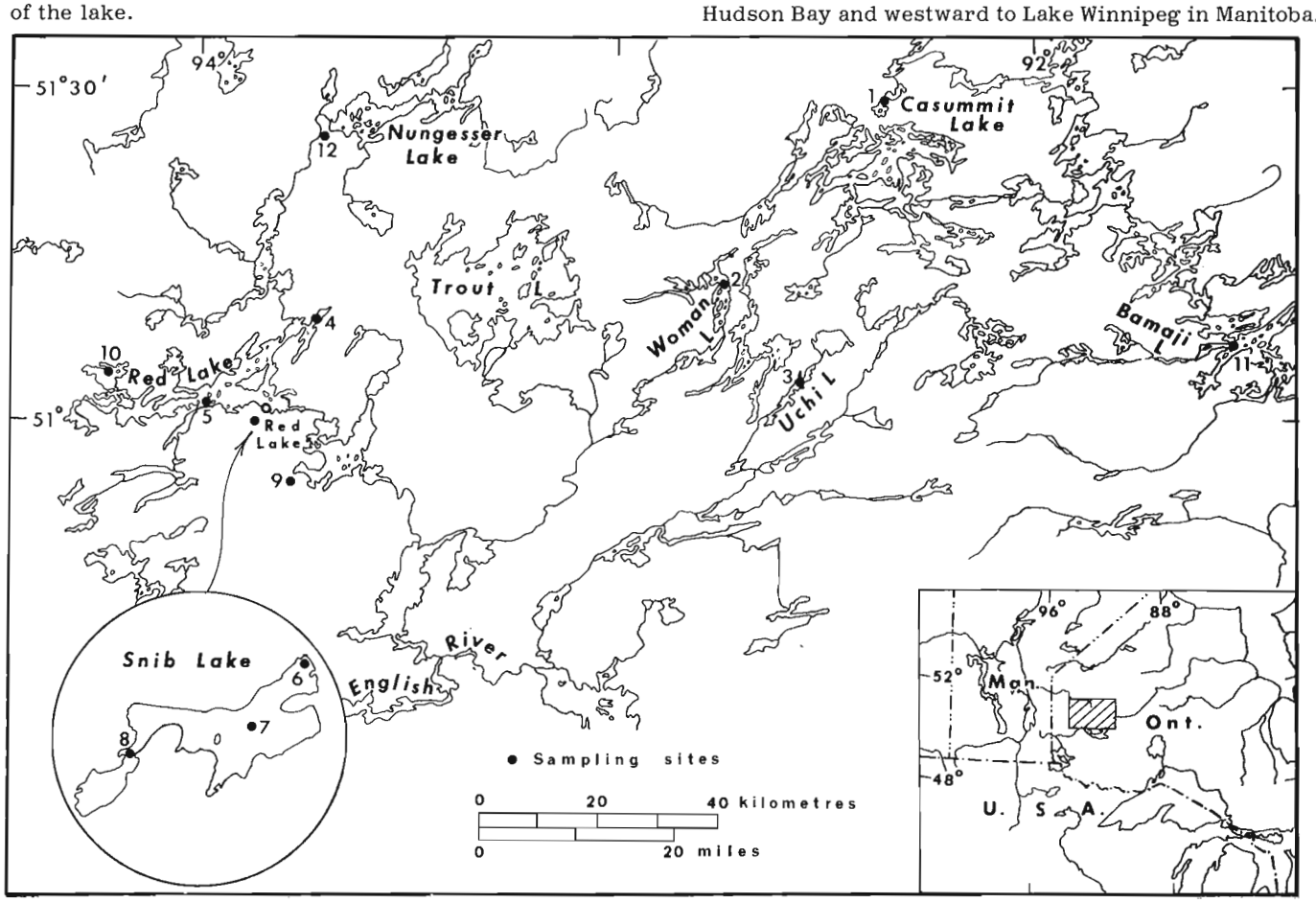

Figure 1. Map showing location of sampling sites.

Table 1

Site No.	Lake Name	N Lat.	W Long.
1	Casummit Lake	51°29'15"	92°22'25"
2	Woman Lake	51°13'20"	92°45'00"
3	Uchi Lake	51°04'25"	92°33'55"
4	Red Lake East Bay	51°09'50"	93°42'05"
5	Red Lake	51°02'00"	93°57'50"
6	Snib Lake	51°00'10"	93°51'25"
7	Snib Lake	51°00'00"	93°51'50"
8	Snib Lake	50°59'55"	93°52'20"
9	unnamed lake	50°55'35"	93°46'20"
10	Red Lake, Pipestone Bay	51°04'45"	94°11'15"
11	Bamaji Lake	51°07'	91°33'
12	Bog surface west of Nungesser Lake	51°26'	93°43'

The surficial geology of the area has been mapped by Prest (1973) and Zoltai (1961). Surficial deposits formed by the retreating Wisconsin ice include gently undulating ground moraine, end and interlobate moraines, eskers, kames, and outwash deltas, partly reworked by wave action of glacial Lake Agassiz which covered the area as the ice retreated. Lake silts and clays deposited in the lake partially blanket the glacial deposits and bedrock, and fill many of the valleys.

Climate

Northwestern Ontario in general has a severe continental climate with cold winters and warm summers (Thomas, 1953; Meteorological Branch, 1960, 1967). A mean January daily temperature of -20°C, a mean July daily temperature of 18°C, and a yearly average of about 1°C characterize the area. Winter lows may be below -45°C and summer highs above 32°C. At Red Lake the mean total precipitation is about 19 inches with 13 inches falling as rain and the remainder as snow. There are short summers with a frost free period of less than 100 days but the temperature and precipitation promote fairly good growth. Some summers have dry periods which make the forest susceptible to fires by lightning.

Vegetation

Three sections of the Boreal Forest Region as described by Rowe (1972) meet in the Red Lake district, namely, the Lower English River, the Upper English River and the Northern Coniferous sections. All of the sites are within the borders of the last section except for the Snib Lake sites which are in the first section. Since only the northern extremity of the Lower English River section is involved and the Upper English River section is somewhat to the southeast, the vegetational characteristics are those of the Northern Coniferous section. Because certain elements of the other two sections may be present in the pollen assemblages, however, some features of these sections are described.

Black spruce (*Picea mariana*) is the dominant species associated in wet lowlands with tamarack (*Larix laricina*), and on dry uplands with jack pine (*Pinus banksiana*) and white birch (*Betula papyrifera*); the latter two species are particularly abundant in areas disturbed by fire. White spruce (*Picea glauca*), balsam fir (*Abies balsamea*), trembling aspen (*Populus tremuloides*), and balsam poplar (*Populus balsamifera*) occur on better soils and on valley slopes. To the south these species commonly occur with jack pine and black spruce on upland sites or form mixed stands themselves. Red and white pine (*Pinus resinosa* and *P. strobus*) occur to the southeast along with large-tooth aspen (*Populus grandidentata*) and eastern white cedar (*Thuja occidentalis*).

Results

Table 2 lists the palynological results for the 12 sites examined. Pollen percentages were calculated on the basis of total pollen grains and spores, exclusive of aquatics, equalling 100. The pollen sum also is shown in the table.

All sites yielded pollen assemblages dominated by pine (*Pinus*) and spruce (*Picea*) with lesser amounts of birch (*Betula*) and alder (*Alnus*) and a variety of other taxa in minor amounts. Among the pine pollen only small numbers were identifiable as white pine type. The majority were identified as either jack pine/red pine type, or, if the area between the bladders was not present or the grain too poorly preserved, as a species of pine (*Pinus* sp.). The latter group, however, commonly had the general appearance of jack pine pollen. In the latter two sites (11 and 12) the counts were made several years ago and the criteria of presence or absence of verrucae on the distal side of the grain between the bladders was not used then for identification. Differentiation was made on size and appearance only. When the percentages of undifferentiated pine and jack pine are totalled, the results are fairly consistent and range between about 34 and 56 per cent except for site 12 where the extremely high percentage probably is due to its close proximity to the Lac Seul moraine (Prest, 1963) which supports abundant jack pine. Sites 1 and 3 are the farthest removed from any morainic or esker ridges, and they show the smallest percentages of pine.

Except for the very low percentages at site 12, where pine is overrepresented, spruce values generally range between 20 and 30 per cent with a low of 17 per cent and a high of 34 per cent. Birch and alder percentages are variable and reflect the scattered occurrences of these genera, with the higher values indicating a close proximity to a local source. Although balsam fir, tamarack, trembling aspen, and balsam poplar occur in the area, their pollen representation

TABLE 2

Pollen Spectra

Taxa	Site No.* 1	2	3	4	5	6	7	8	9	10	11	12
Trees												
Picea	26.7	29.7	28.8	30.6	25.8	33.6	20.9	28.9	17.4	25.9	28.6	7.2
Pinus	13.7	26.0	17.2	25.9	16.1	7.9	14.3	5.5	4.9	24.0		
P. strobus	0.8	1.6	0.7	1.4	2.1	1.4	1.3	1.2	0.9	2.2	1.8	
P. banksiana/resinosa	20.3	16.8	21.1	23.8	37.6	35.0	31.5	39.9	41.0	31.8	54.6	70.9
Abies balsamea	1.4	0.8	0.7	0.7	1.2	1.9	0.3	1.2		0.3	0.9	
Tsuga canadensis											+	
Larix laricina	0.6		1.5	0.7		0.5	2.5	1.9	0.3		1.8	
Betula	12.3	4.1	12.2	4.9	3.0	4.9	10.9	6.0	13.7	1.3	4.6	11.4
Populus	0.3		0.2		0.6	0.5		0.2	0.6			
Quercus	1.1	0.5	0.7	0.2	0.6	1.4	0.5	0.5	0.9	0.6	0.5	
Ulmus		0.3	0.2	0.2					0.3		+	
Carya			0.2									
Acer					0.9							
Fraxinus			0.4		0.3	0.2		0.2	+	0.3		
Carpinus/Ostrya	0.3		0.2	0.2	0.3							
Platanus					0.3							
Juglans							0.3					
Shrubs												
Taxus			0.2									
Juniperus						0.2						
Alnus	12.3	6.5	8.3	3.9	6.7	5.6	10.9	8.2	9.6	2.8	2.3	6.3
Salix	0.6	1.4	0.4	0.5	0.9	0.2	0.8	0.2	1.2	0.6	+	
Corylus				0.2		0.2	0.3					0.4
Myrica			0.2									
Viburnum									0.3			
Rhamnus		0.3										
Herbs												
Ericaceae									0.6			0.4
Gramineae	2.0	3.0	0.7	0.5	0.9	1.6	0.3	0.5	2.6	2.2	0.5	
Tubuliflorae	0.3		0.4	0.2	0.6	0.2	1.3	0.2			0.5	
Ambrosieae	2.8	3.0	1.1	0.7	0.6	2.6	0.5	0.7	1.2	1.6	1.4	0.8
Artemisia	1.7	0.8	1.7	2.1	0.3	0.7	2.5	1.4	1.2	1.6	1.4	1.3
Chenopodiineae	1.4	2.7	0.9	0.7	0.6	0.9	0.3	0.7	0.9	2.5	1.4	0.4
Sarcobatus			0.4					0.7				
Rosaceae	0.3	0.3	0.2			0.3						
Caryophyllaceae				0.2								
Thalictrum	0.3		0.4									
Urtica		0.3						0.2				
Rumex	0.3											
Caltha								0.2				
Campanulaceae									0.3			
Leguminosae									0.3			
Lycopodium			0.2	0.2								0.8
L. annotinum	0.6	0.5		0.5	0.3	0.5	0.3		0.6			
L. clavatum				0.2	0.3			0.5	+	0.3		
L. complanatum/tristachyum		0.3								0.3		
Pteridophyta	0.3	0.3		0.2				0.2	0.6	0.3		
Polypodiaceae		0.3	0.2	0.7			0.3	0.2	+	0.3		
Unidentified		0.8	0.4	0.5				0.2	0.9	1.3		
Pollen Sum (no. of grains)	359	370	459	432	330	429	393	416	344	321	220	237
Aquatics												
Cyperaceae	0.8	0.8	0.7		1.2	0.2	0.3		2.6	0.6		
Typha				0.2		0.2		0.2	2.4			
Sparaganium							0.3	0.2				
Potamogeton									0.3			
Nuphar									0.3			
Nymphaea									+		0.5	
Isoetes	9.2	2.4	2.6	0.2	0.3			0.2		2.5		
Sphagnum	2.0	1.1	1.3	0.5	3.0	0.5	1.3	0.7	0.9	2.5	1.8	0.4

Percentages are based on total pollen (pollen sum) excluding aquatics.

+ – present

*Pollen counts for sites no. 1-10 by L. Wilson, sites 11 and 12 by R.J. Mott

is very low. Several other hardwood genera are represented as low frequencies, indicating long distance transport from sources outside the area.

Shrub genera, other than alder, are very sparse. Willow (*Salix*) is the only genus consistently present, although in small amounts. Among the herb pollen taxa, grasses (Gramineae), wormwood (*Artemisia*), chenopods (Chenopodiineae), and ragweed type (*Ambrosieae*) are present at almost all sites. Ragweed type pollen may have been blown into the area from a considerable distance, but the others indicate some open areas are available to support these taxa. *Sarcobatus* is another genus whose presence is accounted for by long distance transport, whereas the remaining taxa listed with the herbs are probably present in small numbers in the area.

Aquatic taxa are sparsely represented and even *Sphagnum* spores, although consistently present, are not abundant even at the one bog site.

Summary

The boreal forest of the Red Lake district of northwestern Ontario is dominated by black spruce and jack pine with admixed white birch and tamarack plus white spruce, balsam fir, trembling aspen, and balsam poplar on better sites. This forest type is represented by pollen assemblages high in pine, mainly jack pine, spruce, birch, and alder. Pine pollen is generally overrepresented, especially where the sampling sites are in close proximity to pine stands on rocky outcrops, moraines, and eskers. Spruce pollen reflects its general abundance in the landscape. Birch frequencies are indicative of its scattered occurrence and may be overrepresented at some sites. In contrast, alder is locally abundant on some wet sites but is not generally abundant; it is represented by low percentages similar to birch. Other genera found in the forests, namely, balsam fir, trembling aspen, and balsam poplar are underrepresented in the pollen assemblages.

References

Bostock, H.S.
1970: Physiographic subdivisions of Canada; *in* Geology and Economic Minerals of Canada, R.J. Douglas (ed.), Geol. Surv. Can., Econ. Geol. Report No. 1, 5th ed., p. 10-30.

Meteorological Branch
1960: The climate of Canada; Meteorological Br., Air Services, Can. Dept. Transport, Toronto, Ontario, 74 p.

1967: Temperature and precipitation tables for Ontario, v. IV; Meteorological Br., Can. Dept. Transport, Toronto, Ontario, 44 p.

Prest, V.K.
1963: Red Lake-Lansdowne House area, northwestern Ontario, surficial geology; Geol. Surv. Can., Paper 63-6, 23 p.

Rowe, J.S.
1972: Forest regions of Canada; Can. Dept. Environment, Can. Forestry Service, Publ. No. 1300, 172 p.

Terasmae, J.
1967: Postglacial chronology and forest history in the northern Lake Huron and Lake Superior regions; Quaternary Paleoecology Proc. VII Congr. Internatl. Assoc. Quat. Res., E.J. Cushing and H.E. Wright, Jr. (eds.), v. 7, p. 45-58.

Thomas, M.K.
1953: Climatological atlas of Canada; Meteorological Div., Can. Dept. Transport and Div. Bldg. Res., Nat. Res. Council, N.R.C. No. 3151, 253 p.

Timperly, M.H., Jonasson, I.R. and Allan, R.J.
1973: Sub-aquatic organic gels; a medium for geochemical prospecting in the southern Canadian Shield; *in* Report of Activities, Part A, Geol. Surv. Can., Paper 73-1, Pt. A, p. 58-62.

Zoltai, S.C.
1961: Glacial history of part of northwestern Ontario; Proc. Geol. Assoc. Can., v. 13, p. 61-63.

34. SURFICIAL SEDIMENTS OF THE NORTHERN STRAIT OF GEORGIA, BRITISH COLUMBIA

Project 740063

J. J. Clague
Terrain Sciences Division, Vancouver

Introduction

During 1974 sediment sampling was carried out in the northern Strait of Georgia as part of a study of the Quaternary geology of the area (Clague, 1975). One hundred and ninety-eight grab samples collected from the sea floor over a regular grid (Fig. 1) have been analyzed for sediment particle size, and one hundred of these samples have been analyzed for organic and total carbon.

This report presents the results and some environmental and sedimentologic implications of these analyses. The sediments of the northern Strait of Georgia are objectively grouped according to their grain-size

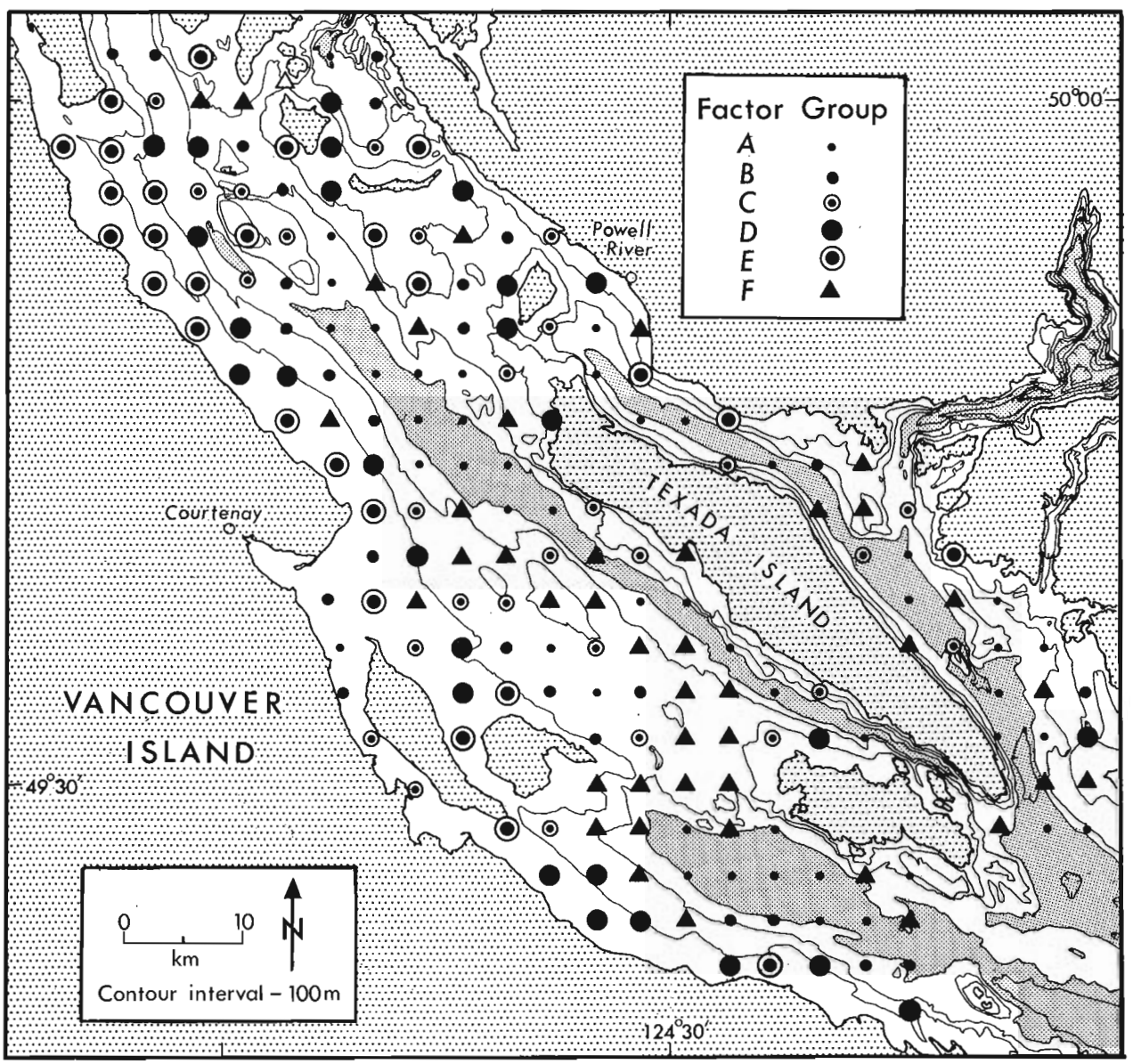

Figure 1. Bathymetric map of northern Strait of Georgia showing locations of analyzed samples and sediment character determined from factor analysis. Groups A through F are discussed in the text. Depths greater than 300 m are fine stippled; land areas are coarse stippled.

distributions. Although defined on granulometric criteria, each sediment group is characterized by other parameters such as carbon content, depth, and distance from the immediate sediment source. These parameters are correlated with the hydraulic energy at the depositional site. The analytical methods described in this report thus provide information on sedimentologic patterns and processes as well as a summary of the granulometry of a collection of samples. Sample suites from different geographic areas and environments may be readily compared using these procedures.

Methods

Sediment samples were collected from the *C. S. S. Vector* using a Shipek grab sampler. Grain-size distributions were determined by standard sieve and pipette methods. Organic and total carbon within the subgravel size fraction were measured by Leco carbon analyzer (Shaw, 1959).

Granulometric data were subjected to factor analysis, a statistical tool which groups related samples. The factor procedure used here (Q-mode) compares samples in terms of granulometric variables (Klovan, 1966). Variables in the data matrix are the weight per cent of each whole-phi class from -6 to 9 phi (64 to .002 mm).

Factor analysis reduces the complexity of the original data by creating linear combinations (factors) of the granulometric variables which account for as much of the original variance as possible. A three-factor model which accounts for 82 per cent of the original variance was selected for data presentation. These three factors are also present in four- and five-factor models which explain 88 and 91 per cent of the variance, respectively. The additional factors in higher level models account for small amounts of total variance and are not easily interpreted.

Table 1. Varimax factor score matrix

Grain-size fraction (phi)	Factor 1	Factor 2	Factor 3
-5 to -6	-.627	-.386	-.010
-4 to -5	-1.295	-.512	.157
-3 to -4	-1.469	-.590	.208
-2 to -3	-1.498	-.539	.311
-1 to -2	-1.416	-.515	.309
0 to -1	-1.525	-.645	.191
1 to 0	-1.230	-.723	-.597
2 to 1	-.512	-.270	-1.428
3 to 2	-.316	1.034	-1.220
4 to 3	-.663	2.240	.317
5 to 4	-.963	1.975	1.949
6 to 5	.038	-.188	1.792
7 to 6	.528	-.879	1.202
8 to 7	.623	-.991	1.044
9 to 8	.540	-.937	1.088

Results and Discussion

Table 1 is the varimax factor score matrix for all northern Strait of Georgia sediment samples. Values in the table are measures of the degree of association of variables (in this case grain-size classes) and factors. High positive values indicate strong positive correlation between a grain-size class and a factor; high negative values indicate negative correlation between variable and factor. The factor score matrix shows that Factor 1 is characterized by high negative loadings on coarse grained sand and gravel and positive loadings on silt and clay; Factor 2 has high positive values for coarse grained silt and fine grained sand; and Factor 3 is characterized by high negative loadings on fine to medium grained sand and high positive loadings on silt.

Table 2. Summary of factor group characteristics

Sediment group	Grain size: Mean	Grain size: Standard deviation	Water depth* (m)	Organic carbon* (%)	Environmental interpretation: Distance from source	Environmental interpretation: Energy at depositional site
A	9.1 (0.3)	2.7 (0.2)	310 (60)	2.0 (0.4)	↑	↓
B	7.9 (0.4)	3.3 (0.3)	210 (60)	1.8 (0.3)		
C	5.4 (0.4)	2.6 (0.5)	150 (30)	1.0 (0.4)	Increasing	Increasing
D	3.6 (0.4)	0.9 (0.3)	100 (40)	0.7 (0.5)		
E	2.3 (0.4)	0.8 (0.2)	70 (60)	0.3 (0.1)	↓	↓
F	2.1 (2.0)	4.6 (1.3)	150 (80)	0.7 (0.2)	†	†

Note: values in table are mean and standard deviation (latter in parentheses) for samples plotted in Figure 3.

*Samples from Comox Harbour, southeast of Courtenay, are excluded; these samples are muds occurring at water depths less than 50 m and containing up to 8% organic carbon. Mean carbon values are per cent of sediment finer than 2 mm.

†Many diamictons of Group F are not in equilibrium with the existing energy regime; they are relict sediments of glacial origin.

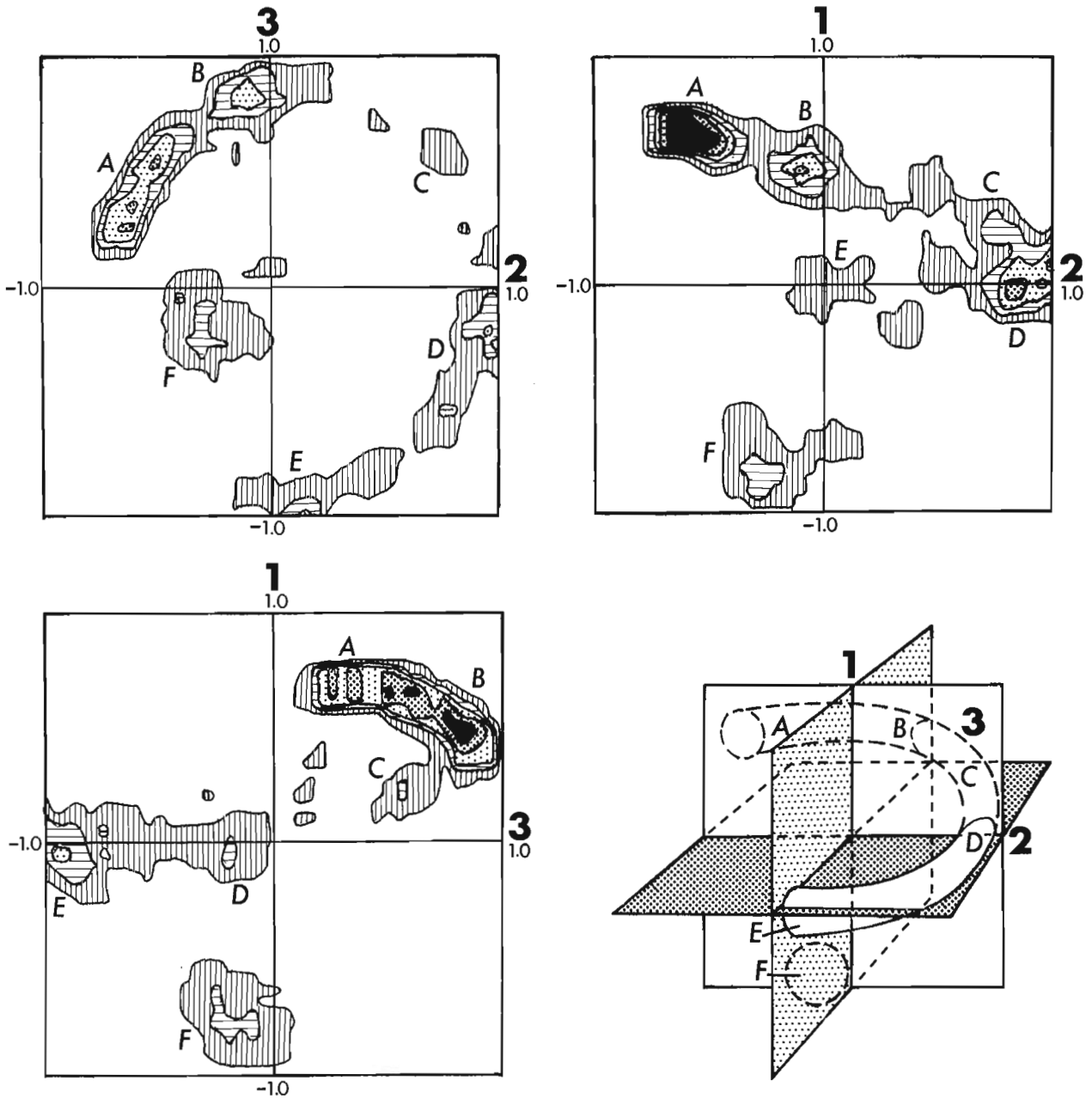

Figure 2. Plots of factor scores for analyzed samples. Upper left--Factor 2 vs. Factor 3; upper right--Factor 1 vs. Factor 2; lower left--Factor 1 vs. Factor 3. Contours indicate density of sample points within two-dimensional factor space and are 2-4-6-8-10 per cent per 1 per cent area (number of samples = 198). These plots are orthogonal sections through three-dimensional factor space which is shown in the lower right illustration. Sample concentrations A through F have characteristic grain-size distributions illustrated in Figure 3.

Loadings in the varimax factor score matrix indicate the relationship between variables and factors for the entire sample suite. In contrast, factor scores are measures of the degree of association of individual samples and factor axes. High positive and negative scores on a factor indicate close association with the positive and negative components, respectively, of the factor axis. The characteristics of, and relationships among, sediment samples from the northern Strait of Georgia are shown by plotting samples in the three-dimensional space of the factor model. The position of each sample in this space is defined by its scores on three orthogonal factor axes. Figure 2 shows the density of sample points projected into various planar sections through this three-dimensional space. Also shown is a diagrammatic three-dimensional representation of sample positions in this space.

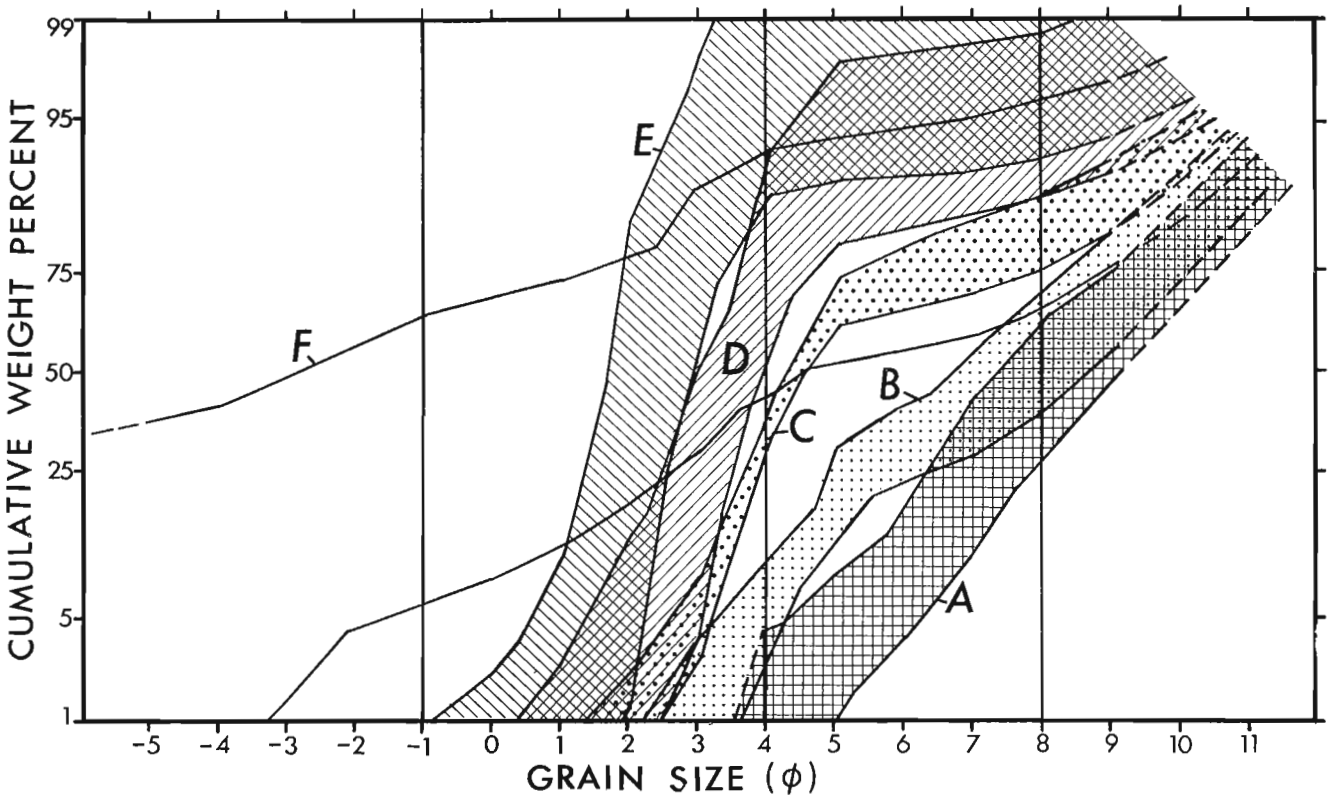

Figure 3. Grain-size distributions of factor groups. Field limits have been determined from cumulative curves of samples corresponding to concentrations A through F, Figure 2. Sample sizes: A = 42, B = 18, C = 7, D = 24, E = 21, F = 30. Vertical lines at -1, 4, and 8 phi (2, . 063, and . 004 mm, respectively) separate gravel, sand, silt, and clay fields.

Figure 2 indicates that samples are concentrated in a band, best described as a partial helix; an isolated group of samples (F in Fig. 2) occurs at the negative end of the Factor 1 axis. Although there is a continuum of samples along the helix, peaks in sample density are evident, namely at positions A through E (Fig. 2). Each of these clusters consists of samples with similar grain-size distributions (Fig. 3). In addition there is a progressive change in sediment character along the helix. The groups represent sediment types which can be mapped and which are significant in terms of sediment genesis and dispersal.

Samples which are not clearly associated with any of Groups A through F are excluded from Figure 3. Some of these samples are located between two groups on the helix, whereas others fall outside the helix and away from Group F. In Figure 1 these samples are placed in those factor groups with which they are most closely affiliated.

Group A includes samples with the highest positive scores on Factor 1 (Fig. 2). These sediments are very poorly sorted, silty clay. * They occur on the sea floor in the deepest basins of the northern Strait of Georgia (Fig. 1).

Group B, represented in the factor model by samples with the highest positive scores on Factor 3, includes very poorly sorted, clayey silt and silty clay with about 3 to 15 per cent sand. Group B sediments are transitional to those of A, but, in general, occur at lesser depths.

Group C is a weak cluster of samples located on the helix between Factor 3 positive and Factor 2 positive. This segment of the helix includes very poorly sorted sand-silt-clay mixtures and silty sand. Group C sediments are most common at intermediate depths along the margins of basins floored by Groups A and B.

Group D, characterized by high positive scores on Factor 2, includes moderately to poorly sorted, silty sand at shallow to intermediate depths adjacent to coastal areas. In shallow water these sediments are transitional to well and moderately sorted sand (Group E). Group E sediments (samples with high Factor 3 negative scores) are most common along the Vancouver Island coast, but also occur as aprons around islands and banks consisting of unconsolidated sediments.

The helix containing sample clusters A through E is a continuum characterized by decreasing phi mean grain size and water depth (Table 2). Standard deviation increases slightly from Group A to Group B, then decreases from B to E, in agreement with similar trends in sorting observed by Folk and Ward (1957) and Damiani and Thomas (1974). These differences in

* Sorting after Folk (1968); sediment types after Shepard (1954).

sediment texture are attributed to variations in hydraulic energy at the depositional site. Winnowing, mixing, and selective sorting caused by currents and waves control the textural characteristics of the sediments. Energy at the depositional site increases progressively from A to E along the helix. The lowest energy regime is represented by silty clay in deep basins, and the highest energy regime by clean gravel and sand in shallow coastal waters.

Organic carbon content, in general, is positively correlated with phi mean grain size and clay content (Table 2). A similar relationship has been noted by other workers (for example, Thomas, 1969; Pharo, 1972) and has been attributed to adsorption of organic matter by phyllosilicates (Hahn and Stumm, 1970).

Organic carbon in clayey basin sediments in the northern Strait of Georgia is higher than that of texturally similar sediments in the central and southern Strait. Pharo (1972, Table XI) reports values of less than 2.0 per cent for organic carbon in silty clay of the central Georgia Depression, whereas the organic carbon content in the study area commonly exceeds 2.0 per cent. This may be due to differences in the sedimentation rate between the two areas; organic matter is increasingly diluted as the terrigenous sedimentation rate increases. Sediments with unusually high organic carbon content (up to 8 per cent) occur in Comox Harbour southeast of Courtenay, and in the vicinity of Powell River. These high carbon values are due, in part, to organic matter in sewage and to plant tissue introduced by the pulp and paper industry.

Major sources of marine sediments in the northern Strait of Georgia are coastal bluffs and shallow submarine banks. Clean gravel and sand of the coastal zone are lag deposits formed mainly by the erosion of bluffs of unconsolidated sediment. In this environment wave and current energy is sufficiently high to prevent the deposition of silt and clay. Mud is carried in suspension into deeper water and is deposited as hydraulic energy decreases. Some sand is transported in traction into deeper water, but represents a minor constituent of basin sediments. Rivers and streams flowing into the northern Georgia Depression are, only locally, important suppliers of sediment. Basin sediments south of the study area include detritus of Fraser River origin. Because most basins within the northern Strait of Georgia are separated by rock sills and constrictions from the main basins in the central and southern Strait, turbidites originating off the Fraser River are not present over much of the study area. Thus, any sediment of Fraser River origin in the northern Strait of Georgia must be transported as dispersed clay particles and mixed in the water column with suspended detritus of local origin.

Local current patterns, steep sea-floor slopes, and complex bathymetry result in exceptions to the general positive relationships among phi mean grain size, water depth, and distance from source (Table 3). For example, at the northwest corner of the study area, tidal currents are sufficiently strong to prevent the deposition of silt and clay in water depths up to about 230 m. Sediments found here are mainly clean sand and gravelly sand. In the constricted parts of deep troughs Holocene sediments are thin, whereas in adjacent broad basins at the same depths they are locally thicker than 175 m. Bottom currents in the constricted zones apparently are strong enough to maintain mud in suspension. On the other hand, silty clay and clayey silt are the dominant bottom sediments at water depths less than 50 m southeast of Courtenay where a sedimentologic subsystem is separated from the Strait of Georgia by an island and a shallow bar mantled by sand and gravel.

Slopes bordering Texada Island and the British Columbia mainland are steep, locally averaging more than 45 degrees. Coarse sediment is introduced into deep water on such slopes. Some sand-silt-clay mixtures and diamictons may thus form by the mixing of shallow water sand and gravel, and deep water mud. This may account for the strongly bimodal grain-size distributions of many diamictons (Group F). Diamicton exposed on ridge crests and relatively flat areas of the sea floor is of glacial and glaciomarine origin and is not in equilibrium with the present energy regime. Diamictons are the most poorly sorted sediments in the Strait of Georgia and those with the largest depth range (Table 2).

Factor analysis does not discriminate between diamicton and gravel. This probably is due to the fact that only a few gravel samples have been recovered and included for statistical processing, whereas diamicton samples are strongly represented in the data matrix. Some gravel and sandy gravel in the northern Strait of Georgia may form by the winnowing of fines from marine diamicton. At any rate, sorted gravelly

Table 3. Correlation coefficient matrix

	SD	Gravel	Sand	Silt	Clay	TC	OC	DS	Depth
Mean	.074	-.631	-.682	.723	.895	.545	.459	.385	.642
Standard deviation (SD)		.378	-.466	.148	.289	-.068	-.086	.275	.326
Gravel			-.060	-.410	-.325	-.302	-.269	-.042	-.181
Sand				-.730	-.854	-.585	-.510	-.437	-.616
Silt					.613	.728	.683	.309	.318
Clay						.477	.385	.429	.772
Total carbon (TC)							.982	-.102	.083
Organic carbon (OC)								-.144	.003
Distance from source (DS)									.554

sediments are distributed in close association with Group A sand and thus are included with that group in Figure 1.

Conclusions

Factor analysis places sediments of the northern Strait of Georgia into groups of similar texture which can be interpreted in terms of hydraulic energy at the depositional site. It also provides a concise and thorough description of a sample suite and establishes a basis for comparison with suites from different geographic areas and environments.

Holocene sediments of the northern Strait of Georgia largely are derived from local sources including coastal bluffs and shallow submarine banks consisting of unconsolidated sediment. Streams and rivers are, only locally, important suppliers of sediment.

The distribution of Holocene sediments is controlled, in part, by current and wave patterns, by bathymetry, and by the location of bluffs and banks of older unconsolidated sediment. In general, with increasing depth and distance from source, sediment becomes finer and more poorly sorted, and carbon content increases. However, some of the coarsest and most poorly sorted sediments (diamictons) are not in equilibrium with the present energy regime within the Strait of Georgia, but rather are of glacial or glaciomarine origin.

Acknowledgments

Grain-size analyses were performed by Heather Mowat of the Geological Survey of Canada and carbon analyses by Can Test Ltd., Vancouver, British Columbia.

References

Clague, J.J.
1975: Quaternary geology, northern Strait of Georgia, British Columbia; *in* Report of Activities, Part A, Geol. Surv. Can., Paper 75-1, Pt. A, p. 397-400.

Damiani, V. and Thomas, R.L.
1974: The surficial sediments of the Big Bay section of the Bay of Quinte, Lake Ontario; Can. J. Earth Sci., v. 11, p. 1562-1576.

Folk, R.L.
1968: Petrology of sedimentary rocks; Austin, Texas, Hemphill's, 170 p.

Folk, R.L. and Ward, W.C.
1957: Brazos River bar: a study in the significance of grain size parameters; J. Sediment. Petrol., v. 27, p. 3-26.

Hahn, H.H. and Stumm, W.
1970: The role of coagulation in natural waters; Am. J. Sci., v. 268, p. 354-368.

Klovan, J.E.
1966: The use of factor analysis in determining depositional environments from grain-size distributions; J. Sediment. Petrol., v. 36, p. 115-125.

Pharo, C.H.
1972: Sediments of the central and southern Strait of Georgia, British Columbia; unpubl. Ph.D. thesis, Univ. British Columbia, 290 p.

Shaw, K.
1959: Determination of organic carbon in soil and plant material; J. Soil Sci., v. 10, p. 316-326.

Shepard, F.P.
1954: Nomenclature based on sand-silt ratios; J. Sediment. Petrol., v. 24, p. 151-158.

Thomas, R.L.
1969: A note on the relationship of grain size, clay content, quartz, and organic carbon in some Lake Erie and Lake Ontario sediments; J. Sediment. Petrol., v. 39, p. 803-809.

35. SEDIMENTARY PROCESSES AND SEDIMENTS, BABBAGE RIVER DELTA, YUKON COAST

Project 740086

D. L. Forbes[1]
Terrain Sciences Division

Field work between mid-May and late August 1974 initiated a study of deltaic sedimentation at the joint outlet of the Babbage River and Deep Creek in Phillips Bay, Yukon coast (69°15'N, 138°25'W) (*see* Lewis, 1975 for location map). The study is intended to document river-marine interaction in an arctic context, with emphasis on system responses to storms or floods of varying pattern, magnitude, and frequency. It supplements several regional reconnaissance studies undertaken in recent years (McDonald and Lewis, 1973; Lewis, 1975). Results may help to identify potential hazards for, and effects of, proposed exploration or construction activities in the region. The project is closely associated with work on coastal processes in the Kay Point area (Lewis, 1975). Investigations during the first season were concentrated on surface sediments and morphology, spring breakup, and seasonal flow patterns in the rivers feeding the delta.

The subaerial Babbage delta (25 km^2) and adjacent estuary (15 km^2) receive drainage and sediment from a 5000 km^2 catchment on the Barn Mountains and Yukon Coastal Plain. Some marine sediment, including a large amount of driftwood, is also incorporated in the delta. Data on total water and sediment discharge from the drainage basin are lacking, but indirect estimates (Church, 1971) suggest maximum probable floods of 910 m^3/sec. for the Babbage above Deep Creek and 220 m^3/sec. for Deep Creek. Total annual precipitation averages 200 mm (1962-1971, Shingle Point), and four months (June-September) have average temperatures over 0°C. Most sediment movement probably occurs between river breakup in late May and freezeup sometime after September. Occasional severe storms, however, may flood the delta even during winter (R. Mackenzie, pers. comm.). The frequency and relative impact of such events remain to be determined. The 1970-storm study (Canada, Department of Public Works, 1971) indicated a 3 m tide associated with a storm of estimated 25-year return period.

Morphology and Sediments

Surface sediments of the delta and estuary were sampled on a coarse rectangular grid (1000 x 500 m). This extensive sample was supplemented with detailed sampling at selected sites. Channel sediments, predominantly sand, were sampled at cross-sections (Fig. 1). Gravel, present in both rivers above the delta, is absent from delta channels.

A generalized surface facies map of the subaerial delta and surroundings is given in Figure 1. Intertidal surfaces are essentially unvegetated. Sediments of this facies range from silt to sand, with rare ice-rafted gravel, little driftwood, and occasional clasts of peat. Bedforms exposed at low water attest to upstream sand movement on channel bars under low-stage flood-tide conditions. Initial impressions suggest that the intertidal flats may be expanding in places at the expense of the delta plain (Fig. 1). The latter, as mapped here, includes all surfaces subject to storm-surge flooding, the upper limit defined by the highest line of marine driftwood (2 to 3 m above mean high tide). The lower delta plain, generally less than 1 m above mean high tide, comprises vegetated levees and interlevee flats and partially vegetated shallow flood basins, interspersed with numerous tidal ponds and connecting channels. Levees, except along minor channels, have negligible relief; vegetation mapping (Lewis, 1975) revealed little consistent contrast between levee and interlevee flora and a complex distribution of the few species present over the floodplain. Channel banks in floodplain deposits expose stratified silt and organic detritus, including some large driftwood logs. Included in the delta plain facies are scattered higher surfaces, inactive levees flanking abandoned channels, and a major abandoned channel at the head of the delta, all subject to driftwood accumulation under occasional storm flooding. Alluvial surfaces in the valley above the highest storm line (Fig. 1) are associated with a variety of sediments: from channel gravels of the braided Crow River on the south to fine-grained overbank deposits of Deep Creek on the north. Polygonal ice-wedge structures are common on this facies; winter or spring accumulation of wind-blown sediment, apparently derived from channel bars, was noted along some banks.

Peat (Fig. 1) outcrops extensively at or near sea level around the estuary and on the delta plain, and occurs beneath silts in cutbank exposures in and above the delta. Its age is unknown at time of writing.

The Kay Point area was overriden by ice at least once during the Quaternary but lay 25 km beyond the presumed late-Wisconsin limit at King Point (Hughes, 1972). The upland surface (Fig. 1) flanking the delta and extending to Niakolik and Kay points is composed of undifferentiated glacial or pro-glacial sediments. Beach sands and gravels of Niakolik and Kay spits are primarily derived from this unit through rapid cliff erosion (McDonald and Lewis, 1973; Lewis, 1975).

Rates of extension and landward migration of the Kay Point spit (under investigation by C. P. Lewis) are clearly relevant to any interpretation of long-term trends in the delta and estuary. A borehole at the delta front (Fig. 1) was logged as follows (from surface at sea level):

[1]Department of Geography, University of British Columbia, Vancouver, B.C.

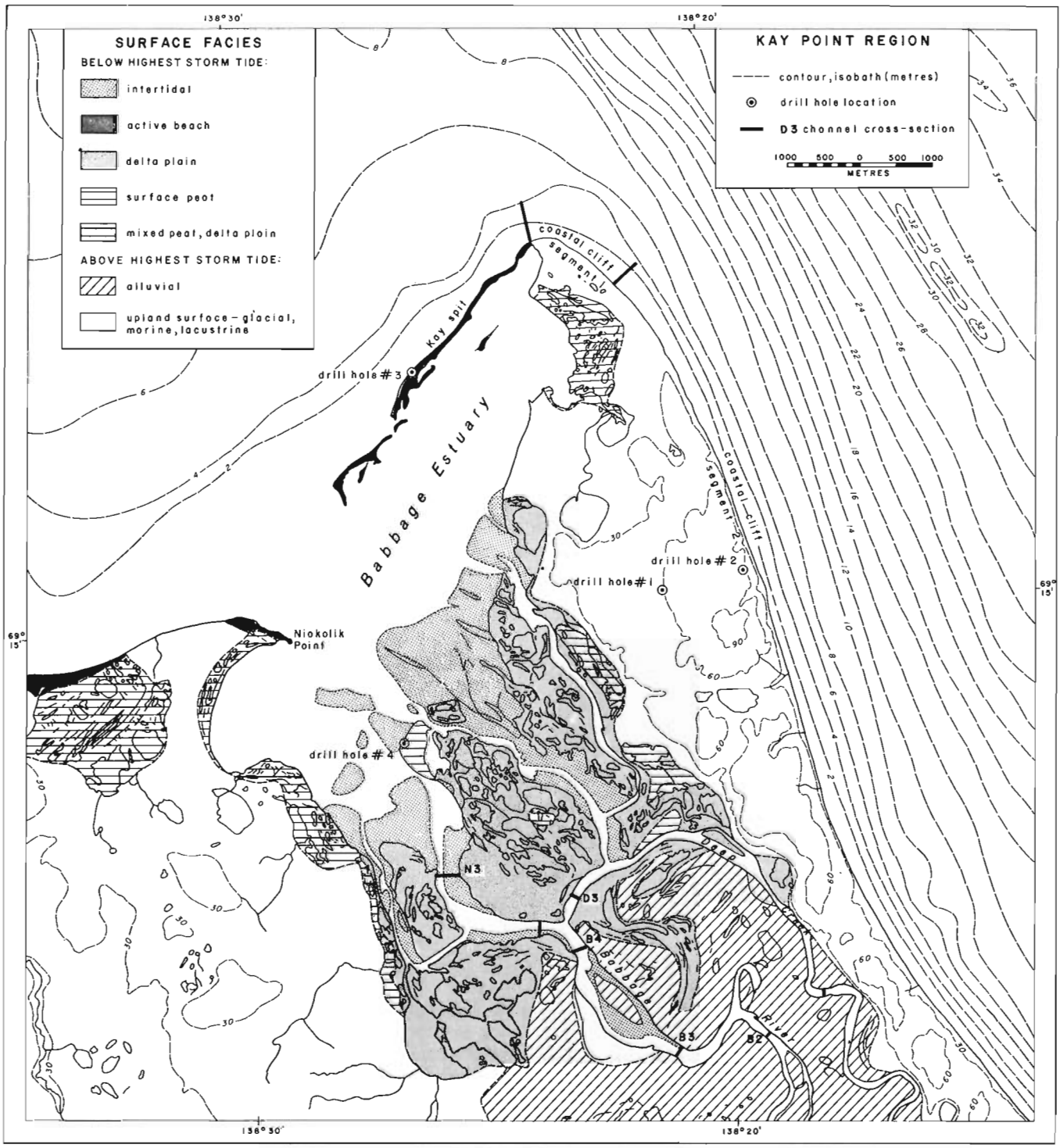

Figure 1. Kay Point Region: Generalized Surface Facies.

0 to 2.6 m: peat, medium sand with ice (30-40% by volume)
2.6 to 6.1 m: ice (90-100% by volume)
below 6.1 m: medium-grained gravel with ice (less than 20% by volume)
22.9 m: abundant salt water.

The gravel may derive from the Crow or Babbage rivers, but is more probably fluvioglacial valley fill associated with the King Point glacierization.

A preliminary hydrographic survey of the estuary and nearshore zone, using high frequency echo sounder and side scan sonar (Lewis, 1975), was extended in August up the main delta distributary channel, where it supplemented data from channel cross-section. Scour holes up to 7.5 m deep were encountered in delta channels.

Hand probing at section N3 (Fig. 1) in August revealed frozen substrate 0.5 to 2 m beneath the channel bottom at least to 3 m depth and possibly continuing beneath the thalweg at 5.5 m. McDonald and Lewis (1973) interpreted as frozen ground a prominent reflector observed in some July echograms from Babbage delta channels.

Breakup, River Discharge and Sediment Transport

A breakup and flood sequence similar to that reported from Alaskan rivers (Barnes and Reimnitz, 1972; Walker, 1974) was observed on rivers of the Yukon north slope in 1974. Three phases were distinguished: (1) pre-breakup flooding over winter ice; (2) breakup accompanied and followed by snowmelt flooding with pronounced diurnal fluctuation; (3) general flow recession interrupted by brief storm floods.

Phase 1 began on the Babbage above the delta on May 16, 1974; flow in the Firth River had already advanced over ice to Nunaluk Spit, but other rivers along the coast, including the Malcolm, Spring, Running, and Blow, showed no evidence of flow. Pre-breakup flooding in the Blow River delta began by May 18 and was well advanced by May 30 in the Malcolm and Spring rivers. On the Babbage, the flow front advanced about 3 km per day, and by May 20 covered the southern part of the estuary and a zone of sea ice outside the spit, out to or beyond the 2 m isobath; at the same time, winter ice in some channels had begun to lift. Ice in the delta channels floated but remained in place until mid-June or later; repeated frosts produced fresh ice cover behind and around the floating winter ice throughout the early part of the month.

At B2 (Fig. 1) above the delta, channel ice approximately 1 m thick began to lift on May 28 but remained in the reach until June 1. Soundings to bottomfast ice suggested a late autumn water level 3.5 m below the top of the cutbank. Stage following May 27 fluctuated between 2.8 and 2.2 m below bank top, rising to a peak of 1.9 m on June 8 and again on June 10. Snow against cutbanks indicated no previous higher flooding. The June 8 peak produced the first extensive flooding of the delta plain and flooded the entire estuary over the ice. The estuary ice subsequently floated and finally cleared by July 9. Ice remained close against the seaward side of Kay Point spit until the last week in July. It should be noted, however, that 1974 breakup in the Beaufort Sea was exceptionally late.

Continuous stage records were obtained for Deep Creek from July 4 to August 22 and for Babbage River at B1 (McDonald and Lewis, 1973) over the same period with some breaks. The data indicate an initially strong dirunal fluctuation on both streams, diminishing with time, but persisting into August. The general reduction in discharge throughout the record was interrupted by brief floods on five occasions: the largest, August 13-15, produced a rise in stage at B1 of 125 cm in 48 hours, 100 cm of which occurred in 14 hours. Discharge through B1 exceeded 60 m^3/sec. during less than 10 per cent of the record, and 20 m^3/sec. during 75 per cent of the 50-day period. Deep Creek showed the same pattern as the Babbage, but with lower, more attenuated peaks. Discharge to the delta probably ceases in late autumn or early winter, although extensive icings on the Crow and upper Babbage in August attest to winter discharge at some points in the basin.

Suspended sediment concentrations during breakup flooding at B2 (Fig. 1) varied from 50 mg/l on June 2 to less than 5 mg/l on June 6 to a maximum of 300 mg/l twelve hours after the flood peak on June 8. Later in June, suspended sediment concentrations were generally higher in Deep Creek than in the Babbage: typical values on 19 June at D3 and B4 (Fig. 1) were 100 and 10 mg/l respectively. Except for temporary flood increases, suspended sediment discharge also declined through the summer, with concentrations in August being generally less than 1 mg/l.

Limited bedload movement occurs over bottomfast ice prior to breakup. Soundings encountered hard ice surfaces with only occasional patches of sediment, except above late autumn water levels, where the bottom was soft. Emergent bottom ice is generally clean, but carries rare patches of sand with some gravel. Exceptionally, well formed asymmetrical ripples occur in the upper surface of bottomfast ice; the lee faces of some ripples carry thin slip-face accumulations of sand, but the ripple surface is apparently thermo-erosional in origin. Clearly, bottomfast ice on the channel bed inhibits scour during pre-breakup flooding. Peak spring discharge may occur after breakup. The extent to which scour then may be inhibited by a frozen channel perimeter remains an important unanswered question.

In mid-July preliminary measurements of salinity, conductivity, and temperature (using a YSI S-C-T meter) showed maximum salinity in the estuary of 2.5‰ behind Kay Point Spit, and minimum salinity of 0.2‰ in river water off Naikolik Point. Water temperatures varied from 7.0°C in river water to 2.5°C in water of intermediate salinity off the end of Kay Point Spit. Water depths in the estuary rarely exceed 2 m. No significant vertical variations in salinity, conductivity or temperature were encountered.

References

Barnes, P. W. and Reimnitz, E.
1972: River overflow onto the sea ice off the northern coast of Alaska, spring (1972); Abstract, Am. Geophys. Union, Trans., v. 53, p. 1020.

Canada, Department of Public Works
1971: Beaufort Sea storm - investigation of effects in the Mackenzie Delta region; unpubl. report, 23 p.

Church, M. A.
1971: Reconnaissance of hydrology and fluvial characteristics of rivers in northern Alaska and northern Yukon Territory; Report prepared for Mackenzie Valley Pipeline Research Limited, 197 p.

Hughes, O. L.
1972: Surficial geology of northern Yukon Territory and northwestern District of Mackenzie, Northwest Territories; Geol. Surv. Can., Paper 69-36, 11p.

Lewis, C. P.
1975: Sediments and sedimentary processes, Yukon Beaufort Sea coast; *in* Report of Activities, Part B, Geol. Surv. Can., Paper 75-1, Pt. B.

McDonald, B. C. and Lewis, C. P.
1973: Geomorphic and sedimentologic processes of rivers and coast, Yukon coastal plain; Environmental-Social Committee, Northern Pipelines, Task Force on Northern Oil Development, Goverment of Canada, Report No. 73-39, 245 p.

Walker, H. J.
1974: The Colville River and the Beaufort Sea: some interactions; *in* The Coast and Shelf of the Beaufort Sea, J. C. Reed and J. E. Sater (eds.), Arctic Inst. North Am., Arlington, p. 513-540.

Project 740062

D. Grieve and K. Fletcher[1]
Terrain Sciences Division

Introduction

This project was initiated under contract to the Geological Survey of Canada in close collaboration with an ongoing study of sedimentation at the Fraser River Delta front (Luternauer, 1975a). Distribution of Co, Cu, Fe, Mn, Ni, Pb, and Zn have been determined for surficial sediments of the Fraser River Delta tidal flats and upper foreslope. The study is intended to provide geochemical maps and baseline data on factors influencing metal dispersion in the delta. Sampling was carried out before, during, and following the 1974 freshet in conjunction with Dr. J. Luternauer of the Terrain Sciences Division, Vancouver (Luternauer, 1975a, 1975b).

Sampling and Analytical Procedures

Tidal flats were sampled at low tides using a Canadian Coast Guard Hovercraft equipped with a Decca Radar system. Samples of the top centimetre of sediment were collected by hand and placed in high wet strength kraft bags. The upper foreslope was sampled from a Department of Transport launch (equipped with a Trisponder navigational system) using a Shipek grab sampler with a stainless steel bucket.

All samples were air-dried at 70°C for 48 hours, disaggregated, and sieved through an 80-mesh nylon sieve (2.5 phi). Samples from February through June were digested in a 4:1 nitric-perchloric acid mixture, evaporated to dryness over an air-bath, taken up in 1.5M HCl, and analyzed for Co, Cu, Fe, Mn, Ni, Pb, and Zn with a Perkin-Elmer 303 atomic absorption spectrophotometer. Background correction was used for determination of Co, Ni, and Pb.

For samples collected in February and March, weight per cent sand in the minus 80-mesh fraction (% sand) was determined by wet sieving through a 270-mesh nylon sieve (4.25 phi). Organic content of minus 80-mesh material was estimated as per cent weight loss on ignition (% LI) after heating for four hours at 550°C in a muffle furnace.

Table 1

Metal content, per cent sand (% sand), and loss on ignition (% LI) for Fraser Delta sediments (minus 80-mesh fraction)

Element (ppm)	Tidal flats (February)		Foreslope (March)	
	$\bar{x}$	s	$\bar{x}$	s
Co	11.3	1.56	13.3	1.77
Cu	17.2	7.75	30.0	13.1
Mn	310.7	55.7	327.3	55.6
Ni	43.5	7.80	47.9	6.30
Pb	5.8	9.08	10.7	7.77
Zn	52.8	11.0	77.1	21.7
Fe(%)	1.85	0.27	2.34	0.47
% Sand	81.6	21.6	45.5	31.8
% LI	1.83	1.02	3.52	1.96
No. of samples	68		218	

$\bar{x}$ = mean; s = standard deviation

Data Processing

Means and standard deviations for Co, Cu, Fe, Mn, Ni, Pb, and Zn were calculated for each sample series and corresponding correlation matrices obtained using UBC TRIP (Bjerring and Seagraves, 1974). Multiple regression equations were obtained (by the same program) for the February and March series. Fe, Mn, % sand, and % LI were independent variables for the regression analyses.

Results and Discussion

No significant differences were found in overall metal content of sediments collected at different times. Comparison of tidal flat and foreslope sediments, collected in February and March respectively, clearly indicates that the latter are relatively enriched in most

Table 2
Correlation matrix for foreslope sediments (minus 80-mesh fraction: n = 218)

	Co	Cu	Fe	Me	Ni	Pb	Zn	Li
Cu	.69							
Fe	.78	.85						
Mn	.68	.76	.85					
Ni	.53	.11	.38	.43				
Pb	.55	.87	.68	.67	-.01			
Zn	.70	.93	.89	.82	.19	.85		
LI	.45	.68	.66	.59	.08	.52	.70	
Sand	-.70	-.92	-.87	-.68	-.09	-.76	-.90	-.69

[1]Dept. of Geological Sciences, University of British Columbia, Vancouver, B.C.

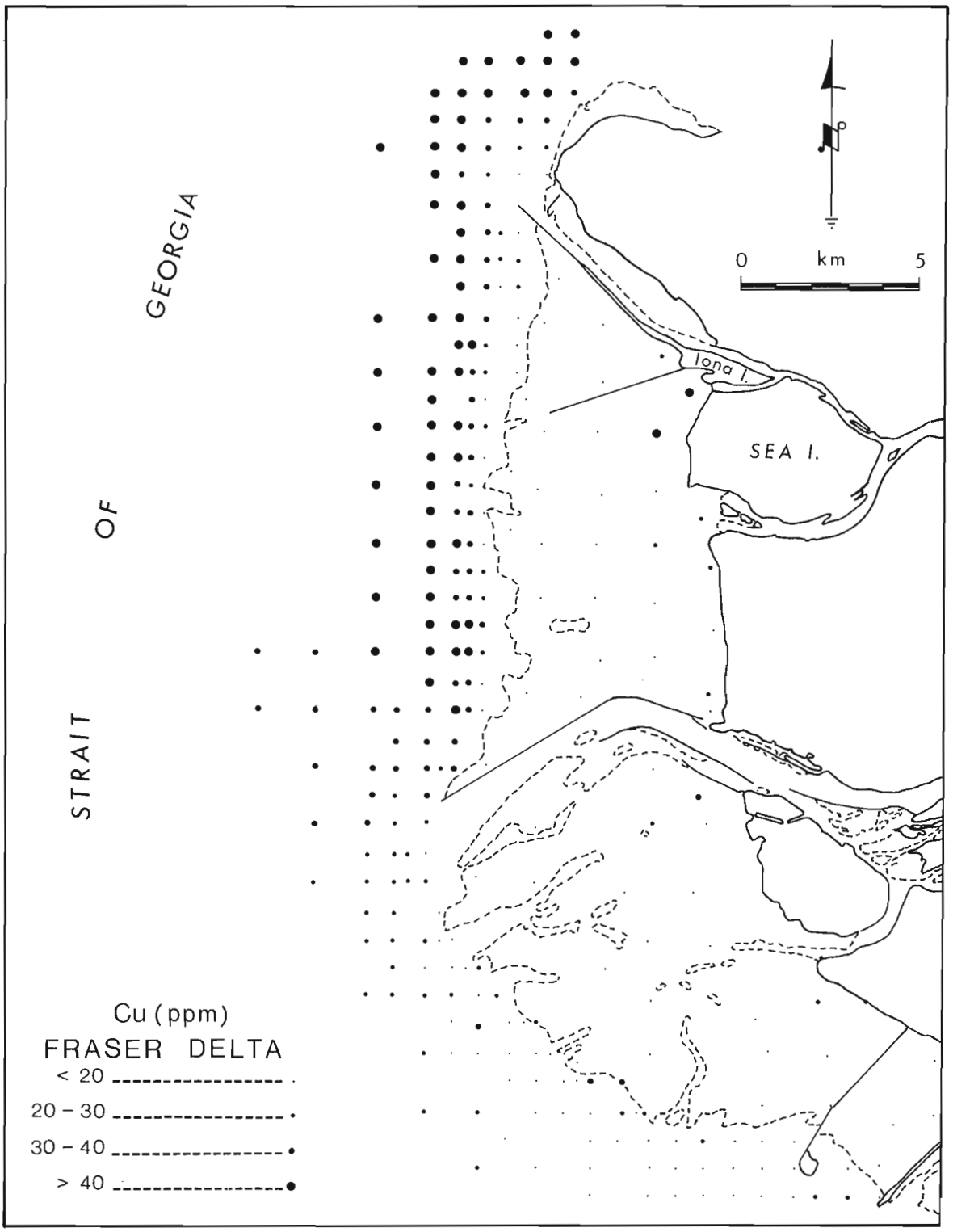

Figure 1. Cu (ppm) in surficial sediments of the Fraser River Delta tidal flats and upper foreslope, February and March, 1974.

Table 3

Multiple regression equations for foreslope sediments (minus 80-mesh fraction; n = 218)

Dependent variable	Regression	Per cent variance accounted for (R^2)
Co	= 6.4548 + 2.94 Fe	60%
Cu	= 29.9390 + 5.8956 Fe - 0.3026 Sand	85%
Ni	= -0.7848 + 16.9150 Fe + 0.1990 Sand	38%
Pb	= 3.8429 + 0.0403 Mn - 0.1377 Sand	62%
Zn	= 48.4373 + 0.1484 Mn - 0.4362 Sand	88%

of the trace metals determined (Table 1; Fig. 1). In the case of Cu (Fig. 1) it is also apparent that concentrations generally increase westwards and northwards on the foreslope. Similar patterns are shown by Zn, Fe, Mn, Pb, and Co (but not Ni) and appear to follow the general trend for sediment grain size on the foreslope to decrease westwards and northwards.

Two tidal flat stations in the vicinity of Iona and Sea Islands have high Cu values (Fig. 1). Pb and Zn values also are enhanced at these locations.

Correlation studies disclose very strong positive correlations with Cu, Pb, and Zn, and, with the exception of Ni, only slightly weaker correlations between other element pairs (Table 2). In addition, correlations of trace metals (except Ni) with Fe and % sand are strongly positive and negative, respectively. These relationships further are emphasized by multiple regression analysis, which shows that up to 80 per cent or more of trace metal variance can be explained in terms of fluctuations in Fe, Mn, and sand content (Table 3). It is hoped that analysis of residuals around the regression equations will identify areas where metal concentrations are poorly explained by the independent variables, and other factors, such as man's activities, may be significant.

Conclusion

On the basis of metal-distribution maps and correlation analysis, it appears that distribution of Co, Cu, Pb, and Zn in surficial sediments from the tidal flats and foreslope is closely related to distribution of fine grained material. Whether this association represents adsorption of metals onto clay mineral surfaces, or involvement of metals with other materials, which may in turn be related to the fine fraction of the sediment (such as hydrous Fe- and Mn-oxides or organic material), as yet is unknown. Further study will be undertaken to ascertain the relative importance of various geochemical processes in concentrating trace metals in this shallow marine sedimentary environment.

References

Bjerring, J.H. and Seagraves, P.
1974: UBC TRIP: Triangular Regression Package; Univ. of B.C. Computing Centre, 120 p.

Luternauer, J.L.
1975a: Fraser Delta sedimentation, Vancouver, British Columbia; *in* Report of Activites, Part A, Geol. Surv. Can., Paper 75-1, Pt. A, p. 467-468.

1975b: Fraser Delta sedimentation, Vancouver, British Columbia; *in* Report of Activities, Part B, Geol. Surv. Can., Paper 75-1, Pt. B.

Project 720079

C.P. Lewis
Terrain Sciences Division

The nature of the Yukon Beaufort Sea coastal zone has been conditioned primarily by erosion and redistribution of the unconsolidated Quaternary sediments of the Yukon coastal plain. Three major coastal types can be distinguished: (a) steep cliffs fronted by narrow beaches, (b) spits and barriers, and (c) arcuate, estuarine and fan deltas of Yukon coastal plain rivers.

A 1972 reconnaissance investigation (McDonald and Lewis, 1973) suggested that the Yukon coast has undergone general retreat in recent years. Erosion of coastal cliffs has been rapid, particularly where the sediments contain considerable pore, wedge, or massive ice. Material derived from this erosion and from the coastal plain rivers is dispersed by well developed longshore currents to four main sediment sinks: (a) Demarction Bay, (b) between Herschel Island and the mainland, (c) Phillips Bay, and (d) Shoalwater Bay (Fig. 1). Photogrammetric data indicate recent extension of spits and barriers, evidence of this longshore movement of sediment.

Objectives of the Project

The 1972 study raised many questions about the detailed nature, magnitude, and frequency of processes and responses in this arctic coastal zone, questions which could best be answered by a longer term instrumented study at a representative sample location. Kay Point (Fig. 1) was chosen as the sample site because it offers a wide range of coastal features in a small area. Specific studies include: (a) erosion of and sediment transport from the coastal cliffs southeast of the Point, (b) growth and migration of Kay spit, (c) morphology, hydraulics, and sedimentology of the Babbage River delta, and estuarine delta of the Mackenzie type, and (d) sediment transport and deposition in Phillips Bay (Fig. 1, inset). The Babbage delta study is being undertaken as a separate but closely related project and is reported on in Forbes (1975).

The second objective of 1974 field work was to examine the geological aspects of coastal susceptibility to oil spills, a part of the joint industry-government Beaufort Sea study of the potential environmental hazards of proposed exploratory offshore drilling. The degree and duration of damage to the coastal zone resulting from such a spill is dependent primarily on: (a) whether or not the oil reaches the coastline, (b) the frequency and duration of inundation of coastal features by sea water containing oil, and (c) the reaction between the oil, once present, and the sediments, vegetation, and wildlife which make up the coastal zone. In this context, the intention of this study was to determine the geometry, sediments, vegetation, and stability of those coastal features most susceptible to inundation by sea water. Studies were carried out on the spits at Shingle and Kay points, on Nunaluk spit in the Firth River region, on the Blow and Babbage river deltas and, as examples of sediment source areas, on cliff segments at Shingle Point and Kay Point.

Field Studies, Kay Point

Initial investigations in the Kay Point region were oriented primarily towards establishing a grid network for data collection and obtaining the detailed background information necessary for process-response studies.

The coastal cliff southeast of Kay Point may be divided into two segments (Fig. 1, inset). In segment 1, the cliff is 5 to 10 m high, vertical, commonly undercut and has no visible beach at normal water levels. A generalized section is given in Figure 2a. Retreat is rapid (25 to 90 m in 16 to 18 years: McDonald and Lewis, 1973) and is controlled by melting and gullying along ice wedge lines, undercutting, and subsequent block slumping. In segment 2 the cliff rises to 90 to 100 m, becomes less steep, changes in stratigraphy, and is fronted by pocket beaches. A 60 m drill log section taken in March 1974 is shown in Figure 2b. Sediments are finer and ice content higher than in segment 1. Ground ice slumps and associated mudflows play an important role in retreat which has been in the order of 25 to 50 m over the last 16-18 years (McDonald and Lewis, 1973).

Much of the sand and gravel eroded from the cliff segments is carried northwest around Kay Point and deposited on Kay spit (Fig. 1, inset). The linear feature is approximately 4.9 km long, averages 61 m in subaerial width, and consists largely of gravelly sand deposited over estuarine sandy silts. A March 1974 drillhole (Fig. 1, inset) showed sand and medium gravel to a depth of 5.2 m, gravel decreasing to zero at 10.7 m and silt content increasing with depth. Permanently frozen ground exists along the length of the spit but the drillhole penetrated a thin talik (unfrozen zone) beginning at 11.0 m.

The spit protects much of the Babbage estuary from marine wave activity and appears to be quite active, having extended about 400 m and retreated on line with Kay Point between 1952 and 1970 (McDonald and Lewis, 1973). Most sediment movement occurs during storm surges when the sea may rise several metres above the astronomical tide of 0.7 m and completely inundate the spit. The transport of sediment is also greatly influenced by sea ice, both directly, through the movement of sediment by ice push - observed in 1972 but not in 1974 - and indirectly, through the effect of the ice on storm surges and associated wave activity. During 1974 ice conditions were among the worst on record. The sea ice remained solid off Kay spit until late July and, although broken,

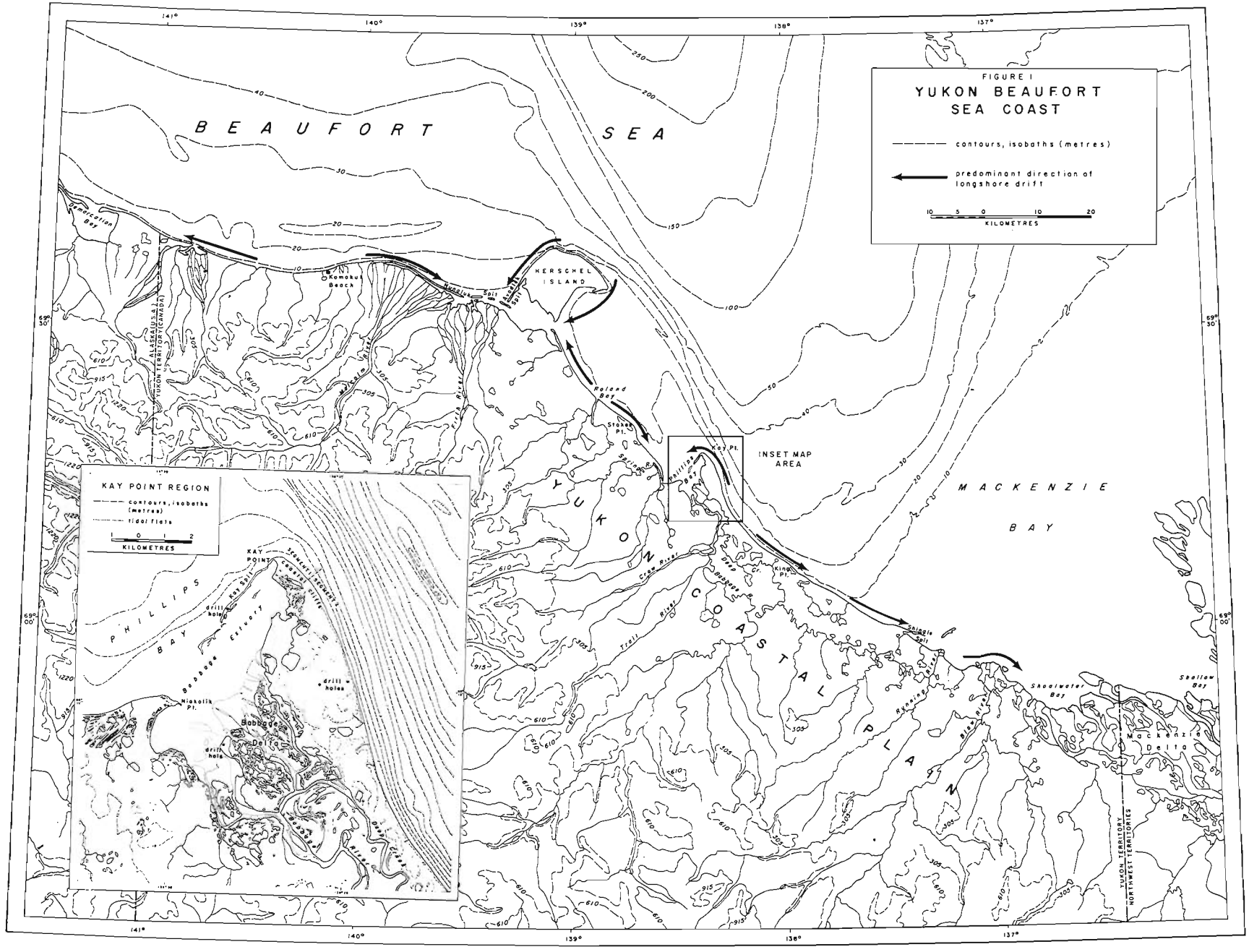
FIGURE I
YUKON BEAUFORT SEA COAST
contours, isobaths (metres)
predominant direction of longshore drift
10 5 0 10 20
KILOMETRES
BEAUFORT SEA
MACKENZIE BAY
YUKON COASTAL PLAIN
PHILLIPS BAY
KERSCHEL ISLAND
INSET MAP AREA
KAY POINT REGION
contours, isobaths (metres)
tidal flats
0 1 2
KILOMETRES
KAY POINT
Kay Spit
drill holes
Babbage Estuary
Babbage Delta
Niakoliik Pt.
Komakuk Beach
Spring Pt.
Stokes Pt.
Roland Bay
Phillips Bay
Key Pt.
King Pt.
Shingle Spit
Shallow Bay
Shoalwater Bay
Mackenzie Delta
Malcolm River
Crow River
Trail River
Rapids River
Blow River
YUKON TERRITORY
NORTHWEST TERRITORIES
ALASKA (U.S.A.)
YUKON TERRITORY (CANADA)
141°
140°
139°
138°
137°
69° 30'
69° 00'

persisted nearshore for the rest of the summer. A storm on August 20-21 caused only a slight surge and only small waves because of the very short ice-free fetch. Because of the ice protection the upper foreshore of the spit beach maintained its winter profile throughout the open water season.

Off both the cliff and the spit, bathymetric profiles are concave upward with the 5 m isobath 150 to 200 m from the cliff shoreline and two to three times this distance from the spit. One or two nearshore bars, 0.5 to 1.0 m in height, parallel the spit for most of its length and occasional sand wave fields with lee faces towards shore lie seaward of the bars. Side scan sonar proved useful even in very shallow water and showed little evidence of ice scour out to the 10 m isobath, the maximum depth scanned. Behind Kay spit, the Babbage estuary is both very shallow and flat; except nearshore, water depths are consistently in the 1 to 2 m range and only one bar, 500 m from the spit and parallel to it, was found. Neither echo sounding nor side scan data showed any evidence of strudel scour (Reimnitz *et al.*, 1974) in the estuary or nearshore although the phenomenon was observed near the distal end of Kay spit in June 1972 (McDonald and Lewis, 1973) and again in June 1974.

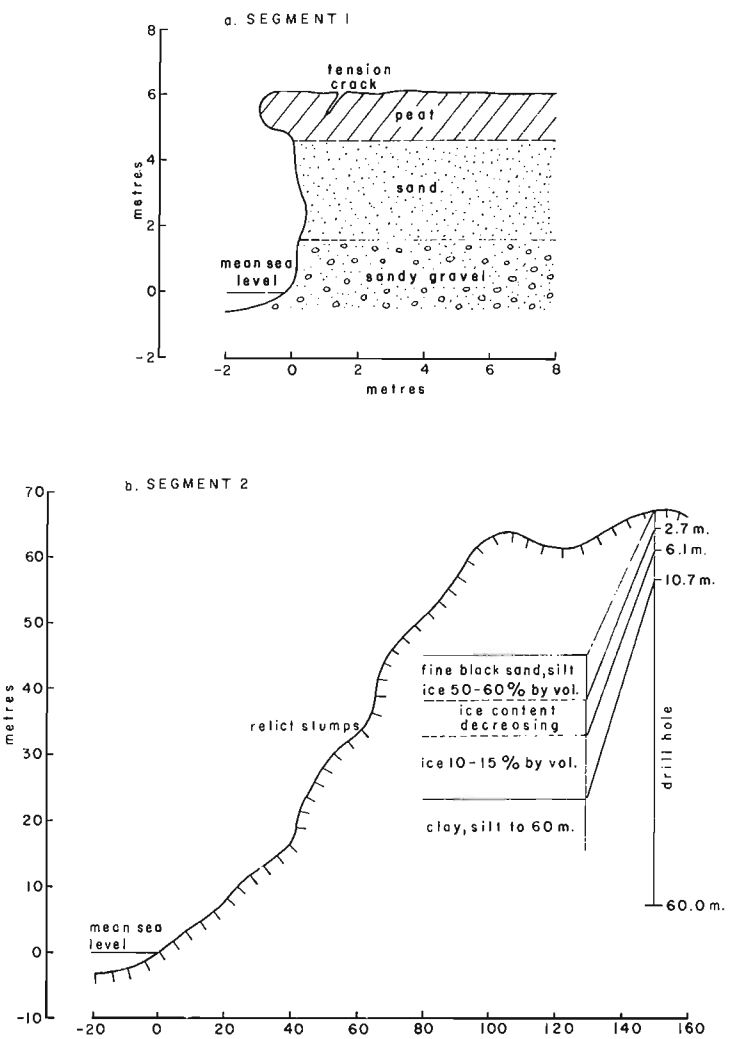

Figure 2. Generalized sections and stratigraphy, cliffs southeast of Kay Point.

Seismic refraction data collected in the Babbage estuary and off the spit and cliffs is discussed in Carson *et al.* (1975) and a tentative post-Pleistocene sedimentary history for the area is proposed. The refraction data, together with drill logs and ground temperature information from 60 m thermistor cables installed in March 1974 also will be used in the development and testing of a model of the perturbation in the ground temperature field caused by the presence and migration of the coastal cliff and spit.

Field Studies, Coastal Susceptibility to Oil Spills

Field work for this component of the project was designed to augment the 1972 reconnaissance study (McDonald and Lewis, 1973) by looking in more detail at major examples of coastal types. The research design used in each region investigated was made consistent with that being used in the Kay Point process-response study so that comparisons and, perhaps, extrapolations could most easily be made.

The approach taken was spatially hierarchical in nature with progressively more detailed work being done with each step down in the hierarchy. The highest level, the region, was defined as the segment of coastline providing sediment to each of the nearshore sediment sinks discussed earlier (Fig. 1). Within each region studied, areas - i.e. coastal types such as cliff segments, major spits and bars, deltas, etc. - were selected and examined in more detail. Intensive field work was carried out in two to four 80 m wide zones in an area, each zone extending, if practical, from the offshore-nearshore boundary (10 m isobath) well into the backshore (beyond the limit of marine activity).

The geomorphic data collected in a zone include the following:

(a) sketch map and photographs - of general topography, major geomorphic features, abrupt changes in sediment properties, etc.,

(b) subaerial stratum boundaries - between portions of the zone which appear homogeneous with respect to type or gradient of processes, e.g. foreshore, backshore, and subdivisions of each,

(c) subaerial profile surveys - three to five, oriented normal to the trend of the shoreline,

(d) subaerial sediment samples - five surface samples in each stratum positioned systematically along the zonal centre-line,

(e) active layer thicknesses - mean of five probings at each sediment sample site,

(f) bathymetric profiles - high frequency echo sounding and side scan sonar along the extension of the zonal centre-line to the offshore-nearshore boundary,

(g) submarine stratum boundaries - as for subaerial, subdivisions of nearshore strata,

(h) submarine grab samples - as for subaerial.

These data will be used to produce a topographic map of each zone, to estimate mean grain size and grain size gradient for the zone and for each stratum within it and, when data for all zones in an area are combined to infer areal gradients and the type and nature of active processes.

The three spit areas studied - Shingle, Kay and Nunaluk (Fig. 1) - are among the most prominent depositional features found along the Yukon coast. Of these, Kay has already been discussed. Shingle and Nunaluk are longer, wider and higher (Table 1) but are similar in form and, with localized exceptions, in the presence of both sand and gravel sediment types. The lower berm elevation of Kay spit may be due to the protection against the dominant southeasterly moving storm waves offered by Herschel Island and the bar between it and Kay Point (Fig. 1). It does not appear to be related to nearshore slope (Table 1).

Typical subaerial profiles and sediment types for each spit are shown in Figure 3. Four morphologic components (sampling strata) are common to most of the spit zones examined: foreshore, backshore I, backshore II, and lagoon shore. The significance of the surveyed foreshore geometry is difficult to evaluate because the upper portion is relict, undisturbed during the 1974 open water season. Berm elevation over the length of all spits is relatively constant except for a sudden drop from the end of the main Nunaluk spit to the distal islands (Fig. 3). Behind the berm crest, the backshore I stratum consists of washover deposits which overlie older backshore II sediments. The boundary between the two is commonly an abrupt scarp. In the proximal zones of Shingle and Nunaluk spits, the washover deposits appear to be trangressing possible evidence of shoreline retreat. The lagoon shore stratum in all cases is lower and displays fewer and smaller ridges than the foreshore because of shallow depths, seldom exceeding 2 m and short fetch in the lagoons.

No consistent pattern of lengthwise variation in mean sediment size is apparent among the spits. Preliminary observations show Shingle to be relatively constant along its length, Kay coarsest at its proximal end and constant thereafter, and Nunaluk with a gradual increase towards its distal end and a sharp decrease to almost pure sand on the second and third distal islands. Laterally, the foreshore stratum is both coarsest and most variable. Backshore II is much finer than backshore I with silt commonly present in addition to the usual sand and some gravel. Mean size increases on the lagoon shore, but not to foreshore levels. These lateral changes are normal for spits at any latitude.

Nearshore bars exist off both Shingle and Kay but are neither numerous nor prominent. No bars were found off the attached segment of Nunaluk spit in 1972 but a complex system of bars and channels existed seaward and between the distal islands, probably due to, at least in part, Firth River discharge (McDonald and Lewis, 1973). Little evidence of ice scour was found in the nearshore areas of any of the spits; this phenomenon apparently ceases at about the 10 m isobath where winter shorefast ice begins (J.M. Shearer, pers. comm.). Nor were significant ice-related features observed on the spit beaches in 1974 but Alaskan observations (Hume and Schalk, 1964 and 1973; etc.) and 1972 observations on Kay spit (McDonald and Lewis, 1973) suggest that 1974 was an unusual year in this regard.

Deltas of Yukon north slope rivers are another important type of depositional feature found along the coast. Two were studied in 1974: the Babbage, discussed in detail in Forbes (1975) and the Blow. Blow River is slightly smaller than Babbage River with a total basin area of 3700 km^2 and an estimated mean peak annual discharge of 144 m^3/sec. (McDonald and Lewis, 1973). Its delta has a surface area of about 50 km^2 (Walker and McCloy, 1969) and is arcuate in form, protruding out from the coastal cliffs rather than being protected by them as is the case for the estuarine Babbage delta.

Except in outline and exposure, the two delta plains are quite similar. Both contain several major distributary channels, extensive vegetated interlevee flats and numerous lakes, some with connecting channels to the distributaries. In the lower deltas, levees are almost indistinguishable, their heights seldom exceeding 0.5 m. Because of its proximity to the Mackenzie, much more driftwood has been stranded on the surface of the

Table 1

Yukon Coast Spit Morphometry

Spit	Length (km)	Mean Subaerial Width (m)	Mean Berm Height (m)	Foreshore[a] Slope	Nearshore[b] Slope
Shingle	5.4	141	1.53	0.085	0.006
Kay	4.9	61	0.96	0.066	0.010
Nunaluk	12.2	163	1.49	0.041	0.017

[a] Berm crest to shoreline

[b] Shoreline to 5 m isobath

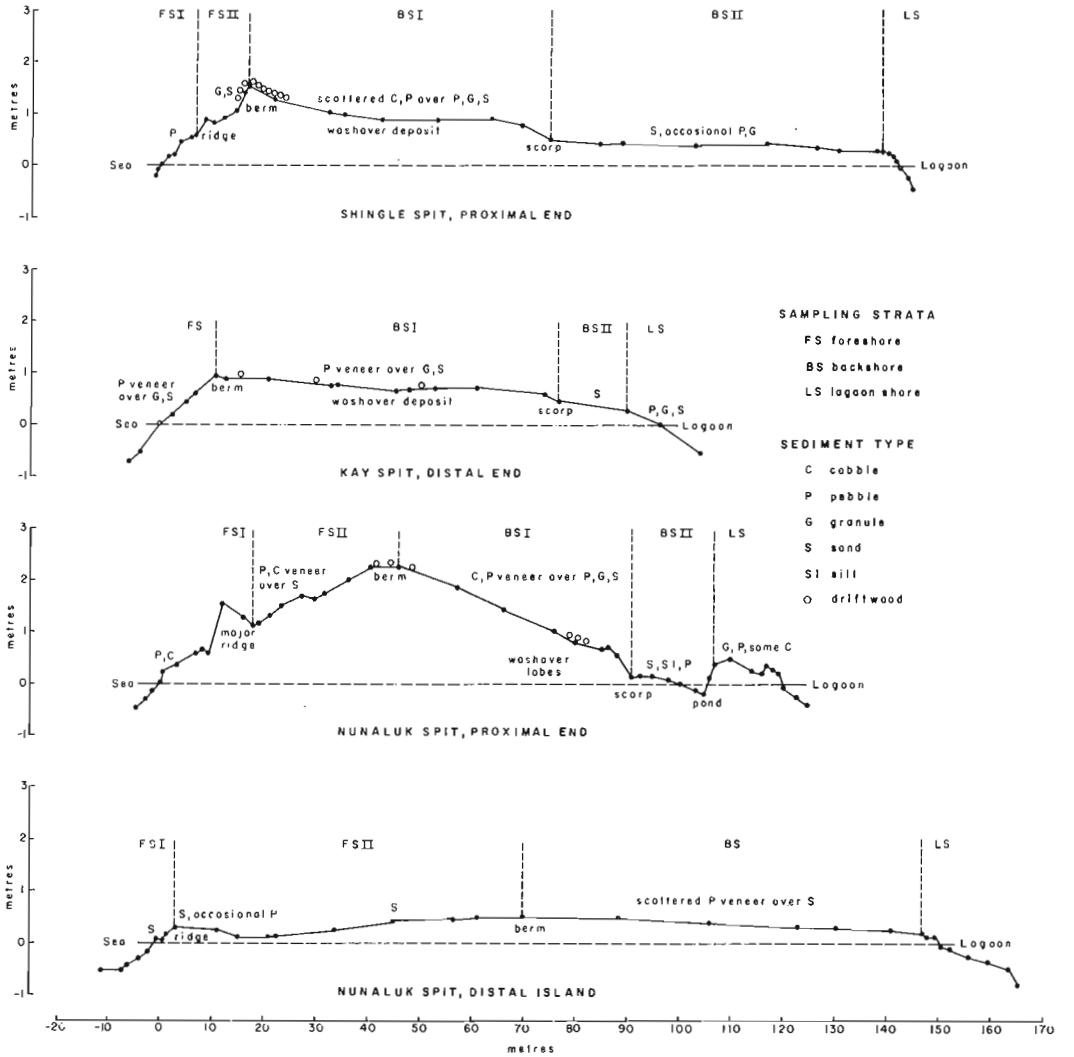

Figure 3. Selected cross-sections with sediment types, Yukon Coast spits.

Blow delta than on the Babbage. The highest driftwood line on the Blow was formed during a storm surge which reached more than 2 m above mean sea level and covered considerably more than 50 per cent of the subaerial delta surface.

Texturally, the two deltas also are alike. Fine gravel in the upper Blow delta changes abruptly to silt in the lower (Walker and McCloy, 1969). Organic detritus, however, appears to be more prominent in the Blow than in the Babbage. All lower delta plain samples show a high percentage of organics with low scarps (up to 0.8 m in height) cut into the vegetated delta front, and alluvial islands being composed almost entirely of organic material.

These scarps, together with the absence of significant intertidal flats, except near the mouths of active distributaries, suggest retreat of the subaerial front of the Blow delta, perhaps even more rapidly than the Babbage. Water depths off the front of the Blow are very shallow however, so the retreat may be more apparent, than real, depending upon the location of distributary mouths. At one site near the major western distributary mouth, water depth was less than 1.0 m out to 1.2 km offshore, increased in a series of steps to 2.5 m at 1.3 km, and was constant at 2.5 m to at least 2.1 km from shore.

Between Shingle Point and Blow delta the coastline is cliffed except at the delta of Running River. East of Running River a largely unvegetated gravel scarp, gullyed at intervals along its length, rises at an angle of 32 to 35 degrees to an elevation of 15 to 20 m. Sediment eroded from this scarp is moved eastward along the narrow beach which fronts it and is the source of gravel found in a sequence of beach ridges on the western Blow River delta. West of Running River the scarp reaches elevations of more than 30 m but is less steep, mostly vegetated, and composed predominantly of silts. Material reaches sea level primarily by mudflows and by erosion in gullies. This cliff segment is similar in many ways to segment 2 at Kay Point.

In addition to the geomorphological and sedimentological studies, botanical work was carried out in connection with the surveyed profiles at Shingle Point, Kay Point, and Nunaluk spit. Collections of all vascular plants and representative bryophytes were made for all areas studied. The distribution of the vegetation was examined in relation to the varied geomorphic units within each study zone using a quadrat method for continuous vegetated areas and by the line transect method for discontinuous areas. The collections presently are being identified and, when completed, plant communities present will be described and discussed in terms of their geomorphic significance (J.M. Teversham, pers. comm.).

Lastly, electrical resistivity sounding and profiling were completed on Shingle, Kay, Spring River (Fig. 1), and Nunaluk spits. The aim of this experiment was to test the usefulness of this geophysical method in distinguishing the top and bottom of permafrost and the thickness of gravel in coastal spits. The data are presently being analyzed but it appears that, because of the configuration of permafrost and the stratigraphic situation, gravel thicknesses cannot be defined.

References

Carson, J.M., Junter, J.A. and Lewis, C.P.
1975: Marine seismic refraction profiling, Kay Point, Yukon Territory; *in* Report of Activities, Part B, Geol. Surv. Can., Paper 75-1, Pt. B.

Forbes, D.L.
1975: Sedimentary processes and sediments, Babbage River delta, Yukon coast; *in* Report of Activities, Part B, Geol. Surv. Can., Paper 75-1, Pt. B.

Hume, J.D. and Schalk, M.
1964: The effects of ice-push on Arctic beaches; Am. J. Sci., v. 262, p. 267-273.

1973: The effects of ice on the beach and nearshore, Point Barrow, arctic Alaska; Partial final report, U.S. Office of Naval Research Subcontract ONR-413, 413a2, Arctic Inst. North Am., 29 p.

McDonald, B.C. and Lewis, C.P.
1973: Geomorphic and sedimentologic processes of rivers and coast, Yukon coastal plain; Environmental-Social Committee, Northern Pipelines, Task Force on Northern Oil Development, Government of Canada, Report No. 73-39, 245 p.

Reimnitz, E., Rodeick, C.A. and Wolf, S.C.
1974: Strudel scour: a unique arctic marine geologic phenomenon; J. Sed. Petrol., v. 44, p. 409-420.

Walker, H.J. and McCloy, J.M.
1969: Morphologic change in two arctic deltas; Arctic Inst. North Am., Res. Paper No. 49, 91 p.

Project 740062

John L. Luternauer
Terrain Sciences Division, Vancouver

The first series of sediment sampling operations for this project, initiated in 1974, (Luternauer, 1975) was completed with the October-November postfreshet sediment surveys of the western delta front slope and tidal flats. A postfreshet bathymetric survey of the delta slope was completed by the Canadian Hydrographic Service in September over the same portions of the slope which had been surveyed earlier (in March and April) generally to a depth of 200 m. However, for all areas, except that off the mouth of the main channel (Fig. 1), the revisory survey extended only to the 100 m contour. Mortimer (1975) has described in detail field operations involved in the surveys and, in a discussion of data quality, suggests that, in general, differences of less than 1 m between surveys may not represent real changes. Figure 1 presents a summary of the changes in bathymetry observed on a series of comparable profiles from the two surveys. Vertical changes in bathymetry generally do not exceed 2 m except off the main channel (Figs. 1 and 2), where there is evidence of considerable freshet related scouring and filling, and off North Arm (Fig. 1) where a double check of navigational and sounding equipment undertaken by Mortimer confirmed that the sea floor here shoaled at least 1 m over a large area, and possible as much as 3 or 4 m over more restricted sections.

A total of 322 samples collected during five sampling trips over the tidal flats between March and November (hence, spanning the freshet) have been completely analyzed for grain size. As of March 1st, statistical parameters have been computer calculated only for those samples obtained during June (mid-freshet) and October-November (postfreshet). The changes noted in the mean grain size for these two periods are qualitatively represented in Figure 1. All samples for which the mean size was identical or differed by no more than 0.1 Ø are considered not to exhibit significant differences.

An examination of mean grain size changes reveals that suspended sediment discharged during the freshet has been deposited primarily to the south of the main

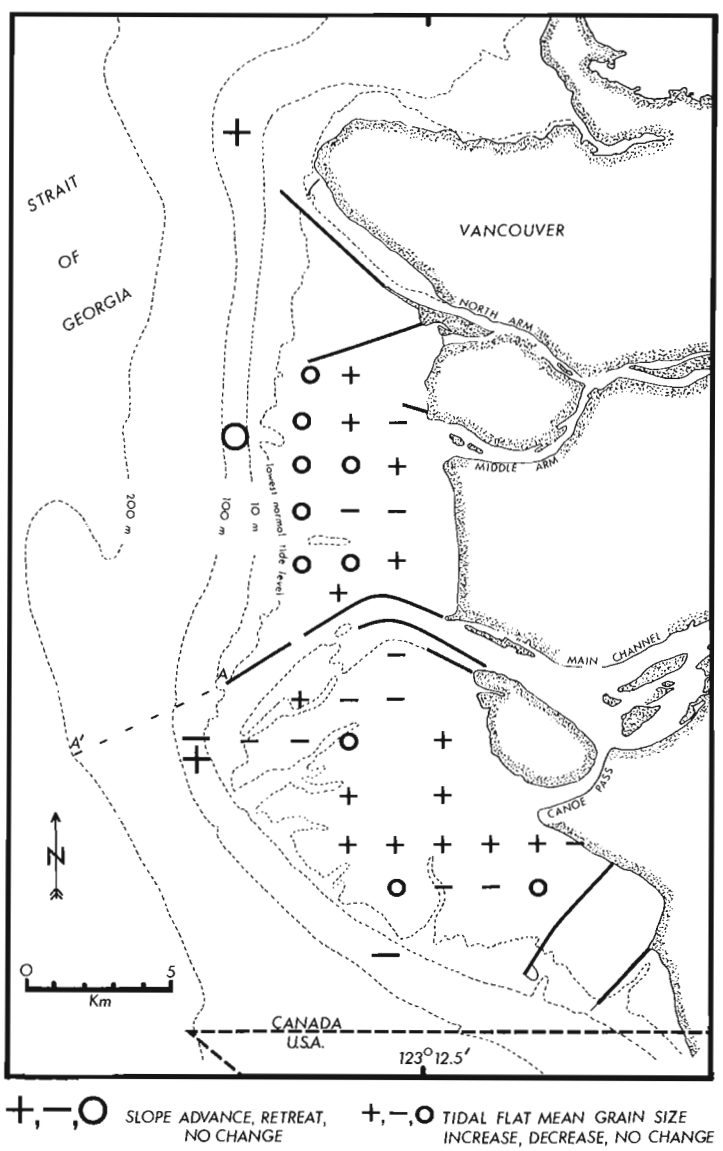

Figure 1.

Short term morphologica and sedimentary changes along the western delta front of the Fraser River. Slope morphologic changes represent advances and retreats occurring over the 1974 freshet period (May-August). These were determined from Canadian Hydrographic Service prefreshet and postfreshet bathymetric surveys (the latter survey extended only to the 100 m contour except off the main channel where both surveys extended to the 200 m contour). Symbols are laterally centres over section of slope described. Tidal flat sedimentary changes represent differences in mean grain size of samples collected at mid-freshet and postfreshet periods. A - A' indicates location of bathymetric profiles in Figure 2. Solid lines crossing tidal flats represent jetties, breakwaters, and causeways.

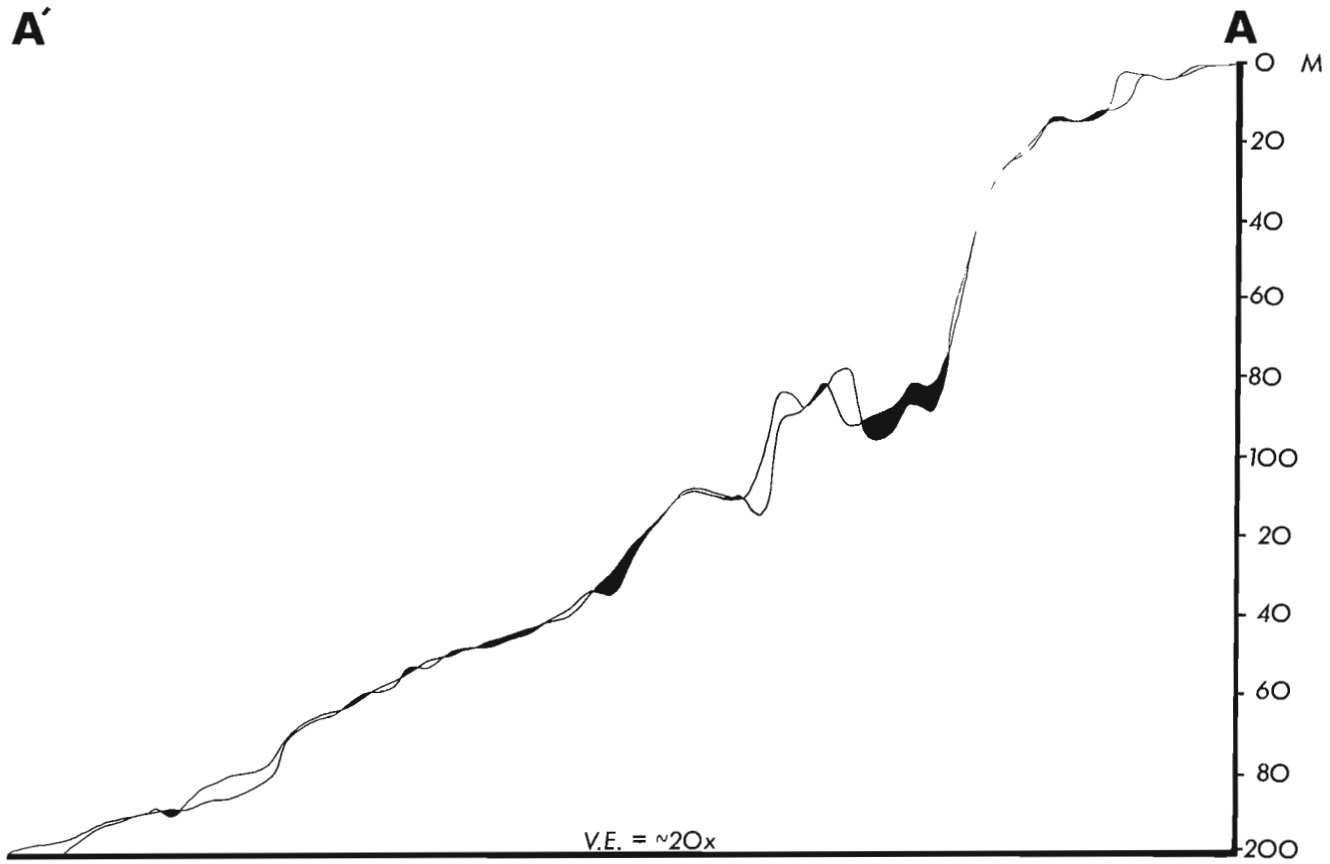

Figure 2. Comparison of prefreshet and postfreshet bathymetric profiles from the same location over the canyoned slope off the main channel of the Fraser River. Blackened segments represent sites of erosion, clear intervals, sites of deposition. Refer to Figure 1 for location of profiles.

channel. The evident increased coarseness of sediment about the mouth of Canoe Pass (Fig. 1) suggests that this distributary may be a significant supplier of the sand critical to the maintenance of the stability of these tidal flat banks. The presence of an unfilled borrow hole at the lower reaches of Middle Arm (Fig. 1) likely prevents the bulk of the traction load in the river (consisting mostly of sand) from reaching the tidal flats. This may, in part, explain the lack of change in the mean size of many of the sediments along the edge of the flats off this distributary. However, some of the coarsest sediments on the western delta front tidal flats, and available in the lower estuary (1.5 - 2.0 ϕ) (0.250 - 0.353 mm), are to be found in this area and it is probable that if grain size were to change, it would have to be through the infusion of finer suspended sediment. This, in turn, is not likely insofar as waves and tidal currents coupled with longshore drift, induced by breaking internal waves (Thomson, in press), probably sweep finer sediment clear of this portion of the flats.

The role of freshet discharge on tidal flat sedimentation should become more sharply delineated as the remaining three series of samples are computer analyzed.

Analysis of prefreshet and postfreshet series of slope samples (Luternauer, 1975) will be completed by early April, 1975. Grieve and Fletcher (1975) described the preliminary results of a study of trace metals in samples collected for this project.

Acknowledgments

All grain size analyses were carried out by Heather Mowat at the Terrain Sciences Laboratory in Vancouver.

References

Grieve, D. and Fletcher, K.
1975: Trace metals in Fraser Delta sediments; *in* Report of Activities, Part B, Geol. Surv. Can., Paper 75-1, Pt. B.

Luternauer, J.L.
1975: Fraser Delta sedimentation, Vancouver, B.C.; *in* Report of Activities, Part A, Geol. Surv. Can., Paper 75-1, Pt. A, p. 467.

Mortimer, A.R.
1975: Final field report, shore party, B.C., March 4 to October 10, 1974; Canadian Hydrographic Service, Pacific Region, unpaged.

Thomson, R.E.
Longshore current generation by internal waves in Georgia Strait; Can. J. Earth Sci. (in press)

39. THE STABILITY OF PERMAFROST AND RECENT CLIMATIC CHANGE IN THE MACKENZIE VALLEY, N.W.T.

Project 680047

J. Ross Mackay[1]
Terrain Sciences Division

Introduction

Numerous writers have discussed the global warming which has occurred from the late 1800s to the 1940s, with a subsequent cooling trend (e.g., Bryson, 1974; Burns, 1973; McKay, 1970; Mitchell, 1963). Although the record has come primarily from air temperatures, recent climatic change is also preserved in many deep borehole temperature profiles (e.g., Cermak, 1971; Cermak and Jessop, 1971; Jessop and Judge, 1971; Judge, 1973a, 1973b; Taylor and Judge, 1974). Lachenbruch and Marshall (1969) have calculated from deep borehole measurements at Barrow and Cape Simpson, Alaska that the mean annual ground temperature rose by about 4°C during the warming period, and the temperature has since cooled by about 1°C. The warming at Norman Wells, N.W.T. as determined from the upward projection of linear profiles below a depth of 50 m (Garland and Lennox, 1962; Hemstock, 1953; Imperial Oil Ltd., pers. comm., 1966 temperature measurements) averages about 3°C. Approximately the same change has occurred at Fort Providence, N.W.T. (Judge, 1973a). Along the western arctic coast, temperature measurements to a depth of 60 m at several drillhole sites show a temperature inversion at depth. A warming trend is seen at Resolute, Cornwallis Island (Cook, 1958), and elsewhere in the Arctic (Gold and Lachenbruch, 1973; Judge, 1973b; Taylor and Judge, 1974). Mackenzie Valley air temperature records for Fort McPherson, Fort Good Hope, and Fort Simpson are remarkably consistent in showing a mean annual air temperature drop of at least 2°C since 1950 (Burns, 1973). There is the good probability, therefore, that mean annual ground temperatures in the Mackenzie Valley increased by about 3°C during the warm period (late 1800s to the 1940s) and have since decreased by 1°C or more. A similar warming and cooling trend also has been observed in the U.S.S.R. with new permafrost having grown in nonpermafrost areas in the past 30 years (e.g., Belopukhova, 1973). It is the purpose of this paper to comment upon the stability of permafrost in the Mackenzie Valley in terms of the climatic change of the past century.

Continuous and Discontinuous Permafrost

The boundary between continuous and discontinuous permafrost in Canda has been defined as the -5°C mean annual ground temperature isotherm as measured just below the level of "zero" annual temperature change, or at about the 15 or 20 m depth (Brown, 1970). Mean annual ground temperatures can easily vary by several degrees within a horizontal distance of a few hundred metres because of local differences in topography, vegetation, snow cover, drainage, and so forth.

The temperature data in Figure 1 have been compiled from published (Judge, 1973a; Mackay, 1967, 1974; Taylor and Judge, 1974) and unpublished ground temperature records. The circled temperature values indicate the approximate positions of the present "average" mean annual ground temperature isotherms in the Mackenzie Valley. The deviation from the average is estimated at about ± 1.5°C. If ground temperatures were 3°C colder 100 years ago, and the present north-south temperature gradient prevailed, then 100 years ago the southern boundary of continuous permafrost may have been as far south as Fort Norman, N.W.T., in contrast to its present location near Arctic Red River, N.W.T., about two hundred miles farther north. A century ago, areas between Wrigley, N.W.T. and Fort Providence, N.W.T. would have had extensive permafrost in contrast to the patches of today. If the ground temperatures along the western arctic coast were likewise 3°C colder, then conditions 100 years ago would have been much more severe and like those now experienced in Banks and Victoria islands.

Suggested Permafrost Changes

If the southern boundary of continuous permafrost shifted northwards a couple of hundred miles in the past century, the thickness of permafrost in present areas of continuous permafrost would have remained unchanged. However, where permafrost was thin (e.g. 10 m) at the beginning of the warming period, thaw at the top and bottom of permafrost either would have thawed all of the permafrost, or else left only relict patches at depth. For example, permafrost perhaps 30 m thick in the Fort Providence, N.W.T. area has completely thawed during the warming trend (Judge, 1973a).

Burns (1973), in discussing climatic trends in the Mackenzie Valley, points out that the mean January air temperatures have exhibited the general trend of a 2.8°C increase from 1920 to 1930, dropping 1.7°C during 1930 to 1940, thence increasing 3.9°C into the late forties, again decreasing by 4.4°C into the late fifties, rising 2.8°C to the mid-sixties, and once again falling by 2.8°C by 1970. As the July temperatures changed little, the mean annual air temperature change would then be approximately half the January change.

[1]Department of Geography, University of British Columbia, Vancouver, B.C., V6T 1W5

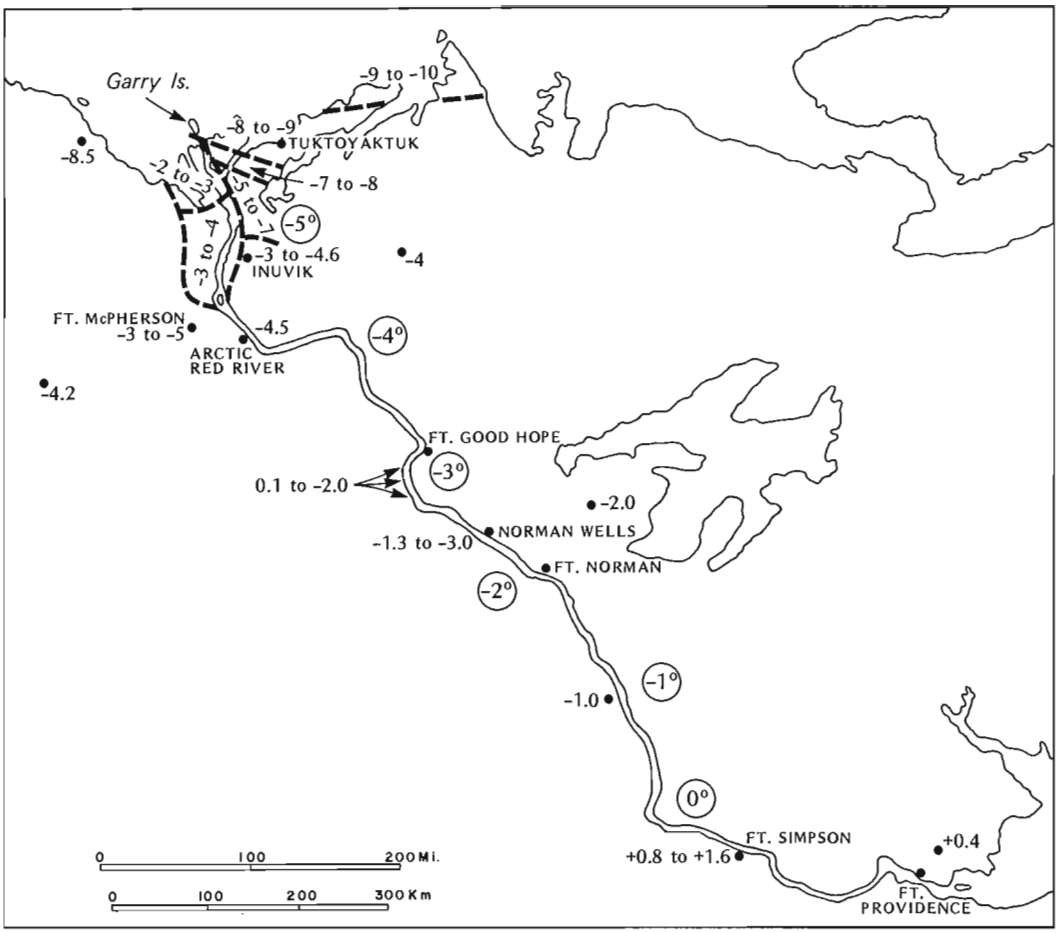

Figure 1. The circled numbers indicate the approximate mean annual ground temperatures in ^{o}C. At any given area, a temperature range of $\pm$ 1.5^{o}C is quite possible.

The rate of any new permafrost growth would depend, of course, upon many factors such as the surface and subsurface ground temperatures and the soil properties in the frozen and unfrozen state. As a very rough estimate, the depth of permafrost growth in saturated fine sands for a step surface temperature change of from 0^{o}C to -1^{o}C would be about

$$z \approx \sqrt{t}$$

where z is the permafrost depth in metres and t is time in years.

Thus, with a post-1950 cooling trend, thin permafrost a few metres thick has probably grown in many areas of the upper Mackenzie Valley. In the U.S.S.R., recent growth of 2 to 3 metres of permafrost has been encountered over extensive areas (Belopukhova, 1973). In addition to such changes in the horizontal distribution and vertical continuity of permafrost other changes may have occurred, viz.:

Thermokarst Features

Partial or complete degradation of warm permafrost, especially in the extensive ice-rich lake clay plains and glacial tills, should be recognizable in thermokarst lakes and depressions. Some of the numerous recently active thaw lakes in the upper Mackenzie Valley may be a response to the climatic change.

Active Layer Thickness

The active layer thickness at any given site would always have been in quasi-equilibrium with any climatic change. The extent of active layer thaw can be estimated from Figure 2 in which the approximate thaw depth for vegetated earth hummocks and their depressions (Tàrnocai, 1973; Zoltai and Tarnocai, 1974), and also for bare sand and gravel, are plotted. If Figure 2 is used to estimate past thaw depths, then a 3^{o}C warming would have thickened the active layer about 20 to 50 per cent. The amount to which the active layer deepened would depend not only on a change in mean annual temperature, but also on whether both summer and winter temperatures changed, or only one. The frequent occurrence of tilted trees and cryoturbated soils (e.g. Zoltai and Pettapiece, 1974) found associated with hummocks points to their instability, but whether the instability has resulted from recent climatic change is unknown.

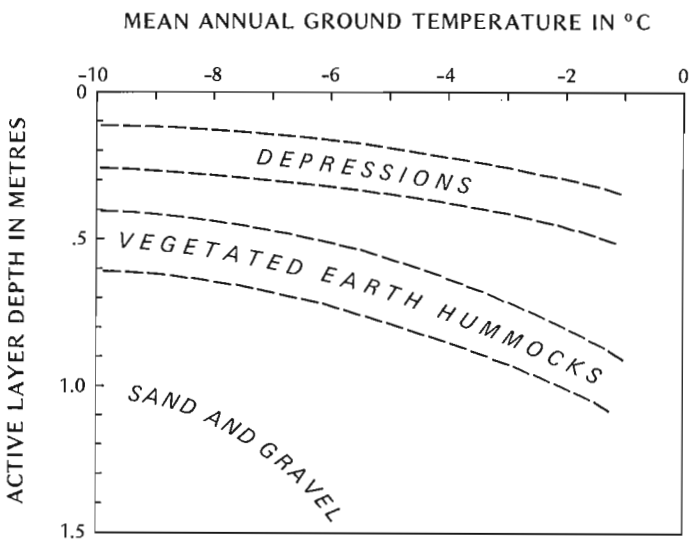

Figure 2. Approximate thicknesses of the active layer for the Mackenzie Valley and western arctic coast for different soil types and vegetation. The data for vegetated earth hummocks and their depressions are from Tarnocai (1973), Zoltai and Tarnocai (1974), and field measurements. The data for sand and gravel are from field measurements on bare or nearly bare areas.

Any climatic cooling which results in a thinning of the active layer at a given site will produce an upward rise of the permafrost table which can only occur by the incorporation into permafrost of soil and ice seasonally frozen at the bottom of the active layer (Mackay, 1972). The type of ice which forms varies according to the relative movements of the downward and upward moving freezing planes in the active layer (e. g. Vtyurina, 1973) and the undulations of the frost table. Therefore, changes in the thickness of the active layer should also be mirrored in ice-rich soil at the top of permafrost.

Ice Wedges

Active ice wedges are most abundant in areas of continuous permafrost with a mean annual ground temperature of -5°C or lower (Péwé, 1966). The present southern limit of active ice wedges appears to be between Inuvik, N. W. T. and Arctic Red River, N. W. T. The ice wedges near Inuvik have troughs so overgrown with vegetation that cracking must be infrequent. By contrast, ice-wedge polygons become conspicuous landscape features north of Inuvik. At Garry Island, N. W. T., 150 km to the northwest of Inuvik, where the mean annual ground temperature is -8°C, about 40 per cent of the ice wedges crack each winter. Although the cracking of ice wedges is not solely a function of ground temperature, it seems probable that a warming of 3°C to temperatures above -5°C would have been sufficient to cause many active ice wedges to become dormant. An active layer thickening would then have truncated the tops of ice wedges beneath the polygon troughs. With a return to colder conditions, rejuvenation may have occurred. Indeed, a few ice wedges north of Inuvik appear to show recent rejuvenation, but the evidence is not conclusive.

Mass Movements

No study has been carried out linking mass movements (e. g. slides restricted to the active layer, flows involving the thaw of ice-rich soils, etc.) to climatic change. It would seem unusual, however, if some mass movements did not occur in response to a thickened active layer and the melting of ice-rich soil at the top of permafrost.

Conclusions

There seems to be the good probability that mean annual ground temperatures in the Mackenzie Valley increased by as much as 3°C from the late 1800s to the 1940s, with possibly a 1°C decrease since then. If this change did occur, then the southern boundary of continuous permafrost one hundred years ago may have been as far south as Fort Norman, N. W. T. The warming, with a northward shift in "permafrost conditions" likely was accompanied by partial to complete disappearance of permafrost in many areas of the upper Mackenzie Valley to give some of the extensive nonpermafrost areas of today. Expected warming changes should be recognizable in: relict permafrost at depth; young thermokarst lakes; thermal erosion; thickening of the active layer; truncation of some ice-wedge tops and increasing inactivity; mass movements; cryoturbation features; and so forth. A cooling trend should be shown by: new growth of permafrost in the upper Mackenzie Valley; thinning of the active layer; growth of aggradational ice at the top of permafrost; rejuvenation of inactive ice wedges; and so forth. Irrespective of any climatic change in the past century, there is excellent evidence from thaw unconformities, deep root penetration into permafrost, buried organic material in permafrost, and fossil, truncated, and rejuvenated ice wedges along the western arctic coast to show that permafrost shifts, exceeding that of the last 100 years, have occurred before.

References

Belopukhova, E. B.
1973: Features of the contemporary development of the permafrost of Western Siberia (in Russian); U. S. S. R. Acad. of Sci., Yakutsk, Proc. Perm. Conf., v. 2, p. 84-86.

Brown, R. J. E.
1970: Permafrost in Canada; University of Toronto Press, Toronto, 234 p.

Bryson, R. A.
1974: A perspective on climatic change; Science, v. 184, p. 753-760.

Burns, B. M.
1973: The climate of the Mackenzie Valley — Beaufort Sea, v. 1; Environment Canada Climatologic Studies Number 24, Toronto, 227 p.

Cermak, V.
1971: Underground temperature and inferred climatic temperature of the past millenium; Paleogeogr. Palaeoclimatol. Palaeoecol., v. 10, p. 1-19.

Cermak, V. and Jessop, A. M.
1971: Heat flow, heat generation and crustal temperature in the Kapuskasing area of the Canadian Shield; Tectonophysics, v. 11, p. 287-303.

Cook, F. A.
1958: Temperatures in permafrost at Resolute, N. W. T.; Geograph. Bull., No. 12, Ottawa, p. 5-18.

Garland, G. D. and Lennox, D. H.
1962: Heat flow in western Canada; Roy. Astron. Soc., Geophys. J., v. 6, p. 245-262.

Gold, L. W. and Lachenbruch, A. H.
1973: Thermal conditions in permafrost - a review of North American literature; Permafrost, North American Contribution, Second Int. Conf., Yakutsk, U. S. S. R.; Washington, Nat. Acad. Sci., p. 3-25.

Hemstock, R. A.
1953: Permafrost at Norman Wells, N. W. T.; Imperial Oil Ltd., Calgary, 100 p.

Jessop, A. M. and Judge, A. S.
1971: Five measurements of heat flow in southern Canada; Can. J. Earth Sci., v. 8, p. 711-716.

Judge, A. S.
1973a: The thermal regime of the Mackenzie Valley: observations of the natural state; Environmental-Social Program, Task Force on Northern Oil Development, Rept. No. 73-38, 177 p.

1973b: Deep temperature observations in the Canadian north; Permafrost, North American Contribution, Second Int. Conf., Yakutsk, U. S. S. R.; Washington, Nat. Acad. Sci., p. 35-40.

Lachenbruch, A. H. and Marshall, B. V.
1969: Heat flow in the Arctic; Arctic, v. 22, p. 300-311.

Mackay, J. R.
1967: Permafrost depths, lower Mackenzie Valley, Northwest Territories; Arctic, v. 20, p. 21-26.

1972: The world of underground ice; Annals Assoc. Am. Geog., v. 62, p. 1-22.

1974: Seismic shot holes and ground temperatures, Mackenzie Delta area, Northwest Territories; *in* Report of Activities, Part A, Geol. Surv. Can., Paper 74-1, Pt. A, p. 389-390.

McKay, G. A.
1970: Climate: a critical factor in the tundra; Trans. Roy. Soc. Can., ser. 4, v. 8, p. 405-412.

Mitchell, J. M.
1963: On the world-wide pattern of secular temperature change; *in* Changes of Climate, Proc. Rome Symposium, UNESCO, p. 161-181.

Péwé, T. L.
1966: Ice-wedges in Alaska - classification, distribution, and climatic significance; Proc. Permafrost Int. Conf., Lafayett, Indiana, 1973; Washington, Nat. Acad. Sci., Nat. Res. Council, Publ. No. 1287, p. 76-81.

Tarnocai, C.
1973: Soils of the Mackenzie River area; Environmental-Social Program, Task Force on Northern Oil Development, Rept. No. 73-26, 136 p.

Taylor, A. E. and Judge, A. S.
1974: Canadian geothermal data collection - Northern Wells, 1955 to February 1974; Energy, Mines and Resources, Earth Physics Branch, Geothermal Series No. 1, 171 p.

Vtyurina, E. A.
1973: Cryogenous texture of soils in the layer of seasonal thawing (in Russian); U. S. S. R. Acad. Sci., Yakutsk, Proc. Perm. Conf., v. 3, p. 60-65.

Zoltai, S. C. and Pettapiece, W. W.
1974: Tree distribution on perennially frozen earth hummocks; Arctic and Alpine Res., v. 6, p. 403-411.

Zoltai, S. C. and Tarnocai, C.
1974: Soils and vegetation of hummocky terrain; Environmental-Social Program, Task Force on Northern Oil development, Rept. No. 74-5, 86 p.

SOME RESISTIVITY SURVEYS OF PERMAFROST THICKNESS, TUKTOYAKTUK PENINSULA, N.W.T.

Project 680047

J. Ross Mackay[1]
Terrain Sciences Division

Some resistivity surveys have been carried out in Tuktoyaktuk Peninsula, N.W.T. (Fig. 1) in a variety of terrain types and thermal conditions. The objective has been to determine, if possible, permafrost thicknesses (Mackay, 1971, 1972). The general procedure has been to carry out surveys at sites where permafrost depths either were known or could be estimated, and additional supplementary data were available on soil type, ground temperature, and geomorphic history. Permafrost depths have been obtained primarily from drillhole logs, temperature measurements in drillholes, and from downhole logging surveys carried out by industry. Subsurface stratigraphy has come largely from shothole and drill logs, ground temperatures from temperature cables (Mackay, 1974), and the geomorphic history from field studies.

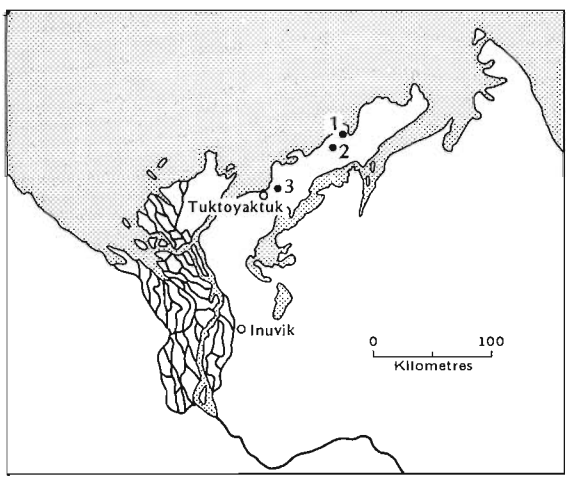

Figure 1. Location map showing Sites 1, 2, and 3.

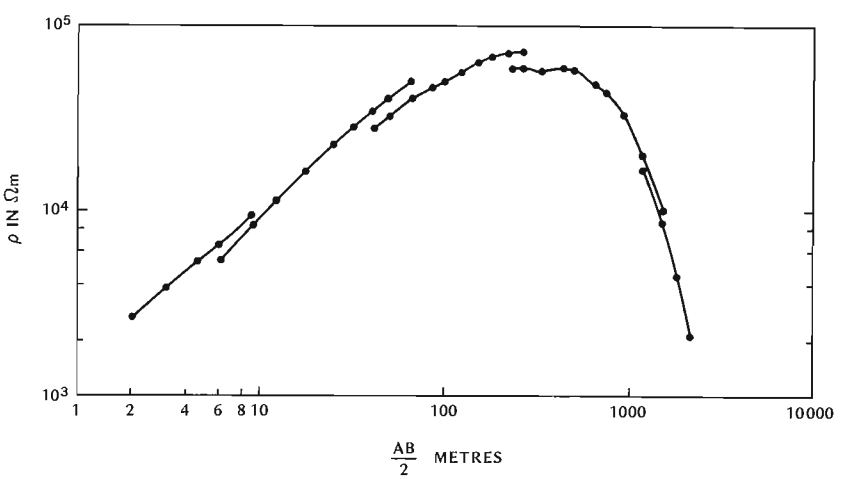

Figure 2.

Schlumberger curve for Site 1, Fig. 1. The apparent resistivity (ρ) is in ohm metres (Ωm); $\frac{AB}{2}$ is half the total electrode separation which, in the present example, slightly exceeded 4000 metres for the maximum separation.

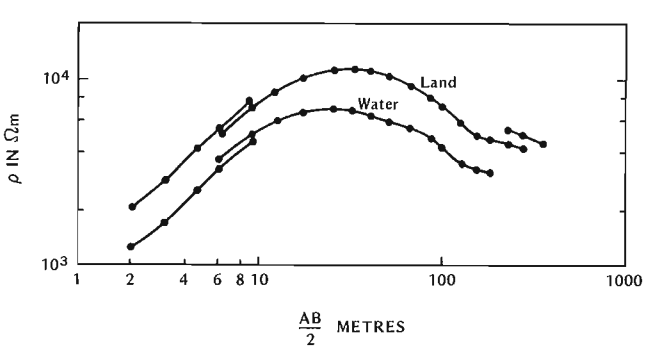

Figure 3.

Schlumberger curves for Site 2, Fig. 1. The "land" and "water" curves were run parallel to a lake shore, with centres 3 m from shore, one on land, and the other in water.

[1]Department of Geography, University of British Columbia, Vancouver, B.C., V6T 1W5

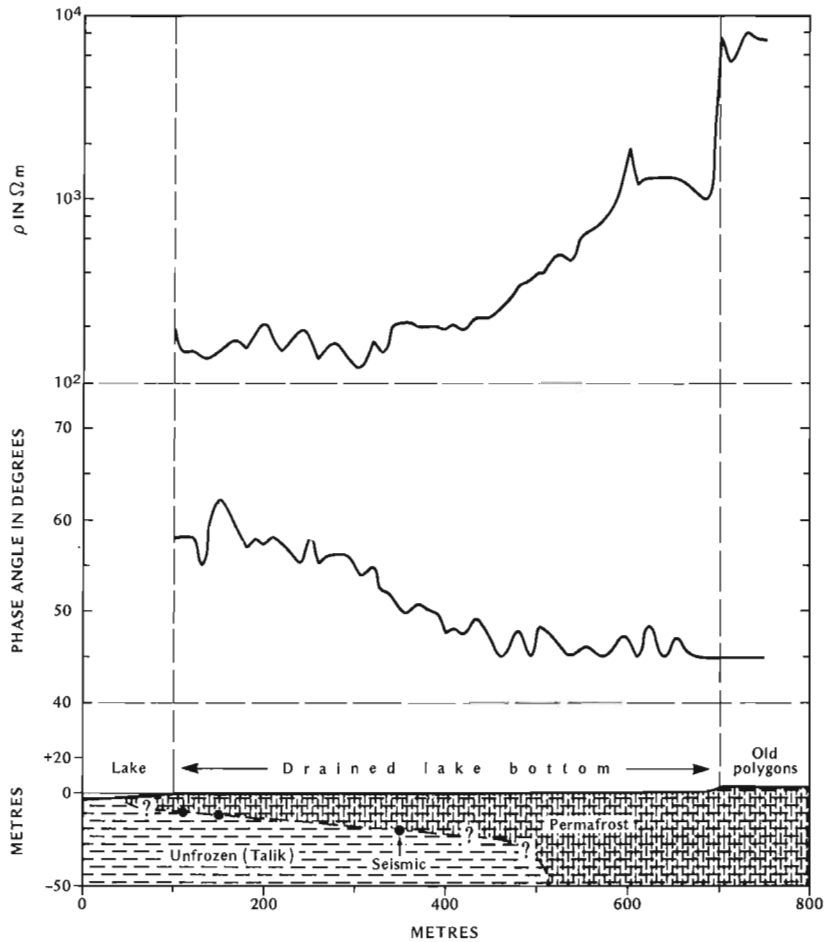

Figure 4. EM16-R profiles at Site 2, Fig. 1.

Two resistivity systems have been used, viz, a low frequency Scintrex RAC-8 unit and Geonic EM16-R VLF electromagnetic unit. The EM16-R unit was used with Station NPG (Seattle, Washington) at a frequency of 18.6 kHz. The RAC-8 was used mainly with the Schlumberger and the Wenner configurations and to a lesser extent with a double dipole array (Bates, 1973). Electrodes were half-inch diameter steel or copper rods. Although porous pots were carried in the field in case contact problems arose, they were not used. No problems were encountered with a completely saturated active layer.

Despite the relative ease with which soundings and profiles could be carried out in the field, the interpretation of the results has been difficult, for at least two reasons. First, the published curves rarely are suitable for determining the depth of permafrost. If a three layer case is assumed - active layer, permafrost, unfrozen material beneath permafrost - the ranges of the resistivity values and depths of the published curves are commonly too low for many permafrost conditions where resistivity and depth contrasts between the active layer and permafrost are great. Consequently, it has been necessary to extend the Schlumberger K-type three layer curves (e.g. van Dam and Meulenkamp, 1969) to cover a greater range of data. Second, problems in curve matching may also arise from the well-known temperature dependence of the unfrozen water content of fine-grained soils. When temperatures are close to $0^{\circ}C$, the resistivity contrast between frozen and unfrozen clays may be negligible because the pore water of clay freezes over a temperature range. For coarse-grained soils just below $0^{\circ}C$, the resistivity rise is abrupt because most of the pore water freezes between $0^{\circ}C$ and $-1^{\circ}C$. To illustrate, the mean annual ground temperature on poorly drained lake bottoms and flats may be as much as $5^{\circ}C$ warmer than the drier, rolling tundra sites. Consequently, a typical poorly drained site, with a mean annual ground temperature of $-5^{\circ}C$, will have the lower half of permafrost between about $-2.5^{\circ}C$ and $0^{\circ}C$ in which temperature range contrasts between frozen and unfrozen fine-grained soils may be slight. The resistivity of permafrost then would be underestimated, and curve matching made difficult.

Site 1. Thick Permafrost

Figure 2 shows one of several RAC-8 resistivity soundings in an exceptionally flat plain, free of lake interference, south of Point Atkinson, N.W.T. The active layer, in fairly dry sands, was about 0.7 m thick. The subsurface material is believed to be composed of sands, silts, and gravels. The maximum

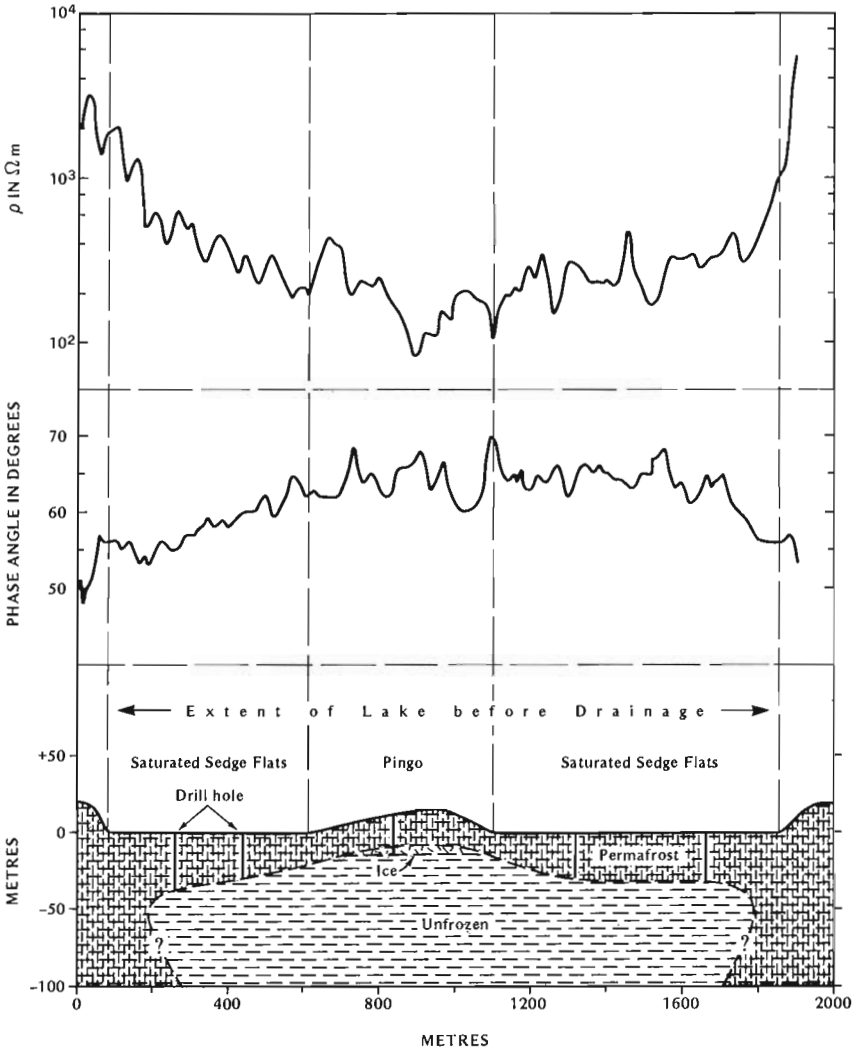

Figure 5. EM16-R profiles at Site 3, Fig. 1.

current used was 10 ma. The curve fits (visually) a Schlumberger K-type three layer curve with resistivities (top: middle: bottom) of 1: 75: 1 and thicknesses (top: middle) of 1: 400. The preceding gives a top layer resistivity of about 10^3 Ωm, middle layer of about 75 x 10^3 Ωm, and a permafrost thickness of about 300 m. There are no deep temperature measurements in the area, but several downhole logging surveys 10 to 15 km to the southwest indicate a permafrost thickness of about 500 m.

Site 2. Thin Permafrost

Figures 3 and 4 show RAC-8 soundings and EM16-R profiles across a lake bottom where permafrost is about 10 to 15 m thick. The site is the bottom of a lake which became partially drained in about 1958 or 1959. Shotholes in 1969 penetrated permafrost at a depth of 10 to 12 m and a seismic survey of permafrost depths in 1971 showed good agreement with the 1969 shothole depths. The subsurface material is sand and silt, to a depth of at least 20 m.

Two Schlumberger curves are shown in Figure 3. The lines were run parallel to the lake shore. The centres for the "land" and "water" curves were each 3 m from the shore. The electrodes for the water sounding were inserted vertically into the lake bottom in 10 to 15 cm of water. A visual fit to published curves (van Dam and Meulenkamp, 1969) indicates a K-type three layer curve with resistivities (top: middle: bottom) of 1: 15: 3 for the land and thicknesses (top: middle) of 1: 12. The "land" curve gives resistivities of 1.5 x 10^3 Ωm and 23 x 10^3 Ωm for the active layer and permafrost, respectively, with thicknesses of 1.3 m and 15 m. Corresponding resistivity data for the "water" curve are 10^3 Ωm and 15 x 10^3 Ωm and thicknesses of 1.6 m and 13 m. The depths for the active layer and permafrost are good, but not much can be said about the resistivities except that they seem reasonable.

The EM16-R profiles in Figure 4 were run at right angles to the lake and old shoreline. The profiles are fairly typical of similar sites mapped elsewhere, but the interpretation of the curves, at present, cannot be carried out. The increase in permafrost thickness as the old lake shore is approached is evidenced by a rapid rise in apparent resistivity and a decline in phase angle to about 45 degrees.

Site 3. Permafrost of Intermediate Thickness

Figure 5 shows EM16-R resistivity and phase angle profiles across a drained lake bottom and pingo (ice-cored hill). The average permafrost thickness, plotted from some ten drillholes, is 30 to 40 m. About 5 to 10 m of a silty clay overlie a medium-grained sand. The apparent resistivity and phase angle profiles show the same pattern as in Figure 4, with an increase in resistivity and a decrease in phase angle as permafrost thickens towards the old shoreline. RAC-8 soundings were carried out on the lake bottom, but the results were poor because once the electrode separation (AB) approached 1000 m, lake-edge effects from thick permafrost were detected.

Conclusions

Resistivity measurements have been used with varying success in the estimation of permafrost thickness in Tuktoyaktuk Peninsula. Numerous soundings in Tuktoyaktuk Peninsula, Richard's Island, and the Mackenzie Delta show that a total electrode (AB) length of about 15 to 20 times the depth of permafrost is required to yield a good sounding curve. If permafrost is several hundred metres deep, therefore, it is very difficult to find homogeneous terrain, free of large lakes, sufficiently extensive for a sounding. Lake taliks have an appreciable effect on apparent resistivities even when the lakes lie beyond the AB electrodes. In drained lake bottoms, soundings may be difficult because of "edge" effects of thick lake shore permafrost. A saturated active layer does not interfere with resistivity surveys. Visual curve matching is difficult because of the limits of the published curves and the possible lack of marked resistivity contrasts between frozen and unfrozen soils at near zero temperatures. The VLF profiles, with the EM16-R, show recognizable patterns between thick and thin permafrost, but depth interpretation has not been attempted. However, a sufficient number of profiles have been run to show that the trends of Figures 4 and 5 can be repeated over and over again. A rising resistivity profile coupled with a decrease in phase angle commonly indicates thickening permafrost.

Acknowledgments

The writer would like to thank L. S. Collett and W. J. Scott for helpful comments on the paper.

References

Bates, E. R.
1973: Detection of subsurface cavities; U. S. Army Engineer Waterways Experiment Station, Vicksburg, Mississippi, 63 p. and appendix.

Mackay, J. R.
1971: Geomorphic processes, Mackenzie Valley, Arctic Coast, District of Mackenzie; *in* Report of Activities, Paper 71-1, Pt. A, p. 189-190.

1972: Geomorphic processes, Mackenzie Valley, Arctic Coast, District of Mackenzie (107 B, C, D); *in* Report of Activities, Part A, Geol. Surv. Can., Paper 72-1, Pt. A, p. 192-194.

1974: Seismic shot holes and ground temperatures, Mackenzie Delta area, Northwest Territories; *in* Report of Activities, Part A, Geol. Surv. Can., Paper 74-1, Pt. A, p. 389-390.

van Dam, J. D. and Meulenkamp, J. J.
1969: Standard graphs for resistivity prospecting; European Association of Exploration Geophysicists.

Project 680047

J.D. Root[1]
Terrain Sciences Division

The coast for 22 km north of Tuktoyaktuk, N.W.T. and for 26 km west-southwest was examined for exposures of ice wedges. The north and west coast of Pelly Island, N.W.T., 120 km northwest of Tuktoyaktuk also was visited.

Representative areas were mapped in topographic detail at 1:2000 using a plane table. Generally, the width of an ice-wedge trough approximated the width of the ice wedge at the contact with overlying sediment in the trough bottom. However, ice wedges are common on slopes where no surface expression of a trough is visible. Slopes as little as 4 degrees were observed to have a well defined ice-wedge network with no trough pattern visible on the surface or on aerial photographs.

"Fortress Polygons"

In areas that have had recent local lowering of the drainage base level, an unusual form of ice-wedge polygons may be found. The ice-wedge ice melts from the top down during the course of the summer thaw. A lowered local drainage base level allows drainage of meltwater from the tops of the ice wedges instead of the more common ponding and subsequent refreezing. The drainage results in marked V-shaped troughs sometimes two to three times deeper than wide. The drainage also contributes to the development of polygonal ground in which the ice wedges have squat, vertical-sided, square-topped walls of sediment and organic matter immediately adjacent to the ice wedges and flat low centres in between. The "walls" are remarkably consistent in width and height and are commonly about one metre high and one metre wide. The exact origin of these fortress polygons is not understood, although local drainage base lowering is an important aspect.

Summary Data on Ice Wedges

The analysis of data collected on ice wedges so far suggests the following:

1. Generally the trough size is directly related to ice-wedge width.
2. Trough size bears no apparent relationship to the depth of penetration of the ice wedge.
3. Slopes as little as 4 degrees can have no indication of ice-wedge troughs although ice wedges are present beneath the surface.
4. The size of ice wedges within an area of similar terrain representation on aerial photographs can be extremely variable in width, depth, and cross-sectional shape.
5. In areas of local drainage, thermal erosion by running water commonly can incise irregular-shaped, canyon-like structures in ice-wedge ice. These thermally eroded structures may refill with water and produce ice with a distinctly different character to the usual near-vertically foliated ice of the ice wedge.
6. In general, ice-wedge polygons developed in sandy materials tend to have a pronounced rectangular pattern. Ice-wedge polygons in stony ice-rich clays tend to be large, both wide and deep. Ice wedges that are part of a small ice-wedge polygon tend to be small, thin, and less deep.
7. Ice wedges control much of the coastal retreat along the coast examined around Tuktoyaktuk.

Depth of Thaw

The depth to the frost table was measured by probing with a steel rod at each of the selected ice-wedge sites. Measurements were made at one metre intervals over a 50 metre course, orientated east-west at various time intervals. The depth of penetration of the thawing plane (D) in centimetres can be described reasonably by

$$D = 2T^{n} \qquad (1)$$

where T is the time in days since thaw began (usually coincident with snow cover disappearance) and 'n' is a constant with values between 0.65 and 0.84. Generally 0.70 was found useful for most areas. The value of n = 0.84 was found good for sites devoid of vegetation. The value 0.65 was found good for ice-wedge polygonal ground terrain. The value 0.70 was found good for hummocky non-polygonal ground. The relationship (1) gave a description within 10 per cent of actual observed values for the first 50 to 60 days of thaw. After this time, the relationship is much less reliable as freeze-back from the underlying frost table begins.

[1]Department of Geography, University of British Columbia, Vancouver, B.C., V6T 1W5

42. SOIL MOISTURE RELATIONSHIPS, SELECTED MAP-AREAS, MACKENZIE VALLEY, N.W.T.

Project 730026

D.E. Lawrence[1]
Terrain Sciences Division

Information from geotechnical boreholes was used in an attempt to establish the relationship between natural soil moisture, soil type, and depth of sample below surface in several areas within the Mackenzie Valley (Norman Wells 96 E, Fort McPherson-Arctic Red River 106 M and N, and Aklavik 107 B). Preliminary analysis shows that a relationship exists between natural soil moisture and depth below surface for various fine grained soil types. Information from boreholes, which were drilled in the past several years by consulting engineering firms and federal agencies for scientific and engineering studies, comprised the base information for the study (96 E - 1325 holes, 106 M and N - 775 holes, 107 B - 812 holes). The data form part of the Mackenzie Valley Geotechnical Data Bank which contains information from over 7200 boreholes (Lawrence, 1974 a, b, c). Updating is currently underway and will bring the total to approximately 10 000 boreholes.

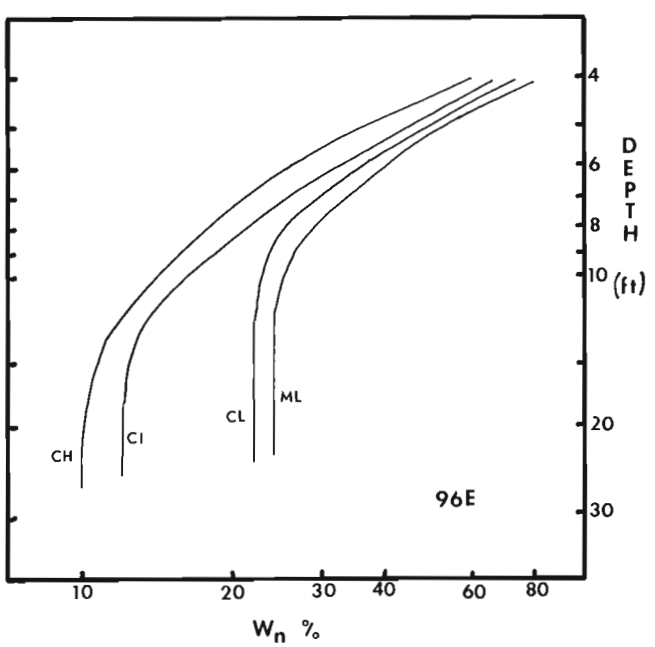

Figure 1. Natural soil moisture vs. depth below surface for various fine grained soil types (Norman Wells 96 E).

The information soon will be available on magnetic tape through the Geological Survey's open file system.

For some of the fine grained mineral soil classes of the modified unified system (CL, ML, CI, CH), a natural moisture vs. depth of sample plot was constructed, one for each of the three map-areas (Figs. 1, 2, 3). Lack of data on some soil types did not permit meaningful analysis and thus they do not appear in the plots. The unified classification of soils permits a wide range of materials within a single class; moisture may be contained as either water or ice, in the case of the latter it may be segregated or within the soil voids. In addition, other factors also influence the amount of moisture in the soils, i.e. availability of moisture, porosity, permeability, associated material types, presence of permafrost, active layer thickness, etc. No attempt was made to isolate the effects of the above factors before plotting, no preferential selection or refinement of the data was made to exclude the influence of any parameters which may have a bearing on soil moisture. It should be noted that the curves are means, the dispersion about the mean in some cases is considerable. This is undoubtedly due to the fact that no preferential selection of data was undertaken.

The curves have certain common attributes:

(1) a limiting value of moisture at depth,
(2) in most cases a well-defined inflection point,
(3) an exponential rise in moisture near the surface.

In all cases the moisture curves show a limiting value at depths greater than about 15 feet; beyond this depth there does not seem to be any significant change in mean values of moisture. CL and ML soils seem to be particularly consistent with respect to this limiting value of moisture, in the range of 16 to 24 per cent for the three areas. The ML soils always show greater moisture values for a given depth as compared to CL soils for a given area. For both map-areas 106 M-N and 96 E, the ML and CL curves are very similar; however, for 107 B there is considerable divergence. CI and CH soils showed lower limiting moisture values than the other soil types, which perhaps reflects the lower permeability of these soil types.

Inflection points of the CL and ML curves for 106 M-N and 96 E (Figs. 1 and 2) show a well defined break at about 8 feet. CH and CI inflection points are at a greater depth, about 15 feet. For curves of 107 B (Fig. 3) the inflection points are less well defined, at about 6 feet for ML and CL soils and about 4 feet for CI

[1]Department of Indian and Northern Affairs.

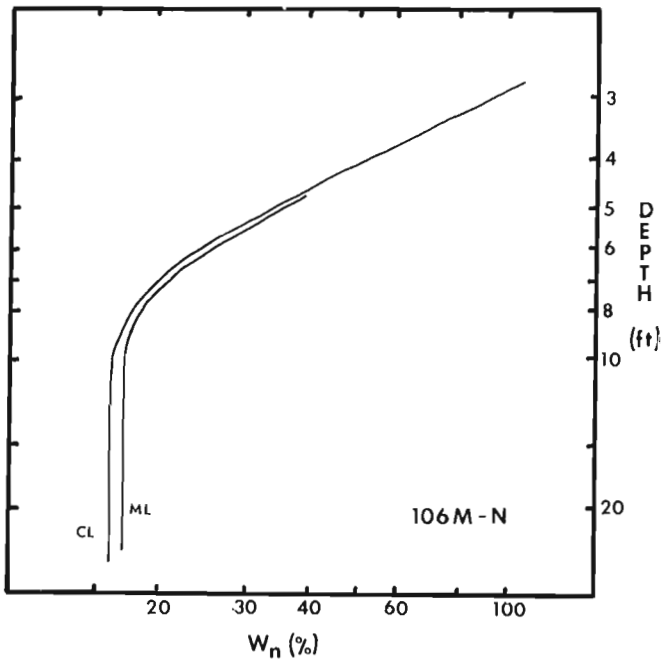

Figure 2. Natural soil moisture vs. depth below surface for various fine grained soil types (Fort McPherson-Arctic Red River 106 M and N).

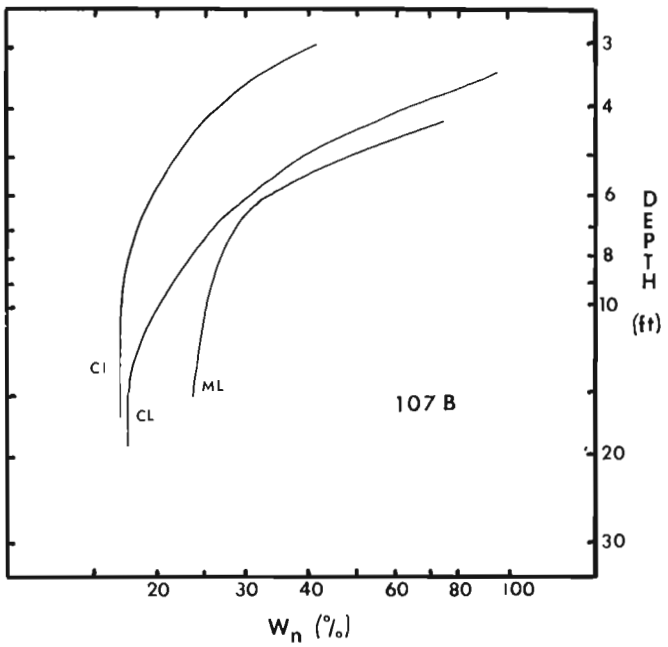

Figure 3. Natural soil moisture vs. depth below surface for various fine grained soil types (Aklavik 107 B),

soils. This may reflect the depth to which surface thawing affects soil moisture. Active layer thicknesses at their summer maximums extend to about half the depth of the observed inflection points for each area. The northernmost area, 107 B, has shallow inflection points consistent with shallow thaw depths in this more northern area.

All curves show an exponential rise in moisture towards the surface. This is to be expected in a permafrost environment where moisture penetration into the soil is restricted by ice in soil voids and in addition, is held at or near the surface by the vegetation mat.

Refinement of the moisture depth plots by carefully selecting data from similar moisture environments and by using a more rigorous soil classification would be useful. The information so derived would be extremely useful in calculations of estimates for thaw settlement and related foundation design calculations in the Mackenzie Valley.

References

Lawrence, D.E.

1974a: Geological review of geotechnical data Mackenzie Valley; *in* Report of Activities, Part A, Geol. Surv. Can., Paper 74-1, Pt. A, p. 281.

1974b: Geological review of geotechnical data Mackenzie Valley; prepared for Mackenzie Highway Environmental Working Group, Dept. of Indian and Northern Affairs, 63 p.

1974c: Mackenzie Valley Geotechnical Data Bank; *in* computer use in projects of the Geological Survey of Canada, T. Gordon and W.W. Hutchison (eds.), Geol. Surv. Can., Paper 74-60, 100 p.

43. GROUNDWATER FLOW IN THE PERMAFROST ACTIVE LAYER, INUVIK, N.W.T.

Project 690054

A. Lissey[1]
Terrain Sciences Division

In September 1972 an experiment was begun at Inuvik, N.W.T. to determine the feasibility of measuring the rate and direction of groundwater flow through the permafrost active layer using very shallow piezometers installed in a heavily bulldozed test plot (Heginbottom, 1973). The piezometers were installed in three nests of ten each, on a site sloping southwards at about 7 per cent. Each piezometer in a nest was screened at a different depth, with the vertical distance between screens set at 10 cm and the deepest piezometer within each nest completed at 100 cm. It was found that the use of such piezometers is a suitable method of measuring groundwater movement within the permafrost active layer.

Falling head tests performed on seven piezometers shortly after installation were analyzed by the basic time lag method, assuming isotropic conditions (Hvorslev, 1952). The results of the analyses show that the average hydraulic conductivity for peat soils in the test area is 1.45×10^{-3} cm per sec., while for till (mineral) soils it is 3.11×10^{-5} cm per sec.

Weekly measurements of the total hydraulic head in all piezometers were taken during the period September 25, 1972 to November 29, 1972. Readings were discontinued during the winter months, but were resumed on June 8, 1973. Daily measurements were taken until June 19, 1973, followed by weekly readings until October 23, 1973. Evaluation of the hydrographs for 1973 suggests a cycle of events in the groundwater regime of the active layer, with four distinct segments: weeks 21-25, weeks 26-28, weeks 29-40, and week 41 through approximately week 20 of the following year. The characteristics of each phase are illustrated graphically in Figure 1. It must be emphasized that this cycle is typical only for disturbed areas.

Phase 1 (weeks 21-25, 1973) begins with the first spring day recording a mean daily air temperature above freezing. This phase is characterized in the test plot by a continuous rapid thaw and downward movement of the frost table, a slow decline in the elevation of the water table during the first part of the phase, with a more rapid decline towards the end of the phase. Snowmelt and rainfall, primarily on the plot itself, contribute to very rapid recharge during the first part of this phase. This is indicated by sudden rises in the water table corresponding to specific rainfall events. This type of recharge occurs so quickly that no lasting vertically downward head gradients can be established. The overall effect is a thickening of the zone of saturation which, coupled with the rapid thickening of the thawed ground due to the melting of ground ice, results in a slow decline of the water table. It is believed that throughout Phase 1 very little water flows out of or into areas adjacent to the plot because the insulating effects of the undisturbed vegetation cover delay thawing and melting outside the plot. Besides recharge by rainfall tending to raise the water table and downward movement of the frost table tending to lower the water table, the only movement of groundwater affecting the position of the water table during this phase is a lateral transfer of water downslope towards the lower portions of the plot itself. This transfer tends to drain the higher portions of the plot. Without recharge by rainfall within the plot or by groundwater flow out of the adjacent upslope area, this transfer tends to lower the water table in the higher portions of the plot even more rapidly than the rate at which the depth of thaw increases.

Phase 2 (weeks 26-28, 1973) begins on the date on which the water table in the plot attains its lowest elevation due to the decline characteristic of Phase 1. During Phase 2, completion of snowmelt, thawing of the active layer, and groundwater recharge occur in the undisturbed terrain around the plot in a manner similar to that of Phase 1 in the plot itself. The only difference is that the rates of downward movement of both the frost table and the water table in the undisturbed terrain must be considerably slower due to the insulating effects of the surface vegetation mat. Within the plot this phase is characterized by a slightly less rapid downward movement of the frost table and a rapid increase in the elevation of the water table such that the thickness of the zone of saturation increases quickly. This requires more water to flow into the plot than flows out. Inflow is accomplished partly by the commencement of groundwater drainage out of the undisturbed terrain upslope and partly by infiltration within the plot of surface runoff derived from continuing snowmelt in the undisturbed terrain upslope. Outflow from the lower end of the plot is believed to be minimal because the elevation of the frost table in the undisturbed terrain downslope would still be above that of the water table within the lower portion of the plot.

Phase 3 (weeks 29-40, 1973) begins on the date the water table first rises to within 12 cm of the ground surface in the plot, marking the end of the rapid water table rise of Phase 2. Phase 3 is characterized by a relatively slow but continued downward movement of the frost table to a depth of more than 1 m, and by a relatively stable water table position. Except for the slight change in storage within the plot, this requires a state of equilibrium between the amount of water that flows into the plot and the amount that flows out. Inflow during this phase consists of direct recharge by rainfall on the surface of the plot and of groundwater drainage out of the undisturbed terrain upslope. Outflow is believed to consist primarily of groundwater

[1]Department of Geological Sciences, Brock University, St. Catharines, Ontario.

drainage out of the plot which should be possible now because the frost table in the undisturbed terrain downslope should have declined to a level below that of the water table at the lower end of the plot.

Phase 4 (week 40, 1973 to probably week 21, 1974) begins on the first autumn day recording a mean daily air temperature below freezing. This phase is characterized in the plot by a refreezing of the active layer both downwards from the ground surface and upwards from the base of the active layer, and by a very rapid decline in the height of the water table. This requires that more water flow out of the plot than flow in. It is believed that inflow is reduced to a minimum because most of the precipitation occurring during this phase is snow and because any precipitation that could contribute to inflow, either by direct recharge within the plot or by recharge within the undisturbed terrain upslope, cannot penetrate the frozen surface. Outflow, however, would continue unabated until refreezing of the soil downwards from the ground surface merged with soil refreezing upwards from the base of the active layer. Depending on the thickness of the unfrozen ground surface in the undisturbed terrain downslope from the plot, the amount of groundwater influx due to drainage of the undisturbed terrain upslope from the plot, and the permeability of the materials concerned, the plot could be completely drained by this outflow before the active layer is entirely refrozen.

In an earlier report (Heginbottom, 1973) it was thought that the strong, vertically upward head gradient measured in 1972 during this phase of events was indicative of groundwater movement towards the freezing front. The complete 1973 hydrograph casts some doubt on this conclusion, because the situation was not duplicated during the fall of 1973. The 1973 readings should indicate the natural flow conditions more reliably than the 1972 readings because none of the piezometers were subject to any lag effects of vigorous development of falling head tests. Hence, it is now felt that most of the water table decline characteristic of Phase 4 is due to drainage of the soil rather than movement of water towards the freezing front.

The data for this report were obtained partly as a result of investigations carried out under the Environmental-Social Program, Northern Pipelines, Task Force on Northern Oil Development, Government of Canada.

References

Heginbottom, J.A.
1973: Erosion in a permafrost environment; *in* Report of Activities, Part A, Geol. Surv. Can., Paper 73-1, Pt. A, p. 225-226.

Hvorslev, M.J.
1952: Time lag and soil permeability in groundwater observations; U.S. Army Corps Eng., Waterways Experiment Station, Vicksburg, Miss., Bull. 36, 50 p.

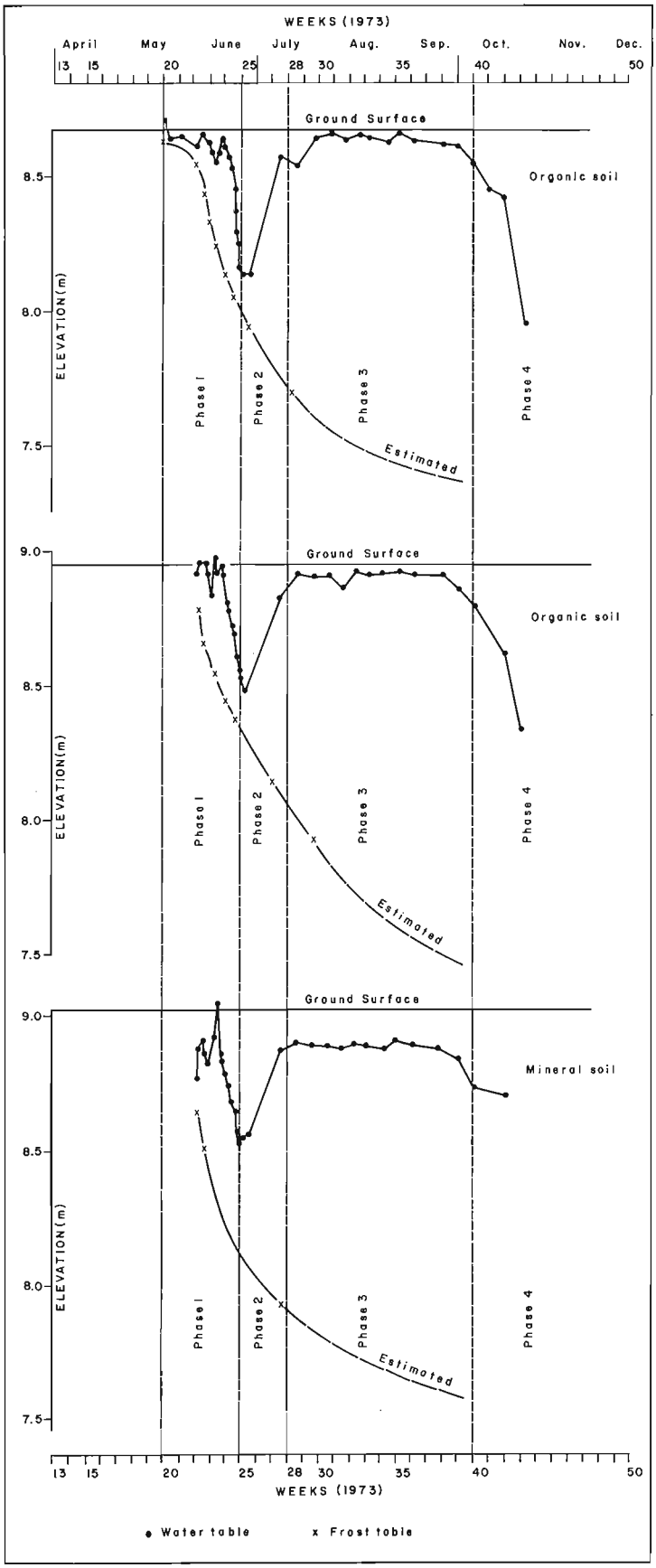

Figure 1 (opposite)

Thickness of zone of saturation at three test plots.

44. TUNDRA FIRES, SOUTHEAST DISTRICT OF KEEWATIN

Project 730013

W. W. Shilts
Terrain Sciences Division

In the summer of 1973 many observations were made of tundra fires during the course of terrain mapping and drift sampling in southeastern District of Keewatin (Fig. 1). It was observed that fires burned in distinctive patterns and at rates controlled by vegetation patterns that are controlled, in turn, by various types of patterned ground. Later examination of ERTS-1 (Earth Resources Technology Satellite) images created in 1973 led to the discovery of several additional burned areas that were not actually observed on the ground (Fig. 2). In view of the observations by Wein (1974, p. 12) that very little is known about tundra fire frequency and that some long-time arctic workers even deny their importance, it is considered timely to add observations of eastern arctic fires to the preliminary list tabulated by Wein (1974) (Table 1).

The period of July-August 1973 was unusually hot and dry in Keewatin (Fig. 9), and communications with exploration company personnel and local residents suggest that May and June were equally hot and dry. By late July much of the tundra vegetation was dry and brown and consequently, easily ignited. Thus, shortly after a violent thunderstorm at 0500 hours on August 2, 1973, at least three major fires were observed burning within a fifty mile radius of Kaminak Lake. At least one fire that was observed was inadvertently started by humas, even after precautions had been taken to prevent it (Table 1).

Patterns and Rates of Burning

Fires were observed to burn through vegetation on all types of terrain common to the tundra in eastern Keewatin, even those with sparse vegetation of low fuel potential. The patterned ground (Shilts, 1974) that characterizes this region, however, exerts a strong influence on the patterns and rates of burning.

Mud boils: Till or marine silty-clay terrains are covered by mud boils (Fig. 3), which are bare or lichen-covered soil patches surrounded by circular turf ridges composed of stones, compressed dead plant matter, and living plants (mostly mosses and shrubs). The circular ridges stand 10 to 30 cm above the mineral soil surface of the mud boil and overlie wedges of damp peaty material to depths of 50 to 100 cm below the mud boil surface. The turf circles and their underlying peaty wedges intersect each other forming a vein-like net of circular mesh. Where fires burn into this type of terrain, which is the most prominent type found in southeastern Keewatin, they burn slowly and intensely through this vegetal net (Fig. 4), destroying the turf ridges and burning 10 to 30 cm into the underlying peaty wedges (Figs. 5, 6). An observed rate of burning was 10 to 20 acres in about 8 days, but this rate may be too low because fire-fighting equipment was used to control it.

Polygonal ground in depressions or valleys: This type of terrain is generally wet and covered by a relatively luxuriant growth of grasses, sedges, and mosses which may be growing on peat from 25 cm to > 1 m in thickness. Although the terrain is damp and growth is luxurious, large quantities of dried grasses from past seasons may form a mat at the base of the new growth. Fire burns rapidly and superficially through this type of terrain, fueled mainly by the dried grass mat. A rate of advance of over one metre per minute was observed against a 10 to 15 km per hour wind where such a fire was burning through a dried lake bed (Fig. 7). These types of fires seem to consume mostly the surface grasses, skipping over matted-down grasses of caribou trails and rarely burning more than a centimetre or two of the damp peaty substrate. When fire does consume the damp peat, however, as around the edges of lakes, spectacular clouds of steam and smoke may be released (Fig. 8).

Rock outcrops, eskers, raised beaches, etc.: Fuel is very scarce on these types of terrains but fires were observed on all of them. Because of the patchiness of the vegetation, however, fires rarely spread for any distance through such areas and are not likely to originate in them as to be spread to them from major fires in adjacent mud boil covered or polygonal terrain.

Conclusions

No follow-up work has been done on the fires observed during 1973 so that conclusions about their long-term effects on the terrain presently cannot be substantiated. It is suspected, however, that the rapidly burning fires in old lake beds and polygonal ground produce minimal long-term terrain disturbance and usually promote more luxuriant growth in succeeding seasons due to temporarily increased availability of nutrients. The species composition of the plant community undoubtedly changes too, but because the underlying peaty deposits are largely undisturbed, it is thought that effects on the permafrost table are minimal, except, perhaps, immediately after a fire when the black ash cover may absorb more radiation than normal, depressing the permafrost table.

The hot, intense burning of peaty material and live vegetation around the mud boils, however, has potential for long-term disturbance by altering the depth and configuration of the permafrost surface and

Figure 1.

Location of fires observed in summer of 1973. Numbers are keyed to Table 1 where additional details can be found. Temperature-precipitation measurements of Figure 2 were made at the northwest corner of Kaminak Lake, indicated on map.

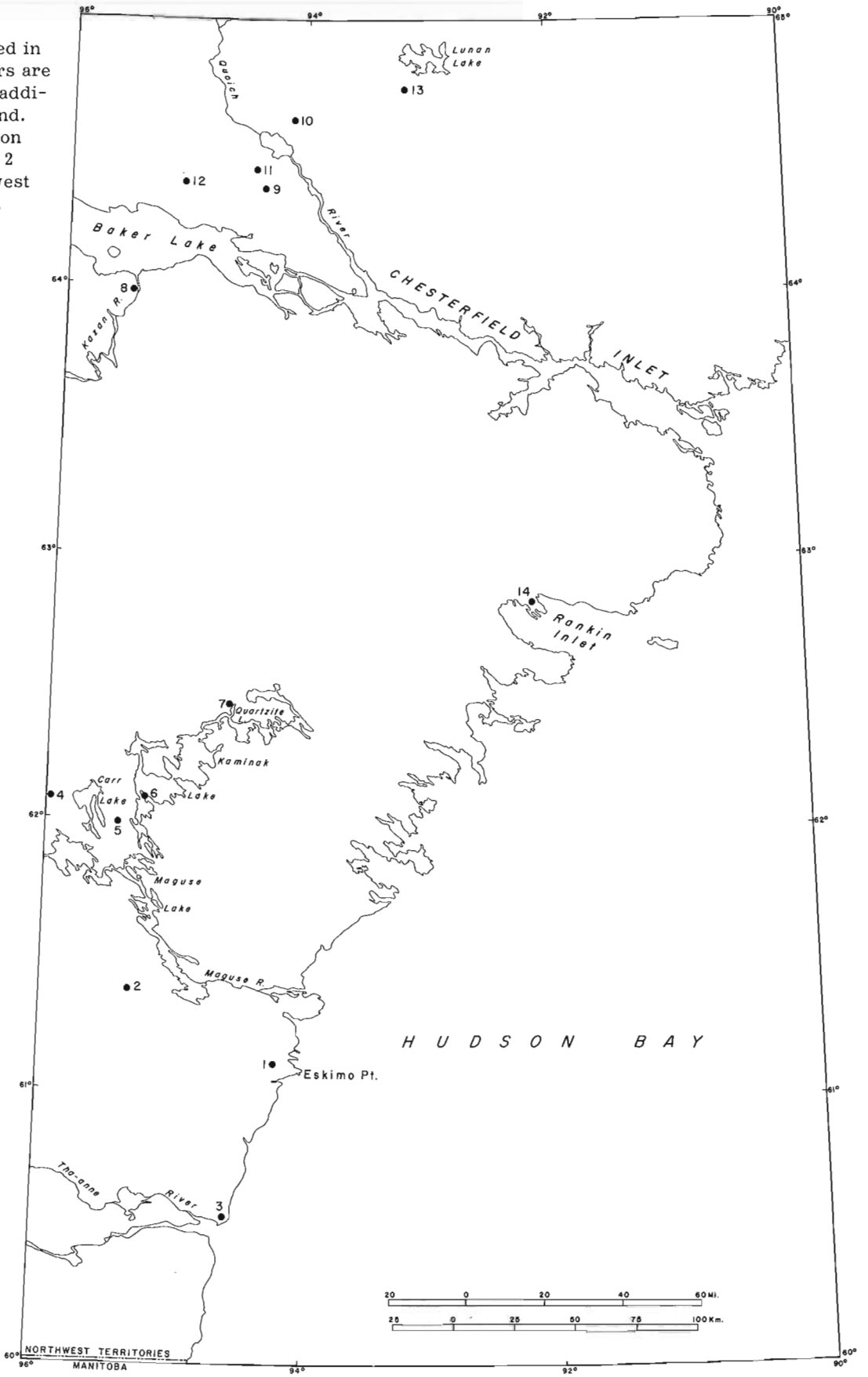

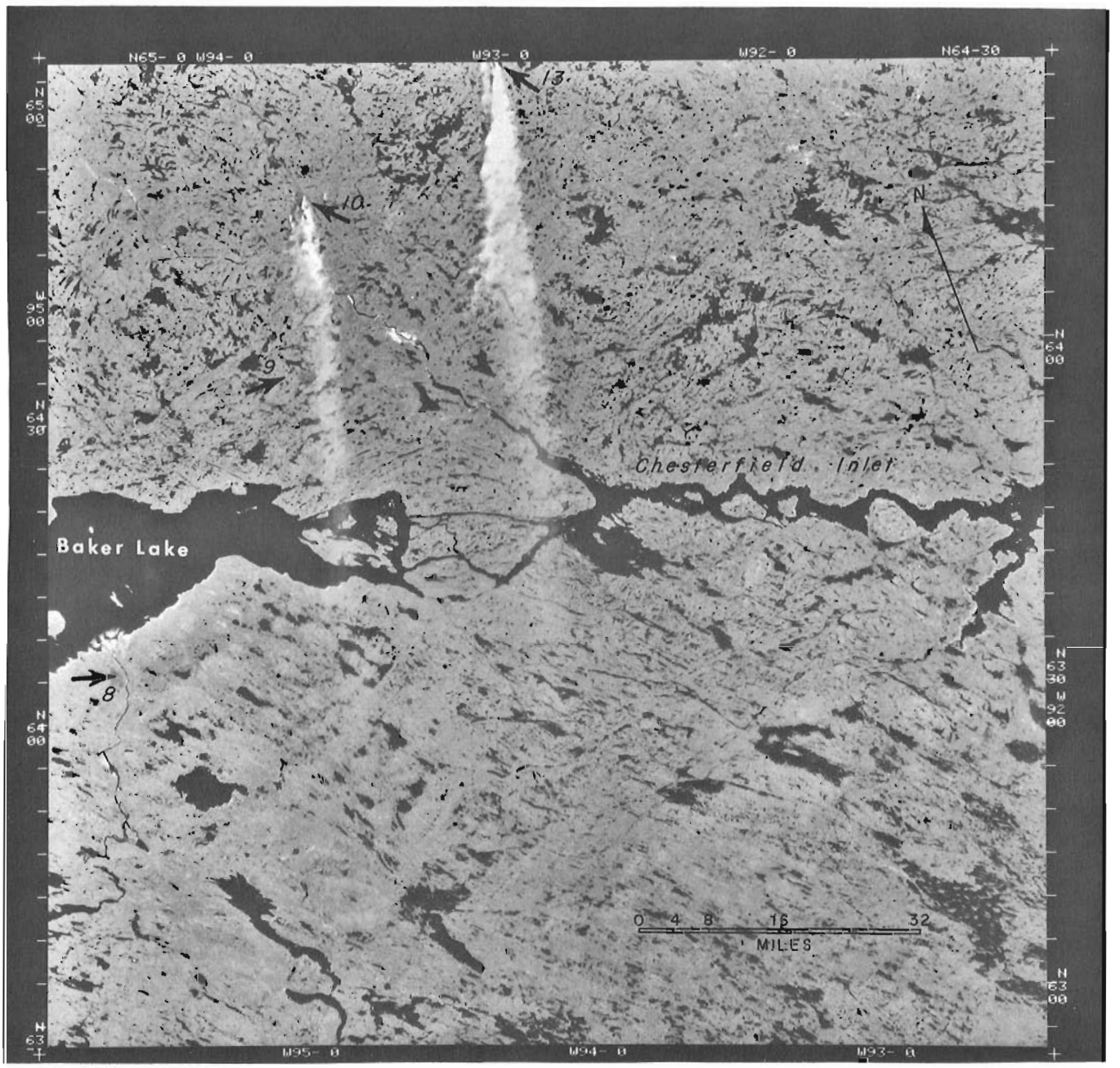

Figure 2. ERTS-1 image showing actively burning and extinguished tundra fires in Baker Lake region of Keewatin, July 29, 1973. Numbers refer to fires described in Table 1 (ERTS-1 image 1371-17121, band 5).

Figure 3.

Aerial view of typical mud boil covered till plain illustrating bare or lichen-covered mineral soil patches within circular turf ridges. Note sharp contact with polygonal terrain underlain by peat over marine sand. Turf circles average 2 to 3 m diameter. (GSC-202321-C).

Figure 4.

Actively burning turf ridge around mud boil. Centre of mud boil is behind burning grass. Smoke in background is from already burned-out turf on other side of mud boil. (GSC-202321-S).

Figure 5.

Ground view of burnt turf hummocks showing relatively untouched mud boil centres. Helicopter is in an unburnt area. (GSC-202446-H).

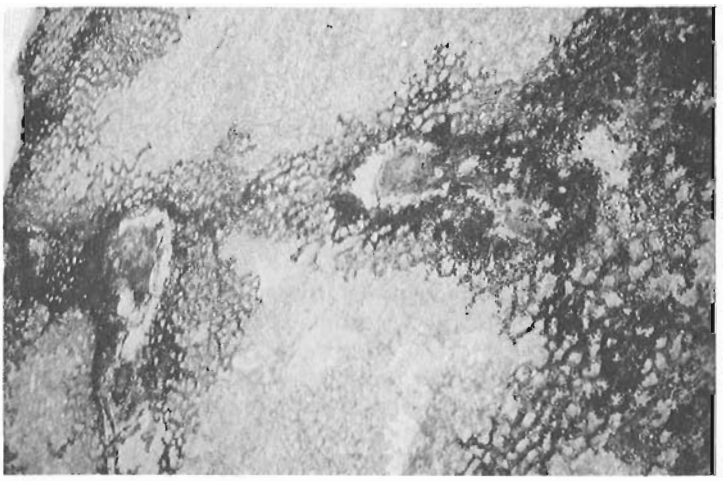

Figure 6.

Typical pattern on burned out mud boils; note centres are untouched by fire. Mud boils are formed almost exclusively on till (as in these photos) but can be found on marine silty clay. (GSC-202445-N).

Figure 7.

Aerial view from 500 feet altitude of lake bed burning. Fire is advancing in lobate form opposite direction of light wind. Lines in black area are probably caribou trails where packed down grass does not burn readily. Pervasive black ash cover is typical of scar in damp, grass-sedge covered area. (GSC-202321-R).

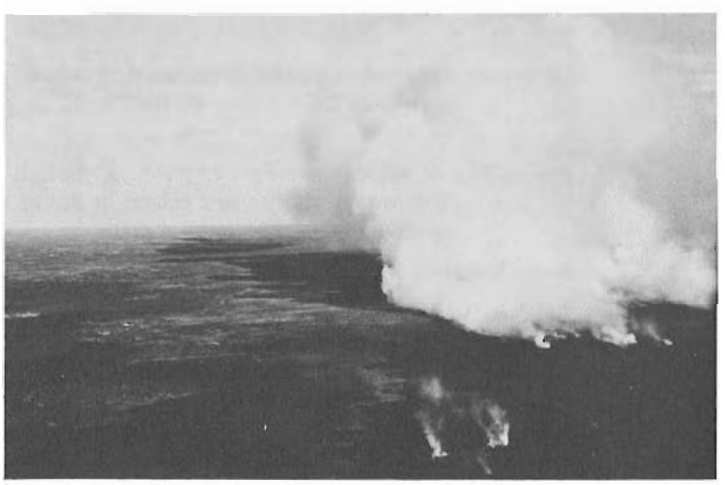

Figure 8.

General view of Fire no. 5, actively burning. "Smoke" is mostly steam created as fire is burning into wet grass-sedge at edge of a lake. Smoke cloud reached altitudes of 1000 to 2000 feet on this day. (GSC-202447-H).

TABLE 1

Listing of tundra fires, 1973

Fire no. 1 - Eskimo Point area

Location: West of Eskimo Point; NTS 55 E

Possibility of relocation: poor to fair

Size: 10 to 50 acres

Terrain: Drumlinized till plain (??)

Vegetation: Unknown

Date: Between May 1 - July 20, 1973

Cause: Unknown

Weather: Dry - hot to cool

Remarks: Seen from air after burnt out, but not marked on map. Settlement manager was aware of fire and may have more details.

Fire no. 2

Location: 12 miles west of south end of Maguse Lake, 48 miles west-northwest of Eskimo Point; NTS 55 E; 61°22'N, 95°26'W

Possibility of relocation: Excellent

Size: Approximately 6 square miles

Terrain/vegetation: Grass-sedge peat on alluvium; dwarf willow/birch and grass in raised rims around mud boils formed on till of drumlinized till plain; most of area is grass-sedge of flat, drained lake bed; dried grasses of lake bed were burning violently with flames 2 to 4 m high at time of observation but dried grass formed mat through which luxuriant cover of grass-sedge was growing. Several types of terrain burned over.

Date: Observed burning fiercely on August 15, 1973; probably extinguished on or about August 18-19 by heavy rain.

Cause: Unknown, probably lightning

Weather: Dry, hot

Remarks: Several colour air and ground photos of fire and surrounding terrain are available. Limits of total burn determined from ERTS-1 images created September 3, 1973. "Dried" lake bed was completely saturated a few centimetres below sediment surface and "quaked" when walked on. Burning was much more rapid in lake bed and alluvial flats than on adjacent mud boil covered till

---

Fire no. 3

Location: North side of mouth of Tha-anne River; NTS 55 D; 60°32'N, 94°35'W

Possibility of relocation: Excellent

Size: Approximately 9 square miles

Terrain/vegetation: Brown Moss, Caribou Moss, grass-sedge on bouldery sand of emerging Tha-anne Delta. Heavy development of low sandy beaches on flat sandy surfaces; brown, moss-like plant in shallow depressions seemed to have burned preferentially. Flood plains of small streams were not burned, unlike Fire no. 2 where burning seemed to have followed flood plains.

Date: Fire was completely out when observed on August 22, 1973. Fire scar evident on ERTS-1 image of July 27, thus area burned before that date - perhaps May to mid-June (ERTS-1, E1405-17012).

Cause: Unknown

Weather: Dry

Remarks: Terrain of the coastal strip is quite different in vegetation associations, sediment type, and morphology from locales of other fires. The area is a recently emerged marine tidal flat.

Fire no. 4

Location: Approximately 6½ miles west of northwest corner of Carr Lake; NTS 65 I; 62°09'N, 96°01'W

Possibility of relocation: Fair to good. Although the fire was visited a few times, it never was accurately recorded on a map.

Size: Estimated at 10 to 20 acres

Terrain/vegetation: Till plain covered by mud boils; fire burned in raised turf ridges around boils; vegetation in ridges is grass-sedge and dwarf willow-birch, various bushes.

Date: Observed burning on July 28, 1973 but probably started about July 24-25, 1973. Probably extinguished by heavy (0.5") rainfall morning of August 2 but possibly extinguished by hoses before that.

Cause: Human; drillers stopped while moving from one site to another to brew tea with blow-torch; ignited turf and thought they had extinguished it but next day fire had spread along turf ridges.

Fire no. 4 (cont.)

Weather: Very dry

Remarks: Fire burned slowly and intensely only along turf network that circles mud boils. Sticky orange ash formed around mud boils but sparse lichens and grasses on mud boil surfaces unburnt. Mud boils left as high mud islands surrounded by low ash moats. Burned area not visible on ERTS-1

Fire no. 5

Location: Between south ends of Carr and Kaminak Lakes; NTS 55 L, 55 E; 62°00'N, 95°25-30'W

Possibility of relocation: Excellent

Size: Approximately 5 square miles

Terrain/vegetaion: This fire burned across almost every type of terrain common in the Kaminak area and through nearly every assemblage of tundra vegetation common to terrain units of the area. Burning was even observed on a sparsely vegetated esker. Great clouds of steam were released when grassy-sedge areas close to lakes were burned. Terrain units in burned area are mud boils, frost-cracked alluvium/lake sediment, marine modified, frost-cracked esker.

Date: Probably started during thunderstorm that occurred around 0500 hours on August 2, 1973. It was observed burning nearly every day thereafter until August 19 when ground observation revealed only a few scattered mud boils smouldering. Probably extinguished between 1800 hours August 17 and 0800 hours August 18 when 0.7" rain fell.

Cause: Probably started by lightning during violent thunderstorm of August 2.

Weather: Dry with traces of rain on August 4, 11, 13, 14, 15, 16.

Remarks: This fire is documented by numerous ground and air photos and is prominently visible on ERTS-1 images from 1973. Some stations were laid out on August 19 to measure mud boil movement in burned and nonburned areas. The fire burned across all units of what could be called a "typical" tundra landscape in the Kaminak Lake region.

Fire no. 6

Location: On peninsula south of large island in southwestern part of Kaminak Lake; NTS 55 L; 62°07'N, 95°20'W

Possibility of relocation: Good to excellent

Fire no. 6 (cont.)

Size: Approximately 1/8 to 1/10 square miles

Terrain/vegetation: Till surface with mud boils and outcrop.

Date: First observed burning on August 13, 1973, and was out by August 19.

Cause: Possibly started by lightning but weather was clear for two days preceding 13th. At time of observation it was thought that the dead calm followed by southerly winds on the 12th may have blown burning debris from Fire no. 5 to this area, causing fire.

Weather: Dry, hot

Remarks: This fire was not visited on ground and details are sketchy.

Fire no. 7

Location: Just north of Quartzite Lake; NTS 55 L; 62°26'N, 95°43'W

Possibility of relocation: Poor to fair

Size: 10 acres (?)

Terrain/vegetation: Very sparse vegetation in bouldery outcrop areas; very little soil

Date: August 1973

Cause: Probably lightning

Weather: Dry

Remarks: This fire was observed once but precise location and details of terrain have been lost.

Fire no. 8

Location: West side of mouth of Kazan River at Baker Lake; NTS 55 M, 56 D; 64°00'N, 95°30'W

Possibility of relocation: Excellent

Size: Approximately 4 square miles

Terrain/vegetation: Fire burning in dwarf birch, lichen moss vegetation on a till plain apparently reworked by marine washing. A.N. Boydell reports that vegetation is growing on a peaty mat ~ 10 cm thick that overlies 65 cm of coarse sand and gravel overlying 10 cm of saturated silty sand to permafrost at depth 75 to 85 cm. Depth to permafrost averages 80 cm in burned and unburned areas at point of observation on July 25, 28, and 31, 1973.

Date: Burning on July 28, but seemed to be mostly out by July 30. Time of starting unknown but after June 24, 1973.

Fire no. 8 (cont.)

Cause: Unknown, probably lightning

Weather: Dry, hot

Remarks: A.N. Boydell visited burnt area three times, made ground observations (ERTS-1, E1426-17165).

Fire no. 9

Location: 21 miles north of Christopher Island (Baker Lake); NTS 56 D; 64°22'N, 94°22'W

Possibility of relocation: Excellent

Size: Approximately 3 square miles

Terrain/vegetation: Not observed; tundra

Date: Observed burning on July 30, 1973 (ERTS-1) but was almost out. Started after June 24.

Cause: Unknown, probably lightning.

Weather: Dry, hot

Remarks: Not observed on ground, identified only on ERTS-1 image (E-1372-17175).

Fire no. 10

Location: North of Quoich River, 40 miles north-northeast of Christopher Island (Baker Lake); NTS 56 D; 64°37'N, 94°10'W

Possibility of relocation: Excellent

Size: 12-15 square miles

Terrain/vegetation: Not observed; tundra

Date: Observed burning fiercely on July 29, 1973; started after June 24, 1973.

Cause: Unknown, probably lightning

Weather: Dry, hot

Remarks: Observed burning on ERTS-1 image (E-1371-17121).

Fire no. 11

Location: 28 miles north of Christopher Island (Baker Lake); NTS 56 D; 64°26'N, 94°25'W

Possibility of relocation: Good-excellent

Size: Approximately 1.5 square miles

Terrain/vegetation: Not observed

Date: Was not burning on July 29, probably started July 30 and burned out sometime between August 1 and August 20, 1973.

Fire no. 11 (cont.)

Cause: Unknown

Weather: Dry, hot

Remarks: Seen on ERTS-1 images (E-1372-17175, E-1426-17165).

Fire no. 12

Location: 25-30 miles northwest of Christopher Island (Baker Lake); NTS 56 D; 64°23'N, 95°05'W

Possibility of Relocation: Excellent

Size: 3-4 square miles

Terrain/vegetation: Unknown

Date: Observed burning (ERTS-1) on July 29, 1973.

Cause: Unknown

Weather: Dry, hot

Remarks: Seen on ERTS-1 image (E-1373-17233).

Fire no. 13

Location: Just south of Lunan Lake; NTS 56 C; 64°45'N, 93°15'W

Possibility of relocation: Excellent

Size: 5-6 square miles

Terrain/vegetation: Unknown; tundra

Date: Observed burning fiercely July 29, 1973 (ERTS-1).

Cause: Unknown

Weather: Dry, hot

Remarks: Seen on ERTS-1 images (E-1370-17062; E-1371-17121).

Fire no. 14

Location: Near Rankin Inlet; NTS 55 K

Possibility of relocation: Unknown

Size: "Several acres"

Terrain/vegetation: Unknown; tundra

Date: July or August, 1973

Cause: Human

Weather: Dry, warm

Remarks: Reported by resident.

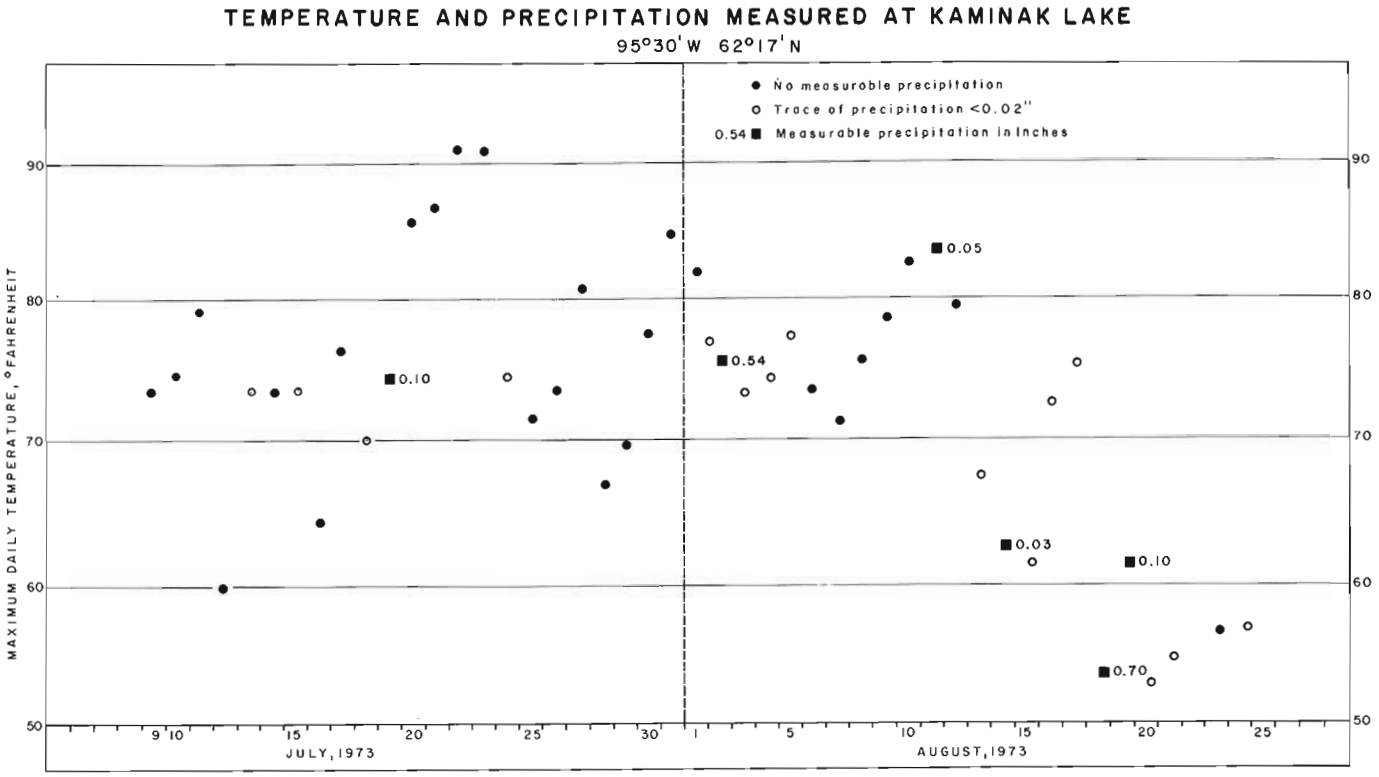

Figure 9. Variations of maximum daily temperatures and daily precipitation at Kaminak Lake, July-August 1973.

by removing rigid support from the sides of the mud islands that occupy the interstices of this vegetation net. The degree of activation of mud boils by removal of this vegetal support is probably proportional to the slope on which the mud boils occur. Mineral material that is trapped in the vegetation circles, which acts as a sort of filter to trap sediment carried by runoff from mud boil centres, may undergo considerable mineralogical alteration as a result of the heat. A sticky grey to orange ash occupied the troughs left by burned-out turf circles. This ash was not sampled but was thought to have a high content of mineral soil.

Finally, it can be concluded that tundra fires are a common phenomenon in this area where upwards of 50 square miles of terrain was burnt in 1973 within the search area of approximately 55 000 square miles. If this amount of burning took place randomly only once in every ten years for the past 4000 years (which can be taken as the average time since most of the area has emerged from glacier or marine water cover), nearly the entire search area would have been burnt over at least once. Thus, it is possible that fire may play a hitherto unsuspectedly important role in influencing periglacial and soil-forming processes in this part of the tundra.

The region described in this paper is adjacent to the possible route of the proposed eastern arctic gas pipeline and will support, in addition, over one hundred persons engaged in uranium and base metal exploration in summer, 1975. It should be emphasized that increased human activity in this terrain is likely to increase the frequency of tundra fires as has been pointed out by Wein (1974, p. 2). Thus, every effort should be made (1) to avoid creating situations where fires are likely to start and (2) to study the possible long-term effects of fires on various terrain types.

References

Wein, R. W.
1974: Recovery of vegetation in Arctic regions after burning; Environmental-Social Comm., Northern Pipelines Task Force on Northern Oil Develop., Rept. No. 74-6, p. 1-41.

Shilts, W. W.
1974: Physical and chemical properties of unconsolidated sediments in permanently frozen terrain, District of Keewatin; *in* Report of Activites, Part A, Geol. Surv. Can., Paper 74-1, Pt. A, p. 229-235.

45. COMPUTER-COMPILED DESCRIPTIONS OF STRATIGRAPHIC SECTIONS

Project 730057

J. D. Aitken and D. A. Carswell[1]
Institute of Sedimentary and Petroleum Geology, Calgary

Introduction

Most active field stratigraphers have in their possession the field notes for a number of described stratigraphic sections as yet unpublished. With few exceptions, these notes are neither sufficiently legible nor sufficiently explicit to be of use to anyone, except through the active intervention of their author; they are valuable but inaccessible components of the total geoscience base.

The principal reason for this situation is that the process of compiling field observations into publishable form is so time-consuming. For instance, the method followed by Aitken over the past decade or so has been as follows:

1. Do the basic arithmetic (Unit number, thickness, height above base, total formation thickness) and enter the figures directly into the field notes in contrasting ink.
2. Dictate the section (in "backward" sequence, top to base) slowly into a dictaphone, emphasizing careful diction, and spelling technical terms where necessary. This step depends absolutely on the services of an experienced geological typist.
3. Have the dictation transcribed in standard format.
4. Edit.
5. Resubmit for final typing as a finished manuscript.

These procedures easily can consume as much of the geologist's office time as the original data-gathering did field time, or even more.

Prior to the field season of 1974, with advice from several computer programmers and active users of computers, Aitken designed a set of machine-processable forms (Figs. 1, 3, 4) for gathering stratigraphic data, and a lexicon (Fig. 2) for use with them. The objectives were threefold:

1. To record data in a more rigorously quantitative form than previously.
2. To stabilize the language of description.
3. To permit machine printout of the described section in standard Geological Survey format.

[1]Geodit, Calgary.

Input Forms

For various reasons, the eighty-column limitation of single punch-cards was accepted in the design of the input forms, i.e., input per card is limited to a total of 80 digits or letters. This appears, *post facto*, to have been a sound decision, although it meant that some kinds of data could not be entered in retrievable form. The forms were printed on 5- x 9¼-inch stock, and punched so as to fit standard loose-leaf binders (the convenient ZIP No. 1069 is used on the outcrop, and the compact, cheaper and safer GSC No. 214-E is used for permanent storage).

The lexicon (Fig. 2) was reproduced on resistant white film for durability. It was tailored especially to the character of the Proterozoic strata that are Aitken's particular field of investigation. Vacant spaces are left for the addition of terms that were unanticipated when the lexicon was written; the sample illustrated shows the terms written-in to date. For projects dealing with markedly different rocks, e.g., Mississippian carbonates or Cretaceous clastics, whole sections of the lexicon may be changed as required, so long as the program subroutines, which serve as "dictionaries", are changed to fit.

Aitken converted to metric measurements at the inception of the Proterozoic study. The present program records thickness in metres but also prints out equivalents in feet (to the nearest whole foot). If measurements are recorded in feet, a simple change in the program is required so that metric equivalents also will be printed out.

The design of the Unit Card and the compilation program "FMLIST" impose a rigid "style" on the description. A given unit of description can contain from one to n lithologies, e.g., it might consist of a% lithology 1, b% lithology 2, and c% lithology 3 (1, 2, 3, etc. always in decreasing order of abundance). At this level, the lithologies are given in simple terms chosen from the list, "Lithology Type", in the lexicon. For further description, each lithology can be designated "as below (above)" (col. 32), or may be fully described, either as a clastic rock (cols. 36 - 48) or a nonclastic rock (cols. 49-65), but not both. A unit of n lithologies requires the completion of n Unit Cards. Each of the n should bear the Section Number (cols. 9-11) and must bear the Unit Number (cols. 12-14), but only the first card for the unit (Lithology No. 1) need bear the formation name and "footage" of the top and base. Abundant room has been left for "Remarks", to include such things as colour, weathering colour, sedimentary structures, etc., codification of which

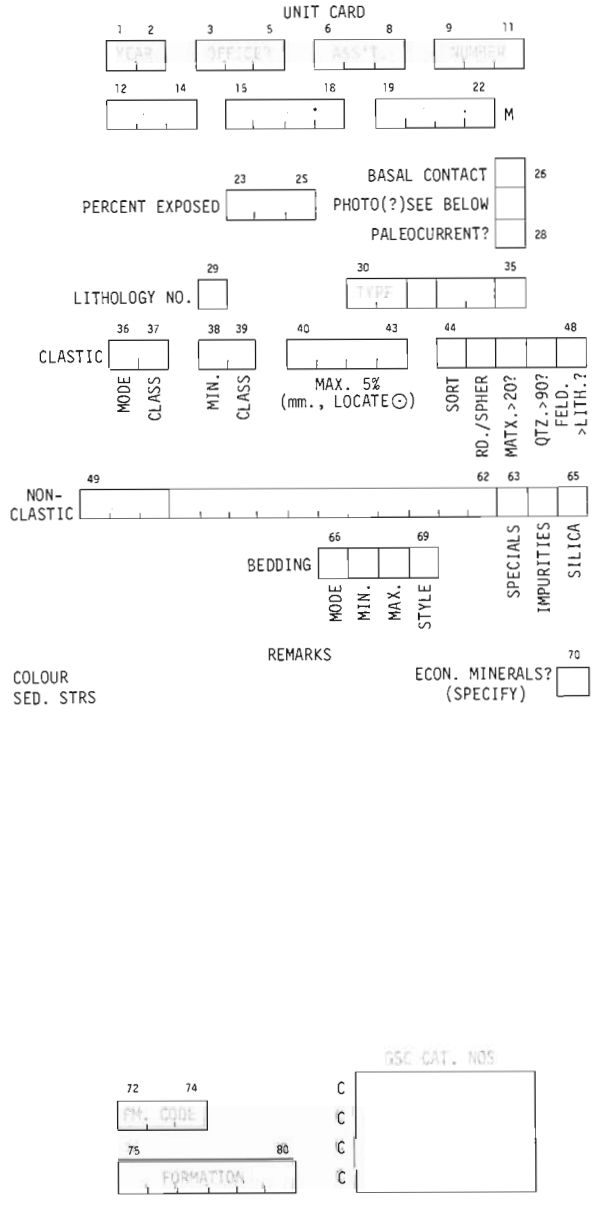

Institute of Sedimentary and Petroleum Geology
3303 - 33rd Street N.W.
Calgary, Alberta

Fig. 1. Unit Card for input of descriptive data (see text)

26 BASAL CONTACT:
0 NOT NOTED
1 EROSIONAL
2 ABRUPT
3 GRADATIONAL, CONTINUOUS
4 GRADATIONAL, MIXED
5 TRIVIAL

30 LITHOLOGY TYPE:

31 CLASTICS:
00 COVERED
01 SHALE
02 MUDSTONE
03 ARGILLITE
04 SLATE
05 SILTSTONE
06 SANDSTONE
07 CONGLOMERATE
08 DIAMICTITE
09 BRECCIA (NON-CARB.)

NONCLASTICS:
11 LIMESTONE
12 DOLOSTONE
13 OTHER CARBONATE
14 CHERT
15 GYPSUM
16 ANHYDRITE
17 IRON-FORMATION
18 CARBONACEOUS ROCK
19

VOLCANICS:
21 ACID FLOW
22 INTERMEDIATE FLOW
23 BASIC FLOW
24 ACID PYROCLASTIC
25 INTERMEDIATE PYROCLASTIC
26 BASIC PYROCLASTIC

INTRUSIVE IGNEOUS:
31 ACID INTRUSIVE
32 INTERMEDIATE
33 BASIC INTRUSIVE

OTHER:
41
42
43

32 "AS BELOW":
BLANK - NO
1 AS BELOW STRATIGRAPHICALLY
2 AS ABOVE

35 SAMPLES:
0 NONE
1 LITHOLOGICAL
2 BIOLOGICAL
3 ORIENTED
4 RADIOMETRIC

36 TO **39** GRADE SCALE CODE:
BB >256 MM BOULDER
LC 128-256 LARGE COBBLE
SC 64-128 SMALL COBBLE
VP 32-64 VERY LARGE PEBBLE
LP 16-32 LARGE PEBBLE
MP 8-16 MEDIUM PEBBLE
SP 4-8 SMALL PEBBLE
GR 2-4 GRANULE
VC 1-2 VERY COARSE SAND
CS 1/2-1 COARSE SAND
MS 1/4-1/2 MEDIUM SAND
FS 1/8-1/4 FINE SAND
VF 1/16-1/8 VERY FINE SAND
ST 1/256-1/16 SILT
CL <1/256 CLAY

44 SORTING:
0 NOT DETERMINED
1 EXCELLENT
2 GOOD
3 FAIR
4 POOR
5 DIAMICT (UNSORTED)

45 ROUNDING, SPHERICITY:
0 NOT DETERMINED
1 EXCELLENT
2 GOOD
3 FAIR
4 POOR
5 SUBANGULAR
6 ANGULAR

46 **47** **48**
BLANK = NO STATEMENT
Y = YES
N = NO

49 TO **51** NONCLASTIC ROCK NAMES:

	LIMESTONE	DOLOMITE, DOLOMITIZED
A. CARBONATES		
	011 CALCILUTITE	511
	012 CALCISILTITE	512
	013 WACKESTONE	513
	021 CALCARENITE-GRAINSTONE	521
	022 CALCARENITE-PACKSTONE	522
	031 CALCIRUDITE-GRAINSTONE	531
	032 CALCIRUDITE-PACKSTONE	532
	033 CALCIRUDITE-WACKESTONE	533
	041 LAMINITE	541
	042 STROMATOLITE LAMINITE	542
	043 STROMATOLITE BED (HEADS)	543
	044 THROMBOLITE BED (HEADS)	544
	045 THROMBOLITIC BED	545
	051 BRECCIA, COLLAPSE	551
	052 BRECCIA, DETRITAL	552
	046 MOLAR TOOTH	546
	CRYSTALLINE CARBONATE, ORIGIN UNDETERMINED	
	061 >16 MM MEGACRYSTALLINE	561
	062 4.0-16 MM VERY COARSELY CRYSTALLINE	562
	063 1.0-4.0 MM COARSELY CRYSTALLINE	563
	064 0.25-1.0 MM MEDIUM CRYSTALLINE	564
	065 0.06-0.25 MM FINELY CRYSTALLINE	565
	066 0.015-0.06 MM VERY FINELY CRYSTALLINE	566
	067 <0.015 MM MICROCRYSTALLINE	567
B. NON-CARBONATES		
	071 GYPSUM	
	072 ANHYDRITE	
	073 HALITE	
	081 IRON-FORMATION	
	082 SILICA-ROCK	

63 "SPECIAL BODIES":
1 OOLITES
2 ONCOLITES
3 STROMATOLITES
4 PELLETS
5 INTRACLASTS

64 IMPURITIES:
1 CLAY 4 CALCAREOUS
2 SILT 5 DOLOMITIC
3 SAND

65 SILICA (IN CARBONATES):
1 CHERT NODULES
2 CHERT BEDS
3 IRREGULAR CHERT MASSES
4 SPONGY SILICIFICATION
5 SELECTIVE SILICIFICATION
6 SILICEOUS

66 BEDDING:
1 <0.3 CM THINLY LAMINATED
2 0.3-1.0 CM LAMINATED
3 1.0-3 CM VERY THIN BEDDED
4 3-10 CM THIN BEDDED
5 10-30 CM MEDIUM BEDDED
6 30-100 CM THICK BEDDED
7 >100 CM VERY THICK BEDDED
8 NON-BEDDED

69 BEDDING STYLE:
1 PLANAR
2 LENTICULAR
3 NODULAR
4 WAVY
5 CRINKLY

Fig. 2. Lexicon, for use with Unit Card

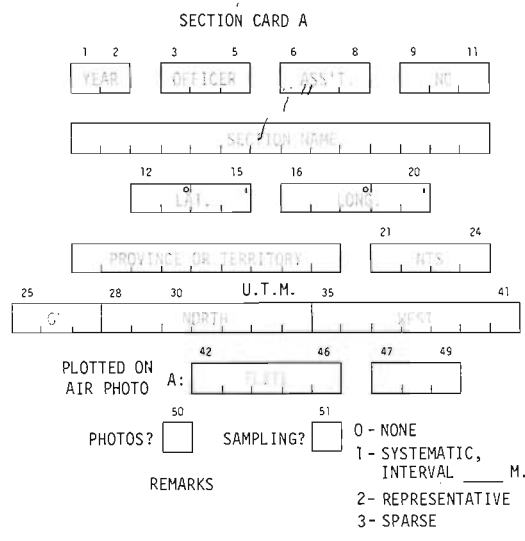

LINE (ROUTE) OF MEASUREMENT:

ATTITUDE OF SECTION

CARD NO. 80 [1]

[ ] ? SECT. PREV. VISITED? (GIVE REF.)

Institute of Sedimentary and Petroleum Geology
3303 - 33rd Street N.W.
Calgary, Alberta

Fig. 3. Section Card A (one per section)

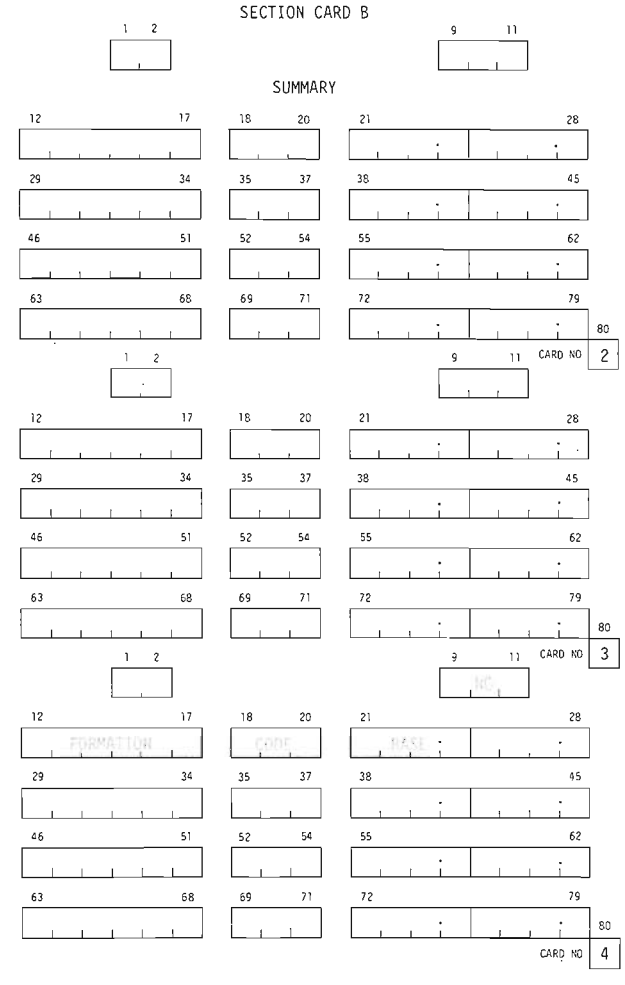

Institute of Sedimentary and Petroleum Geology
3303 - 33rd Street N.W.
Calgary, Alberta

Fig. 4. Section Card B (one per section)

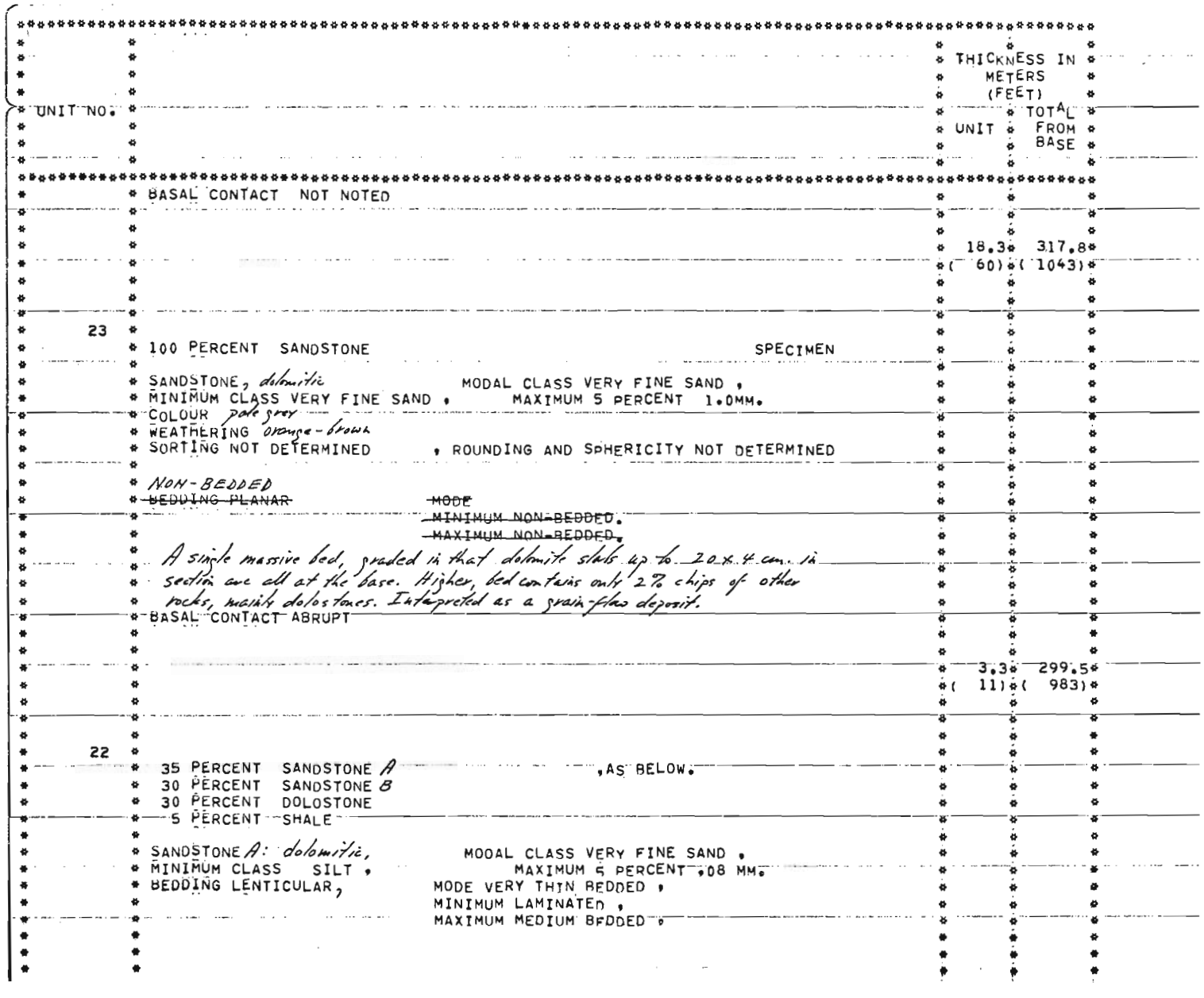

UNIT NO.		THICKNESS IN METERS (FEET) UNIT	TOTAL FROM BASE
	BASAL CONTACT NOT NOTED		
		18.3 (60)	317.8 (1043)
23	100 PERCENT SANDSTONE SPECIMEN		
	SANDSTONE, dolomitic MODAL CLASS VERY FINE SAND ,		
	MINIMUM CLASS VERY FINE SAND , MAXIMUM 5 PERCENT 1.0MM.		
	COLOUR pale grey		
	WEATHERING orange-brown		
	SORTING NOT DETERMINED , ROUNDING AND SPHERICITY NOT DETERMINED		
	NON-BEDDED		
	~~BEDDING PLANAR~~ ~~MODE~~		
	~~MINIMUM NON-BEDDED.~~		
	~~MAXIMUM NON-BEDDED.~~		
	A single massive bed, graded in that dolomite slabs up to 20x4 cm. in section are all at the base. Higher, bed contains only 2% chips of other rocks, mainly dolostones. Interpreted as a grain-flow deposit.		
	BASAL CONTACT ABRUPT		
		3.3 (11)	299.5 (983)
22	35 PERCENT SANDSTONE A ,AS BELOW.		
	30 PERCENT SANDSTONE B		
	30 PERCENT DOLOSTONE		
	5 PERCENT SHALE		
	SANDSTONE A: dolomitic, MODAL CLASS VERY FINE SAND ,		
	MINIMUM CLASS SILT , MAXIMUM 5 PERCENT .08 MM.		
	BEDDING LENTICULAR, MODE VERY THIN BEDDED ,		
	MINIMUM LAMINATED ,		
	MAXIMUM MEDIUM BEDDED .		

Fig. 5. An example of edited machine printout.

Fig. 5. (cont'd).

UNIT NO.		THICKNESS IN METERS (FEET) UNIT	TOTAL FROM BASE
	SANDSTONE B: MODAL CLASS MEDIUM SAND ,		
	MINIMUM CLASS VERY FINE SAND , MAXIMUM 5 PERCENT 0.8 MM,		
	COLOUR pale brownish grey		
	~~WEATHERING~~		
	~~SORTING NOT DETERMINED~~ ~~, ROUNDING AND SPHERICITY NOT DETERMINED~~		
	BEDDING LENTICULAR MODE MEDIUM BEDDED ,		
	MINIMUM THIN BEDDED ,		
	MAXIMUM THICK BEDDED ,		
	Massive.		
	High-angle tangential cross-lamination, in sets 8-25 cm. thick.		
	Dolostone and shale chips abundant. Individual sandstones visibly tapering-out.		
	DOLOSTONE EX-~~CUTITE~~ calcilutite		
	mostly very silty-sandy.		
	~~IMPURITIES , SILT~~ SILICEOUS		
	Prominent molar-tooth structure. Very fine-crystalline.		
	COLOUR medium grey		
	WEATHERING orange		
	BEDDING LENTICULAR MODE MEDIUM BEDDED ,		
	MINIMUM VERY THIN BEDDED ,		
	MAXIMUM THICK BEDDED ,		
	Cross-laminated.		
	SHALE, slaty MODAL CLASS CLAY ,		
	MINIMUM CLASS CLAY , MAXIMUM 5 PERCENT .04 MM.		
	COLOUR black		
	WEATHERING black		
	~~SORTING NOT DETERMINED~~ ~~, ROUNDING AND SPHERICITY NOT DETERMINED~~		
	BEDDING MODE VERY THIN BEDDED ,		
	MINIMUM LAMINATED ,		
	MAXIMUM THIN BEDDED ,		
	Occurs mostly as partings		
	BASAL CONTACT EROSIONAL		
		9.7 (32)	296.2 (972)

would lead to a clumsy and inevitably incomplete lexicon and exceed the self-imposed 80-column limit. Use of the Unit Card is explained in the Appendix.

In addition to the stack of Unit Cards that describe the section, one Section Card A and one Section Card B are required per section. These provide data on location and sampling and a summary of the formations encountered and their thickness and bounding "footages" (recorded thicknesses increase continuously and cumulatively from base to top of section); they thus contain the information printed out as the head block for the section.

The system provides for the measurement, under a single section number, of up to 999.9 m of strata comprising up to 12 formations or informal units.

Field Test

The input documents were tested by using them to record data on five stratigraphic sections measured and described during July, 1974. Progress was slow during the first two days, while the correct habits were being learned and the codes for the various parameters memorized through use. Once familiarity with the system had been acquired, the rate of progress (metres of strata described per working day) did not exceed about 60 per cent of Aitken's former rate while taking unstructured notes. The time penalty is by no means entirely attributable to the requirements of the format, because the description was detailed and highly quantified. Furthermore, the procedure creates a data-bank that is accessible by computer, thus making possible kinds of data analysis that were impractical before.

The Program

The program, identified as FMLIST, is written in Fortran IV for a C.D.C. 6400 with Extended Core Storage (E.C.S.). All of the data cards are read in and written out to E.C.S., and the need for sorting is thus eliminated. During this pass, all the unit thicknesses and formation-thicknesses are calculated. At the end of each formation, all of the thicknesses as well as the access keys for individual units are also stored in E.C.S. Only the header cards and a 36-word pointer list are retained in memory as well as the working storage areas. The program currently runs at 25 000 octal words of Central Memory (or 10 752 decimal words). The E.C.S. size can be computed for each run at approximately 10 words per card.

The present limitations of the program are set as 12 formations, 100 units and 10 lithologies, giving a possible maximum of 12 000 data cards per job. Each of these limitations could be extended easily with only minor program modifications to enlarge the scratch storage. This would of course increase the Central Memory requirement. The maximum possible number of data cards per job at this installation is just over 20 000 cards due to the limit of E.C.S. available. The Geodigit installation has 250 000 words of E.C.S. some of which is used by the system, leaving just over 200 000 (decimal) words available.

If changes were required in the dictionary definitions, these could be keyed to the individual officer's designation with the sets of dictionaries written as overlays. This would allow many dictionary sets to be available but no increase in Central Memory or E.C.S. storage requirements.

As an example of the run costs, for a card deck of 106 cards (7 system control cards, and 99 data cards), the cost was $10.65 or about $0.108 for each of the 99 data cards. The costs will vary slightly depending on the amount of print to be generated but 11 cents per card would be a good average to use as a guide.

The capital cost of the program for analyst time and computer time was under $1500.

Initial Results

Following de-bugging of the program and modification of the printout format as suggested by several early trials, the five stratigraphic sections described using the machine-input cards were machine-compiled with complete success.

The printout (Fig. 5) is open-spaced to permit editing and additions, as illustrated. Editing consists of reviewing each Unit Card against the printout, to add by hand details such as colouring, sedimentary structures, and GSC catalogue numbers, to complete abbreviated formation names, and to delete non-significant printout. An example of the latter would be a mudstone or siltstone for which blanks in Columns 44 and 45 would be printed out as "sorting (roundness/sphericity) not determined". Additions and deletions are made directly on the printout, which then serves as the copy for final typing for publication, or as a document that can be read by any potential user.

We can recommend the FMLIST system to any field stratigrapher who is willing to accept a modest sacrifice of time at the outcrop in order to acquire quantified data that can be easily compiled quickly and into formal descriptions of stratigraphic sections.

Appendix

Explanation of the Unit Card

1. Numbers appended to the "boxes" are the Column Numbers; they indicate the punch-card column under which the punch-card operator will enter the digit or letter in the "box".
2. Columns 1-11. Section or station designation in standard form: Year (75); Officer Identifier (-AC, BAA, etc.) in cols. 3-5; Assistant's Initials in cols. 6-8 (only if the assistant is the responsible geologist); Number (cumulative from 001 in each calendar year).
3. Columns 12-14. Number of the unit of description. Each formation commences with Unit 1 at its base.
4. Columns 15-22. Base, top, of unit of description, to nearest 0.1 m. Must not exceed 999.9 m. If section will exceed 999 m, the section number must be changed at the first formation contact below 999 m, and measurement recommenced at zero m.

5. Columns 23-25. Per cent exposed. Option: Lithologies 1 to n may total 100% in a unit that is less than 100% exposed, or "covered" (code 00 in cols. 30, 31) may be treated as a lithology, with a percentage assigned.
6. Column 26. Basal contact (of unit of description). Choose one digit from List 26 of Lexicon.
7. Columns 27, 28. Blank answers "no", 1 answers "yes". Photo roll/exposure number and subject should be entered under "Remarks". A paleocurrent data card has been designed and printed, but no program for printout has been written to date. A positive response indicates that a sample of paleocurrent data has been collected.
8. Column 29. Lithology number. Lithology 1, 2, 3, ... n of the n lithologies that make up the unit of description. Lithology 1 is the most abundant, n the least abundant. The lithology number indicated in col. 29 is the one described in cols. 30 to 70 of the same card.
9. Columns 30, 31. Lithology type, a simple term chosen from List 30, 31 of Lexicon.
10. Column 32. "As described". Enter 1 for "as below", 2 for "as above" (in the stratigraphic sense). An empty box leads on to a full description of the lithology.
11. Columns 33, 34. "%"; enter the percentage of the unit occupied by the lithology identified in col. 29. For 100%, enter 00.
12. Column 35. "Specimen" (sample); chosen one from List 35. Computer will read blank as "none".
13. Columns 36-48. Data on clastic lithology. If a clastic lithology is indicated in cols. 30, 31, the computer will scan cols. 36-48. If a non-clastic lithology code appears in 30, 31, the computer will ignore 36-48 and scan cols. 49-65 instead, for data on a non-clastic lithology.
14. Columns 36-43. Granulometry of clastics. Choose "modal class" and "minimum class" (Wentworth scale) from List "Grade Scale Code" of Lexicon. In cols. 40-43, enter in mm the estimated average particle diameter of the coarsest 5% of the rock. The decimal point must be entered, and occupies one block.

    In silt-grade and finer sediments, grain-size cannot be measured in the field, however, it may be worthwhile to complete 36 to 43 giving your best guess, against the time when you may wish to retrieve a granulometry profile of the section by computer.
15. Columns 44, 45. Sorting, roundness/sphericity. Choose appropriate digit from each of Lists 44, 45.
16. Columns 46, 47, 48. Each of these boxes asks a question:
    - 46 - Is matrix more than 20%?
    - 47 - Is quartz more than 90% (of rock)?
    - 48 - Does feldspar content exceed content of lithic clasts?

    Answer Y for "yes", N for "no". If box is blank, printout will make no statement about these parameters.

    The answers to these three questions permit the assignment of a name to any sandstone, in most classifications.
17. Columns 49-65. Data on nonclastic rocks. See note 13, above.
18. Columns 49-51. "Code". Choose and enter the code for a rock-type chosen from List "Nonclastic Rock Names", of Lexicon. This is mostly for future retrieval purposes, but serves as a check against the following item.
19. Columns 52-62. "Name". Enter the rock name as you wish it to appear in the printout. The choice of names or classifications is unlimited, but must not exceed eleven letters; abbreviation is commonly necessary. The printout will print back precisely what you enter here, provided you use the English alphabet.
20. Columns 63-65. "Special Bodies", impurities, silica. Choose one each from Lists 63 to 65, or leave box blank where appropriate.
21. Columns 66-69. Bedding detail (clastics and nonclastics). Enter modal bed thickness class, minimum bed thickness class, and maximum bed thickness class, coded from List 66, "Bedding". In col. 69, enter bedding "style", coded from List 69.
22. Column 70. "Economic Minerals?". Enter 1 for "Yes", to have computer print "Economic Minerals". Blank will give no response. Mineral name must be entered under "Remarks", to be added to printout by hand.
23. Columns 72-74. "Formation Code". This is for retrieval purposes. It appears that the best solution is for each user to create and keep up-to-date a code designed for his specific project. Geologists dealing with the same stratigraphic units should of course agree among themselves on a common code between them.
24. Columns 75-80. "Formation Name". Enter the formation name, or if that exceeds six letters, an abbreviation, which will have to be completed by hand on the printout. The position of this entry was chosen to facilitate manual scanning of the field notes by riffling the note deck.

DO NOT FORGET COMPUTERESE! Zero is 0
Letter O is Ø
One is 1
i is I
Two is 2
Z is Ƶ

46. EUREKA SOUND FORMATION AT FLAT SOUND, AXEL HEIBERG ISLAND, AND CHRONOLOGY OF THE EUREKAN OROGENY

Project 710003

H. R. Balkwill, R. M. Bustin and W. S. Hopkins, Jr.
Institute of Sedimentary and Petroleum Geology, Calgary

Introduction

Stratigraphic and structural studies of Mesozoic and Tertiary rocks on eastern Axel Heiberg Island and central Ellesmere Island were conducted in July, 1974 (Balkwill and Bustin, 1975). During this program, Bustin measured, sampled, and studied several sections of the Eureka Sound Formation (Troelsen, 1950; Tozer, 1963). Structural and stratigraphic relationships of this sandstone-dominated, Upper Cretaceous, Paleocene and Eocene succession are critical in elucidating the chronology of tectonism during the Eurekan Orogeny (Thorsteinsson and Tozer, 1970, p. 585-586) a major episode of Tertiary uplift, folding and faulting in the eastern part of Sverdrup Basin and environs. A section of Eureka Sound strata along the western shore of Flat Sound (80°12'N; 89°05'W) is near the centre of this structurally disrupted terrane, and provides significant data in this study.

Thorsteinsson and Trettin (1972) compiled the geology of the immediate region of Flat Sound, and Thorsteinsson (1971a, b) published maps for neighboring parts of eastern Axel Heiberg Island. Princess Margaret Arch (Gould and deMille, 1964; Trettin, 1972, p. 134), a northwest-trending uplifted block of Cretaceous and older rocks, forms the dominant structural element of Axel Heiberg Island (Fig. 1b). Northwest-trending Stolz Fault disrupts the eastern flank of the arch. Tertiary rocks immediately east of the fault lie paraconformably, or with regional discordance, on several Mesozoic formations.

Eureka Sound Formation at Flat Sound

About 200 m (660 feet) of well-exposed Eureka Sound strata dip about 50 degrees eastward along the eastern shore of Flat Sound (Figs. 1a, 1b). Basal Eureka Sound sandstone lies paraconformably on dark grey silty shale and grey sandstone which, because of microfaunal content (J. H. Wall, pers. comm., 1974) and stratigraphic position, are tentatively assigned to the lower part of the Awingak Formation. Elsewhere in the eastern part of Sverdrup Basin, rocks in the lower part of the Awingak Formation are probably of Oxfordian age (Tozer, 1970, Fig. X-12). The top of the Eureka Sound section at Flat Sound is the present erosional surface.

Eureka Sound rocks at Flat Sound are similar, lithologically, to the middle and upper parts of a very thick section of Eureka Sound strata near Slidre Fiord, Ellesmere Island (Fig. 1b). They contrast, however, with the lowermost part of the latter section, which is gradational upward from marine, black Kanguk Formation shale (Balkwill and Bustin, 1975, Fig. 2). Sedimentary structures, the presence of carbonized logs and thin coal beds, absence of marine faunas, and regional lithofacies indicate that Eureka Sound strata at Flat Sound were deposited on a moderate to low-gradient alluvial plain. Hopkins examined microfloras from the succession (GSC locs. C-34675 to C-34679; Fig. 1a); all of the samples contained abundant and well-preserved, uppermost Paleocene or lower Eocene palynomorphs.

Regional Considerations

From the foregoing evidence, the hiatus beneath Eureka Sound rocks at Flat Sound likely extends from lower Upper Jurassic to upper Paleocene. In nearby parts of eastern Sverdrup basin, as at Slidre Fiord, Ellesmere Island (Thorsteinsson, 1971c), or at Strand Fiord, western Axel Heiberg Island (Thorsteinsson, 1971a), a succession of rocks ranging in thickness from about 1200 m to 3000 m (4000 feet to 10 000 feet) - comprising the upper part of the Awingak Formation, and the Deer Bay, Isachsen, Christopher, Hassel, and Kanguk formations, and marine strata of the lowermost Eureka Sound Formation - lie between lower Awingak strata and Paleocene/Eocene beds. There are no indications in the regional geometry and facies of those formations to suggest significant regional uplift before late Maastrichtian. Thus, the hiatus beneath Eureka Sound rocks at Flat Sound marks a tectonic phase of uplift of the eastern flank of Princess Margaret Arch (Fig. 1b) in latest Cretaceous - early Tertiary time. Structural gradients on the order of 10-20 m/km (several tens of feet per mile) were developed in east-central Axel Heiberg Island as a result of this event. The event is nearly contemporaneous with, and is similar in style, to uplift of Cornwall Arch (Fig. 1b), a northwest-trending, possibly basement-cored regional element in the central part of Sverdrup Basin (Balkwill, 1974).

Uplift and tectonism along Cornwall Arch seems to have ended by middle Eocene, inasmuch as lower or middle Eocene rocks along the crest of the arch are not folded. But the Maastrichtian/late Paleocene phase of uplift along the eastern flank of Princess Margaret Arch was a prelude to a second, widespread, climatic compressional phase, throughout the eastern part of Sverdrup Basin and its environs, which produced large folds and faults in Eocene and older rocks (exemplified by the steeply dipping Eocene rocks at Flat Sound). This was followed by a third, more subdued phase of renewed uplift and local normal faulting of the eastern flank of Princess Margaret Arch, accompanied by syntectonic deposition of coarse clastics (Balkwill and Bustin, 1975).

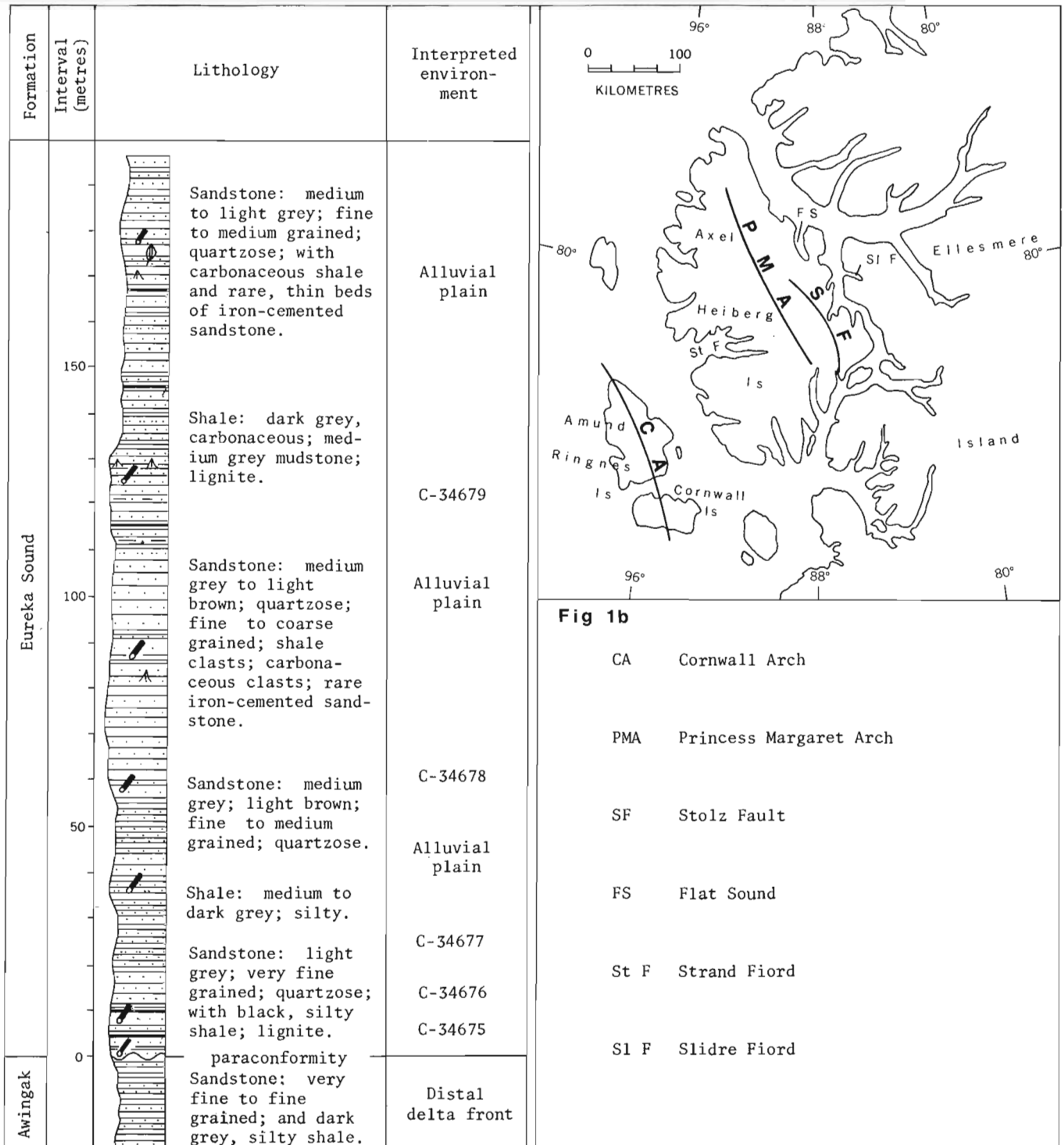

Fig 1a

Fig 1b

CA	Cornwall Arch
PMA	Princess Margaret Arch
SF	Stolz Fault
FS	Flat Sound
St F	Strand Fiord
Sl F	Slidre Fiord

Figure 1a. Eureka Sound Formation at Flat Sound, Axel Heiberg Island (Lat. 80°12'N; Long. 89°05'W).

Figure 1b. Major tectonic elements, eastern Sverdrup Basin.

In summary, three phases of the Eurekan Orogeny can be recognized from structural-stratigraphic relationships in east-central Axel Heiberg Island: a late Maastrichtian/late Paleocene phase of local uplift; a (?) middle Eocene/Oligocene phase of regional compression; and a Miocene/(?)Pliocene phase of local uplift. Distinction of the chronology and kinematics of these phases of the Eurekan Orogeny elsewhere, may be significant for interpretation of plate motions and other regional crustal activity in the Arctic.

References

Balkwill, H.R.
1974: Structure and tectonics of Cornwall Arch, Amund Ringnes and Cornwall Islands, Arctic Archipelago *in* Proceedings Volume, 1973 Symposium on the Geology of the Canadian Arctic; Geol. Assoc. Can./Can. Soc. Pet. Geol., p. 39-62.

Balkwill, H.R. and Bustin, R.M.
1975: Stratigraphic and structural studies, central Ellesmere Island and eastern Axel Heiberg Island, District of Franklin; *in* Report of Activities, April to October 1974, Geol. Surv. Can., Paper 75-1, Pt. A, p. 513-517.

Gould, D.B. and deMille, G.
1964: Piercement structures in the Arctic Island; Bull. Can. Pet. Geol., v. 12, p. 719-753.

Thorsteinsson, R.
1971a: Geology, Strand Fiord, District of Franklin; Geol. Surv. Can., Map 1301A.

Thorsteinsson, R. (cont'd.)
1971b: Geology, Eureka Sound North, District of Franklin; Geol. Surv. Can., Map 1302A.

1971c: Geology, Slidre Fiord, District of Franklin; Geol. Surv. Can., Map 1298A.

Thorsteinsson, R. and Tozer, E.T.
1970: Geology of the Arctic Archipelago *in* Geology and economic minerals of Canada; Douglas, R.J.W., ed., Geol. Surv. Can., Econ. Geol. Rept. No. 1, 5th ed., p. 548-590.

Thorsteinsson, R. and Trettin, H.P.
1972: Geology, Bukken Fiord, District of Franklin; Geol. Surv. Can., Map 1310A.

Tozer, E.T.
1963: Mesozoic and Tertiary stratigraphy, western Ellesmere Island and Axel Heiberg Island, District of Franklin; Geol. Surv. Can., Paper 63-30.

1970: Geology of the Arctic Archipelago: Mesozoic *in* Geology and economic minerals of Canada; Douglas, R.J.W., ed., Geol. Surv. Can., Econ. Geol. Rept. No. 1, 5th ed., p. 574-584.

Trettin, H.P.
1972: The Innuitian Province *in* Variations in tectonic styles in Canada; (Price, R.A. and Douglas, R.J.W., eds.); Geol. Assoc. Can., Spec. Paper no. 11, p. 83-179.

Troelsen, J.C.
1950: Contribution to the geology of northwest Greenland, Ellesmere and Axel Heiberg Islands; Medd. om Grønland, v. 147, no. 7.

UPPER PALEOZOIC CARBONATES AND EVAPORITES IN THE SVERDRUP BASIN, CANADIAN ARCTIC ARCHIPELAGO

Project 720060

Graham R. Davies
Institute of Sedimentary and Petroleum Geology, Calgary

Introduction

During a lecture tour in late November and early December, 1974, two talks were presented at eight universities in eastern Canada and the northeastern United States. As one of these talks introduced some new data on the stratigraphy and sedimentology of upper Paleozoic rocks in the Canadian Arctic Islands, an expanded version of the abstract for that talk is reproduced here, with selected figures and references. Field work for this project was conducted jointly with W. W. Nassichuk (Project 680064).

Summary

The Sverdrup depositional trough (Fig. 1) is an elongate depression superimposed on the folded and eroded rocks of the Franklinian Geosyncline; it is filled with sedimentary rocks ranging in age inclusively from Mississippian to Tertiary. The upper Paleozoic succession is characterized by an association of red beds, evaporites, shelf carbonates, and basinal carbonates and shales (Thorsteinsson, 1974). The Mesozoic and Tertiary section is dominated by sandstone and shale; major gas discoveries in the Arctic Islands are confined to the Mesozoic rocks.

The exposed Carboniferous (Upper Mississippian-Pennsylvanian) to Lower Permian succession in the axial zone of the Sverdrup trough (on Ellesmere Island) is composed from the base upward of fluviomarine red beds of the Borup Fiord Formation, sulphate evaporites of the Otto Fiord Formation, and deep-water cherty carbonates and shales of the Hare Fiord Formation (Fig. 2). The evaporites and basinal sediments grade laterally into shelf carbonates of shallow-water aspect (Nansen Formation), which in turn interfinger with red beds at the depositional margins of the Sverdrup Basin. Spectacular examples of facies changes are exposed along the walls of some fiords (Figs. 3, 4).

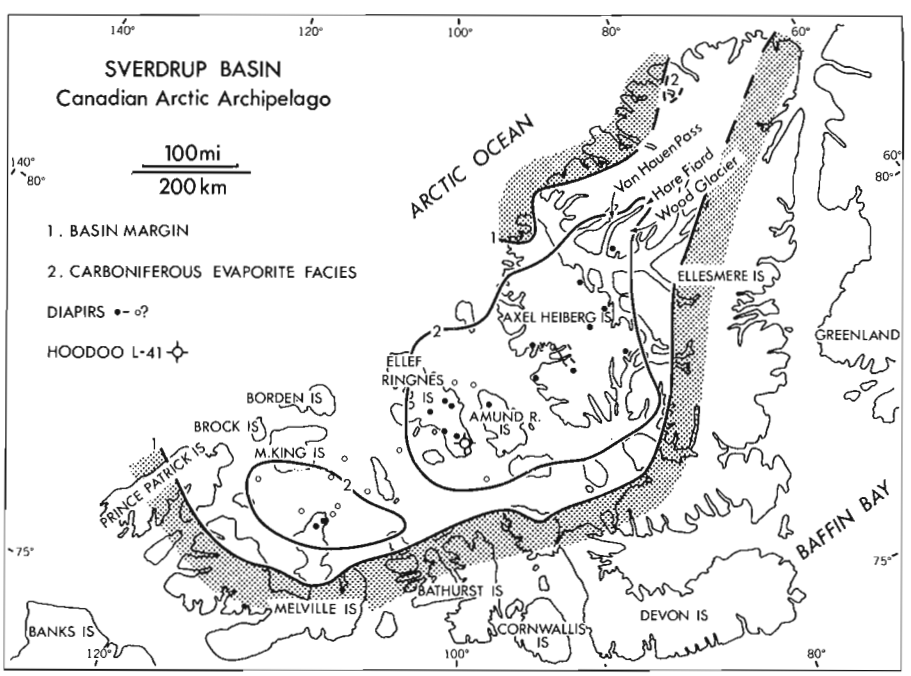

Figure 1.

Localities, boundaries of the Sverdrup Basin, and distribution of Carboniferous Otto Fiord evaporites (modified from Meneley *et al.*, 1974). Major exposures of upper Paleozoic carbonates discussed in this summary are confined to northwestern Axel Heiberg and northwestern Ellesmere islands. Offshore anomalies interpreted as diapirs (O?) are from Plauchut (1971).

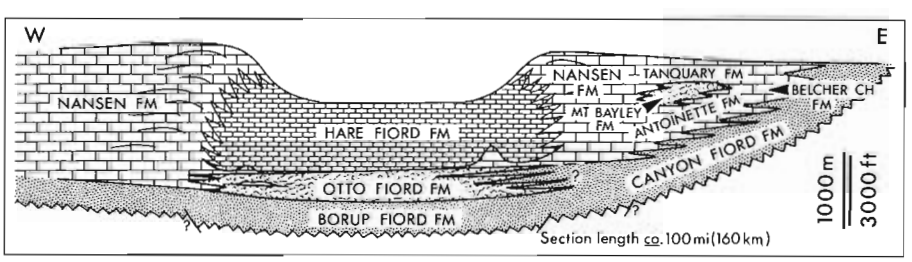

Figure 2.

Schematic restored east-west cross-section across the northern Sverdrup Basin in the vicinity of northeastern Hare Fiord (Fig. 1) on Ellesmere Island (modified from Thorsteinsson, 1974).

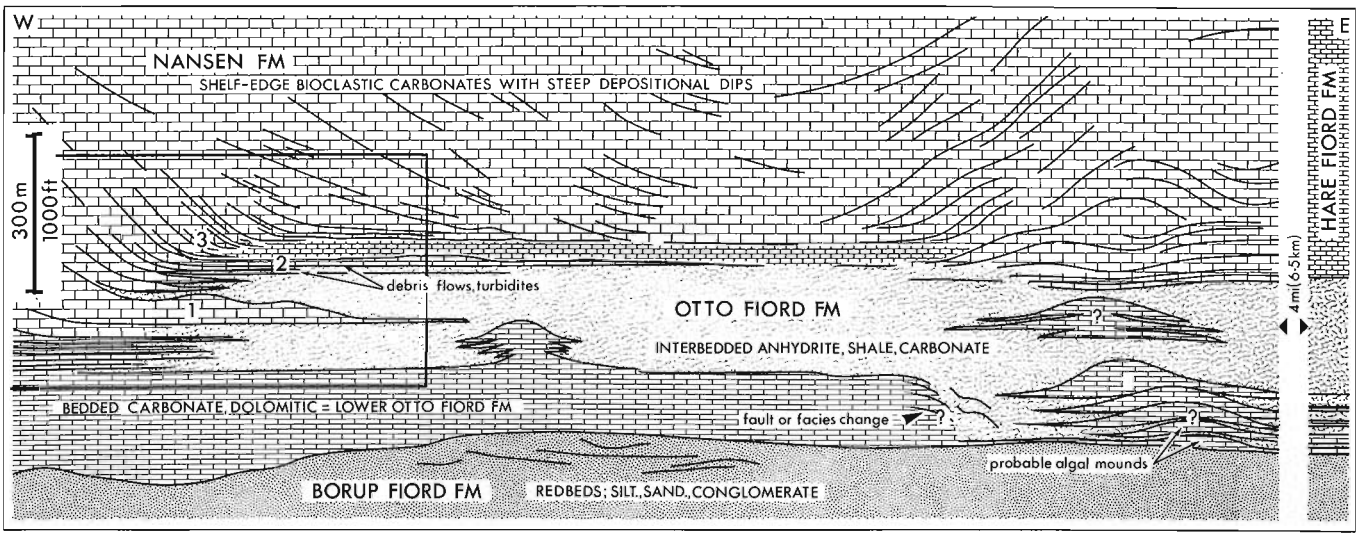

Figure 3. Simplified sketch from colour slides of Otto Fiord anhydrite to Nansen carbonate facies change near the northwestern margin of the central evaporite belt (Fig. 1), along cliffs east of Girty Creek on the north side of eastern Hare Fiord. Lowermost anhydrite beds thin out into horizontally-bedded carbonates (lower left); higher anhydrite beds thin out and abut against flank beds of shelf-edge carbonates, and in part are interbedded with carbonate turbidites and debris flows. As the succession is regressive, the Otto Fiord evaporites here are overlain by a thin unit of Hare Fiord Formation ("basinal" facies) and then a thick mass of Nansen shelf carbonate; note the steep depositional bedding in the Nansen carbonates with reversals of dip reflecting local mounding. A few miles to the east, the Otto Fiord evaporites are overlain directly by Hare Fiord rocks (section at right; *see* Davies, 1974a; Fig. 3A). Geometry of mounds shown at right (?) is interpretive. Block outline at left locates Figure 4.

Figure 4.

Photograph of facies change at western end of Figure 3; measured section located in gully at centre. Note carbonate beds 1, 2, 3 (keyed to Fig. 3), some of which are turbidites and debris flows, that grade (left) into steeply-dipping shelf-edge carbonates. Carbonate unit 1 thins out eastward (right) and its place is taken by bedded anhydrite. For scale, *see* Figure 3.

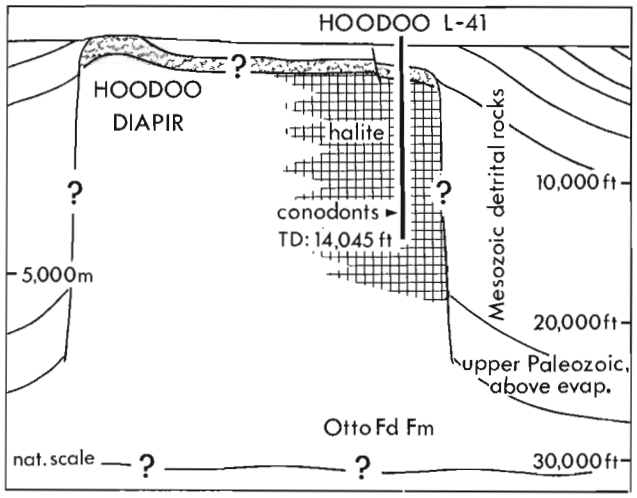

Figure 5.

Schematic cross-section across Hoodoo diapir on Ellef Ringnes Island (Fig. 1) showing relationship to the section in the Hoodoo L-41 (Imperial, Panarctic, Home and others) well. Configuration of diapir is schematic and is not based on geophysical data. Upper Paleozoic conodonts from core at about 12 600 ft (3840 m) establish correlation with the Otto Fiord Formation as the halite source (P. Bender, pers. comm., 1973).

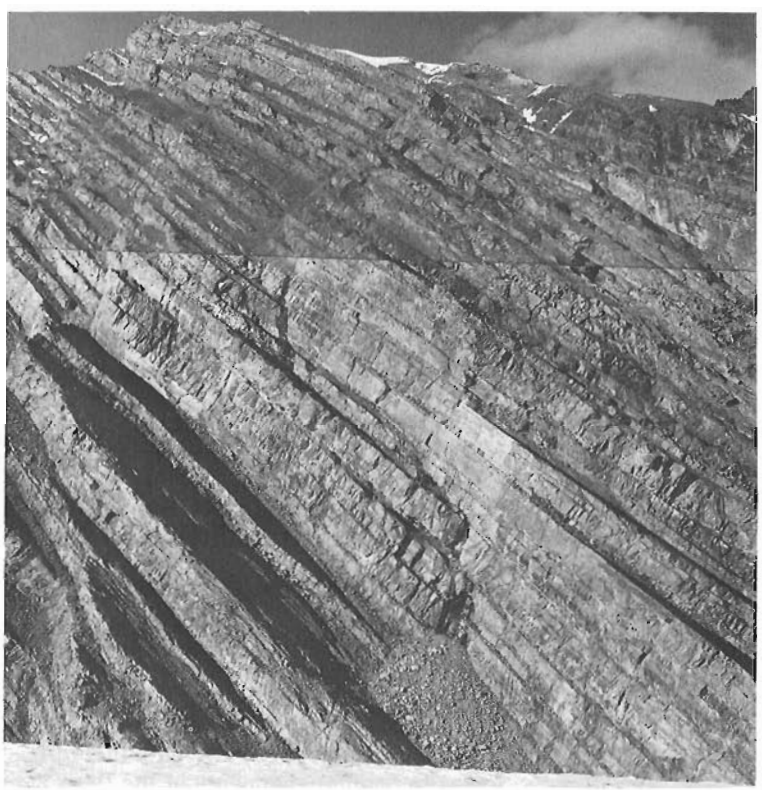

Figure 6.

Regularly-bedded, cyclic shelf carbonates of the Nansen Formation (Pennsylvanian to Lower Permian) near Oobloyah Bay, northwestern Ellesmere Island. Biogenic mounds, common near the outer shelf edge, are absent in this section. Fusulinid wackestones and packstones, and rounded-grain to oolitic grainstones are two common rock types in this section. Many units are dolomitized, enhancing porosity and permeability.

In outcrop on Ellesmere Island, the Upper Mississippian to lower Middle Pennsylvanian Otto Fiord Formation is composed of up to 1500 feet (460 m) of thick cyclic sequences of anhydrite and limestone, and of anhydrite, mudstone, sandstone and limestone (Davies, 1974a; Davies and Nassichuk, in press; and in preparation). Carbonate mounds, characterized by dasycladacean algae, are associated with some cycles (Davies, 1974a, Fig. 3B). The proposed depositional model for the Otto Fiord sediments requires carbonate accumulation during transgression to a deep marine maximum, followed by deposition of anhydrite-halite and prograding coarsening-upward detrital sediments during regression (Davies and Nassichuk, in press). Mosaic anhydrite occurs interbedded between deep-marine carbonates and bedded anhydrite of subaqueous origin – the mosaic fabric formed apparently by early diagenetic replacive and displacive growth of sulphate nodules below the sediment-water interface in a subaqueous hypersaline environment (cf. subaerial or sabkha environments). Sulphur isotope geochemistry of the Otto Fiord anhydrite is discussed in Davies and Krouse (1975a).

Figure 7.

"Waulsortian"-type Pennsylvanian carbonate mounds (light grey) in the Blue Mountains, east of Hare Fiord, looking north-northeast. Mounds are characterized by fenestrate bryozoans with a variety of early cement fabrics. They are overlain by argillaceous carbonates and shales of the Hare Fiord Formation (dark grey, right).

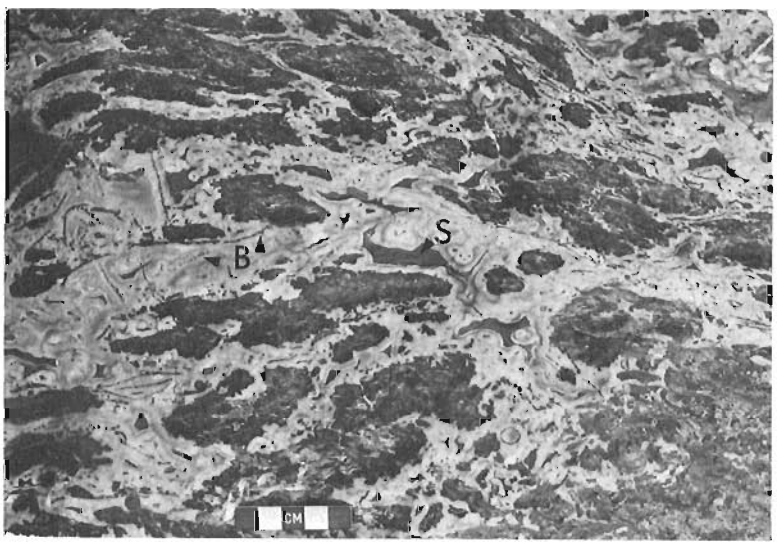

Figure 8.

Fabric of Pennsylvanian "Waulsortian"-type carbonate mound. Fenestrate bryozoan fronds (B) and primary carbonate sediment (irregular dark grey patches) are cemented by multigeneration fibrous calcite (white) of very early, probably submarine, origin (Davies and Krouse, 1975b). Dolomitized late-generation internal sediment (S) fills post-cement pore systems fed from sediment-filled fractures (Davies, 1974b).

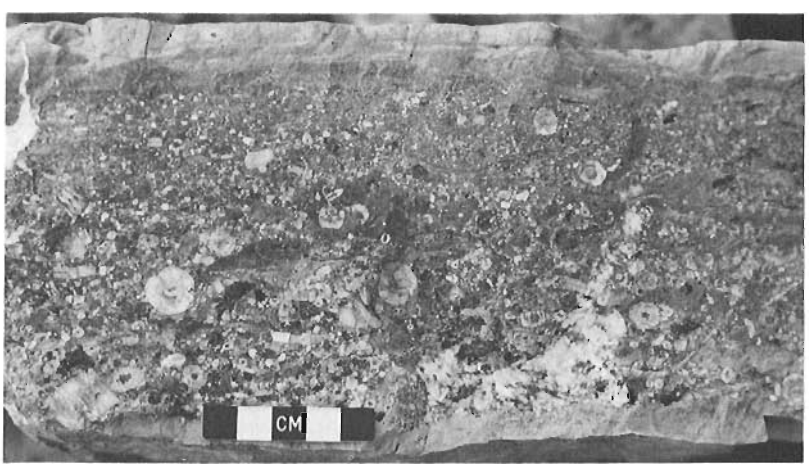

Figure 9.

Graded bed of crinoid debris and carbonate lithoclasts, typical of carbonate turbidites found in basinal sediments of the Hare Fiord Formation near shelf-edge transitions. This example is from the facies change near Girty Creek (Fig. 3, left centre). Mixed microfaunas (conodonts) representing several different ages are found in some of these beds of retransported carbonate.

Recently released well data confirm the presence of a halite facies of the Otto Fiord Formation in the subsurface of the structurally deeper sector of the basin; 12 000 feet (3660 m) of halite were penetrated in the Hoodoo L-41 well drilled on the flank of a diapir on Ellef Ringnes Island (Figs. 1, 5). The Otto Fiord Formation is the source of many diapirs and structural piercements in the axial zone of the Sverdrup Basin (Fig. 1), yet only anhydrite is exposed at the surface.

Figure 10.

Carbonate debris sheet interbedded in thin-bedded cherty carbonates of deep-water aspect in the Hare Fiord Formation, east of van Hauen Pass on Ellesmere Island (Davies and Schmidt, in press). The debris sheets are composed of angular lithoclasts of cemented shallow water bioclastic carbonates of shelf aspect, mixed with lithoclasts of slope and deeper water origin, and often with a spicular argillaceous matrix. Debris unit in foreground is 30 feet (10 m) thick.

The Pennsylvanian to Lower Permian shelf carbonates are well bedded, cyclic, bioclastic and oolitic limestones (Fig. 6), with extensive dolomitization in some areas. Close to the shelf-to-trough (shelf edge) transition, massive organogenic units and mounds are more common. Significant contributors to biostromes and mounds are fenestrate bryozoans (Pennsylvanian; Figs. 7, 8), phylloid algae (Pennsylvanian to Lower Permian) and the hydrozoan? Palaeoaplysina (Lower Permian; Davies and Nassichuk, 1973). Many of these shelf-edge buildups and other carbonate mounds had high primary depositional porosities, now obliterated by several types of calcite cement (Davies and Krouse, 1975b, Figs. 1, 2, 3). The earliest multigeneration cements, preserved as fibrous or radiaxial fibrous calcite, are interpreted on the basis of fabrics, isotopes (Davies and Krouse, 1975b) and elemental composition, to have been early submarine cements (Davies, 1974b), analogous to cements found recently in modern coralgal reefs. Steep flank beds of shelf-edge build-ups and mounds contain clasts cemented by the same type of calcite.

Where the shelf-edge to basin transition is abrupt, considerable topographic relief probably existed between the shelf and the basin floor. Graded clastic carbonates (turbidites, Fig. 9), debris flows (Fig. 10), and large displaced blocks of carbonate of shallow water origin found interbedded with basinal cherty limestones of the Hare Fiord Formation, probably were derived from these high-relief shelf edges (Davies and Schmidt, in press).

Some exposures of well-bedded cherty (spicular) carbonates and shales of Hare Fiord type, representing a deep-water shelf-slope facies in the axial zone of the basin, contain very large penecontemporaneous structures, interpreted to be gravity-induced submarine slides that have removed catastrophically up to 400 feet (120 m) of section (Davies, 1975; Davies and Nassichuk, 1975). The slide scars subsequently were infilled with cherty limestones and shales in units which thicken into the scar. Apparently similar structures are found in slope carbonate facies elsewhere.

High relief, aridity, and lack of vegetation combine to make many northern Arctic exposures of carbonates and evaporites classic "textbook" illustrations of megastructures and facies relationships.

References

Davies, G. R.

1974a: Paleozoic evaporites of the Canadian Arctic Archipelago *in* Fourth symposium on salt, Houston, 1973; Coogan, A. H., ed.; N. Ohio Geol. Soc., v. 1, p. 119-125.

1974b: Submarine cementation, fracturing, and internal sedimentation in Pennsylvanian-Permian carbonate build-ups, Arctic Archipelago; Am. Assoc. Pet. Geol., Ann. Meeting, Abs., v. 1, p. 25.

1975: Penecontemporaneous slide and fill megastructures in upper Paleozoic slope-facies carbonates, Arctic Canada; Am. Assoc. Pet. Geol., Ann. Meeting, Abs. Vol.

Davies, G. R. and Krouse, H. R.

1975a: Sulphur isotope composition of Paleozoic sulphate evaporites, Arctic Archipelago; *in* Report of Activities, Pt. B, Geol. Surv. Can., Paper 75-1, Pt. B, p. 221

Davies, G. R. and Krouse, H. R. (cont'd.)
1975b: Carbon and oxygen isotopic composition of upper Paleozoic carbonate cements, Arctic Archipelago - preliminary data and interpretation; *in* Report of Activities, Pt. B, Geol. Surv. Can., Paper 75-1, Pt. B, p. 221.

Davies, G. R. and Nassichuk, W. W.
1973: The hydrozoan? Palaeoaplysina from the upper Paleozoic of Ellesmere Island, Arctic Canada; J. Paleontol., v. 47, no. 2, p. 251-265.

1975: Gravity-slide megastructures in deep-water carbonates of the Hare Fiord Formation, upper Paleozoic of Ellesmere Island; *in* Report of Activities, Pt. B, Geol. Surv. Can., Paper 75-1, Pt. B, p. 227.

Davies, G. R. and Schmidt, V.
Gravity-displaced shallow-water carbonate sediments in Pennsylvanian to Permian basinal facies of the Sverdrup Basin, Arctic Archipelago; Bull. Can. Pet. Geol. (in press)

Meneley, R. A., Henao, D. and Merritt, R. K.
1974: The northwest margin of the Sverdrup Basin; Can. Soc. Pet. Geol., Symp. on Canada's Continental Margins, Abs., p. 74.

Plauchut, B. P.
1971: Geology of the Sverdrup Basin; Bull. Can. Pet. Geol., v. 19, p. 659-679.

Thorsteinsson, R.
1974: Carboniferous and Permian stratigraphy of Axel Heiberg Island and western Ellesmere Island, Canadian Arctic Archipelago; Geol. Surv. Can., Bull. 224.

48. CARBON AND OXYGEN ISOTOPIC COMPOSITION OF LATE PALEOZOIC CALCITE CEMENTS, CANADIAN ARCTIC ARCHIPELAGO – PRELIMINARY RESULTS AND INTERPRETATION

Project 720060

Graham R. Davies and H. R. Krouse[1]
Institute of Sedimentary and Petroleum Geology, Calgary

Introduction

The Pennsylvanian to Lower Permian stratigraphic succession in the Sverdrup Basin of the Arctic Archipelago is dominated by a carbonate shelf facies (Nansen Formation) and a coeval carbonate and shale trough facies (Hare Fiord Formation; Thorsteinsson, 1974). Biogenic carbonate mounds and lenses are found within the Nansen shelf facies, particularly towards the outer shelf edge; these mounds are characterized by an abundance of fenestrate bryozoans (Middle Pennsylvanian), phylloid algae (Late Pennsylvanian to Early Permian) and the enigmatic organism Palaeoaplysina (latest Pennsylvanian to Early Permian; Davies and Nassichuk, 1973a, 1973b). Spectacular bryozoan mounds or "reefs" ("Waulsortian" facies) also are found at the base of the Hare Fiord Formation at a number of localities. The biogenic carbonates, exposed best on northwestern Ellesmere Island, often contain fabrics indicative of extremely high primary depositional porosities of shelter type (Figs. 1, 2, 3). Their potential as reservoir rocks, however, has been destroyed by extensive cementation and infilling of the primary pore systems by early diagenetic cements, preserved now as fibrous and radiaxial fibrous (Bathurst, 1971; Kendall and Tucker, 1973) calcite, and by late sparry calcite. Examination of large polished rock slabs, thin sections and stained peels from the various mound types suggests that many of the fibrous calcite cements were precipitated as very early, multigeneration isopachous layers in irregular, interconnected cavity systems, without pendant or other geopetal precipitational fabrics indicative of vadose (partly air-filled pore-space) conditions. Cement generations often predate or alternate with layers of internal carbonate sediment containing marine microorganisms. In total, fabric relationships indicate a very early (penecontemporaneous) submarine origin for much of the fibrous calcite cement or its precursor (Davies, 1974).

The validity of this interpretation is enhanced by the recognition, particularly within the last five years, of early submarine cementation as a normal and pervasive process in modern porous coralgal reefs (Shinn, 1971; Ginsburg and Schroeder, 1973; Ginsburg and James, 1973; Goreau and Land, 1974). Cement fabrics and cement-internal sediment relationships in these modern reefs serve as analogs and process models for many of the late Paleozoic cements in Arctic carbonates.

Additional insight into the origin of carbonate cements may be gained by chemical and isotopic analyses. Elemental analyses by electron microprobe have provided some clues to origin; these analyses, near completion, will not be discussed here. Carbon and oxygen isotope analyses add support to the interpretation of early submarine origin (that is, precipitation from marine water) for the cements. This paper is a preliminary report and discussion of $\delta^{13}C$ and $\delta^{18}O$ isotope data from the Arctic Paleozoic cements and related carbonate deposits. A complete documentation of all aspects of the cement fabrics, composition and isotope geochemistry is in preparation (Davies, Ghent, Krouse, in prep.).

Carbon and oxygen isotopes in carbonate rocks

Carbon has two stable isotopes, ^{12}C ("light" isotope) with an abundance of 98.9%, and ^{13}C ("heavy", 1.1%). Oxygen has three stable isotopes, ^{16}O ("lightest", 99.7%), ^{17}O (0.04%), ^{18}O ("heaviest", 0.2%). The $^{13}C/^{12}C$ and $^{18}O/^{16}O$ ratios in carbonate rocks are measured by mass spectrometer using CO_2 gas generated from the carbonate sample by reaction with phosphoric acid. Most of the 50 paired carbon-oxygen analyses reported in this paper were run in the Stable Isotope Laboratory of the Department of Physics, University of Calgary (others by Marathon Oil Co., *see* Acknowledgments). Carbon and oxygen isotope ratios in this paper are expressed as per mil deviation from the ratio in the PDB standard (Cretaceous Peedee Formation belemnite):

$$\delta \text{ (delta) } ^{13}C \text{ or } ^{18}O‰ = \frac{R \text{ (sample)} - R \text{ (standard)}}{R \text{ (standard)}} \times 10^3$$

where R is the isotope ratio for either element. (Oxygen isotope data elsewhere may be expressed relative to Standard Mean Ocean Water (SMOW); $\delta^{18}O$ SMOW = ($\delta^{18}O$ PDB x 1.03) + 29.5.)

It is beyond the intent of this report to consider the variables of initial isotopic composition of waters, biogenic and physical fractionations, and other factors that affect the isotopic composition of a carbonate solid precipitated from solution. A general "frame of reference" for ^{13}C and ^{18}O isotope data in limestones is provided by Keith and Weber (1964), based on analyses of 500 samples divided into marine and freshwater groupings. The means for $\delta^{13}C$ and $\delta^{18}O$ for each genetic limestone grouping have been added to Figure 5 to provide a reference base for the Arctic Paleozoic data.

The principal generalizations relevant to the present interpretations and discussion are:

(a) calcium carbonate precipitated from normal marine sea water in relatively shallow environments will tend to be enriched in ^{13}C (positive $\delta^{13}C$ values)

[1]Department of Physics, University of Calgary.

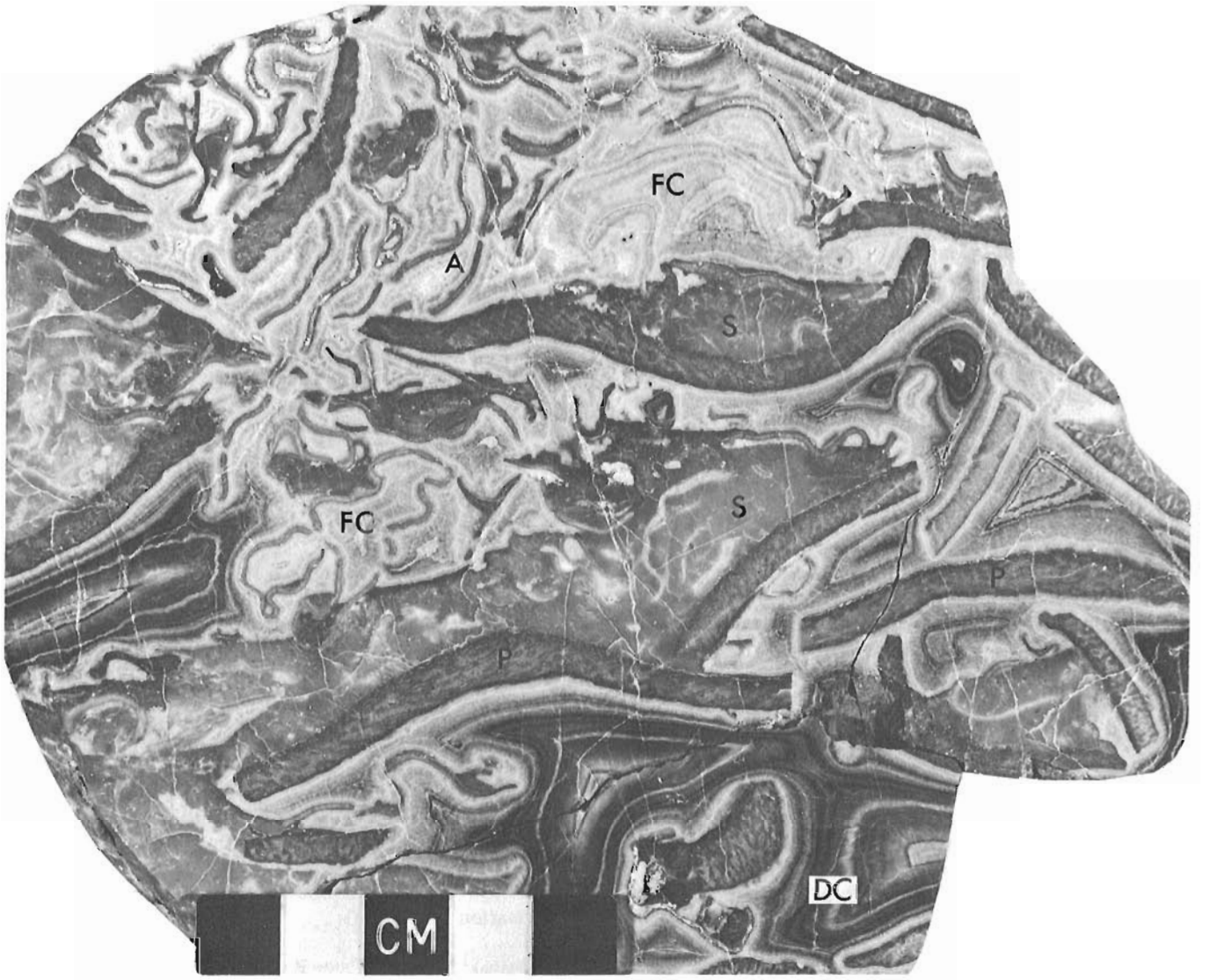

Figure 1. Fibrous calcite cements in Palaeoaplysina - phylloid algal boundstone of Early Permian age from the Nansen Formation, Girty Creek section, eastern Hare Fiord, Ellesmere Island. Note broken Palaeoaplysina plates (P) with internal canal system and ponded primary wackestone sediment (S), and thinner phylloid algal plates (A). Multilayered fibrous and radiaxial fibrous calcite (FC) fills the original shelter and inter-plate pore system. Later generations of cement are darker coloured than earlier generations (DC).

and slightly depleted to slightly enriched in ^{18}O (Fig. 5). Submarine aragonite and magnesium calcite cements in modern coralgal reefs generally lie within the range $\delta\,^{13}C$ +2 to 4.5°/oo, and $\delta\,^{18}O$ 0 to +2 (Goreau and Land, 1974; and others).

(b) carbonate precipitated from fresh or brackish waters tends to have negative $\delta\,^{13}C$ and $\delta\,^{18}O$ values, with the degree of depletion in the heavy isotopes dependent in part on the organic (photosynthetic) processes and reactions.

(c) for Paleozoic carbonates, diagenetic processes may have altered the original isotopic composition. Oxygen isotopes particularly may have been altered due to exchange reactions with connate or other "non-marine" and fresh waters depleted in ^{18}O. However, data from the Arctic carbonates suggest that the carbon isotopic composition has not been greatly affected by later equilibrium reactions with "fresh" waters.

The isotope data

Carbon and oxygen isotope data from the Arctic Paleozoic carbonates are cross-plotted in Figure 5. The following major trends are apparent:

1. Calcites from a brachiopod valve and from a composite sample of bryozoan zoaria lie in the range $\delta\,^{13}C$ +5.5 to +6.3°/oo, and $\delta\,^{18}O$ −1.9 to -3.3°/oo. The original mineralogy of these grains was calcite or calcite-dominant; although they have been altered diagenetically, original skeletal fabrics are preserved (solution-moldic phase discounted). As these grains

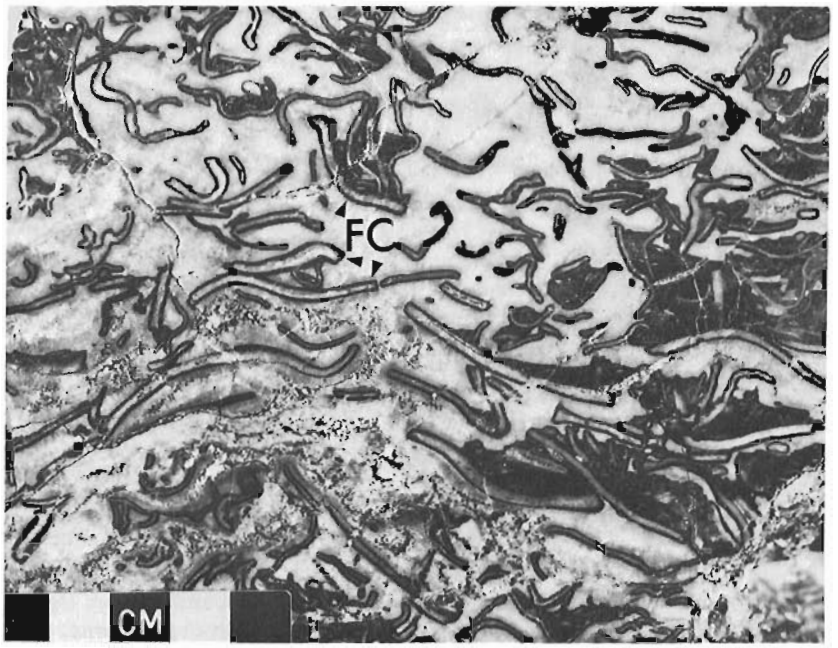

Figure 2.

Fibrous calcite and later cements in phylloid-algal boundstone of Late Pennsylvanian or Early Permian age from the Nansen Formation, Girty Creek section, eastern Hare Fiord, Ellesmere Island. Broken plates of phylloid algae, some with ponded wackestone sediment, are cemented together in a loosely packed framework by a thin layer of dark-coloured radiaxial fibrous calcite (FC). Remaining original pore space has been filled by calcite with a replacement sparry fabric (predates 'spar' of Fig. 5).

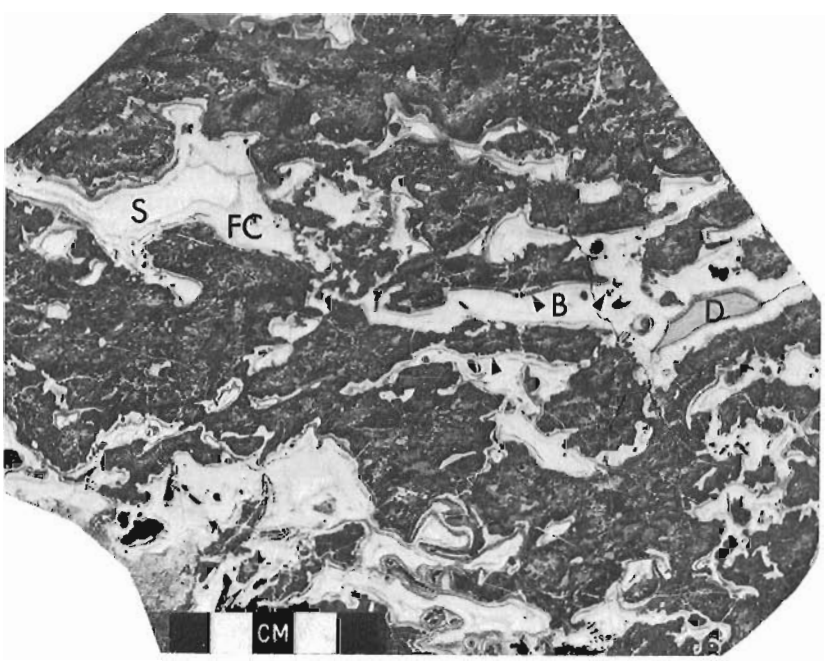

Figure 3.

Fabric typical of "Waulsortian"-type carbonate mounds characterized by abundance of fenestrate bryozoans. Irregular dark patches are primary skeletal wackestone sediment, with irregular pore systems filled with light-coloured fibrous calcite (FC), later dolomitized sediment fill (D), and late diagenetic calcite spar (S). Bryozoan zoaria are visible at (B); many form part of primary shelter pore spaces.

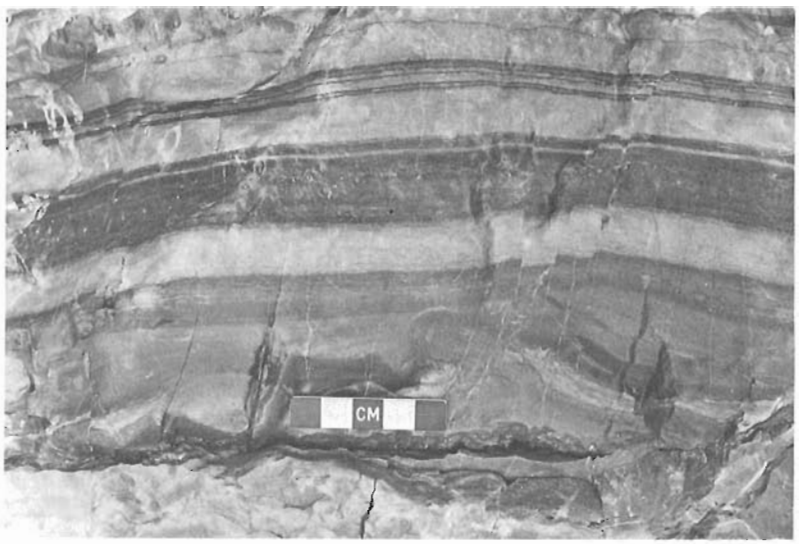

Figure 4.

Thick layer of rim cement lining one wall of a large fracture in a mid-Pennsylvanian bryozoan mound near Wood Glacier, northwestern Ellesmere Island. Darker layers contain organic-like structures and micro-fabrics.

unquestionably are of marine biogenic origin, their enrichment in ^{13}C, and the level of that enrichment serves as a check on expected ^{13}C enrichment in contemporaneous marine precipitates (allowing for different fractionation reactions for the two products). Similarly, the slight depletion in ^{18}O gives a sense of the degree of possible exchange between oxygen in the original marine carbonate and later ^{18}O-deficient waters.

2. The fibrous and radiaxial-fibrous calcites, established from fabric studies to be diagenetic replacements of very early cements, have $\delta^{13}C$ +4.8 to +6.2‰ (mean +5.6 +0.5‰) and $\delta^{18}O$ -1 to -7‰ (mean -4.1 +1.9‰). Nearly half of the analyses fall close to the data for skeletal grains of undoubted marine origin, and lie within a more limited, low-negative range for $\delta^{18}O$. The overall greater range in $\delta^{18}O$ towards more negative values, compared with the limited and high-positive range for $\delta^{13}C$, probably reflects the influence of late diagenetic oxygen isotope exchange with ^{18}O-deficient water. These data, particularly the few ^{13}C, are consistent with, and add support to, the marine-origin interpretation for the primary cement.

3. Radial to acicular calcites (dark radial, Fig. 5) forming dark coloured botryoidal masses if fractures and cavities, and radiating fabrics apparently of replacive type (not illustrated in this paper), have a slightly greater range in $\delta^{13}C$ than fibrous cements — from +4.7 to +7.4 (mean +5.9 ± 0.7‰). The range for $\delta^{18}O$ is more limited, from -1.3 to -5.3 (mean -3.1 ± 1.2‰. Some of the botryoidal radial calcites occur in large fractures lined by calcite cements (*see* 4, following); however, sedimentological and stratigraphical relationships show that many if not all fractures of this type predate burial by overlying sediments (and thus were relatively early). Other examples of dark radial calcite predate fibrous and radiaxial fibrous cements. The isotopic data suggest marine origin for some if not all of the radial calcites. However, the possibility that ^{13}C was derived from the host marine limestones must be considered (*see* later section).

4. Fracture rim cements, characterized by multi-generation layers of calcite colour-banded from light to dark grey (Fig. 4), possibly with organic encrustations, lie close to the isotopic composition of fibrous calcite cements (Fig. 5). Again, a marine source for this type of cement is suggested by the ^{13}C data and to a less extent by the ^{18}O data. Fractures lined by this type of cement in bryozoan mounds frequently are filled with bedded dolomitized crinoidal sediment derived from the overlying and partly enclosing Hare Fiord Formation ("basinal" carbonates, grading to shale). The fractures and associated cement linings thus predate burial of the mounds. Submarine fracturing of modern coralgal reefs has been documented by Shinn (1971).

5. Two samples of internal sediment composed of pelletoidal packstones with scattered ostracodes and foraminiferids that occur interlayered with early fibrous calcite cements in bryozoan mounds have $\delta^{13}C$ of +4.6 to +6.3‰, and $\delta^{18}O$ of about -8‰. Sedimentological relationships suggest that the internal sediment was of early (penecontemporaneous) marine origin; the high positive $\delta^{13}C$ values support this, while the more negative $\delta^{18}O$ value provides a cautionary note.

6. A single sample (sedimentary dyke, Fig. 4) from the sedimentary fill of a cement-lined fracture in a bryozoan mound has a $\delta^{13}C$ value of +4.5‰ and $\delta^{18}O$ of -11.7. The rock is an undolomitized, pink-coloured pelletoidal limestone. The depletion in ^{18}O suggests the strong influence of isotopic exchange with freshwater or of water deficient in ^{18}O, perhaps enhanced by the porosity and permeability of the relatively uncompacted sediment fill in a fracture in impermeable rock.

7. Sparry calcites, always post-dating earlier fibrous cements and internal sediments and often zoned with ferroan calcite, exhibit a wide range of $\delta^{13}C$ and $\delta^{18}O$ values. To these samples may be added the two sparry vein calcites (vein, Fig. 5). $\delta^{13}C$ in the calcite spars ranges from about +6.5 to -20.8‰, $\delta^{18}O$

ranges from -3.2 to -13.3‰. Once again, however, the majority of samples lie in the range of $\delta^{13}C$ from +4 to +6.5‰, and thus are comparable in ^{13}C to the fibrous cement. As these spars are later diagenetic products, precipitated from connate and (or) other water of various origins, the range of $\delta^{18}O$ values and the depletion in ^{18}O are expected. The high $\delta^{13}C$ values were not expected; evaluation of the possible mechanisms precipitation from marine-like waters during burial diagenesis; derivation of ^{13}C from the host marine carbonates; later isotopic exchange with ^{13}C-enriched waters; other processes) for this enrichment will be followed up in a later paper (Davies, Ghent, Krouse, in prep.).

Conclusion

The isotopic data obtained from the fibrous calcite cements support the interpretation of an early marine origin for the precursor cements, reinforcing fabric evidence and analogies with submarine cementation in modern reefs. Anomalies requiring further attention and analysis are the overall high positive $\delta^{13}C$ values for all the calcite types in these limestones (with a few exceptions). Have later generations of carbonate cements and spar derived their carbon from the host marine carbonate, thus perpetuating the original enrichment in ^{13}C? Alternatively, have many, or all, of the carbonate species undergone isotopic exchange with waters enriched in ^{13}C? If the latter, the entire basis

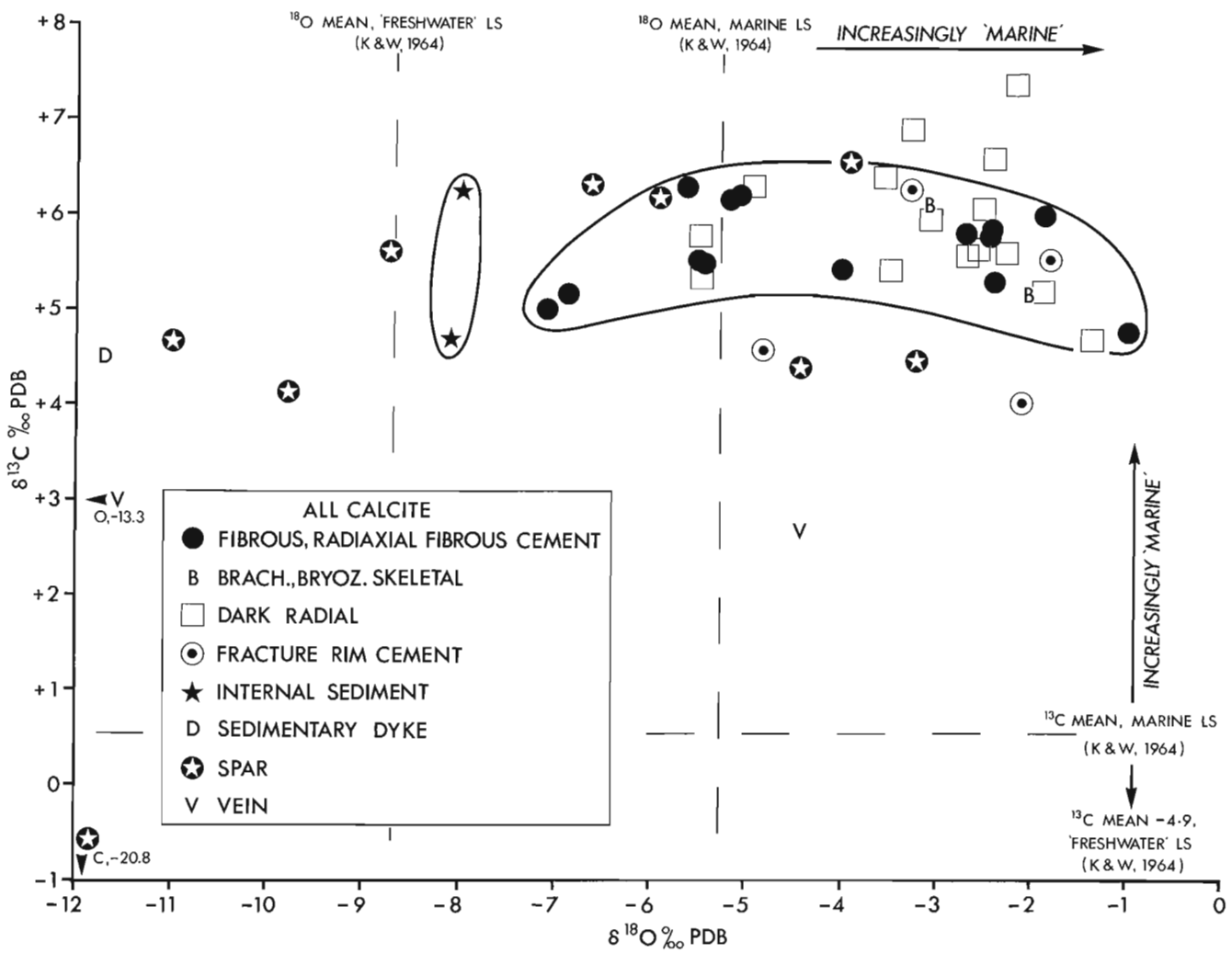

Figure 5. Plot of $\delta^{13}C$ and $\delta^{18}O$ data for about 50 samples of cement and associated calcite types in Pennsylvanian and lower Permian carbonates on Ellesmere Island. Six samples were analyzed by the Marathon Laboratory in Denver (*see* Acknowledgments); all others were analyzed at the Stable Isotope Laboratory, University of Calgary. Data for dolomites are not plotted. Means for $\delta^{13}C$ and $\delta^{18}O$ in 500 limestone samples divided into marine and freshwater genetic groupings by Keith and Weber (1964) are plotted on the figure as a frame of reference.

of interpretation must be re-evaluated. A full discussion of factors possibly controlling or contributing to the isotopic composition of these Paleozoic carbonates will be given in Davies, Ghent, Krouse (in prep.).

Acknowledgments

Dr. P.W. Choquette, Denver Research Center of Marathon Oil Company, encouraged the first author (G.R. Davies) to apply isotope geochemistry to the study of the Arctic Paleozoic cements. Through arrangements made by Choquette, the first analyses (6) of selected samples were run in the Marathon laboratory, and established the high $\delta^{13}C$ value of the fibrous cements; the Marathon data are included in Figure 5.

References

Bathurst, G.C.
1971: Carbonate sediments and their diagenesis; Developments in Sedimentology, v. 12, Elsevier, New York.

Davies, G.R.
1974: Submarine cementation, fracturing, and internal sedimentation in Pennsylvanian-Permian carbonate buildups, Arctic Archipelago; Am. Assoc. Pet. Geol., Abs., v. 1, p. 25.

Davies, G.R. and Nassichuk, W.W.
1973a: The hydrozoan ?Palaeoaplysina from the upper Paleozoic of Ellesmere Island, Arctic Canada; J. Paleontol., v. 47, no. 2, p. 251-265.

1973b: Upper Paleozoic carbonate mounds of the Sverdrup Basin, Arctic Canada (Abs.); Can. Soc. Pet. Geol., Geol. Assoc. Can., Arctic Symposium, Abstracts Vol., p. 7.

Ginsburg, R.N. and James, N.P.
1973: British Honduras by submarine; Geotimes, May 1973, p. 23-24.

Ginsburg, R.N. and Schroeder, J.H.
1973: Growth and submarine fossilization of algal cup reefs, Bermuda; Sedimentology, v. 20, p. 575-614.

Goreau, T.F. and Land, L.S.
1974: Fore-reef morphology and depositional processes, North Jamaica, *in* Laporte, L.F. (ed.), Reefs in time and space, Soc. Econ. Paleontol. Mineral., Spec. Publ. 18, p. 77-89.

Keith, M.L. and Weber, J.N.
1964: Carbon and oxygen isotopic composition of selected limestones and fossils; Geochim. Cosmochim. Acta, v. 28, p. 1787-1816.

Kendall, A.C. and Tucker, M.E.
1973: Radiaxial fibrous calcite: a replacement after acicular carbonate; Sedimentology, v. 20, no. 3, p. 365-389.

Shinn, E.A.
1971: Aspects of diagenesis of algal cup reefs in Bermuda; Gulf Coast Assoc. Geol. Soc., Trans., 21st Ann. Meet., v. 21, p. 387-394.

Thorsteinsson, R.
1974: Carboniferous and Permian stratigraphy of Axel Heiberg Island and western Ellesmere Island, Canadian Arctic Archipelago; Geol. Surv. Can., Bull. 224.

49. SULPHUR ISOTOPE DISTRIBUTION IN PALEOZOIC SULPHATE EVAPORITES, CANADIAN ARCTIC ARCHIPELAGO

Project 720060

Graham R. Davies and H. R. Krouse[1]
Institute of Sedimentary and Petroleum Geology, Calgary

Introduction and Summary

Sulphur isotope geochemistry has been used with varying success in studies of organic geochemistry, sulphide ore genesis, geothermometry, the composition of igneous and extra-terrestrial rocks, precipitational and diagenetic processes in modern and ancient calcium sulphate deposits, and for "dating" (relative) displaced evaporitic sulphate rocks. In this paper, we summarize the results of our own preliminary sulphur isotope analyses of Paleozoic sulphate evaporites from the Canadian Arctic Archipelago, plus available isotope data from Arctic Paleozoic evaporites from other sources. Our objectives in this initial survey were to determine whether the sulphur isotope composition of the Arctic Paleozoic evaporites is consistent with published data for other Paleozoic evaporites, and whether isotope geochemistry contributes to the interpretation of depositional (precipitational) processes for the Arctic gypsum-anhydrite minerals.

Three main points emerge:

1. The $\delta\,^{34}S$ values of Precambrian, Cambrian, Early and Middle Ordovician, Early and Middle Devonian, Early and Middle Pennsylvanian, and Early Permian anhydrite (or gypsum) from the Arctic Islands conform closely to the sulphur isotope age curve of Holser and Kaplan (1966), Nielsen (1972), and others. This distribution adds further substantiation to the documented fluctuation of sulphur isotope composition in sulphate evaporites, thus also of sulphate in sea water, during Paleozoic time.

2. On a smaller scale, Early to early Middle Pennsylvanian (Otto Fiord Formation) and early Permian (Mt. Bayley Formation) anhydrites appear to follow a crude trend of decreasing enrichment in ^{34}S with decreasing age. Values for $\delta\,^{34}S$ range between 16 and 18°/oo for the earliest Pennsylvanian samples, to a mean of about 14.5°/oo for the late Early to early Middle Pennsylvanian, and a mean of 13.9°/oo for the Early Permian. However, scatter between analyses throughout the section, including reversals in apparent trend, and particularly between very closely spaced samples (*see* 3, following), reduce the validity of this interpretation. The trend, if real, is roughly parallel to the curve for published data on upper Paleozoic sulphates (Holser and Kaplan, 1966; Claypool *et al.*, 1972).

3. Sequential analyses through two rhythmic beds (28 cm thick) of anhydrite in the Otto Fiord Formation, at a stratigraphic level probably of mid-Early Pennsylvanian age, reveal a variation in $\delta\,^{34}S$ from 11.8°/oo to 17.7°/oo, but with an apparent consistent vertical trend from about 16°/oo at the base of each rhythm to 12°/oo or 12.5°/oo at the top. As each bedding unit or rhythm of anhydrite contains structures interpreted to be pseudomorphic after large crystals of gypsum, the inference is made that the decrease in ^{34}S from the base to the top of the crystal-pseudomorph layer reflects, in part, isotopic fractionation during crystallization of gypsum in a semi-closed brine system.

Sulphur Isotopes

Of the four stable isotopes of sulphur, only ^{32}S (95% abundance) and ^{34}S (4.2%) commonly are investigated. Sulphur isotope abundances are measured by mass spectrometry, and are expressed as per mil deviation from a standard (sulphur in troilite from a meteorite), as δ (del) ^{34}S°/oo:

$$\delta\,^{34}\text{o/oo} = \frac{^{34}S/^{32}S \text{ sample} - {}^{34}S/^{32}S \text{ standard}}{^{34}S/^{32}S \text{ standard}} \times 10^3$$

If a sample is enriched in the heavier ^{34}S isotope relative to the standard, $\delta\,^{34}S$°/oo will be positive. If it is depleted in ^{34}S relative to the standard, $\delta\,^{34}S$°/oo will be negative. As a generalization, sulphur in sea water sulphates and in evaporitic sulphate materials is enriched in ^{34}S relative to the standard (modern sea water sulphate has a $\delta\,^{34}S$ composition of +20°/oo); in contrast, sulphur in sulphides (pyrite, etc.) may be isotopically light due to processes such as strong isotope fractionation during bacterial reduction of sulphates, favouring the incorporation of ^{32}S into sulphides.

Sulphur isotope ratios of evaporitic sulphate minerals plotted against geological age (Fig. 1) reveal a marked variation in distribution, particularly in Paleozoic evaporites (Holser and Kaplan, 1966; and others). This variation of at least 20°/oo between Cambro-Ordovician and Permian time may reflect major secular variations in concentration of total dissolved sulphate in the oceans (or perhaps potential variations; Rees, 1970). Perhaps one of the most significant aspects of this possible corollary, in view of apparent "evaporite maxima" in the Paleozoic, is that conditions favouring precipitation of calcium sulphate may have been enhanced during Paleozoic time by increased ionic concentrations of SO_4^{--} in sea water; the present (geochemistry of sea water) may not be the key to the past.

Most of the new isotope data presented in this paper are from the Stable Isotope Laboratory of the Department of Physics, University of Calgary; sources for other data are given in Table 1.

[1]Department of Physics, University of Calgary.

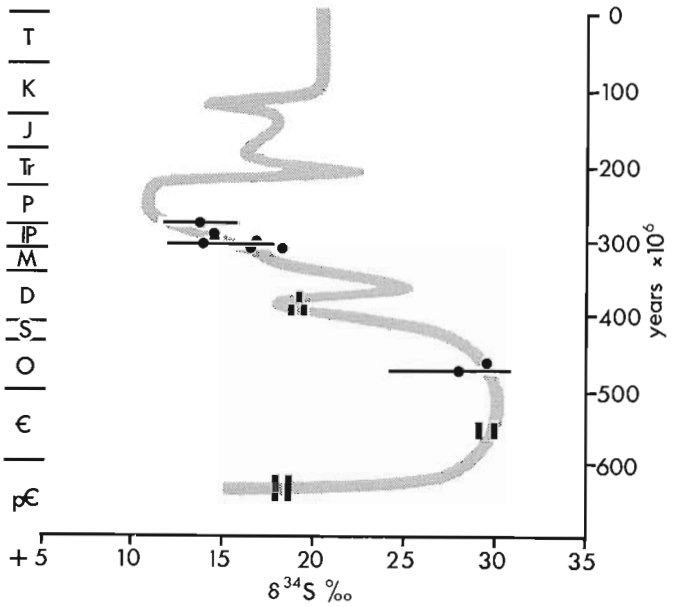

Figure 1. Sulphur isotope data from Arctic Paleozoic evaporites plotted over the isotope age curve (stipple) of Holser and Kaplan (1966); Arctic data and sources are listed in Table 1. The height of vertical bars express stratigraphic age uncertainty. Circles are individual analyses; horizontal bars with superimposed circles represent range and mean, respectively, of grouped data (Table 1). Note the general conformity between the curve and Arctic data, particularly for individual values and means of grouped analyses.

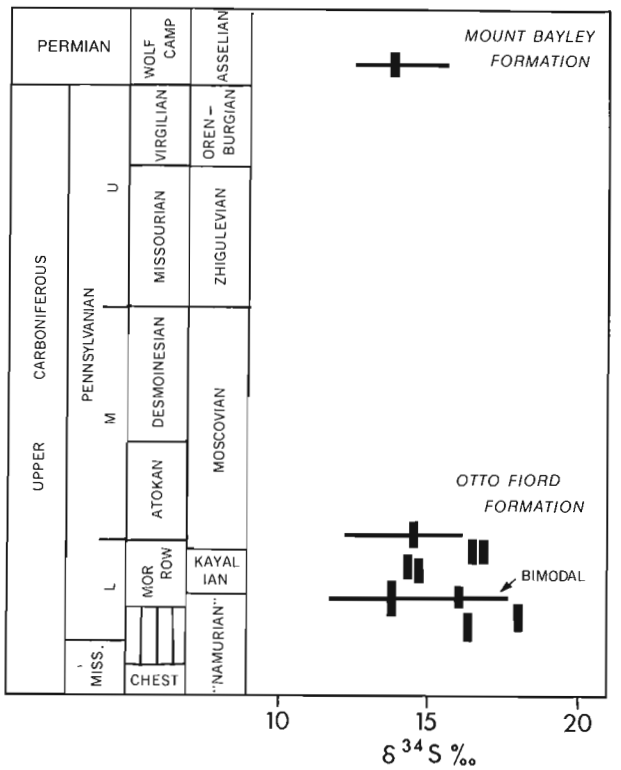

Figure 2. Plot of $\delta^{34}S$ data for anhydrite from the Otto Fiord Formation and Mt. Bayley Formation in the general time span Early to Middle Pennsylvanian and Early Permian. Vertical height of bars expresses stratigraphic uncertainty for individual samples. Horizontal bars and superimposed vertical bars express range and mean, respectively of grouped data. If means and individuals are considered, there is a crude decrease in $\delta^{34}S$ from earliest Pennsylvanian to Early Permian; if minimum $\delta^{34}S$ values are chosen as closer to sea water isotope composition, the trend is reversed.

Variation of sulphur isotopic composition of sulphate evaporites during Paleozoic time

Figure 1 is a compilation of previously published sulphur isotope data for Phanerozoic sulphates (Holser and Kaplan, 1966; Claypool *et al.*, 1972), and of available data from Arctic evaporites. The source and results of the Arctic analyses are summarized in Table 1; a brief outline of the geology and distribution of most of the source rocks for these samples is given in Davies (1974). It is apparent that the Arctic data, particularly averaged data for stratigraphically closely spaced samples, conform closely to the established curve. This adds further weight to the validity of the curve as a reflection of secular variations in sea water chemistry (ionic concentration of dissolved SO_4^{--}), particularly in Paleozoic time. To a sedimentologist, the general trend of decreasing enrichment in the heavier ^{34}S isotope relative to ^{32}S from Cambro-Ordovician time to Permian time, corresponding to a time of periodic major evaporite deposition (Ordovician, Devonian, Mississippian-Pennsylvanian, Permian) is too strong to be ignored. If, by fractionation, sulphate evaporites preferentially lock up some of the available ^{34}S relative to ^{32}S, the remaining sea water or brine should show a progressive decrease in the $^{34}S/^{32}S$ ratio; that is, sulphates precipitating subsequently from this sea water would have a lower $\delta^{34}S$ value than the first precipitate. Does this mechanism operate on a global scale, and over long periods of geological time? If so, is it a major factor producing the trend of declining $\delta^{34}S$ value through Paleozoic time? Although a preliminary reading of available literature suggests this is too simple an explanation, and that bacterial reduction of sulphate is the dominant process controlling $^{34}S/^{32}S$ composition, the sulphur isotope age curve has far greater significance than being simply a reflection of isotope ratio variations.

Isotopic composition of upper Paleozoic anhydrites

Thirty-one isotopic analyses have been run using anhydrite samples from the Upper Mississippian to Middle Pennsylvanian Otto Fiord Formation and the Lower Permian Mt. Bayley Formation (Fig. 2). Both of these evaporite formations were deposited within the Sverdrup

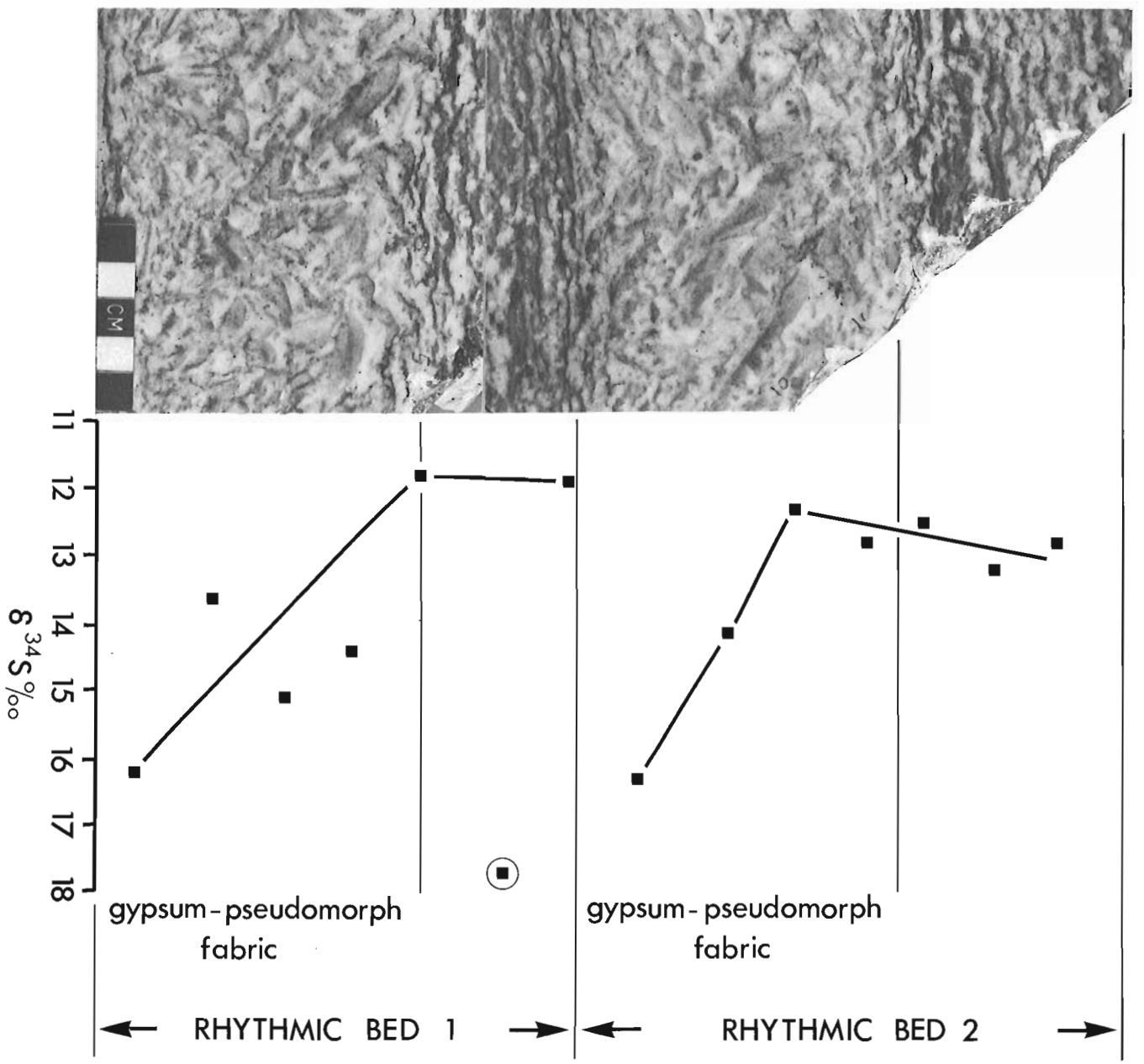

Figure 3. Plot of $\delta^{34}S$ for 14 samples through two rhythmic beds of anhydrite from the Otto Fiord Formation, at van Hauen Pass, Ellesmere Island. The beds probably are middle Early Pennsylvanian in age. Pseudomorphs after gypsum crystals are outlined by carbonate inclusions in the lower subunit of each bed (photograph, left). The inclined bars emphasize the apparent trend of decrease in $\delta^{34}S$ upward through the crystal-pseudomorph unit.

TABLE 1

$\delta^{34}S$ in Paleozoic sulphates, Arctic Archipelago

Age	Formation	Location	No. of Samples	Ref.	$\delta^{34}S$‰	Anal.
Permian, Asselian	Mt. Bayley	Ellesmere	7	DX-1972	13.9 ± 1.25	Krouse[1]
Pennsylvanian, ?earliest Middle	Otto Fiord	Ellesmere	4	DX-1972	14.5 ±	"
Pennsylvanian, latest Early	Otto Fiord	Ellesmere	2	DX-1971	16.7	"
Pennsylvanian, mid-Early	Otto Fiord	Ellesmere	2	DX-1971	14.5	"
Pennsylvanian, mid-Early	Otto Fiord	Ellesmere	14	DX-1971	13.9 ± 1.9	"
Pennsylvanian, earliest Early	Otto Fiord	Ellesmere	1	DX-1971	18.0	"
Pennsylvanian, earliest Early	Otto Fiord	Ellesmere	1	DX-1971	16.3	
Devonian, Middle (or late Early)	Blue Fiord equiv.	Ellesmere	1	KI-71	19.0	"
Devonian, Early	?	Ellesmere	1	TM-72	19.2	"
Ordovician, Middle	Bay Fiord	Devon	1	KI-71	29.3	"
Ordovician, mid-Early	Baumann Fiord	Ellesmere	15	GM-7-8	27.9 ± 1.8	Adler[2]
Cambrian, ?Middle	Ooyahgah	Devon	1	SL-23-1	29.0	Thode et al.[3]
			1	SL-23-2	30.0	"
Precambrian, ?Hadrynian	?Minto Inlet	Victoria	1	TC-18	17.8	Krouse
			1	TC-18	18.3	"

1. H.R. Krouse, Stable Isotope Lab., Dept. Physics, Univ. Calgary.
2. H.H. Adler, U.S. Atomic Energy Commission, Washington; samples coll. G.D. Mossop.
3. Thode and Monster (1965); Dept. Chemistry, McMaster Univ.

sedimentary Basin of the Arctic Archipelago (Thorsteinsson, 1974). Samples were collected from outcrops of the two units on central and northwestern Ellesmere Island. The analyses are listed in Table 1 in stratigraphic order with approximate age assignments.

As a generalization, there is a poorly-defined decrease in $\delta^{34}S$ from the oldest sampled anhydrites of earliest Pennsylvanian age to the youngest, of Asselian age (Fig. 2). This trend approximates the published data for the same time span (Holser and Kaplan, 1966; and others). The overall average for 24 samples from the Early to early Middle Pennsylvanian is $\delta^{34}S = 14.6 \pm 1.9$‰, within a range of 11.8 to 18.0‰. Depending on the weighting given to a closely-spaced set of analyses with a bimodal distribution about 60 m above the base of the Otto Fiord sample sequence, the mean for the early to mid-Early Pennsylvanian may range from 16.7‰ to 14.3‰. The mean of 4 analyses from anhydrite possibly as young as earliest Moscovian (earliest Middle Pennsylvanian) is 14.5‰, and for 7 samples from the Early Permian, 13.9 ± 1.3‰. However, departures from this crude trend, and wide

variance within closely-spaced analyses (for example, a range of 11.8 to 17.7°/oo in 14 analyses over a 28-cm interval), detract from the degree of confidence in the apparent trend. Indeed, if minimum $\delta^{34}S$ values are chosen, the trend would be reversed (Fig. 2).

Intra-bed variations of $\delta^{34}S$ in Pennsylvanian anhydrite

Analyses of 14 samples spaced at regular intervals though two beds of Otto Fiord anhydrite totalling 28 cm in thickness, reveal an overall variation in $\delta^{34}S$ from 11.8 to 17.7°/oo, with an apparently consistent and repeated trend of decreasing $\delta^{34}S$ from 16.2 or 16.3°/oo at the base of each bed, to a mean of 12 to 12.5°/oo near the top (Fig. 3). The mean for all the analyses is 13.9 ± 1.9°/oo. The age of the beds is estimated to be middle Early Pennsylvanian (Zone 20; Morrowan).

Each bed occurs as a couplet, with the lower layer containing inclusion-defined fabrics interpreted to be pseudomorphic after large, subvertical to inclined gypsum crystals (Davies, 1974, Fig. 3E). The trend of decreasing $\delta^{34}S$, allied to the interpreted primary gypsum crystal fabric, suggests that fractionation occurred during crystallization of the gypsum, leading to a progressive "lightening" of sulphate in the residual brines and consequent reduced $\delta^{34}S$ in later-forming crystals. The differential of about 4°/oo is greater than the expected fractionation occurring during crystallization of gypsum as documented by Thode and Monster (1965) and Nielsen (1972). Kinetic and other factors may have played a significant role in reduction of ^{34}S levels in the precipitating brine. However, Butler *et al.* (1973) present new data from modern calcium sulphates of the Trucial Coast to show that fractionation during crystallization and crystal growth of gypsum in the range 3 to 4°/oo $\delta^{34}S$ occurs at an advanced stage of brine evolution and precipitation. It is significant that Butler *et al.* (ibid.) found a vertical trend of increasing $\delta^{34}S$ values in the sabkha sulphate sequence, and suggest that this trend might be used to identify supratidal cycles in sulphate evaporites. In contrast, the reverse trend documented in this paper occurs in bedded sulphate evaporites interpreted to be of submarine origin (Davies and Nassichuk, in press). The trend of decreasing $\delta^{34}S$ in the Otto Fiord anhydrite beds suggest that crystallization and growth of gypsum, precursor of anhydrite, occurred in a semi-closed or closed brine system without access to "infinite" oceanic sources of dissolved sulphate.

Future Research

Possible lines of study, some of which may be pursued, include analyses of anhydrite samples throughout the Otto Fiord Formation with more precise paleontological control, detailed analyses of other bedded units, $\delta^{18}O$ analysis of sulphates in the same samples, and $\delta^{34}S$ and $\delta^{18}O$ analysis of Miocene and other bedded gypsum deposits analogous in crystal fabric to the pseudomorph fabrics in the Otto Fiord beds.

Acknowledgments

We thank Hans Adler (U.S. Atomic Energy Commission) and Grant Mossop for the data on Baumann Fiord sulphates, and H.G. Thode and J. Monster (McMaster University) for data from lower Paleozoic Arctic evaporites, some of which have been used in this paper.

References

Butler, G.P., Krouse, R.H. and Mitchell, R.
1973: Sulphur-isotope geochemistry of an arid, supratidal evaporite environment, Trucial Coast *in* Purser, B.H., ed., The Persian Gulf. Holocene carbonate sedimentation and diagenesis in a shallow epicontinental sea; Springer-Verlag, New York, p. 453-462.

Claypool, G.E., Holser, W.T., Kaplan, I.R., Sakai, H. and Zak, I.
1972: Sulfur and oxygen isotope geochemistry of evaporite sulfates (Abs.); Geol. Soc. Am., Abs., v. 4, no. 7, p. 473.

Davies, G.R.
1974: Paleozoic evaporites of the Canadian Arctic Archipelago; Fourth Symp. Salt, Houston, v. I, p. 119-125.

Holser, W.T. and Kaplan, I.R.
1966: Isotope geochemistry of sedimentary sulfates; Chem. Geol., v. 1, p. 93-135.

Nielsen, H.
1972: Sulphur isotopes and the formation of evaporite deposits *in* Geology of saline deposits; Proc. Hanover Symp., 1968, p. 91-102.

Rees, C.E.
1970: The sulphur isotope balance of the ocean: an improved model; Earth Planet. Sci. Lett., v. 7, p. 366-370.

Thode, H.G. and Monster, J.
1965: Sulfur-isotope geochemistry of petroleum, evaporites, and ancient seas *in* Fluids in subsurface environments, Young, A. and Galley, J.E., eds.; Am. Assoc. Pet. Geol., Mem. 4, p. 367-377.

Thorsteinsson, R.
1974: Carboniferous and Permian stratigraphy of Axel Heiberg Island and Western Ellesmere Island, Canadian Arctic Archipelago; Geol. Surv. Can., Bull. 224.

50. GRAVITY-SLIDE MEGASTRUCTURES IN DEEP-WATER CARBONATES OF THE PENNSYLVANIAN-PERMIAN HARE FIORD FORMATION, OF ELLESMERE ISLAND

Projects 720060 and 680064

Graham R. Davies and W. W. Nassichuk
Institute of Sedimentary and Petroleum Geology, Calgary

Introduction

Pennsylvanian and Permian rocks are exposed in spectacular but relatively inaccessible cliffs 900 m (300 ft.) high and 13 km (8 miles) long facing Otto Fiord on the north side of Svartfjeld Peninsula in northwestern Ellesmere Island (Fig. 1). Formations contained within the cliff sequence, from bottom to top, are the Hare Fiord Formation (Middle Pennsylvanian to Lower Permian), composed of dark coloured, cherty, argillaceous carbonates and shales, the van Hauen Formation (Lower Permian) containing dark coloured siltstones and cherts, and the Degerböls Formation (Upper Permian), composed of lighter coloured carbonates and siltstones. All formations show a remarkably uniform medium bedding; the Hare Fiord Formation is estimated to be 800 m (2300 ft.) thick, the van Hauen 100 m (300 ft.) and the Degerböls 30 m (100 ft.). As shown in Figure 1, the cliff exposure probably is less than 15 km (10 miles) south of a major east-west trending facies boundary separating deeper water shales and carbonates of the Hare Fiord Formation to the south from shelf carbonates of the coeval Nansen Formation to the north. The type section of the Hare Fiord Formation, 50 km (30 miles) to the northeast, is in a comparable position relative to this facies boundary. Certain gross bedding characteristics of the Hare Fiord Formation in the cliffs on the north coast of Svartfjeld Peninsula resemble bedding in middle units of the Nansen Formation in the type area east of the head of Hare Fiord, but we consider overall lithologies to be of Hare Fiord rather than Nansen aspect.

The Hare Fiord Formation in the cliff exposure and adjacent areas previously had been designated the Nansen Formation in four Geological Survey of Canada maps by Thorsteinsson and others that corner on the cliff area: Map 1305A, Cape Stallworthy; Map 1309A,

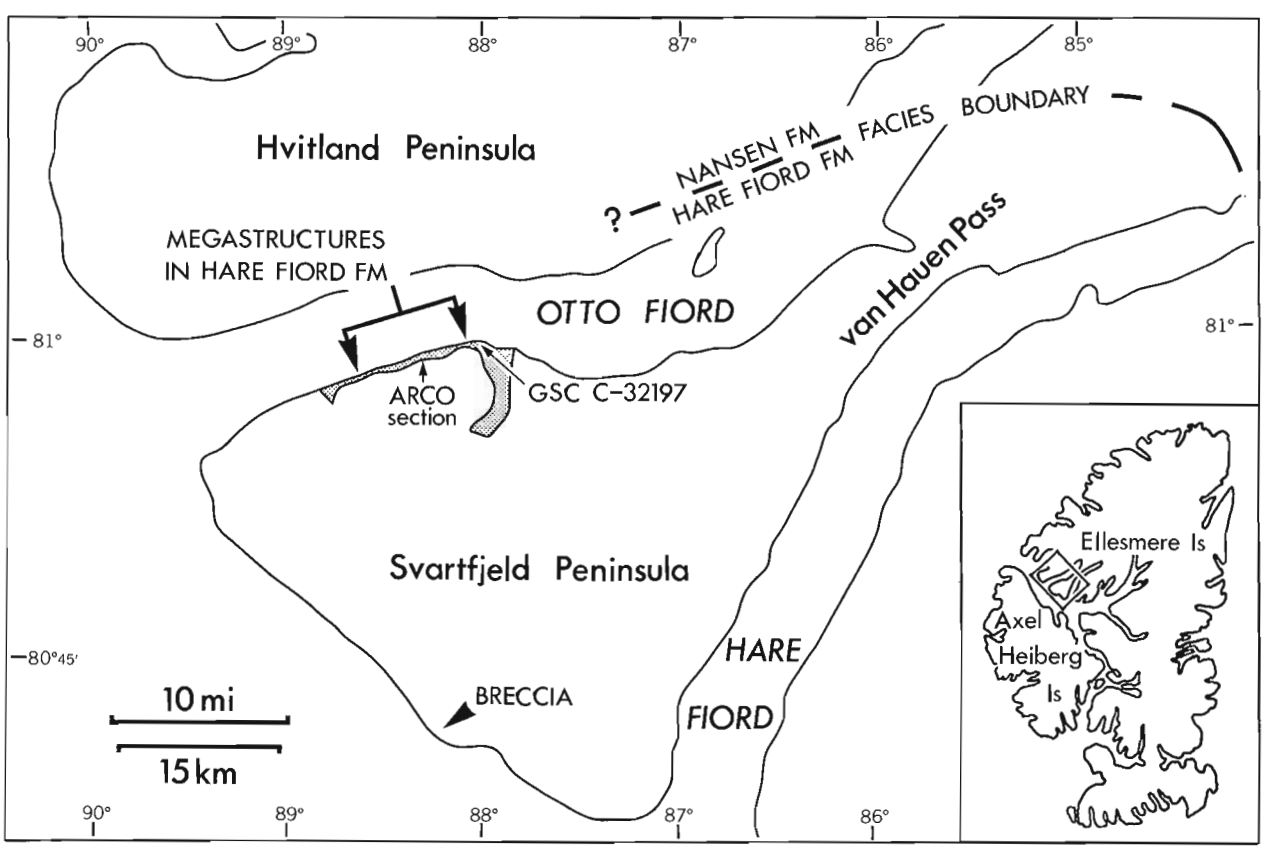

Figure 1. Locality map, northwestern Ellesmere Island. Only the general distribution of exposed Hare Fiord Formation rocks in the immediate area of the cliff section containing megastructures is shown. The extension of the shelf-to-trough facies boundary westward may parallel Otto Fiord, or swing northwestward across Hvitland Peninsula.

Figure 2. Part of a large "slide and fill" megastructure in the Svartfjeld cliff section of the Hare Fiord Formation. Width of view is estimated to be about 120 m (400 ft.) ± 10 per cent; scale estimated from length of shadow of helicopter on cliff face. At least 120 m (400 ft.) of vertical section was removed by this slide; only a small part is seen in this photograph. Note the angular relationship between "footwall" beds and overlying rocks, thinning and pinch-out of some beds immediately above the slide surface, and general thickening downdip of beds. Beds at the top of the visible section are parallel to beds below the slide. Dark beds and dark irregular pods are cherty carbonates.

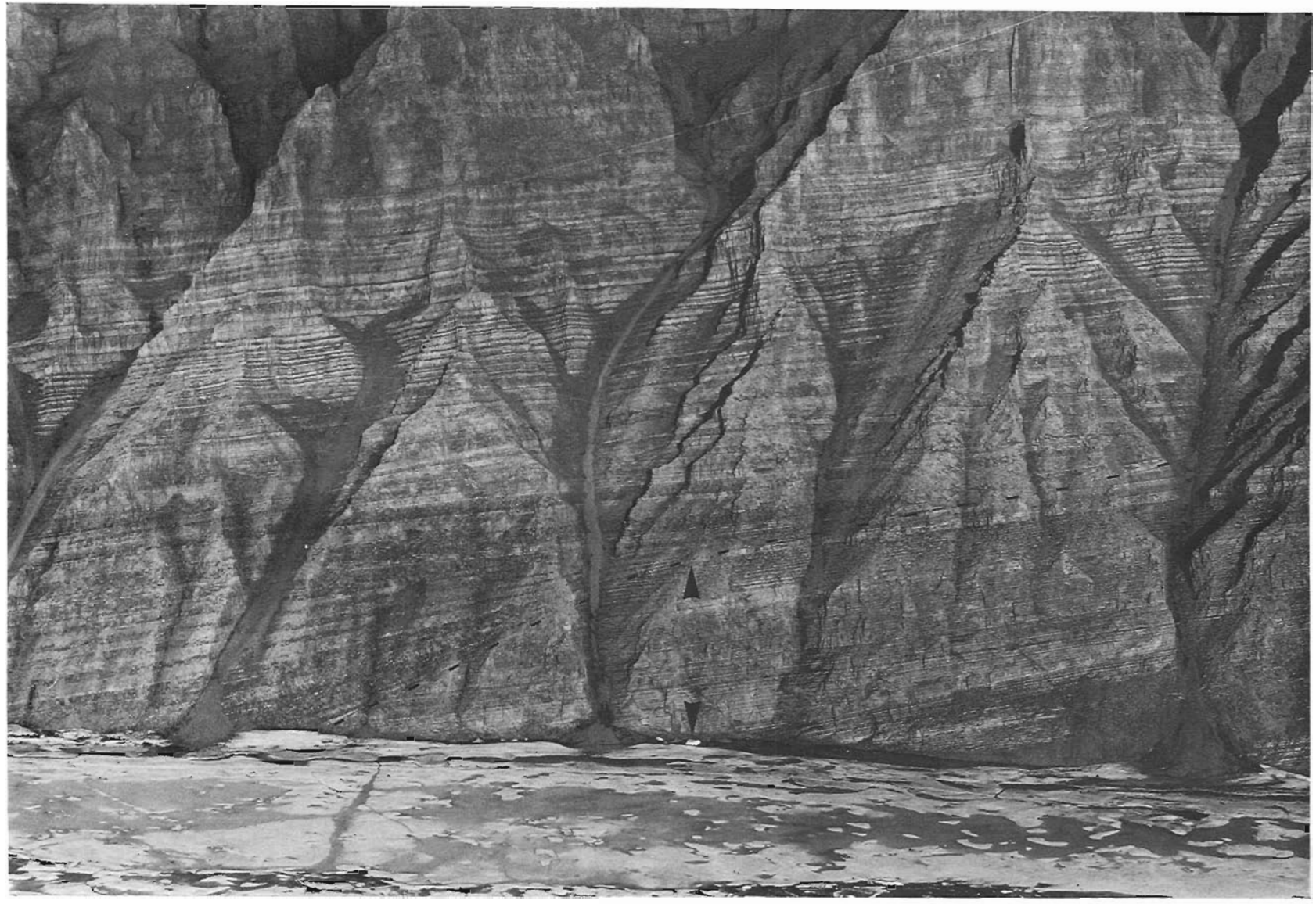

Figure 3. Another "slide and fill" megastructure partly covered by fiord sea ice, with several less obvious discontinuities, probably also submarine slides, higher in the section. Field of view is 460 m (1500 ft.) wide; vertical distance between arrows is 60 m (200 ft.). Note pronounced thickening downdip of sediments filling the slide scar.

Figure 4.

Photomicrograph of carbonate bed in the Hare Fiord Formation at GSC locality C-32197 (Fig. 1). Note wackestone texture, with bryozoans, crinoids (partly silicified) and thin-shelled brachiopods in a dolomitized, siliceous spicular matrix.

Otto Fiord; Map 1310A, Bukken Fiord; and Map 1311A, Greely Fiord West.

Spectacular, large-scale intraformational discontinuities or unconformities were observed from the air in the cliff exposures of the Hare Fiord Formation. These discontinuities apparently are the result of gravity slides followed subsequently by infilling of the slide scar by sediments.

Aerial photography of these megastructures (Figs. 2, 3) was followed by limited sampling of the lower part of the Hare Fiord Formation at one of the few accessible exposures. Our samples have since been augmented by additional samples taken from another incomplete section by geologists of Atlantic Richfield Canada Ltd.; we are grateful to C. Johnson and D. Folk of Atlantic Richfield for samples provided and other stratigraphic information.

A description of the megastructures in abstract form has been published elsewhere (Davies, in press); a more complete description with additional photographic documentation is planned.

Regional and local stratigraphy and facies

Regional stratigraphic facies relationships for the Carboniferous (Upper Mississippian through Pennsylvanian) to Lower Permian succession in the northern part of the Sverdrup Basin have been documented by Thorsteinsson (1974). In the axial Basinal Clastic and Evaporite Belt (ibid., 1974, Fig. 3), evaporites of the Otto Fiord Formation are overlain by cherty carbonates, siltstones and shales of the Mid-Pennsylvanian to Lower Permian Hare Fiord Formation, the principal upper Paleozoic trough-filling deep-water sedimentary unit in the Sverdrup Basin. The Hare Fiord Formation is characterized by dark coloured, well-bedded rocks of thin to medium bed thickness. In contrast, the shelf carbonates of the coeval Pennsylvanian to Early Permian Nansen Formation, forming the Northwestern Carbonate Belt (ibid., 1974, Fig. 3) flanking the axial trough, generally are light coloured carbonates of shallow-water aspect; carbonates range from well-bedded deposits of medium thickness to massive biogenic units.

Thin sections (Fig. 4) of resistant carbonate beds from the Hare Fiord Formation at the eastern end of the cliff exposure (GSC loc. C-32197, Fig. 1) reveal a bioclastic wackestone texture with partly silicified crinoid ossicles, fenestrate and other bryozoan zoaria, and thin-shelled brachiopod valves enclosed in a dolomitized (fine crystalline) and silicified spicular matrix. Lithologically, these rocks are similar to Hare Fiord rocks in the type section at van Hauen Pass (Fig. 1), and at other localities.

The base of the Hare Fiord Formation in the fiord cliff section is not exposed above the sea ice in the fiord. Immediately east of locality C-32197 (Fig. 1), anhydrite from the underlying Otto Fiord Formation is intruded and exposed in a fault zone, but is not exposed in the area in normal stratigraphic succession.

Biochronology of the Hare Fiord Formation

The Hare Fiord Formation ranges from Middle Pennsylvanian, Atokan (Moscovian) to Early Permian (Artinskian) age (Spinosa and Nassichuk, 1971; Nassichuk, 1975). Brachiopods have been recovered from three localities within the Hare Fiord Formation in the cliffs of Svartfjeld Peninsula and these have been identified by Carter (pers. comm., 1975) as follows:

GSC locality C-32197 (Fig. 1); talus collection, 122 m (400 ft.) above base of section:

Stenoscisma sp.
Age: Middle Pennsylvanian to Early Permian

GSC locality C-39368 (ARCO Section, Fig. 1); 6 m (20 ft.) above top of Hare Fiord Formation:

Chonetinella sp.
Age: Early Permian

GSC locality C-39367 (ARCO Section, Fig. 1); 46 m (150 ft.) below top of Hare Fiord Formation:

Cancrinella sp.
Rugivestis sp.
Martinia sp.
Age: Early Permian (Wolfcampian)

Megastructures

The large-scale structures in the Svartfjeld cliff exposure of the Hare Fiord Formation are distinguished initially by the angular discordance between large packages of well-bedded rocks of similar lithology (Figs. 2, 3). Larger individual structures affect up to 120 m (400 ft.) of vertical section and are at least 920 m (3000 ft.) long. A more detailed examination, particularly of colour photographs, shows that:

1. The plane of discordance or unconformity is a concave-upward curved surface that becomes progressively less steep in angle of dip downsection, until it runs parallel with and becomes indistinguishable from the underlying undisturbed beds; this listric geometry is characteristic of land-slide and other rotational gravity-slide failure surfaces. The horizontal or paralled-to-bedding component of the discontinuity surface may coincide with an original shale parting or bed between cherty carbonate beds.
2. The discontinuity surface truncates sharply the underlying beds ("footwall"), apparently with no soft-sediment or other type of deformation of the truncated bed, or evidence for local scouring below the general level of the listric discontinuity surface.
3. Beds deposited above the inclined part of discontinuities lie with angular (unconformable) relationship to the "footwall" beds and thicken down depositional dip (Figs. 2, 3). Where the discontinuity eventually becomes planar and parallel with "footwall" bedding, the overlapping beds are conformable (actual disconformity) to the underlying beds - apparent conformity, yet in fact a disconformity recognizable only by tracing individual beds along strike, or possibly by detailed paleontological study. Where dips of overlying beds are steep, the lowermost beds immediately above the discontinuity surface may thin or pinch out (Fig. 2). Because of the differential "fill" effect of the downdip thickening of beds, the depositional dip of overlying beds becomes progressively less steep up-section, until finally the younger beds are parallel with the original "footwall" beds and the structure is "buried".

Discussion, interpretation and significance

The size of the structures, their occurrence in sediments of deep-water aspect relatively close to the trough margin (the trough-to-shelf facies boundary, projected; Fig. 1), their probable position in a foreslope setting, the listric shape of the discontinuity surface, the sharpness of the truncation of beds and the lack of evidence for irregular erosional surfaces or of reverse-dipping rotated blocks above the discontinuities, argue against an erosional (submarine canyon?) or growth-fault (?) origin for the structures, and favour a gravity slide process in which up to 120 m (400 ft.) of section has been removed catastrophically by slope failure and redeposited "downslope" in deeper water of the trough axis. That gravity-displacement and redeposition of shelf and foreslope sediments in the Hare Fiord Formation has occurred elsewhere within the basin on a less spectacular but significant scale is documented by Davies and Schmidt (in press). The only example of possible redeposited Hare Fiord slope-facies rocks known to the authors that might be derived from the area of the Svartfjeld cliff structures was found by Atlantic Richfield geologists in 1974 (*see* Acknowledgments) at a locality on the coast of Svartfjeld Peninsula about 32 km (20 miles) south of the cliff exposures. At that locality (Fig. 1, "breccia"), sedimentary breccias of Hare Fiord-like lithoclasts occur as discontinuous deposits within normally bedded Hare Fiord rocks; these breccias may represent part of the sediment package displaced by gravity slides.

The slide scars, seen in the cliff face only in two dimensions, but probably arcuate in plan view and concave "downslope", subsequently were filled with sediments lithologically similar to the underlying rocks - spicular, slightly argillaceous lime muds, some pelletoidal, with varying amounts of crinoid, bryozoan and brachiopod skeletal debris. Crude fining-upward size grading of bioclasts in some of the carbonate beds suggests a turbidite-like transport and depositional mechanism, but are not comparable to the development of carbonate turbidites in other occurrences of the Hare Fiord Formation on Ellesmere Island (Davies and Schmidt, in press).

The carbonate sediments may have been weakly to strongly indurated at an early diagenetic stage by remobilization of specule silica into chert (similar to modern silica-rich oceanic sediments), and possibly by partial replacement of the lime mud matrix by finely crystalline authigenic dolomite. Early lithification, not necessarily complete, is suggested by the sharp truncation of beds by the slide surface.

The "slide and fill" (Davies, in press) megastructures in the Hare Fiord Formation are of more than local significance. Because of their exposure on steep, high-relief fiord walls under arid Arctic weathering conditions, the two-dimensional geometry of the entire slide structure and overlying sediment fill may be documented by oblique aerial photographs. Unfortunately, most of the section is inaccessible for sampling. Wilson (1969) has recognized probably similar "cut and fill" or slump structures in lime mudstones at localities in Europe, Montana, and the Guadalupe Mountains of Texas-New Mexico, and considers them to be characteristic of deep-water carbonate facies; rarely, however, can the geometry and nature of these structures be fully documented because of incomplete exposures under more temperate climatic conditions. The Arctic megastructures, when documented more fully, may serve as illustrative models for the phenomenon in other areas.

Probable submarine slides in siliceous and carbonate rocks of deep-water aspect have been described by a number of authors (Cox and Pratt, 1973; and others). Seismic profiles across modern continental shelves, specifically continental slopes, show submarine slumping and sliding (with geometric relationships comparable to the Hare Fiord structures) to be common in that tectono-sedimentary setting (Lewis, 1971; Normark, 1974; others). Earthquakes often are cited as possible triggering mechanisms for these modern submarine slope failures.

A more complete description of the Hare Fiord megastructures is planned, with emphasis on photographic documentation and on analogs in modern continental slope sediments.

References

Cox, D. P. and Pratt, W. P.
1973: Submarine chert-argillite slide breccia of Paleozoic age in the southern Klamath Mountains, California; Bull. Geol. Soc. Am., v. 84, p. 1423-1438.

Davies, G. R.
Penecontemporaneous slide and fill megastructures in upper Paleozoic slope-facies carbonates, Arctic Canada (Abs.); Am. Assoc. Pet. Geol., Abs. Vol., Ann. Meeting, 1975. (in press)

Davies, G. R. and Schmidt, V.
Gravity-displaced shallow-water carbonate sediments in Pennsylvanian to Permian basinal facies of the Sverdrup Basin, Arctic Archipelago; Bull. Can. Pet. Geol. (in press)

Lewis, K. B.
1971: Slumping on a continental slope inclined at 1° - 4°; Sedimentology, v. 16, p. 97-110.

Nassichuk, W. W.
1975: Carboniferous ammonoids and stratigraphy in the Canadian Arctic Archipelago; Geol. Surv. Can., Bull. 237.

Normark, W. R.
1974: Ranger submarine slide, northern Sebastian Vizcaino Bay, Baja California, Mexico; Bull. Geol. Soc. Am., v. 85, p. 781-784.

Spinosa, Claude and Nassichuk, W. W.
1971: The Permian ammonoid Stacheoceras discovered on Ellesmere Island, Canadian Arctic; Geol. Surv. Can., Bull. 197, p. 89-93.

Thorsteinsson, R.
1974: Carboniferous and Permian stratigraphy of Axel Heiberg Island and Western Ellesmere Island, Canadian Arctic Archipelago; Geol. Surv. Can., Bull. 224.

Wilson, J. L.
1969: Microfacies and sedimentary structures in "deeper water" lime mudstones *in* Friedman, G. M. (ed.), Depositional Environments in Carbonate rocks, a symposium; Soc. Econ. Paleontol. Mineral., Spec. Publ., 14, p. 4-19.

A TROPICAL ORDOVICIAN GRAPTOLITE FAUNA FROM NEAR THE NORTH POLE

Project 500029

D. E. Jackson[1]
Institute of Sedimentary and Petroleum Geology, Calgary

Introduction

The biprovincial nature of Early Ordovician graptolites was recognized as long ago as 1932 by Harris and Keble in Australia. Since that time, the Pacific Faunal Province has become widely recognized in U. S. S. R. and China, as well as in North America. By contrast, the Atlantic Province is restricted to Scandinavia, England, Wales and northwestern Europe. However, the total number of areas in the world for which graptolite data are available is less than thirty, and vast areas apparently are devoid of graptolites of this age. This paper shows for the first time that the Franklinian Geosyncline lay within the Pacific Province and discusses the implications of this.

In 1971, Thorsteinsson and Norford (*in* Trettin, 1971, p. 44, 46) recorded two suites of graptolites from the Hazen Formation near St. Patrick Bay (GSC loc. C-66) and at Mount Pullen (GSC loc. C-65) in northeastern Ellesmere Island. These faunas were deposited in the axial part of the Franklinian Geosyncline between the Pearya Geanticline on the northwest and the miogeosynclinal shelf on the southeast. Trettin (1971) postulates that this non-volcanic trough developed in an ensialic position. The state of preservation of these fossils is quite good in spite of a well-developed slaty cleavage. Recent studies by the author indicate that *Isograptus* cf. *I. victoriae divergens* Harris (Fig. 1D) and *Tetragraptus* sp. (not illustrated are present in GSC locality C-65 and that GSC locality C-66 contains *Isograptus* cf. *I. caduceus australis* Cooper (Fig. 1A), *I. victoriae maximodivergens* Harris (not illustrated), *Glyptograptus* cf. *G. austrodentatus* Harris and Keble (Fig. 1B), *Skiagraptus gnomonicus* (Harris and Keble) (Fig. 1C), *Glossograptus* cf. *G. echinatus* Ruedemann (Fig. 1E) and *Glyptograptus* sp. (Fig. 1F). These faunas have clear affinities with the Pacific Province and are assigned to the *I. caduceus* Zone (upper Arenigian) sensu Jackson (1964), which can be correlated with the Yapeenian Stage in Australia.

Various explanations have been proposed to account for the provincial distribution patterns of Ordovician epipelagic graptolite faunas. By far the most common explanation is that linking the distribution patterns to surface-water temperature. However, little progress was possible until geophysicists provided data on the positioning of continents and the paleoequator during Ordovician time. Skevington (1974) has provided the best demonstration to date that these provinces are controlled primarily by temperature. Using the Smith *et al.* (1973) reconstruction of positions of continents through Cambrian-Early Ordovician time, Skevington showed that all known localities of Pacific faunas straddled the paleoequator whereas the Atlantic Province is confined to latitudes higher than 30 degrees south and therefore is regarded as a temperature-water fauna. Using knowledge of how temperature affects the morphology and distribution of invertebrate faunas in present day oceans, Skevington (1974) explained the high generic diversity of the Pacific Province as being in accord with the general rule that taxonomic diversity increases from high latitudes to low latitudes. This explains why the Pacific Province contains several endemic genera (e. g. *Cardiograptus, Paraglossograptus, Pseudobryograptus, Sinograptus* and *Allograptus*), whereas the Atlantic Province has none.

Apart from diversity, it would be surprising if graptolite morphology was not affected by temperature. Planktonic protists living in warm waters today are notably more spinose than colder water forms of the same species. This tendency has been regarded as an adaptation to counteract the less buoyant nature of warm water. An analogy exists in the Llanvirn graptolite genus *Holmograptus*. *Holmograptus spinosus* (Ruedemann) is a biramous graptolite with dorsal spines developed on the prothecal fold and prominent ventral spines on the thecal apertures. It is restricted to the tropical Pacific Province where it is recorded from Australia, China, Canada, USA and western Ireland under a variety of names (*see* Archer and Skevington, 1973). In the Atlantic Province, the allopatric species (or subspecies) is *Holmograptus lentus* Tornquist which is comparable to *H. spinosus* in all characteristics except spines. This species is known from Peru, Norway and Belgium. Two other notably "spinose" species, *Sinograptus typicalis* Mu and *Paraglossograptus tentaculatus* (J. Hall), from Llanvirn beds in the Pacific Province have no equivalents in the Atlantic Province.

Another general tendency among ectothermic animals living in cold water is that they attain larger sizes than conspecific warm-water forms. Bouček (1972, p. 266) proposed that an inverse relationship existed between rhabdosomal size and water temperature (and density). However, it is difficult to arrive at a meaningful conclusion on the significance of size as the quantitative data are lacking. Comparing published data on co-provincial species such as *Tetragraptus approximatus, T. fruticosus, Didymograptus extensus, D. hirundo* and *Tristichograptus ensiformis* from the Arenig, forms from the Atlantic Province do not appear to be larger than their Pacific representatives. It is true that the largest multiramose species (*Temnograptus multiplex* Nicholson), the largest deflexed didymograptid (*Didymograptus* v-*fractus volucer* Nicholson), and the largest pendent didymograptid [*Didymograptus murchisoni* (Beck)] all are confined to the Atlantic

[1]The Open University, Milton Keynes, England.

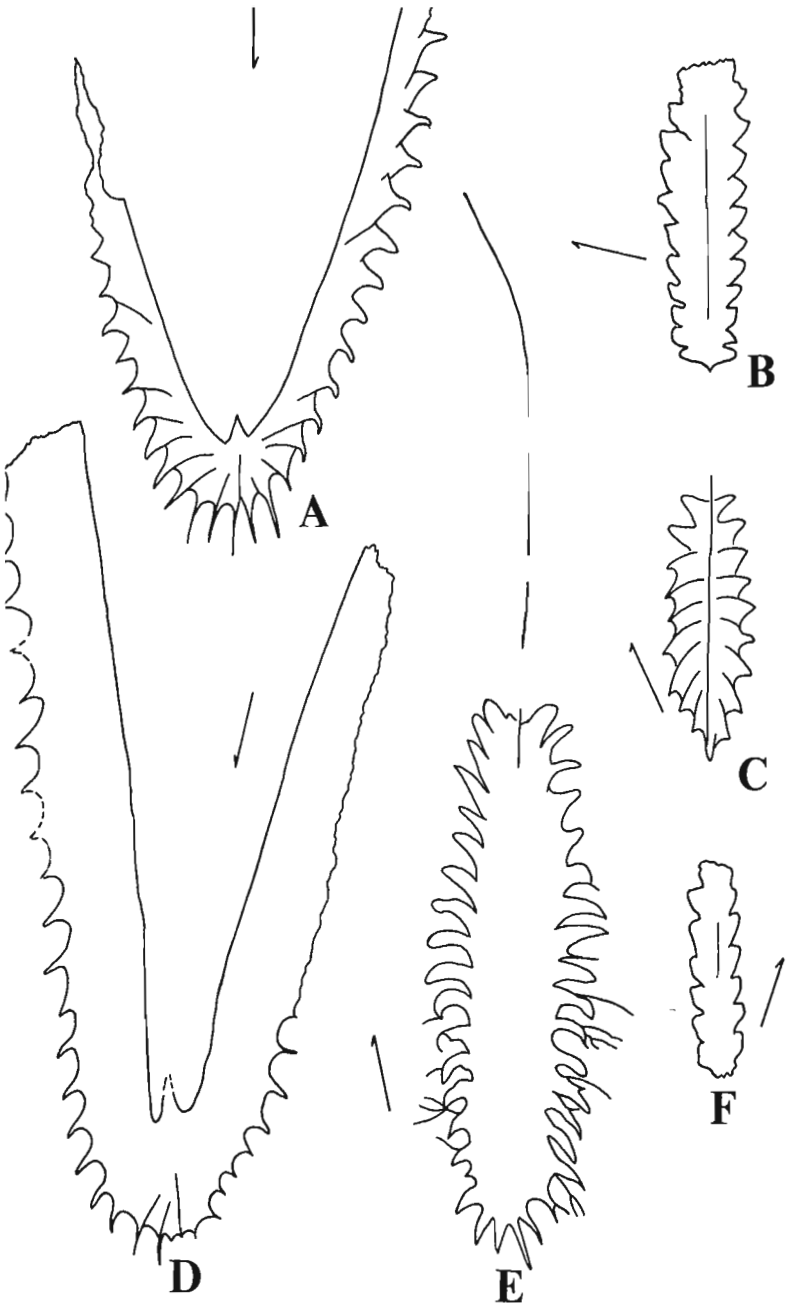

Figure 1.

A *Isograptus* cf. *I. caduceus australis* Cooper (GSC hypotype 42539);

B *Glyptograptus* cf. *G. austrodentatus* Harris and Keble (GSC hypotype 42540);

C *Skiagraptus gnomonicus* (Harris and Keble) (GSC hypotype 42541);

D *Isograptus* cf. *I. victoriae divergens* Harris (GSC hypotype 42542);

E *Glossograptus echinatus* Ruedemann (GSC hypotype 42543);

F *Glyptograptus* sp. (GSC hypotype 42544).

All figures x6.5; bars equal 1 mm.

Province. An equally plausible explanation is that size is related to phyletic age. This phenomenon has been demonstrated recently to occur amongst isograptids from Australia (Cooper, 1973, p. 103).

In conclusion, the Ellesmere Island graptolite assemblage is compatible with the geophysicists' positioning of the paleoequator (Fig. 2). Using the theoretical model of oceanic circulation proposed by Munk (1950), it is reasonable to assume that the Franklinian and Cordilleran Geosynclines of North America were swept by westward-flowing surface currents analogous with todays North Equatorial Current. In accordance with the map of Smith *et al.* (1973, Fig. 2), such a current would be part of a large Pacific gyre which brought genera such as *Sinograptus*, *Pseudobryograptus* and *Parabrograptus* from China to western Canada (but apparently not to Texas, Australia or New Zealand). The configuration and alignment of these coastlines north of the equator were such as to ensure similar thermal regimes and a corresponding uniformity of faunas. Such does not appear to have been the case in the southern paleohemisphere where coastlines of South America, North America, Europe, Africa and USSR would produce a complicated circulatory pattern and several latitudinal provinces or subprovinces. This could explain the differences in composition of faunas in Argentine, eastern North America, England-Wales and Norway.

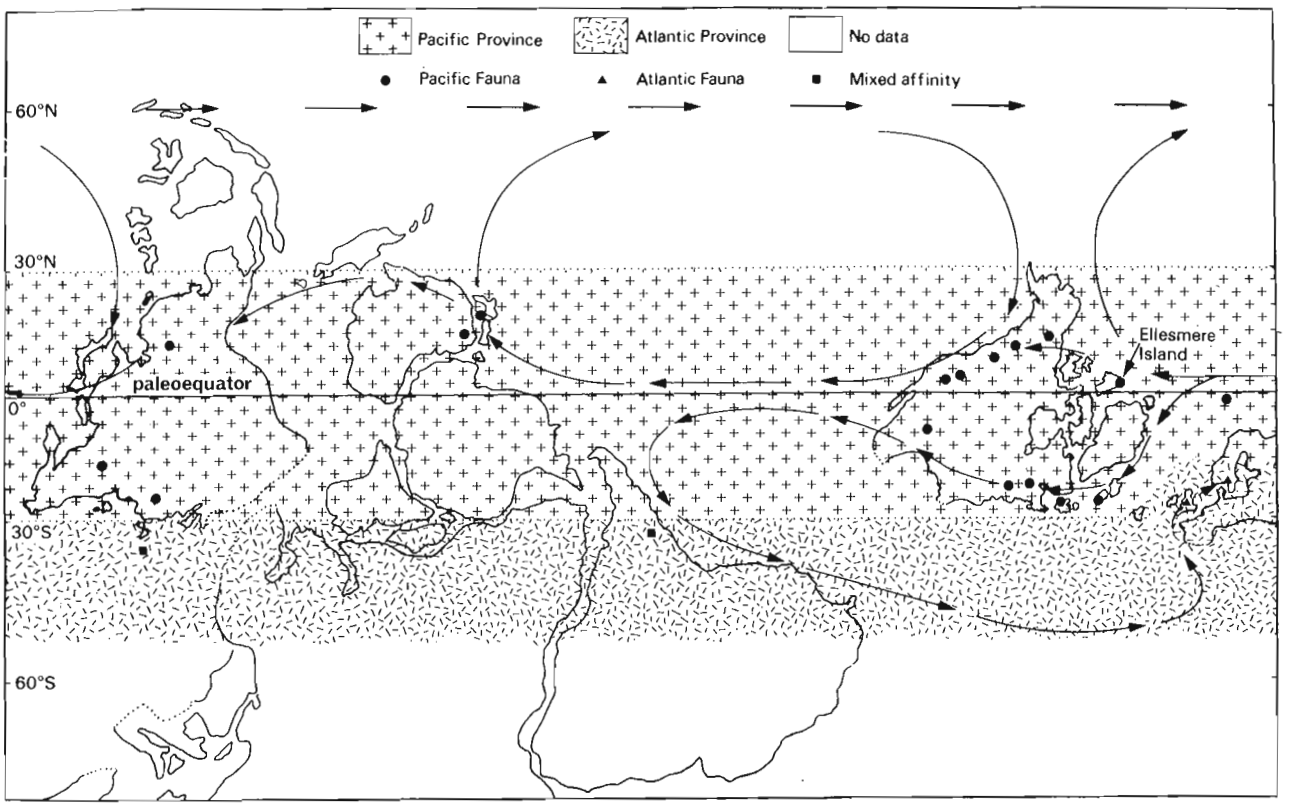

Figure 2. Positions of continents (after Smith *et al.*, 1973), distribution of Pacific and Atlantic graptolite faunas and postulated oceanic circulatory patterns during Early Ordovician time.

References

Archer, J.B. and Skevington, D.
1973: The morphology and systematics of '*Didymograptus*' *spinosus* Ruedemann, 1904, and allied species from the Lower Ordovician; Geol. Mag., v. 110, p. 43-54.

Bouček, B.
1972: The paleogeography of Lower Ordovician graptolite faunas: a possible evidence of continental drift; 24th Int. Geol. Congr., Sec. 7, Paleontology, p. 266-272.

Cooper, R.A.
1973: Taxonomy and evolution of *Isograptus* Moberg in Australia; Palaeontology, v. 16, p. 45-115.

Harris, W.J. and Keble, R.A.
1932: Victorian graptolite zones; Proc. Roy. Soc. Victoria, v. 44, p. 25-48.

Jackson, D.E.
1964: Observations on the sequence and correlation of Lower and Middle Ordovician graptolite faunas of North America; Bull. Geol. Soc. Am., v. 75, p. 523-534.

Munk, W.H.
1950: On the wind-driven ocean circulation; J. Meteorol., v. 7, p. 79-93.

Skevington, D.
1974: Controls influencing the composition and distribution of Ordovician graptolite faunal provinces *in* Graptolite studies in honour of O.M.B. Bulman; Palaeontol. Assoc. London, Spec. Papers in Palaeontology, no. 13, p. 59-73.

Smith, A.G., Briden, J.C. and Drewry, G.E.
1973: Phanerozoic world maps *in* Organisms and continents through time; Palaeont. Assoc. London, Spec. Papers in Palaeontology, no. 12, p. 1-42.

Trettin, H.P.
1971: Geology of lower Paleozoic formations, Hazen Plateau and southern Grant Land Mountains, Ellesmere Island, Arctic Archipelago; Geol. Surv. Can., Bull. 203.

52. SHARP MOUNTAIN FORMATION (NEW); A SHORELINE FACIES OF THE UPPER APTIAN-LOWER ALBIAN FLYSCH DIVISION, EASTERN KEELE RANGE, YUKON TERRITORY (NTS-117-O)

Project 550004

J. A. Jeletzky
Institute of Sedimentary and Petroleum Geology, Ottawa

Introduction and Acknowledgments

The purpose of this paper is to describe and to name formally a lithologically distinctive, paleogeographically and stratigraphically important lower Albian conglomerate unit delimiting the western shoreline of the early Albian flysch trough of the Porcupine Plateau. This unit, so far has been only briefly discussed and paleogeographically interpreted by the writer (Jeletzky, 1972, 1975, p. 26-27, Fig. 16).

The field work was carried out in July 1971 from the camp of Shell Oil Canada Ltd. situated at Whitefish Lake, northern Yukon Territory and camp facilities, air support, and field assistants were provided by Shell Oil Canada Ltd., Calgary. This assistance and co-operation are deeply appreciated. All fossils listed in this paper have been identified and dated by the writer.

Historical Remarks

The conglomerate unit described in this paper has been known for some time to geologists of the oil industry and those of the Geological Survey of Canada. However, no diagnostic fossils had been found prior to the writer's survey and the unit was assigned either a Permian (Operation Porcupine; Geol. Surv. Can., Map 10-1963) or a late Devonian (Bassett and Stout, 1967, p. 750, Fig. 11) age.

Geographic Distribution

The principal outcrop-area of the lower Albian conglomerate unit discussed here is the quasicontinuous ridge-like belt on and around the slopes of 3395-foot-high Sharp Mountain (= Molar Peak of early industrial geologists) that is about 7 miles long and up to 3 miles wide. Outside of this outcrop belt intermittent ridge-forming outcrops of the conglomerate unit have been traced from the air and on aerial photographs for another 6 to 7 miles west-southwestward. Toward the northeast the intermittent conglomerate ridges are definitely traceable for only 2 to 3 miles beyond the principal outcrop belt. However, they appear to extend north-northeastward all the way to Porcupine River where isolated exposures of lithologically similar and apparently correlative conglomerates were described by Norford (1964, p. 119, 120, units 6, 7). According to D.K. Norris (written communication of March 4, 1975) regional studies strongly suggest that these conglomerates may well be lateral equivalents of those occurring on Sharp Mountain. Possible outcrop-areas of the unit outside of eastern Keele Range are discussed below in connection with its paleogeographical interpretation.

Stratigraphy and Depositional Environment

The type section

The conglomerate unit is named herewith the Sharp Mountain Formation after the mountain of that name. That section (Field No. JA-F71-34/1-9) of the formation measured across the northwestern slope of Sharp Mountain beginning with the point on its crest situated about 550 yards northeast of the summit and continuing for about ¾ mile north-northeastward along the divide separating nameless westward and eastward flowing creeks is designated the type section of the formation (*see* Fig. 1). A panoramic view of this section with the principal lithological units indicated, is shown in Figure 2. This section was previously mentioned and graphically summarized by Jeletzky (1975, Fig. 5). The downward sequence from Sharp Mountain's crest is as follows:

Sharp Mountain Formation (type section)

7. Pebble conglomerate, mottled-light-brown-grey or green or, less commonly, bright orange, mostly fine to very fine (1/8- to ½-inch pebbles are prevalent) and grading commonly into coarse grit; sizable pods and 1- to 6-inch-thick interbeds of somewhat coarser (¼- to 1-inch) pebble conglomerate occur locally; pebbles are predominantly fairly rounded to subangular but the conglomerate includes a fair ratio of subangular to angular finer pebbles and grit particles; the conglomerate is roughly estimated to include 55 to 60 per cent of black to grey chert pebbles, 20 to 25 per cent of white pebbles probably belonging to milky chert according to F. G. Young (written communication of March 4, 1975), 10 to 15 per cent of quartz pebbles and 5 to 15 per cent of various metamorphic and clastic rocks; the abundant gritty to very coarse sandy matrix consists almost exclusively of poorly sorted and rounded, prevalent chert and subordinate feldspar grains; conglomerate is moderately hard to fairly friable, fairly tightly to tightly packed (mostly clast-supported) but not silicified, it is mostly poor in cement (mostly ferruginous), has a fair to good porosity in the outcrop and is thinly to medium (2- to 18-inch beds) fairly regularly to lenticularly bedded; regular attitude 095°/42°S; no graded bedding or other signs of turbiditic redeposition or plastic flow redeposition were seen; some ¼- to 1-inch-thick, lenticular interbeds and pods of bright orange-weathering, strongly ferruginous,

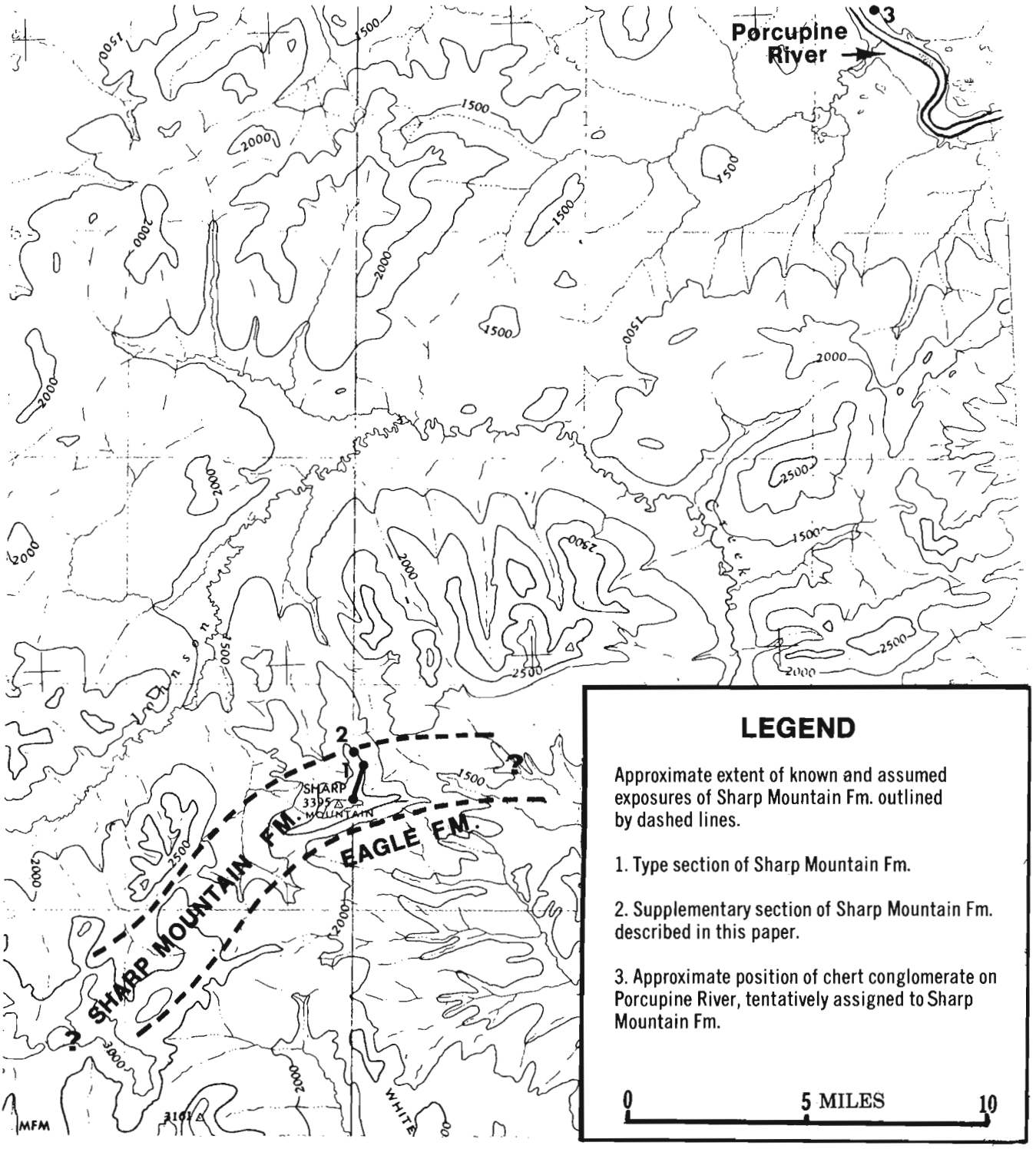

Figure 1. Sketch map of Sharp Mountain area, adapted from Old Crow sheet (116O-116N E½) of the 1: 250 000 scale topo maps, showing the known or assumed outcrops of Sharp Mountain Formation and the described sections.

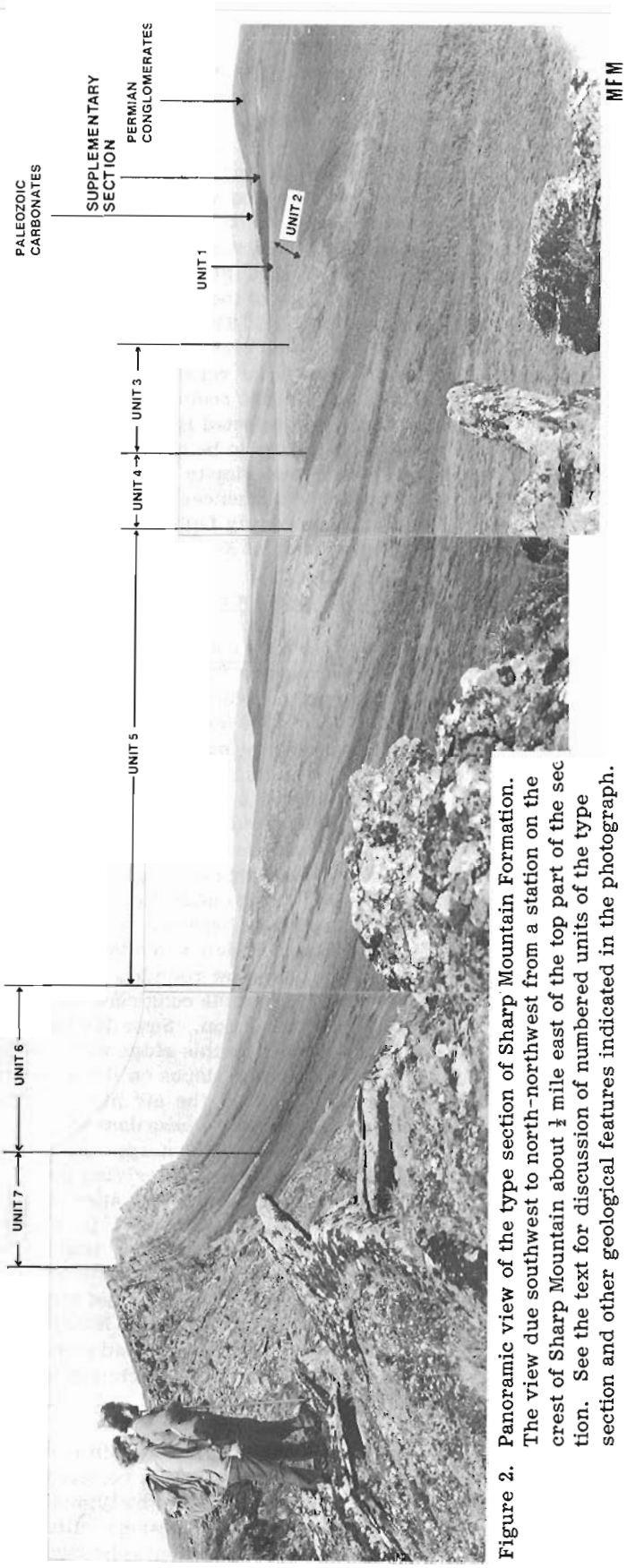

Figure 2. Panoramic view of the type section of Sharp Mountain Formation. The view due southwest to north-northwest from a station on the crest of Sharp Mountain about ½ mile east of the top part of the sec tion. See the text for discussion of numbered units of the type section and other geological features indicated in the photograph.

hard, fine grained lithic (greywacke) sandstone or sandy siltstone ("clay ironstone") with scattered grit particles and fine pebbles occur at irregular intervals; one of these interbeds occurring 352 feet below the unit's top has yielded fragments of a regularly and closely ribbed (?Albian), specifically indeterminate *Inoceramus* and an indeterminate pectenid (GSC loc. 87670); only some fragments of lithified wood were found elsewhere; top covered on the southeastern side of the mountain; base covered and possibly faulted on its lower slope; visible 490 feet.

6. A completely covered interval on the lower part of northwestern slope of Sharp Mountain and at its base; this possibly faulted interval is believed to be underlain either by friable conglomerates or possibly by argillaceous rocks; it is estimated to correspond to an about 865-foot-thick section assuming the attitude as in unit 7.

5. Pebble conglomerate lithologically similar to that of unit 7 but intercalated with a considerable number of irregularly recurring, interbeds and up to 100-foot-thick members of friable, recessively weathering, fine pebble conglomerate and rare 1- to 4-inch-thick beds of light brownish grey, weathering buff, fine to medium grained, locally carbonaceous, poorly rounded and sorted, lithic (greywacke-type) sandstone containing poor marine pelecypods (GSC loc. 87671); some bedding surfaces of these sandstones carry medium-sized (6-10 inch across) asymmetrical ripple-marks; the lower bedding surfaces are locally covered by flute cast-like markings; the unit is disturbed by faulting and the attitudes vary from 235°/70°SE to ± 90° to 070°/45°S; lower contact covered and probably faulted judging by the disturbed state of rocks of the unit; forms a hogsback on the crest of the above mentioned divide; visible 690 feet (approx.).

4. A completely covered interval at the top of the divide; this almost certainly faulted interval is believed to be underlain either by friable conglomerates or possibly by argillaceous rocks; width of the interval across the prevalent strike of rocks 155 feet.

3. Irregular, often lenticular, thin to medium (beds 1- to 12-inches-thick) interbedding of: a) Pebble conglomerate, light brown to rust-coloured, strongly ferruginous, fine to very fine, moderately hard to friable; mostly very rich in sandy to silty matrix and locally grades into pebbly grit; the lithology is similar to that of units 5 and 7, except for the presence of pebbles of characteristic Devonian pebble conglomerate rich in fine to very fine clasts of semitransparent blue grey chert; and b) Sandstone, light whitish grey or cream coloured; light to dark brown or light rust weathering, ferruginous; sandstone is predominantly fine grained but with a variable admixture of medium to coarse grains, grit particles, fine to very fine pebbles, angular fragments of dull grey carbonaceous to coaly shale and 1/8- to ½-inch flattened clay balls; some grains, pebble size clasts, rare specks, laminae and ¼- to ½-inch-thick interbeds of black shiny coal were noted; sandstone is moderately hard and dense but not quartzite-like and has some interstitial porosity; no crossbedding or ripple-marks noted; regular attitude is 045°/17°SE and the rocks are undisturbed otherwise;

the sandstone is roughly estimated to contain 30 to 40 per cent of white grains tentatively identified as feldspar grains in the field but probably belonging to white chert according to F. G. Young (written communication of March 4, 1975). F. G. Young had found only about 5 per cent of feldspar in the thin section of the unit studied by himself. Some 25 to 30 per cent of dark mineral (mostly chert), 10 to 15 per cent of orange coloured limonite grains, and a considerable ratio of lithic fragments; fragments of fossil wood and poor fragments of carbonized plants, including some ferns, conifers and ?dicotyledonous leaves, occur locally; rich and variegated macroinvertebrate fauna found at several levels (GSC loc. 87672, 87673, 87675, and 87676) includes early (presumably early early) Albian *Sonneratia* Bayle 1878 s. lato (including *Tetrahoplites* Casey 1952 and *Hemisonneratia* Casey, 1952, sp. indet., *Lima* (*Limatula*) sp., *Pecten* (*Entolium*) sp., ?*Inoceramus* sp., ?*Arctica* sp., *Modiolus* sp., and a rhynchonellid brachiopod; ammonites are commonly fragmentary while other macroinvertebrates are mostly disarticulated and/or fragmentary; this indicates a postmortal accumulation and burial in a high energy marginal marine environment (upper littoral or ?supratidal deposit); presence of brachiopods and an apparent absence of oysters suggest a normal salinity environment; the unit forms a low hogsback across the crest of the above mentioned divide (*see* Fig. 2); base and top covered; visible 40 feet (approx.)

2. A completely covered interval across the crest of the divide; this probably unfaulted (judging by low dips and undisturbed state of rocks on both sides) interval is believed to conceal a disconformable contact of Sharp Mountain Formation with the underlying Unnamed Upper Jurassic sandstone unit of Jeletzky (1974, p. 2, 7-8); width across prevalent strike 620 feet.

Unnamed Upper Jurassic sandstone

1. Sandstone, light yellow to bright orange when fresh, weathers dirty white to light grey with yellow specks and spots, fine (mostly) to medium grained, hard and fairly dense but not quartzite-like and with a good interstitial porosity; poorly sorted and rounded, most grains being subangular to angular; predominantly quartzose but contains a considerable (10 to 20 per cent) admixture of white grains of (?)kaolinized feldspar, orange limonite grains and those of dark mineral; almost devoid of silty particles; commonly more or less carbonaceous and contains partings, laminae and ¼- to 1-inch interbeds of dark grey to dull grey carbonaceous sandstone rich in small plant fragments; massive-looking to heavily and indistinctly bedded and fractures blocky to chunky; outcrops poor and only frost-heaved rock was seen; attitude appears to be approximately as last but it could not be measured exactly; marine pelecypods resembling *Astarte* (s. lato) sp. were found some 53 feet stratigraphically below visible top (GSC loc. 87676) and a poorly preserved ?*Buchia* (*Anaucella*) sp. of an apparent late Oxfordian to early Kimmeridgian age was collected by F. G. Young in 1972 from some part of the unit (GSC loc. no. 89210, writer's identification); base covered, visible 106 feet (approx.).

The above described type section of Sharp Mountain Formation is incomplete (both contacts are covered), the exposures are intermittent, and the rocks are locally faulted. However, all exposed ridge-forming conglomeratic units (i.e. units 7, 5, and 3) are lithologically distinctive. Moreover all of the section forms part of the southwestern limb of a major anticline. Therefore the section appears to be structurally conformable and fundamentally continuous throughout, in spite of a local steepening and disturbance of the persistently southward dipping rocks (Fig. 2). This suggests a minor scale of faults disturbing the section (especially unit 5) and the absence of either major repetition or a major faulting out of rocks within the section. Because of the above considerations, the selected type section of Sharp Mountain Formation is judged to be quite serviceable. Furthermore, it is much superior to any other section known to the author and the chances of discovering a better type section in a strongly faulted and at the same time poorly exposed terrain of Keele Range are poor.

Thickness and contact relationships

Because of the apparently continuous nature of the type section of Sharp Mountain Formation, its conglomeratic rocks (including the covered intervals 6 and 4) are inferred to be at least 2000 feet thick. The complete thickness of the formation appears to be greater yet. A couple of hundred feet of its rocks may be concealed within the covered interval 2 separating unit 3 from the exposed top of the Unnamed Upper Jurassic sandstone (*see* above). An undetermined but apparently small (? a few hundred feet) thickness of Sharp Mountain conglomerate is believed to underlie the completely covered, relatively gentle southeastern slope (a dip-slope) of Sharp Mountain, which extends for about ¾ mile across the strike, as a low rounded ridge at the foot of this slope is built of pebble conglomerate similar to that of unit 7 of the type section. Some 100 feet of this conglomerate is exposed in this ridge with the top concealed in the forested lower slopes on the southern side of the ridge. Judging by the air photographs, the disconformable and probably discordant contact of Sharp Mountain Formation with what appears to be (from distant observation only) the overlying poorly exposed but characteristically striped clastics of the Eagle Plain Formation of Mountjoy (1967, p. 5), is situated only a few hundred feet farther downslope. The here discussed conglomerate ridge is therefore inferred to be only two to three hundred feet stratigraphically below the upper contact of the Sharp Mountain Formation. The above described stratigraphical relationships suggest that the total thickness of the formation within its principal outcrop belt is in the order of 2500 to 3000 feet.

The lower contact of the Sharp Mountain Formation was not seen anywhere. However, it is believed to be at least erosionally disconformable in the type section of the formation (*see* in preceding section). Distant observation and analysis of air photographs suggest

that the formation overlies unconformably Permian and ?older Paleozoic rocks in some sections situated to the west of the principal outcrop belt.

Other sections

The previously mentioned conglomerate ridges occurring northeastward and southwestward of the principal outcrop belt of the Sharp Mountain Formation appear to be built exclusively of the weathering-resistant pebble conglomerate equivalent to the unit 7 of the type section, judging by a few spot checks and the analysis of air photographs. The thickness of the unit appears to be comparable to that of the type section in the southwest. However, the unit appears to decrease in thickness to some 300 feet at the easternmost point visited which is about 4 miles northeast of the type section. Only small, poorly exposed outcrops of rocks equivalent to those of units 5 and 3 of the type section have been observed in the above mentioned supplementary sections of Sharp Mountain Formation. None of the supplementary outcrops visited adds anything essential to the information provided by the above described type section of Sharp Mountain Formation.

The only known section of the Sharp Mountain Formation exposing rocks lithologically different from those of the type section outcrops in a short south-trending ravine situated about 300 yards northeastward of the base of the above described type section (*see* in the right background of Fig. 2). The descending succession is:

Sharp Mountain Formation

2. Sandstone, greenish yellow, olive tinged, weathers dull orange, very fine grained, often grades into very sandy siltstone, lithic and feldspathic, moderately well rounded and sorted (subrounded grains predominate), hard and dense with but little interstitial porosity or more or less silicified; indistinctly and heavily bedded, weathers medium rubbly; more or less carbonaceous and locally contains some small coaly fragments of plants; rare small fragments of shells occur locally but no identifiable macroinvertebrates seen; outcrops poor and almost completely covered by rubble; attitude is believed to be similar to that of unit 1 but could not be measured exactly; base covered and believed to be cut off by a strong strike fault; top covered and definitely faulted because of the appearance of outcrops of mid-Paleozoic carbonates and ?Permian conglomerates closely to the west and northwest of the section's top (*see* in the extreme right background of Fig. 2); visible 33 feet (est.).

1. Conglomerate, pebble, dull brown grey, weathers same, fine to very fine (pebbles 1/8- to ¼-inch predominant); pebbles consist almost exclusively of chert (?85 to 90 per cent) with various argillaceous and arenaceous (mainly sandstone) pebbles comprising the rest; pebbles range from fairly well rounded to angular and the matrix ranges from fine sandy (dark brown to dull brown grey) to silty (sandy siltstone); the structure of conglomerate varies from sparsely pebbly, matrix supported (grading into pebbly mudstone) to tightly packed, clast-supported; these two varieties alternate in a somewhat cyclical fashion; conglomerate is strongly ferruginous, friable to moderately hard and medium to heavily (6-inch to 5-foot beds) and somewhat indistinctly bedded; general attitude 280°/18°N but the rocks are closely jointed, commonly strongly slickensided and locally contorted; base covered, visible 175 feet (approx.).

Because of the northern dip of rocks in the above described section, it appears to form part of the faulted northern flank of the previously mentioned anticline on the southern part of which the type section of Sharp Mountain Formation was measured. The above described section occurs in close proximity of the exposures of the Unnamed Upper Jurassic sandstone (i.e. unit 1 of the type section) which occupies the axial part of the anticline (*see* Fig. 2). Therefore this section is believed to correspond to part or all of the covered interval 2 of the type section.

Age and correlation

The ammonite fauna of unit 3 of the type section of Sharp Mountain Formation represents the *Sonneratia* (sensu lato) n. sp. A fauna widespread in northern Yukon and Mackenzie Lowland regions (*see* Jeletzky, 1964, p. 74, pl. XXIII, fig. 1, corr. table; this paper Fig. 3). This fauna is correlative with either (most likely) the upper part of the *Leymeriella tardefurcata* zone or ?the lower part of *Douvilleiceras mammillatum* zone of the European standard. Therefore it is either early early or late early Albian in terms of the generally accepted subdivision of the Albian stage in Europe (*see* Casey, 1961, p. 495; this paper Fig. 3). However, the *Sonneratia* (s. lato) n. sp. A fauna is of a later lower (i.e. Leymeriellan) or ?early middle (i.e. Douvilleiceratan) Albian age in terms of the formerly popular but now generally abandoned subdivision of the European Albian introduced by Spath (1923). This subdivision was used by all Canadian workers, including the writer (Jeletzky, 1964, corr. table; 1968, p. 14-17), until it fell into disfavour in Europe.

The Canadian zone of *Sonneratia* (sensu lato) n. sp. A is older than any part of the generalized late early Albian (formerly early middle Albian; *see* Jeletzky, 1968, p. 14-17) zone of *Beudanticeras affine* and *Arcthoplites* (= *Lemuroceras auctorum*) spp. of Central and Arctic Canada which is now known to include the *Cleoniceras* (*Grycia*) cf. *C. subbaylei* zone of Jeletzky (1964, Table 1) as a faunal facies.

So far as is known, *Sonneratia* (sensu lato) n. sp. A zone is the oldest Albian zone in Canada. It may or may not overlie immediately the late Aptian *Tropaeum australe* and *Aucellina aptiensis-caucasica* zone (*see* Jeletzky, 1964, Table 1).

Outside of Sharp Mountain Formation the index fossils of *Sonneratia* (sensu lato) n. sp. A zone have been found in Chert conglomerate and Upper shale-siltstone units of the Upper Aptian-Lower Albian flysch division of the Porcupine Plain-Richardson Mountain Trough (Jeletzky, 1971a, p. 210; 1975, p. 94; Young,

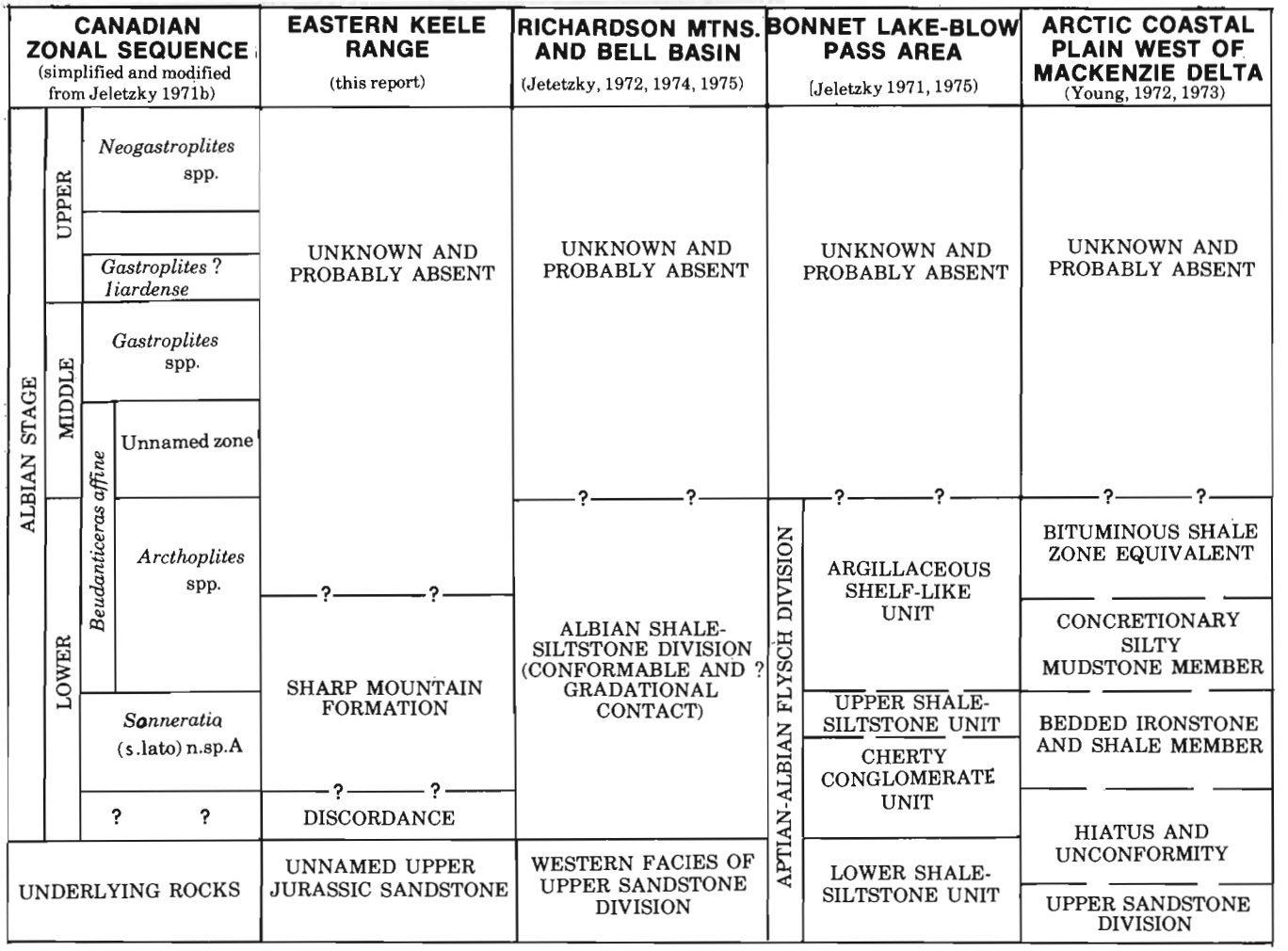

Figure 3. Age and correlation of Sharp Mountain Formation. MFM

1973, p. 280), in the shelf deposits of the Albian shale-siltstone division (Jeletzky, 1974, p. 17; Jeletzky, *in* Barnes *et al.*, 1974, p. 6-7 and unpublished), and in those of the Bedded ironstone and shale member of Young (1972, p. 232, Fig. 1; unpublished internal fossil reports of the writer).

None of the other units of the Sharp Mountain Formation yielded diagnostic fossils. However, they are unlikely to be appreciably older or younger than unit 3 for the following reasons:

1. Coarse clastics of Sharp Mountain Formation are closely similar lithologically and environmentally throughout. Therefore, they appear to be a product of a single cycle of sedimentation (*compare* under 2).

2. As pointed out by Jeletzky (1971a, p. 209; 1975, p. 26-27 and in the section on depositional environment below), all Albian conglomeratic units encountered in northern and west-central Yukon appear to be approximately contemporary units. They are products of a single cycle of deposition of coarse clastics along the western margin of Porcupine Plain-Richardson Mountain Trough in response to the strong but shortlived latest Aptian orogenic pulse.

3. No Albian rocks younger than *Beudanticeras affine* and *Arcthoplites* spp. zone are known to exist anywhere in northern and west-central Yukon and adjacent parts of the Mackenzie District (Jeletzky, 1971b, p. 45, Fig. 10; 1975, p. 41). The mid- to late Albian time was apparently a period of a pronounced uplift and erosion throughout this region. Because of the above considerations the younger and older (i.e. units 1 and 2 of supplementary section) units of the Sharp Mountain Formation are tentatively assigned either the same age as or a slightly younger age (i.e. zone of *Beudanticeras affine* and *Arcthoplites* spp.) than unit 3 (*see* Fig. 3).

Depositional environment and paleogeographical significance

As already pointed out, the sandstone-conglomerate unit 3 of the type section is an upper littoral to ?supratidal deposit. The evidence of its shallow water marine fauna is corroborated by the presence of coaly to carbonaceous, plant-bearing sandstone, thin layers of coal, and flattened clay balls.

Conglomeratic units 5 and 7 of the type section and their equivalents elsewhere in the area are also interpreted as largely or ?entirely littoral to supratidal deposits because of the local presence of well preserved, and hence not redeposited, shallow water marine pelecypods and the local presence of large scale ripplemarks combined with an apparently complete absence of graded bedding, slump phenomena, and pebbly mudstones. However, unit 1 of the above described supplementary section, presumably representing the basal part of Sharp Mountain Formation, is of an undetermined, possibly deeper water origin.

The extremely poorly exposed upper part of Sharp Mountain Formation overlying unit 7 is more likely an alluvial than a shallow marine deposit because of an apparently complete absence of marine fossils and interbeds of clay ironstone.

As pointed out elsewhere (Jeletzky, 1975, p. 26-27, Fig. 16; this paper, Fig. 3), the littoral to ?alluvial conglomerates of Sharp Mountain Formation occur westward of a wide belt of essentially contemporary outer neritic to bathyal sediments occupying the eastern and central parts of the early Albian Porcupine Plain-Richardson Mountain Trough. These conglomerates are accordingly interpreted as an erosional remnant of the originally continuous belt of littoral to alluvial gravel masses which were rapidly accumulating within a narrow western shelf and/or lowland plain of this trough. This shelf and plain zone must have fringed the strongly uplifted and rapidly wasting early Albian generation of Keele-Old Crow landmass because of the almost entirely rudaceous character of its sediments and the presence of thick flyschoid sediments immediately east of it.

Because of the lithology and discordant superposition on the Unnamed Upper Jurassic sandstone and older rocks, the conglomerates of Sharp Mountain Formation reflect the previously reported (Jeletzky, 1971a, p. 209; 1975, p. 26-27) drastic change in the depositional-tectonical regime of southern and western parts of the Porcupine Plain-Richardson Mountain Trough caused by the strong late Aptian tectonic movements.

The now known outcrops of the Sharp Mountain Formation delimit the approximate position of only a short segment of the early Albian western shoreline of the Porcupine Plain-Richardson Mountain Trough (*see* Jeletzky, 1975, p. 26-27, Fig. 16; this paper Fig. 1) situated within eastern Keele Range. Elsewhere the former position of this shoreline can only be inferred from the distribution of outcrop areas of the approximately contemporary deeper water rocks, such as flysch and deep water conglomerates, known to be restricted to the narrow western zone of this strongly asymmetrical, foredeep-like trough.

South of Keele Range the early Albian shoreline of Keele-Old Crow landmass may be placed north of extensive outcrop-areas of flysch-like, thick late Aptian to early Albian rocks in the headwaters of Kandik River (Jeletzky, 1971a, p. 219-220; 1975, Fig. 16). These deep water sediments apparently were deposited within a sublatitudinal strait connecting the early Albian Porcupine Plain-Richardson Mountain Trough with the Charley River (= Kandik River) basin in Central Alaska. South of Kandik River Basin the trough apparently ended blindly within the present northern Ogilvie and Wernecke mountains.

On the southeastern slope of Keele Range the western shoreline of early Albian Keele-Old Crow landmass may be placed to the west of an extensive outcrop-area of thick flyschoid and conglomeratic (?deep water only) early Albian rocks outcropping in the basins of Cody Creek and Fishing Branch of Porcupine River (*see* Jeletzky, 1975, Fig. 16). The presence of lithologically closely similar, presumably early Albian, flyschoid rocks to the northwest of Cody Creek in the headwaters of Lord Creek and Bluefish River (Jeletzky, 1972) suggests the existence of a presumably narrow western embayment of the Porcupine Plain-Richardson Mountain Trough within the western part of Keele Range. This embayment presumably ended blindly east of the Yukon-Alaska boundary as indicated in Jeletzky's (1975, Fig. 16) paleogeographical map.

The inferred presence of above mentioned early Albian embayment and the southwest-northeast orientation of the outcrop-belt of Sharp Mountain conglomerates suggest a strong eastward bulging of the early Albian Keele-Old Crow landmass in the eastern Keele Range-middle Porcupine River area. In this area the shape and extent of the early Albian generation of Keele-Old Crow landmass apparently was similar to those of its Late Jurassic and early Early Cretaceous predecessors (*see* Jeletzky, 1975, Figs. 10, 11, 16). Judging by the known distribution of the lower Albian flysch and pebble conglomerates in the Bonnet Lake-Blow Pass area (Jeletzky, 1971a, p. 209-210; 1975, p. 26-27, Fig. 16), this eastward protruding peninsula of the early Albian generation of Keele-Old Crow landmass extended eastward and northward well beyond the middle Porcupine River and the present Old Crow Range, including at least the western part of Old Crow Flats and Barn Mountains. It must be pointed out in this connection that the early lower Albian Chert conglomerate unit of the Upper Aptian-Lower Albian flysch division of the Bonnet Lake-Blow Pass area (Jeletzky, 1971a, p. 209-210) cannot be placed in the Sharp Mountain Formation on lithological and environmental grounds. As pointed out by Jeletzky (1975, p. 26-27), these conglomerates form part of early lower Albian deep sea fans deposited at the base of a steep western continental slope of Porcupine Plain-Richardson Mountain Trough by some kind of plastic sediment flow. These conglomerates differ from those of Sharp Mountain Formation in the occurrence within a thick deep water (?upper bathyal) flysch sequence, the abundance of argillaceous matrix, common presence of pebbly mudstones, and the apparently completely unfossiliferous character. These deep water conglomerates are interpreted as products of redeposition of the now completely destroyed (? or still undiscovered) shallow water to piedmont conglomerates equivalent to Sharp Mountain Formation which were deposited farther westward on a narrow western shelf of the early early Albian sea in the Bonnet Lake-Blow Pass area (*see* Jeletzky, 1975, Figs. 16, 22). These shallow water conglomerates equivalent to the Sharp Mountain Formation are possibly

preserved locally farther north on the Yukon's north slope (i.e. northeast of Mount Fitton, in the highlands between Blow River and Purkis Creek, etc.) as pointed out by Jeletzky (1975, p. 26). However, the data available (Young, 1972, p. 230; 1973, p. 280) are insufficient for a definitive interpretation of these conglomerates.

References

Barnes, C.R., Brideaux, W.W., Chamney, T.P., Clowser, D.R., Dunay, R.E., Fisher, M.J., Fritz, W.H., Hopkins, Jr., William S., Jeletzky, J.A., McGregor, D.C., Norford, B.S., Norris, A.W., Pedder, A.E.H., Rauwerda, P.J., Sherrington, P.F., Sliter, W.V., Tozer, E.T., Uyeno, T.T. and Waterhouse, J.B.
1974: Biostratigraphic determinations of fossils from the subsurface of the Northwest and Yukon Territories; Geol. Surv. Can., Paper 74-11.

Bassett, H.G. and Stout, J.G.
1967: Devonian of Western Canada, Intern. Symposium on the Devonian System, Calgary; Am. Assoc. Pet. Geol., v. 1, p. 717-752.

Casey, R.
1961: The stratigraphical palaeontology of the Lower Greensand; Palaeontology, v. 3, Part 4, p. 487-621.

Jeletzky, J.A.
1964: Illustrations of Canadian fossils. Cretaceous of Western and Arctic Canada. Lower Cretaceous index fossils of the Canadian sedimentary basins; Geol. Surv. Can., Paper 64-11, 100 p.

1968: Macrofossil zones of the marine Cretaceous of the Western Interior of Canada and their correlation with the zones and stages of Europe and the Western Interior of the United States; Geol. Surv. Can., Paper 67-72, 66 p.

1971a: Stratigraphy, facies and paleogeography of Mesozoic rocks of northern and west-central Yukon; *in* Report of Activities, April to October 1970, Geol. Surv. Can., Paper 71-1, Pt. A, p. 203-221.

Jeletzky, J.A. (cont'd.)
1971b: Marine Cretaceous biotic provinces and paleogeography of Western and Arctic Canada; illustrated by a detailed study of ammonites; Geol. Surv. Can., Paper 70-22.

1972: Stratigraphy, facies and paleogeography of Mesozoic and Tertiary rocks of northern Yukon and northwest Mackenzie District, N.W.T.; Geol. Surv. Can., Open File 82.

1974: Contribution to the Jurassic and Cretaceous geology of northern Yukon Territory and District of Mackenzie, Northwest Territories; Geol. Surv. Can., Paper 74-10.

1975: Jurassic and Lower Cretaceous paleogeography and depositional tectonics of Porcupine Plateau, adjacent areas of north Yukon and Mackenzie District, N.W.T.; Geol. Surv. Can., Paper 74-16.

Mountjoy, E.W.
1967: Upper Cretaceous and Tertiary stratigraphy, northern Yukon Territory and northwestern District of Mackenzie; Geol. Surv. Can., Paper 66-16.

Norford, B.S.
1964: Reconnaissance of the Ordovician and Silurian rocks of northern Yukon Territory; Geol. Surv. Can., Paper 63-39.

Spath, L.F.
1923: On the ammonite horizons of the Gault and contiguous deposits. Appendix II, in Summ. Progr.; Geol. Surv. U.K. for 1922, p. 139-149.

Young, F.G.
1972: Cretaceous stratigraphy between Blow and Fish Rivers, Yukon Territory; *in* Report of Activities, April to October 1971, Geol. Surv. Can., Paper 72-1, Pt. A, p. 229-235.

1973: Jurassic and Cretaceous stratigraphy between Babbage and Blow Rivers, Yukon Territory; *in* Report of Activities, April to October 1972, Geol. Surv. Can., Paper 73-1, Pt. A, p. 277-281.

53. UPPER DEER BAY FORMATION (BERRIASIAN-VALANGINIAN) OF SVERDRUP BASIN AND BIOSTRATIGRAPHY OF THE ARCTIC VALANGINIAN

Project 550004

Edwin Kemper[1]
Institute of Sedimentary and Petroleum Geology, Calgary

Introduction and Acknowledgments

The results described here were obtained during field work financed by Bundesministerium für Forschung und Technologie of the Federal German Republic. This research was carried out under the title of a joint project organized by the Geological Survey of Canada and the Bundesanstalt für Geowissenschaften und Rohstoffe. The field work was carried out in July 1974 with the logistic support of the Geological Survey field party led by H. R. Balkwill.

The object of the field work was to measure and study geological profiles in the upper part (Berriasian and Valanginian) of the Deer Bay Formation and to make a bed-by-bed collection of rock samples and fossils. An attempt was made to fit into these profiles fossil materials previously collected by officers of the Geological Survey of Canada and others; stratigraphic data accompanying some collections is limited. This important objective was largely achieved. The previously collected and the newly collected materials together provide a good but still incomplete basis for

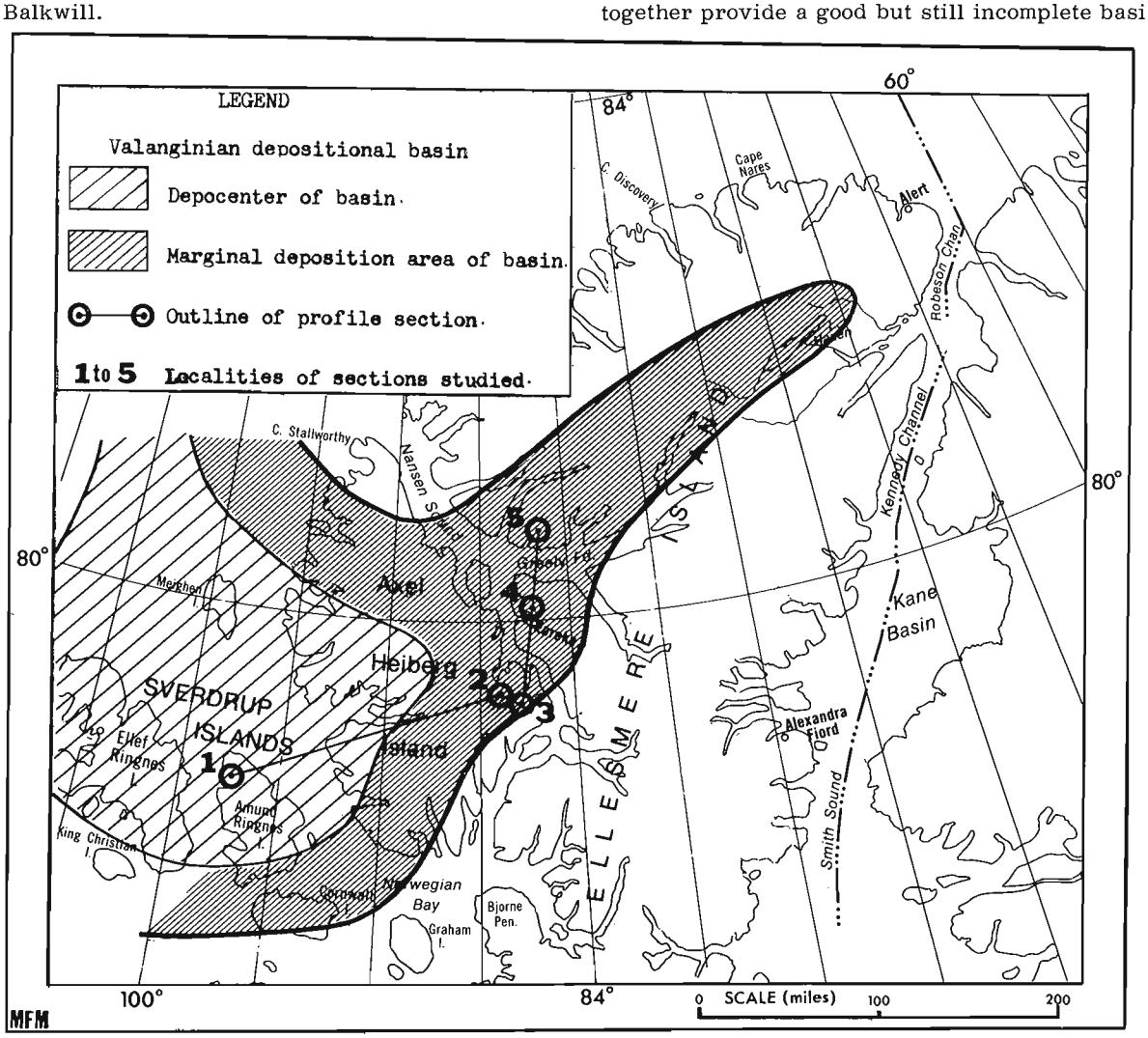

Figure 1. Key map with localities and different depositional areas.

[1]Bundesanstalt für Geowissenschaften und Rohstoffe, Hannover, Federal German Republic.

a refined paleontological subdivision, as well as for regional and intercontinental correlation, of the upper Deer Bay Formation.

The writer uses this opportunity to offer his sincere thanks to all who made this project possible and who have contributed to its completion. Special thanks are due to J. A. Jeletzky of the Geological Survey of Canada for discussing with the writer Canadian fossils and rocks concerned with this study prior to the field work being done, and for the translation of this article into English.

The identification and preliminary biostratigraphic evaluation of collected fossils was carried out in co-operation with J. A. Jeletzky. The results of the joint effort included herein represent the first phase of a planned co-operative biostratigraphical and paleontological study of mega-invertebrates (in particular ammonites) of the upper Deer Bay Formation in conjunction with closely related Valanginian ammonite faunas of northwestern Germany. The subdivision and dating of the investigated beds was facilitated greatly by the perusal of previously published paleontological-stratigraphical papers of Jeletzky (e.g. 1964, 1965, 1971, 1973), particularly those dealing with *Buchia* species.

Definition of Deer Bay and Isachsen Formations

The name Deer Bay Formation was proposed by Heywood (1957, p. 9) who defined it as follows: *This formation is composed of black, laminated shale and silty shale that is poorly consolidated and very closely jointed. Thick- to thin-bedded massive shale beds occur throughout the formation and buff weathering thin-bedded limestone beds 4 to 30 inches thick are present near the top. Numerous calcite concretions and rosettes occur throughout the formation but are most common in the lower part of the exposed section. The base of the formation is not exposed, therefore only the upper 600 feet have been mapped.* According to Tozer (*in* Thorsteinsson and Tozer, 1970, p. 582), the age of this formation ranges from the Volgian to the upper Valanginian. The name "*Buchia* shale" would have been much more suitable for the Deer Bay Formation, as the presence of *Buchia* species is the most characteristic feature of this marine succession of beds. On Spitzbergen, very similar beds contemporary with the Deer Bay Formation were named, therefore, "*Aucella* shale" (*Buchia* = *Aucella*).

The Deer Bay Formation is overlain by the Isachsen Formation (Heywood, 1957). According to Tozer (*in* Thorsteinsson and Tozer, 1970, p. 582), the Isachsen Formation *normally consists of light coloured, quartzose sandstone, grit and conglomerate, with interbeds of dark siltstone, shale and coal. A non-marine environment of deposition is indicated for all but the thin marine beds near the base.*

The Isachsen Formation includes beds ranging from upper Valanginian to lower Aptian. The stratotypes of the two formations discussed above are situated on Ellef Ringnes Island (Fig. 1).

Areas Studied and the Quality of Profiles

The field work was carried out in western Ellesmere Island and eastern Axel Heiberg Island from a base camp situated at the Eureka Weather Station. Only a few days were devoted to the study of Amund Ringnes Island profiles from a fly camp on that island. A definitive solution of some problems defined in the previous section depends on a continuation of field work on Amund Ringnes Island and its extension to Ellef Ringnes Island. Biostratigraphic work carried out on the profiles of Ellesmere and Axel Heiberg islands was hindered considerably because of poorly preserved megafossils. Definitive identifications of fossils from these areas were possible only in exceptional instances but, on Amund Ringnes Island, ammonites were well preserved. So far it is impossible to explain these important regional differences in the preservation of megafossils.

Field work was hindered also by the lack of consolidation of argillaceous sediments of the Deer Bay Formation. This resulted in strong solifluction which caused difficulties and formed a potential source of errors in the measuring and study of profiles. Even the narrow elevated ridges were covered by rock fragments. Because of the presence of this material, it was often impossible to recognize definitively whether or not the sediment is autochthonous and whether or not it contains concretions of the "hedgehog" type. The following text is concerned with the interpretation of the following localities and profiles (Fig. 1):

1. Unnamed hills and creeks (profile 11): northern part of Amund Ringnes Island; 78°38'20"N, 97°56'W and 78°38'35"N, 97°52'W.
2. Locality south of Buchanan Lake (profile 8): Axel Heiberg Island, Eureka Sound north map-area (Map 1302A); 79°22'10"N, 87°45'W.
3. Whitsunday Bay Anticline (profile 9): Axel Heiberg Island, Eureka Sound north map-area (Map 1302A); 79°18'20"N, 86°39'W.
4. Reptile Creek (profiles 1, 2, 5, 6, 10): Ellesmere Island, Greely Fiord west map-area (Map 1311A); the profile of Figure 2 is a combination of five individual profiles situated between 80°02'50"N, 85°46'W and 80°00'18"N, 85°52'W.
5. Blackwelder Mountains (profile 3): Ellesmere Island, Greely Fiord west map-area (Map 1311A); 80°39'30"N, 84°59'W.

The localities 2-5 are situated in the eastern marginal part of the basin (Fig. 1). Of these localities, locality 3 is near the Valanginian coastline. Locality 1 typifies profiles in the central part of the basin.

Sediments, Fauna and Paleoclimate

A dark grey shale is the predominant sediment throughout the basin; it is more or less silty and also may be sandy, especially in the upper part of the unit. These uppermost micaceous layers are also darker

coloured (blackish grey). The Valanginian part of the Deer Bay Formation may be represented by sand on eastern Axel Heiberg Island (Fig. 2). In the lower part of the Valanginian (i.e. in the beds with *Tollia* and *Temnoptychites*), the shale sequence contains units which break into fine layers when weathered, probably as a result of minimal bioturbation. However, there are no indications of definitively anaerobic conditions on the sea bottom. This type of sediment is well represented in the Blackwelder Mountains of northern Ellesmere Island and on northern Amund Ringnes Island and is of minimal importance for correlation. These rocks, which are widespread in the Valanginian, have also been reported from Spitzbergen.

The grey shale of the report-area contains sideritic layers that are represented either by brownish coloured bands or by layers of clay-ironstone concretions. The average thickness of sideritic layers is about 10 cm. However, thickness of 50 cm may occur, especially where isolated lenses are involved. The bank-like deposition of siderites is especially apparent in the lower Valanginian of the Blackwelder Mountains.

The clay-ironstone layers are unsuitable for correlation purposes; the profile in the Blackwelder Mountains contains, for example, three times as many layers as the succession at Reptile Creek.

Irregularly distributed "cannonball" concretions which are usually of fist size are remarkable. These concretions are characteristic of the uppermost beds of the Deer Bay Formation where they often contain *Buchia* of the *B. inflata-bulloides* species group. These scattered "cannonball" concretions occur most commonly in the Blackwelder Mountains and on Amund Ringnes Island. All types of nodules observed in the investigated sections of the Deer Bay Formation are genuine siderites; calcite is either absent or present only in small amounts.

The most characteristic lithological feature of the formation is the presence of aggregates of crystals (composite euhedrons) - so-called "hedgehogs" - which grew within argillaceous sediments. An adequate name would be polar euhedrons. Such "euhedrons" do not occur in the Lower Cretaceous of Europe. They are present in huge numbers in many beds of the Valanginian part of the Deer Bay Formation and their distribution in the sections is indicated on Figure 2.

The origin of polar euhedrons will be discussed in another paper devoted to this subject (Kemper and Schmitz, in prep.). They are interpreted as indicators of a cold-water environment.

The beds with polar euhedrons are normally devoid of fossils. If a fauna is present, it consists of giant *Buchias* and large gastropods, a typical cold-water assemblage.

The units containing polar euhedrons are mostly rather thick: 2 to 20 m; thinner beds are rare. Except for a 1- to 2-cm-thick layer in the Upper Jurassic of the Blackwelder Mountains, the "hedgehogs" are restricted to the shale facies of the Valanginian from the upper part of the Lower Valanginian on (LEB on Fig. 2). They do not occur in nearshore sands (Whitsunday Bay Anticline).

If the hypothesis proposed here is accepted, one has to postulate the prevalence of Arctic-Boreal climatic conditions from the lower to the lower upper Valanginian in the Sverdrup Basin. The beds with euhedrons may be used with some caution for correlation purposes. Valanginian beds may be easily distinguished from Upper Jurassic and Berriasian beds by means of euhedrons but it must be pointed out that the euhedrons also occur in the Albian Christopher Formation.

Upper Deer Bay Formation is characterized by a mass occurrence of driftwood (compare Heywood, 1957) which contrasts with its much less common occurrence in the European Lower Cretaceous. Similar accumulations of driftwood occur in the recent Beaufort Sea. In the Lower Cretaceous of the Lower Saxonian Basin driftwood is normally strongly affected by small pholadids. However, pholadids are rare and, at the same time, much larger in the Valanginian of Sverdrup Basin. The above mass accumulation of driftwood in the Deer Bay Formation, Sverdrup Basin appears to be attributable to the decrease of its mega- and microbiological destruction under the cold-water conditions.

During the Valanginian, faunal character was directly influenced by climatic conditions. Jeletzky (1971, p. 14) points out: ... *the Lower Cretaceous invertebrate faunas of the North American Boreal Province ... are characterized by their lack of diversity. These strongly to extremely depauperated faunas are, as a rule, dominated by only a few, or even a single molluscan species that occur in great abundance.* This conclusion is especially applicable to the cold climatic phases which are characterized by a maximum development of euhedron concretions. In such time, the faunas disappeared either completely or nearly completely. Following a temperature increase, immigrant faunas, invariably dominated by *Buchia* forms, appeared.

The immigration of such expressly southern faunas as lytoceratids, *Buchia* ex gr. *B. crassicollis* (Keyserling) and *Homolsomites* ex gr. *H. quatsinoensis* (Whiteaves) apparently had taken place only under favourable climatic conditions in the upper beds of the lower upper Valanginian. According to J.A. Jeletzky (internal fossil reports and pers. comm., 1974), these "southern" fossils apparently only occur in lower upper Valanginian beds with "cannonball" concretions. These faunas immigrated partly from the seas of western North America (Jeletzky, 1971) and partly (?predominantly) either from the European-Greenland or Siberian seas. The warming up trend reached its maximum during the time of deposition of the Isachsen Formation (cf. rich vegetation, presence of coal).

Because of the above considerations, the dating, subdivision and correlation of the upper Deer Bay Formation depends on fossils alone. Among mega-invertebrates, ammonites and *Buchia* have the greatest biostratigraphic value (*see* Jeletzky, 1973). The value of ammonites in the Eureka area is diminished by their rarity and poor preservation but, on Amund Ringnes Island, it is possible to work out a zonal standard for the Valanginian of the Sverdrup Basin based on ammonites.

Buchias are the most widespread components of the boreal fossil faunas. They occur in many beds of dark grey shale in a flattened and hence mostly indeterminate condition. Undeformed and therefore readily determinable specimens can, generally speaking, only be obtained from the clay-ironstone bands and concretions. Belemnites are relatively common and widespread, but are nearly always corroded or disintegrated. This poor state of preservation makes it impossible to collect identifiable material systematically.

The occurrence of characteristic cold-water assemblages of mega-invertebrates deserves mention. The associations are confined to shales and are in some cases associated with polar euhedrons. The shell matter is generally not preserved on fossils. Several species of giant gastropods of the family Trochidae are present but large specimens of *Buchia* are the prevalent components of most such faunas. Pectinidae (among others *Camptonectes* sp.) are present also. In Reptile Creek, faunas that are especially typical of a cold-water environment occur in beds which have yielded *Temnoptychites novosemelica* (Sokolov) and *Tollia* species.

Biostratigraphic Subdivision of the Valanginian of Sverdrup Basin

As has already repeatedly been stressed by Jeletzky (1973), only *Buchia* and ammonite species can be utilized effectively for subdividing the Valanginian. Satisfactory results are expected, but they must be preceded by additional taxonomic research and by supplementary bed-by-bed collecting.

In contrast with the Upper Jurassic and the Berriasian, the existing subdivision of the Valanginian into *Buchia* zones is still too coarse. A single zone of *Buchia keyserlingi* (Lahusen) comprises, in accordance with the present concept of the species, two-thirds to four-fifths of the Valanginian. This amounts to about 400 m on Amund Ringnes Island (Fig. 2).

The younger *Buchia* ex gr. *B. inflata-sublaevis-bulloides* appear late in the upper half of the lower upper Valanginian ("bull" on Fig. 2). At least in the central part of the basin, this species group still occurs far up into the deposits of Isachsen Formation. Further detailed research will probably permit a specific and subspecific subdivision of these broad species groups of *Buchia*. However, it is not expected that the Valanginian can be subdivided into more than four units on the basis of *Buchia*.

The knowledge of distribution and time-ranges of important ammonite species was considerably extended only on Amund Ringnes Island. Even there, however, there are thick units that are devoid of fossils. An early Valanginian fauna of the profile measured on Amund Ringnes Island includes, according to the latest identifications of Jeletzky (written comm., 1974), exclusively Tolliinae; namely *Temnoptychites* ex gr. *T. lgowensis-syzranenzis-simplex*, *Tollia* ex gr. *T. mira* Voronets - ?*mutabilis* Stanton, and *Russanovia diptycha* (Keyserling). *Tollia* and *Temnoptychites* occur also in profiles measured on Axel Heiberg and Ellesmere Island (*see* Jeletzky, 1973). The *Tollia* and *Temnoptychites* faunas are therefore the best known of all ammonites thus far recorded. *Platylenticeras* and/or *Pseudogarnieria* have not been found in the Sverdrup Basin but are known from Spitzbergen.

The nearest younger ammonite fauna on Amund Ringnes Island occurs 230 m stratigraphically higher than the *Tollia* and *Temnoptychites* beds mentioned above. It includes several specimens of *Polyptychites stubendorffi* (Schmidt) and allied forms, which is a very typical group of Arctic-Boreal polyptychitids, and one *Euryptychites* sp. A similar fauna occurs 20 m higher. *Polyptychites keyserlingi* (Neymayr and Uhlig) was not found but was previously found on Amund Ringnes Island (Jeletzky, 1973, Pl. 3, figs. 2a, b). Jeletzky (written comm., 1975) believes that *P. keyserlingi* may be restricted to younger beds containing *Prodichotomites* in association with *P. sphaeroidalis* Koenen (= *P. tschekanowskii* Pavlow) as it is associated with *P. sphaeroidalis* in an older collection (GSC loc. 82695).

After another unfossiliferous interval of 120 m, a layer of large sphaeroidal concretions with a different ammonite fauna occurs. This fauna is dominated by large-size *Prodichotomites* species. According to Jeletzky and the writer, these species are comparable and, in one instance [e.g. *Dichotomites* (*Prodichotomites*) *polytomus* (Koenen)], conspecific with some species from the Lower Saxonian Basin of northwest Germany (i.e. fauna of Hollwede). Jeletzky and the writer believe that the *Prodichotomites* lineage is a characteristically Arctic group of ammonites, which replaces in Arctic regions the lineage of the parallel-flanked, more slender, and mostly smaller *Dichotomites* (*Dichotomites*). *Prodichotomites* lineage evolves into forms with a shell which exhibits *Craspedites*-like features. However, these forms are olcostephanid homoeomorphs, which have nothing to do either with the craspeditids or with the early Valanginian *Neocraspedites*.

All "dichotomitids" figured in the Russian literature and all *Dichotomites* mentioned and figured from Arctic Canada (e.g. Jeletzky, 1973, p. 68, Pl. 2, figs. 1a-c) belong to this boreal *Prodichotomites* lineage. The branching off of the subgenus *Prodichotomites* Kemper (1973) from *Polyptychites* may be demonstrated in all details on the material of the German Hollwede locality.

Jeletzky and the writer wish to point out in this connection that the correlation of the above-mentioned Canadian *Prodichotomites* fauna with that of the Hollwede locality (and also with that of Spitzbergen; *see* below) is further strengthened by the presence at both localities of large, almost spherical *Polyptychites* forms referable to *Polyptychites sphaeroidalis* (Koenen, 1909) (= *P. tschekanowskii* Pavlow, 1914). Therefore, this fauna is correlative with that of the basal *Dichotomites* Beds of northwestern Germany as already recognized by Jeletzky (1973).

The next younger beds (Fig. 2) are characterized by large, discus-like ammonites which Jeletzky (1973) considers to be closely allied to but probably not conspecific with *Homolsomites quatsinoensis* (Whiteaves).

They are immigrants from the North Pacific Province of North America (Jeletzky, 1971) where they occur in the *Buchia crassicollis* Zone (Jeletzky, 1973). This species is still accompanied by *Buchia keyserlingi* (Lahusen). The definite identification of *Homolsomites* in the lower part of the upper Valanginian is significant, as many Russian workers are inclined to place the beds containing *Homolsomites* species (e.g. *H. bojarkensis* Shulgina) into the uppermost Valanginian or even into the lower Hauterivian (cf. Jeletzky, 1973, p. 73).

Buchia keyserlingi continues to exist in the basal part of the shales overlying the *Homolsomites*-bearing sequence. Still higher in the section, 70-90 m below the base of the Isachsen Formation, two young shells of *Dichotomites* (*Prodichotomites*) were collected which seem to belong to the same species group as the above-mentioned forms. There is no trace of Hauterivian fossils.

The previously discussed argillaceous sequence, which had thus far yielded only *Dichotomites* (*Prodichotomites*) and *Homolsomites* in the lower part, is about 140 m thick. The uppermost part of this shaly upper Valanginian sequence is rich in scattered "cannonball" concretions containing *Buchia* of the *B.* aff. *inflata-sublaevis* species group. In the upward direction, the sequence tends to become enriched in sandy inclusions.

Thorsteinssonoceras ellesmerensis Jeletzky was not found on Amund Ringnes Island but, in the Blackwelder Mountains, it occurs a few metres stratigraphically above the occurrences of *Temnoptychites novosemelica* (Sokolov). *Thorsteinssonoceras ellesmerensis* seems to be a species belonging in the upper part of the *Tollia* and *Temnoptychites* Beds (Fig. 2).

The presence of unfossiliferous intervals and an insufficient knowledge of ammonites within the report-area makes it impossible to formulate a sufficiently reliable zonal subdivision based on ammonites. However, the following preliminary and tentative downward subdivision of the Valanginian can be suggested at present:

3. *Prodichotomites* Beds (lower upper Valanginian)
   - *Prodichotomites* spp.
   - *Homolsomites* cf. *H. quatsinoensis* (Whiteaves)
   - *Polyptychites sphaeroidalis* (Koenen) (near the base)
   - ?*Polyptychites keyserlingi* (Neumayr and Uhlig) (near the base)
2. *Polyptychites* Beds (middle Valanginian)
   - *Polyptychites stubendorffi* (Schmidt) and allied forms
1. *Tollia* and *Temnoptychites* Beds (lower Valanginian)

Comparison of Profiles and Depositional History of Sverdrup Basin

A comparison of measured profiles is made difficult by the absence or poor preservation of fossils. Some important conclusions are possible, however, especially those concerning the presence of hiatuses in the Berriasian and the changes of thicknesses of the upper Deer Bay Formation between the central part of the basin and its eastern margin. Thorsteinsson and Tozer's (1970, p. 581) suggestion that sedimentation was continuous through the Late Jurassic and early Early Cretaceous does not agree with the results obtained by the writer. These results, however, explain Jeletzky's (1973, Fig. 2) observation of a total absence of late Berriasian index fossils in Sverdrup Basin.

A complete section of the Berriasian could be expected in the central part of the basin on Amund Ringnes Island. Unfortunately there was no opportunity to extend the measuring and bed-by-bed collecting of the Valanginian profile on Amund Ringnes Island down into the Berriasian rocks. In the eastern marginal parts of the basin (Fig. 2), the Berriasian is either absent or only incompletely represented.

The presence of the Berriasian remains unproven in Reptile Creek (Fig. 1, No. 4). In this section, it may either be absent entirely or represented by less than about 20 m of silty and unfossiliferous shale. A similar stratigraphic situation occurs in the Blackwelder Mountains (Fig. 1, No. 5). There, a bed of brownish grey shale with silt and sand inclusions, about 3 m thick, occurs at the same level. It may be interpreted as a transgressive basal bed of either latest Berriasian or more likely earliest Valanginian on the Late Jurassic.

Unlike the unfossiliferous localities described above, the profile south of Buchanan Lake (Fig. 1, No. 2) yielded a rich but poorly preserved fauna. There the beds with *Tollia* spp. and *Buchia keyserlingi* Lahusen occur only a few metres stratigraphically above the beds with *Praetollia antiqua* Jeletzky and the latest Jurassic or earliest Berriasian *Buchia* species. Jeletzky (1973, p. 47, 50, 52, Fig. 3; and pers. comm., 1975) maintains that the lower Berriasian *Buchia okensis sensu stricto* and *Craspedites* (?*Subcraspedites*) aff. *C. suprasubditus* fauna occurs between the uppermost Jurassic *Praetollia antiqua* Jeletzky bed and the Valanginian beds with *Tollia* spp. and *Buchia keyserlingi* in the Buchanan Lake sections, including those measured by the writer. Therefore, it is necessary to suggest a transgression of the lower Valanginian upon the lowermost Berriasian or on the transition beds Berriasian/upper Volgian. It should be noted in this connection that thick units of the lower Valanginian exhibit a considerable admixture of silt particles in this profile.

The conditions described above also permit a logical interpretation of observations made in the profile of the Whitsunday Bay Anticline (Fig. 1, no. 3) which is situated about 20 km southeast of the Buchanan Lake profile (loc. 2). There, a sandstone succession with some thick layers of clay-ironstone concretions was placed in the Isachsen Formation. These sands overlie the Deer Bay shale, the highest beds of which have yielded the latest Late Jurassic *Buchia* species. If the lowermost sands of the Whitsunday Bay Anticline can be correlated with the silty shales of the previous locality, as is suggested by the available fossils, the lower sandstone sequence of the Whitsunday Bay Anticline has to

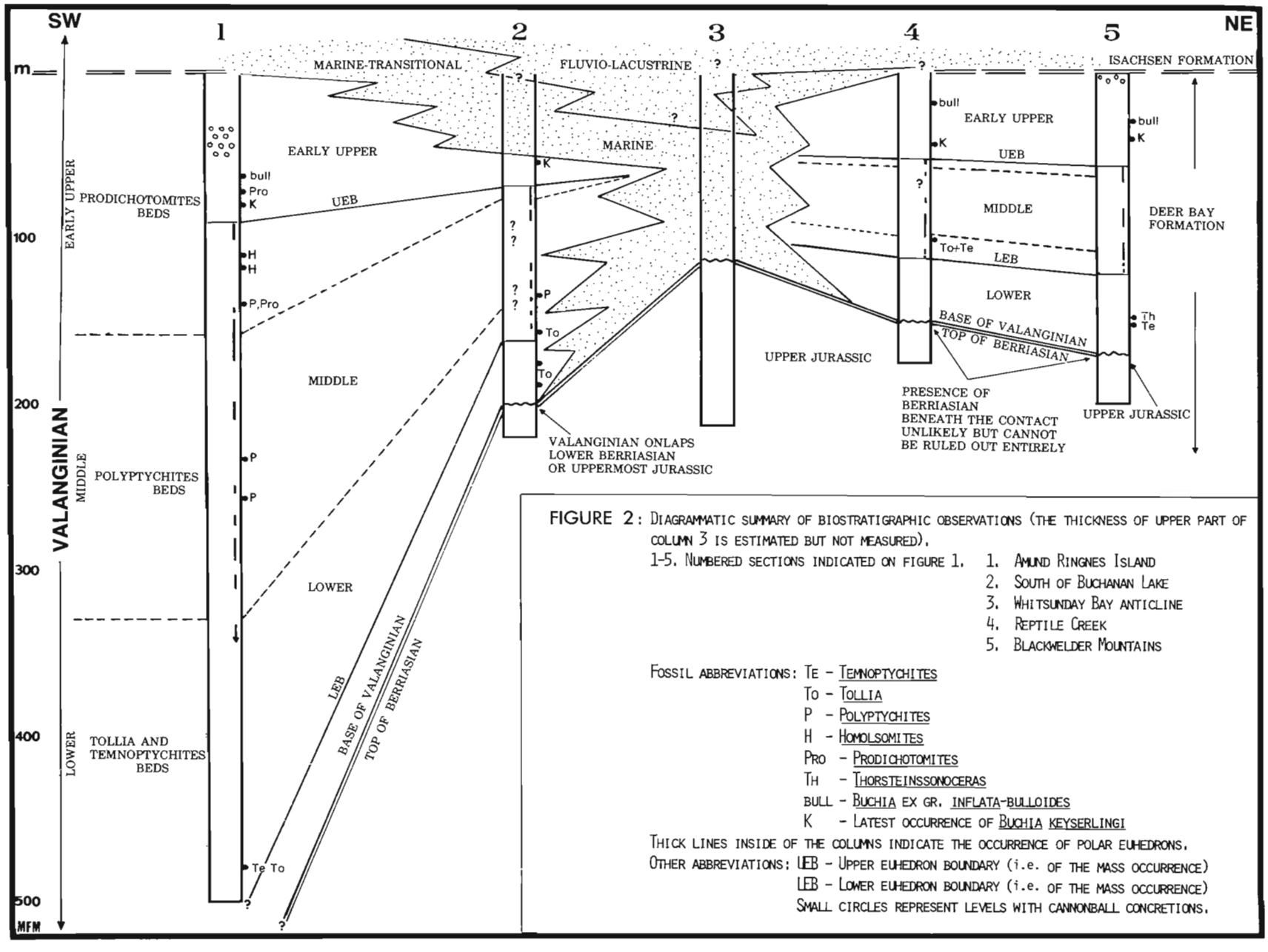

FIGURE 2: DIAGRAMMATIC SUMMARY OF BIOSTRATIGRAPHIC OBSERVATIONS (THE THICKNESS OF UPPER PART OF COLUMN 3 IS ESTIMATED BUT NOT MEASURED).

1-5. NUMBERED SECTIONS INDICATED ON FIGURE 1.

1. AMUND RINGNES ISLAND
2. SOUTH OF BUCHANAN LAKE
3. WHITSUNDAY BAY ANTICLINE
4. REPTILE CREEK
5. BLACKWELDER MOUNTAINS

FOSSIL ABBREVIATIONS: TE - TEMNOPTYCHITES
TO - TOLLIA
P - POLYPTYCHITES
H - HOMOLSOMITES
PRO - PRODICHOTOMITES
TH - THORSTEINSSONOCERAS
BULL - BUCHIA EX GR. INFLATA-BULLOIDES
K - LATEST OCCURRENCE OF BUCHIA KEYSERLINGI

THICK LINES INSIDE OF THE COLUMNS INDICATE THE OCCURRENCE OF POLAR EUHEDRONS.

OTHER ABBREVIATIONS: UEB - UPPER EUHEDRON BOUNDARY (i.e. OF THE MASS OCCURRENCE)
LEB - LOWER EUHEDRON BOUNDARY (i.e. OF THE MASS OCCURRENCE)
SMALL CIRCLES REPRESENT LEVELS WITH CANNONBALL CONCRETIONS.

be interpreted as a sandy, near coastal facies of the Valanginian which overlaps transgressively the argillaceous Upper Jurassic rocks (Fig. 2). Higher in the profile, the grain sizes revert to silt to fine sand values. Therefore, the basal transgressive sand in the Whitsunday Bay Anticline appears to correspond to the sandstone member, about 40 m thick, which was mentioned by Tozer (1963, p. 25) from the middle part of the Deer Bay Formation on southern Axel Heiberg Island (Glacier Fiord area).

In this context, the following conclusion of Thorsteinsson and Tozer (1970, p. 582) acquires a new meaning: *The fossil record for the Mould Bay Formation of Prince Patrick Island is far less complete than that for the Deer Bay shales for it includes only Lower Volgian and Upper Valanginian. Upper Volgian, Berriasian, and much of Valanginian time are not demonstrably represented.*

In contrast with the incomplete development of the Berriasian, or even its absence, the Valanginian part of the Deer Bay Formation is completely developed everywhere in the area. Thicknesses of more than 500 m occur in the central part of the basin (Amund Ringnes Island). These thicknesses decrease to between 150 and 200 m in eastern Axel Heiberg Island and western Ellesmere Island (Fig. 2).

According to Thorsteinsson and Tozer (1970, p. 581, Fig. x-12), great thicknesses appear to be present in the western part of Axel Heiberg Island as the total thickness of Deer Bay shale there is stated to be about 900 m. Figure 2 clearly indicates prominent variations in thickness of the total Deer Bay shale on Axel Heiberg Island. The data available indicate the presence of a depositionally positive region with a westward convexity of the shoreline in the area of southeastern Axel Heiberg Island (Fig. 1). In the eastern marginal areas of Sverdrup Basin, uplifts of Berriasian time were accompanied by interruptions of deposition and/or erosion. These uplifts were followed by a transgressive deposition of lower Valanginian sands or silts. The presence of *Buchia* cf. *B. keyserlingi* within the sandstones on southern Axel Heiberg Island (Tozer, 1963, p. 63) indicates that this transgression has definitely occurred in this area in the early Valanginian. This transgression possibly occurred somewhat later in the region of the Whitsunday Bay Anticline.

It has been suggested that the actual upper boundary of the Valanginian occurs within the Isachsen Formation (Jeletzky, 1973). The position of the boundary cannot be recognized there because of the absence of reliable fossils. Because of the absence of ammonites in the uppermost Deer Bay shales and the presence there of only a few unstudied *Buchia*, it is difficult also to date definitively the time of appearance of the Isachsen facies; that is, the regressive sand facies. Such an analysis is made more difficult moreover by the polygenetic nature of this sand facies, which extends from the marine coastal sand to the fluvio-lacustrine deposits with coal seams (Fig. 2). As is indicated on Figure 2, based on latest occurrences of *Buchia* ex gr. *B. keyserlingi:* absence of *B.* ex gr. *B. inflata-bulloides* : bull, -UEB boundary and absence of the "cannonball" member, the sand facies appeared early in the east (Ellesmere and eastern Axel Heiberg islands) within the previously mentioned positive region. It was followed apparently by a migration of the sand facies toward the centre of the basin, to Amund Ringnes Island and Blackwelder Mountains.

The lower sands of the Isachsen Formation are marine and transitional to the uppermost beds of Deer Bay Formation, at least south of Buchanan Lake and on Amund Ringnes Island. During the temporal migration of sand facies toward the central part of the basin, the deposition of littoral marine sands preceded that of the fluvio-lacustrine sands. In the east (e. g. at the Fosheim Anticline and at Reptile Creek?), however, the fluvio-lacustrine sediments may overlie the Deer Bay shale with an erosional-transgressive contact.

Interregional Correlation

Because endemic developments seem to be either absent or insignificant in the Sverdrup Basin, one would expect that evidence for faunal connections with adjacent marine basins would be apparent (Jeletzky, 1971, 1973). Since the relationships with the Yukon region and with the Pacific regions of North America have been discussed comprehensively by Jeletzky (1973), the writer will concentrate on the comparison of Sverdrup Basin faunas and stratigraphy with those of Spitzbergen. The Valanginian ammonite fauna of Spitzbergen was analyzed earlier by Frebold (1929) whose conclusions must naturally be brought up to date.

The lower Lower Cretaceous of Spitzbergen is not only characterized by close faunal relationships with that of the Sverdrup Basin but lithostratigraphical development within the two regions also is similar. This conclusion may lend support to ideas that Spitzbergen and Ellesmere Island were proximal in the early Early Cretaceous as postulated by theoreticians of continental drift (e. g. Bullard *et al.*, 1965, Fig. 7; Callomon *et al.*, 1972, Fig. 8).

After the older workers introduced the very appropriate term "*Aucella* shales" (*Aucella* = *Buchia*) for a succession of dark grey shales equivalent to the Deer Bay Formation, numerous formation and member names have been recently introduced for rock units of Spitzbergen (e. g. Parker, 1967). The name "Rurikfjellet Formation" was, for example, introduced for the Valanginian part of "*Aucella* shales". Comprehensive data about lithostratigraphy of the beds concerned have been provided by Hoel and Orvin (1937) and Pchelina (1965a, b).

The Rurikfjellet Formation transgressively overlies older beds, predominantly those of the Volgian Stage. The older Valanginian beds contain, just as they do in Sverdrup Basin, dark grey shales that split into fine lamellae. The content of silty particles fluctuates but the content of silt and sand particles generally increases upward. Beds with clay-ironstone concretions are common. According to Pchelina (1965a), "stellate nodules of anthracolite are highly characteristic" of the higher beds (?) of the formation. These

nodules are, without doubt, polar euhedrons! The exposures were probably poor because these nodules were not observed in the older beds of the formation. Furthermore, "cannonball" concretions occur in the uppermost beds of the unit just as they do in the Sverdrup Basin. Judging by the sparse information provided by Pchelina (1965a), the lithostratigraphy of the Rurikfjellet Formation exhibits an extraordinary similarity with that of the Sverdrup Basin Valanginian. Some faunal data are contradictory, but they can be interpreted differently than was done by Pchelina (ibid.). The presence of *Buchia crassicollis* (Keyserling) really does not represent a contradiction, as this fossil could have been derived from the youngest part of the "bituminous siltstone" (Pchelina, 1965b). However, the identification of "*Simbirskites* ex gr. *decheni*" makes a comparison with Sverdrup Basin difficult. Exact identification evidently was impossible and poorly preserved fossils of that type could have actually belonged to the misidentified inner whorls of *Polyptychites sphaeroidalis* (Koenen). A Hauterivian age for beds with scattered "cannonball" concretions occurring on Spitzbergen therefore can be considered improbable. It should be noted in this connection that the fossil data are extremely scarce in the modern literature on the lower Lower Cretaceous of Spitzbergen. This contrasts strongly with the older literature (*see* especially Frebold, 1929; Frebold and Stoll, 1937; Sokolov and Bodylevsky, 1931; Hoel and Orvin, 1937).

The Valanginian ammonite faunas of Sverdrup Basin and Spitzbergen appear to be identical, so far as known (e.g. Frebold, 1929; Sokolov and Bodylevsky, 1931). *Polyptychites* species, including *P.* ex gr. *P. stubendorffi* (Schmidt), among others, characterize the middle Valanginian of both regions while the representatives of *Prodichotomites* lineage characterize the upper Valanginian. *Polyptychites sphaeroidalis* Koenen characterizes the basal part of the upper Valanginian in both regions.

The re-interpretation of the fossil content of the lower Valanginian is more difficult because only a few illustrations of fossils are available. As pointed out by Jeletzky (written comm., 1975), the occurrence of previously misidentified *Thorsteinssonoceras ellesmerensis* on Spitzbergen (*see* Jeletzky, 1965, p. 12) attests to the presence there of beds correlative with the upper part of *Temnoptychites* beds of Sverdrup Basin. The presence on Spitzbergen of beds equivalent to *Tollia* and *Temnoptychites* beds of Sverdrup Basin also is indicated by the mention of the *Stenomphala* Zone containing *Temnoptychites* and *Peregrinoceras* species by Hoel and Orvin (1937). Most diagnostic of the presence of the older Valanginian beds on Spitzbergen is the presence of widely umbilicated polyptychitids (Frebold and Stoll, 1937; Hoel and Orvin, 1937) and also that of *Platylenticeras* (or *Pseudogarnieria*?) species (Sokolov and Bodylevsky, 1931, p. 26). The presence of *Platylenticeras* and some *Polyptychites* species strongly indicate the existence of connections with middle European basins.

It is these lower Valanginian beds which onlap the Volgian beds and those of other systems on Spitzbergen. The Berriasian either is primarily absent or subsequently was destroyed. Jeletzky (1964, p. 34, Pl. III, figs. 1, 3; pers. comm., 1975) maintains, however, that "*Polyptychites*" *hoeli* Frebold 1929 is an early Berriasian craspeditid closely related to *Craspedites* (?*Subcraspedites*) aff. *C. suprasubditus* (Bogoslowsky) of the Sverdrup Basin. The early Valanginian transgression recognized in the marginal areas of the Sverdrup Basin (*see* previous section of this paper) therefore is present also on Spitzbergen. This transgression apparently was a very important event in the Arctic depositional basins. However, one has to take into consideration that the Spitzbergen basin was characterized by a marginal depositional environment. It must be assumed that the Berriasian was represented fully in the central parts of the Arctic sedimentary basins. The Cretaceous transgression began in the Berriasian, as indicated, in particular, by observations in East Greenland (Surlyk, 1973, p. 89). This transgression then reached its acme in the Valanginian. As in Spitzbergen, only the western marginal region of the basin of East Greenland and Scandinavia is available for study in Greenland; it is characterized by shelf environment with coastal and shallow neritic environments.

Our knowledge of the Valanginian in East Greenland is still very sparse. Donovan (1953) described an early Valanginian ammonite fauna from Traill Island which was placed more recently in the latest early Valanginian by Jeletzky (1973, p. 67). The latest interpretation of the Valanginian record is provided by Donovan (1964, p. 11). The Berriasian was, in contrast, intensively studied recently (Surlyk, 1973). A good review of the paleogeographical situation was provided by Donovan (*in* Callomon *et al.*, 1972, Fig. 8). These workers have made an important observation of such southern ammonite genera as *Phylloceras, Lytoceras,* etc. in the region. The Valanginian faunas of Greenland are, therefore, transitional to the southern faunas, as should have been expected by their paleogeographical position.

As stressed by Frebold (1951, p. 134, 135) and Jeletzky (1961, p. 539, 543), another extremely important common feature of Arctic Early Cretaceous basins is the occurrence of a strong and widespread regression, which began in the late Valanginian and was accompanied by an increase of temperature. This regression had resulted locally in the erosion and nondeposition (e.g. East Greenland) in Hauterivian and Barremian time. Elsewhere it caused the deposition of paludal sediments during the Hauterivian and Berremian; for example the Isachsen Formation (Sverdrup Basin) or Helvetiafjellet Formation (Spitzbergen). The marine deposition was resumed only in the Aptian.

Only marginal areas of the Early Cretaceous depositional basins characterized by the absence or incompleteness of the Berriasian and, in part, by thin and sandy facies of the Valanginian are preserved in Spitzbergen, East Greenland, and Ellesmere Island. The thick succession of correlative beds outcropping in the central part of Sverdrup Basin is, therefore, of decisive importance for the understanding of the Lower Cretaceous

stratigraphy of the Arctic, especially as this very succession contains well-preserved ammonite faunas. The investigation of the Berriasian in this area (e. g. on Ellef Ringnes and Amund Ringnes islands) would have been of particular importance, because insufficient scattered observations are available about these rocks in the central part of Sverdrup Basin. Additional investigations in the Valanginian part of Deer Bay Formation of the area are likewise needed.

References

Bullard, E., Everett, J.E. and Smith, A.G.
1965: The fit of the continents around the Atlantic; Roy. Soc. London, Phil. Trans., 258, ser. A, no. 1088, p. 41-51.

Callomon, J.H., Donovan, D.T. and Trümpy, R.
1972: An annotated map of the Permian and Mesozoic Formations of East Greenland; Medd. om Grønland, v. 168, no. 3, p. 1-35.

Donovan, D.T.
1953: The Jurassic and Cretaceous stratigraphy and palaeontology of Traill Ø, East Greenland; Medd. om Grønland, v. 111, no. 4, p. 1-150.

1964: Stratigraphy and ammonite fauna of the Volgian and Berriasian rocks of East Greenland; Medd. om Grønland, v. 154, no. 4, p. 1-34.

Frebold, H.
1929: Ammoniten aus dem Valanginien von Spitzbergen; Skrift. Svalbard Ishavet, v. 21, p. 1-24.

1951: Geologie des Barentsschelfes; Abhandl. Deutsch. Akad. Wiss. Berlin, Kl. Math. u. allg. Naturwiss. Jahrg 1950, no. 5, Abhandl. zur Geotektonik no. 4.

Frebold, H. and Stoll, E.
1937: Das Festungsprofil auf Spitzbergen. III. Stratigraphie und Fauna des Jura und der Unterkreide; Skrift. Svalbard Ishavet, v. 68, p. 1-85.

Heywood, W.W.
1957: Isachsen area, Ellef Ringnes Island, District of Franklin, Northwest Territories; Geol. Surv. Can., Paper 56-8.

Hoel, A. and Orvin, A.K.
1937: Das Festungsprofil auf Spitzbergen, Karbon-Kreide; I. Vermessungs-resultate; Skrift. Svalbard Ishavet, v. 18, p. 1-57.

Jeletzky, J.A.
1961: Eastern slope, Richardson Mountains: Cretaceous and Tertiary structural history and regional significance; Geol. of the Arctic, Proc. 1st Int. Symp. on Arctic geology, v. 1, p. 532-583.

Jeletzky, J.A. (cont'd.)
1964: Lower Cretaceous marine index fossils of the sedimentary basins of western and Arctic Canada; Geol. Surv. Can., Paper 64-11.

1965: *Thorsteinssonoceras*; a new craspeditid ammonite from the Valanginian of Ellesmere Island, Arctic Archipelago; Geol. Surv. Can., Bull. 120.

1971: Marine Cretaceous biotic provinces and paleogeography of western and Arctic Canada: illustrated by a detailed study of ammonites; Geol. Surv. Can., Paper 70-22.

1973: Biochronology of the marine boreal latest Jurassic, Berriasian and Valanginian in Canada *in* The boreal Lower Cretaceous (Casey, R. and Rawson, P.F., eds.); Liverpool, p. 41-80.

Kemper, E.
1971: Zur Abgrenzung und Unterteilung des Valanginium ("Valendis"); Newsl. Stratigr., v. 1, no. 4, p. 45-58.

1973: The Valanginian and Hauterivian stages in northwest Germany *in* The boreal Lower Cretaceous (Casey, R. and Rawson, P.F., eds.); Liverpool, p. 327-344.

Kemper, E. and Schmitz, H.H.
1975: Stellate nodules (polar-marine mud euhedrons) from the upper Deer Bay Formation (Valanginian) of Arctic Canada; Geol. Surv. Can. (In preparation.)

Parker, J.R.
1967: The Jurassic and Cretaceous sequence in Spitzbergen; Geol. Mag., v. 104, no. 5, p. 487-505.

Pchelina, T.M.
1965a: Stratigraphy and composition of the Mesozoic deposits in central Westspitzbergen *in* Geology of Spitzbergen (V.N. Sokolov, ed.), Leningrad, v. 1, p. 131-154 (in Translation of National Lending Library).

1965b: Mesozoic deposits around Van Keulenfjorden Westspitzbergen *in* Geology of Spitzbergen (V.N. Sokolov, ed.); Leningrad, v. 1, p. 155-180 (in Translation of National Lending Library).

Sokolov, D.N. and Bodylevsky, V.I.
1931: Jura-und Kreidefaunen von Spitzbergen; Skrift. Svalbard Ishavet., v. 35, p. 1-151.

Surlyk, F.
1973: The Jurassic-Cretaceous boundary in Jameson Land, East Greenland *in* The boreal Lower Cretaceous (Casey, R., and Rawson, P.F., eds.); Liverpool, p. 81-100.

Thorsteinsson, R. and Tozer, E. T.
1970: Geology of the Arctic Archipelago *in* Geology and economic minerals of Canada; Geol. Surv. Can., Econ. Geol. Rept. No. 1, p. 549-590.

Tozer, E. T.
1963: Mesozoic and Tertiary stratigraphy, western Ellesmere Island and Axel Heiberg Island, District of Franklin; Geol. Surv. Can., Paper 63-30.

54. CORRELATION OF LOWER PALEOZIC SUBSURFACE SECTIONS, DEVON, CORNWALLIS, AND SOMERSET ISLANDS, DISTRICT OF FRANKLIN

Ulrich Mayr

Institute of Sedimentary and Petroleum Geology, Calgary

The stratigraphy of several wells in the eastern Arctic Islands is under study. Results for Imp. IOE Panarctic *et al.* Devon E-45, Panarctic Deminex Cornwallis Central Dome K-40, Lobitos *et al.* Resolute Bay L-41, and Panarctic Deminex Garnier O-21 are summarized in Figure 1. The correlations are based to a large degree on macro- and microfossils obtained from the wells.

Core 6 at the bottom of the Cornwallis Central Dome well yielded Upper Cambrian trilobites (identifications by W.H. Fritz) and the section below 5327 feet (1624.7 metres) has been assigned to the Parrish Glacier Formation. The top of the formation is drawn above a red and green shale interval; this is similar to field practice of J.Wm. Kerr (pers. comm.) on Grinnell Peninsula. The Gallery Formation is presumed to be at least partially of Late Cambrian age and to correlate in part with the Parrish Glacier Formation.

The upper part of the Turner Cliffs Formation in the Garnier well yielded Lower Ordovician conodonts, thus indicating its correlation with the Copes Bay Formation. Equivalents of the Baumann Fiord Formation probably are not present in the well and in the Admiralty Inlet area, and the contact between the Turner Cliffs and Ship Point formations is considered to be a disconformity.

The Bay Fiord, Thumb Mountain, Irene Bay, and Allen Bay formations can be traced into the Garnier well and are recognizable as subdivisions (Trettin, 1969, p. 30, 33) of the Baillarge Formation. The relationships are listed below in Table 1. The change from the formations of the Cornwallis Island area to the Baillarge Formation is a change in stratigraphic nomenclature and is indicated as a straight, dashed line on Figure 1.

Conodonts from the upper part of the Garnier well are presently being processed, so the relationships between the Leopold – Cape Crauford and Read Bay – Cape Storm Formations are not known with certainty. The upper boundary of the Cape Storm Formation is gradational and shown as a facies change on Figure 1. The age range of the facies change appears to be limited to early Ludlow.

Reference

Trettin, H.P.
1969: Lower Palaeozoic sediments of northwestern Baffin Island, District of Franklin; Geol. Surv. Can., Bull 157.

Table 1

Cornwallis Island	Panarctic Deminex Garnier O-21 Feet (Metres)	Admiralty Inlet
Allen Bay Fm.	2674 - 4150 (815.6 - 1265.8)	Baillarge Formation Member B, units 7-3
Irene Bay Fm.	4150 - 4216 (1265.8 - 1285.9)	Baillarge Formation Member B, unit 2
Thumb Mountain Fm.	4216 - 4594 (1285.9 - 1401.2)	Baillarge Formation Member B, unit 1
Bay Fiord Fm. (part)	4594 - 5238 (1401.2 - 1597.6)	Baillarge Formation Member A

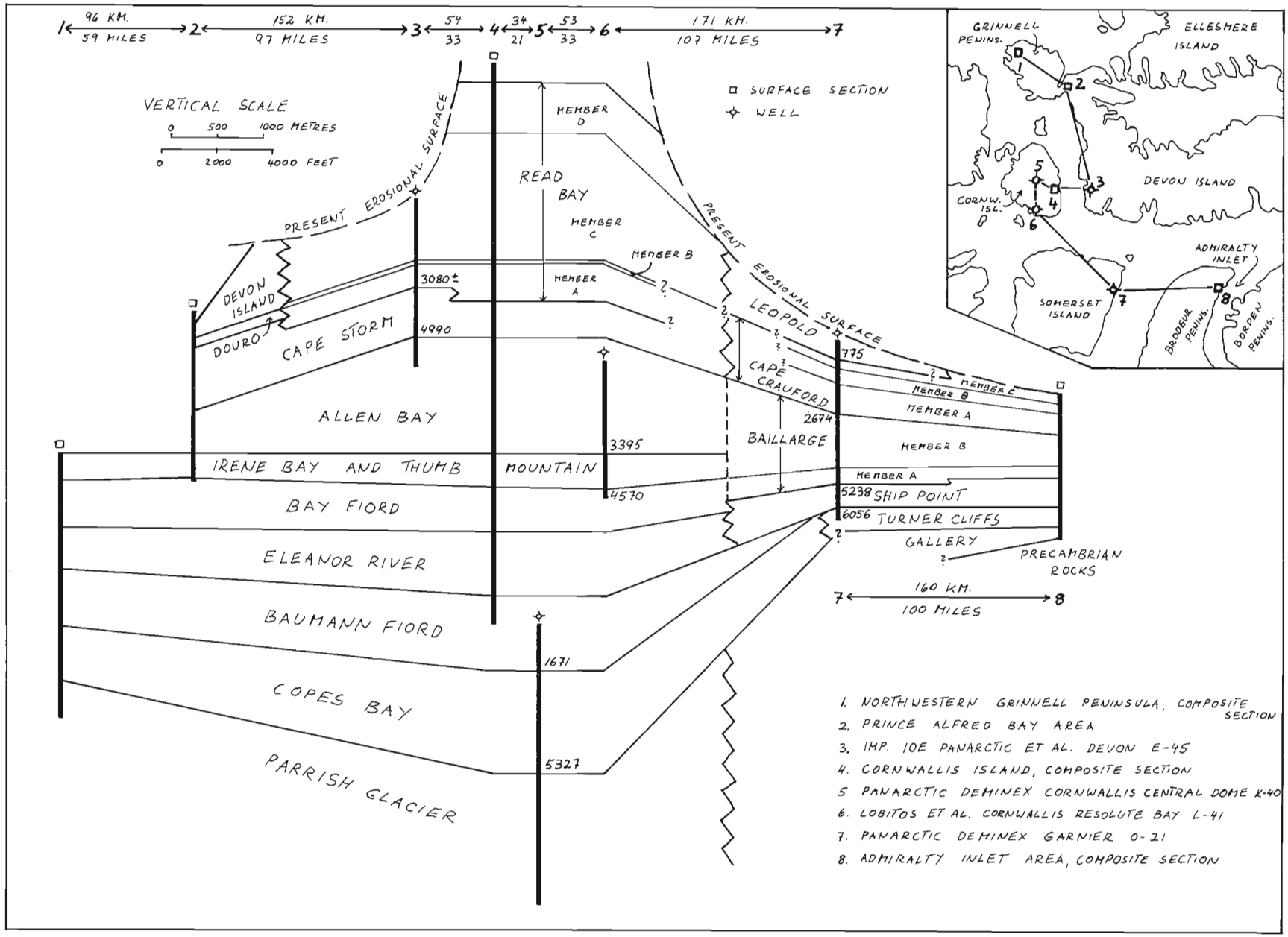

Figure 1. Generalized stratigraphic cross-section, Grinnell Peninsula to Admiralty Inlet area.

55. STRATIGRAPHY OF THE DEMINEX CGDC FOC AMOCO ORKSUT I-44 WELL

Project 720061

Andrew D. Miall
Institute of Sedimentary and Petroleum Geology, Calgary

Introduction

This well, at 72°24'N and 122°42'W, was the fourth well to be drilled on Banks Island. It was released from confidential status on March 28th, 1975. Samples and cores have been logged by the writer and a number of palynological and micropaleontological determinations have been obtained for different levels in the well. A summary of the stratigraphy is given below. The stratigraphy of the three earlier wells are described by Miall (1974a, b) and these data have been incorporated into regional syntheses covering the entire Banks Island area (Miall, in press; in prep.).

Paleozoic Stratigraphy

The lower 4100 feet (1250 m) of the section at the Orksut well consists of Paleozoic strata. Four units have been recognized; all are Devonian in age with the possible exception of the oldest, which may be all, or in part, of Silurian age. Tops, depths and thicknesses of these units are given in Table 1.

The unnamed dolomite formation consists of 322 feet (98 m) of very fine grained, medium to dark brown grey, argillaceous, dense, dolomite. The overlying unit is 164 feet (50 m) thick; it is similar in lithology but includes shale interbeds. Channel samples were taken from the unwashed cuttings in both units and processed for conodonts by T.T. Uyeno, with little success. The age of the two unnamed formations is therefore unknown. Their stratigraphic position beneath the Blue Fiord Formation suggests an Early Devonian age, with the earliest beds possibly as old as Late Silurian.

The Blue Formation consists of 2269 feet (692 m) of limestone and dolomite, with minor intercalated shale beds near the top of the formation. The upper 300 feet (100 m) consists predominantly of pale to medium brown-grey limestone containing brachiopods, *Tentaculites* and *Styliolina*. Below a depth of 7600 feet (2320 m), dolomite rhombs are present; these increase in abundance downward and, below 7800 feet (2380 m), the formation consists almost exclusively of dolomite. Several channel samples were taken from the section

Table 1

Table of formations in the Orksut I-44 well

Age	Formation	Member	log depth feet (metres)	subsea elevation feet (metres)	thickness feet (metres)
Miocene-recent	Beaufort and surficial deposits		0 (0)	448 (137)	553 (169)
Paleocene-Eocene	Eureka Sound	sand-shale mbr.	553 (169)	-105 (-32)	1 857 (566)
		shale mbr.	2 410 (734)	-1 962 (-598)	600 (183)
Campanian-Maastrichtian	Kanguk	upper ss. mbr.	3 010 (917)	-2 562 (-781)	45 (14)
		upper shale mbr.	3 055 (931)	-2 607 (-795)	835 (254)
		lower ss. mbr.	3 890 (1 186)	-3 442 (-1 049)	96 (29)
		lower shale mbr.	3 986 (1 215)	-3 538 (-1 078)	244 (74)
		spherulitic carbonate	4 230 (1 289)	-3 782 (-1 153)	trace
Albian	Christopher		4 230 (1 289)	-3 782 (-1 153)	140 (43)
Aptian	Isachsen		4 370 (1 332)	-3 922 (-1 195)	313 (95)
Oxfordian-Valanginian	Mould Bay		4 683 (1 427)	-4 235 (-1 291)	657 (200)
Bajocian-Oxfordian	Wilkie Point		5 340 (1 628)	-4 892 (-1 491)	660 (201)
Eifelian-Givetian	Orksut		6 000 (1 829)	-5 552 (-1 693)	1 285 (392)
?Siegenian-Eifelian	Blue Fiord		7 285 (2 221)	-6 837 (-2 084)	2 269 (692)
Lower Devonian	unnamed dolomite-shale		9 554 (2 913)	-9 106 (-2 776)	164 (50)
?Silurian-Devonian	unnamed dolomite		9 718 (2 963)	-9 270 (-2 826)	322 (98)
		TD	10 040 (3 061)	-9 592 (-2 924)	

and analyzed for conodonts, but only one sample yielded sufficient identifiable material for an age to be assigned. This was a sample from the interval between 9010 and 9110 feet (2746-2777 m), dated by T.T. Uyeno as Emsian, probably late Emsian. Based on regional stratigraphic correlations (Miall, in prep.), the formation is assigned a ?Siegenian to Eifelian age range.

The uppermost 1285 feet (392 m) of Paleozoic beds at the Orksut well are assigned to a new unit, the Orksut Formation, as defined in Miall (in prep.). Shale is the predominant rock type. It is dark grey, variably silty, variably calcareous, slightly micaceous, and contains minor amounts of disseminated pyrite. Thin intercalated beds of dark grey, argillaceous limestone are present at the top of the succession. Palynological samples from the topmost beds have yielded a Givetian, probably late Givetian age (identifications by D.C. McGregor), and the formation is assigned an Eifelian to Givetian age range at this locality. The Orksut is, therefore, a stratigraphic equivalent of part of the Melville Island Group.

Mesozoic and Tertiary Stratigraphy

The Jurassic Mould Bay and Wilkie Point formations are recognized on the basis of foraminiferal identifications by T.P. Chamney. Both units are much more argillaceous than in their type areas. The Wilkie Point Formation consists of 660 feet (201 m) of silty, dark grey, slightly calcareous shale with minor interbeds of dark grey, argillaceous, slightly glauconitic siltstone. A clean, quartzose sandstone, 50 feet (15 m) in thickness, occurs at the base of the succession. The Mould Bay Formation consists of 657 feet (200 m) of medium grey to grey green, silty, slightly micaceous, noncalcareous shale. Pyrite is a common accessory. Foraminifera and pelecypod fragments are abundant in both the Jurassic units.

The Cretaceous Isachsen Formation comprises interbedded sandstone, siltstone and shale with minor coal beds. The sandstone is medium to very coarse grained and pebbly, quartzose, and pale in colour. Gamma ray log interpretation suggests the presence of fining-upward cycles, probably fluvial in origin, and the whole formation appears to become finer upward from pebbly sandstone at the base to silty shales at the top. The lithologic assemblage is similar to that present at the surface in parts of southern Banks Island, especially the Sandhill River area, but contains a considerably higher percentage of argillaceous and silty beds than does the Isachsen in southeastern and northern Banks Island. These differences are discussed further in Miall (in press).

The interval between 3986 and 4254 feet (1215-1297 m) was provisionally assigned to the Lower Cretaceous Christopher Formation by Miall (in press). However, further work has shown that most of this part of the succession is Late Cretaceous in age and should be re-assigned to the Kanguk Formation. J.H. Wall states that there are no Early Cretaceous foraminifera in the beds above the Isachsen Formation. Traces of a spherulitic carbonate lithology were found in the cuttings at a depth of 4230 feet (1289 m) and this may represent the same unit that occurs at the Upper-Lower Cretaceous contact in the subsurface of western Banks Island (Miall, 1974c). The shale immediately above the carbonate horizon is slightly bentonitic, which suggests a correlation with the basal bituminous member of the Kanguk Formation. For these reasons, the base of the Kanguk is placed now at a depth of 4230 feet (1289 m).

The Christopher Formation is represented by 140 feet (43 m) of beds, if this interpretation is correct. It will be observed from geophysical logs that the upper 24 feet (7 m) of this interval are shale, and are characterized by slightly greater gamma ray readings and a slightly lower resistivity than the overlying Kanguk Formation. Sandstone and siltstone, with traces of glauconite, occur in the middle of the formation. An Albian, possibly Late Albian age has been indicated by W.S. Hopkins, Jr. from palynological samples taken from a core through these sandy beds.

Throughout Banks Island, the Christopher-Kanguk contact is a disconformity. It would seem that, at the Orksut well, mid-Cretaceous erosion was more than usually pronounced, and that only a thin erosional remnant of the Christopher Formation remains. The Hassel Formation is absent.

The Kanguk Formation is 1220 feet (372 m) thick; it consists predominantly of shale, but two sandstone members also are present. The shale is pale grey, slightly silty, calcareous to noncalcareous, slightly micaceous, slightly glauconitic. Pyrite and siderite are present throughout. The lower sandstone unit comprises very fine grained, pale grey sandstone with interbeds of dark grey, micaceous shale; the upper sandstone member consists of very fine grained sandstone with argillaceous siltstone. The lower sandstone member is correlated tentatively with the sandstone unit in the lower part of the Kanguk Formation at the Uminmak well (Miall, 1974c). The upper sandstone member is correlated with the "white sand" of Jutard and Plauchut (1973). J.H. Wall reports the presence in the Kanguk Formation of a foraminiferal succession ranging in age from Campanian to Maastrichtian.

The Eureka Sound Formation consists of similar rock types to those present in Northern Banks Basin. There is a lower shale and silty shale member and an upper member comprising sand, shale, silt and coal. Much of the succession is marked by coarsening-upward cycles similar to those present in surface exposures and in the subsurface of western Banks Island (Miall, in press). The lower shale member was sampled for foraminifera by J.H. Wall, with no success. The unit probably is largely nonmarine, as reported by Jutard and Plauchut (1973).

The upper 553 feet (169 m) of beds comprise coarse gravels, sand and soft mudstone. No geophysical logs are available for these uppermost beds, and the writer was not able, from cuttings alone, to separate the Beaufort Formation from surficial deposits. Both are presumed to be present.

References

Jutard, G. and Plauchut, B.P.
1973: Cretaceous and Tertiary stratigraphy northern Banks Island *in* Proceedings of the Symposium on the Geology of the Canadian Arctic, Aitken, J.D., eds.; Geol. Assoc. Can. and Can. Soc. Pet. Geol., p. 203-219.

Miall, A.D.
1974a: Stratigraphy of the Elf *et al.* Storkerson Bay A-15 well; *in* Report of Activities, April to October 1973, Geol. Surv. Can., Paper 74-1, Pt. A, p. 335-336.

1974b: Subsurface geology of western Banks Island; *in* Report of Activities, November 1973 to March 1974, Geol. Surv. Can., Paper 74-1, Pt. B, p. 278-281.

Miall, A.D. (cont'd.)
1974c: Manganese spherulites at an intra-Cretaceous disconformity, Banks Island, Northwest Territories; Can. J. Earth Sci., v. 11, p. 1704-1716.

Post-Paleozoic geology of Banks, Prince Patrick and Eglinton Islands, Arctic Canada; *in* Can. Soc. Pet. Geol., Mem. 4. (in press)

Proterozoic and Paleozoic geology of Banks Island, Arctic Canada; Geol. Surv. Can., Bull. (available as Open File Report 260). (in prep.)

56. THE FLORIDA AQUIFER: A POSSIBLE MODEL FOR A DEVONIAN PALEOAQUIFER IN NORTHEASTERN BRITISH COLUMBIA

Project 630017

D. W. Morrow
Institute of Sedimentary and Petroleum Geology, Calgary

Introduction

The Stone Formation of northeastern British Columbia is composed of thick-bedded, light grey dolomite and is up to 600 m thick. It is overlain by the Dunedin Formation which is a sequence of medium-bedded, dark grey limestone and is up to 350 m thick. Figure 1 shows where these and other thick Devonian carbonate units in northeastern British Columbia pass northward and westward to shale of the Besa River Formation.

Taylor and MacKenzie (1970, p. 11) have described a facies of the Stone Formation that is characterized by dolomite breccias. In the mountains of northeastern British Columbia, where the Stone Formation outcrops, this facies extends northward from about 58°N to about 59°30'N (Fig. 1).

The author spent two weeks at the end of the 1974 field season with G. C. Taylor, R. W. Macqueen and R. I. Thompson in northeastern British Columbia. During this time the breccias in the Stone Formation, which are described in some detail by Taylor *et al.* (1974), were examined at both One-Ten Creek and Sulphur Creek (Fig. 1).

Stone Formation Breccias

Tabular, largely conformable sheets of breccia up to 4 m thick and several to hundreds of metres long occur throughout the dolomite breccia facies of the Stone Formation. Sharp, angular fragments of grey Stone dolomite are cemented with very coarsely crystalline, white dolomite or calcite in these breccias. The thicker, more extensive sheets consist largely of breccia blocks that have undergone little or no displacement relative to each other (i. e., mosaic or crackle breccia). Figure 2 shows an example of one of these laterally extensive sheets. Thinner, less extensive breccia bodies contain a higher proportion of rubble breccia in which individual fragments are oriented randomly (Taylor *et al.*, 1974, Figs. 2 and 8). Near the head of Sulphur Creek (Fig. 1), breccia zones were observed throughout the lower 50 m of the Stone Formation, but are abundant only in the lower 30 m. At One-Ten Creek, breccia zones occur in the upper rather than the lower part of the formation.

Taylor *et al.* (1974) suggested that these breccias were possibly the result of subsurface solution in the Stone Formation that occurred before deposition of the overlying Dunedin Formation. An objection to this interpretation is the lack of any karst features at the Stone-Dunedin contact. At One-Ten Creek this contact is conformable and gradational over several metres, although breccia bodies in the Stone Formation occur near the contact. Only south of 57°N does the Dunedin Formation overlie the Stone Formation with an abrupt, slightly angular unconformity (Taylor and MacKenzie, 1970). However, no karst features are reported from within the Stone Formation or at its contact with the Dunedin Formation in this region. Similarly, no karst features or breccias have been reported from the Chinchaga Formation in the subsurface of northeastern British Columbia. This formation is probably correlative with the Stone Formation and part of the Dunedin Formation (Griffin, 1967).

It is important to note that the mineralized breccia body at Robb Lake is south of the main area of breccia development in the Stone Formation (Fig. 1). This may be an indication that the breccias at Robb Lake are genetically distinct from the breccias in the Stone Formation farther north.

Stone and Dunedin Formations Buttress Structures

In support of their assertion of pre-Dunedin breccia development in the Stone Formation, Taylor *et al.* (1974) note the absence of breccias or solution features of the type typical of the Stone Formation in the Dunedin Formation. However, both the Stone and Dunedin formations contain near-vertical sheets of dolomite and limestone breccia that are oriented perpendicular to bedding (Fig. 3). These were described briefly by Taylor *et al.* (1974) and called buttress structures because folds of Laramide age immediately adjacent to them appear to be crumpled (Fig. 3). These rare, but impressive structures are tens of metres wide, hundreds of metres high and up to a kilometer or more long (Taylor *et al.*, 1974).

At One-Ten Creek, one of these structures occurs in the Dunedin Formation (Fig. 4a). It appears to be formed of blocks of Dunedin limestone up to 1. 5 m long that are randomly oriented (i. e. rubble breccia) and set in a recrystallized, grey, lime mud matrix. Another of these buttress structures was observed 20 km south of Sulphur Creek (Fig. 3). This particular breccia body occurs in the Stone Formation and may be capped by basal beds of the Dunedin Formation (G. C. Taylor, pers. comm.). Figure 4a shows the stratigraphic position of both this breccia sheet and the one at One-Ten Creek as well as their position relative to the more typical Stone Formation breccias.

The rubble debris in these buttress structures is similar in appearance to that observed in present-day underground sinks. Monument Mountain in Wyandotte cave in southern Indiana is a good example of a collapsed pile of debris that largely fills an underground sink. The ceiling of the cavern is 11 m above the 42-m-high collapsed pile of rock which form the mountain (Thornbury, 1954, p. 339).

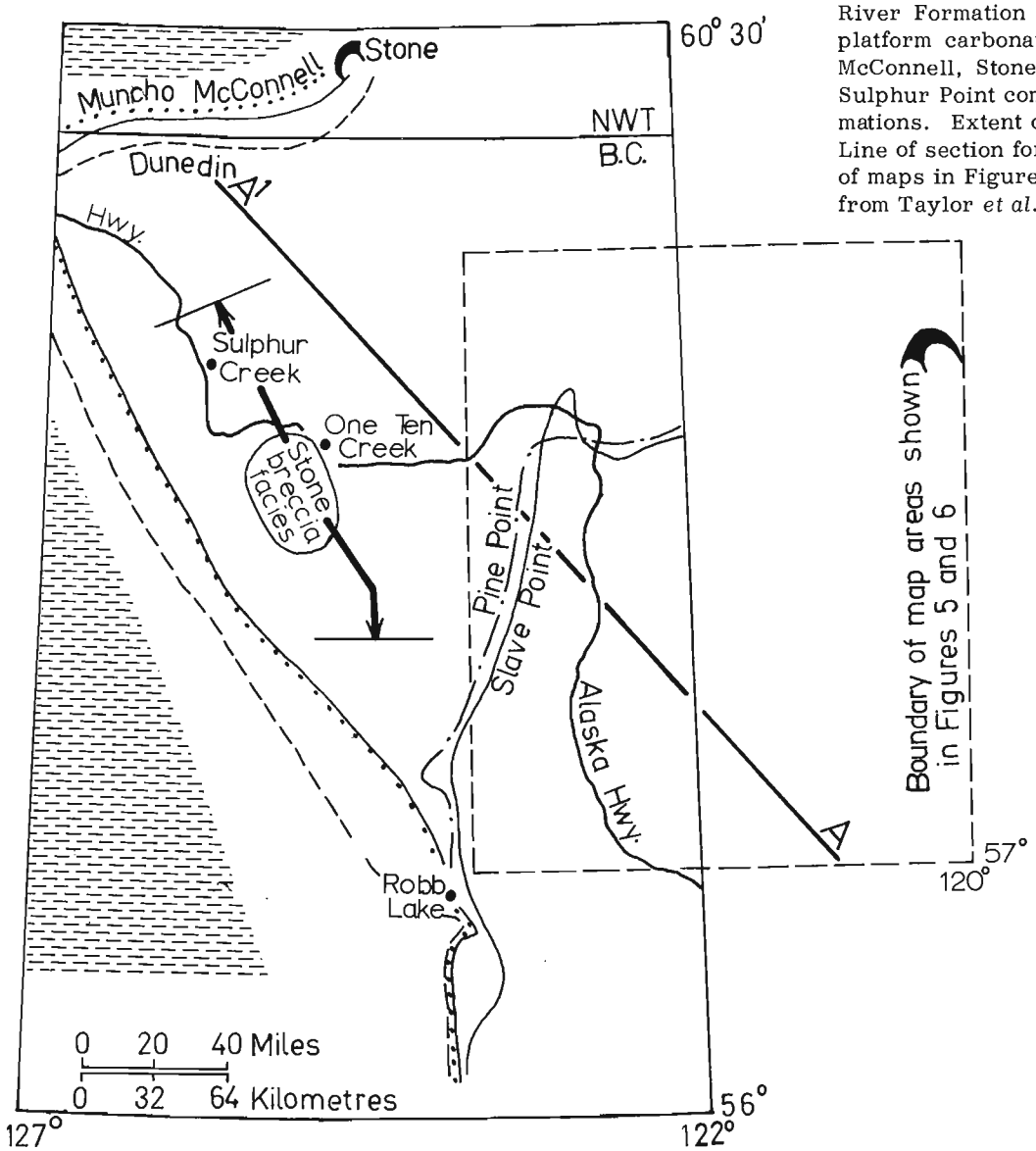

Figure 1. Map of northeastern British Columbia showing locations of Devonian facies changes. Besa River Formation shales occur northwest of platform carbonates formed by the Muncho-McConnell, Stone, Pine Point (Pine Point and Sulphur Point combined), and Slave Point formations. Extent of Stone breccia facies is shown. Line of section for Figure 4a (AA^1) and the area of maps in Figures 5 and 6 are shown. Adapted from Taylor *et al.* (1974).

The Florida Aquifer--A Model for Devonian Groundwater

The Florida Aquifer (Kohout, 1965) is the main zone of underground seaward fresh and brackish water flow in the Florida Peninsula. This aquifer is composed of porous and permeable Tertiary limestone and dolomitic limestone that underlie Florida, and parts of South Carolina, Georgia, and Alabama. In southern Florida, the main part of the aquifer extends from about 300 m to about 1050 m below sea level (Fig. 4b). Freshwater filled underground caverns are developed at depths between 570 m (1900 ft.) and 990 m (3300 ft.) below sea level. This zone of cavern development, termed the Boulder zone by drillers, is populated by many caverns 1 to 2 m in height and one large 28-m-high cavern (Kohout, 1965, p. 262).

Recently, fresh and brackish water in this aquifer has been found beneath the sea floor on the Florida-Hatteras Slope (Manheim, 1967), 120 km offshore from Jacksonville, Florida (Fig. 4b). Additional evidence (Manheim, 1967) suggests that submarine discharge of fresh water occurs more than 200 km offshore on the sea floor at depths exceeding 500 m. This submarine discharge may originate from sinkhole-shaped depressions that are about 50 m deep. Manheim (1967) suggests that submarine sapping by fresh or brackish water outflow may have formed these depressions. Many large sinkhole-shaped depressions occur still farther offshore on the Blake Plateau in water depths up to 800 m.

Figure 2.

A typical zone of breccia in the Stone Formation at Sulphur Creek. The large angular blocks are only slightly (crackle breccia) to moderately (mosaic breccia) displaced relative to each other. Coarsely crystalline white calcite and dolomite form the white interfragment matrix.

Figure 3.

View of a vertically oriented buttress structure breccia sheet exposed in a valley wall 20 km south of Sulphur Creek. Breccia sheet is several tens of metres wide here. Blocks of all shapes and sizes that are oriented randomly (rubble breccia) form this breccia. Grey, recrystallized carbonate mud forms the interfragment matrix.

Kohout (1965) described the movement of groundwater in the Florida Aquifer. Downward movement of groundwater with sinkhole development occurs beneath the emergent recharge area. Downward movement is followed by lateral movement downdip along the aquifer accompanied by subsurface lateral cavern development in the Boulder Zone (Fig. 4b). The geothermal gradient causes this groundwater to be heated during its lateral movement at depth. The resultant density change aids the upward dispersion of the groundwater near the seaward edge of the aquifer (Fig. 4b). It seems possible that groundwater along the upper, seaward edge of the Florida Aquifer with its strong, upward directed movement, would tend to form solution cavities with long vertical rather than long lateral dimensions. In this respect, an analogy may be drawn with the upland recharge area where downward percolating groundwater forms sinks hundreds of feet deep with near vertical walls.

Application of the Aquifer Model

Figure 4a illustrates a possible application of the Florida Aquifer model to groundwater flow after deposition of the Stone and Dunedin formations in northeastern British Columbia. The regression that accompanied deposition of the Watt Mountain Formation deltaic sandstone and shale (Fig. 5) may have exposed nearly all of the underlying Sulphur Point Formation limestone to subaerial erosion (Griffin, 1967). The severe brecciation of the Sulphur Point Formation and the infiltration of green shale between large breccia clasts (Griffin, 1967; and unpublished core studies by the author) suggest that this formation underwent a significant period of subaerial erosion and karst formation. The isopach map of the Sulphur Point Formation shown in Figure 6 displays a very irregular contour pattern including several closed depressions that are difficult to interpret as reflecting a depositional pattern. Instead, however,

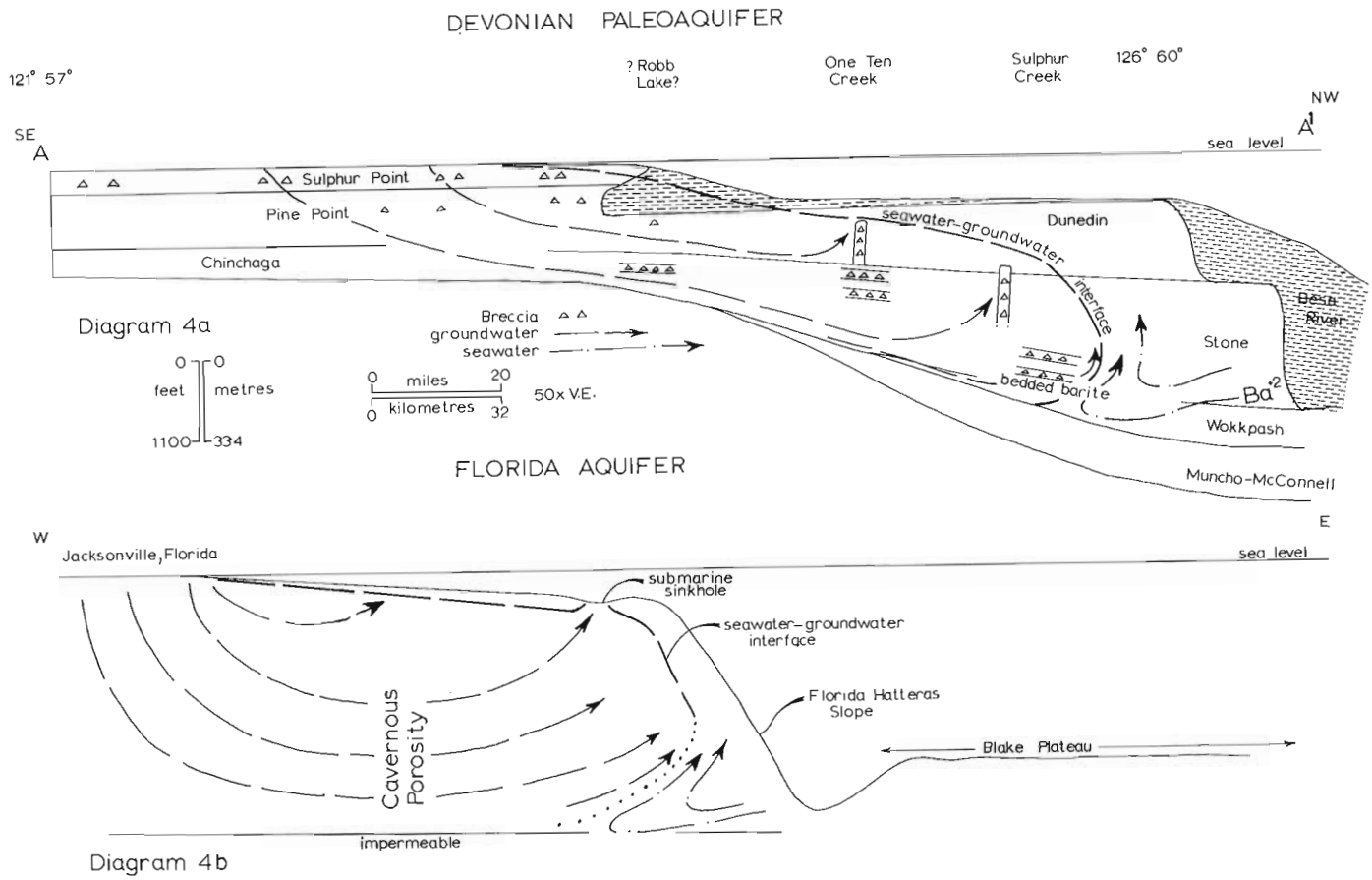

Figure 4. Diagram 4a shows the units that may have been involved in the development of a Devonian paleoaquifer. The variety of breccias in the Sulphur Point, Stone and Dunedin formations may be all the result of the movement of fresh groundwater through this paleoaquifer. Barite mineralization may have occurred at the base of the seaward end of the aquifer where barium charged seawater derived solutions first came into contact with deep groundwater of the aquifer.
Diagram 4b shows the Florida Aquifer as it exists underneath and seaward of Jacksonville, Florida. Adapted from Kohout (1965) and Manheim (1967).

the isopach contour pattern may reflect thickness variations due to karst. Closed depressions may represent partly infilled sinkholes.

This evidence suggests that a large part of northeastern British Columbia was an area of considerable freshwater recharge during and somewhat after deposition of the Watt Mountain and Sulphur Point formations. A recharge area of this large size may have promoted the growth of a regional aquifer similar to the present-day Florida Aquifer (Fig. 4a). The laterally extensive and conformable breccias in the Stone Formation at One-Ten and Sulphur creeks may reflect the development at depth of laterally extensive solution caverns similar to those in the Florida Aquifer. Large sheets of rock may have detached from the roofs of these low, broad caverns to form the crackle and mosaic breccias (Fig. 2) typical of the Stone Formation at these localities. Upward flowing groundwater in the upper, seaward part of the aquifer may have favoured the development of deep vertical sinks. The buttress structure breccias in the Stone and Dunedin formations may be the infills of these offshore underground sinks (Fig. 4a).

G. C. Taylor (pers. comm., 1975) found that these vertical breccia sheets or buttress structures trend uniformly northeast-southwest. He suggested that individual breccia sheets may be oriented along pre-existing fractures. The inferred karst sinkhole depressions in the Sulphur Point Formation are elongate in a northeast-southwest direction also (Fig. 6) and may reflect a similar structural control.

The lower stratigraphic position of the top of the buttress structure breccia near Sulphur Creek, relative to the stratigraphic position of the buttress structure breccia observed at One-Ten Creek, may reflect the progressive offshore lowering of the ancient freshwater-seawater interface (Fig. 4a). The absence of breccias, other than those of penecontemporaneous

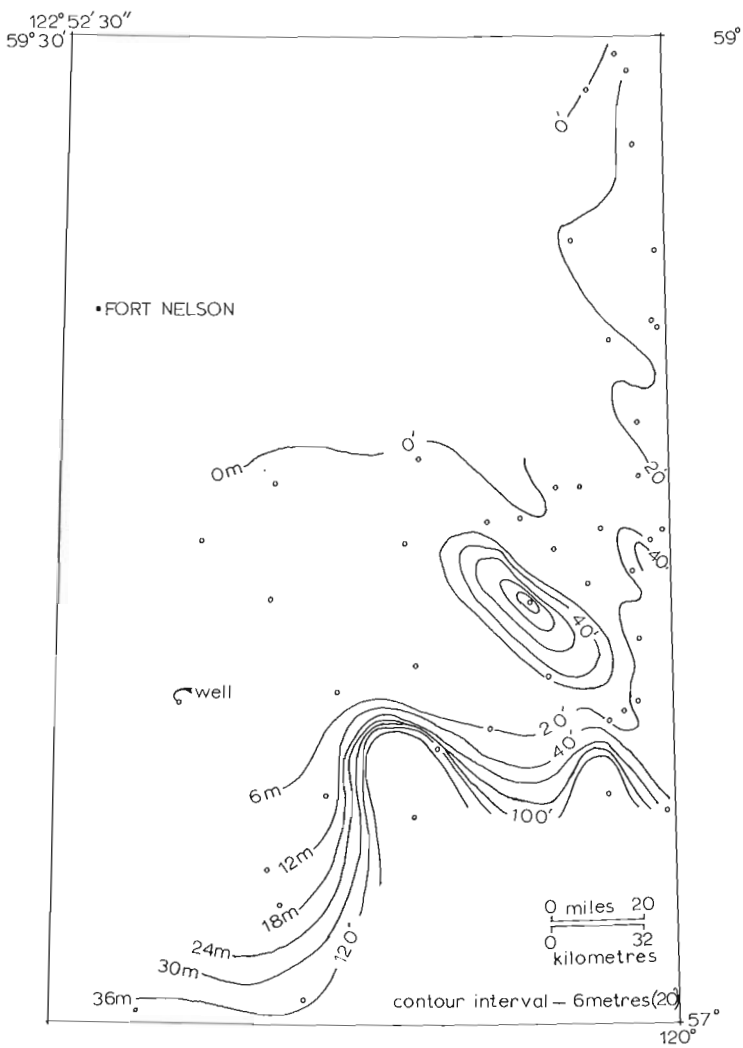

Figure 5. Isopach map of the Watt Mountain Formation in northeastern British Columbia. Note the northwest-facing sandstone delta lobes of this formation. Northwest beyond the delta lobes the Watt Mountain Formation is formed of green shale. Adapted from Morrow (1970).

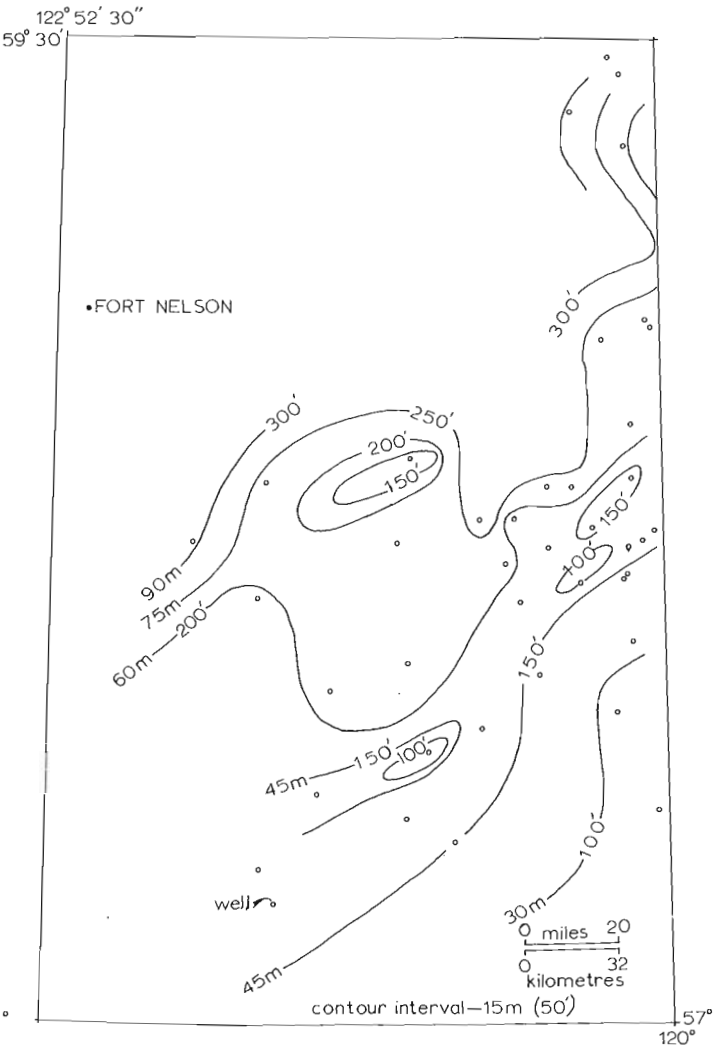

Figure 6. Isopach map of the Sulphur Point Formation in northeastern British Columbia. Note the northeast-southwest trend of the elongate sinkhole-shaped closed depressions. Adapted from Morrow (1970).

sedimentary origin, in the Stone and Dunedin formations northwest of Sulphur Creek may indicate that Sulphur Creek is near the seaward limit of this Devonian paleoaquifer (Fig. 4a).

Taylor *et al.* (1974) mention that the development of solution cavities in dolomite is uncommon. However, solution of limestone beds and their dolomitization are contemporaneous processes in the Florida Aquifer (Kohout, 1965). This is the result of the subsurface mixing of fresh groundwater with between 5 per cent and 30 per cent seawater, which leads to undersaturation with respect to calcite, but supersaturation with respect to dolomite (Badiozamani, 1973). It is possible that the development of solution caverns in the Stone Formation was contemporaneous with dolomitization rather than post-dolomitization.

Barite Mineralization Related to the Devonian Paleoaquifer

The occurrence of barite and other minerals in the Stone and Dunedin formations has been described by Taylor *et al.* (1974). However, the only place where barite forms a predominant rock constituent is at Sulphur Creek. Here, the basal 15 m of the Stone Formation consist of medium-bedded white barite with minor dolomite (Fig. 4a). No bedded barite has been observed elsewhere.

The stratigraphic and geographic position of this barite deposit suggests that it formed at the base of the seaward edge of the fluctuating fresh groundwater-seawater interface in the Devonian paleoaquifer. In the Florida Aquifer, seawater-derived connate solutions

are continually brought into contact with fresh groundwater at the base of the seaward edge of the aquifer (Kohout, 1965; and Fig. 4b). It is possible that a long period of barite deposition occurred in this part of the paleoaquifer as a result of the extensive mixing of seawater-derived solutions and fresh groundwater.

Plummer (1971) showed that reducing, somewhat acid solutions that contain H_2S as the dominant sulphur species are capable of retaining large amounts of barium in solution. Barium solubility abruptly decreases where such solutions mix with fresh groundwater. Barium deposition occurs following the overall reaction

$$Ba^{2+} + H_2S + CaCO_3 + 2O_2 = Ca^{2+} + BaSO_4 + CO_2 + H_2O.$$

The highly radioactive pyritiferous shales (i.e. Muskwa Member) at the base of the thick Besa River Formation which overlies the Dunedin Formation (Fig. 4a) may indicate that the seawater circulating in the sediments offshore from the Devonian paleoaquifer was predominantly acid and reducing. In some areas of northeastern British Columbia, these radioactive basal shales contain numerous zones, up to 6.3 cm thick, of authigenic barite crystals (Griffin, 1965, p. 45). This may be direct evidence of the barium-bearing capacity of the seawater in which these shales were deposited.

References

Badiozamani, K.
1973: The dorag dolomitization model--application to the Middle Ordovician of Wisconsin; J. Sediment. Petrol., v. 43, no. 9, p. 965-984.

Griffin, D.L.
1965: The Devonian Slave Point, Beaverhill Lake, and Muskwa Formations of northeastern British Columbia and adjacent areas; B.C. Dept. Mines Pet. Resour., Bull. 50.

Griffin, D.L. (cont'd.)
1967: Devonian of northeastern British Columbia *in* Intern. Symp. on the Devonian System, Alberta Soc. Pet. Geol., v. 1, p. 803-826.

Kohout, F.A.
1965: A hypothesis concerning cyclic flow of salt water related to geothermal heating in the Floridan aquifer; Trans. N.Y. Acad. Sci., v. 28, no. 2, p. 249-271.

Manheim, F.T.
1967: Evidence for submarine discharge of water on the Atlantic Continental Slope of the southern United States, and suggestions for further search; Trans. N.Y. Acad. Sci., v. 29, no. 7, p. 839-853.

Morrow, D.W.
1970: Stratigraphy and petrography of the Elk Point Group, northeast British Columbia; unpubl. M.A. thesis, Univ. of Texas.

Plummer, A.N.
1971: Barite deposition in Central Kentucky; Econ. Geol., v. 66, p. 252-258.

Taylor, G.C. and MacKenzie, W.S.
1970: Devonian stratigraphy of northeastern British Columbia; Geol. Surv. Can., Bull. 186.

Taylor, G.C., Macqueen, R.W. and Thompson, R.I.
1974: Facies changes, breccias, and mineralization in Devonian rocks of Rocky Mountains, northeastern British Columbia (94B, K, N) *in* Rept. of Activities, Part A, April to October, 1974; Geol. Surv. Can., Paper 75-1, Pt. A, p. 577-585.

Thornbury, W.D.
1954: Principles of geomorphology; John Wiley and Sons, New York.

57. MARKERS WITHIN CRETACEOUS ROCKS AS INDICATED BY MECHANICAL LOGS FROM BOREHOLES IN THE MACKENZIE DELTA AREA, NORTHWEST TERRITORIES

Part A. Borehole markers, stratigraphic and sedimentological correlation tools.
Part B. Their relationship to chemical and mineralogical properties of the rocks.

Project 710036

D. W. Myhr
Institute of Sedimentary and Petroleum Geology, Calgary

Introduction

Several Gamma Ray Log and Dual Induction – Laterolog markers were identified in strata of Albian and Late Cretaceous age. These were correlated among boreholes on the northeastern part of Tuktoyaktuk Peninsula (Fig. 1), over a distance of 61.14 km (38 miles). Lithologic and biostratigraphic data, in conjunction with the identified log markers, delineated changes in radioactive content of strata, faults, stratigraphic discontinuities, thickness variations within the succession, assisted in the correlation of formation boundaries (Fig. 3, and Table 3).

Samples from the IOE Atkinson M-33 borehole (Lat. 69°42'28"N, Long. 131°54'43"W), and several cores from nearby wells were examined (Table 1 and Fig. 2) for lithologic data. Core samples were analyzed for qualitative and semi-quantitative compositional data, in order to identify and compare the mineral assemblages (Table 2) and geochemistry of "normal" and "highly" radioactive strata.

PART A. BOREHOLE MARKERS, STRATIGRAPHIC AND SEDIMENTOLOGICAL CORRELATION TOOLS

Identification and Type

Mechanical log markers, within boreholes on northeastern Tuktoyaktuk Peninsula, are the result of significant changes in radioactivity and resistivity of the rock units.

Two types of mechanical logs were used for identification of the borehole markers. These are displayed on Figures 2 and 3 and include, in order of importance: (a) the Gamma Ray Log, and (b) the Dual Induction - Laterolog. Both can be used to identify markers "A" and "B" (Fig. 2), whereas only the Gamma Ray Log can be used for the remaining markers ("C" to "F", Fig. 3). A biostratigraphic marker, the first occurrence of *Inoceramus* columnals, was chosen from samples (Table 3) and from a cored interval (Table 1) in the IOE Natagnak H-50 borehole.

Stratigraphy and Geological Setting

The borehole markers were identified on logs from wells which penetrated rocks of Middle Albian, ?Turonian, Santonian and Upper Campanian to Maastrichtian age (Chamney, 1973, and *in* Barnes *et al.*, 1974; Brideaux, pers. comm.); the sequence divided by a regional pre-Late Cretaceous unconformity at the top of the Albian ("Morden" unconformity, Chamney, 1969b). These epicontinental, shallow marine deposits outcrop in Anderson Plain where they are represented by the Horton River Formation (Albian), Smoking Hills Formation (Coniacian — Campanian) and Mason River Formation (Campanian to Maastrichtian) (Yorath *et al.*, in press; McIntyre, 1974; Brideaux and Fisher, in press).

In the subsurface the contact between the Horton River Formation and overlying Smoking Hills Formation is identified by changes in lithology, mechanical log character (Marker "E" in Figs. 2 and 3), and microfossil assemblages (Chamney, 1973a, b). The contact between the subsurface equivalents of the Smoking Hills Formation and Mason River Formation is chosen at Marker "D" (datum in Fig. 3). This marker represents the first occurrence of bentonitic shale, and corresponds approximately with the uppermost part of a microfossil assemblage (Chamney, 1973) representative of the Smoking Hills Formation (formerly Bituminous Zone *in* Yorath *et al.*, 1969). These shales grade downward into highly radioactive, bentonitic (?tuffaceous), bituminous shale and less radioactive, *Inoceramus*-bearing shales; the basal contact of the formation marked by approximately 3 m (10 feet) of "highly" radioactive, bituminous? shale (Fig. 3). In contrast, outcrops of the Smoking Hills Formation commonly consist of jarosite beds, interstratified with black, bituminous shales, and earthy hematite beds. These lithologies occur where the formation has undergone combustion as bocannes. Secondary gypsum crystals are common and a discontinuous basal conglomerate occurs locally (Yorath *et al.*, 1969, and in press).

The study-area (Fig. 1) overlies a paleotopographic high that is part of the northeasterly trending Aklavik Arch Complex (Yorath *et al.*, 1975). The arch has undergone multiple movements which culminated in Laramide time with dislocation by mainly down-to-basin faults of variable stratigraphic separation (Eskimo Lakes Fault Zone *in* Cote *et al.*, in press).

Correlation of Borehole Markers

Of the seven Gamma Ray Log markers identified (Table 3) only four are correlative over the whole of

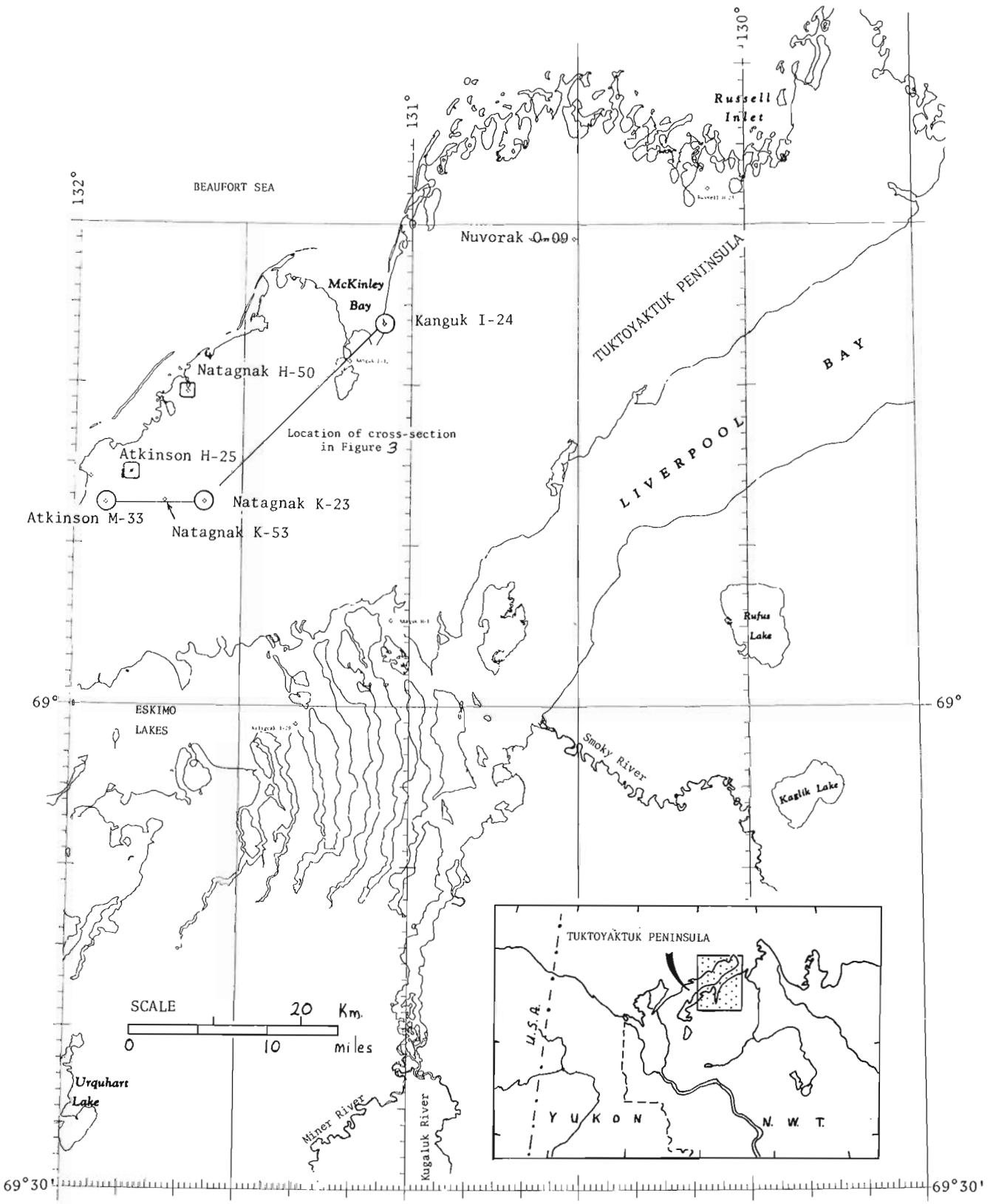

Figure 1. Location map of pertinent boreholes, northern portion of Tuktoyaktuk Peninsula.

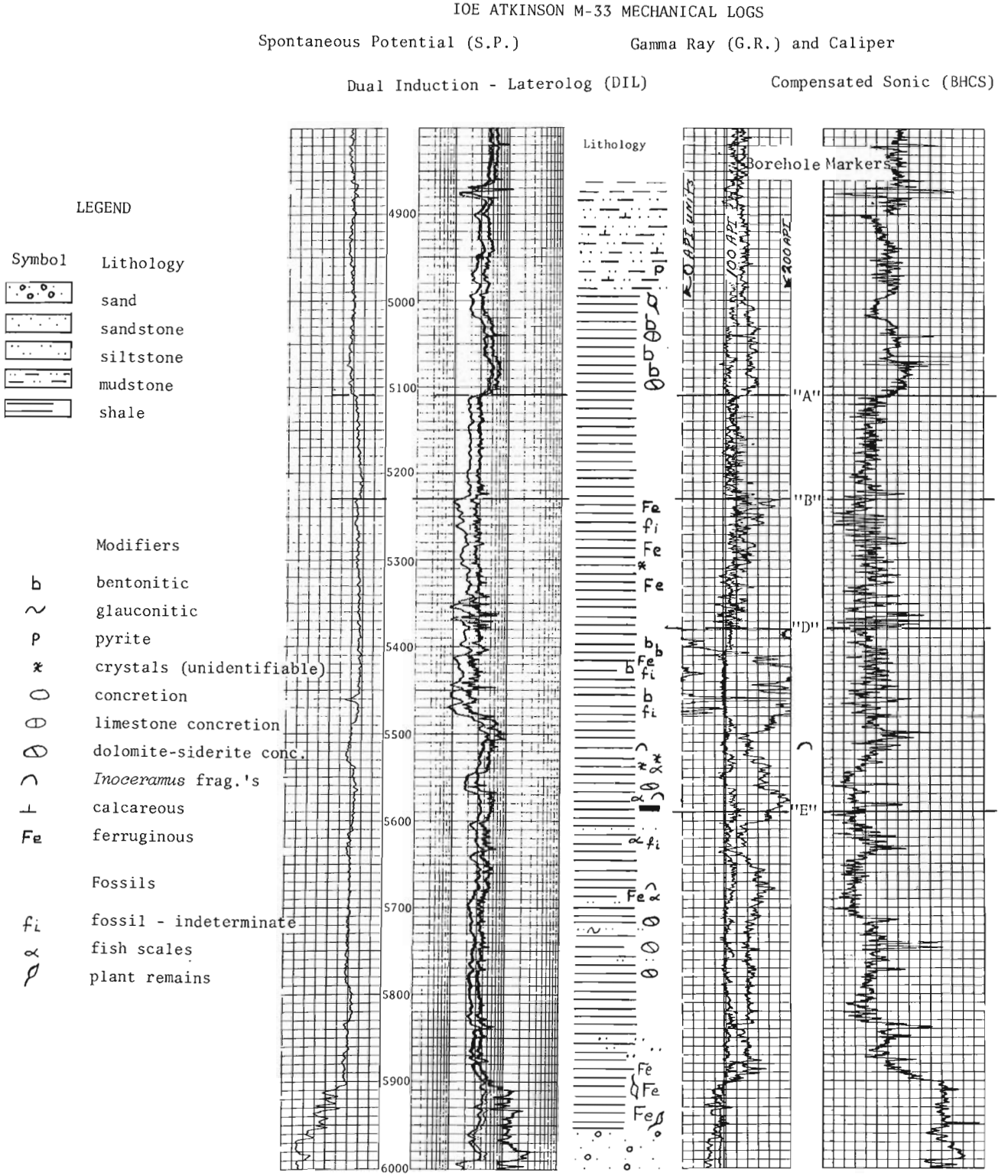

Figure 2. A comparison of mechanical log response and lithology from the IOE Atkinson M-33 borehole.

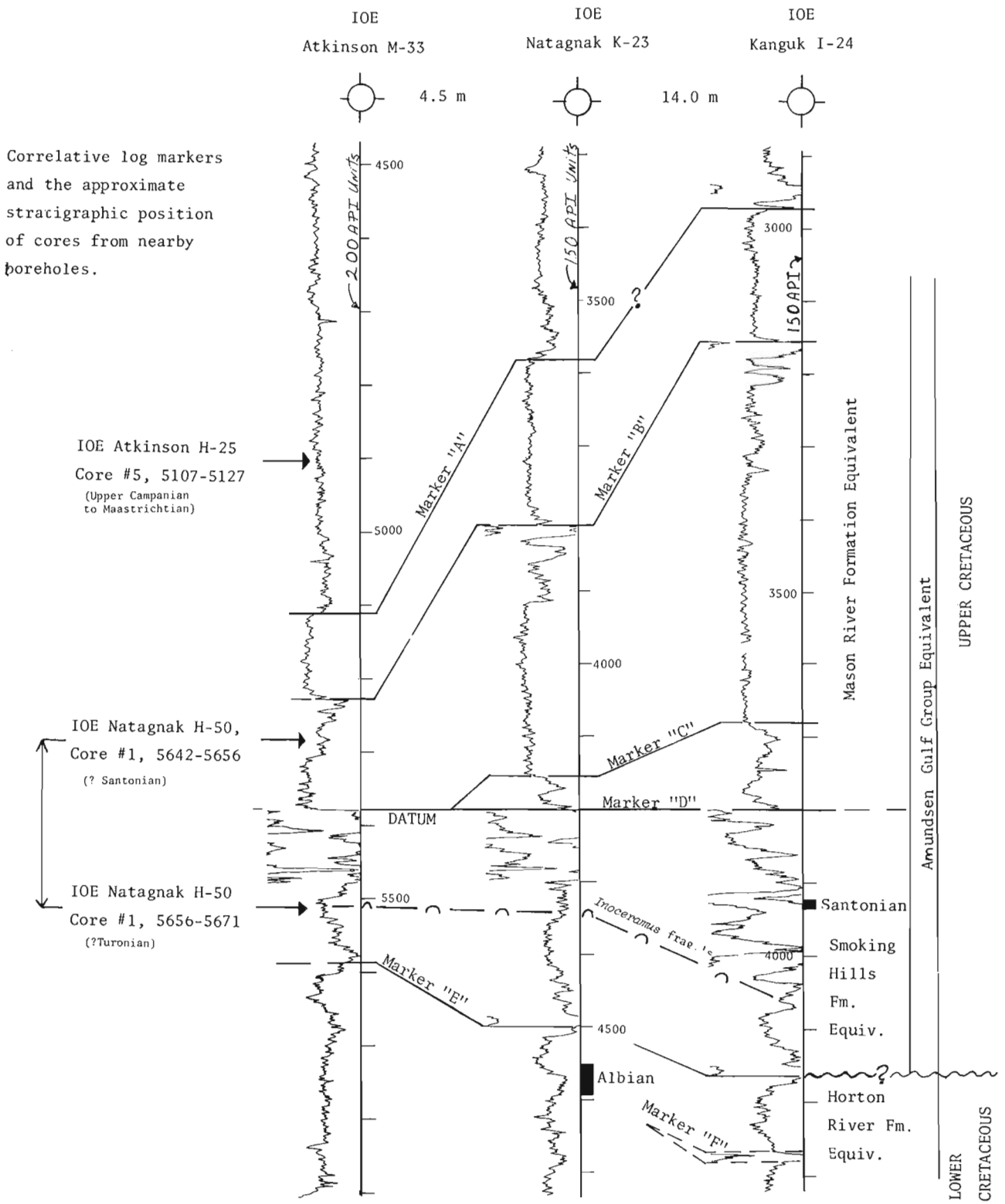

Figure 3. Correlation of Gamma Ray (G.R.) Log markers and a Biostratigraphic marker in three boreholes, Tuktoyaktuk Peninsula, N.W.T.

Table 1

Stratigraphy and Lithology of cored intervals pertinent to Figure 3 and Table 2

Well Name	Location	Core No. and Depth (metres)	Lithology	Formation Equivalent (Yorath *et al.*, in press) and Age
IOE Atkinson H-25	69°44'20"N 131°50'06"W	No. 5; 5107 ft - 5127 ft (1557.6 m - 1563.7 m)	Shale; dark greenish grey, massive.	Mason River (U. Campanian to Maastrichtian)
IOE Natagnak H-50	69°49'27"N 131°40'11"W	No. 1; 5642 ft - 5671 ft (1720.8 m - 1729.7 m)	Shale; light olive grey, silty grades into dark grey to black shale, with trace of bentonite, fissile and contorted.	Mason River (?Santonian) 5656 ft (1696 m)
			Shale; medium dark grey, with three brownish grey claystone concretions. *Inoceramus* fragments at 5657 ft - 5671 ft.	Smoking Hills (?Turonian)
IOE Kanguk I-24	69°53'40"N 131°05'12"W	No. 2; 3924 ft - 3936 ft (1196.8 m - 1200.5 m)	Bentonite; tuffaceous bluish white to light bluish grey, grades into shale; dark grey, bituminous with fossil hash microlaminae (?fish remains indurated).	Smoking Hills (Santonian)
IOE Natagnak K-23	69°42'31"N 131°36'44"W	No. 1; 4552 ft - 4592 ft (1388.4 m - 1400.6 m)	Shale; medium to dark grey, trace fossil fragments (fish remains, brachiopod), pyrite infilling burrows, two limestone nodules.	Horton River (Albian)

the study area (Fig. 3). The contact between the Smoking Hills Formation and Mason River Formation was chosen as the datum in Figure 3 because of its distinct mechanical log character (Marker "D"); marked by an obvious change in lithology (Fig. 2). The character of the markers suggest volcanism and physical changes (transgression) and/or chemical changes (aerobic⇌anaerobic conditions) in the Cretaceous seas.

Stratigraphic and Sedimentological Implications

Several conclusions may be drawn from the correlation of markers in Figure 3. These are: (a) Marker "F" (255 API units) in the IOE Kanguk I-24 borehole (69°54'N, 131°05'W) grades laterally into "normal" radioactive shale (≈80 API units) in a southeasterly direction; (b) Marker "E" is regionally correlative and represents thin (≈3 m, 10 ft), radioactive, bituminous? shale at base of the Smoking Hills Formation; (c) Marker "C" is absent in the IOE Atkinson M-33 borehole suggesting non-deposition of equivalent strata (note stratigraphic condensation between Marker "D" and "C" in adjacent boreholes); (d) significant depositional thickening occurred in the vicinity of the IOE Kanguk I-24 borehole; post-Marker "D" to Marker "B" time, (e) stratigraphic condensation also is evident between Marker "B" and Marker "A" in the IOE Atkinson M-33 borehole.

In addition, cored intervals from nearby boreholes (IOE Atkinson H-25 borehole, and IOE Natagnak H-50 borehole) may be correlated with equivalent strata of the IOE Atkinson M-33 borehole, as displayed on the left hand side of Figure 3.

The presence of a fault in No. 1 (1697 m, 5656 ft.) of the IOE Natagnak H-50 borehole (69°49'27"N, 131° 40'11"W) accounts for missing section in the cored interval, as displayed in Figure 3. Evidence of this structural discontinuity is based on (a) an abrupt change in lithology and bedding character forms contorted black shale to massive shale (Table 1), (b) the "moderately" radioactive log character of the upper 4.2 m (14 ft.) is characteristic of strata below the "B"

Table 2.

Mineral analysis of core samples from four boreholes on Tuktoyaktuk Peninsula, N.W.T.

Well Name and Sample No. and depth (pit)	Mineral Analysis from X-ray Diffraction Methods													
	Clay Minerals				Silicates			Carbonates			Sulfates			Stratigraphy
	Montmorillonite and/or mixed layers	Illite	Clinoptilolite	Kaolinite/ Chlorite	Crystalline Quartz	Feldspars	Christobalite	Calcite	Dolomite	Siderite	Jarosite	Pyrite	Total (%)	Formation & Age
1 Atkinson H-25 (5108') 4.2		16		11	63	9		?5					100	Mason River Fm. Equiv. (U. Camp. to Maast.)
2 Natagnak H-50 (5643) 9.1	18				82								100	Mason River Fm. Equiv. (?Santonian)
3 Natagnak H-50 (5650) 4.1	?Tr	12		7	78							3	100	Mason River Fm. Equiv. (?Santonian)
4 Kanguk I-24 (3925) 5.8	42		14		7	3	28				6		100	Smoking Hills Fm. Equiv. (Santonian)
5 Kanguk I-24 (3936) 3.2	17	4			46	7		5	3	2		16	100	Smoking Hills Fm. Equiv. (Santonian)
6 Natagnak K-23 (4555) 8.3		12		12	72			Tr	Tr			4	100	Horton River Fm. Equiv. (Albian)

marker (establishes the stratigraphic position of the hanging wall) combined with the lithology of the lower few feet (massive shale with *Inoceramus* fragments), establishes the stratigraphic position of the footwall, and (c) the absence of the Coniacian stage (Table 1).

Table 3 displays the depth at which correlative log markers were encountered in boreholes of the study-area. An interpretation as to the absence (x) of these markers is as follows: (1) Marker "G"; decrease in amount of radioactive material, related to a change in lithology, (2) Marker "F"; same interpretation as Marker "G" (refer to Fig. 3), (3) IOE Atkinson H-25 borehole; absence of markers "E", "D", "C" - due to one or more faults (this well is located within the Eskimo Lakes Fault Zone, Gulf geologists in Oilweek, 1974), (4) IOE Natagnak H-50; absence of Marker "E" - due to a fault or, less likely, a facies change; Markers "D" and "C" - absence pertaining to a fault (previously discussed), and (5) IOE Atkinson M-33 borehole; absence of Marker "C" - nondeposition. These interpretations are based on visual examination of geophysical logs (dipmeter surveys, Gamma Ray Logs), core examination (Table 1), biostratigraphy of the IOE Atkinson H-25 borehole (Imperial Oil geologists in Oilweek, 1972; Brideaux, W.W., pers. comm.), and sample examination (Table 3).

PART B. BOREHOLE MARKERS AND THEIR RELATIONSHIP TO CHEMICAL AND MINERALOGICAL PROPERTIES OF THE ROCKS

The mechanical log markers correlate with changes in lithology from shale⇌bentonitic shale, or bituminous shale (Fig. 2). The amount of gamma radiation emitted by these rocks is recorded in API units on the Gamma Ray Log and is dependent on rock density and weight concentration of radioactive material in the formation; such as the radioactive elements of the uranium and thorium series and the radioactive potassium isotope, ^{40}K (Schlumberger, 1972).

Analytical Methods and Results

The following analyses were done to determine if there is any relationship between mineral assemblages, uranium content (U_3O_8) and organic carbon content within "highly" radioactive rock units. Less radioactive rocks were also sampled for comparison.

X-ray diffraction analysis was used to obtain semi-quantitative, mineralogical composition of samples from

Table 3.

Depth and type of correlative markers within boreholes on northeastern Tuktoyaktuk Peninsula, N.W.T.

Markers chosen from geophysical logs in the IOE Kanguk I-24 borehole (69°54'N, 131°05'W)		Boreholes with Correlative Log Markers (x denotes absence of the marker)						Formation Equivalent after (Yorath *et al.*, in press)	
Type of Log used and Depth i) Gamma Ray (G.R.) ii) Dual Induction-Laterlog (DIL)		IOE Nuvorak O-09	IOE Natagnak K-23	IOE Natagnak K-53	IOE Atkinson M-33	IOE Atkinson H-25	IOE Natagnak H-50		
		69°59'N 130°31'W	69°43'N 131°37'W	69°43'N 131°44'W	69°43'N 131°55'W	69°44'N 131°51'W	69°49'N 131°40'W	Map-areas Franklin Bay (97C) Malloch Hill (97F)	
Marker "A"	G.R. 2975 ft (907.4 m)	G.R. 1830 ft (558.2 m)	G.R., DIL 3580 ft (1091.9 m)	G.R., DIL 4580 ft (1396.9 m)	G.R., DIL 5110 ft (1558.6 m)	G.R., DIL 5340 ft (1628.7 m)	G.R., DIL 5410 ft (1650.1 m)		AMUNDSEN GULF GROUP
Marker "B"	G.R., DIL 3158 ft (963.2 m)	G.R. ?2020 ft (616.1 m)	G.R., DIL 3805 ft (1160.6 m)	G.R., DIL 4755 ft (1450.3 m)	G.R., DIL 5230 ft (1595.2 m)	G.R., DIL 5405 ft (1648.6 m)	G.R., DIL 5585 ft (1703.4 m)	Mason River	
Marker "C"	G.R. 3690 ft (1125.5 m)	G.R. 2870 ft (875.4 m)	G.R. 4150 ft (1265.8 m)	G.R. 5028 ft (1533.5 m)	x	x	x		
Marker "D"	G.R. 3797 ft (1158.1 m)	G.R. 2950 ft (1032.5 m)	G.R. 4205 ft (1282.5 m)	G.R. 5050 ft (1767.5 m)	G.R. 5380 ft (1640.9 m)	x	x	Smoking Hills	
First occurrence of *Inoceramus* columnals	samples 4080 ft (1244.4 m)	samples 3000 ft (915 m)	samples 4350 ft (1326.8 m)	samples 5140 ft (1542 m)	samples 5510 ft (1680.6 m)	samples 5520 ft (1683.6 m)	core 5657 ft (1725.4 m)		
Marker "E"	G.R. 4160 ft (1268.8 m)	G.R. 3140 ft (957.7 m)	G.R. 4500 ft (1372.5 m)	G.R. 5320 ft (1622.6 m)	G.R. ?5590 ft (1705.0 m)	x	x		
Marker "F"	G.R. 4270 ft (1302.4 m)	G.R. 3205 ft (977.5 m)	x	G.R. 5390 ft (1644 m)	x	x	x	Horton River	
	x	Marker "G" G.R. 3337 ft (1017.8 m)	x	x	x	x	x		

cores (Table 2) whose lithology and relative position within the stratigraphic framework are illustrated in Table 1 and Figure 3. Uranium analyses were determined by atomic absorption spectrophotometry and organic carbon by Leco induction equipment. These procedures are described by Foscolos and Barefoot (1970a), and supplemented by notes pertaining to methodology and accuracy of data in Macqueen *et al.* (1975).

Mineralogical results in Table 2 show that the samples have a high crystalline quartz content (except for sample No. 4) and contain a variable clay mineral assemblage. Montmorillonite and/or mixed layer clays are present in three samples (No. 2, No. 4, No. 5) of which samples No. 4 and No. 5 are from a radioactive zone of high (150-400 API units) gamma ray counts (Fig. 3). Sample No. 4 (tuffaceous bentonite, 150 API units) is composed mainly of bentonitic clay (42% montmorillonite) with volcanic glass (28% cristobalite) and an authigenic zeolite; rich in silica and alkalic components (14% clinoptilolite - $Na_2K_2CaAl_6Si_{30}O_{72}.24H_2O$). A comparison of sample lithology with the Gamma Ray Log response indicates that bentonitic shales are "slightly" radioactive (above Marker "A", Fig. 2) to "highly" radioactive (below Marker "D" in Fig. 2). A plausible source for the radioactive material may have been the erosion of terrestrial rocks and transportation to the sea by rivers and streams and/or diagenetic enrichment from formation pore waters during sediment compaction (Vine and Tourtelot, 1970).

Sample No. 4 also contains jarosite (6%), an abundant mineral in outcrops of the Smoking Hills Formation. Jarosite (hydrous potassium iron sulphate), is an oxidation product of rocks enriched in montmorillonite and pyrite (Foscolos, A.E., pers. comm.). Therefore, one would expect equivalent subsurface rocks to consist of bentonite, bentonitic shale, and pyritic, organic-rich shales.

Pyrite is present in three samples analyzed and is most abundant in sample No. 5 (16%) which is a dark grey, organic (5.9%), "highly" radioactive shale (225 API units) from the subsurface equivalents of the Smoking Hills Formation. Swanson (1961) noted that shale with dark colour hues, such as dark grey (N3), greyish black (N2), and dark hues of brown (5YR2/1) is commonly enriched in iron sulphides and radioactive elements, which are correlative in the subsurface with radioactive lithologies recognizable on Gamma Ray Logs (Mapel, 1956; Tourtelot, 1956).

Well Name	Sample Depth	U_3O_8 (ppm)	% Organic Carbon	API units	Lithology
IOE Atkinson H-25	5108 ft. (1532.4 m)	2	1.1	80	dark greenish grey shale
IOE Kanguk I-24	3925 ft. (1197.1 m)	6	0.32	135	bentonite
IOE Kanguk I-24	3936 ft. (1200.5 m)	7	5.9	225	dark grey, pyritic shale
IOE Natagnak K-23	4555 ft. (1389.3 m)	2	2.3	80	medium to dark grey shale

Various authors, as listed in a selected annotated bibliography prepared by Fix (1958) and Tourtelot (1970) have shown that "black shales" contain high amounts of organic (carbon and mineral) and radioactive material. This relationship was tested on four samples in order to quantify the amount of uranium and organic carbon with respect to lithology and measured radioactivity (API units). The analysis was done by R.R. Barefoot (int. rep. chem. 74-14, 16) and is tabulated below with the samples arranged in stratigraphic order, similar to the cored intervals in Table 1.

Uranium content is highest (6 ppm - 7 ppm) within the "highly" radioactive lithologies of the Smoking Hills Formation equivalent, whereas the "normal" radioactive shale contains lesser amounts of uranium (2 ppm). The percentage of organic carbon content is relatively low in the less radioactive shales and bentonite samples, but is substantially higher in the pyritic, "highly" radioactive shale sample (API units = 225).

The relationship between relatively high amounts of radioactive material and high content of organic carbon and mineral matter in pelitic lithologies has been extensively documented in an annotated bibliography by Tourtelot (1970). In general, radioactive material is most common in marine, black shales enriched in organic matter, pyrite, phosphates (Swanson, 1961) and metallic elements (Vine and Tourtelot, 1970). Swanson (ibid.) has thoroughly documented several processes which may explain the emplacement of radioactive material in shales of this type. The most plausible one is reduction of uranium from sea water in an anaerobic environment, enriched in organic matter and hydrogen sulphide (reducing agent) with a low pH (acidic) and negative Eh. The organic-rich shales of the Smoking Hills Formation probably were deposited in a similar environment as evidenced by the marine, restricted fossil assemblage (Chamney, *in* Barnes *et al.*, 1974), the thin, black shale beds acting as a source for uranium enrichment of other interstratified lithologies (Vine *et al.*, 1970), which may explain, in part, the "highly" radioactive nature of the bentonite and bentonitic shales in core No. 1 of the IOE Kanguk I-24 borehole.

In conclusion, rocks enriched in montmorillonite (and/or mixed layer clays), organic carbon and pyrite are generally more radioactive as evidenced by comparatively high API counts on the Gamma Ray Log, and by radioactive elemental analysis.

Radioactive lithologies include organic-rich shales ("black" shales, "bituminous" shales), bentonitic shale and bentonite. Rocks of this nature are common constituents of the Smoking Hills Formation (especially in the subsurface), and to a lesser degree, the Horton River Formation and Mason River Formation (Yorath *et al.*, 1969, and in press).

Acknowledgments

The writer benefitted greatly from critical comments by C.J. Yorath and A.D. Miall. Analytical work and helpful discussion was contributed by A.E. Foscolos, R.R. Barefoot and A.G. Heinrich.

References

Barnes, C.R., Brideaux, W.W., Chamney, T.P., Clowser, D.R., Dunary, R.E., Fisher, M.J., Fritz, W.H., Hopkins, William S., Jr., Jeletzky, J.A., McGregor, D.C., Norford, B.S., Norris, A.W., Pedder, A.E.H., Rauwerda, J., Sherrington, P.E. Sliter, W.V., Tozer, E.T., Uyeno, T.T. and Waterhouse, J.B.
1974: Biostratigraphic determinations of fossils from the subsurface of the Northwest and Yukon Territories; Geol. Surv. Can., Paper 74-11.

Brideaux, W.W. and Fisher, M.J.
Upper Jurassic - Lower Cretaceous dinoflagellate assemblages from Arctic Canada; Geol. Surv. Can., Open File Rept. 253. (in press)

Chamney, T.P.
1969b: Microfossil study points to prospective anomalies; Oilweek, v. 20, no. 5, p. 7-8.

1973a: Tuktoyaktuk Peninsula Tertiary and Mesozoic biostratigraphic correlation; *in* Report of Activities, November 1972 to March 1973, Geol. Surv. Can., Paper 73-1B, p. 171-178.

1973b: The boreal Lower Cretaceous; *in* The proceedings of an international symposium organized by Queen Mary College (Univ. of London) and the Institute of Geological Sciences, ed. by: R. Casey and P.F. Rawson in The Boreal Lowest Cretaceous, 1972, p. 19-40.

Cote, R.P., Lerand, M.M. and Rector, R.J.
Geology of the Lower Cretaceous Parsons Lake Gas Field, Mackenzie Delta, Northwest Territories, *in* Canada's Continental Margins and Offshore Petroleum Exploration, ed. by C.J. Yorath; Can. Soc. Pet. Geol., Mem. no. 4. (in press)

Fix, C.E.
1958: Selected annotated bibliography of the geology and occurrence of uranium-bearing marine black shales in the United States; U.S. Geol. Surv. Bull. 1059-F, p. 163-325.

Foscolos, A.E. and Barefoot, R.R.
1970a: A rapid determination of total organic and inorganic carbon in shales and carbonates; A rapid determination of total sulphur in rocks and minerals; Geol. Surv. Can., Paper 70-11.

Mapel, W.J.
1956: Uraniferous black shales in the northern Rocky Mountains and Great Plains Regions: Intern. Conf. on Peaceful Uses of Atomic Energy, Geneva, 1955, Proc., v. 6, Geology of uranium and thorium, p. 445-451; U.S. Geol. Surv., Prof. Paper 300, p. 469-476.

Macqueen, R.W., Williams, G.K., Barefoot, R.R. and Foscolos, A.E.
1975: Devonian metalliferous shales, Pine Point Region, District of Mackenzie; *in* Report of Activities, April to October 1974, Geol. Surv. Can., Paper 75-1, Pt. A, p. 553-556.

McIntyre, D.J.
1974: Palynology of an Upper Cretaceous Section, Horton River, District of Mackenzie, N.W.T.; Geol. Surv. Can., Paper 74-14, p. 3-4.

Oilweek
1974: Gulf Parsons data focuses attention on Delta's Eskimo Lakes Fault Zone; Oilweek, v. 25, no. 5, March 18, 1974, p. 39-42.

Schlumberger Limited
1972: Schlumberger Log Interpretation, Principles; The Gamma Ray Log, v. 1, p. 57-59.

Swanson, V.E.
1961: Geology and geochemistry of uranium in marine black shales; A Review; U.S. Geol. Surv., Prof. Paper 356-C, p. 67-110.

Tourtelot, E.G.
1970: Selected annotated bibliography of minor-element content of marine black shales and related sedimentary rocks, 1930-65; U.S. Geol. Surv., Bull. 1293, p. 1-118.

Vine, J.D. and Tourtelot, E.G.
1970: Geochemistry of black shale deposits - a summary report; Econ. Geol., v. 65, p. 253-272.

Yorath, C.J., Balkwill, H.R. and Klassen, R.W.
1969: Geology of the eastern part of the Northern Interior and Arctic Coastal Plains, Northwest Territories; Geol. Surv. Can., Paper 68-27, p. 14-22.

Franklin Bay (97C) and Malloch Hill (97F) map-areas, District of Mackenzie; Geol. Surv. Can., Paper 74-36. (in press)

Yorath, C.J., Myhr, D.W. and Young, F.G.
1975: Geology of the Beaufort-Mackenzie Basin; Geol. Surv. Can., Open File Rept. 251.

58. THE STRATIGRAPHIC SIGNIFICANCE OF PERMIAN AMMONOIDS ON ELLESMERE ISLAND

Project 680064

W. W. Nassichuk
Institute of Sedimentary and Petroleum Geology, Calgary

Ammonoids constitute a rather small proportion of invertebrate megafossil specimens of marine origin that have been recovered from Permian rocks in the Sverdrup Basin but biochronologic data derived from them have contributed significantly to a general understanding of Permian stratigraphic relationships. Although ammonoids are known from the oldest Permian (Asselian) rocks in the Sverdrup Basin, they assume a special importance for correlating rocks of Artinskian and younger ages. Beginning in the early Artinskian, clastic deposition in the Sverdrup Basin was far more extensive than it had been during earlier Permian time. The beginning of this episode of clastic deposition coincided, more or less, with the disappearance of fusulinaceans from boreal regions of the world. Whereas data from fusulinaceans serve particularly well for correlating pre-Artinskian strata in the Sverdrup Basin, ammonoids and brachiopods have been used exclusively for correlating younger Permian rocks.

Early Permian ammonoids are abundant and have been rather completely documented from Bjorne Peninsula on southwestern Ellesmere Island and in the Hare Fiord and Blue Mountains regions of northwestern Ellesmere Island. On Bjorne Peninsula, a number of species of late Sakmarian or early Artinskian age were described by Nassichuk *et al.* (1966) from strata mapped as Assistance Formation by Thorsteinsson and Kerr (1972). In the following, the merits of reassigning so-called "Assistance" rocks on Bjorne Peninsula to a new, as yet unnamed formation are discussed. At Hare Fiord and in the Blue Mountains, some 12 km (7.5 miles) east of Hare Fiord, Asselian and Artinskian species were described from the Hare Fiord Formation by Nassichuk and Spinosa (1972) and by Spinosa and Nassichuk (1971). Although ammonoids of Artinskian and Roadian ages are known to occur at a number of localities elsewhere in western regions of Ellesmere Island, between Hamilton Peninsula in the north and Raanes Peninsula in the south, none have been described in the literature. Similarly, Roadian ammonoids from the van Hauen Formation in the Blue Mountains have not been described. The purpose of this report is to discuss stratigraphic implications of the little-known ammonoids from the latter regions but, for completeness, a brief stratigraphic review of previously described occurrences at Bjorne Peninsula and in the general vicinity of Hare Fiord is included.

All Permian ammonoid localities on southwestern and western Ellesmere Island, between Bjorne Peninsula and Hamilton Peninsula, are in formations which contain sandstone with minor limestone interbeds and which occur near the eastern margin of the Sverdrup Basin. The oldest (late Sakmarian or early Artinskian) ammonoids in this area occur in a new, unnamed formation east of Blind Fiord and on Bjorne Peninsula; in the latter area the new formation was designated the "Assistance" Formation by Thorsteinsson and Kerr (1972). Ammonoids of a comparable age are also known from the Tanquary Formation near Mount Bridgeman in the "Sawtooth Range" south of Cañon Fiord. The youngest (Roadian) ammonoids from western Ellesmere Island occur in the Assistance Formation (of typical Assistance aspect) on Hamilton Peninsula. All other ammonoids from Ellesmere Island, that is, Asselian and Artinskian species from the Hare Fiord Formation in the Hare Fiord-Blue Mountains region as well as Roadian species from the van Hauen Formation in the Blue Mountains, were recovered from concretionary shale and bioclastic limestone that reflect deposition in a relatively deeper part of the basin. Whereas the Hare Fiord Formation and the older (Carboniferous) evaporitic Otto Fiord Formation constitute Thorsteinsson's (1974) Basinal Clastic and Evaporitic Belt, the younger and particularly transgressive van Hauen Formation overlies not only Hare Fiord rocks in that belt but also rocks contained within Thorsteinsson's (ibid.) Northwestern Carbonate Belt to the northwest and the "Southeastern Carbonate Belt" to the southeast. As defined, none of Thorsteinsson's (ibid.) facies belts include rocks that are younger than early Artinskian.

Thorsteinsson (1974) presented a comprehensive discussion of strata that he assigned to the "Assistance" Formation on Bjorne Peninsula; thus, the need for more than a general statement of relationships of that formation is precluded here. It is particularly clear from Thorsteinsson's (ibid.) work that the general lithology and age of much of the so-called "Assistance" Formation on Bjorne Peninsula differs from the Assistance Formation in its type area at Grinnell Peninsula, Devon Island. In the latter area, the Assistance Formation occurs proximal to the southern edge of the basin and contains 70 m (220 ft.) of calcareous sandstone with bands of concretionary limestone; a prominent disconformity, reflecting transgressive overlap, occurs between the Assistance and the underlying Belcher Channel Formation. The Belcher Channel Formation consists of bioclastic limestone and minor sandstone and contains early Artinskian fusulinaceans in its upper part (Harker and Thorsteinsson, 1960). The top of the type section of the Assistance Formation is a Recent erosional surface. Locally, a rather thick accumulation of unconsolidated green "glauconitic" sandstone occurs at the surface in the type area and this may imply the former presence of the Trold Fiord Formation, which is characterized by green glauconitic sandstone and which is known to rest on the Assistance Formation elsewhere in southern and eastern regions of the Sverdrup Basin. Although most ammonoids from the type Assistance Formation indicate a latest Early Permian (Roadian) age (Nassichuk *et al.*,

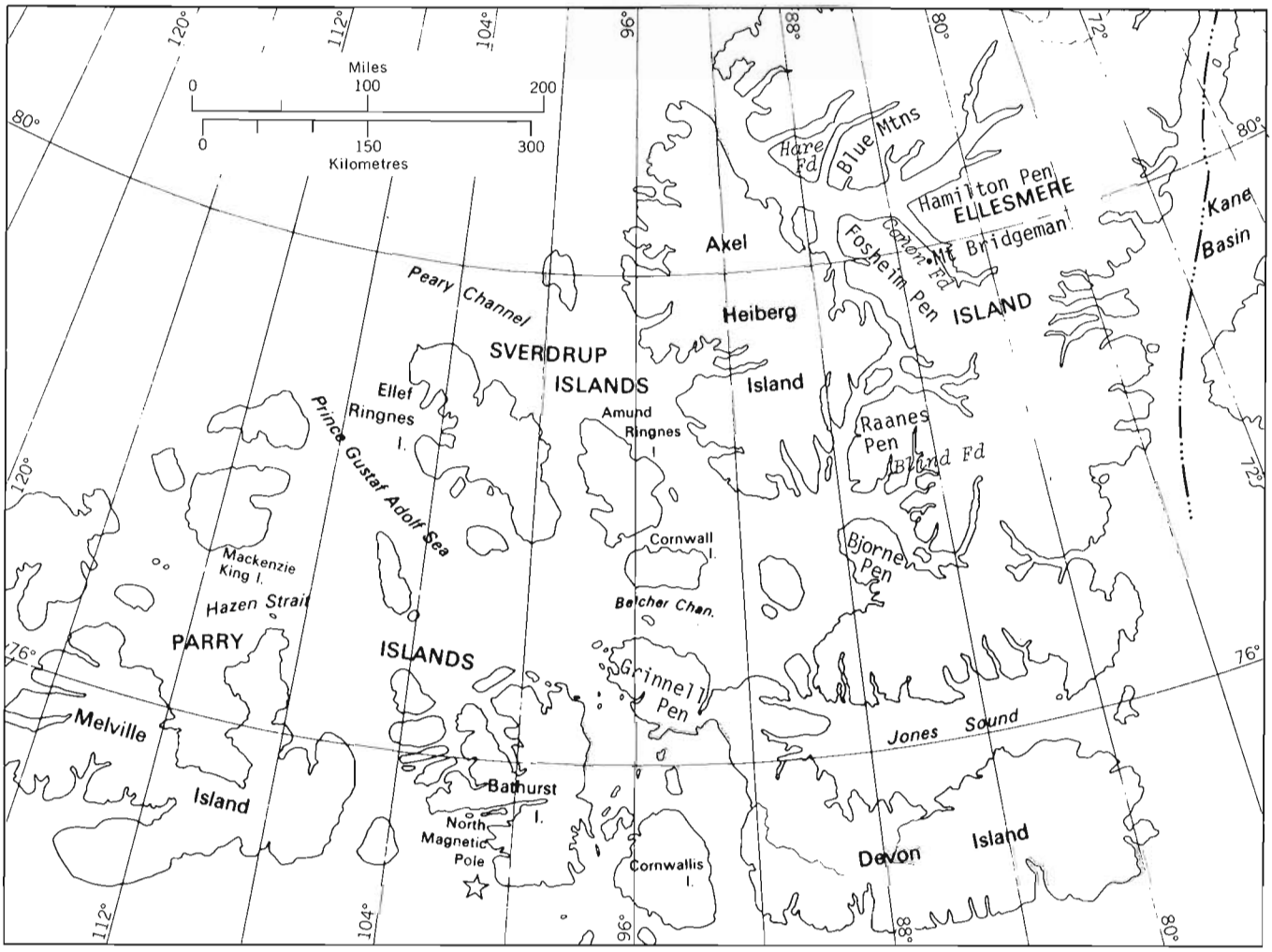

Figure 1. General reference map for Ellesmere Island and adjacent Islands.

1966), slightly older (Baigendzhinian) forms also may be represented (Nassichuk, 1970).

On Bjorne Peninsula, rocks that have been mapped as "Assistance" Formation include more than 330 m (1000 ft.) of shale, calcareous sandstone and limestone. The formation rests conformably on the Belcher Channel Formation and contains, in its middle part, a variety of late Sakmarian or early Artinskian ammonoids and brachiopods (Thorsteinsson, 1974). Post-Artinskian fossils have not yet been reported from the upper part of the "Assistance" on Bjorne Peninsula and a rather prominent disconformity may exist locally between that formation and the overlying Degerböls Formation of probable late Roadian or slightly younger Wordian age. Thorsteinsson (1974) suggested that the "Assistance" Formation on Bjorne Peninsula might logically be considered either a new formation or a deeper water continuation of typical Assistance rocks. Whereas Thorsteinsson (ibid.) preferred the latter procedure and and retained usage of Assistance Formation on Bjorne Peninsula, the present author favours the former and is currently preparing a paper to formally accommodate so-called "Assistance" rocks on Bjorne Peninsula as a new formation.

Rocks identical to the "Assistance" Formation on Bjorne Peninsula are rather widespread north of Bjorne Peninsula and are particularly well exposed above the Belcher Channel Formation east of the head of Blind Fiord. In that area, the late Sakmarian or early Artinskian ammonoid *Neoshumardites* sp. occurs near the bottom of the formation, and brachiopods of typical Assistance aspect (Waterhouse, pers. comm., 1974) occur near its top. Moreover, east of the head of Blind Fiord, the new, unnamed formation is overlain by a thin succession of siltstone and shale belonging to the upper part of the van Hauen Formation. A few miles to the west, however, on the west side of Blind Fiord, it can be seen that the sandstone and limestone of the new formation have graded to the darker weathering shale of the lower part of the van Hauen Formation (Member A of the van Hauen; Thorsteinsson, 1974), which rests directly on the Belcher Channel Formation.

Several ammonoids from the type area of the Assistance Formation that indicate a Roadian age, including

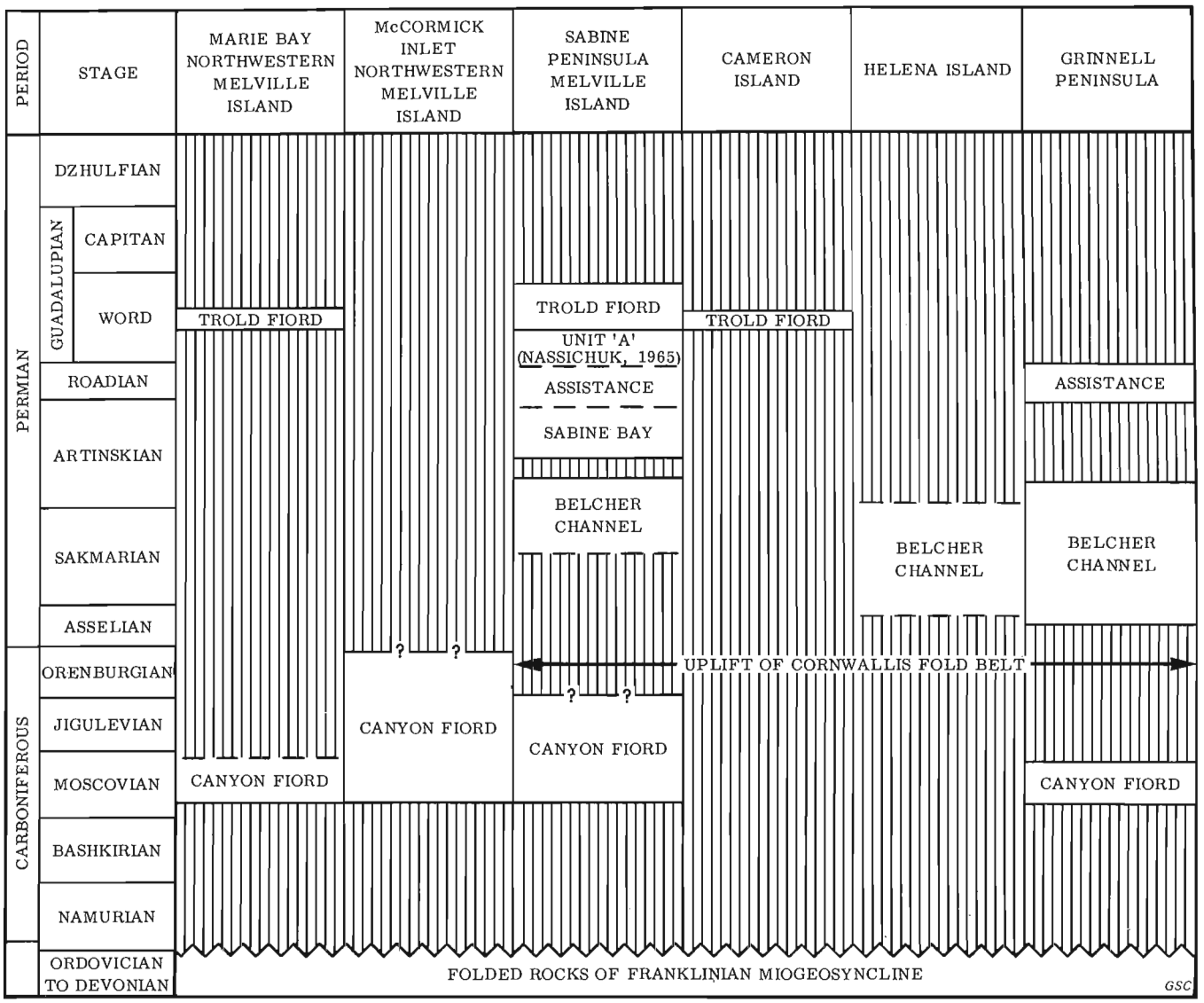

Figure 2. Correlation chart for Carboniferous and Permian rocks along the southern margin of the Sverdrup Basin.

representatives of *Daubichites* Popow and *Sverdrupites* Nassichuk, also occur in the Assistance Formation on Melville Island (Nassichuk, 1970) and at Hamilton Peninsula (this report). Furthermore, the same genera are known from the van Hauen Formation in the Blue Mountains of Ellesmere Island (this report). Additionally, the elasmobranch *Helicoprion* sp. occurs in the van Hauen Formation at Blind Fiord (Nassichuk and Spinosa, 1970) as well as the type section of the Assistance Formation (Nassichuk, 1971).

Whereas much of the van Hauen Formation is coeval with the type Assistance Formation, it must be stressed that locally the van Hauen probably embraces rocks that are slightly younger as well as slightly older than typical Assistance rocks. Evidence for both of the latter contingencies may be available from west of Blind Fiord where the van Hauen Formation rests conformably on carbonate rocks of Sakmarian age that were provisionally assigned to the Nansen Formation by Thorsteinsson (1974) and to the Belcher Channel Formation by Nassichuk (1975). It has already been stated that, to the east, the shale of the van Hauen Formation grades to argillaceous limestone and sandstone of a new unnamed formation of probable early Artinskian (pre-typical Assistance) age. Waterhouse (pers. comm., 1971) identified brachiopods from near the top of the van Hauen Formation at Blind Fiord and suggested that they were "slightly younger" than typical Assistance brachiopod faunas.

Finally, a single ammonoid species, *Uraloceras burtiense* (Voinova), occurs near the top of the Tanquary Formation on the southeast side of Mount Bridgeman, south of Cañon Fiord. The Tanquary Formation sensu stricto is contained within Thorsteinsson's (1974) Marginal Clastic and Carbonate Belt. In the Mount Bridgeman area, the Tanquary Formation attains its maximum thickness of 822 m (2740 ft.) measured between the underlying Mount Bayley Formation of Asselian age

and the overlying Sabine Bay Formation of Artinskian age (Thorsteinsson, 1974). The lower half of the formation includes a rhythmic alternation of resistant limestone and recessive shale while the upper half, reminiscent of "Assistance" rocks (= new formation) at Bjorne Peninsula and Blind Fiord, contains a uniform succession of thin-bedded calcareous sandstone and argillaceous limestone. Thorsteinsson (1974) reported the Artinskian fusulinacean *Schwagerina* sp. aff. *S. hyperborea* (Salter) from within 15 m (50 ft.) of the top of the Tanquary in the Mount Bridgeman area; the ammonoid *Uraloceras burtiense* (Voinova) was found near the top of the formation at a nearby locality but its precise position relative to *S. hyperborea* is unknown.

All the known ammonoids from Ellesmere Island, their stratigraphic positions, and ages are cited in the following summary.

A: Bjorne Peninsula, southwestern Ellesmere Island:

1. "Assistance Formation" - GSC locality 57719; 275 m (915 ft.) above base of the "Assistance" Formation (= unnamed formation) on eastern Bjorne Peninsula, less than 10 km (6 miles) west of Baumann Fiord (73°36'50"N, 86°13'W); *see* Section 52 of Thorsteinsson (1974).
   Neoshumardites cf. *N. sakmarae* (Ruzhencev)
   Paragastrioceras aff. *P. jossae* (de Verneuil)
   Uraloceras burtiense (Voinova)
   Uraloceras involutum (Voinova)
   Metalegoceras crenatum Nassichuk, Furnish and Glenister
   ?*Neopronorites* sp.
   Prothalassoceras sp.
   Age: Ammonoids at this locality lack elements that are sufficiently distinctive to discriminate between a late Sakmarian (Sterlitimakian) or early Artinskian (Aktastinian) age. Other fossil groups, however, tend to favour an early Artinskian age. Thorsteinsson (1974) indicated that early Artinskian fusulinaceans occur near the top of the underlying Belcher Channel Formation in the Bjorne Peninsula region and Waterhouse (*in* Thorsteinsson, 1974) favoured an early Artinskian age for the following brachiopods found in the "Assistance" Formation, directly associated with the previously-listed ammonoids at GSC locality 57719.
   orthotetacean
   echinoconchid, possibly *Bathymyonia* sp.
   Kutorginella sp.
   Linoproductus simensis (Tschernyschew)
   Yakovlevia sp.
   Septacamera mutabilis Tschernyschew
   Camerisma sp. aff. *C. pentameroides* (Tschernyschew)
   Orulgania sp. or *Pseudosyrinx* sp.
   Spiriferella polaris (Wiman)
   Martinia sp.

2. "Assistance Formation" - GSC locality C-1895; ammonoid talus collection from near the top of the "Assistance" Formation (= new unnamed formation), 6 km (3.75 miles) due east of Great Bear Cape, southwestern Bjorne Peninsula.
   Uraloceras burtiense (Voinova)
   Uraloceras involutum (Voinova)
   Age: late Sakmarian (Sterlitmakian) or early Artinskian (Aktastinian).

B: Blind Fiord, western Ellesmere Island:

On the east side of Blind Fiord, an unnamed formation of argillaceous limestone and sandstone closely comparable to "Assistance" rocks on Bjorne Peninsula occurs above the Belcher Channel Formation and below the van Hauen Formation; *see* Note 5 in Thorsteinsson, Tozer and Kerr (1972). The new formation is of the order of 300 m (1000 ft.) thick a few miles northeast of the head of Blind Fiord and is replete with a variety of fossils, particularly brachiopods.

Although ammonoids from the new formation at Blind Fiord lack sufficient diversity to provide an age more precise than "late Sakmarian or early Artinskian", brachiopods are diversified and abundant at a number of localities near the base of the formation and, for all of those collections, Waterhouse (pers. comm., 1970) suggested a definite Artinskian, probably an early Artinskian age. Similarly, Waterhouse (pers. comm., 1974) suggested a late Kungurian age for brachiopods collected from several localities near the top of the formation, directly beneath the van Hauen Formation. Thus, the new formation ranges from early Artinskian to Roadian; that is, it is equivalent both to so-called "Assistance" rocks on Bjorne Peninsula (Artinskian) and to typical Assistance rocks at Grinnell Peninsula (Roadian).

1. Unnamed formation - GSC locality C-10514; ammonoids from 105 m (350 ft.) above the base of an unnamed formation, 6.4 km (4 miles) northeast of the head of Blind Fiord (78°24'30"N, 85°35'W).
   Neoshumardites cf. *N. sakmarae* (Ruzhencev)
   Age: late Sakmarian (Sterlitimakian) or early Artinskian (Aktastinian).

C: Mount Bridgeman, western Ellesmere Island:

On the southeast side of Mount Bridgeman (Fig. 1), the Tanquary Formation has a thickness of 822 m (2740 ft.); it occurs above the Mount Bayley Formation of latest Pennsylvanian (Orenburgian) and/or earliest Permian (Asselian) age and the Sabine Bay Formation of Artinskian age. Thorsteinsson (1974) reported the fusulinid *Schwagerina* sp. aff. *S. hyperborea* (Salter) from within 15 m (50 ft.) of the top of the formation on the southeast side of Mount Bridgeman and that species is indicative of an early Artinskian age. The section that yielded ammonoids near Mount Bridgeman is about 0.8 km (0.5 mile) along strike to the west of Thorsteinsson's (ibid.) fusulinid locality. Ammonoids were found in a section of the Tanquary Formation that did not

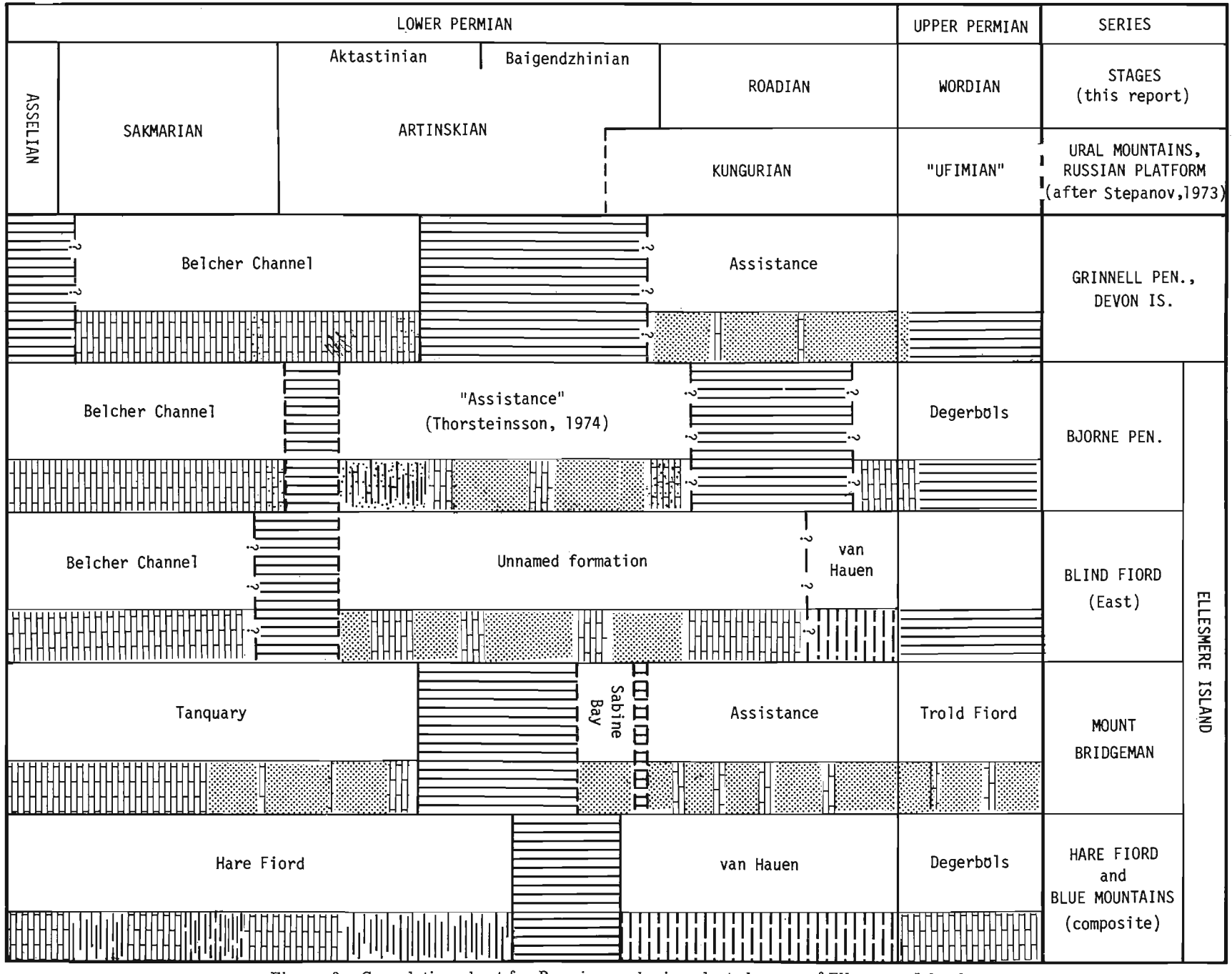

Figure 3. Correlation chart for Permian rocks in selected areas of Ellesmere Island.

yield the diagnostic *S. hyperborea* and so the position of ammonoids relative to that important fusulinid is uncertain.

1. Tanquary Formation - GSC locality C-39365; 9 m (30 ft.) below the top of the Tanquary Formation on the south side of Mount Bridgeman, 9 km (5.6 miles) from the nearest (western) shore of Cañon Fiord (71°51'30"N, 82°38'W). The locality is 0.8 km (0.5 mile) from Thorsteinsson's (1974) Section 56.
   Uraloceras burtiense (Voinova)
   Age: late Sakmarian (Sterlitimakian) or early Artinskian (Aktastinian).

D: Hamilton Peninsula, western Ellesmere Island:

1. Assistance Formation - GSC locality C-39374; 'talus' collection from a solifluction slope on a terrace 8 km (5 miles) northeast of Tschernyschew River (80°19'30"N, 81°00'00"W). The source of materials is uncertain but the Tanquary, Sabine Bay and Assistance formations ('true' Assistance) crop out in the immediate vicinity. Fossils are preserved in an olive-grey sandstone that resembles typical Assistance sandstones:
   Sverdrupites sp. indet.
   Age: Roadian.

2. Assistance Formation - GSC locality C-37487; talus collection from near the base of the Assistance Formation ('true' Assistance), 8.6 km (5.6 miles) east-northeast of the mid-point of the delta formed by East Cape River (80°02'30"N, 81°44'30"W).
   Daubichites fortieri (Harker)
   Age: Roadian.

E: Blue Mountains, northern Ellesmere Island:

1. Hare Fiord Formation - GSC locality C-4320; 456 m (1550 ft.) above the top of the "Tellevak Limestone" member of the Hare Fiord Formation on the west side of the Blue Mountains, 11.6 m (7.28 miles) southeast of Hare Fiord (80°43'30"N, 85° 40'W). Ammonoids occur in concretions in a black shale sequence in the upper member of the Hare Fiord Formation.
   Stacheoceras n. sp. Spinosa and Nassichuk, 1971
   Paragastrioceras n. sp. Nassichuk, Furnish and Glenister, 1966
   Popanoceras sp.
   ?*Neocrimites* sp.
   Age: Artinskian.

2. Hare Fiord Formation - GSC locality 47869; is on the same shale slope as the previous locality and for all practical purposes occupies the same stratigraphic level.
   Paragastrioceras n. sp. Nassichuk, Furnish and Glenister, 1966.
   Age: Artinskian.

3. van Hauen Formation - GSC locality C-39375; 360 m (1200 ft.) below the top of the van Hauen Formation about 600 m (2000 ft.) stratigraphically above the two previously listed Hare Fiord Formation localities. The lower part of the van Hauen Formation in which this locality occurs consists of dark-weathering siltstone and shale and is gradational with the underlying Hare Fiord Formation of similar composition. The formations can be distinguished one from the other only with considerable difficulty in this area and hence a stratigraphic measurement from the top of the van Hauen rather than from the base is given here. In this area, the Hare Fiord and van Hauen formations have a combined thickness of 1590 m (5300 ft.); of this thickness, about 1200 m (4000 ft.) belong to the Hare Fiord Formation.
   Ammonoids are: *Sverdrupites harkeri* (Ruzhencev)
   Daubichites fortieri (Harker)
   Age: Roadian.

F: Hare Fiord, northern Ellesmere Island:

1. Hare Fiord Formation - GSC locality C-4088; 300 m (1000 ft.) above the base of the Hare Fiord Formation, 13.6 km (8.5 miles) northeast of van Hauen Pass (81°07'05"N, 85°01'W).
   Somoholites cf. *S. artus* Ruzhencev
   Kargalites sp.
   Neopronorites sp.
   Agathiceras sp.
   Age: Asselian.

2. Hare Fiord Formation - GSC locality C-4093; approximately 300 m (1000 ft.) above the base of the Hare Fiord Formation, 11.5 km (7.2 miles) northeast of van Hauen Pass (81°06'15"N, 85°07'W).
   Neopronorites sp.
   Agathiceras sp.
   Age: Asselian.

3. Hare Fiord Formation - GSC locality 58302; is estimated to be some 180 m (600 ft.) below the top of the Hare Fiord Formation, 3.2 km (2 miles) west of Stepanov Creek and 1.6 km (1 mile) north of Hare Fiord (81°07'30"N, 84°18'00"W).
   Paragastrioceras n. sp. Nassichuk, Furnish and Glenister, 1966
   Age: Artinskian.

References

Harker, P. and Thorsteinsson, R.
1960: Permian rocks and faunas of Grinnell Peninsula, Arctic Archipelago; Geol. Surv. Can., Mem. 309.

Nassichuk, W.W.
1970: Permian ammonoids from Devon and Melville Islands, Canadian Arctic Archipelago; J. Paleontol., v. 44, no. 1, p. 77-97, pls. 19-22.

Nassichuk, W.W. (cont'd.)
1971: *Helicoprion* and *Physonemus*, Permian vertebrates from the Assistance Formation, Canadian Arctic Archipelago; Geol. Surv. Can., Bull. 192, p. 83-93.

1975: Carboniferous ammonoids and stratigraphy in the Canadian Arctic Archipelago; Geol. Surv. Can., Bull. 237.

Nassichuk, W.W., Furnish, W.M. and Glenister, Brian F.
1966: The Permian ammonoids of Arctic Canada; Geol. Surv. Can., Bull. 131.

Nassichuk, W.W. and Spinosa, Claude
1970: *Helicoprion* sp., a Permian Elasmobranch from Ellesmere Island, Canadian Arctic; J. Paleontol., v. 44, p. 1130-1132.

1972: Early Permian (Asselian) ammonoids from the Hare Fiord Formation, northern Ellesmere Island; J. Paleontol., v. 46, no. 4, p. 536-544, Pl. 1.

Spinosa, Claude and Nassichuk, W.W.
1971: The Permian ammonoid *Stacheoceras* discovered on Ellesmere Island, Canadian Arctic; Geol. Surv. Can., Bull. 192, p. 89-93.

Thorsteinsson, R.
1974: Carboniferous and Permian stratigraphy of Axel Heiberg Island and western Ellesmere Island, Canadian Arctic Archipelago; Geol. Surv. Can., Bull. 224.

Thorsteinsson, R. and Kerr, J.W.
1972: Geology Baumann Fiord, District of Franklin; Geol. Surv. Can., Map 1312A (Scale 1:250 000).

Thorsteinsson, R., Tozer, E.T. and Kerr, J.W.
1972: Geology Eureka Sound South, District of Franklin; Geol. Surv. Can., Map 1300A (Scale 1:250 000).

59. SEQUENCE AND RELATIONSHIPS OF THREE LOWER DEVONIAN CORAL FAUNAS FROM YUKON TERRITORY

Project 680093

A. E. H. Pedder
Institute of Sedimentary and Petroleum Geology, Calgary

One of the aims of Project 680093 is to establish the sequence of Lower Devonian corals faunas in northwestern Canada. Although results are still of a preliminary nature, five, possibly as many as seven, such faunas are already evident. The purposes of the present communication are to make three of these known, so that they can be used immediately in biostratigraphic work, and to document their biogeographic relationships, which are of special interest in regard to the Lower Devonian coral sequence recently established in Nevada by Merriam (1973a-1974b).

The Lower Devonian coral faunas of Nevada, Yukon Territory and Alaska (Churkin and Brabb, 1968) are correlated with reasonable ease within the framework of conodont sequences established in the same areas by Klapper, Lane and Ormiston. They are not, however, easily related to the standard European stages.

Corals associated with the *Pedavis pesavis* conodont assemblage in Yukon Territory are illustrated by Figures 2 to 21. Quite clearly this fauna is very different from the coral fauna associated with *P. pesavis* in the breccia member of the Windmill Limestone in Nevada. The fauna of this breccia member is Merriam's "Silurian" E fauna and comprises *Stylopleura berthiaumi* Merriam, *S. nevadensis* (Merriam), *Kodonophyllum mulleri* Merriam, *Mucophyllum oliveri* Merriam, *Dubrovia simpsoni* (Merriam) (includes Merriam's *Chonophyllum* sp. cf. *C. simpsoni*), *D.* sp. (= *Ryderophyllum*? sp. of Merriam), *Neostringophyllum* sp. broad sense (= *Cyathactis*? sp. of Merriam), *Neomphyma nevadensis* (Merriam), "*Salairophyllum*?" sp., *Kozlowiaphyllum johnsoni* (Merriam), *K.* spp., *Aphroidophyllum* sp. (Figs. 56, 57 of this work), *Cystiphyllum* sp. and *Rhizophyllum* sp. cf. *R. enorme* Etheridge (Oliver, 1964, Figs. 153. 5a, b). Unlike other late Lochkovian Old World coral faunas, this one is almost completely dominated by Silurian hold-overs, and it is not at all surprising that Merriam regarded it as Silurian. On the other hand, data, given in the systematic notes appended below, indicate that the coral fauna associated with *P. pesavis* in Yukon Territory is similar to the Old World faunas of Europe, Asia and Australia.

Figures 22 to 38 depict corals occurring with the late form of *Eognathodus sulcatus* in Yukon Territory. At the generic level they are typical of other Old World coral faunas of comparable age, but differ, even at family level, from the corals associated with late *sulcatus* conodonts in Nevada (Merriam's Devonian B fauna), which consist entirely of species of an endemic halliid genus, known as *Kobeha.*

	STAGES		CONODONT FAUNAS	NEVADA CORAL FAUNAS	YUKON CORAL FAUNAS
DEVONIAN	EMSIAN		perbonus n. subsp.	Devonian D3	
		ZLICHOVIAN	perbonus s.s. 9	Devonian D2	
		PRAGIAN	dehiscens 8	Devonian D1	dehiscens associates
			dehiscens 7	Devonian C	
	SEIGENIAN ?		late sulcatus 6	Devonian B	late sulcatus associates
	?		early sulcatus 5	Devonian A	
LOWER	GEDINNIAN	LOCHKOVIAN	pesavis 4	"Silurian" E	pesavis associates
			Spathognathodus n. sp. 3		
			eurekaensis 2	"Silurian" D	
			woschmidti 1		

Figure 1.

Relationships between Yukon and Nevada coral and conodont sequences, and Lower Devonian stages. The Nevada coral faunas are those of Merriam (1973a-1974b), while the conodont sequence is that recognized by Klapper (*in* Klapper *et al.*, 1971; Lenz and Pedder, 1972; Perry *et al.*, 1974; Klapper and Murphy, 1975) in both Nevada and Yukon Territory. Correlations with the Bohemian and Rhenish stages are approximate. They rely heavily on the works of Carls (1969), Carls *et al.* (1972) and a personal communication from R. Thorsteinsson, to the effect that pteraspids, associated with *Pedavis pesavis* and brachiopods of the *Quadrithyris* Zone on Prince of Wales Island in the Canadian Arctic, are of a similar biologic grade as *Protopteraspis primaeva* and *P. gosseleti,* which in the Ardennes and Artois are of Middle Gedinnian age.

Illustrations of the corals associated with late occurrences of *Polygnathus dehiscens* in Yukon Territory are given in Figures 39 to 55. Again, at generic level, the fauna has obvious Old World affinities. It also differs remarkably from the corals associated with late occurrences of *P. dehiscens* in Nevada (Merriam's Devonian D1 fauna), as these include *Breviphrentis* spp., *Papiliophyllum elegantulum* n. subsp., "*Bethanyphyllum*?" sp. and "*Sinospongophyllum*" sp.

It is evident that initial studies of late Lochkovian and Pragian coral faunas in Nevada and Yukon Territory fully support the notion of distinct faunal realms during late Lochkovian and Pragian times in Cordilleran North America. In the terminology of Boucot (1975, p. 311-332) these are the Nevadan Subprovince of the Eastern Americas Realm and the Old World Realm.

SYSTEMATIC NOTES

Family Laccophyllidae Grabau

Genus *Barrandeophyllum* Počta, 1902

Type species. *B. perplexum* Počta. Type stratum Pragian or Zlichovian; originally cited as "calcaire de la bande g 1, à Hlubočep". Hlubočep Valley is just south of Prague, Czechoslovakia.

Remarks. Species of *Barrandeophyllum* resemble those of *Syringaxon*, the difference being that in *Barrandeophyllum* tabulae are developed within, as well as between, pairs of contratingent septa. Most species of *Barrandeophyllum* have thinner septa than those found in *Syringaxon*, although the specimen from late *sulcatus*-bearing beds at Royal Creek is exceptional in this respect.

In central Asia *Barrandeophyllum* ranges from Pridolian (Upper Arg Beds and correlatives of Tadzhikistan) to Eifelian (Kryukova Beds of the Mountain Altai and correlatives in the Dzhungar-Balkhash region). In Europe its known range is Pragian (Koněprusy Lst., Czechoslovakia; Erbsloch Grauwacke, Germany) to late Emsian (Daleje Shales, Czechoslovakia; Lauterberg Lst., Germany) and possibly early Eifelian in France (Chalonnes Lst.). Definite Eifelian occurrences are known in the Urals. Other known occurrences are Emsian and Eifelian in Morocco, and Lochkovian (Boola Beds) and Pragian (Coopers Creek Lst.) in Australia. The Pragian occurrence reported here is the first record of the genus in North America.

New laccophyllid gen. and sp.

A small coral from *pesavis*-bearing beds at Royal Creek resembles species of both *Barrandeophyllum* and *Petraia*, but is unlikely to belong to either of these genera, because of its prominent fossulae. It is further differentiated from *Barrandeophyllum* in lacking an aulos, and from *Petraia* in possessing numerous tabulae within the loculi formed by the contratingent major and minor septa.

Family Stauriidae Edwards and Haime

Genus *Fasciphyllum* Schlüter, 1885

Type species. *Fascicularia conglomerata* Schlüter. The lectotype is from the early Givetian Fleringer Schichten, near Hillesheim, Germany.

Remarks. This fasciculate genus has a narrow

Figures 2-21 (opposite)

Corals of *pesavis*-bearing beds of Yukon Territory.

Figures 2, 5. *Spongophyllum* sp. cf. *S. rosiforme* (Zheltonogova), x4, GSC 42566, Loc. 69301.

Figures 3, 4. *Xystriphyllum* n. sp., x3, GSC 42567, Loc. C-12890.

Figures 6, 9. *Pseudamplexus* sp. cf. *P. bohemicus* (Počta), x1.5, GSC 42568 (6) and GSC 42569 (9); both Loc. C-12890.

Figures 7, 8. new gen. and sp., cf. "*Pseudomicroplasma*" *multilobata* Spasskiy, x2, GSC 42570, Loc. 69301.

Figures 10, 11, 13. new laccophyllid gen. and sp., x3, GSC 42571, Loc. C-4264.

Figures 12, 16. *Dubrovia* n. sp., x1.5, GSC 42572, Loc. C-4271.

Figure 14. *Lyrielasma* sp., x3, GSC 42573, Loc. C-4264.

Figures 15, 19. *Lyrielasma*? sp., x3, GSC 42574, Loc. C-12891.

Figures 17, 18. new phaceloid arachnophyllid gen. and sp., x2, GSC 42575, Loc. C-4264.

Figures 20, 21. *Pseudogrypophyllum* sp., x3, GSC 42576, Loc. C-4272.

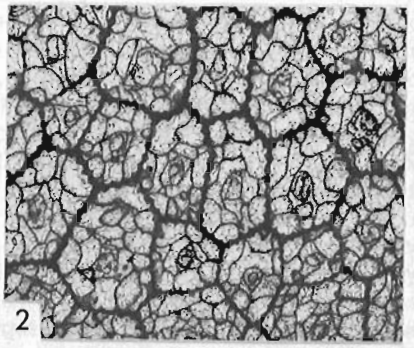
2

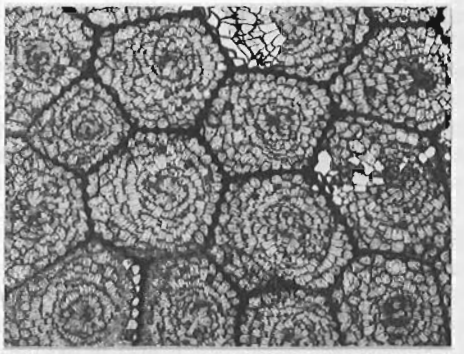
3

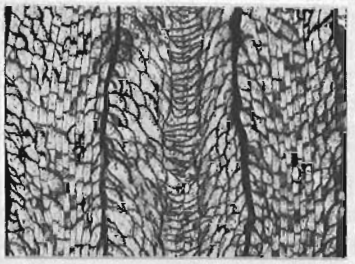
4

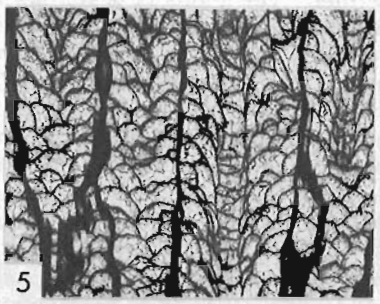
5

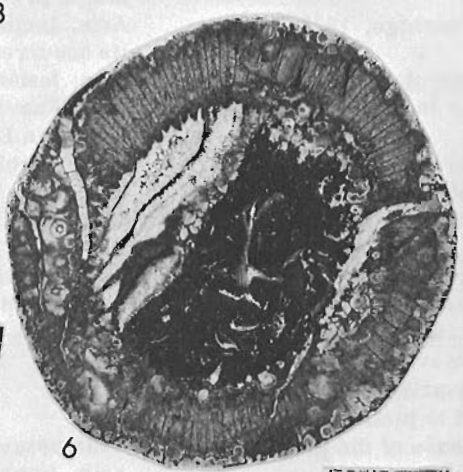
6

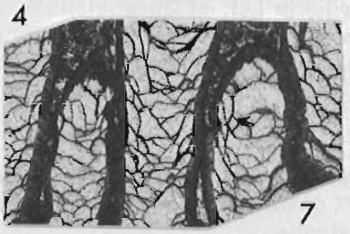
7

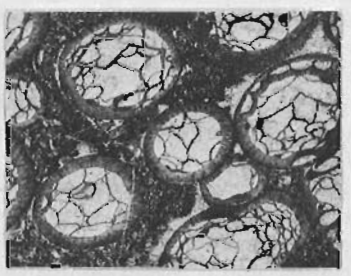
8


9


10


11

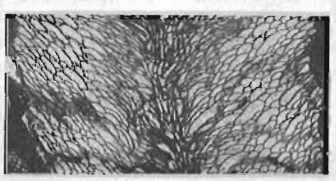
12

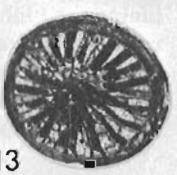
13

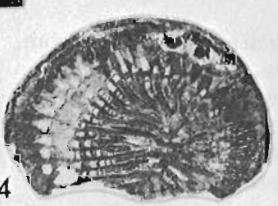
14

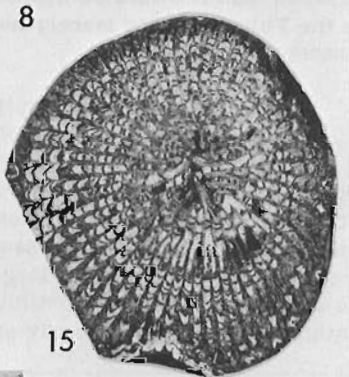
15

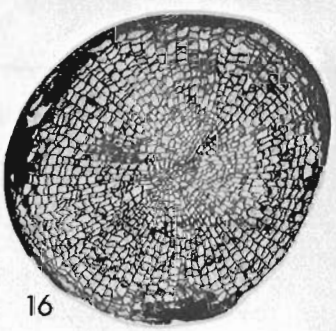
16

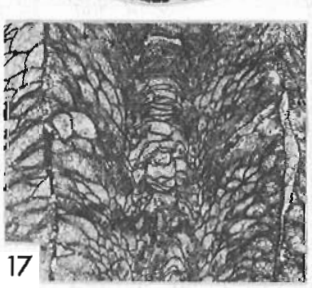
17


18


19

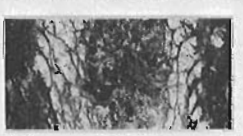
20

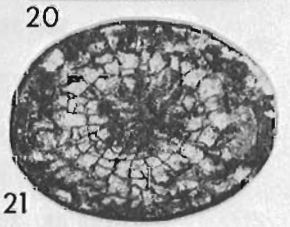
21

peripheral stereozone and a complete, or incomplete, series of relatively large elongate dissepiments. The septa may bear vepreculae and the cardinal and counter septa may be longer than other major septa. The genus is probably a junior synonym of *Battersbyia*, but the type species of *Battersbyia* is poorly understood.

Fasciphyllum is known from scattered occurrences in Europe, Asia and Australia, that range in age from Pragian (Upper Turk-Parida Suite of Tadzhikistan; Coopers Creek Lst. of Victoria) to Givetian (Carnic Alps; Burdekin Lst. of Queensland). Prior to the discovery of a species in late Pragian strata at Royal Creek, the genus was unknown in North America.

Genus *Vepresiphyllum* Etheridge, 1920

Type species. *V. falciforme* Etheridge. Zlichovian part of the Taemas Limestone, Wee Jasper area, N.S.W., Australia.

Remarks. Features most characteristic of this stauriid genus, are the highly vepreculate septa and sagging tabulae. The species from late *sulcatus*-bearing limestones at Royal Creek is new and is the first known outside Australia. It was first identified (Lenz and Pedder, 1972, p. 16) as n. gen. cf. *Vepresiphyllum*, because of the presence of dissepiments, which are entirely absent from the type species. However, the development of dissepiments in other stauriids is extremely variable, and it would be difficult to justify a new genus for the Yukon species merely because of the presence of some dissepiments.

Family Mucophyllidae Hill

Genus *Pseudamplexus* Weissermel, 1897

Type species. *Zaphrentis ligeriensis* Barrois. Emsian, Erbray Limestone, Erbray, France.

Remarks. The corallum in Pseudamplexus is trochoid to cylindrical and usually large and solitary. Septa are short and typically constituted of coarse rhabdacanthine trabeculae. In early species, including the type, they are poorly differentiated and contiguous for most of their length, thus forming a peripheral stereozone; in late species they may be clearly differentiated into major and minor orders and may taper adaxially, creating interseptal loculi. The tabulae are broad, locally complete, and generally form flat tabularial surfaces. Dissepiments are extremely rare, evidently completely absent from some species.

Pselophyllum Počta, 1902 and *Pseudotryplasma* Ivaniya, 1958 are synonymous with *Pseudamplexus*, but the Silurian genus *Pseudomphyma* Wedekind, 1927, which has also been regarded synonymous, has a tabular fossula and sclerenchymal thickening of the septa, and is probably distinct. The genus is best known in Asia, including the Urals and Novaya Zemlya, where its occurrences are Pridolian (Kunzhak Beds, Tadzhikistan; lower Petropavlov Suite, central Urals) to Givetian (Anavar Beds, Tadzhikistan). It is also well known in Europe and Australia, where it ranges from early Lochkovian (Borshchov Beds, Podolia; Nemingha Lst., N.S.W.) to late Emsian (Erbray Lst., France; Sulcor Lst., N.S.W.). Its range in Yukon Territory is Lochkovian to Zlichovian, but in Alaska, which is the only other region of North America where it has been found, it is apparently confined to Pragian strata.

Family Arachnophyllidae Dybowski

New phaceloid gen. and sp.

This *pesavis* associate from Royal Creek, was identified as n. kyphophyllid gen. and sp. by Lenz and Pedder (1972, p. 22). It differs from *Kyphophyllum* in being phaceloid rather than solitary. In this respect it resembles *Strombodes*, but the type species of that genus has a wide tabularium and narrow dissepimentarium, which is redeveloped subsequent to numerous rejuvenescenses. Furthermore each of the rejuvenescenses is preceded by a marked flaring of the marginarium. These features strongly suggest *Strombodes* to be an endophyllid.

Figures 22-38 (opposite)

Corals of late *sulcatus*-bearing beds of Yukon Territory.

Figures 22, 24. *Pseudamplexus* n. sp., x1.5, GSC 42577, Loc. C-4281.

Figures 23, 25. *Patridophyllum* n. sp., x1.5, GSC 42578, Loc. 69304.

Figures 26, 30. *Dohmophyllum* sp., x1.5, GSC 42579, Loc. C-4282.

Figures 27, 28. *Lyrielasma* sp., x3, GSC 42580, Loc. C-4283.

Figures 29, 32. *Xystriphyllum* n. sp., x3, GSC 42581, Loc. C-4282.

Figures 31,33,36. *Barrandeophyllum* sp., x3, GSC 42582, Loc. C-4283.

Figures 34, 37. new solitary arachnophyllid gen. and sp., x3, (34) GSC 42583, Loc. 69303; (37) GSC 42584, Loc. 67547.

Figures 35, 38. *Vepresiphyllum* n. sp., x5, GSC 42585, Loc. C-4281.

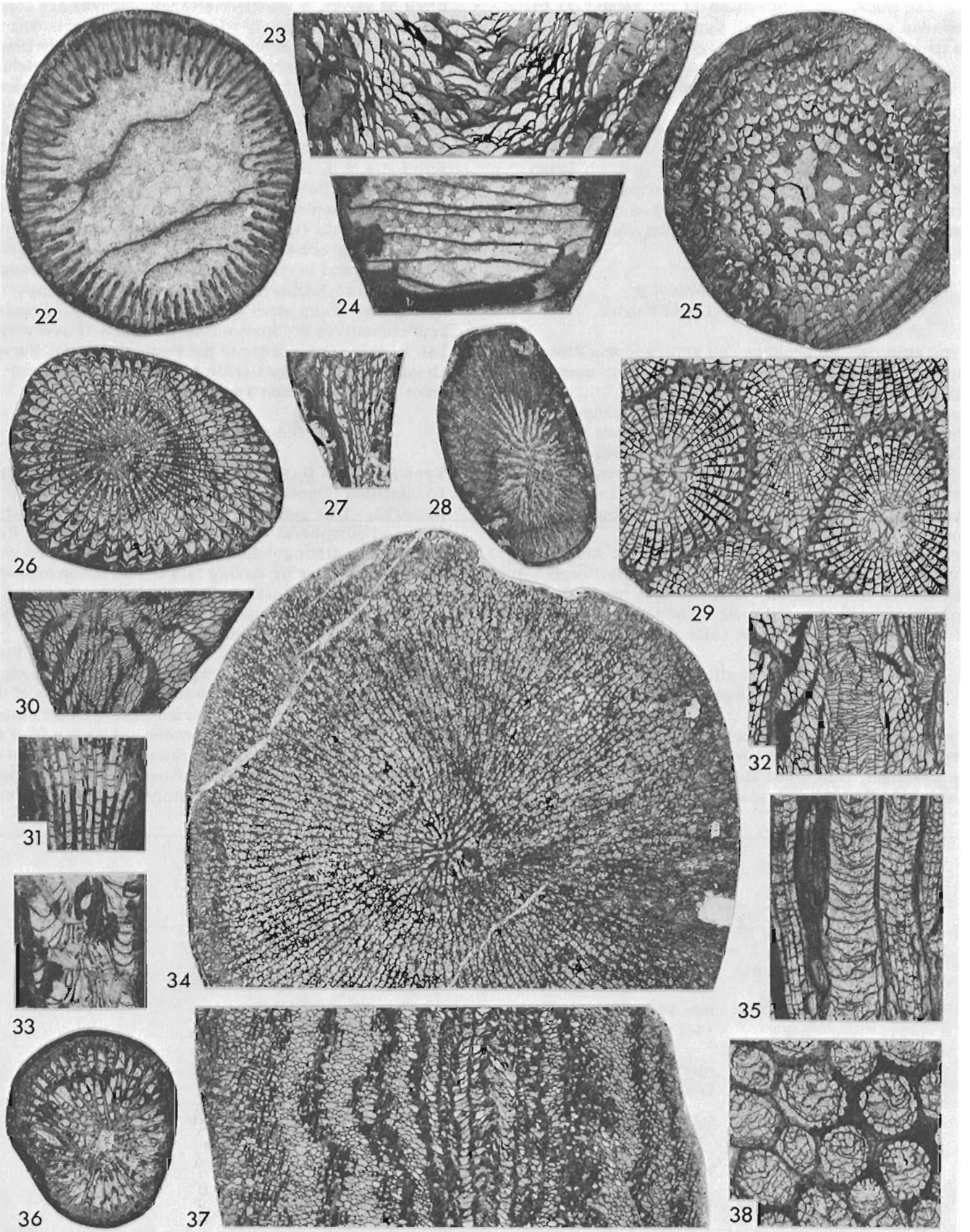
22
23
24
25
26
27
28
29
30
31
32
33
34
35
36
37
38

The Royal Creek specimen is not related to the Nevadan species ascribed to *Kyphophyllum* by Merriam, as they are more correctly assigned to *Neomphyma*.

New solitary gen. and sp.

This coral from late *sulcatus*-bearing beds resembles the genus *Ramulophyllum* and may have developed from it since *Ramulophyllum* occurs in Lochkovian strata in Kazakhstan. It differs in having a much wider dissepimentarium and better developed septa in the axial region. It was listed as *Ramulopyllum* (sic) by Lenz and Pedder (1972, p. 16).

Family Disphyllidae Hill
Genus *Martinophyllum* Jell and Pedder, 1969

Type species. *M. ornatum* Jell and Pedder. Probable late Lochkovian, Martin's Well Limestone, northern Queensland, Australia.
Remarks. *Martinophyllum* differs from *Hexagonaria* and *Argutastrea* in having long trabecular fibres diverging only slightly from the trabecular axes. It is widely distributed in limestones of late Lochkovian and Pragian age in eastern Australia, and has recently been figured from Pragian strata in southern China and the Mountain Altai region of Russia. In North America it is presently known only from Alaska and Yukon Territory, where its range is late Pragian and Zlichovian (Salmontrout, Michelle and lower Ogilvie Formations and correlatives). The latest occurrence is apparently in late Emsian beds of the central Urals.

Family Spongophyllidae Dybowski
Genus *Spongophyllum* Edwards and Haime, 1851

Type species. *S. sedgwicki* Edwards and Haime. The provisional neotype is a pebble specimen, believed to be Devonian, from south Devonshire, England.
Remarks. Royal Creek specimens, identified as *Spongophyllum* sp. cf. *S. rosiforme* (Zheltonogova) are cerioid, and have relatively wide dissempimentaria composed almost exclusively of presepiments. Very likely they should be referred to a new genus, distinguished from true *Spongophyllum* by its highly reduced major septa, and from *Neomphyma* by its cerioid form. The oldest spongophylloids of this type may be Wenlockian (limestone outcropping near Kiturin, Manchuria; Ozbak-Kuh Lst., N.E. Iran); Ludlovian occurrences are certain (Kawauti Series, Japan; Kosor Lst., Czechoslovakia). Spongophyllids of this sort are known also from Pridolian strata (Kunzhak Beds of Tadzhikistan), and reached their acme in Lochkovian strata, in Australia (Nemingha and lower Garra Lst.), Asia (Tomchumysh, Shishkat and Remnev Beds), Urals (Siyak, upper Petropavlov Suite etc.) and Yukon Territory. Pragian representatives are known from Australia (Silverwood Lst.), Asia (Ganin Beds of the Mountain Altai), Europe (Seewarte Lst. of the Carnic Alps), Alaska (Salmontrout Lst.) and Yukon Territory.

Genus *Dubrovia* Zheltonogova, 1960

Type species. *D. dubroviensis* Zheltonogova. Early Lochkovian, Tomchumysh Beds, Salair, U.S.S.R.
Remarks. This genus is characterized by its solitary form and peripheral withdrawal of at least some of its septa. It is distinguished from the closely related genus *Spongophylloides* by having larger and fewer presepiments, and from *Dohmophyllum* in having a predominantly inwardly sloping dissepimentarium, that invariably lacks naotic presepiments.

The genus may be as old as Wenlockian in the Tarbagatay Range of the southern Altai, and it is undoubtedly present in the Ludlovian Durnay Beds of the Pripolar Urals and Upper Silurian Borovyshkin Suite of the Altai. Pridolian occurrences are known from the Baltic (Kaugatuma Beds of Saaremaa Island), Podolia (Skala Beds), Vaygach Island (Greben Beds), Pripolar Urals (Greben Beds), and possibly Iran (Upper Niur

---

Figures 39-55 (opposite)

Corals of *dehiscens*-bearing beds of Yukon Territory.

Figures 39, 40. *Martinophyllum* n. sp., x3, GSC 42586, Loc. 67543.

Figures 41-43. *Fasciphyllum* sp., x4, GSC 42587, Loc. C-12894.

Figures 44, 45. new solitary cystiphyllid gen. and sp., x2, GSC 42588 (44) and GSC 42589 (45); both Loc. C-12694.

Figures 46, 49. new cerioid cystiphyllid gen. and sp., x3, GSC 42590, Loc. 69314.

Figures 47, 48. *Xystriphyllum* n. sp., x3, GSC 42591, Loc. C-12894.

Figures 50, 52. *Pseudamplexus* n. sp., x1.5, GSC 42592, Loc. C-12694.

Figures 51, 53. *Dohmophyllum* sp., x1.5, GSC 42593, Loc. C-26750.

Figures 54, 55. *Taimyrophyllum* n. sp., x3, GSC 42594, Loc. C-12894.

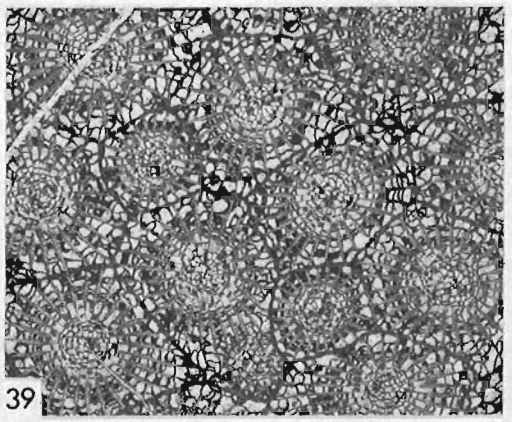
39

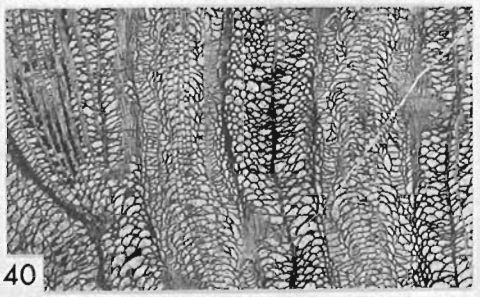
40

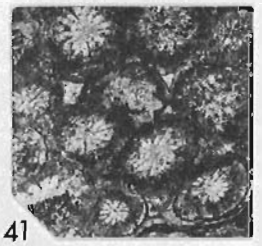
41


42


43

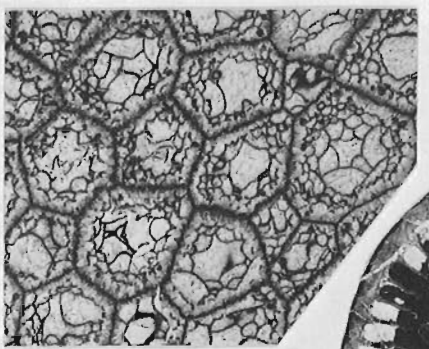
46

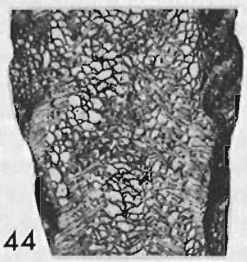
44

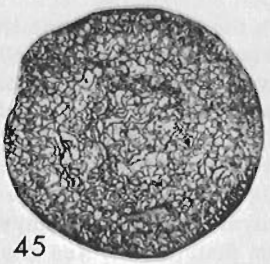
45

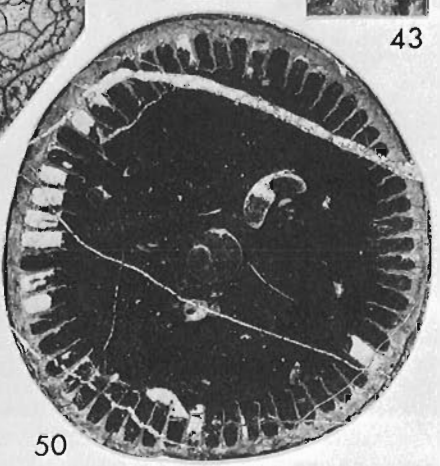
50

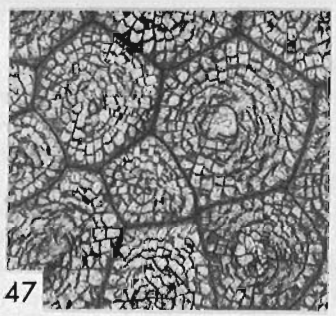
47

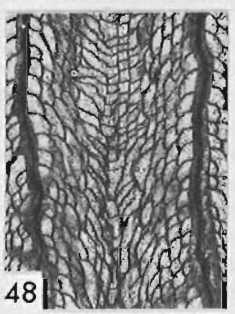
48

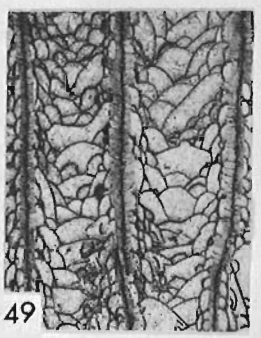
49

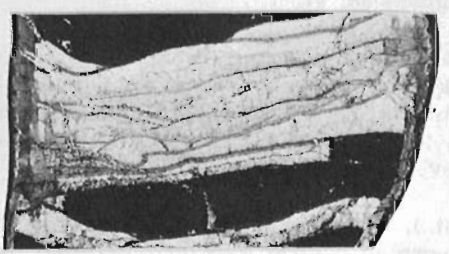
52

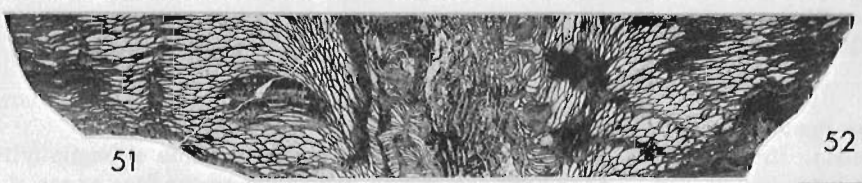
51

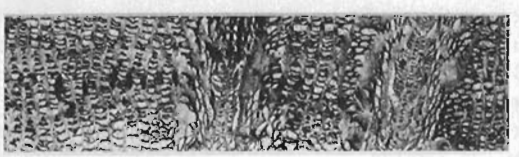
54

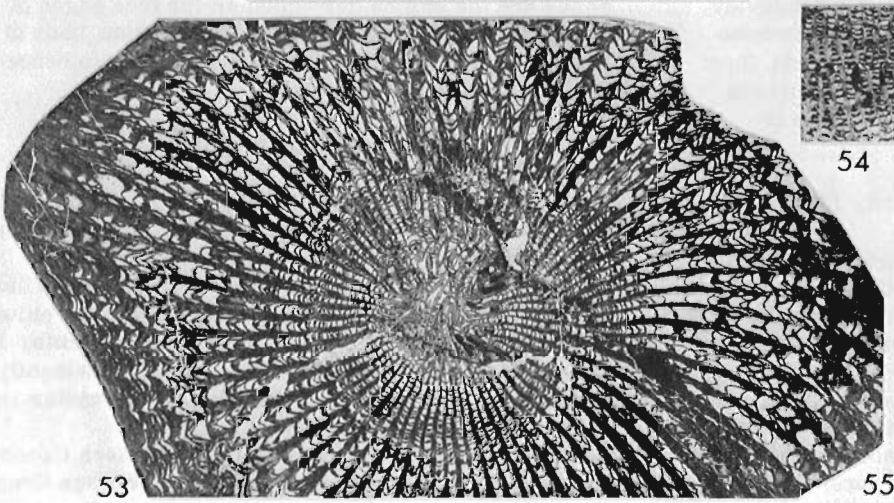
53

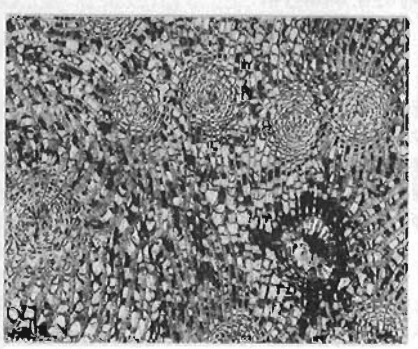
55

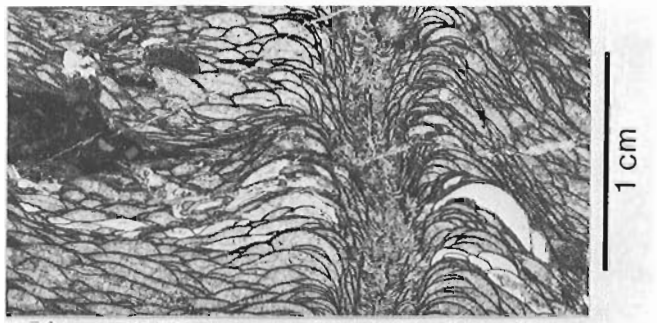

56

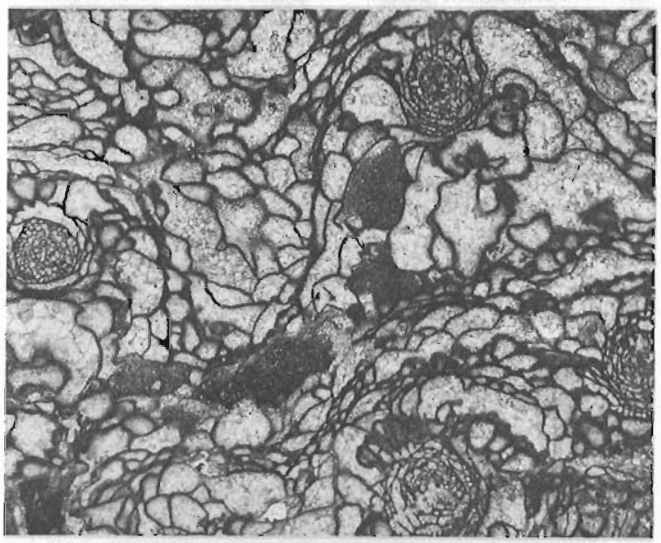

57

Figures 56, 57.

Aphroidophyllum sp., USNM 219172, talus from *pesavis*-bearing breccia member of the Windmill Limestone. Coal Canyon, 300 m from entrance on east side, SE ¼ sec. 17, T. 25 N., R. 49 E. Horse Creek Valley Quadrangle, Nevada.

Lst.). Lochkovian strata containing the genus are known in central Asia (Tomchumysh Beds), Urals (lower Siyak Beds; Sarayna and upper Petropavlov Suites), Chernyshev Ridge (Vaygach Beds), Podolia (Borshchov Beds), Yukon Territory and Nevada (breccia member of the Windmill Limestone). *Dubrovia* is also present in the Pragian Lower Valnev Beds of Novaya Zemlya.

Genus *Dohmophyllum* Wedekind, 1923

Type species. *D. involutum* Wedekind. Eifelian, Junckerberg Schichten, Rhenish Mountains, Germany.
Remarks. *Dohmophyllum* is distinguished from *Acanthophyllum* only by its relatively wider dissepimentarium in adult stages.

Faunal lists suggest that the genus may be present in Pridolian (Kunzhak) beds in Tadzhikistan, but the earliest documented occurrences are late Lochkovian (Kshtut Beds, Tadzhikistan; *pesavis* coral fauna, Yukon Territory). From Pragian to Eifelian times the genus was widely distributed in asiatic Russia, the Urals and western Canada; it is also known in Eifelian strata (Beiliu Stage) of south China. It is not known from younger beds in any of these regions. In Europe the known range of *Dohmophyllum* is Eifelian to Givetian, and in Australia, Zlichovian (*perbonus*-bearing limestones) to Givetian.

Genus *Lyrielasma* Hill, 1939

Type species. *L. chapmani* Pedder. Middle Pragian, Lilydale Limestone, Victoria, Australia.
Remarks. This and several related genera are in need of revision. Provisionally, *Lyrielasma* retains solitary to fasciculate subcylindrical spongophyllids having a narrow steeply inclined dissepimentarium and peripheral septal stereozone. *Salairophyllum* is a synonym, although the specimen, tentatively identified as such by Merriam, from the Windmill breccia of Nevada, is excessively carinate and probably not congeneric.

The genus is first known from Pridolian strata in Yukon Territory. Occurrences in the succeeding Lochkovian have been documented in Yukon Territory, the Urals (middle Petropavlov Suite and equivalents) and central Asia (Tomchumysh and Kshtut Beds). Maximum distribution was attained in Pragian times, when the genus was distributed in Yukon Territory, Alaska (Salmontrout Lst.), Novaya Zemlya (lower Valnev Beds), the Urals (*K. conjugula* and upper Siyak Beds), Czechoslovakia (Koněprusy Lst.), Carnic Alps (Seewarte Lst.), Asia (Ganin and Kireev Beds, Turk-Parida Suite and Dzhidalin Supersuite) and Australia. Later Early Devonian and Eifelian occurrences are known in France (Chalonnes Lst.), the Urals and Australia (Sulcor and Moore Creek Lst.); the latest occurrence of the genus is in the Givetian Broken River Formation of northern Queensland.

Genus *Pseudogrypophyllum* Cherepnina, 1968

Type species. *P. limatum* Cherepnina. Lochkovian, Remnev Beds, Mountain Altai, U.S.S.R.
Remarks. The salient feature of this spongophyllid genus are the spines developed on the free edges of the septa. Specimens from late Lochkovian beds at Royal Creek constitute only the second known occurrence of the genus.

Genus *Xystriphyllum* Hill, 1939

Type species. *Cyathophyllum dunstani*. Zlichovian, Douglas Creek Limestone, near Clermont, Queensland, Australia.
Remarks. *Xystriphyllum* is a cerioid spongophyllid having two or more rows of dissepiments and either lacking, or possessing only a few presepiments. It differs from *Entelophylloides* in having prominently expanded septal bases, and from *Kozlowiaphyllum* in having far fewer presepiments.

The genus is well represented in western Canada in rocks ranging in age from Pridolian (Prongs Creek Formation) to early Givetian (Winnipegosis Formation).

It may be present in Pridolian beds (*Eccentricosta jerseyensis* Zone of the Keyser Formation) in Maryland and also in strata of Lochkovian age in Tadzhikistan (Kshtut Beds) and Australia (Nemingha Lst.), but in regions other than western Canada, the oldest documented occurrences are Pragian (Salmontrout Lst., Alaska; Kalnev Beds, Novaya Zemlya; Taribigaya Beds, Taymyr; the Urals; Dzhidalin Supersuite, Tadzhikistan; Coopers Creek Lst., Australia). Later Early Devonian occurrences are known in Alaska (McCan Hill Chert and Salmontrout Lst.), southern Urals, Czechoslovakia (Koněprusy Lst.), central Asia (Salairka Beds) and Australia (Taemas, Sulcor and Douglas Creek Lst.). The known Eifelian distribution is western Canada (Hume Lst.), the Urals, Germany (Junkerberg Schichten), central Asia where it is especially common (Shandin, Rakitina and Shivertin Beds) and Australia (Moore Creek and Broken River Lst.). The latest appearance of the genus is probably in the Givetian Biya Beds of the southern Urals.

Genus *Taimyrophyllum* Chernyshev, 1941

Type species. *T. speciosum* Chernyshev. Pragian, Daksana Beds, Tareya River, Taymyr, U.S.S.R.
Remarks. The species associated with the *dehiscens* conodont fauna at Royal Creek is new, but closely resembles unnamed forms, with narrow tabularia and thick septa, occurring in probable late Lochkovian strata in Australia (lower Garra Beds) and early to late Pragian beds in Alaska (Salmontrout Lst.). A less similar species occurs in the Zlichovian, or later part of the Ogilvie Formation of Yukon Territory. Other dissimilar species are known from the lower Devonian of the Salair (late Pragian Malobachat Beds) and the Russian Far East, and also from Eifelian deposits in western Canada (Hume Formation) and Nevada (Merriam's Devonian fauna F). The latest known occurrence of the genus is in the Givetian part of the Timor Limestone of New South Wales.

Genus *Aphroidophyllum* Lenz, 1961

Type species. *A. howelli* Lenz. Late Eifelian, Hume Formation (*dysmorphostrota* Zone), Lac à Jacques, District of Mackenzie, Canada.
Remarks. Opportunity is taken to figure a new species from Merriam's Nevada "Silurian" fauna E, as it further emphasizes differences between the late Lochkovian coral faunas of Nevada and Yukon Territory. Its aphroid corallum, narrow tabularia and strongly excert dissepimentaria are reminiscent of the genus *Zenophila* [typified by *Z. walli* (Etheridge) from the Ludlovian Silverdale Formation, near Yass, New South Wales], however, the septa are dilated and flanged in the axial region, and exhibit naotic tendencies in the inner dissepimentarium. These features suggest that it is better accommodated in *Aphroidophyllum*, although no link is known between it and the Eifelian species of western Canada and Kuznetsk Basin.

Family Cystiphyllidae Edwards and Haime
Genus *Patridophyllum* Ulitina, 1963

Type species. *P. paternum* Ulitina. Late Eifelian, River Arpa, Trans Caucasus, U.S.S.R.
Remarks. The septa in this genus consist of coarse monacanthine trabeculae and are laterally contiguous through most, if not all, the corallum.

The new Pragian species from late *sulcatus*-bearing beds at Royal Creek, is intermediate in age between early occurrences of the genus in the Pridolian Skala Beds of Podolia and the Lochkovian Pribalkhash and Nadaynasuy Beds of Kazakhstan, and later Eifelian occurrences in the Kuznetsk Basin and Trans Caucasus.

New gen. and sp., cf.
"*Pseudomicroplasma*" *multitabulata* Spassky

This phaceloid cystimorph from the *pesavis*-bearing part of the Royal Creek sections is characterized by having a distinct peripheral septal stereozone and almost no sclerenchymal investment of the vesicular surfaces. It was identified as cf. *Microplasma* sp. by Lenz and Pedder (1972, p. 15, 22) and is congeneric with a form from the "Koblenzian" of the southern Urals, described under the name of *Pseudomicroplasma multitabulata*. The Yukon and Urals species, however, belong to neither *Microplasma* nor *Pseudomicroplasma*.

New cerioid gen. and sp.

This is similar to the preceding genus but is cerioid. Several similar Lower Devonian corals from western Canada await description.

New solitary gen. and sp.

Solitary cystiphyllids from the *dehiscens*-bearing Michelle Formation resemble species of *Hedstroemophyllum, Holmophyllia* and *Gukoviphyllum*. They differ from *Hedstroemophyllum* in having more closely spaced septal spines, and from *Holmophyllia* and *Gukoviphyllum* in having monacanthine, rather than rhabdacanthine or flabellicanthine trabeculae.

FOSSIL LOCALITY DATA

Co-ordinates of the centres of the Royal Creek sections are as follows:

Royal Creek 1: 64°46'22"N, 135°12'36"W
Royal Creek 2: 64°46'38"N, 135°14'12"W
Royal Creek 3: 64°45'54"N, 135°09'54"W

Full faunal lists, including revised conodont identifications by G. Klapper are given for Royal Creek sections 1 and 2 in Lenz and Pedder, 1972, p. 12-23. Corals from the short Royal Creek 3 section occur with *Polygnathus dehiscens*, identified by Klapper, and overlie the type occurrence of *Monograptus*

yukonensis. Evidence for the age of the Michelle Formation has been presented by Ludvigsen (1970) and Lane (1974, p. 722); since C-12694 comes from high in the formation it is regarded as equivalent to Klapper's fauna 8, rather than 7. R.W. Macqueen estimates that C-26750 is stratigraphically equivalent to C-26749, obtained in the same area, which contains a species of *Martinophyllum* found elsewhere only in the later *P. dehiscens* fauna. The age of C-12894 is based on the similarity of the megafauna to that occurring in the upper part of Royal Creek 3, as well as on associated conodonts, including *P. dehiscens*, identified by T.T. Uyeno.

Name and date refer to collector and date of collection. Collection numbers are GSC Locality numbers. No satisfactory stratigraphic terminology is at present available for the Royal Creek sections.

Pedavis pesavis Collections

69301. Royal Creek 1; 105.5-108.9 m (346-357 feet) above base of section.
A.C. Lenz, 1965.

C-4264. Royal Creek 2; 194.9-198.2 m (639-650 feet) above base of section.
A.E.H. Pedder, 1969.

C-4271. Royal Creek 1; 98.2-98.8 m (322-324 feet) above base of section.
A.E.H. Pedder, 1969.

C-4272. Royal Creek 1; 105.5-106.1 m (346-348 feet) above base of section.
A.E.H. Pedder, 1969.

C-12890. Royal Creek 2; 194.9-197.9 m (639-649 feet) above base of section.
A.E.H. Pedder, 1971.

C-12891. Royal Creek 2; 198.2 m (650 feet) above base of section.
A.E.H. Pedder, 1971.

Late *Eognathodus sulcatus* Collections

69304. Royal Creek 1; 231.8-235.5 m (760-772 feet) above base of section.
A.C. Lenz, 1965.

C-4281. Royal Creek 1; 210.3-211.4 m (690-693 feet) above base of section.
A.E.H. Pedder, 1969.

C-4282. Royal Creek 1; 231.8-235.5 m (760-772 feet) above base of section.
A.E.H. Pedder, 1969.

C-4283. Royal Creek 1; 240.3-250.1 m (788-820 feet) above base of section.
A.E.H. Pedder, 1969.

Polygnathus dehiscens Collections

67543. Royal Creek 3. A.C. Lenz, 1962.
69314. Royal Creek 3. A.C. Lenz, 1965.
C-12694. Michelle Formation, upper 15 m (49.2 feet), Ogilvie Mountains, 65°40'30"N, 136°57'00"W. R. Ludvigsen, 1971.
C-12894. Royal Creek headwaters, 64°45'40"N, 135°11'00"W. A.E.H. Pedder, 1971.
C-26750. Unnamed carbonate, west flank of Royal Mountain, 65°03'N, 135°05'W. R.W. Macqueen, 1973.

References

Boucot, A.J.
1975: Evolution and extinction rate controls; Develop. Palaeont. Stratig., v. 1.

Carls, P.
1969: Die Conodonten des tieferen Unter-Devons der Guadarrama (Mittel-Spanien) und die Stellung des Grenzbereiches Lochkovium/Pragium nach der rheinischen Gliederung; Senckenbergiana lethaea, Bd. 50, p. 303-355.

Carls, P., Gandl, J., Gross-Uffenorde, H., Jahnke, H. and Walliser, O.
1972: Neue Daten zur Grenze Unter-/Mittel-Devon; Newsletters on Stratigraphy, v. 2, p. 115-147.

Churkin, M. and Brabb, E.E.
1968: Devonian rocks of the Yukon-Porcupine Rivers area and their tectonic relation to other Devonian sequences in Alaska; Int. Symp. Devonian System, Calgary, 1967 (D.H. Oswald, ed.), v. 2, p. 227-258.

Klapper, G. and Murphy, M.A.
1975: Silurian-Lower Devonian conodant sequence in the Roberts Mountains Formation of central Nevada; Univ. Calif. Pub. Geol. Sci., v. 111.

Klapper, G., Sandberg, C.A., Collinson, C., Huddle, J.W., Orr, R.W., Rickard, L.V., Schumacher, D., Seddon, G. and Uyeno, T.T.
1971: North American Devonian conodont biostratigraphy; Geol. Soc. Am., Mem. 127, p. 285-316.

Lane, H.R.
1974: *Icriodus taimyricus* (Conodonta) from the Salmontrout Limestone (Lower Devonian), Alaska; J. Paleontol., v. 48, p. 721-726.

Lane, H.R. and Ormiston, A.R.
1973: Biostratigraphy of the Salmontrout Limestone, east-central Alaska; Geol. Soc. Am., Abstracts with programs, v. 5, p. 330.

Lenz, A.C. and Pedder, A.E.H.
1972: Lower and Middle Paleozoic sediments and paleontology of Royal Creek and Peel River, Yukon, and Powell Creek, N.W.T.; Int. Geol. Congr., Guidebook, Field Excursion A-14.

Ludvigsen, R.
1970: Age and fauna of the Michelle Formation, northern Yukon Territory; Bull. Can. Pet. Geol., v. 18, p. 407-429.

Merriam, C. W.
1973a: Paleontology and stratigraphy of the Rabbit Hill Limestone and Lone Mountain Dolomite of central Nevada; U. S. Geol. Surv., Prof. Paper 808.

1973b: Middle Devonian rugose corals of the central Great Basin; U. S. Geol. Surv., Prof. Paper 799.

1974a: Silurian rugose corals of the central and southwest Great Basin; U.S. Geol. Surv., Prof. Paper 777.

Merriam, C. W. (cont'd.)
1974b: Lower and Lower Middle Devonian rugose corals of the central Great Basin; U.S. Geol. Surv., Prof. Paper 805.

Oliver, W. A.
1964: New occurrences of the Rugose coral *Rhizophyllum* in North America; U. S. Geol. Surv., Prof. Paper 475-D, p. 149-158.

Perry, D. G., Klapper, G. and Lenz, A. C.
1974: Age of the Ogilvie Formation (Devonian), northern Yukon: based primarily on the occurrence of brachiopods and conodonts; Can. J. Earth Sci., v. 11, p. 1055-1097.

60. LITHOFACIES ANALYSIS OF CORES FROM THE BORDEN ISLAND FORMATION, DRAKE POINT, MELVILLE ISLAND

Project 710069

G.E. Reinson
Institute of Sedimentary and Petroleum Geology, Calgary

Introduction

A project on the subsurface geology of Sabine Peninsula, Melville Island, was undertaken recently by the writer, and the initial investigations are reported here. The two cores described in this paper cover the Jurassic gas-bearing sandstone interval in the Panarctic Tenneco *et al.*, Por Drake F-16 and Panarctic Por Homestead Drake E-78 boreholes (Fig. 1). The publication of these brief descriptions and preliminary interpretations is warranted because of the diverse depositional histories recorded in, and the complex sedimentary environments represented by, the lithologies within the cores.

The interval from 3640 to 3845 feet below K.B. elevation in the Panarctic Drake Point L-67 borehole (Fig. 2), has been assigned to the Borden Island Formation in the Schedule of Wells for 1970-1972 (Department of Indian Affairs and Northern Development, 1973). The sequence above this interval has been designated as the Savik Formation, and the sequence below it, as the Schei Point Formation (Department of Indian Affairs and Northern Development, op. cit.). This interval can be correlated through both the F-16 and E-78 boreholes, and the cores from both wells, when combined, provide an almost complete lithological record of the Borden Island Formation in the subsurface of this region (Fig. 3).

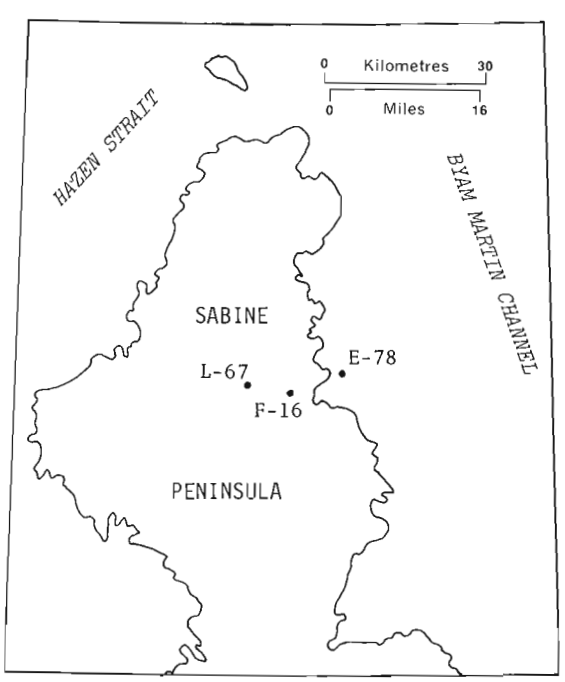

Figure 1. Index map showing locations of boreholes under discussion.

Three major lithofacies can be recognized within the Borden Island Formation. They comprise an oolitic iron-formation facies at the base, a cyclic quartzose sandstone-siltstone facies in the middle, and a glauconite facies at the top. All three facies give characteristic and distinctive responses on logs (Fig. 2), and preliminary subsurface correlation suggests that they are continuous in a direction parallel to the Sverdrup Basin margin, across the Sabine Peninsula region.

Facies Descriptions and Environmental Interpretations

Oolitic Iron-Formation Facies

This lithofacies is essentially a ferruginous, oolitic sequence, about 32 feet (10 m) thick, which has a conglomeratic-like appearance. It is composed mainly of dark reddish brown, medium to coarse grained ooliths with lesser amounts of granule- to pebble-size reddish brown chert and yellowish brown claystone rock fragments, embedded in a dark green to green grey, aphanitic matrix. Preliminary mineralogical analyses (supplied by K.J. Roy) of the oolitic grains indicate that they are composed mainly of goethite with lesser amounts of siderite. However, extensive petrographic, X-ray, and analytical work is yet to be done to establish in detail the mineralogy and chemistry of both the ooliths and matrix material.

Oolitic ironstone of the type encountered here is similar to those found in the Jurassic of Great Britain (Hallam, 1966; Brookfield, 1971; Whitehead *et al.*, 1952; Taylor, 1949), which are classified as the minette type of iron-formation by Gross (1965). It is considered that such deposits formed in shallow marine environments, in the transition zone between sand-silt and clay deposition. They usually have thick sandstone as their shoreline equivalent, and shale as their offshore equivalent.

From analogy of the British Jurassic ironstones, it is considered that the oolitic facies of the Borden Island Formation formed in a transitional nearshore environment during a minor regressive phase, or near stillstand of the sea.

The basal contact of this facies forms an abrupt erosional surface with the underlying dark grey blocky shale of the Schei Point Formation. The upper contact of the oolitic facies with the overlying cyclic sandstone-siltstone is rather sharp; it appears there may be a depositional break either at this contact or at the top of the calcareous siltstone units of the basal part of the cyclic sandstone-siltstone facies (Fig. 4). A small

(about 3 cm thick) red brown nodular band of dense, sideritic-ferruginous claystone occurs at every one of these above-mentioned contacts.

Cyclic Sandstone-Siltstone Facies

This lithofacies is about 100 feet (30.5 m) thick, consisting predominantly of light brown, fine grained quartzose sandstone, with interbeds of interlaminated yellow grey sandstone-siltstone, and interlaminated green grey siltstone-claystone. The sequence is a series of coarsening-upward cycles, the base of each cycle being represented by the fine grained siltstone-claystone interbeds (Fig. 4).

Hydroplastic deformational structures such as contorted bedding, flaser bedding and convolute laminae occur in the interlaminated claystone-siltstone-sandstone beds, but evidence of bioturbation is scarce. The fine grained quartzose sandstone beds are generally well sorted, with parallel laminations and micro-cross-laminations, being the dominant sedimentary structure. Faintly laminated and structureless beds occur in the upper parts of some sandstone intervals also.

Natural gas occurs in this facies, and in particular, in the laminated and massive, well sorted, well rounded quartzose sandstones. Effective porosity is highest in this facies compared to the glauconite and ironstone facies above and below (Fig. 2), because of the clean, predominantly monomineralic and mature character of these sandstones.

The vertical sequence of sedimentary structures and textures in each cycle of the sandstone-siltstone facies is similar to that in vertical sequences of Mesozoic and Holocene barrier complexes as described by many authors including Davies *et al.* (1971), Campbell (1971), and Bernard *et al.* (1962). Therefore, it is interpreted as representing a pulsating series of barrier-bar or barrier-coastline accretionary stages during a major regressive marine cycle of deposition. Diverse depositional subenvironments are present in the nearshore zone, and this is apparent just from the two cores examined. The F-16 core contains a series of normal prograding beach-shoreface sequences, whereas the E-78 core contains what appears to be an eolian sequence which is capped by tidal inlet (channel) deposits, in addition to the beach-shoreface successions. It is highly likely that a variety of nearshore marine and coastal plain sediments are present in this facies along its depositional strike. The shoreline fluctuations, recorded by the cycles in this facies may reflect major migrations of prograding fluvio-deltaic and/or inter-deltaic-barrier complexes in adjacent areas, rather than widespread eustatic changes in sea level.

Glauconite Facies

This lithofacies is about 70 feet (21 m) thick, and has an abrupt contact with the underlying cyclic sandstone-siltstone facies (Fig. 2). Grey phosphatic nodules, and dark brown, dense ferruginous nodules form a thin resistant band at the base of this facies, and a similar resistant band occurs at the top of the lower unit within this facies (Fig. 4). The lower unit consists of a coarsening-upward sequence of olive grey siltstone, interlaminated siltstone-mudstone, and finally glauconitic, quartzose pale olive, fine to medium grained sandstone. Most of this unit is bioturbated, the intensity of bioturbation increasing downward.

The upper unit within the glauconite facies consists largely of greenish grey, fine to medium grained sandstone, which gives way upward to interbedded green grey sandstone and green grey claystone, and finally to green grey claystone of the overlying lower Savik Formation. The green colour of the whole lithofacies is likely due to its high glauconite content, but petrographic and mineralogical analyses are yet to be done to ascertain whether other green mineral phases are present.

Glauconite formation is favoured by low sedimentation rates such as are provided during marine transgressions, thus this mineral is often associated with

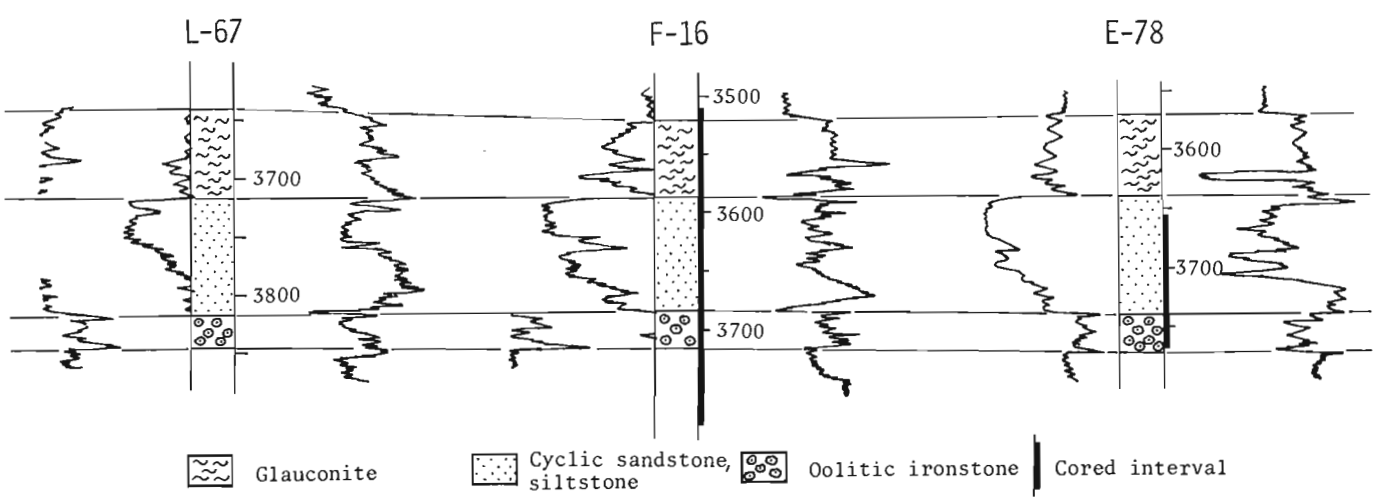

Figure 2. Correlation of lithofacies of Borden Island Formation on gamma ray-sonic logs.

unconformities (McRae, 1972). The glauconite facies of the Borden Island Formation is interpreted as representing deposition during a major transgression. The unconformity at the base accompanied by phosphatic and ferruginous nodules, suggests that initial transgression occurred very rapidly, probably in response to some eustatic event. The top of the lower unit of this lithofacies may mark the start of a second rapid transgressive pulse. This may be indicated by the lower unit which represents a regressive shoreface sedimentary sequence (Fig. 4), that appears to have undergone intense glauconitization after deposition.

The Borden Island Formation in the type area of Borden Island, as defined by Thorsteinsson and Tozer (1964), consists of about 200 feet (61 m) of glauconitic sandstone, which contains hard ferruginous bands and grey phosphatic nodules. The Borden Island Formation is not exposed on Sabine Peninsula, according to Thorsteinsson and Tozer, who consider that it was overstepped by succeeding Jurassic formations. Their

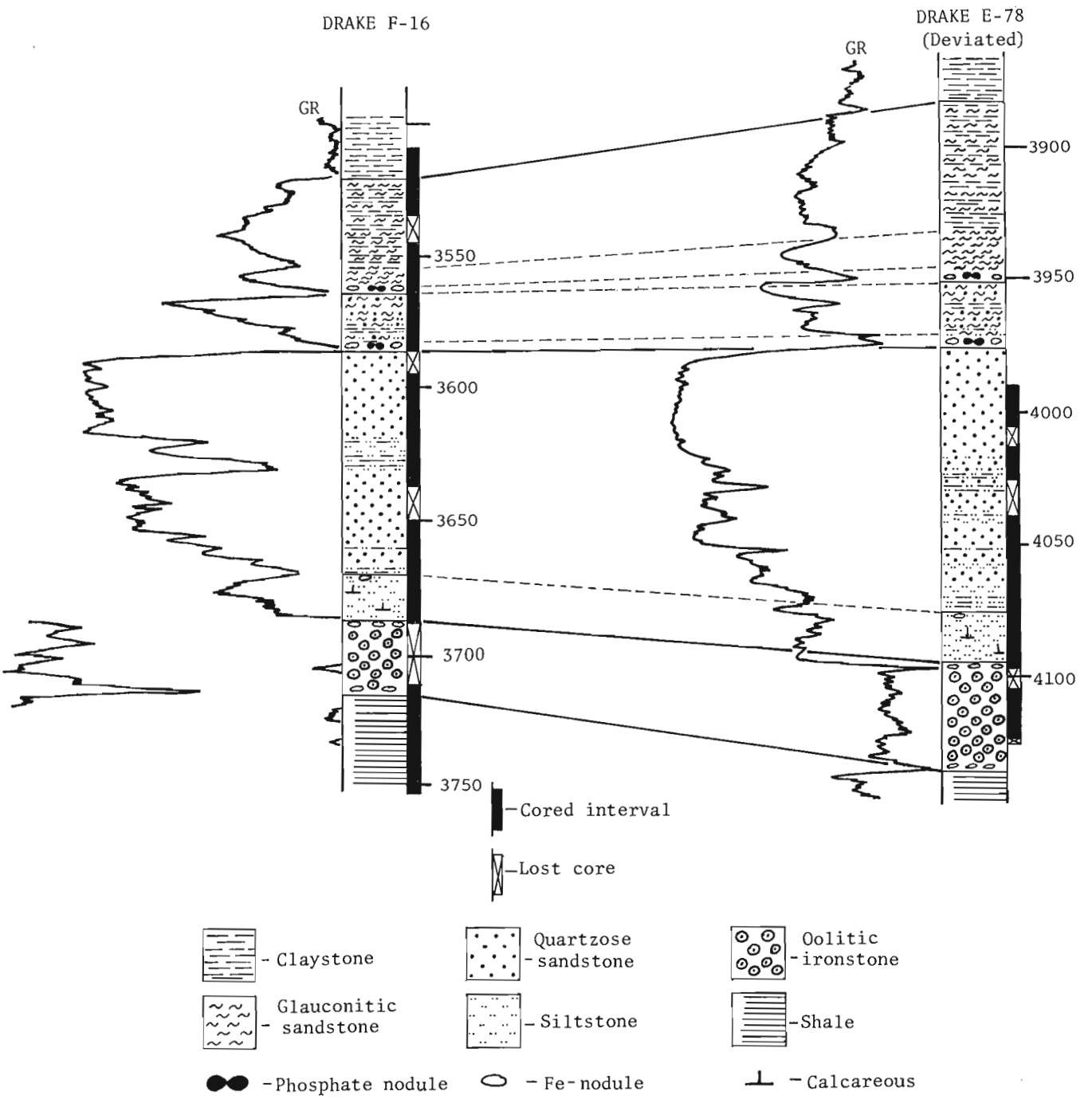

Figure 3. Detailed lithologic correlation of Borden Island Formation in F-16 and E-78 boreholes.

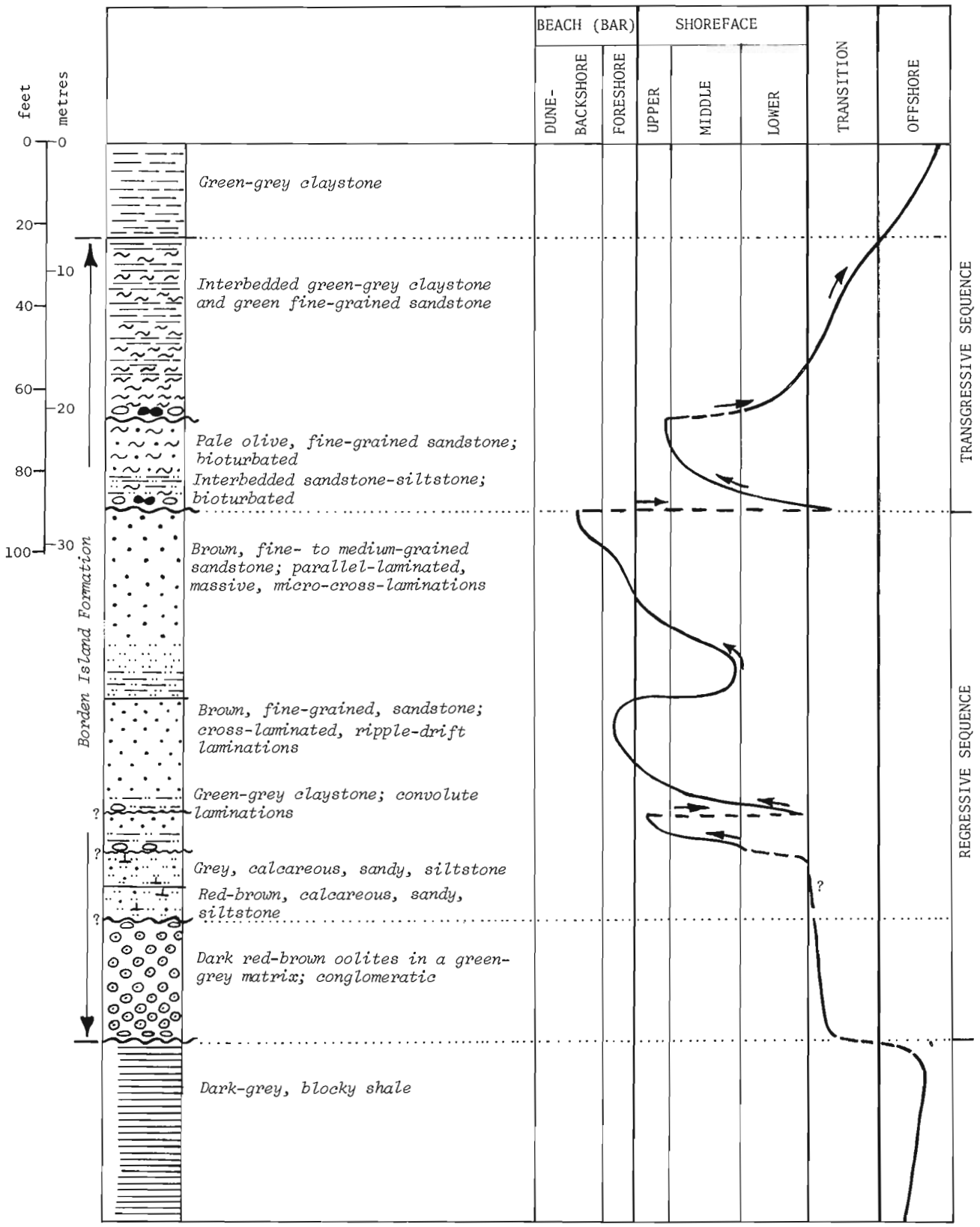

Figure 4. Environmental interpretation of lithologic sequence in F-16 borehole.

descriptions from the type area, however, compare favourably with the glauconite facies encountered in the subsurface cores on Sabine Peninsula, which is only 70 feet (21 m) thick. This suggests that the cyclic sandstone-siltstone facies is probably in part, a shoreward lateral equivalent of the marine glauconite facies.

The environmental interpretations presented here are preliminary, as only preliminary descriptions of lithology have been completed to date. Further work on the subsurface stratigraphy of the western part of the Sverdrup Basin, and on the petrography, mineralogy, and chemistry of these rocks is being undertaken, and is needed, to substantiate the depositional history of the Borden Island Formation and equivalent rocks in this region. This diversified suite of rocks certainly warrants detailed study and documentation because of its regional hydrocarbon potential.

Drs. H.R. Balkwill and K.J. Roy introduced the writer to the Mesozoic of the Sverdrup Basin, and also commented on this preliminary report.

References

Bernard, H.A., LeBlanc, R.J. and Major, C.F.
1962: Recent and Pleistocene geology of southeast Texas, field excursion No. 3 *in* Geology of the Gulf Coast and central Texas and guidebook of excursions; Geol. Soc. Am. Ann. Mtg. Guidebook, p. 175-224.

Brookfield, M.
1971: An alternative to the 'clastic trap' interpretation of oolitic ironstone facies; Geol. Mag., v. 108, p. 137-143.

Campbell, C.V.
1971: Depositional model - Upper Cretaceous Gallup Beach Shoreline, Ship Rock area, Northwestern New Mexico; J. Sediment. Petrol., v. 41, p. 395-409.

Davies, D.K., Ethridge, F.G. and Berg, R.R.
1971: Recognition of Barrier Environments; Bull. Am. Assoc. Pet. Geol., v. 55, p. 550-565.

Department of Indian Affairs and Northern Development
1973: Schedule of Wells, 1970-72, North of 60; Ottawa, Information Canada.

Gross, G.A.
1965: Geology of iron deposits in Canada, v. 1, General geology and evaluation of iron deposits; Geol. Surv. Can., Econ. Geol. Rept. 22.

Hallam, A.
1966: Depositional environment of British Liassic ironstones considered in the context of their facies relationships; Nature, v. 209, p. 1306-1309.

McRae, S.G.
1972: Glauconite; Earth-Science Review, v. 8, p. 397-440.

Taylor, J.H.
1949: Petrology of the Northampton Sand Ironstone Formation; Mem. Geol. Surv. G. Brit.

Thorsteinsson, R. and Tozer, E.T.
1964: Western Queen Elizabeth Islands, Arctic Archipelago; Geol. Surv. Can., Mem. 332.

Whitehead, T.H., Anderson, W., Wilson, V., Wray, D.A. and Dunham, K.C.
1952: The Liassic Ironstones; Mem. Geol. Surv. G. Brit.

61. ESSAI DE SYNTHESE DES DONNEES DE SONDAGES DE L' "UPPER ELK POINT" (DEVONIEN MOYEN) DES CHAMPS DE RAINBOW ET DE ZAMA (NORD-OUEST de L'ALBERTA): CHRONOLOGIE DES FORMATIONS "MUSKEG" ET "UPPER KEG RIVER"

Projet 740027[1]

Jean-Claude Tranchant
Institut de géologie sédimentaire et pétrolière, Calgary.

Introduction

Ce projet, commencé en novembre 1973, concerne l'étude stratigraphique du sous-groupe "Upper Elk Point", appartenant au Dévonien moyen, de la région de Rainbow-Zama. La série repose sur les évaporites de la formation Chinchaga. Elle se compose d'une unité lithologique carbonatée ou Keg River, puis d'évaporites (Muskeg) et de carbonates (Sulphur Point), et se termine par des argiles (Watt Mountain), qui précèdent la formation Slave Point carbonatée. Le "Rainbow member" a été défini comme étant l'équivalent récifal, partiellement ou totalement, des carbonates "Upper Keg River".

Au point de vue géographique, la région en cours d'étude s'arrête au nord à la limite entre l'Alberta et les Territoires du Nord-Ouest (Twp 126; 60°N), à l'ouest à la bordure de la Colombie-Britannique (120°W), au sud du township 106, et à l'est au sixième méridien ouest (118°W). Cette zone, d'une superficie d'environ 25 000 km^2, se situe donc à la terminaison nord-ouest du bassin de l'Elk Point. Elle englobe les deux sous-bassins de Rainbow et de Zama (bassin du Black Creek) et constitue une province pétrolière de type récifal (Perrodon, 1971).

Plus d'un millier de puits, forés pour la plupart depuis la découverte d'hydrocarbures dans le récif "A" du champ de Rainbow nord, en mars 1965 (puits Banff-Aquitaine Rainbow West 7-32-109-8W6), atteignent ou traversent les carbonates "Upper Keg River-Rainbow member". Si les champs de Rainbow et de Zama, notamment les récifs, ont fait l'objet d'études très détaillées de la part de nombreuses sociétés pétrolières, ces travaux restent le plus souvent confidentiels. Quant aux synthèses publiées, elles s'appuient, en général, sur des données fragmentaires.

METHODES D'ETUDE

Jusqu'à présent, près de 500 sondages ont été étudiés à partir de diagraphies (logs "gamma-ray" et "density" essentiellement). Pour obtenir des corrélations fines à partir de niveaux repères définis sur ces diagraphies, la réinterprétation de celles-ci s'avère indispensable. En effet, les informations disponibles (toits des formations) ne sont pas suffisamment détaillées et manquent d'homogénéité.

L'examen des carottes ne peut être que subordonné à celui des diagraphies, qui seules permettent de sélectionner des carottes et de les localiser précisément dans la série stratigraphique considérée. Les diagraphies ne donnent pas seulement des renseignements sur la nature lithologique des formations traversées, mais peuvent aussi, après un étalonnage d'après carottes, apporter des indications tant sur les faciès (Serra, 1973) que sur les phénomènes diagénétiques (Bebout et Maiklem, 1973).

La principale contribution de cette étude sera l'établissement de cartes isopaques détaillées, aussi bien en ce qui concerne le nombre de puits pris en considération, que les intervalles représentés. Les paléogéographies successives ainsi reconstituées devraient permettre de préciser l'évolution des sous-bassins de Rainbow et de Zama, les relations entre ces deux régions, et leurs rapports avec le reste du bassin de l'Elk Point, en cours d'étude par G. Busson (1974).

RESULTATS PRELIMINAIRES

Deux coupes, réalisées d'après diagraphies dans les bassins de Rainbow et de Zama, sont illustrées par la figure 1. Pour le bassin de Zama, la coupe est synthétique; en particulier, le modèle récifal a été construit d'après deux puits, l'un ayant atteint le flanc d'un pinacle (2-25-117-5W6), l'autre la crête d'un second récif (3-7-115-5W6).

Quelle que soit la situation des puits -- récifs, off-reef, avec du sel présent ou non --, la série allant du toit des évaporites du Chinchaga au toit de la formation Watt Mountain (limites considérées comme des lignes-temps) est toujours plus épaisse à Rainbow qu'à Zama. Ceci indique une subsidence moins importante à Zama qu'à Rainbow, et ainsi, sur la figure 1, l'intervalle ab et la formation Slave Point, par exemple, sont plus minces à Zama. Le rapport des épaisseurs est de l'ordre de 1.2 entre les bassins de Rainbow et de Zama (puits 9-24-109-8W6 et 10-21-116-5W6). Les récifs de Rainbow sont environ deux fois plus élevés que les pinacles de Zama, ce que tous les auteurs semblent attribuer, exclusivement, à la subsidence plus forte du bassin de Rainbow.

Dans le champ de Rainbow, une douzaine de sondages ont traversé une couche de sel qui varie de 83 m (272 pieds) au puits 9-24-109-8W6 (fig. 1), à 1 m environ (3 pieds) au puits 9-18-107-8W6 (non figuré sur la coupe). Ce sel est séparé par quelques pieds d'anhydrite de deux bancs dolomitiques, caractéristiques sur diagraphies, l'un à la base (e sur la figure 1), l'autre au toit du sel (d). Au dessus du sel, une succession de lits d'anhydrite et de dolomie a une épaisseur sensiblement égale (ad) dans tous les puits

[1] Projet associé à celui de G. Busson (No. 720065; cf. G. Busson, 1974).

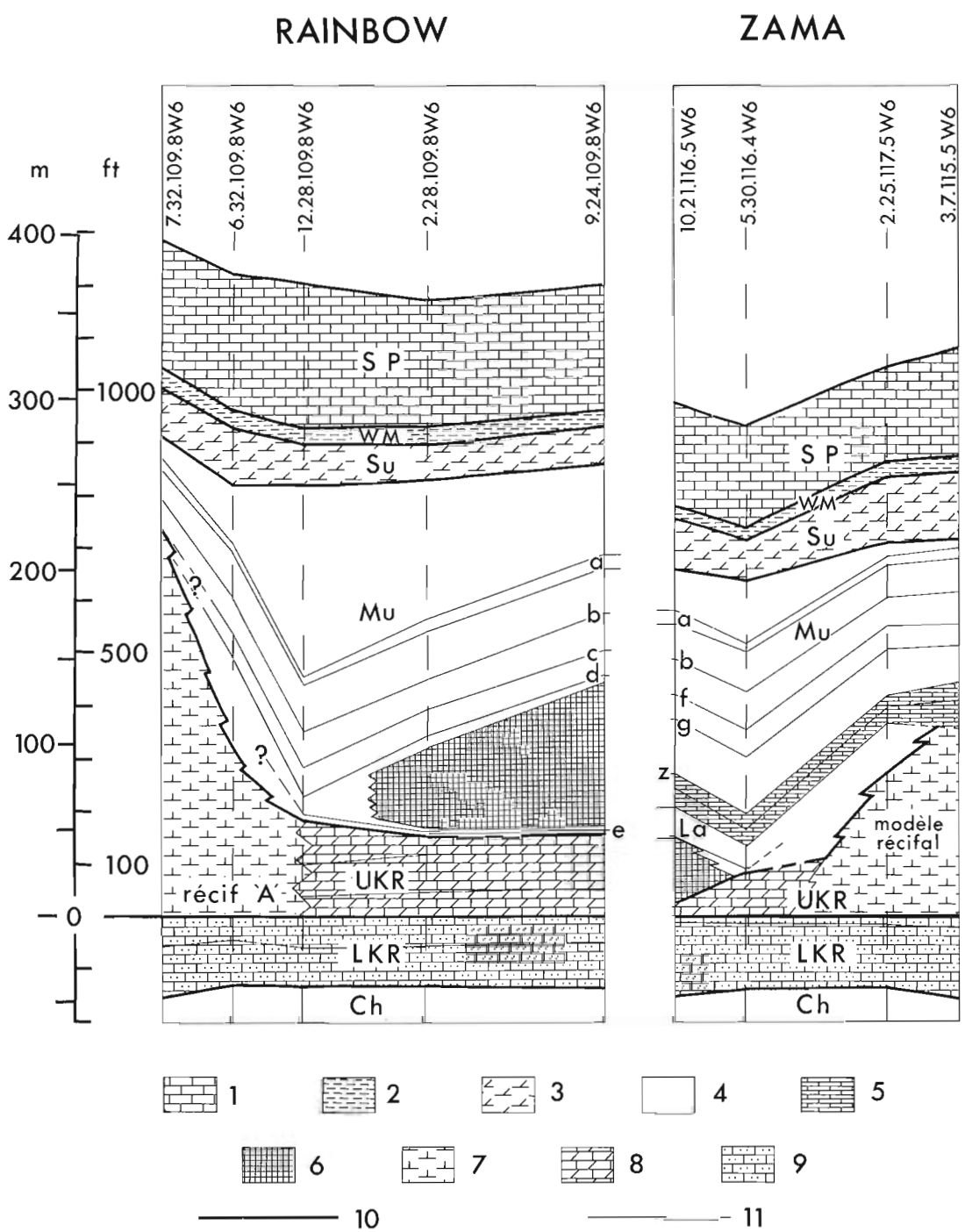

Figure 1. Coupes, d'après diagraphies, dans les bassins de Rainbow et de Zama; 1, carbonates du Slave Point (SP); 2, argiles du Watt Mountain (WM); 3, carbonates de la formation Sulphur Point (Su); 4, anhydrite et dolomie (Mu: Muskeg; La: Lower anhydrite; Ch: Chinchaga); 5, dolomies du "Zama member"; 6, sel; 7, récifs; 8, carbonates "Upper Keg River" (UKR); 9, carbonates du "Lower Keg River" (LKR); 10, limites des formations selon la terminologie habituelle; 11, autres niveaux repères définis sur diagraphies (a; b; c; d; e; f; g; z: toit du "Zama member"). Lithologie simplifiée; plan de référence: toit du "Lower Keg River".

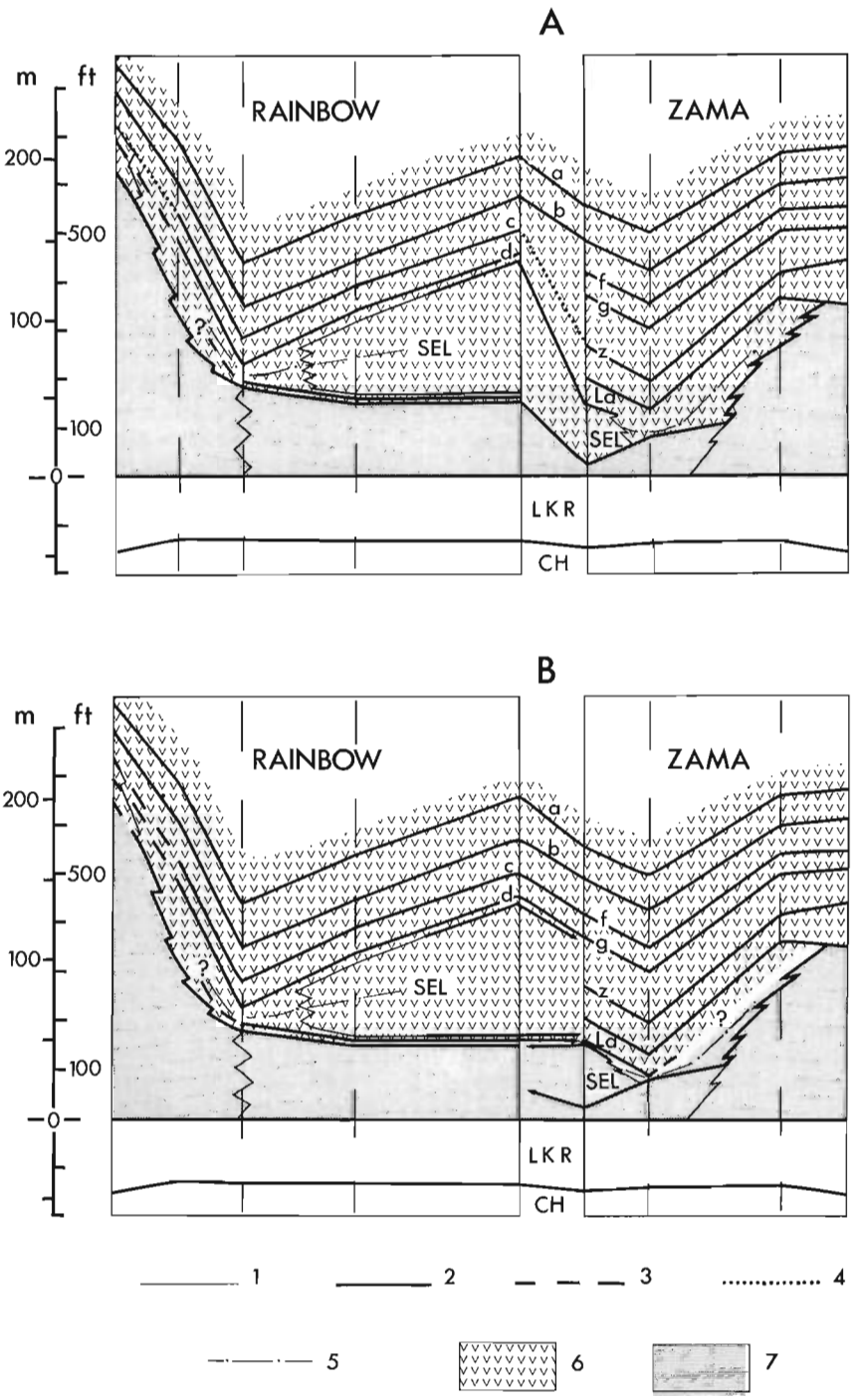

Figure 2. A) Corrélation des coupes de la figure 1 d'après des conclusions des auteurs cités dans le texte.
B) Conclusions et hypothèse 2 (flèches) présentées dans ce rapport.

1, contact lithologique; 2, ligne-temps; 3, ligne-temps approximative; 4, isocrone d'après Bebout et Maiklem (1973); 5, sel dissous; 6, formations d'âge Muskeg; 7, formations d'âge "Upper Keg River" (*voir* figure 1 et texte).

situés entre les récifs. La dissolution du sel est donc postérieure au dépôt du banc a, car sinon elle aurait entraîné des variations notables d'épaisseur de l'intervalle ad (cf. Dumestre, 1969; Barss *et al.*, 1970).

A Zama, le sel, qui n'a été rencontré qu'au puits 10-21-116-5W6, atteint 37 m (123 pieds). De même qu'à Rainbow, la dissolution du sel est postérieure au dépôt du banc a, puisque l'intervalle a-base de la "Lower anhydrite" est constant, du moins lorsque cette "anhydrite inférieure" est comparable, sur diagraphies, à celle qui existe au puits 10-21-116-5W6 (comme c'est le cas du puits 5-30-116-4W6 sur la figure 1).

Une différence fondamentale entre les deux bassins, est la présence à Zama des dolomies du "Zama member" qui recouvrent les sommets des pinacles et qui, entre les récifs, reposent sur la "Lower anhydrite" (fig. 1). McCamis et Griffith (1967, 1968) présument que, dans la région de Rainbow, la partie sommitale des récifs (150 à 250 pieds) est contemporaine du dépôt du "Zama member" à Zama. Barss *et al.* (1970) refusent cette hypothèse, mais ne proposent pas d'équivalent-temps à Rainbow pour le "Zama member". D'après Bebout et Maiklem (1973), durant la sédimentation du "Zama member" dans le bassin de Zama, les crêtes des récifs de Rainbow sont soumises à une altération vadose, tandis que deux types de dolomie se déposent, l'un à la périphérie de ces récifs et l'autre en off-reef.

La figure 2A est l'interprétation de la figure 1, obtenue à partir des conclusions de McCamis et Griffith (1967, 1968), Barss *et al.* (1970), Bebout et Maiklem (1973). Pour tous ces auteurs, à Rainbow comme à Zama, les récifs et leurs équivalents carbonatés en off-reef se sont formés principalement durant le Keg River supérieur, et essentiellement, sinon totalement, avant l'apparition du sel d'âge Muskeg ("Black Creek member"). D'après les corrélations de Bebout et Maiklem (1973), le marqueur c à Rainbow, serait synchrone du toit (z) du "Zama member". Or, l'épaisseur des dolomies c est très faible devant celle du "Zama member". De plus, l'équivalence de ces deux unités implique le synchronisme de dépôt des séquences bc (Rainbow) et bz (Zama). Aucune émersion, aucune érosion, aucune lacune de sédimentation n'est signalée à Rainbow durant cette période; une subsidence plus forte à Zama qu'à Rainbow n'est pas invoquée; les histoires des deux bassins sont toujours considérées comme identiques. Les successions bc et bz sont constituées par une alternance de lits d'anhydrite et de dolomie. La lithologie étant semblable et les deux puits 9-24-109-8W6 et 10-21-116-5W6 étant tous les deux en position off-reef, il est légitime d'admettre une compaction analogue. La dissolution du sel, éventuelle, n'a pas d'influence sur l'épaisseur des intervalles bc et bz, puisqu'elle est postérieure au dépôt du banc a, comme cela a été vu précédemment. A subsidence égale (en fait elle est plus importante à Rainbow), les vitesses de sédimentation seraient approximativement les mêmes. Admettre l'équivalence de ces deux séquences bc et bz revient à postuler, lors de leur dépôt, une subsidence quatre fois plus rapide à Zama qu'à Rainbow. Même en considérant les intervalles b-toit du sel ou a-toit du sel (a représente la "Rainbow dolomite" de Bebout et Maiklem, 1973), la subsidence devrait être respectivement de trois à deux fois plus forte à Zama qu'à Rainbow. Les remarques préalables à propos de la subsidence contredisent cette conclusion, et le dépôt du "Zama member" n'est pas contemporain mais antérieur à celui des dolomies c de Rainbow.

Nos conclusions et l'une de nos hypothèses actuelles sont indiquées par la figure 2B. L'étude des diagraphies et les considérations d'épaisseur nous font admettre l'équivalence des successions cd (Rainbow) et fg (Zama) et non le synchronisme du "Zama member" et des dolomies c. Par conséquent, du sel précipitait encore dans le bassin de Rainbow, alors que de l'anhydrite et de la dolomie se formaient à Zama: le sel de Rainbow est postérieur[1], partiellement au moins, au sel de Zama.

La corrélation des intervalles sous-jacents aux repères d (Rainbow) et g (Zama) est plus difficile, puisque la lithologie et donc les vitesses de sédimentation et la compaction sont différentes, et que, de plus, une partie du sel a pu être dissous en ces deux puits 9-24-109-8W6 et 10-21-116-5W6. Le toit du "Lower Keg River", caractéristique sur les logs "gamma ray", à Rainbow, à Zama et dans la zone intermédiaire, est considéré comme une ligne-temps sur l'ensemble de la région étudiée. Les carbonates "Upper Keg River" entre les récifs de Rainbow, peuvent être divisés en trois unités (fig. 1) d'après les logs "gamma ray", ce qui n'est pas le cas à Zama. Le sel du puits 10-21-116-5W6 repose directement sur les carbonates "Upper Keg River", qui sont extrêmement minces par rapport à leurs homologues de Rainbow. A Rainbow, ces carbonates sont séparés du sel par deux niveaux d'anhydrite encadrant un banc dolomitique (marqueur e sur la fig. 1). Le sel de Zama est apparu plus brutalement et a vraisemblablement commencé à précipiter alors que dans le bassin de Rainbow des carbonates continuaient à se déposer entre les récifs, dont le développement se poursuivait. Dans l'hypothèse où la croissance des sommets des récifs est incompatible avec le dépôt de sel, même à leur base seulement, le sel étant apparu plus précocement à Zama, la sédimentation récifale y avait cessé plus tôt qu'à Rainbow. Si les récifs peuvent continuer à se développer durant la précipitation du sel, la conclusion est identique, compte tenu du décalage de temps dans l'installation du sel dans les deux bassins. En prenant le bassin de Rainbow comme référence temps, les carbonates "Upper Keg River" (récifs et off-reef) de Rainbow sont contemporains de leurs équivalents et du sel à Zama. Ce sel de Zama est, du moins au début, d'âge "Upper Keg River" défini dans le bassin de Rainbow. L'apparition plus précoce du sel à Zama est responsable en partie de la faible hauteur des pinacles de Zama, et explique le peu d'extension en surface de ces récifs. La subsidence moins importante à Zama aurait dû favoriser le développement horizontal des récifs, qui

---

[1] G. Blusson (communication personnelle, 1974) avait émis l'hypothèse que le sel de Rainbow pouvait être postérieur au sel de Zama.

à l'origine se trouvaient dans un milieu très favorable, comme en témoigne la profusion de pinacles. – Pour la distribution et la taille des récifs dans les champs de Rainbow et de Zama, *voir* Klovan, 1974, fig. 11, p. 794.

Dans l'état actuel de cette étude, trois hypothèses peuvent être envisagées:

1) le sel de Zama n'est que partiellement antérieur au sel de Rainbow. La "Lower anhydrite", le "Zama member" et l'intervalle gz (anhydrite et dolomie) sont alors représentés par le dépôt du sel de Rainbow;

2) tout le sel de Zama et les carbonates sous-jacents, correspondent aux carbonates "Upper Keg River" de Rainbow (hypothèse illustrée par la figure 2B). Les conclusions au sujet de la "Lower anhydrite", du "Zama member" et de l'intervalle gz sont les mêmes que dans la première hypothèse; le sel de Zama est entièrement d'âge Keg River supérieur (tel qu'il a été défini à Rainbow), tandis que précédemment il était d'âge Keg River supérieur au départ, puis d'âge Muskeg;

3) à Zama, le sel, la "Lower anhydrite" et le "Zama member" (ce dernier partiellement ou totalement) se sont déposés durant la sédimentation des carbonates "Upper Keg River" de Rainbow; la sucession (gz) de lits d'anhydrite et de dolomie, au dessus du "Zama member" serait seule synchrone du sel de Rainbow.

Nos conclusions et ces trois hypothèses sont en contradiction avec toutes les études réalisées jusqu'à présent (par exemple celles de McCamis et Griffith, 1967, 1968; Barss *et al.*, 1970; Bebout et Maiklem, 1973), dans lesquelles une homogénéité lithologique a été "érigée en instrument de datation" (Busson, 1972). Tous les auteurs ont admis, implicitement, pour les bassins de Rainbow et de Zama, que seuls des carbonates étaient d'âge "Upper Keg River", que le sel ("Black Creek member") était d'âge Muskeg, et que la présence d'anhydrite signifiait un âge Muskeg. La "Lower anhydrite" a été ainsi "datée" du Muskeg, et le "Zama member" aussi par conséquent, ce qui est loin d'être certain (hypothèse 3).

CONCLUSIONS

Le "Zama member" ne peut pas être l'équivalent-temps des dolomies (c) indiquées par Bebout et Maiklem (1973). Contrairement aux affirmations de ces auteurs, notamment, les événements sédimentaires ne sont pas toujours synchrones dans les bassins de Rainbow et de Zama.

Les termes "Muskeg" et "Upper Keg River", tels qu'ils ont été définis jusqu'à présent -- unités lithologiques -- ne devraient avoir aucune signification chronologique, à moins de définir l'âge de ces formations dans un bassin, celui de Rainbow par exemple.

Si plusieurs hypothèses restent possibles, il apparaît cependant que le sel de Rainbow et celui de Zama, de même que les récifs de ces deux bassins, n'ont pas pas une histoire identique.

Le facteur responsable, avec la subsidence, du faible volume de tous les pinacles de Zama, réservoirs d'hydrocarbures, est très vraisemblablement l'apparition plus précoce du sel, dans ce bassin que dans celui de Rainbow, ce qui a fait obstacle au développement vertical et horizontal des récifs.

Bibliographie

Barss, D.L., Copland, A.B. and Ritchie, W.D.
1970: Geology of Middle Devonian reefs, Rainbow area, Alberta, Canada *in* Geology of giant petroleum fields; Am. Assoc. Pet. Geol., Mem. no. 14, p. 19-49.

Bebout, D.G. and Maiklem, W.R.
1973: Ancient anhydrite facies and environments, Middle Devonian Elk Point Basin, Alberta; Bull. Can. Pet. Geol., v. 21, no, 3, p. 287-343.

Busson, G.
1972: Principes, méthodes et résultats d'une étude stratigraphique du Mésozoïque saharien; Mém. Mus. Nat. Hist. Nat., 441 p.

1974: Interprétation et synthèse des données de sondages de l' "Upper Elk Point" (Dévonien moyen du Canada occidental): genèse des évaporites et rapports avec les carbonates; Report of Activities, Part A, April to October 1973; Geol. Surv. Can., Paper 74-1, Pt. A, p. 291-295.

Dumestre, A.
1969: Relations entre hydrocarbures et environnement évaporitique à Rainbow, Alberta (Canada); Rev. Assoc. Fr. Techn. Petr., No. 194, p. 29-46.

Klovan, J.E.
1974: Development of Western Canadian reefs and comparison with Holocene analogues; Bull. Am. Assoc. Pet. Geol., v. 58, no. 5, p. 787-799.

McCamis, J.G. and Griffith, L.S.
1967: Middle Devonian facies relations, Zama area, Alberta; Bull. Can. Petrol. Geol., v. 15, No. 4, p. 434-467 (également, modifié: Bull. Am. Assoc. Pet. Geol., 1968, v. 52, no. 10, p. 1899-1924).

Perrodon, A.
1971: Les provinces pétrolières de type paralique et récifal. Deuxième partie: les provinces récifales; Rev. Inst. Fr. Petr., v. 26, no. 6, p. 521-537.

Serra, O.
1973: Interprétation géologique des diagraphies différées en séries carbonatées (Geological interpretation of different logs in carbonate series); Bull. Centre Rech. Pau-SNPA, v. 7, No. 1, p. 265-284.

62. STRATIGRAPHIC AND SEDIMENTOLOGIC STUDIES IN NORTHEASTERN EAGLE PLAIN, YUKON TERRITORY

Project 710013

F. G. Young
Institute of Sedimentary and Petroleum Geology, Calgary

Preliminary data on stratigraphy, lithofacies, petrography, paleontology, thickness trends and paleocurrents of Upper Devonian and younger rocks in northeastern Eagle Plain (Fig. 1) are provided in this report. This information is used to support the existence of the early Mesozoic Eagle Arch (Moorhouse, 1966), which trended northeasterly from the headwaters of Burnthill Creek to at least as far as Rock River (Fig. 1). This interpretation differs somewhat from that of Jeletzky (1962, 1972, 1974, in press), who concludes that the Porcupine Plain-Richardson Mountain Trough extended roughly north-south through Eagle Plain across the crest of Eagle Arch during Jurassic to pre-Albian, Early Cretaceous time. As evidence for this interpretation, he cites the thick, basinal Jurassic sequence in the lower part of the Molar YT P-34 borehole that was documented by Chamney (*in* Norford *et al.*, 1971). This subsurface section is reinterpreted here on petrographic, lithologic and micropaleontologic grounds to comprise a thick section of Devonian Imperial Formation, and a relatively thin sequence of Jurassic rocks.

The Molar YT P-34 section

The Imperial Formation can be distinguished from the Jurassic and Lower Cretaceous (Neocomian) sequence on the basis of contrasting compositions of their respective sandstones (*see* discussion below and Table 1). Imperial sandstones are enriched in chert, sedimentary rock fragments and argillaceous matrix, whereas those of Jurassic and Neocomian age are quartz-rich, generally well sorted, and winnowed of detrital matrix. Drill cuttings in the Molar YT P-34 well from the depth interval 7650-7900 feet were identified by Chamney (op. cit.) as Late Jurassic (Callovian to Early Oxfordian) in age on the basis of abundant and critical species of Foraminifera. Below this interval his determinations are less definitive, and range from Early to Middle Jurassic in age in the interval 8150-8704 feet. However, the fine-grained, well-sorted, porous quartz arenite (Sample P-34-2, Table 1) in Core No. 13 (7952-7968 ft.) offers a striking contrast to the poorly sorted, brecciated, chert-rich greywacke (Sample P-34-3, Table 1) and interbedded black mudstone of Core No. 14 (8141-8151 ft.), which undoubtedly is a sample of the Imperial Formation.

From the characteristics of drill cuttings and well-logs, the base of the Jurassic is probably unconformable on the Devonian at the 7990-foot level. Chamney's dating of the lowest interval may be explained as due to cavings and recirculation of Jurassic cuttings into the lower depths of the borehole. Unfortunately, palynologic preparations from Core No. 14 yielded only carbonized debris (A. R. Sweet and W. W. Brideaux, pers. comm.).

Hence, the Jurassic section in the Molar well probably comprises an over-all transgressive sequence, 107 m (350 ft.) thick, consisting of condensed, littoral sandstone, 14 m (45 ft.) thick, at the base, and possibly of Early to Middle Jurassic age, overlain by burrowed, marine siltstone up to approximately the 7900-foot level, which in turn is overlain by marine shale of Late Jurassic age. The shale is possibly eroded and truncated below Lower Cretaceous clastics at a depth of 7640 feet.

Eagle Arch

The main lines of evidence in support of the existence of the early Mesozoic Eagle Arch are: (1) progressively older Paleozoic rocks subcrop beneath the sub-Mesozoic unconformity toward the crest of the arch; (2) basal Mesozoic units become thinner toward and progressively onlap over the crest of the arch; and (3) these units consist of littoral and sublittoral deposits.

In the subsurface of the Whitefish Lake area and in outcrops to the east, Mesozoic rocks overlie, in places with angular discordance, the Upper Devonian Imperial Formation (Fig. 1). Southward, beneath Eagle Plain, increasingly younger Paleozoic rock units subcrop below the Mesozoic rocks (Graham, 1973, Fig. 6). Graham also provided seismic evidence showing erosional truncation of the Paleozoic sedimentary record beneath the pre-Mesozoic unconformity from south to north. Northwest from the Whitefish Lake area, a thickening wedge of upper Paleozoic sedimentary rocks is preserved below the Jurassic. This general subcrop distribution of rock units indicates that a broad arch existed in Late Permian and/or Triassic time, resulting in a probable hiatus during most of the Triassic, and contemporaneous erosion of the Lower Permian to Upper Devonian sedimentary record in the crestal area.

Another argument in support of the pre-Jurassic Eagle Arch is the fact that basal Mesozoic units thin and progressively onlap the crest of the arch (Fig. 2). For example, Lower Jurassic sediments unconformably overlie Lower Permian rocks on Porcupine River (Nassichuk, 1971) 16 km (10 miles) downstream from the mouth of Bell River, but 51 km (32 miles) south in the East Pine Creek YT O-78 well, Albian or possibly Aptian shale rests directly on Imperial Formation (micropaleontologic observations of J. H. Wall, pers. comm.). These relationships are in part accountable by positive relief in the crestal portion of the arch, and in part by differential subsidence during Jurassic

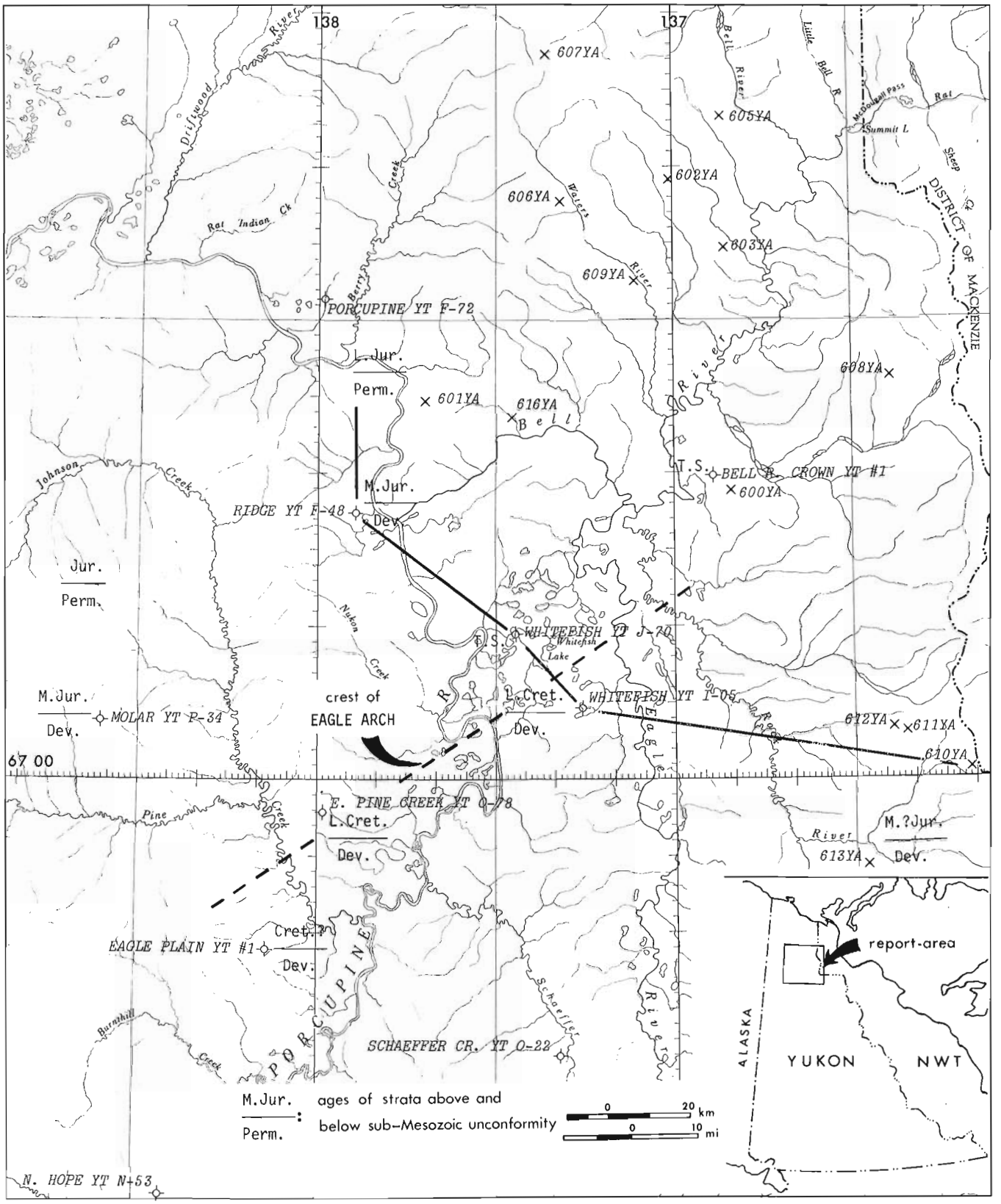

Figure 1. Location map.

Table 1

Petrographic analyses of sandstones, northeastern Eagle Plain.

STRATIGRAPHIC UNITS	SAMPLE NO	PARTICULATES (recalculated to 100%)									MATRIX					Quartz / Chert
		% Vol	Qtz	Cht	Lith	K-Feld	Plag Feld	Carb	Calc	Oth	Void	Qtz Cem	Calc Cem	Det	Oth	
basal Eagle Plain Fm (U Cret)	600 YA-12	76	32	33	16	5	1	11	—	2	—	3	—	21	—	0.97
Lower sandstone div (L Cret	610 YA-18	67	79	15	5	tr	—	1	—	1	—	32	—	1	—	5.4
	602 YA-5	67	85	6	2	1	—	3	—	1	tr	22	—	1	10	13.8
Upper Jurassic sandstone div	606 YA-2	65	92	6	1	—	—	1	—	tr	1	27	—	1	5	16.0
	601 YA-6	66	93	2	1	3	—	1	—	2	3	29	—	2	—	46.5
	F-48-2	65	95	tr	—	4	—	tr	1	tr	—	—	35	tr	—	>100
	P-34-2	58	80	19	—	—	—	—	—	1	6	33	1	1	—	4.2
Imperial Formation (U Devonian)	613 YA-1	72	41	51	5	—	—	3	—	tr	—	5	—	23	—	0.79
	O-78-2	74	39	46	12	—	—	3	—	tr	—	7	—	17	2	0.85
	I-05-2	75	42	35	9	—	tr	4	8	3	—	—	6	19	—	1.17
	P-34-3	75	37	45	6	tr	—	—	10	2	—	—	5	19	1	0.83

(all analyses included over 400 point-counts on samples of very fine to medium-grained sandstones)

and Early Cretaceous time. Thinning of nearshore Jurassic and Neocomian rock units toward the arch-axis does not support the idea that erosion erased basinal early Mesozoic deposits following tectonic uplifts during mid-Cretaceous time (Jeletzky, 1972, p. 9a).

Upper Devonian

The Upper Devonian in the study-area is represented by the Imperial Formation, a thick sequence of interbedded sandstone and shale. This formation was examined in subsurface cores and in outcrop near Rock River (613YA, Fig. 1), where it consists of friable, grey silty shale alternating with argillaceous, fine- to medium-grained sandstone. Bedding soles of the sandstone exhibit flute- and groove-casts, tool-marks, primary lineations, and plant fragments, all of which indicate deposition from turbidity currents, as Glennie (1963) and Gregory (1972) also concluded. As well, graded beds displaying the Bouma turbidite sequence of sedimentary structures were observed both here and in Core No. 5 of the East Pine Creek YT O-78 well. Rare in outcrop are sedimentary breccias consisting of angular clasts of previously deposited sandstone set chaotically in a matrix of mudstone. This type of breccia is particularly striking in cores of the Molar YT P-34 well.

The Imperial sandstone is petrographically distinct from those of Jurassic and Early Cretaceous (Neocomian) age in this area. Martin (1959, p. 2421) noted that "...the sandstones and conglomerates are composed of grains and pebbles of chert and siliceous shale, and quartz, in varying proportions. The combined percentage of chert and siliceous shale is generally greater than the percentage of quartz". Point-count analyses undertaken on Imperial sandstones from cores of Molar YT P-34, Whitefish YT I-05, and East Pine Creek YT O-78 wells, as well as Rock River outcrop samples (Table 1) support Martin's conclusions. Quartz content averages 40 per cent, while the combined chert and sedimentary rock fragment content averages 55 per cent. Carbonate rock fragments are important constituents of some samples. By contrast, sandstones of the Jurassic and Neocomian are far richer in quartz (Table 1) and, in general, more mature texturally and mineralogically (Young, 1973). Norris (1974) suggested that the lower Paleozoic Road River Formation and the Neruokpuk Formation of Romanzof and Barn uplifts were the principal sources of the Imperial Formation.

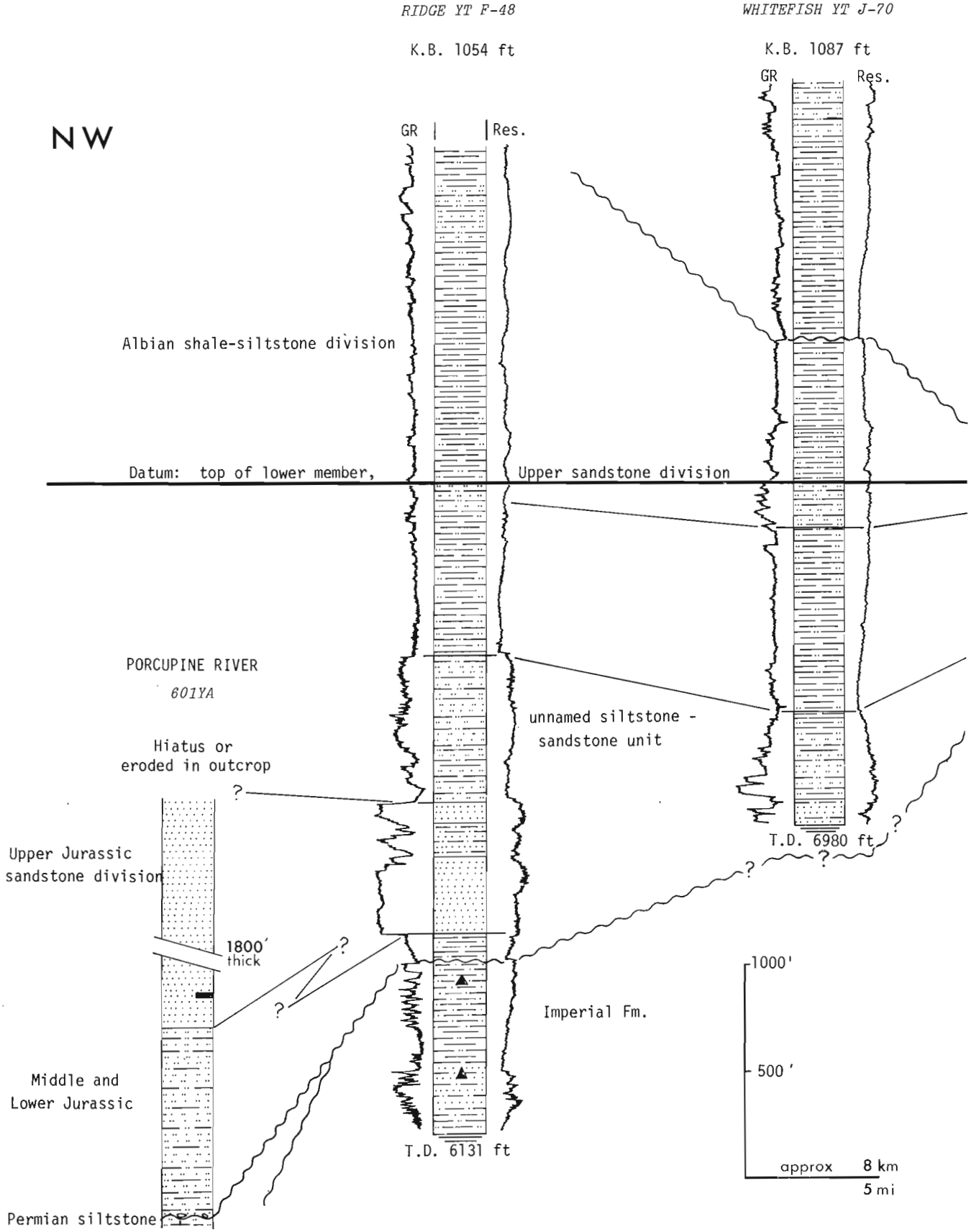
RIDGE YT F-48
K.B. 1054 ft
GR
Res.
WHITEFISH YT J-70
K.B. 1087 ft
GR
Res.
NW
Albian shale-siltstone division
Datum: top of lower member,
Upper sandstone division
PORCUPINE RIVER
601YA
unnamed siltstone - sandstone unit
Hiatus or eroded in outcrop
?
Upper Jurassic sandstone division
1800' thick
?
?
Middle and Lower Jurassic
Permian siltstone
T.D. 6131 ft
T.D. 6980 ft
?
?
?
Imperial Fm.
1000'
500'
approx 8 km
5 mi

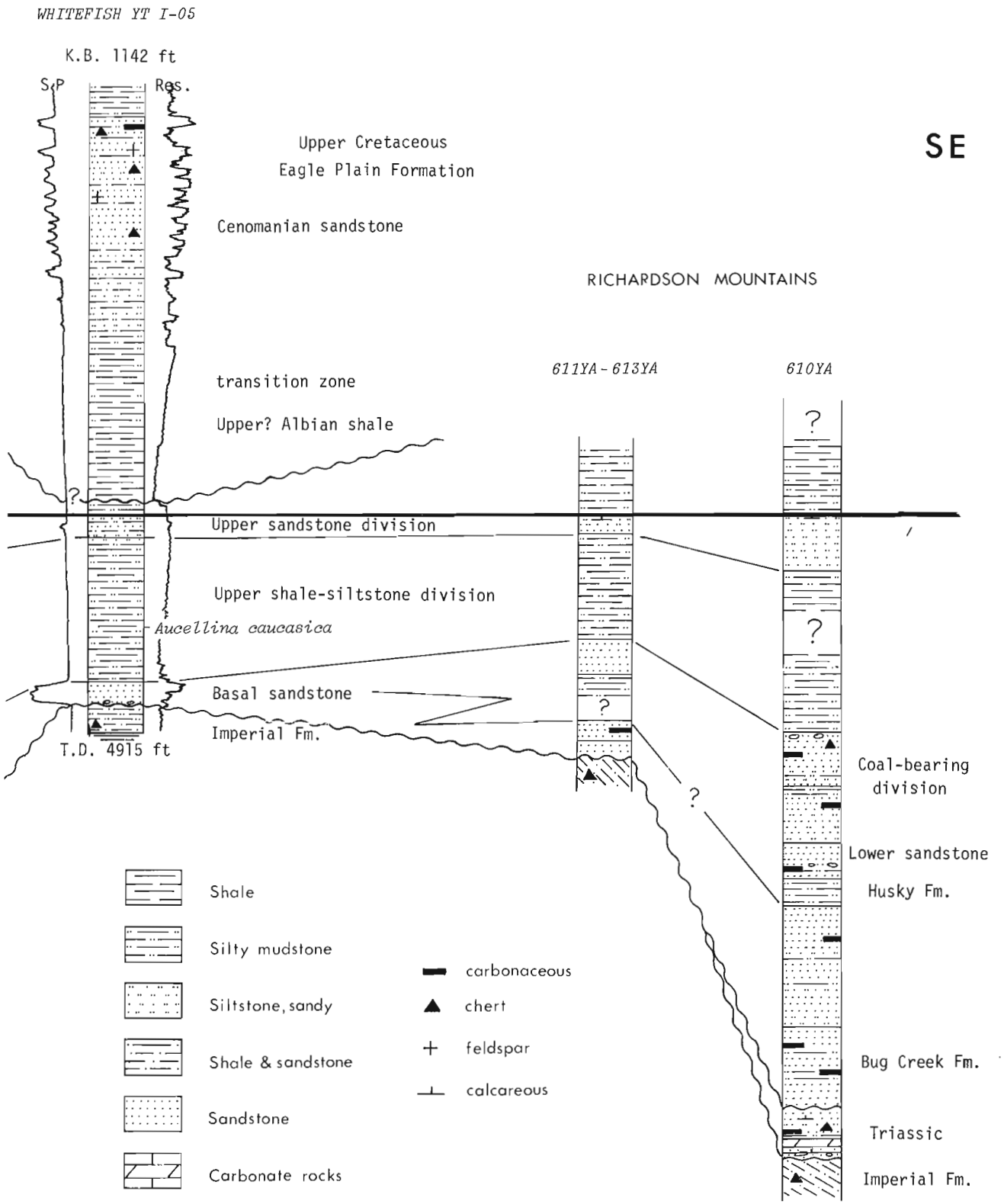

Figure 2. Stratigraphic profile across Eagle Arch, Yukon.

All samples of Imperial shale submitted for palynological and micropaleontological analyses yielded only pyrite and carbonized debris, and were essentially barren. These include samples from Molar YT P-34 (W.W. Brideaux and A.R. Sweet, pers. comm.), and the East Pine Creek YT O-78 and Whitefish YT I-05 wells (J.H. Wall, pers. comm.).

Following deposition of the Imperial Formation, Early Carboniferous tectonism affected the area (Martin, 1959; Knipping, 1960; Bell, 1973), probably in the form of folding and over-thrusting from the northwest.

Upper Paleozoic

Carboniferous rocks become younger southward and subcrop beneath Mesozoic sediments on the south flank of Eagle Arch (Graham, 1973). On the northern flank of the arch, Lower Permian rocks outcrop (Nassichuk, 1971; Bamber and Waterhouse, 1971), and lie unconformably on the Imperial Formation (Gregory, 1972). The Permian rocks were not examined by the writer.

The sub-Mesozoic unconformity

Angular relationships between basal Jurassic beds and underlying Permian rocks are, in most places, impossible to discern although, in the area of Summit Lake Anticline in Richardson Mountains, a small angular discordance is visible (Gregory, 1972). Between basal Jurassic sandstone and the Imperial Formation, however, marked angular differences occur, as, for example, in the Rock River outcrop (613YA, Fig. 1) where almost horizontal Jurassic rocks overlie Imperial rocks that strike north-south, and dip 15-20 degrees westward. Angular discordance of approximately 20 degrees is present between basal Mesozoic gritty sandstone and underlying Imperial Formation in Core No. 5 of Whitefish YT I-05.

Regional upwarping and emergence of Eagle Arch during the Early Permian to Early Jurassic interval (Moorhouse, 1966; Norris, 1974, p. 31) is supported by the abrupt erosional disappearance of Permian rocks below the unconformity, the absence of Triassic rocks, and the low angular relationship between Jurassic and Permian strata.

The surface of the unconformity varies in character from place to place. In the upper Bell River basin, the contact between Middle Jurassic sandstone and siltstone and very similar Permian rocks is difficult to determine (Jeletzky, 1974, p. 7). However, on Porcupine River, Nassichuk (1971, pers. comm.) found Lower Jurassic orange-weathering, pebble conglomerate grading up into quartzose sandstone containing coquinoid lenses above Lower Permian siltstone and shale. The unconformity was penetrated in cores of two boreholes, Whitefish YT I-05 and East Pine Creek YT O-78. At the top of Core No. 5 of the Whitefish YT I-05 well, the basal Mesozoic sandstone is medium grained and contains chert and siltstone grit and flat shale-clasts. The underlying Imperial Formation consists of dark grey shale and minor sandy siltstone with ripple-marks. In Core No. 6 (2536-2596 ft.) of East Pine Creek YT O-78 well, the basal Mesozoic shale formation, believed to be Early Cretaceous (Albian or ?Aptian) in age from log correlations and micropaleontologic observations (J.H. Wall, pers. comm.), becomes bioturbated and increasingly glauconitic and sandy downward in the basal 3 m (10 ft.). The basal 0.6 m (2 ft.) of sandstone contains vertical dwelling burrows, and is fine grained and well sorted, with abundant chert, glauconite, and quartz grains. This is a transgressive vertical sequence, consisting of a thin, basal shoreface deposit overlain by increasingly deeper offshore sediments. The basal sandstone is mixed with leached boulders of underlying Imperial sandstone, which here is coarse to very coarse grained, rich in chert, and argillaceous.

Lower and Middle Jurassic

Middle to lower Upper Jurassic fossiliferous, sandy siltstone occurs on Porcupine River several kilometres downstream from the confluence with Bell River (Jeletzky, 1974, p. 4; and *in* Frebold, 1961, p. 2). This facies has been interpreted by Jeletzky (ibid.) as inner neritic on the basis of its abundant endemic belemnites and pelecypods. Toward the southeast in the subsurface, this unit thins and grades into littoral sandstones which onlap the Eagle Arch (*see* Ridge YT F-48 in Fig. 2). In the Molar YT P-34 well (Core No. 13, 7952-7968 ft.), the basal Jurassic sandstone is very fine to fine grained, quartzitic, well sorted, and contains rare burrows, ripple-drift cross-lamination, and fine moldic porosity. Fifty kilometres (30 miles) west of the Porcupine River locality in the crestal part of Dave Lord Ridge, open-marine Kingak shale of Middle Jurassic age (GSC loc. 55255; fossils identified by J.A. Jeletzky) forms a rubbly outcrop (D.K. Norris, pers. comm.). This distribution of facies supports the existence of a marine strait in Middle Jurassic time in the position and approximate orientation of the present-day Dave Lord Ridge (Kandik-Porcupine trough of Moorhouse, 1966). Its northwestern shoreline is difficult to determine precisely owing to poor preservation.

In the Richardson Mountains in the headwaters of Waters River (607YA, Fig. 1), an area of Middle Jurassic shoaling is indicated by a thick accumulation of shallow-marine sandstone and shale. Fossil belemnites and pelecypods collected by the writer were identified by J.A. Jeletzky as *Pseudoicoelites* ex gr. *P. bidgievi-hibolitoides* (Saks) and *Inoceramus* (*Retroceramus*) ex aff. *I. menneri* Koshelkina (GSC loc. C-29248), indicative of a late Toarcian to middle Bajocian age. These rocks were previously thought to be much younger (Section 116P8, Mountjoy and Proctor, 1969). The thick shale unit above the sandstone now is identified as Husky Formation instead of bluish grey shale division.

Upper Jurassic

Upper Jurassic sandstones were examined to ascertain areal variations in paleocurrent directions, litho-

facies and petrography. Paleocurrent indicators in these rocks are rare, due in part to extensive frost-heaving of outcrops and lichen cover.

On Porcupine River (601YA, Fig. 1), the unnamed Upper Jurassic sandstone (Jeletzky, 1971, Fig. 2) consists of a great thickness of uniform, mature, fine-grained sandstone. The unit is approximately 550 m (1800 ft.) thick and is eroded at the top. In the upper 300 m (1000 ft.), well-sorted sandstone commonly exhibits parallel lamination, primary current lineations, and low-angle cross-stratification with scours. Biogenic features include abundant burrows, including straight, vertical, dwelling burrows such as *Skolithos* and *Diplocraterion*, and fossil belemnites, brachiopods and pelecypods, in part in coquinoid lenses. These structures, together with the dispersed paleocurrent distribution (Fig. 3), indicate an active, shallow-marine to littoral environment, with current flow dominantly toward the northeast.

At Waters River (606YA, Fig. 1), 29 km (18 miles) northeast, the Upper Jurassic sandstone is very fine to fine grained, carbonaceous, and consists of alternating beds of burrowed argillaceous sandstone with unburrowed, horizontally laminated sandstone. The presence of these sets with pelecypods and vertical burrows, including rare feeding burrows, indicate a lower shoreface environment and somewhat deeper marine conditions than those at Porcupine River. Paleocurrents here are also highly dispersed easterly (Fig. 3).

Farther northeast near Bell River(605YA, Fig. 1), the Upper Jurassic section is dominated by dark grey shale and silty mudstone, with minor very fine grained sandstone. This sandstone is in part silty and limonitic with shaly interbeds, and is commonly laminated, burrowed, and carbonaceous. Here paleocurrents are directed toward the northwest, as they are at localities to the south (Fig. 3).

In northern Eagle Plain, the Ridge YT F-48 well penetrated the Upper Jurassic sandstone unit at a depth of 4625 feet. Here, the unit is 183 m (600 ft.) thick, in contrast with the 550 m thickness present

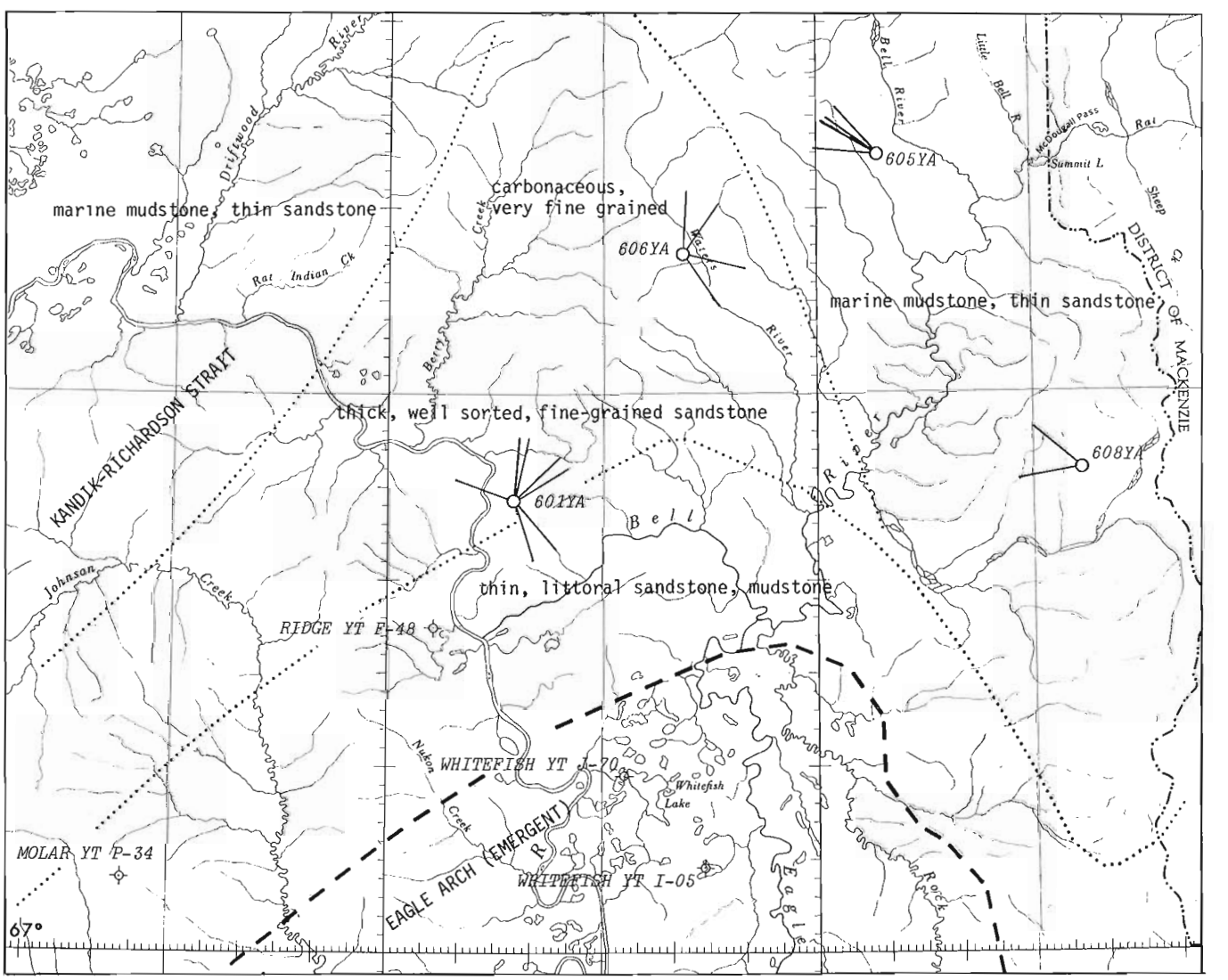

Figure 3. Upper Jurassic lithofacies trends and paleocurrents.

only 8 km (5 miles) to the north (Fig. 2). In Cores No. 1 and 2 (4647-3699 ft.), the sandstone is well sorted, fine grained, with good intergranular porosity, and is highly burrowed and bioturbated, commonly with lined, oblique, two-hole burrows. These features indicate physical and biotic reworking in the shoreface environment.

Upper Jurassic sandstone analyzed from three localities contain on the average 93 per cent quartz, 3 per cent chert, 2 per cent potash feldspar, and trace amounts of glauconite, tourmaline and zircon (Table 1).

The regional trends of paleocurrents, lithofacies, and thicknesses suggest that currents flowed northeasterly through Kandik-Richardson Strait and converged with westerly currents at its mouth in the area of the present-day Waters River (Fig. 3).

Lower Cretaceous (Neocomian)

In the subsurface of northeastern Eagle Plain, the Lower Cretaceous (Neocomian) sequence consists of a basal sandstone unit, which may be Late Jurassic or Neocomian in age, an unnamed sandy siltstone unit and the overlying Upper shale-siltstone division. In both Whitefish wells, the sandstone unit yielded trace amounts of natural gas from drillstem tests. Also, the sandy siltstone tested minor amounts of gas in the depth interval 3950-4230 feet of the Ridge YT F-48 well. Interestingly, these units are approximately correlative with the prolific reservoir rocks of the Parsons gas field (Cote *et al.*, in press), 250 km (155 miles) to the northeast.

Northward in Richardson Mountains, the Upper shale-siltstone division lies unconformably on the Lower sandstone division of Berriasian and Valanginian ages (Jeletzky, 1974, p. 9, 10). The sandy siltstone unit of the subsurface is absent in outcrop, due to either facies change, non-deposition, or erosion northward toward Aklavik Arch. Eastward in southern Richardson Mountains, it may be represented by the estuarine facies of the Coal-bearing division (Jeletzky, 1972).

Sandstones of the Lower sandstone division are richer in chert and slaty rock fragments than the underlying unnamed Upper Jurassic sandstone (Table 1), but are still far leaner in these components than sandstone of the Imperial Formation. A few paleocurrent measurements from the Lower sandstone division (Fig. 4) suggest that a southeastern source was important. This terrain could have supplied chert and sedimentary rock fragments from exposures of the Imperial Formation and younger Paleozoic rocks which underlie much of the Cretaceous in the Peel Plateau region (Norris *et al.*, 1963).

The Upper shale-siltstone division is very thick west of Bell River (602YA, Fig. 1) where Jeletzky (1974, p. 13) measured and described 1280 m (4200 ft.) and the writer measured 1190 m (3900 ft.). However, in wells of northeastern Eagle Plain, its thickness varies from 245 to 410 m (800-1350 ft.). It is probably absent in East Pine Creek YT O-78, presumably because of non-deposition over Eagle Arch.

In Core No. 3 of Whitefish YT I-05 well, at a depth of 4458 feet, the pelecypod *Aucellina caucasica* (Abich, 1851) sensu lato was identified by J.A. Jeletzky (internal rept., 1975; GSC loc. C-38252). According to Jeletzky, this fossil indicates a late Berremian or Aptian age, and generally ranges "from the upper part of the Upper member of the Upper shale-siltstone division to the top of the Upper sandstone division".

The relative thinness of the late Neocomian-?Aptian sections of the subsurface and the identification of the above pelecypod fossil aid in the refinement of Early Cretaceous paleogeography of the area. Because *Aucellina caucasica* occurs only 105 m (350 ft.) above the pre-Mesozoic unconformity in the Whitefish YT I-05 well, and the entire Neocomian section thickens northwestward (Fig. 2), the axis of Jeletzky's (1974, in press) Porcupine Plain-Richardson Mountain Trough must have lain close to the southern edge of Dave Lord Ridge. The Whitefish Lake area probably was emergent on the Eagle Arch until inundated by the late Neocomian marine transgression.

Lower Cretaceous (Aptian-Albian)

The lower member of the Upper sandstone division west of Bell River (602YA, Fig. 1) was described and interpreted by Jeletzky (1974, p. 16) and also examined by the writer. It is 200 m (660 ft.) thick here, and consists of siltstone and very fine grained sandstone containing marine pelecypods, brittle starfish, and bioturbation structures indicative of an offshore marine environment. Cross-laminae and ripple-mark orientations were measured to determine directions of paleocurrents. The dominant directional mode is approximately southerly here (Fig. 4) and is similar at another locality (603YA, Fig. 1), 8 km (5 miles) to the southeast (Fig. 4).

On Barrier Ridge of Richardson Mountains (610YA, Figs. 1, 2), a similar Upper sandstone division facies was encountered, but is only 74 m (243 ft.) thick. Here, flaggy, very fine grained sandstone exhibits low-angle, festoon cross-bedding, and marine pelecypods, and is interbedded with carbonaceous, medium grey, bioturbated siltstone. Paleocurrents measured from cross-stratification are bimodal, diametrically opposed, and oriented northwest-southeast (Fig. 4). This pattern may be due to the ebb and flow of tidal currents or wave breakage and swash (Klein, 1967). Owing to the fine texture of the sediments, the carbonaceous matter, and the presence of coquinoid lenses, a shallow, tide-influenced, brackish to open-marine environment is favoured, possibly within an estuary or bay.

In the subsurface of northeastern Eagle Plain, shale of Aptian age, equivalent to the Upper sandstone division, probably exists in the upper part of the Upper shale-siltstone division; the presence of *Aucellina caucasica* (*see* above discussion) low in the formation supports this view (Fig. 2). Possibly during the early Aptian marine regression and regional tectonic episode, part of the Eagle Arch again became emergent,

leaving a bay or estuary to the east of northern Eagle Plain (Fig. 4).

The upper member of the Upper sandstone division (Jeletzky, 1974, p. 16) west of Bell River (602YA, 609YA, Fig. 1) grades imperceptibly into the Albian shale-siltstone division. Jeletzky (ibid.) measured about 460 m (1500 ft.) below a faulted upper contact near 602YA. The writer traversed an unfaulted section on Waters River (609YA) which was determined graphically to contain 1370 m (4500 ft.) of pelitic rocks between the lower member of the Upper sandstone division and a major fault (Fig. 5). A lower unit, approximately 670 m (2200 ft.) thick, consists of siltstone and silty shale in the basal part, with shale becoming dominant upward. This unit is probably the upper member of the Upper sandstone division (Jeletzky, 1974, p. 16). The siltstone includes both laminated and burrowed varieties, while the silty shale is uniform and bioturbated, and contains marine pelecypods and spherical ironstone nodules.

The overlying 700 m (2300 ft.) consist of very uniform, dark grey slaty shale which contains ironstone concretions at its base, rare chert granules and pebbles, and pyrite nodules. At a stratigraphic level 1220 m (4000 ft.) above the top of the lower member of the Upper sandstone division an ammonite fossil was found, identified by J.A. Jeletzky (GSC loc. C-29255, Rept. No. Km-6-1974-JAJ) as *Arcthoplites* cf. *A. belli* McLearn, belonging to the upper Lower Albian part of the generalized *Arcthoplites* and *Beudanticeras affine* zone. Hence this unit is part of the Albian shale-siltstone division.

The lower part of this unit also was traversed along a small creek flowing into lower Bell River (616YA, Fig. 1). Here, medium to dark grey shale contains numerous ironstone concretions, about one half of which contain ammonite impressions. These were identified by Jeletzky as *Sonneratia* (sensu lato) n. sp. A (GSC locs. C-29263, C-29264) and, according to Jeletzky (Rept. No. Km-6-1974-JAJ), are indicative of an early Early Albian age, older than the generalized *Arcthoplites* and *Beudanticeras affine* zone. The shale here is relatively soft, and contains rare siltstone beds with abundant coaly particles on bedding planes. The

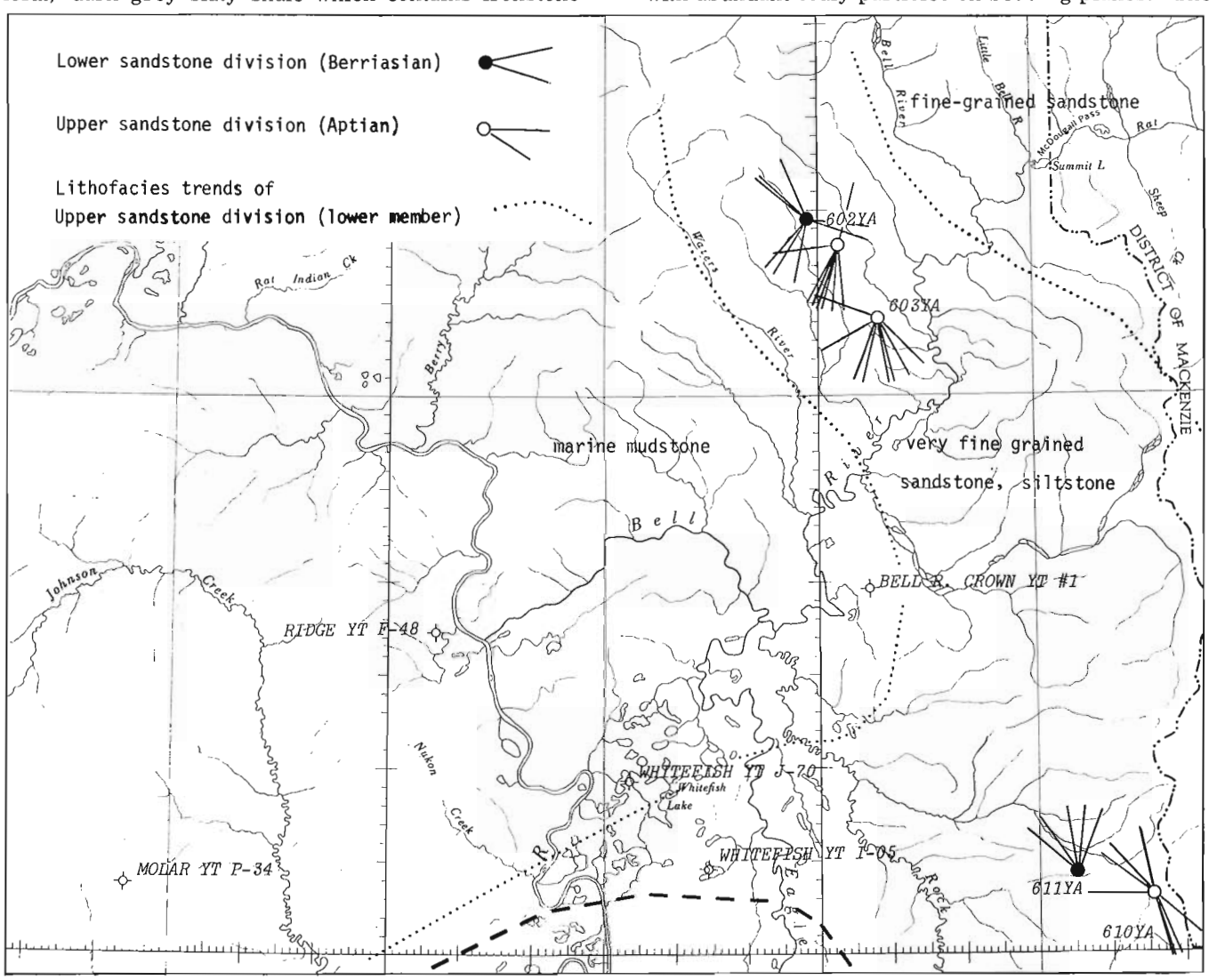

Figure 4. Lower Cretaceous lithofacies trends and paleocurrents.

section becomes gradually younger southward, and is overlain on the south bank of Bell River by ridge-forming, fine-grained sandstone probably of Late Cretaceous (?Cenomanian) age (Mountjoy, 1967, p. 6). As discussed below, the transitional shaly unit just below these sandstones may be Late Albian in age.

Upper Cretaceous

The lower part of the Upper Cretaceous Eagle Plain Formation was studied on a prominent ridge just south of "Pacific" Rat River (600YA, Fig. 1) and was penetrated in the two Whitefish boreholes and the Molar YT P-34 well. The contact relations with the underlying Lower Albian shale are unclear due to lack of exposure of the critical interval and, for the present, poor fossil control in subsurface sections. However, log correlations (Fig. 2) and micropaleontology of the Molar YT P-34 well (Chamney *in* Norford *et al.*, 1971; GSC locs. C-8001 to C-8034) suggest the presence of an unconformity. A coarsening-upward transition zone overlies the Albian shale-siltstone division, and culminates in the unnamed Cenomanian sandstone ("Blackie" sandstone of wildcatters). In the Molar YT P-34 well, this sandstone unit lies abruptly on Albian shale but, at

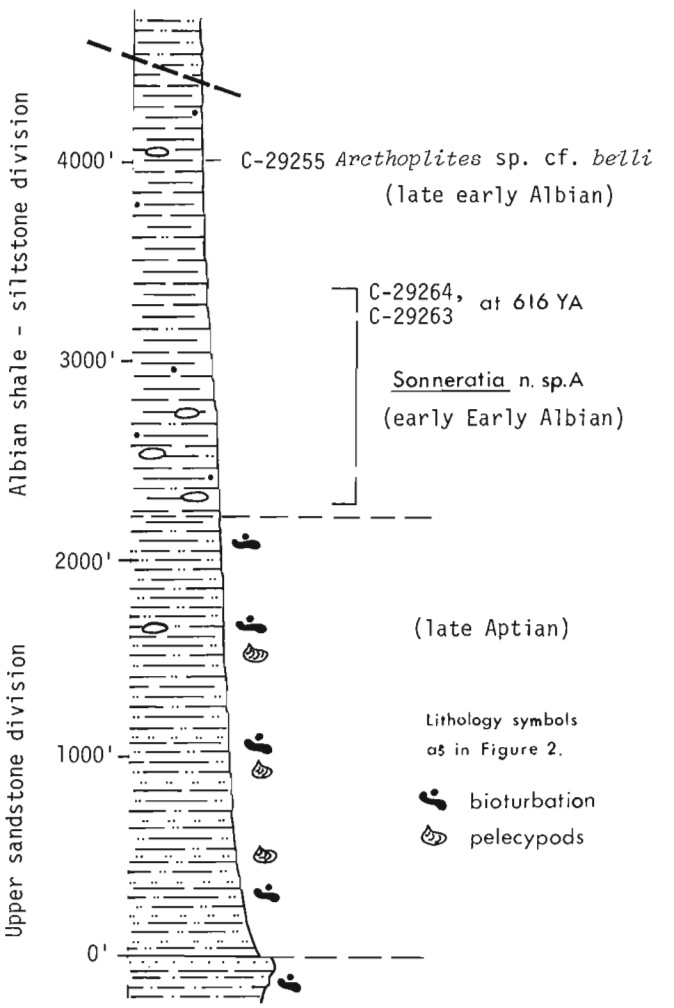

Figure 1. Aptian-Albian section on Waters River, Yukon.

"Pacific" Rat River, the transition zone is approximately 760 m (2500 ft.) thick and the few poorly exposed, broken outcrops indicate the predominance of argillaceous, very fine grained sandstone, mostly bioturbated, and interbedded silty mudstone and calcareous siltstone. The zone is approximately 300 m (1000 ft.) thick, 24 km (15 miles) west and southwest as evidenced by outcrop patterns near Bell River and subsurface control in Whitefish YT J-70 and I-05 wells. Its age may be Late Albian because it contains questionable Albian Foraminifera (J.H. Wall, pers. comm.), and it lies conformably below the unnamed Cenomanian sandstone which contains the Cenomanian or possibly Albian pelecypod *Inoceramus* ex gr. *I. dunveganensis* (Mountjoy, 1967, p. 6), and Cenomanian Foraminifera (Chamney *in* Norford *et al.*, 1971; GSC locs. C-8001 to C-8016).

The "Blackie" sandstone is 210 m (700 ft.) thick in both Whitefish wells, 200 m (660 ft.) in the Molar well, and 64 m (210 ft.) thick, but eroded at the top, in the section measured at 600YA (Fig. 1). Here it consists of well sorted, very fine grained to fine grained sandstone, in part calcareous, with interbedded shaly siltstone. It exhibits parallel lamination, burrows, ripplemarks and, rarely, convolutions. It is similar in texture in cuttings of the Whitefish wells, and also contains coaly plant fragments and *Inoceramus* fragments. Coal seams occur near its top, indicating in part a nonmarine depositional environment. The sandstone is generally rich in chert, particularly black, grey, and green varieties. There is also an abundance of sedimentary rock fragments, plagioclase, and potash feldspar (Table 1). Quartz content seems variable, being greater in relatively finer grained and porous specimens. Its immature composition is similar to molassoid Upper Cretaceous deposits lying to the north (Young, 1973) and suggests derivation from an upland composed of mixed sedimentary and plutonic igneous rocks. Grain-size fining and eastward thickening of the transition zone suggest derivation from the west.

A thick marine shale unit overlies the Blackie sandstone in the area, but this and younger members of the Eagle Plain Formation do not outcrop, and were not studied.

References

Bamber, E.W. and Waterhouse, J.B.
1971: Carboniferous and Permian stratigraphy and paleontology, northern Yukon Territory, Canada; Bull. Can. Pet. Geol., v. 19, p. 29-250.

Bell, J.S.
1973: Late-Paleozoic orogeny in the northern Yukon *in* Proc. of the Symposium on the Geology of the Canadian Arctic, Aitken, J.D. and Glass, D.J., eds.; Geol. Assoc. Can. and Can. Soc. Pet. Geol., p. 23-38.

Cote, R.P., Lerand, M. and Rector, R.J.
Geology of the Lower Cretaceous Parsons Lake Gas Field, Mackenzie Delta, Northwest Terri-

Cote, R. P., Lerand, M. and Rector, R. J. (cont'd.)
tories *in* Proc. of Symposium on Canada's Continental Margins and Offshore Petroleum Exploration, C. J. Yorath, ed.; Can. Soc. Pet. Geol. (in press)

Frebold, H.
1961: The Jurassic faunas of the Canadian Arctic, Middle and Upper Jurassic ammonites; Geol. Surv. Can., Bull. 74.

Glennie, K. W.
1963: An interpretation of turbidites whose sole markings show multiple directional trends; J. Geol., v. 71, p. 525-527.

Graham, A. D.
1973: Carboniferous and Permian stratigraphy, southern Eagle Plain, Yukon Territory, Canada *in* Proc. of the Symposium on the Geology of the Canadian Arctic, Aitken, J. D., and Glass, D. J., eds.; Geol. Assoc. Can. and Can. Soc. Pet. Geol., p. 159-180.

Gregory, J.
1972: The structure and geologic history of the Summit Lake anticline, north Richardson Mountains, Yukon and Northwest Territories; unpublished B. Sc. thesis, Carleton Univ., Ottawa.

Jeletzky, J. A.
1962: Pre-Cretaceous Richardson Mountains trough: its place in the tectonic framework of Arctic Canada and its bearing on some geosynclinal concepts; Trans. Roy. Soc. Can., v. 54, ser. III, p. 55-83.

1971: Stratigraphy, facies and paleogeography of Mesozoic rocks of northern and west-central Yukon; *in* Report of Activities, April to October 1970, Geol. Surv. Can., Paper 71-1, Pt. A, p. 203-221.

1972: Stratigraphy, facies and paleogeography of Mesozoic and Tertiary rocks of northern Yukon and northwestern Mackenzie District, N. W. T.; Geol. Surv. Can., Open File 82.

1974: Contribution to the Jurassic and Cretaceous geology of northern Yukon Territory and District of Mackenzie, Northwest Territories; Geol. Surv. Can., Paper 74-10.

Jurassic and Lower Cretaceous paleogeography and depositional tectonics of Porcupine Plateau and adjacent areas of northern Yukon; Geol. Surv. Can., Paper 74-16 (Open File 203). (in press)

Klein, G. deV.
1967: Paleocurrent analysis in relation to modern marine sediment dispersal patterns; Bull. Am. Assoc. Pet. Geol., v. 51, p. 366-382.

Knipping, H. D.
1960: Late Paleozoic orogeny - northern Yukon; preprint for Am. Assoc. Petrol. Geologists - Alberta Soc. Petrol. Geologists Regional Mtg., Frontiers of Exploration in Canada, Banff, Alberta.

Martin, L. J.
1959: Stratigraphy and depositional tectonics of the north Yukon - lower Mackenzie area, Canada; Bull. Am. Assoc. Pet. Geol., v. 43, p. 2399-2455.

Moorhouse, M. D.
1966: Eagle Plain Basin of Yukon Territory (abstr.); Bull. Am. Assoc. Pet. Geol., v. 50, p. 628.

Mountjoy, E. W.
1967: Upper Cretaceous and Tertiary stratigraphy, northern Yukon Territory and northwestern District of Mackenzie; Geol. Surv. Can., Paper 66-16.

Mountjoy, E. W. and Procter, R. M.
1969: Eleven field descriptions of some Jurassic and Cretaceous rocks in Arctic Plateau and Arctic Coastal Plain; Geol. Surv. Can., Open File 16.

Nassichuk, W. W.
1971: Permian biostratigraphy, northern British Columbia and northern Yukon; *in* Report of Activities, April to October 1970, Geol. Surv. Can., Paper 71-1, Pt. A, p. 103-105.

Norford, B. S., Barss, M. S., Brideaux, W. W., Chamney, T. P., Fritz, W. H., Hopkins, W. S. Jr., Jeletzky, J. A., Pedder, A. E. H. and Uyeno, T. T.
1971: Biostratigraphic determinations of fossils from the subsurface of the Yukon Territory and the District of Mackenzie; Geol. Surv. Can., Paper 71-15.

Norris, D. K.
1974: Structural geometry and geological history of the northern Canadian Cordillera *in* Proc. of the 1973 Nat. Convention, Calgary, Alberta, A. E. Wren and R. B. Cruz, eds.; Can. Soc. Exploration Geophysicists, p. 18-45.

Norris, D. K., Price, R. A. and Mountjoy, E. W.
1963: Northern Yukon Territory and northwestern District of Mackenzie; Geol. Surv. Can., Map 10-1963.

Young, F. G.
1973: Mesozoic epicontinental, flyschoid and molassoid depositional phases of Yukon's north slope *in* Proc. of the Symposium on the Geology of the Canadian Arctic, Aitken, J. D. and Glass, D. J., eds.; Geol. Assoc. Can. and Can. Soc. Pet. Geol., p. 181-202.

ADDENDUM

(The following papers were received after production of this report had begun on April 9, 1975)

63. PRESENT AND FUTURE SATELLITE PROGRAM OF U.S.A.

Project 700089

S. Washkurak
Resource Geophysics and Geochemistry Division

It behoves geoscientists to be aware of present and future developments concerning information from space. This report summarizes various active and planned spacecraft to be launched by the United States through to 1980 at which time Space Shuttle will usher in a new generation of experiments in space science. The report contains information on primary satellite mission, orbit parameter, sensor type and expected performance in ground resolution and wavelength. The information was obtained primarily from bulletins provided by NASA, some scientific journals and a review paper presented at AES, Toronto, in February by C.H. Vermillion of Goddard Space Flight Center, Maryland.

LANDSAT II
Polar Orbit Launched January 1975

The name of ERTS II has been officially changed to LANDSAT II. This is to complement an ocean dynamics satellite named SEASAT "A" which is currently in the design stage. It has also been announced (February) that LANDSAT III is scheduled for launch in 1977. This should provide a continuing program through to 1980 or until an operational satellite called EOS (Earth Observational Satellite) is launched in 1978. LANDSAT II is operating normally including the return beam vidicon but is not routinely scheduled in conjunction with ERTS I to provide double earth coverage (i.e. once every nine days).

EOS
Polar Orbit to be Launched 1978

The Earth Observational Satellite (EOS) to be launched in 1978 into a polar orbit will provide an improved ground resolution of 130 feet compared to LANDSAT II at 260 feet. Ground resolution can be improved by a factor of ten with some modification on board the spacecraft. The biggest strain on hardware is caused by the very high data rate (200 megabit per second) required to transmit the large volume of information produced with a 10-foot ground resolution. For most applications it is not necessary to count the trees.

EOS is expected to have a two frequency dual polarization synthetic aperture radar on board with a ground resolution of 30 metres at both "L" and "X" frequency band. The "L" band at 1700 MHz (wavelength 18 cm) should have some vegetation penetration and indicate percentage moisture content of soil to a few centimetres in depth. The "X" band at 3 cm wavelength system will have complete cloud penetration and provide a comparative measurement capability of wavelength and polarization to enhance characteristic signatures. Total earth coverage is expected every 40 days with a swath width of 55 km. Tradeoffs may be made with swath width, ground resolution, antenna size and power provided on board the spacecraft.

SEOS Equator Synchronous Orbit
To be Launched 1980

A Synchronous Earth Observational Satellite is proposed for launching in 1980 (via Space Shuttle). The unique capability of SEOS will be its pointable telescope that can continuously monitor selected portions of the earth's surface with a subsatellite ground resolution of 100 feet from synchronous orbit. Some applications include tornado watch, hail storm monitoring, and forest fire detection. Unfortunately coverage of Canada will be limited to about 55^{o} North latitude due to distortion as a result of the earth's curvature apparent from synchronous orbit.

SPACE SHUTTLE 1980

The Space Shuttle Program will provide the opportunity for a new generation of experiments in space science. Large aperture antennas in the order of 90 feet in length may be deployed from the space hatch and electronically steered to produce both a 3-dimensional meteorological radar with a fringe benefit of a 2-dimensional radar reflectivity map of the earth's surface with a swath width of 500 km and 1 km ground resolution. The frequency coverage will be extended from 100 MHz to 100 GHz or from 3 metres to 3 mm wavelength.

Having proven that welding of material in space is possible in the "Skylab" experiment, the construction of a large $\frac{1}{2}$-mile parabolic reflector antenna may be undertaken to relay energy (power) via microwave radiation to various isolated locations on earth.

After 1980 most satellite launches will be made via the shuttle orbiter. To justify the cost of the whole project a launch per week will be maintained.

HEAT CAPACITY MAPPER HCM
(1977) Polar Orbit

The heat capacity mapper mission to be launched in 1977 is a relatively small (117 kg) satellite. The sun synchronous orbit will sense the maximum (2 p.m.) and minimum (2 a.m.) of the diurnal thermal cycle at an altitude of 600 km. The thermal inertia which is the ratio of thermal conductivity to the square root of the thermal diffusivity correlates somewhat linearly with density for most geologic materials. The ratio of day night temperature difference to the complement of albedo is dependent on thermal inertia and moisture content. The thermal inertia can be used to discriminate geologic material or moisture content. A 1-cm lichen layer and a 10-cm soil layer produce a surface temperature similar to an infinitely thick soil cover. Clearly then, the thermal inertia mapping is only applicable in areas of good geologic exposure such as the Arctic and Cordilleran regions. Measurement of plant canopy temperature at frequent intervals will determine the transpiration of water and plant life. It will map thermal effluents, both natural and man-made. Frequent coverage of snow fields for water run-off prediction and location and variation of the freeze thaw line over various regions is anticipated.

COASTAL ZONE OCEAN COLOUR SCANNER
CZOC 1978 (Nimbus G) Polar Orbit

The CZOC mapper is designed to map the chlorophyll concentration in water, sediment distribution and a "gelbstaffe" concentration as a salinity indicator. Eighty per cent of the world's oxygen is produced by algae in the top few millimetres of ocean surface. The satellite monitoring of the absorption due to chlorophyll will indicate the extent of possible irreversible damage due to chemical pollutant. Chlorophyll production is sensitive to physiological disturbances including disease or lack of moisture stress conditions. Soil-metal-plant interrelationship is well developed and may provide geologic signatures detectable with the coastal zone mapper.

MEASUREMENT OF AIR POLLUTION MAPS
1978 (Nimbus G) Polar Orbit

Maps will chart the Global distribution of CO, $CH_{(4)}$, SO_2, and NH_3 to track movement of contaminated air masses and study dispersal and scavenging mechanisms. The instrument will employ a Barringer type gas filter correlation technique. Other types of radiometers will monitor O_3, N_2O, NO_2, HNO_3, CH_4 and aerosols in the upper troposphere to middle stratosphere. No geological applications have been mentioned although sensitivities of a few per cent and parts per million have been mentioned.

ELECTRON MICROWAVE SCANNING RADIOMETER
ESMR Nimbus 5 F and G

The primary objectives of the Nimbus Microwave Scanning Radiometer were to derive liquid water content of clouds, observe sea ice type (first year or older) over the polar ice cap and to test the feasibility of inferring surface composition and soil moisture content. The microwave emission is sensed at several wavelengths from 1.5 cm to 4.6 mm giving excellent cloud penetration with a 25-km ground resolution. Besides inferring soil moisture by observing the IR reflectance through the emission window at 11 μm, similar apparent temperature variation may indicate soil moisture content at microwave wavelengths especially below 1 cm. Additional studies are necessary using multifrequency sensors with intensive ground truth directed specifically to relating moisture variations to microwave data. Nimbus 5 is operational with F scheduled for launch in 1975 and G with improved sensors scheduled for 1978.

SEASAT 1978 Polar Orbit

Mission objectives of SEASAT will be to provide a look at the dynamics of the earth's ocean. Areas of prime consideration are: gross topography (a 66-foot depression has already been located over the region of Puerto Rico Trench, site of the Atlantic's deepest point of 27 500 feet); sea state, ocean currents, wave spectra and direction and water temperature. Instruments onboard will include short pulse radar, scatterometer, synthetic aperture radar, visible and microwave radiometers.

HIGH ENERGY ASTRONOMY OBSERVATORY
HEOA-A, 1977 Polar Orbit

The objective of the High Energy Astronomy Observatory will be to conduct research into X-ray Gamma-ray and Cosmic ray astrophysics. The 3000 kilogram spacecraft in polar earth orbit at 200 miles will conduct pointable observations at very high energy and low flux levels. The prime objective will be to conduct an X-ray sky survey. HEAO-A is the first of three satellites planned to be launched from 1977 through to 1979.

The low energy gamma-ray survey experiment will search for phenomena in the energy range from 0.01 to 10 Mev. Determination of intensity and spectra of sources at a sensitivity of 7E-4 photons/cm sq/sec and the position of sources will be fixed to 1 degree for threshold sources.

The instrument package will contain seven detectors shielded by an active collimator anti coincident crystal. Detectors will have a collimated field of view of 20 x 40 degrees. A cesium iodide blocking crystal will be positioned over the aperture to record the back-

ground events in the detector. It is interesting to note that a Mission Definition Group including NASA and ESRO (European Space Research Organization) scientists decided to maximize the scientific gain for a planned Jupiter probe to dedicate 70 per cent of the 40 kg payload to the study of energetic particles and magnetic fields, with the remainder set aside for instruments capable of providing visual, ultraviolet and infrared images.

HAWKEYE 1974
Polar elliptical orbit (Magnetometer)

In 1974 a small (26 kg) spacecraft was launched to study solar wind injection into the magnetosphere by monitoring low energy protons and electrons; the electromagnetic radiation from 10 Hz to 178 KHz as well as a triaxial fluxgate magnetometer. The principal scientist heading the project is J. Van Allen of the University of Utah.

During the Skylab II mission solar observations have shown that previous coronal theory will have to be discarded. It is much more dynamic and may have a near term practical benefit in weather forecasting. It has been discovered that, when the boundary between the magnetic fields in the interplanetary medium sweeps by the earth, there is a profound effect on our weather; it generally correlates with an approximate 10 per cent reduction in large storms in the northern hemisphere.

VIKING 1975 (Mars Probe)

This is a two part spacecraft mission. The imagery obtained from the orbiter vehicle will determine the site for the landing vehicle which is designed to operate for 90 days after landing. The scientific payload for the lander will weigh 2000 pounds. The experiments include seismology, molecular analysis (mass spectrometer) magnetic properties, biology investigation, colour TV as well as an X-ray fluorescence spectrometer. The proportional counters will detect X-rays emitted from samples of the Martian surface materials irradiated by X-rays from radioisotope sources iron 55 and cadmium 109. Surface composition of trace elements will be measured in parts per million and a few per cent for major elements. The orbiter imaging system will have a 40-metre resolution at a reference altitude of 1500 km. The orbiter will weigh 2000 pounds. A second mission Viking B will follow as a complete back up. The information obtained from Viking A will determine the alternate landing site of Viking B.

PIONEER VENUS ORBITER 1978

This 1000-pound spacecraft will orbit Venus for one Venus sidereal year (225 days) to obtain information on the upper and lower Venusian atmosphere and surface global characteristics. Surface profile, roughness, and electrical properties data including derived gravity information and earth based radar backscatter data will be used to produce cartographic and geological maps to a scale of 1 to 5 million. Walter Brown of JPL is the principal scientist for the microwave radar altimeter experiment.

Concluding Remarks

This review mentions only some of the spacecraft and experiments planned by the U. S. which may be of interest to geoscientists. Development of specialized instruments for geophysical use from space, and the parallel improvements in the compactness and reliability of equipment have already contributed to the development of ground instrumentation and ground methods. The United States has spent 440 billion dollars on all aspects of space research in the past 25 years. Undoubtedly there will be an accelerating world-wide pay-off from this in the future.

L. E. Stephens and R. V. Cooper
Gravity Division, Earth Physics Branch, Ottawa

Gravity, magnetic, seismic and bathymetric measurements were made over part of Amundsen Gulf (Fig. 1) from the C. S. S. PARIZEAU during August and September, 1973 (Sandilands and Clarke, 1973). The survey was part of the Natural Resource Mapping Program jointly sponsored by the Department of the Environment and the Department of Energy, Mines and Resources. The gravity survey was the responsibility

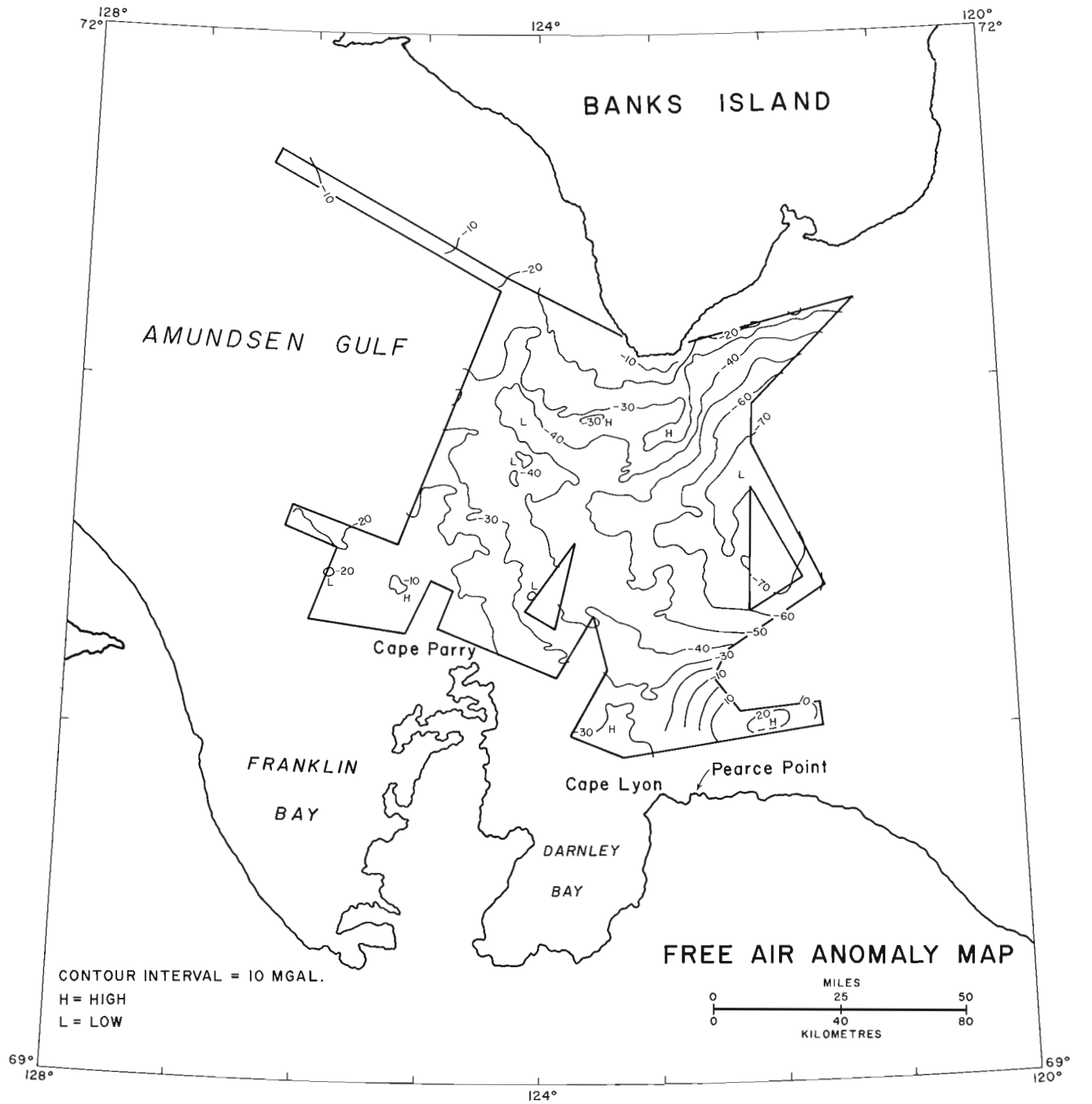

Figure 1. Free air anomaly map of Amundsen Gulf.

of the Earth Physics Branch and the results are briefly described in this paper.

The gravity data were acquired with a LaCoste and Romberg sea gravimeter mounted on a 3-axis inertial platform. Data channels were scanned every 10 seconds with an NLS data acquisition system and recorded on a Digi-Data incremental tape deck. The raw gravity data on magnetic tape were reduced on board ship to preliminary gravity values at five minute intervals using a Nova 1200 computer. The hydrographers submitted a daily punch paper tape consisting of time, bathymetry and geographic co-ordinates at five minute intervals which was subsequently integrated with the observed gravity values to determine preliminary free air anomalies. On return to Ottawa the crossover differences in gravity were adjusted by least squares on the departmental CDC 6400 computer. The standard deviation of the crossover residuals from this adjustment was

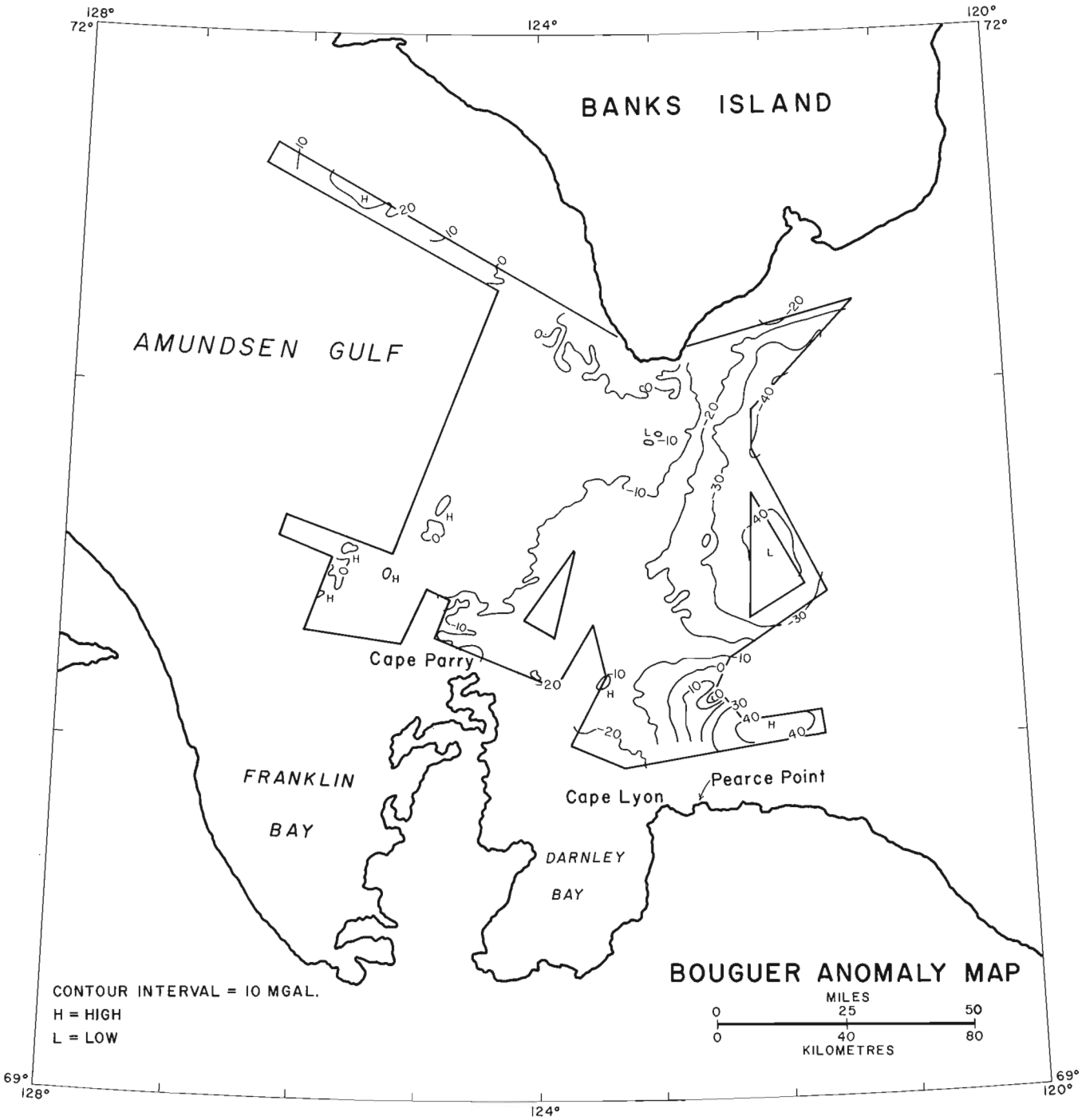

Figure 2. Bouguer anomaly map of Amundsen Gulf.

0.90 mgal. Final gravity values were then computed by adjusting the data between crossovers to the adjusted crossover values.

A Decca navigation chain established by the Polar Continental Shelf Project provided the navigational data which the hydrographers reduced to geographic co-ordinates on board ship using a PDP-8e computer. Simultaneously, the depth sounder accoustic response times were reduced to depth equivalents.

The ship tracks followed Decca lanes which were 0.5 km and 2 km apart with check lines transverse to the lanes every 10 km. Five minute fixes along each line produced station intervals of 1 to 2 km depending on the speed of the ship. The estimated accuracy of the navigational fixes, based on an error lobe analysis, is ± 200 m, while the depths have an accuracy of ± 12 m (about 2% of the depth).

If the errors inherent in the observed gravity, navigation and bathymetry are considered, the overall accuracies of the free air and Bouguer anomalies are about ± 3 mgal and ± 4 mgal, respectively. After screening the gravity data for erroneous readings, a total of 3014 stations was recovered.

Amundsen Gulf is geologically situated at the convergence of the Prince Patrick Uplift (Banks Island), and the Aklavik and Coppermine arches (mainland). Thorsteinsson and Tozer (1960) suggested that the Precambrian inlier of south Banks Island may be related to the Prince Patrick Uplift to the north and possibly to the Precambrian inlier of Darnley Bay across Amundsen Gulf. Precambrian sedimentary basement rocks of the western Arctic Islands are overlain by Paleozoic and Mesozoic sedimentary rocks which have subsequently been disrupted by north and northwest trending extension faults. Surrounding Amundsen Gulf, northwest and northeast trending gabbro-diabase dykes and sills have intruded all Precambrian sedimentary rocks including basalt flows, but have not intruded Paleozoic and Mesozoic sedimentary rocks (Christie, 1964; Yorath *et al.*, 1969).

The most prominent gravity anomalies within the survey area (Figs. 1 and 2) are a north-south trending negative anomaly (low) southeast of Banks Island and an easterly trending positive anomaly (high) northeast of Pearce Point named the Pearce Point high. The western part of the survey area consists of a relatively featureless gravity field. The elongate low anomaly may indicate a sedimentary basin; a similar anomaly on Banks Island (Stephens *et al.*, 1972) may be related to a northerly extension of this basin that has been displaced about 40 km to the east. The Pearce Point high coincides with a high magnetic anomaly (Currie and Tiffin, 1972), as does the Darnley Bay gravity high (Riddihough and Haines, 1972). However, it differs significantly from the Darnley Bay anomaly; it is linear and not circular, and also has an amplitude and horizontal gradients which are half those of the Darnley Bay anomaly. These differences may be related to differences in the composition of the intrusive rocks which must underlie these anomalies. The Darnley Bay anomaly may be associated with an ultrabasic intrusion (Stacey, 1971); the Pearce Point anomaly may be related to a basic intrusion, perhaps with a composition similar to the basalts of the Coppermine Arch or possibly the Muskox Intrusion.

The gravity data in Amundsen Gulf along with other geophysical and geological data support the suggestion that the Coppermine Arch and related geological structures extend to Banks Island (Currie and Tiffin, 1974). The higher gravity gradients between Banks Island and the mainland indicate a shallow Precambrian basement, perhaps uplifted during the Mesozoic (Thorsteinsson and Tozer, 1960) and the north-south gravity anomaly trends within the survey and adjacent areas in the Amundsen Gulf indicate the northward extension of the Coppermine structures.

References

Christie, R.L.
1964: Diabase-gabbro sills and related rocks of Banks Island and Victoria Islands, Arctic Archipelago; Geol. Surv. Can., Bull. 105.

Currie, R.G. and Tiffin, D.L.
1974: Preliminary results of a shipborne magnetic survey in Amundsen Gulf, District of Franklin; *in* Report of Activities, November 1973 to March 1974, Geol. Surv. Can., Paper 74-1, Pt. B, p. 65-67.

Riddihough, R.P. and Haines, G.V.
1972: Magnetic measurements over Darnley Bay, N.W.T.; Can. J. Earth Sci., v. 9, p. 972-978.

Sandilands, R.W. and Clarke, E.B.
1973: Final field report - C.S.S. Parizeau - Queen Charlotte Sound, British Columbia and Amundsen Gulf, N.W.T.; C.H.S., Marine Sciences Br., Dept. Environment, Ottawa.

Stacey, R.A.
1971: Interpretation of the gravity anomaly at Darnley Bay, N.W.T.; Can. J. Earth Sci., v. 8, no. 8, p. 1037-1042.

Stephens, L.E., Sobczak, L.W. and Wainwright, E.S.
1972: Gravity measurements on Banks Island, N.W.T.; Gravity Map Series, Earth Physics Br., No. 150.

Thorsteinsson, R. and Tozer, E.T.
1960: Summary account of structural history of the Canadian Arctic Archipelago since Precambrian times; Geol. Surv. Can., Paper 60-7.

Yorath, C.J., Balkwill, H.R. and Klassen, R.W.
1969: Geology of the eastern part of the northern interior and Arctic coastal plains, N.W.T.; Geol. Surv. Can., Paper 68-27.

65. SUMMARY OF STRATABOUND ZINC-LEAD DEPOSITS OF LITTLE CORNWALLIS AND NEARBY ISLANDS, CANADIAN ARCTIC

Projects 630002, 650003, 670016

J. Wm. Kerr
Institute of Sedimentary and Petroleum Geology, Calgary

Introduction

Two important lead-zinc discoveries of Arvik Mines Ltd. (owned jointly by Cominco Ltd., and Bankeno Mines Ltd.) on Little Cornwallis Island will probably be producing mines in the future. These and other nearby occurrences of lesser or uncertain importance are shown on the index map (Fig. 1) and information on their geological occurrence is summarized by table (Table 1). Much of the information in Column 2 of this table was kindly provided by Cominco Ltd. (T.W. Muraro, pers. comm., 1975).

Drilling and underground development have proven up 20 million tons of 20% combined lead-zinc ore at Polaris, whereas drilling alone at Eclipse has proven up 1 million tons of 13% combined lead-zinc ore (Brown, 1973). According to Sangster (1974) the gross metal value of the Polaris deposit has been determined to exceed $1.5 billion, making it one of the more significant lead-zinc deposits in the world. The other occurrences have not been drilled extensively, and for them available information is primarily from surface mapping.

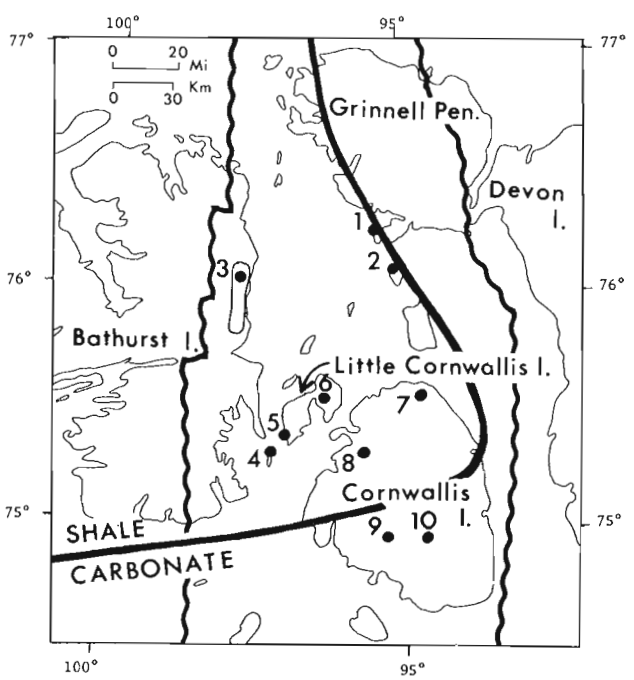

Figure 1. Lead-zinc occurrences of the Canadian Arctic referred to in Table 1. The solid line marks a facies change from the Cape Phillips shale formation to equivalent carbonate units. The wavy lines show the limit of the Cornwallis Fold Belt.

Lead-Zinc Deposits

Four geological circumstances apply to nearly all of the ten mineral occurrences. These four circumstances are listed below, along with a summary of how prevalent they are in the ten occurrences shown on Table 1.

(a) All ten occur in the Cornwallis Fold Belt.
(b) Nine of the ten occur in the Ordovician Thumb Mountain Formation, and all the important ones occur near the top (1, 2, 4, 5, 6).
(c) Eight of the ten occur in the geographic area where the Cape Phillips Formation was deposited.
(d) In at least eight and perhaps all ten cases the host formation is truncated and overlain unconformably by a Lower Devonian formation.

The four circumstances listed above can largely be documented by plotting the mineral occurrences on maps of Thorsteinsson and Kerr (1968); Thorsteinsson (1973), and Kerr (1974). They are based in small part on later unpublished field work by Thorsteinsson and by this writer.

The four unconformities that are known to have affected the Cornwallis Fold Belt are shown in Table 2, along with their age of development and the formation that succeeded each one. It should be noted that the four circumstances listed above apply without exception to occurrences 1 through 8, and that the two exceptions (9 and 10) are small surface showings only.

Figure 2 is a structural cross-section through the Truro Island and Polaris deposits, showing the ages and lithologies of formations involved. All four of the geological circumstances listed above apply to each of these deposits. The deposits occur in the upper part of the Thumb Mountain Formation in the Crozier Strait anticline, a structure that developed in Early Devonian time by the folding that produced unconformities 2 and 3 (Table 2). Only unconformity 3 is exposed in this structure. This area was part of the Franklinian Geosyncline throughout deposition of the Cape Phillips Formation. Later deformations made it more stable so that the Disappointment Bay Formation and younger formations there are stable shelf deposits. Crozier Strait is a deep channel with steep parallel sides. Ruffman (pers. comm., 1975) suggested that this strait basically is a fault zone, and his idea was used in constructing the cross-section (Fig. 2).

The graben suggested in the cross-section doubtless is an oversimplification of the true situation in Crozier Strait. Normal faults have been drawn along

Table 1

Summary of the geology of lead-zinc occurrences of the central Canadian Arctic Islands.
Locations are shown by number on Index Map (Fig. 1).
Unconformities shown by number in Column 5 are those listed in Table 2.

	1	2	3	4	5
No.	Name of showing	Discoveries to date	Host Formation(s)	Relation to Silurian Facies Change	Relation of Thumb Mountain Formation to unconformities
1	Sheills Peninsula	Good shows from surface and drilling	Thumb Mountain	Below Cape Phillips shale belt	Truncated by Unconformity 3
2	Dundas Island	Spectacular surface showing	Thumb Mountain	Below Cape Phillips shale belt	Truncated by Unconformity 3
3	E. Bathurst Island	Minor surface showings	Thumb Mountain	Below Cape Phillips shale belt	Truncated by Unconformity 3
4	Truro Island	Spectacular surface showing	Thumb Mountain	Below Cape Phillips shale belt	Truncated by Unconformity 3
5	Polaris	20 million tons 20% combined Pb-Zn proven by drill and shaft	Thumb Mountain	Below Cape Phillips shale belt	Truncated by Unconformity 3
6	Eclipse	1 million tons 13% combined Pb-Zn proven by drilling	Thumb Mountain	Below Cape Phillips shale belt	Truncated by Unconformity 2
7	Stuart River	Small showings in cores	Thumb Mountain (and Disappointment Bay)	Below Cape Phillips shale belt	Truncated by Unconformity 3
8	Rookery Creek	Small showings in cores	Thumb Mountain, Disappointment Bay and Griper Bay	Below Cape Phillips shale belt	Truncated by Unconformities 3 and 4
9	Taylor River	Small surface showings	Thumb Mountain	Below carbonate belt	Unknown
10	Allen Branch	Small surface showing	Allen Bay	In carbonate belt	Unknown

each of the two inward-facing steeply-sloping submarine slopes of Crozier Strait. This is rather similar to a situation a few miles to the west on eastern Bathurst Island (Kerr, 1974). There a north trending anticline that formed in Early Devonian time had its axis down dropped by a graben of late Cretaceous and possibly Tertiary age. It is not known what if any influence these faults had on the accumulation of ore.

The regional geology and stratigraphy of Little Cornwallis Island has been described by Thorsteinsson and Kerr (1968). A description of the Polaris deposit was given by Muraro (1973) and is summarized below. The Thumb Mountain Formation, normally limestone, is dolomitized around the Polaris deposit. The introduced mineral assemblage at the deposit includes the sulphides galena, sphalerite, pyrite and marcasite, as well as dolomite and calcite spar. Both the sulphides and the spar appeared to Muraro to occupy mainly space that had developed in the host formation by solution and brecciation.

Origin of the Ore deposits

The features of the Arctic deposits described in this paper are similar to the salient features ascribed to Mississippi Valley type deposits by Sangster (1970). Jowett (1975) drew a parallel between the Polaris deposit and Mississippi Valley type deposits, and with Pine Point in particular. The accumulation of these deposits in the Thumb Mountain Formation may have been in karst solution caverns in the manner proposed by Callahan (1964). Caverns could have formed in the Thumb Mountain Formation during one of the Early Devonian erosional events shown in Table 2. The source of metal ions may have been the nearby black shales of the Cape Phillips Formation in the manner suggested at Pine Point by Jackson and Beales (1967).

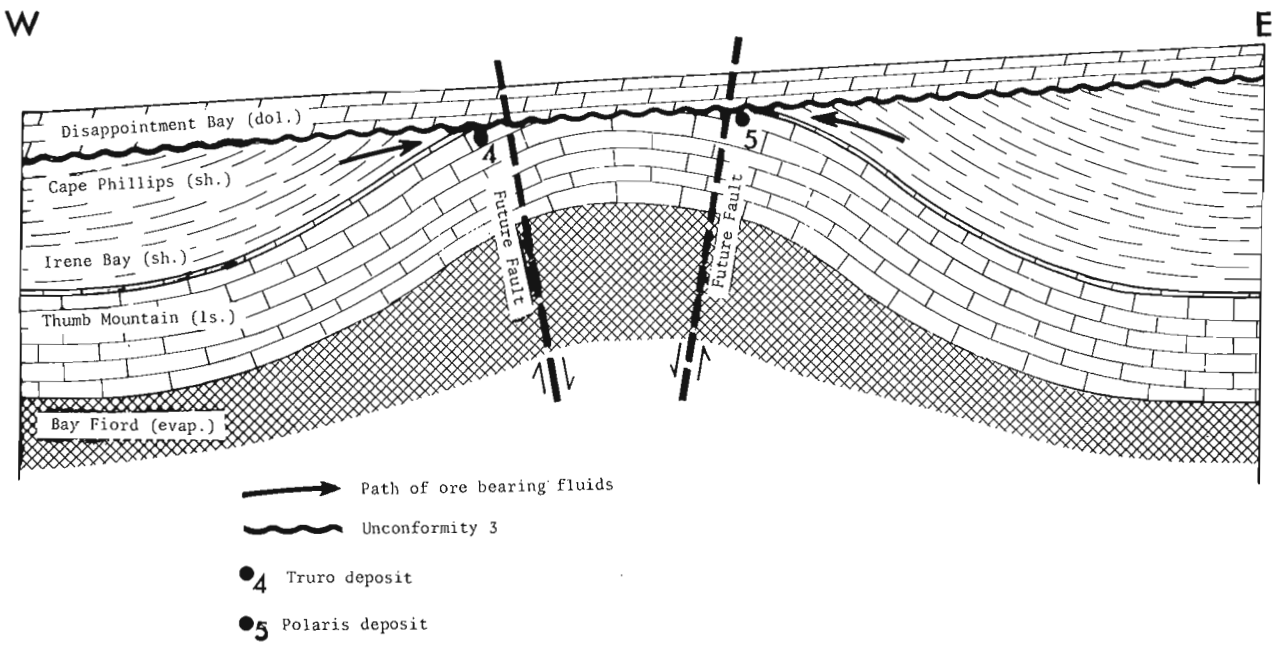

Figure 2. Sketch of the Crozier Strait Anticline in Early Devonian time, when ore is presumed to have formed at the Truro and Polaris deposits. The sites of faults are marked, but they had not yet developed.

Table 2

Unconformities affecting the Cornwallis Fold Belt and referred to in Column 5 of Table 1.

Unconformity No. (Table 1, Col. 5)	Age	Formation Succeeding Unconformity
4	Late Devonian	Griper Bay (quartz sandstone)
3	Early Devonian	Disappointment Bay (dolomite)
2	Early Devonian	Stuart Bay (limestone) or Snowblind Bay (dolomite)
1	Early Silurian	Cape Storm (limestone; Kerr, in press)

References

Brown, M. R.
1973: Cominco opening major new Arctic mines; The Northern Miner, v. 59, no. 4, Apr. 12.

Callahan, William H.
1964: Paleophysiographic premises for prospecting for stratabound base metal mineral deposits in carbonate rocks, Symposium on Mining Geology and the Base Metals, Central Treaty Organization, p. 191-248.

Jackson, S. A. and Beales, F. W.
1967: An aspect of sedimentary basin evolution: The concentration of Mississippi Valley-type ores during late stages of diagenesis; Can. Pet. Geol., Bull., v. 15, no. 4, p. 383-433.

Jowett, E. C.
1975: Nature of the ore-forming fluids of the Polaris lead-zinc deposit, Little Cornwallis Island, N.W.T., from fluid inclusion studies; Can. Inst. Min. Met., Bull., v. 68, no. 755, p. 124-129, March 1975.

Kerr, J. Wm.
1974: Geology of Bathurst Island Group and Byam Martin Island, Arctic Canada (Operation Bathurst Island); Geol. Surv. Can., Mem. 378, 152 p.

Muraro, T.W.
1973: Lead-zinc mining on Little Cornwallis Island; Can. Soc. Explor. Geophys., Proc. First National Convention, Calgary, 1973.

Sangster, D.F.
1970: Metallogenesis of some Canadian lead-zinc deposits in carbonate rocks; Geol. Assoc. Can. Proc., v. 22, p. 27-36.

Sangster, D.F. (cont'd.)
1974: Geology of Canadian lead and zinc deposits; Geol. Surv. Can., Paper 74-1, Part A, p. 141-142.

Thorsteinsson, R.
1973: Prince Alfred Bay (59B), Resolute (58F), Baillie Hamilton Island (58G), Lowther Island (68E) and McDougall Sound (68H) map-areas, Arctic Islands; Geol. Surv. Can., Open File Report 139.

Thorsteinsson, R. and Kerr, J. Wm.
1968: Cornwallis and adjacent smaller islands, Canadian Arctic Archipelago; Geol. Surv. Can., Paper 67-64.

AUTHOR INDEX